

https://dspace.org/

A geometallugical characterisation of the Hwange coalfield: how does coal formation affect coal exploitation?

Maponga, Oliver Josiah

2021
https://hdl.handle.net/10539/31890

Downloaded from a DSpace repository. https://dspace.org/



A GEOMETALLURGICAL CHARACTERISATION OF THE HWANGE COALFIELD: HOW DOES COAL FORMATION AFFECT COAL EXPLOITATION?

Oliver Josiah Maponga

A Thesis submitted School of Chemical and Metallurgical Engineering, Faculty of Engineering and the Built Environment, University of the Witwatersrand, in fulfilment for the degree of Doctor of Philosophy.

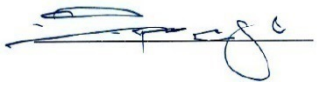
Supervisors:

Prof Rosemary Falcon, Prof Nicola Wagner, and Dr Samson Bada

January 2021

DECLARATION

I declare that this thesis is my own, unaided work. It is being submitted for the Degree of Doctor of Philosophy in the University of the Witwatersrand, Johannesburg. It has not been submitted for any degree or examination in any other University.

Signed:  …. on this …13th…. day of... January ...year …2021.

ABSTRACT

The Hwange Colliery located in northwest Zimbabwe hosts significant coal resources. The mine produces thermal coal for power generation, as well as some of southern Africa's best coking and blend coking coals.

However, since the commissioning of Chaba Opencast and 3 Main Underground Mine in 2005, certain anomalies, which have technological implications, have arisen, and there is need to establish the reasons for these anomalies. Questions posed included: a) Why does the Chaba coal reserve previously classified as coking coal based on cut-offs of a cumulative ash maximum of 15% and cumulative volatile matter minimum of 23.5% fail to produce coking coal in the plant? b) Why do-good coking properties produced in some areas of Hwange Colliery not respond well to conventional coking tests? A compelling need arose to characterise the Hwange coals and estimate the tonnages of the mineable reserves for each of the three coal categories, namely: thermal coal, general purpose coal, and coking coal, thus ensuring Hwange Colliery's preparedness to meet the coal quality demands for a variety of users.

Historical geological data generated by previous exploration programmes and new coal samples representative of the future mining areas and anomalous coals were examined. Coal samples were collected from Hwange Colliery's Chaba and 3 Main Underground mines and key analyses and tests were conducted on them. These included proximate, ultimate, and total sulphur analyses for basic characterisation of the Hwange coals; petrographic analyses to determine coal rank, maceral composition and mineral matter in the coal. XRF analysis was undertaken to determine the ash composition as well as combustion prediction and coking tests.

The geological mapping study revealed that faulting is dominantly listric increasing in intensity westwards and the main coal seam becomes progressively deeper westwards. The footwall of the seam plunges from 850m above sea-level in the northeast to approximately 490m above sea-level in the south-west. Localised topographic highs and lows occur were found within the coalfield. The coal seam is significantly thicker in the pre-coal forming topographically low-lying areas but thins out over topographic highs.

In the analytical investigation, proximate and petrographic analyses of the coal samples revealed that a low-ash, vitrinite-rich coal band occurs near or at the base of the seam, and that

the overlying coals passing progressively up through the seam become richer in ash and inertinite. Based on this sequence, it is suggested that the maceral profile reflects an initially wet swamp environment in early coal-forming times which was progressively replaced by increasingly drier forest swamps. The low-ash basal horizon is significantly thicker in the topographic depressions (up to 6m) but is thinner (1-2 m) where the seam abuts over or against topographic highs, namely, in locations in excess of 600 m above sea level. The mineral matter comprises silicates, sulphides and carbonates, with clay the dominant mineral, particularly towards the top of the coal seam. Combustion tests reveal that the vitrinite-rich basal samples devolatilise at lower temperatures, have lower peak temperatures, and burn out more rapidly than the inertinite-rich samples found higher in the seam. In terms of rank, the Hwange coals are Bituminous and more specifically Medium Rank B and C. No heat effect from sills and dykes has been observed. No specific regional trend in rank has been observed.

With regard to coking attributes, the study revealed that volatile matter is not a good indicator of coking properties. Some Hwange coals yield high volatile matter contents but possess a free swelling index lower than the 3.5, the minimum for most coking coals, while other Hwange coals possess relatively low volatile matter contents and swell to some extent. Proximate analyses alone are, therefore, insufficient to indicate coking capacity in these coals. Of all coals tested, only the lowest part of the seam in the Chaba location yielded a sufficiently high vitrinite content and free swelling index to qualify as a coking coal. The samples higher up the seam, although high in the volatile matter (23.5% and above), have low free swelling indices and vitrinite contents insufficiently high to qualify as coking coal.

The reason for the anomalous swelling capacity in coals that showed good swell, but low volatile matter content appears to be associated with the presence of exudatinite in association with reactive semi-fusinite, fusinite and secretinite. Exudatinite, is a high volatile, viscous material that would have emanated from liptinite and vitrinite at specific levels of rank during coalification, and as a consequence of regional heating. Coals that have high volatiles but do not show swelling capacity simply have vitrinite contents that are too low in proportion to provide any degree of swelling and coking properties.

Based on a review of the extensive borehole data undertaken throughout the Hwange Mine, and the resource and reserve calculations both undertaken in this thesis, it is estimated that the remaining life of mine for coking coal is 43 years, and for thermal coal as used in the agricultural, cement and brick making industries is 39 years. Assuming the production rates

are sustained, Hwange Colliery has the potential to generate in excess of USD 1 277 000 000 per year over the next 43 years.

ACKNOWLEDGEMENTS

I would like to thank Hwange Colliery Company for allowing me to carry out this study on their property and for use of some of the Company facilities during the study.

I am most grateful and indeed indebted to my Supervisors (Professors RMS Falcon, N.J. Wagner and Dr SO Bada), not only for their guidance, but were a great source of encouragement. My repeated appeals for financial assistance, which they generously provided, is immensely appreciated.

I also would like to thank Dr Bada who very willingly assisted during some of the Laboratory work; and Maggie Blair, as well as Gail Gordon, who offered logistical support when this was most needed.

Mention must be made of Zama, Bruce and Janet at Wits University for logistical assistance with regards to Laboratory work.

Thanks, are also due to the Hwange Colliery Company Geology and Coal Laboratory staff for the various technical support which they very willingly offered.

I am greatly indebted to my wife, Marcella, and my three children Carol, Frederick and Anisa; with extended thanks to Anisa who put up with my frequent calls for assistance with ICT systems for which she has a great talent.

Last, but by no means least, my thanks go to fellow postgraduate students, Kundayi Chagwedera, who assisted in various ways.

TABLE OF CONTENTS

DECLARATION ..... **i**

ABSTRACT ..... **ii**

ACKNOWLEDGEMENTS ..... **v**

TABLE OF CONTENTS ..... **vi**

LIST OF FIGURES ..... **xi**

LIST OF TABLES ..... **xv**

CHAPTER ONE: INTRODUCTION **1**

1.1 Motivation for This Study. 1

1.2 General background 2

1.3 Coal and the Coalification Process 9

1.4 Generalisation of the Zimbabwe Coal Deposits 12

1.5 Aim and objectives of the study 14

1.6 Research Questions 14

1.7 Hypothesis 15

1.8 Intended Outcomes 15

1.9 Structure of the thesis 15

CHAPTER TWO: LITERATURE REVIEW **16**

2.1. Introduction 16

2.2. The Zimbabwe Coal Industry 16

2.3. Factors controlling or influencing coalfield development and coal seam attributes in southern Africa 20

2.3.1. Macro-level Factors Affecting Coalfield Development 20

2.3.1.1. Tectonic Framework 20

2.3.1.2. Climate and Flora 25

2.3.1.3. Local Depositional Environments and Sedimentary Controls 32

2.3.2. Micro-factors Affecting Coal Seams 33

2.3.2.1 Characterisation of In-seam Strata 33

2.3.2.2 In-seam Biostratigraphic Subdivisions and Correlations 36

2.3.3 Mid-Zambezi Basin Models 40

2.3.3.1. The Tectonic Model for the Mid-Zambezi Basin 40

2.3.3.2. The new rift concept of the Mid-Zambezi Basin 46

2.3.4 Lithology and coal-quality related to environment of deposition of the K^{2-3} Group 49
2.3.4.1. Information from maceral analysis of coal. 52
2.4 Coal Characterisation 54
2.4.1. Introduction 54
2.4.2. Coal Characterisation 55
2.4.3. Organic Constituent 55
2.4.3.1. Vitrinite Group 56
2.4.3.2. Inertinite Group 58
2.4.3.3. Liptinite Group (Previously known as Exinite group) 60
2.4.4. Mineral Matter 62
2.4.4.1. Syngenetic minerals (primary mineral matter) 63
2.4.4.2. Epigenetic minerals (secondary mineral matter) 64
2.4.5 Microlithotypes 66
2.4.6 Coal Condition 66
2.4.7 Coal Rank 67
2.4.8. Analytical Techniques 68
2.5. Coal Beneficiation 72
2.5.1. Reasons for Coal Beneficiation 72
2.5.2 Broad Steps in Coal Beneficiation 72
2.5.3. Coal Beneficiation Methods (past and present) 74
2.5.3.1. Heavy Medium Separation and Float and Sink (Washability) 74
2.5.3.2. Jigging 77
2.5.3.3. Froth Flotation 77
2.5.4 Beneficiation of Coal for Making Coke 78
2.5.4.1. Coal Beneficiation in Zimbabwe 78
2.6. Coal Utilisation 79
2.6.1. Properties/Factors affecting Coal Utilisation 79
2.6.1.1. Intrinsic factors 79
2.6.1.2 External factors 81
2.6.2 Coal use for Power Generation 82
2.6.3 Coal Carbonisation 82
2.7 Chapter Summary 88
CHAPTER THREE: METHODOLOGY 91
3.1 Introduction 91

3.2. Geological mapping 92
3.2.1 Surface Geological Mapping 92
3.2.2 Underground and Open Pit Geological Mapping 93
3.3 Historical raw coal sample data review and processing 96
3.3.1 Drilling practice 96
3.3.2 Drill core samples quality assurance and quality control 99
3.3.3 Hwange Main Seam Modelling 99
3.4 Coal sampling and sample collection for the current study 101
3.4.1 Description of sample localities 103
3.4.1.1 Chaba Opencast Mine: 103
3.4.1.2 Main underground mine. 103
3.4.2 Sample preparation 104
3.5 Analytical techniques 104
3.5.1. Proximate Analysis 107
3.5.2 Total sulphur analysis 108
3.5.3 Phosphorus 108
3.5.4 Heat Content Analysis 108
3.5.5 Ash Chemistry (XRF) 108
3.5.6 Petrographic Analyses 108
3.6 Coking Tests 109
3.6.1 Dilatation 109
3.6.2 Roga Index 109
3.6.3 Free Swelling Index 109
3.7 Combustion tests using Thermogravimetric Analysis (TGA) 110
3.8 Furnace/Oven Tests 110
3.9 Challenges Faced. 110
3.10 SUMMARY OF THE COAL ANALYSES CONDUCTED DURING THE STUDY 111
CHAPTER THREE: RESULTS AND DISCUSSION 113
4.1 Introduction 113
4.2 Geology of the Hwange Basin 113
4.2.1 Background 113
4.2.2 Description of the area covered by the study. 119
4.2.2.1 Stratigraphy of Hwange Colliery Operational Area 121
4.2.2.2 Structural Geology of Hwange Colliery Mining Area 123

4.2.2.3 Controls on the Hwange Main Seam Thickness 131
Geological Sections along Selected Lines 133
4.2.3 Coal thickness Distribution over the Hwange Concession and Option Area 138
4.2.3.1 Coking Coal 138
4.2.3.2 Thermal Coal 139
4.2.3.3 Free Swelling Index Values of the Mine Site from Historical Drill-hole Data 142
4.3. Implications of Geological Aspects of Hwange Coalfield on Coal Attributes 144
4.3.1. Implications of Palaeotopography on Coal Formation 144
4.3.2 Implications of Tectonics and Structural Geology on Coal Formation and Condition 146
4.4 Coal Characterisation 149
4.4.1. Proximate Analysis 149
4.4.1.1. Proximate Analyses for Chaba Channel 1 and Channel 2 Samples 149
4.4.1.2. Proximate Analyses for 3 Main East Channel Samples 151
4.4.1.3. Proximate analyses for 3 Main South Channel coal samples 151
4.4.1.4 The Hwange Seam Ash Vertical Trend Current Samples and Drill Core Samples 154
4.4.2. Total Sulphur content in Chaba Coal Samples 157
4.4.2.1. Variation of total sulphur along 3 Main East and 3 Main South channels 158
4.4.2.2. Variation of sulphur at 3 Main sites A and B 158
4.4.3. Phosphorus Analyses 159
4.4.3.1. Phosphorus analysis for Chaba Channel 1 and Channel 2 Samples 159
4.4.3.2. Phosphorus content in 3 Main East and 3 Main South channels 160
4.4.3.3. Phosphorus content in 3 Main sites A and B coal 161
4.4.4. Calorific Value analysis 162
4.4.5. XRF Analyses 165
4.4.6 Petrographic Analyses 171
4.4.6.1. Coal Rank determination by Vitrinite Reflectance Analysis (ISO 7404) 171
4.4.6.2. Maceral Analyses 174
4.4.6.3 Mineral Species in Hwange Coal 185
4.4.6.4 Macerals Microscopy 190
4.4.6.5 Microlithotype Analysis 209
4.4.7 Thermogravimetric Analyses: (TGA & DTG) 215
4.4.8 Coking Coal Analysis Tests 219
4.4.8.1 Dilatation 219
4.4.8.2 Free Swelling Index 222
4.4.8.3. Roga Index 223

4.4.9 Furnace tests/Observations 223
4.4.10 Selected Quality Parameters and Coal Classification 231
4.5 Depositional Environment of the Hwange Coal 232
CHAPTER FIVE: ECONOMIC POTENTIAL OF THE HWANGE COAL CONCESSION 234
5.1 Introduction 234
5.2 Estimated in Situ Coal Resource of the Hwange Coal Concession 235
5.2.1 Straight Hwange coking coal (HCC) 235
5.2.2 Blend coal 235
5.2.3 Hwange industrial coal (HIC) 236
5.2.4 Thermal coal (Hwange 920 MW coal-fired electricity generation plant - HPS): 236
5.3 Resource Conversion to Mineable Reserve 237
5.3.1. Strip Mining: 237
5.3.2. Underground Bord and Pillar Mining: 237
5.4. Anticipated Coal Product Demand and Raw Coal Supply 238
5.5 Projected Coal Product Sourcing Requirements 239
5.6 Hwange Colliery Market Structure for coking, blend coal and industrial coal 240
5.7 Hwange Thermal Coal Market 241
5.8 Estimated Remaining Life of Mine 242
5.9 Financial Appraisal 242
CHAPTER SIX: CONCLUSIONS AND RECOMMENDATIONS 244
6.1. Overall summary of the Approach and Methodology to this Research 244
6.2. Controls on the deposition of Hwange Main Seam and its impact on coal quality 246
6.3. Conclusions regarding the Coking Anomalies 247
6.3.1 Chaba coal anomaly 248
6.3.2 Why do some Hwange Low Volatile Coals produce Swelling indices and Coke. 248
6.4. Economic Value of Hwange Coal Resource and Life of Mine 249
6.5. Recommendations 249
CHAPTER SEVEN: REFERENCE LIST 252
APPENDICES 272

LIST OF FIGURES

Figure 1.1: Location of Karoo Basins and some of the coal producing mines in Zimbabwe (Maponga, 2014). 2
Figure.1.2: Location of Zimbabwe's southern Karoo basins in relation to those of South Africa, Botswana and Namibia (Source: Bordy and Catuneanu, 2001). 3
Figure 1.3: Human Development Index versus Electricity Demand. (Source: International Energy Agency, 2004). 4
Figure 1.4: Countries heavily dependent on coal for electricity (Source: IEA Statistics, 2017). ... 5
Figure 1.5: Carbon intensity of industry energy consumption, Zimbabwe 1990 -2018 (Source: IEA Statistics, 2020). 6
Figure 1.6: Status of Special Grants issued for coal exploration and/or mining (after Moyo, 2012) 8
Figure 1.7: Global carbon cycle interrupted for fossil fuel formation. (Source: Arnold, 2013)... 11
Figure 1.8: Coal rank and physico-chemical changes associated with the coalification process (By Steve Greb, © Kentucky Geological Survey, 2013). 12
Figure 1.9: Lithostratigraphic correlation of the Lower Karoo in the Mid-Zambezi Basin (Adapted from Lepper, 1992). Not to scale. 13
Figure 1.10: Economic Aspects of Hwange Main Seam (Source: Maponga 2014). 14
Figure 2.1: Hwange Colliery Company Concession mining blocks. 19
Figure 2.2: Distribution of Karoo basins in south-central Africa (source: Catuneau *et al*. 2005; modified from Johnston *et al.*, 1996; Wescott and Diggens, 1998; Nyambe, 1999; Wopfner, 2002). 22
Figure 2.3: Distribution of the main stratigraphic groups of the main Karoo Basin (source: Wheeler and Götz, 2016; modified after Catuneau, *et al.* 1998) 23
Figure 2.4: Climate reconstruction of the main Karoo Basin based on pollen-producing flora (from Hancox and Götz, 2014; modified after Falcon 1986). 26
Figure 2.5: Major structural features affecting Karoo deposition in Southern Africa during Late Palaeozoic and Early Mesozoic Times (Falcon, 1986). Basins 1: Main Karoo Basin; 2: Botswana Basin; 3: Angolan Basin; 4: Mid Zambezi; 5: Lower Zambezi Basin; 6: Limpopo Basin; 7: Mozambique Basin; 8: Luangwa Basin; 9: Tanzanian Basin; 10: Zaire Basin. 29
Figure 2.6: A cross section through different types of coal-bearing basins associated with the Kaapvaal Craton, South Africa, during the Permian and Triassic Times (after Falcon, 1978c, 1986b; Whateley and Hopkins, 1985). 30
Figure 2.7 a and b: Summary of the No.2 seam stratigraphy using microlithotype petrographic profiles and illustrating vertical zones, subzones, and clastic partings. The sum of vitrite (and clarite) and intermediate categories (vitrinertite and trimacerite) and Inertite forms were used to draw the lithotype profiles. (Source: Falcon, 1989). 35

Figure 2.8: Graphic presentation of the Hwange Concession subseam development based on Drill-hole 1067 proximate analysis (after Pallocks, 1987). 39
Figure 2.9: Location of the Hwange Coalfield in relation to other coalfields and coal-occurrences in the Mid-Zambezi basin, Zimbabwe (I=Insuza, S=Sawmills, T=Tsholotsho) (source: Oesterlen and Lepper, 2005). 43
Figure 2.10: The mobile belts of Central Africa and the distribution of the Karoo Basins (after Orpen *et al*., 1989). Mw = Mwembesi Shear Zone; Mz = Mzarabani Shear Zone; K = Karoo. Mobile belts are identified as follows: A = Damaran; B = Irumide; C = Magondi; D = Lufilian Arc; E = Zambezi; and F = Mozambique Mobile Belt. 44
Figure 2.11: Sketch map of Central African Karoo basins showing their broad-scale geometry (Orpen *et al*., 1989). 46
Figure 2.12: Suggested stages in the development of the Mid-Zambezi Basin (Diagrammatic and not to scale. Source: Oesterlen, 1999). 48
Figure 2.13: The K^{2-3} lithofacies changes at the Hwange coalfields including lithological legend (Source: Oesterlen and Lepper, 2005). 51
Figure 2.14: The formation of vitrinite and inertinite (from Falcon, 2013). 59
Figure 2.15: International classification of coal seam by type – hard coal (after Falcon, 2013).. 62
Figure 2.16: Mineral matter introduction into the peat swamp. 64
Figure 2.17: A Typical TGA and DTG (burning profile) curves (from Norton, 1993). 71
Figure 2.18: Simple burning profile (DTG) showing moisture loss, initiation temperature for volatile matter (IT_{vm}) and fixed carbon (IT_{fc}), peak temperature (PT) and burnout temperature (BT) (from Norton, 1993). 71
Figure 2.19: Broad steps in the beneficiation of coal. 73
Figure 2.20: Geological modelling (as per major customers) of a seam during coal exploration. 74
Figure 2.21: Heavy medium separation plant configuration (from Kubach, 2012). 75
Figure 2.22: Diagram to illustrate the Float and Sink Process (from the US National Commission on Energy Policy, 2008). 76
Figure 2.23: Diagrammatic presentation of the Hwange Colliery Coke works and gas plant operation. (Hwange Colliery Centenary Brochure, 1995). 79
Figure 2.24: Standard profiles of coke buttons and the corresponding Free Swelling Index Number (from ASTM D-720-2010). 84
Figure 2.25: Audibert-Arnu dilatometer curve [ISO Standard 349-1975(E)]. 85
Figure 2.26: Coke Oven Operation: An oven has just been pushed and a quench car, full of incandescent coke, is *en route* to the Quench Station. (Photograph by Morrise, 2005). 88
Figure 3.1: Diagram to illustrate the layout of the off-set mapping method. 95
Figure 3.2: Diagram to illustrate the measurement and plotting of planar geological feature from the off-set Method. 95
Figure 3.3: Location of diamond core drill holes sunk over the Hwange Concession between 1983 and 2015. 98
Figure 3.4: The coal quality compositing procedure 100

Figure 3.5: Localities for the channel samples at Chaba Opencast and 3 Main Underground Mine. 102
Figure 3.6: Chaba Opencast highwall showing location of Channel 2 samples. 103
Figure 3.7: Summary of sampling and preparation steps taken Hwange coal analyses. 105
Figure 3.8: Flowsheet for Hwange coal samples 106
Figure 4.1: Geological map of the dichotomous Hwange Basin (modified from Watson, 1960) 114
Figure 4.2: Hwange Karoo Basin stratigraphy. 116
Figure 4.3: Geology of the area covered by the Hwange Colliery mining operations. 120
Figure 4.4: Log of BH 3901 (Matura Hills) showing the stratigraphy of Hwange Colliery Mining Area. 122
Figure 4.5: Structural plan of Hwange Concession and location of mined-out part of 3 Main showing mapped faults and joints. (Note some joints may well be listric faults). 124
Figure 4.6: Deka Fault juxtaposing pillow lavas of Batoka Basalts (on the left) against the Escapement Grits (on the right). Location: Deka Bridge to Angling Boating Club Camp at the Zambezi River. (blue pen is included for scale). 125
Figure 4.7: Structural map of part of 3 Main Underground Mine showing mapped joints and faults (current study). 128
Figure 4.8: Geological plan of part of Chaba showing location of one of the listric normal faults encountered. 129
Figure 4.9 : Geological section along Chaba coal face to show a listric normal fault. 130
Figure 4.10: Photograph of a highwall at JKL Opencast Block (also known as the Dragline Pit) showing a listric normal fault. 131
Figure 4.11: Hwange Main Coal Seam footwall profile over the Hwange Concession. 132
Figure 4.12: Hwange Concession and Western Areas Coalfield plan showing positions of selected section lines. 134
Figure 4.13: Geological section along section line E –F 135
Figure 4.14: Geological section along section line A – B. 136
Figure 4.15: Geological section along section line C – D (drawn during this study). 137
Figure 4.16: Hwange Concession thickness contour plan for the high grade coking coal. 140
Figure 4.17: Hwange Concession thickness contour plan for the thermal coal. 141
Figure 4.18: Free Swelling Index Value contour plan for 3 Main Underground Block based on borehole data available at time of study. The arrow points in the direction of overburden increase as well as direction of coal seam base plunge. 142
Figure 4.19: Free Swelling Index value contours for JKL Block based on data from historical drill-holes. The arrow points in the direction of overburden increase as well as direction of coal seam base plunge. 143
Figure 4.20: Structural plan of Hwange Concession and location of mined-out part of 3 Main showing mapped faults and joints. (Note some of joints may well be listric faults). 148
Figure 4.21: Variation of total sulphur along Chaba Channel 2. 157

Figure 4.22: Cross-correlation plot of ash yield (%) and calorific value (MJ/kg)..... 164
Figure 4.23: Cross-correlation plot of volatile matter (%) and calorific value (MJ/kg)..... 165
Figure 4.24: Cross-correlation plot of fixed carbon (%) and calorific value (MJ/kg)..... 165
Figure 4.25: Graph for SiO_2 in coal samples from Chaba and 3 Main channels..... 166
Figure 4.26: XRF analysis for Al_2O_3 in coal samples from Chaba and 3 Main channels. 167
Figure 4.27: Graph for CaO in coal samples from Chaba and 3 Main channels. 168
Figure 4.28: Graph for Fe_2O_3 (ferric oxide) in coal samples from Chaba and 3 Main channels.168
Figure 4.29: Graph for TiO_2 in coal samples from Chaba and 3 Main channels..... 169
Figure 4.30: Maceral group analyses (m.m.f) for the three Chaba Channel 1..... 178
Figure 4.31: Maceral group analyses (m.m.f) for the three Chaba Channel 2..... 178
Figure 4.32: Graph to show analyses (m.m.f) for the three maceral groups along 3ME Channel samples..... 182
Figure 4.33: Graph to show analyses (m.m.f) for the three maceral groups along 3MS Channel samples..... 185
Figure 4.34: Mineral species petrographically observed in Chaba Channel 1 samples..... 186
Figure 4.35: Mineral species petrographically observed in Chaba Channel 2 samples..... 186
Figure 4.36: Mineral species observed in 3 Main East samples. 187
Figure 4.37: Mineral species in 3 Main South samples. 187
Figure 4.38: Ash and observed mineral species in Chaba Channel 1 samples. 188
Figure 4.39: Ash and observed mineral species in Chaba Channel 2 samples. 188
Figure 4.40: Ash and observed mineral species in 3 Main East samples. 189
Figure 4.41: Ash and observed mineral species in 3 Main South samples..... 189
Figure 4.42: Microlithotype vertical variation along Chaba Channel 1 (%vol). NB, samples were taken at 3 m intervals vertically up the seam with 1565 representing the lowest sample (0-3 m), and the 1567 representing the top three metres of the seam. 213
Figure 4.43: Microlithotype vertical variation along Chaba Channel 2 (%vol). NB., samples were collected at 1 m intervals from base to top with 0-1 m representing the basal sample and 7-8 m representing the top of coal sample. 213
Figure 4.44: Microlithotype vertical variation along 3 Main East Channel. NB, samples was taken at 30 cm intervals vertically up the seam with 1542 being representing the basal sample (0-30 cm), and the 1553 representing top 30 cm of the channel. 214
Figure 4.45: Microlithotype vertical variation along 3 Main South Channel. 214
Figure 4.46: TGA and DTG for Chaba Channel 2 samples from 0-1 to 3-4 m. 216
Figure 4.47: TGA and DTG for Chaba Channel 2 samples from 4-5 to 7-8 m. 216
Figure 4.48: TGA and DTG for 3ME samples from 0-30cm to 90 -120 cm. 217
Figure 4.49: TGA and DTG for 3ME samples from 240 -270 to 3.30-360 cm. 217
Figure 4.50: TGA and DTG for 3MS samples from 0 -30 to 120-150cm. 218
Figure 4.51: TGA and DTG for 3MS samples from 150 -180 cm to 270-300 cm. 218
Figure 4.52: Coal lumps from lower half (i.e., from base to 4m above seam base) of Chaba Channel 2 showing varying levels of bubble (swellings) development. The lumps on the right in

each pair were heated in the furnace, while the ones on the left were unheated original samples. 225
Figure 4.53: Coal lumps 0-1m and 1-2m and their respective proximate analyses and coking tests results. Arrows point to the sample interval. 226
Figure 4.54: Coal lumps 2-3m and 3-4m and their respective proximate analyse and coking tests resultst Arrows point to the sample interval. 226
Figure 4.55: Coal lumps 4-5 and 5-6 and their respective proximate analyses coking tests results. Arrows point to the sample interval. 227
Figure 4.56: Coal lumps 6-7m and 7-8m and their respective proximate analyses and coking test results. Arrows point to the sample interval. 227
Figure 4.57: Coal lumps from 3 Main sites A and B. 228
Figure 4.58: Furnace and coking tests for 3 Main Site A 229
Figure 4.59: Furnace and coking tests for 3 Main Site B. 230
Figure 4.60: Vitrinite % vs Rank (RoVr) for Chaba Channel 2 samples. 231
Figure 5.1: Anticipated coal products flow model..... 240
Figure 5.2: Hwange coking coal, blend coal, and industrial coal distribution by market. 241

LIST OF TABLES

Table 2.1: Proximate analysis (ash and volatile matter contents) of drill-hole 1067 (after Pallocks, 1987)..... 39
Table 2.2: Mid-Zambezi coalfields and hosting intrabasins. 42
Table 2.3: Maceral analyses from drill-holes Nos. 101 and 107, Lubimbi coalfields (from Thompson, 1981). 53
Table 2.4: Maceral analysis of the coal horizons from Lubimbi coalfields (source; Thompson, (1981). 54
Table 2.5: Vitrinite maceral and their respective forms (source: Wagner, *et al*. 2018, adapted from ICCP System 1994). 57
Table 2.6: Macerals in the inertinite maceral group (source: Wagner *et al.* 2018; adapted from ICCP System 1994 (ICCP, 2001), with some modification) 59
Table 2.7: Macerals in the liptinite maceral group (after Wagner *et al*. 2018)..... 61
Table 2.8: Microlithotypes in coal (Taylor, et al., 1998) 66
Table 2.9: Most common conventional analyses (Falcon and Ham, 1988; Johns and Harris, 2009). 69
Table 2.10: Effects of selected coal properties on combustion (Falcon and Ham, 1988). 80
Table 2.11: Effects of some coal properties on metallurgical processes (Zimmerman, 1979)..... 80
Table 2.12: Comparative Thermal Coal Characteristics in South Africa and Zimbabwe. (Hwange Colliery Marketing Department, 2015)..... 82
Table 2.13: Representative data for the plastic properties of coals (Speight, 2013). 87
Table 2.14: Rough Comparison between FSI and Gray-King Test (after Zimmerman, 1979). ... 87

Table 3.1: Analyses and analytical phases (HCCL = Hwange Colliery Company Limited). 107
Table 3.2: Summary of coal analyses conducted. 112
Table 4.1: Proximate Analysis Results (air dry) for Chaba Channel 1. 150
Table 4.2**:** Results for proximate analyses of the Chaba Channel 2. 150
Table 4.3: Proximate analyses of 3 Main East Channel coal samples 151
Table 4.4: Proximate analyses of 3 Main South Channel coal samples. 152
Table 4.5: Hwange Main Seam proximate analysis, free swelling index (BH006750 core samples). 155
Table 4.6: Hwange seam proximate analysis and Free Swelling Index Free for BH006404 core samples. 156
Table 4.7: Total sulphur analyses for Chaba Channels 1 and 2 coal samples. 157
Table 4.8: Variation of sulphur content along 3 Main East and 3 Main South. 158
Table 4.9: Total sulphur content in coal samples from 3 Main sites A and B. 159
Table 4.10: Vertical distribution of phosphorus values along Chaba channels 1 and 2. 160
Table 4.11: Phosphorus analysis for coal samples collected at 3 Main East and 3 Main South. 161
Table 4.12: Phosphorus analysis for 3 Main sites A and B coal samples. 161
Table 4.13: Calorific values (MJ/kg) ash content (%) for Chaba and 3 Main Mines. 162
Table 4.14: Major oxides in Hwange coal ash (incorporating data from Mapani, *et al*., 2013). 170
Table 4.15: Global major inorganic constituents of coal ash (after Speight, 2013). 170
Table 4.16: Vitrinite reflectance results for Chaba Channel 1 Samples 171
Table 4.17: Vitrinite reflectance results for 3 Main East Channel. 172
Table 4.18: Vitrinite reflectance results for 3MS Channel samples. 172
Table 4.19: Detailed maceral analyses (% by volume) of Chaba channels 1 and 2. 176
Table 4.20: Summary of detailed maceral analyses of Chaba channels 1 and 2. 177
Table 4.21: Maceral group analysis (% by Volume) of 3ME Channel samples. 180
Table 4.22: Summary of detailed maceral analyses of 3ME Channel samples. 181
Table 4.23: Maceral group analysis (% by volume) for 3MS Channel samples. 183
Table 4.24: Summary of detailed maceral analyses for 3MS Channel. 184
Table 4.25: Microlithotype analysis for Chaba Channel 1 samples. 209
Table 4.26: Microlithotype analyses for Chaba Channel 2 samples. 210
Table 4.27: Microlithotype analyses for 3 Main East Channel samples 211
Table 4.28: Microlithotype analyses for 3 Main South Channel samples. 212
Table 4.29: Coking tests for Chaba Channel 2. 219
Table 4.30: Coking tests for 3 Main sites A and B Samples. 220
Table 4.31: Dilatation data for coking coals from areas in the sub-region (Kruger, 2013). 222
Table 5.1: summarises the in-situ resource in categories, by type and height above sea level as calculated from the borehole data used in this thesis. 237
Table 5.2: Mineable coal reserves categorisation by source, type & extraction technology. 238
Table 5.3: Hwange Colliery summary of mineable coal reserves in metric tonnes. 238

Table 5.4: Anticipated coking coal and blend coal products and extraction sourcing requirements 239
Table 5.5: Potential market requirement for Hwange coking coal, blend coal, and industrial coal. 240
Table 5.6: Anticipated thermal coal (HPS) product and demand (in tonnes). 241
Table 5.7: Estimated net value of Hwange Colliery's remaining coal reserve. 243

CHAPTER ONE: INTRODUCTION

1.1 Motivation for This Study.

Hwange Colliery is sited in the northwest of Zimbabwe in the Mid-Zambezi Basin. The relevance of this colliery is that it produces thermal coal for the coal-fired power generation users in Zimbabwe, but, more specifically, it also produces some of the sub-continent of southern Africa's best coking and blend coking coals for coke making for the metallurgical industries in the region.

However, questions are now arising with respect to the current quality of the coals being produced and those yet to be mined in future. Linked to these questions is the query: why do some Hwange coals produce good coking capacity blend materials but do not respond well in conventional coking tests? Furthermore, prior to the commissioning of the Chaba Opencast Mine and the 3-Main Underground Mine, both of which were brought into full production in 2006, all coal mined from the Hwange Colliery property with a cumulative ash maximum of 15%, and a cumulative volatile matter minimum of 23.5%, was defined as coking coal, and indeed such coal produced coked when heated in the absence of oxygen, both at the laboratory- scale and at the actual full-scale coke-works coke battery. But other coals with similar analyses did not produce coke. Such anomalies have considerable technical and economic impacts, not only for the mine and its production, but even more specifically for the metallurgical customer base that draws such specialised coals from this colliery.

The primary purpose of this thesis is three-fold as detailed below.

I. To undertake an in-depth study assessment into:
   a) the nature and performance of the coking coal and thermal coal in two main areas of the mine (the 3 Main Underground and Chaba Opencast); and
   b) the coking capacity in order to establish the reasons for the anomalies that have been identified.

II. To determine the general coal quality distribution across the Hwange Colliery; and

III. To evaluate the techno-economic aspects of the Hwange coal deposit by providing the remaining coal resources expected value(s) of the products yet to be mined, their value to the mine and the remaining life of mine (LOM).

1.2 General background

As an introduction to background knowledge, it is necessary to understand that Zimbabwe's coal measures are an integral part of the region's main Karoo Sequence. The Karoo sediments in Zimbabwe are preserved in two major areas: the Mid-Zambezi and the Save-Limpopo coal basins which occur on either side of the Zimbabwean Craton (Figure 1.1).

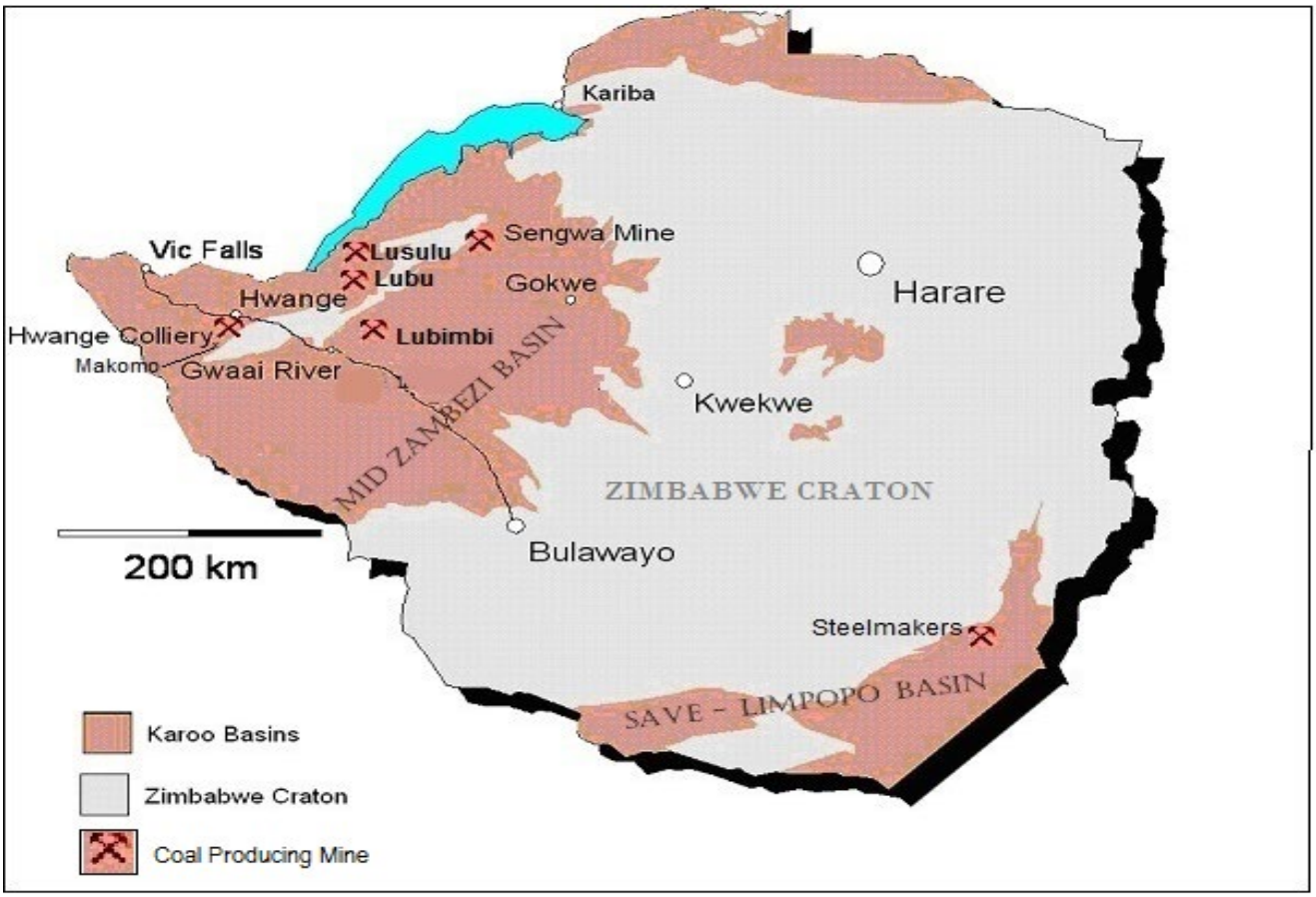


Figure 1.1: Location of Karoo Basins and some of the coal producing mines in Zimbabwe (Maponga, 2014).

The Limpopo area of the Save-Limpopo Basin is made up of the Tuli Basin, (Bordy and Catuneanu, 2001) which occurs on the triple junction of Zimbabwe, Botswana and South Africa; Chipise, which is partly South Africa and partly Zimbabwe; and Nuanetsi which falls wholly in Zimbabwe (Figure 1.2). Tectonically, Zimbabwe's southern Karoo basins (the Limpopo area and the Save) are linked to the Lebombo Basin of South Africa and Mozambique, and this is discussed in detail in Chapter 2, Section 2.2.

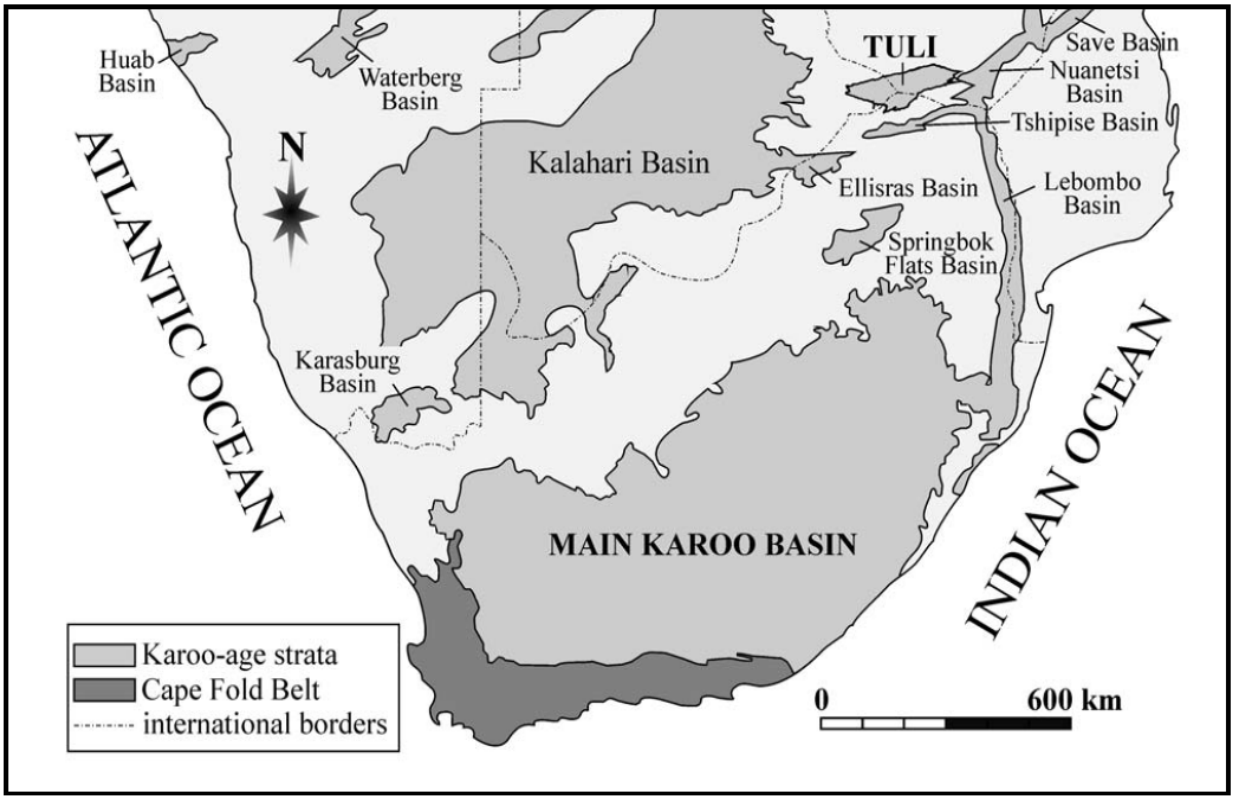


Figure.1.2: Location of Zimbabwe's southern Karoo basins in relation to those of South Africa, Botswana and Namibia (Source: Bordy and Catuneanu, 2001).

The main coal deposits in Zimbabwe lie in the west and northwest of the country, in the Mid-Zambezi Basin (Duguid, 1986a), where significantly thicker and better-quality coal occurs as compared with the coals hosted by the southern coalfields which in general are multiple, thin high ash materials (Duguid, 1986b; Bartholomew, 1992). This northern seam has played a pivotal role in the human and economic development of Zimbabwe, a function that is in tandem with the United Nations Development Programme (UNDP)'s thrust and objectives as embodied in the statements below. The economic and human development of any nation is directly proportional to the production and utilization of energy. The role of energy in development has amply been studied by organisations such as the UNDP (UNDP, 2004). The latter organisation has developed a set of numerical indices designed to measure the stage of human development in individual countries. One such index is Human Development Index (HDI), shown in Figure 1.3. This measures life expectancy at birth; adult literacy and school enrolment; and per capita GDP (adjusted for purchasing power parity). The relevance of the HDI to this thesis lies in the role of coal for human development in Zimbabwe as discussed in the paragraph below.

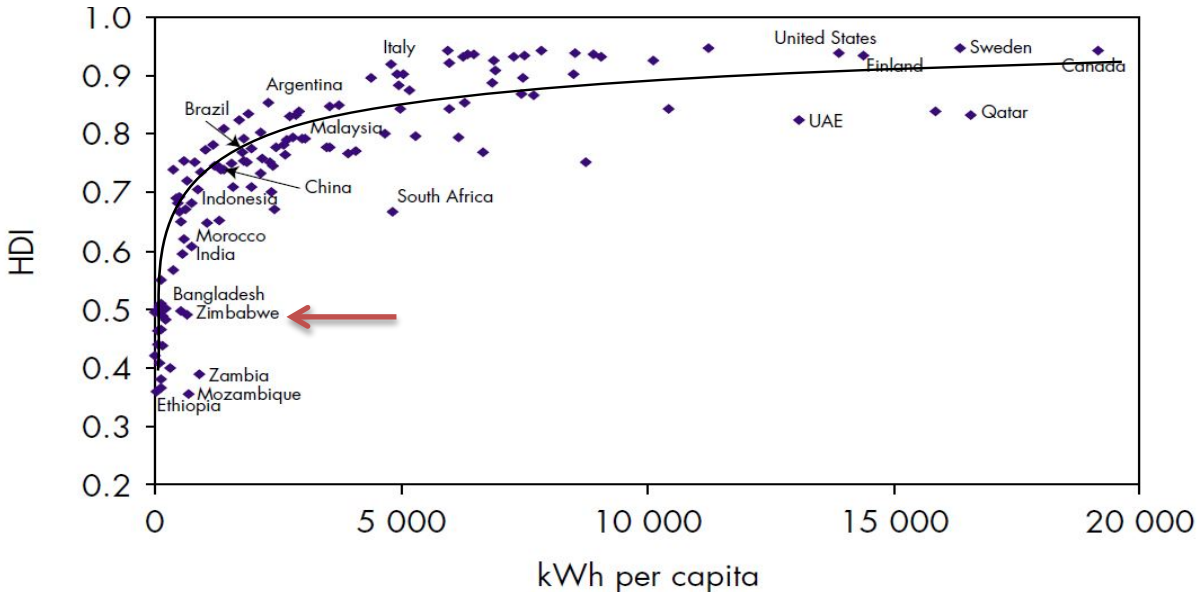


Figure 1.3: Human Development Index versus Electricity Demand. (Source: International Energy Agency, 2004).

Electricity demand is likely to increase if economic growth is experienced, with power prices that are economically acceptable (Exxon Mobil, 2008). Endowed with abundant coal resources, some of which are of high quality, Zimbabwe, a developing country, was reported to be one of the world's top 22 countries with heavy dependence on coal (Figure 1.4) for their energy needs (IEA Statistics, 2017). In fact, from 1902, when the first coal load left the underground mine for the market, up to the commissioning of the Kariba Hydroelectric Power Plant in 1961, the country depended solely on coal for its energy requirements, except for the basic form of energy source such as firewood and cow dung utilized mainly by the rural population.

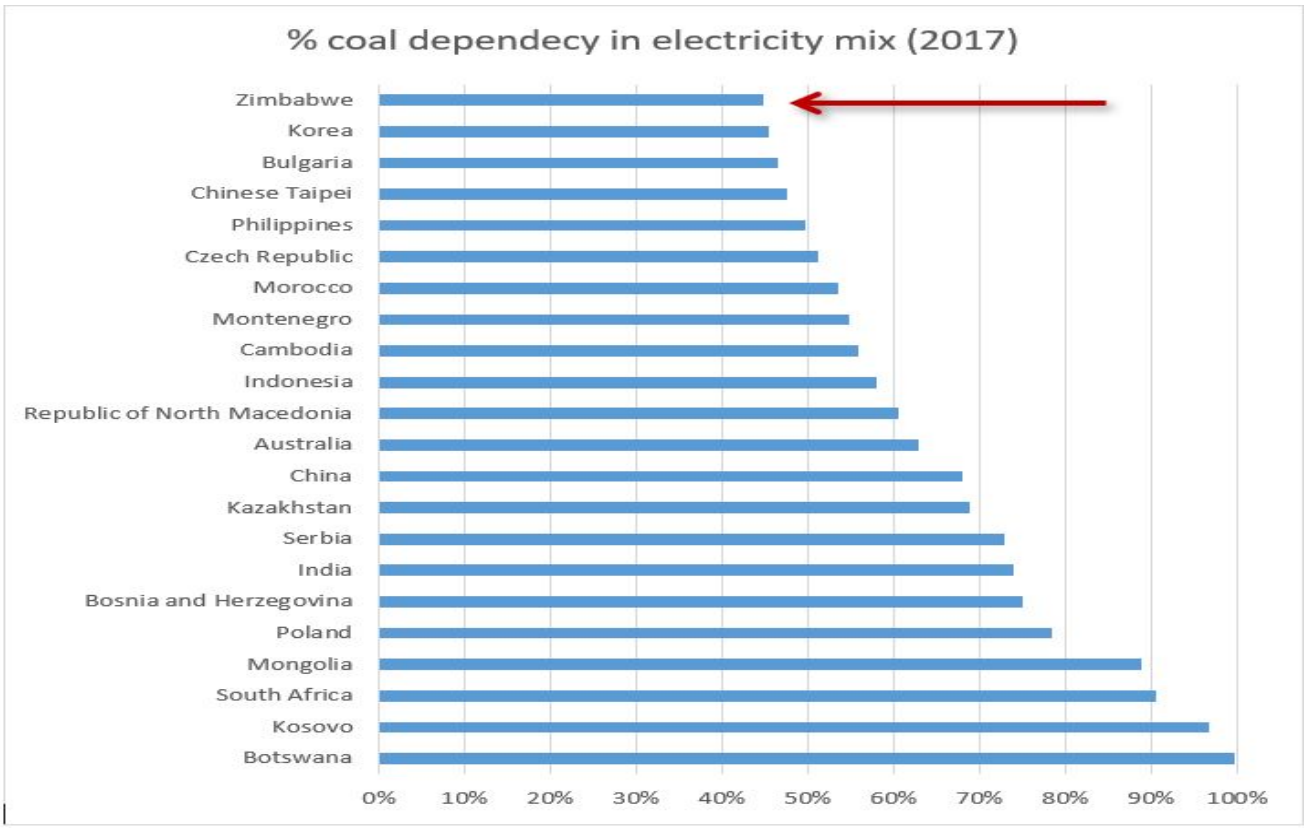


Figure 1.4: Countries heavily dependent on coal for electricity (Source: IEA Statistics, 2017).

While the International Energy Association (IEA Statistics 2016) reports a global drastic decrease in coal combustion over the last decade and that hydro-electricity is playing an increasing role as a source for electricity, in Zimbabwe the coal remained the major source as hydroelectricity has severely been affected by the vagaries of weather. The country's Kariba Hydro-electric Plant has been forced into temporary decommissioning due to the dam water levels falling to below critical levels for power generation. In their report on coal energy consumption in Zimbabwe (IEA Statistics 2020), IEA demonstrate that there has been a downward trend in this fossil fuel consumption from its peak circa 1991 to 2018 (Figure 1.5). This has been attributed not to preference for other sources of energy for power generation, such as hydro-electric plants, but is a result of severe reduction in production rates at the main coal producing company, Hwange Colliery, due to poor business performance of the mining giant.

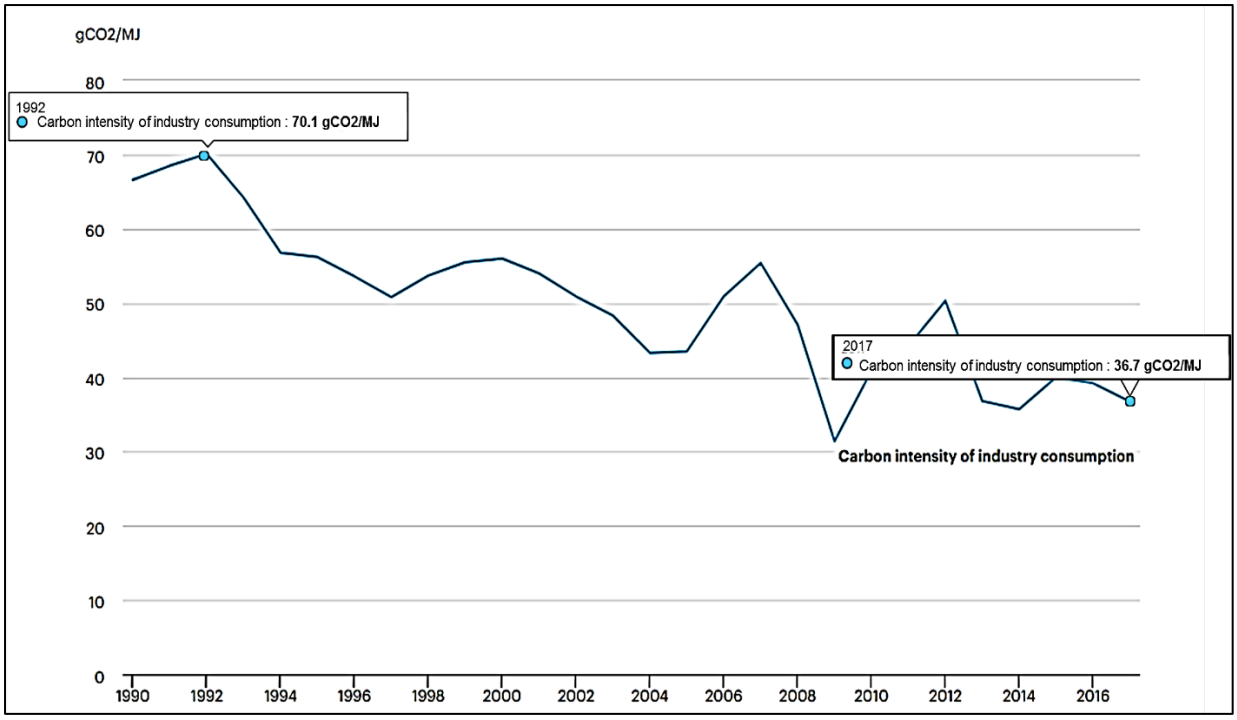


Figure 1.5: Carbon intensity of industry energy consumption, Zimbabwe 1990 -2018 (Source: IEA Statistics, 2020).

Until about 1980, Zimbabwe's solid fossil fuel requirements were met by coal from Hwange Colliery Company who exploited the Hwange coal deposit under an industry monopoly protected by an Act of Parliament known as the Wankie Act (1950). Zimbabwe's coal industry has since been de-regulated, a move that opened flood gates and ushered in stiff competition as the number of new entrants into the coal mining industry continues to increase. These mines are at different stages of development (Figure 1.6). The increase in the number of producers will, more than likely, result in the national coal output surpassing the country's demand.

Hwange Colliery Company Ltd, with its long coal producing history, has invested considerably in its operations in terms of manpower training, mining and beneficiation technology, buildings and other infrastructure, medical services provisions, and the like. The company recently took giant steps to increase its output mainly through technological advancement. These include the use of a fully mechanised bord and pillar underground mining system utilising. In addition to a continuous miner to cut and gather coal simultaneously into a fleet of three shuttle cars, in turn, trams the coal to a high-capacity feeder breaker (Maponga, 2019). Regrettably, this decision was taken against the background of increased competition from new entrants and a subdued local market. The company has since adopted the strategy to penetrate the regional and international markets, while at the same time making all efforts to retain its local market share (Hwange Colliery Company Strategic Plan, 2014). The company will protect its local

market share mainly by virtue of local knowledge, strategic coal pricing, and its current and long-time relationship with the coal market, which facilitates easier access to this sector. In terms of penetrating the regional markets, Zimbabwe has only one country south of it, i.e., South Africa, which currently is its only competitor in the northern markets. However, South Africa's coal must travel more than 1 000km to the northern markets. Thus, in terms of coal transport to markets, Zimbabwean coal has an advantage. Furthermore, Hwange Colliery Company will also capture road traffic bound north empty and will enjoy lower logistical charges than would the South African coal. Zimbabwe belongs to the Common Market for Eastern and Southern Africa (COMESA) which has no tariffs on coal and coke products, while South Africa is not a member of this organisation. Zimbabwe also has strong political links with countries to the north and Hwange Colliery Company will use this to advantage. Internationally, Hwange Colliery will leverage on Asian companies invested in the Zimbabwe extractive sector to get them to buy local coal and coke products. While the coal mining industry in Mozambique is on the increase, production is targeting the Indian and Chinese thermal coal sector taking advantage of the relatively cheaper maritime transport for the relatively lower value thermal coal product; while Hwange Colliery Company would focus on coking coal and coke products.

However, there is an increase in the number of customer complaints against Hwange coal's poor performance in boilers and various related power generation plants. These include "too much flaking in coal" and "poor burning rates" (Hwange Colliery Marketing Department report, 2012). The complaints could be spurred by the fact that the local market now has alternative internal suppliers, or the complainants might be using technologies designed for coal that is different from that of the Hwange Coal Deposit. True or not, Hwange Colliery is finding itself with no other option but to compensate the complainants in a desperate move to retain these customers. The question arises: is the poor coal performance due to the inherent properties of coal or to imposed boiler design or operating conditions? This is a question which, for the moment, Hwange Colliery cannot answer adequately. What is required is that specific coal products need to be matched to the process in which they are to be used.

STATUS OF COAL SPECIAL GRANTS

Various Stages Of Production

1	Hwange Colliery
2	Rio Zim (Sengwa)
3	Steel Makers (Simbi)
4	Tuli Coal Mine
5	Makomo Resources (Entuba)
6	Galpex Mine (Chibondo)

Exploration / Developement Stage

1	Dahlia
2	Hankano
3	Lubimbi
4	Lusulu
5	Lubu
6	Bubi

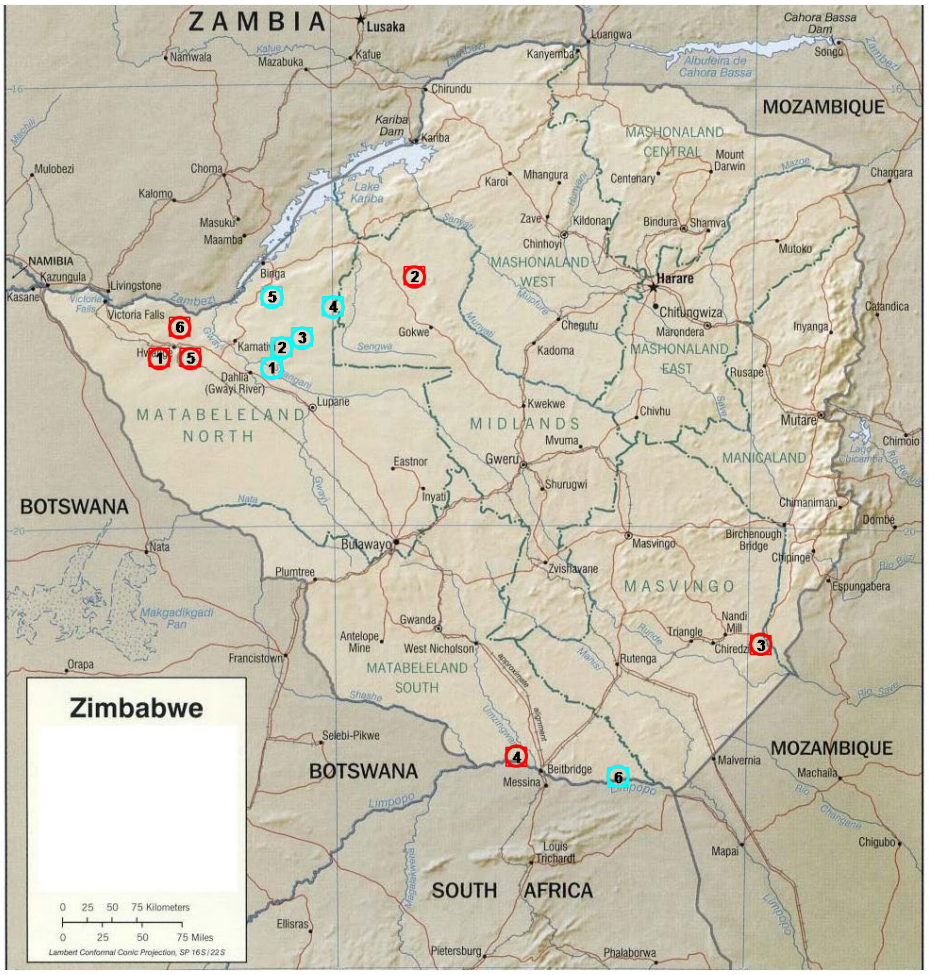


Figure 1.6: Status of Special Grants issued for coal exploration and/or mining (after Moyo, 2012)

The requirements of the regional and international thermal markets in terms of coal attributes are not fully understood, especially for customers who use equipment that burns coal whose attributes differ from those of the Hwange coal deposit. Experience elsewhere has shown that equipment or process technologies designed to combust or make coke from the northern hemisphere (e.g. USA and Europe) may not necessarily be suitable for burning or coking the coals found in the southern hemisphere, e.g. the Gondwana coals found in southern Africa, India and Australia, (Falcon, personal communication). Furthermore, and to demonstrate the existing challenge, in 2012 Hwange colliery's first load of export coking coal destined for the international market was rejected while at Maputo Port Terminal by the intended customer on the grounds of the declared swelling index of 2. On the international market this was considered as non-coking thermal coal yet experience in Zimbabwe showed the coal successfully coked (Source: Hwange Colliery Marketing Department).

These negative occurrences point to the fact that the properties of coal from the Hwange coal deposit are not fully understood. For the Company to penetrate the regional and international

markets, there is an urgent need to investigate and provide scientific proof on the properties of Hwange coal as required by the local and international markets. This is particularly crucial bearing in mind that, for a variety of reasons, coal varies vertically and laterally, within and between coalfields and between coal basins as noted in their physical and chemical attributes and with regard to their constituent organic and inorganic components (Falcon and Falcon, 1987; Chen, 1998). It is imperative that the relationship between the petrographic and mechanical attributes of the Hwange coal is well understood. The relationship between these aspects has been reported to be responsible for various anomalous performances when using some South African coals (Falcon and Falcon, 1987). Understanding of such anomalies and their possible application to the Hwange coal is currently limited. Such technical data, especially that which impacts on the beneficiation and utilization of the Hwange coal and which is often requested by the potential regional and international customers, is not available in the public domain. This is yet to be studied by Hwange Colliery Company, and therefore this study intends to investigate in detail what is responsible for the anomalous performance of Hwange coal.

The above statements and experiences form the core of the current study. In summary, this investigation has been prompted by the need to establish the conditions under which the Hwange coal was initially formed, the subsequent conditions imposed, how these affected the coal quality, and finally, how the subsequent qualities affect coal mining, beneficiation and utilization. Due to the large scope of this research, certain aspects will be identified and dealt with to a greater extent than others in this document.

1.3 Coal and the Coalification Process

Coal is a readily combustible sedimentary rock composed of organic material derived from ancient plant material (Arnold, 2013; Falcon, 2013). It is a heterogeneous substance made up of two main components. Firstly, the organic component, which is made up of macerals, the microscopic organic constituents known as the building blocks of coal. Secondly there are the inorganic constituents which are basically minerals including those found in the mineral categories such as sulphides, silicates, and carbonates. The higher the proportions of organic constituents, the greater the quality of the coal; while the higher the percentage of minerals, the higher the ash content and the poorer the value of the coal.

The organic component of this naturally occurring solid substance, like other hydrocarbons such as oil and natural gas, is made up essentially of carbon and hydrogen and is found

fossilised in rocks (Arnold, 2013). Carbon exists as carbon dioxide in three main environments: in the atmosphere, in water, and in rocks (Arnold, 2013). Living organisms utilise this gas in a variety of ways: for example, plants take in carbon dioxide during photosynthesis and give out oxygen; while animals, on the other hand, take up oxygen and give out carbon dioxide. Upon their deaths, these organisms' decay and some carbon dioxide is released into the atmosphere. Figure 1.7 represents the carbon cycle and the position of the fossil fuel in this cycle is clearly shown.

The process that dead plants undergo to become coal, i.e., coal coalification, is considered to fall into two stages (Pohl, 2011). The first is the peatification stage which takes place in the peat swamp. This is basically a biochemical process that takes place in an environment that is wetland and has an oxidised near-surface layer, with a shallow-depth reducing environment. Plant remains in swamp are decomposed by bacteria, archaea, actinomycetes and fungi (Stach, *et al.,* 1982; Pohl, 2011). Micro-organisms thriving on the organic residues synthesise humic macromolecules (Kögel-Knaber, 1993) and synthesised products vary according to the respective redox environment and the building materials (i.e., substrate) of the plants. Sugars, starch, pectin and protein are rapidly metabolised; while lignin is preferentially attacked by fungi (Hatcher and Clifford, 1997). As the mire, sea or lake floor sinks, a high energy environment is created and sediment slumps in and buries the vegetation, triggering the second phase which is essentially a geochemical one, and is abiotic (Damberger *et al*, 1984; Arnold, 2013). The coalification process *senso stricto* refers to the changes that take place during this second stage. The changes bring about the progressive transformation of peat to lignite, thence into subbituminous and bituminous coals, to anthracites and meta-anthracites (Wagner *et al.,* 2018). The degree of change, i.e., the level which a coal has reached in the coalification series, is referred to as its rank (Falcon, 2013, Wagner *et al*., 2018).

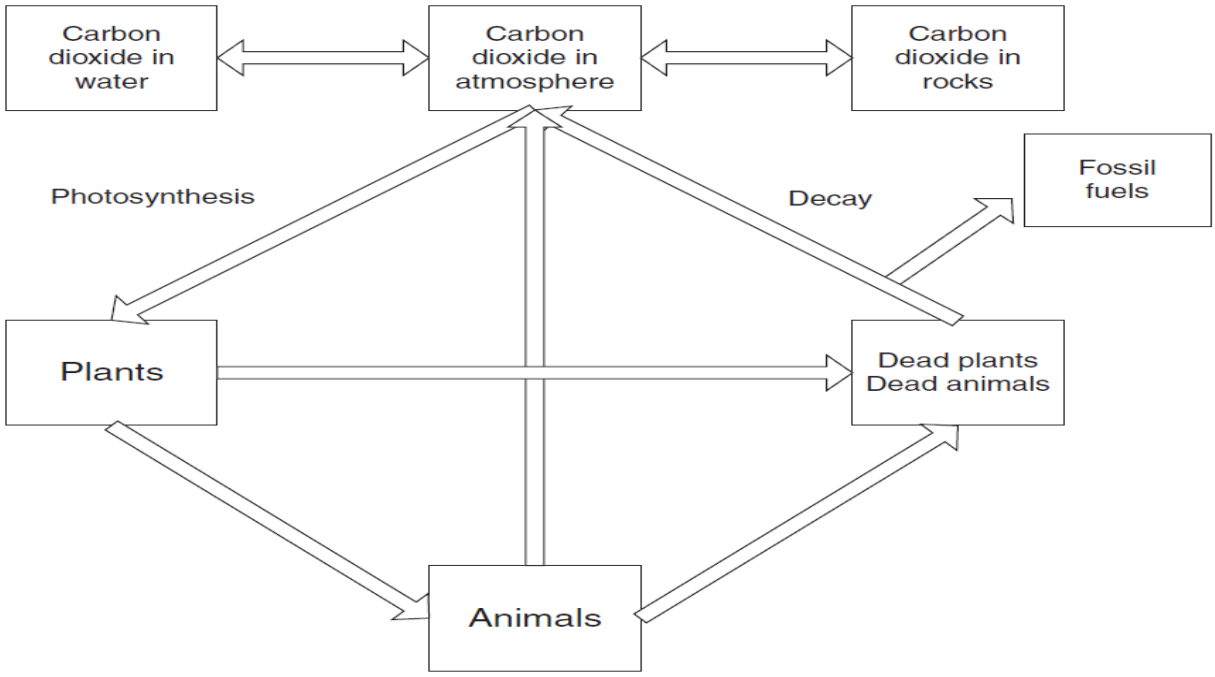


Figure 1.7: Global carbon cycle interrupted for fossil fuel formation. (Source: Arnold, 2013).

In terms of geological environments of occurrence bituminous coal is generally associated with less deformed and mostly flat–lying sedimentary rocks (Bauerman, 1911; Cao *et al*., 2000). In contrast, anthracite is associated with strongly deformed sedimentary rocks which were subjected to high temperatures (170 to 280 ^{0}C) and pressures, i.e. rocks that have been subjected to considerable earth-movement, metamorphic stresses and pressures, such as flanks of great mountain ranges (Bauerman, 1911) or volcanic intrusions. Athracite coal can also be formed by thermal upgrading of the lower rank coals by intrusions of dolerite dykes and sills. Typical examples occur in Kwazulu-Natal where it is estimated 90% of the coal deposits have been affected by dolerite dykes and sills (Snyman and Barclay, 1989).

The coalification process as shown in Figure 1.8 defines the conditions imposed on the swamp vegetation after it has died. In general, the process is marked by a progressive decrease in moisture and volatile functional groups, with consequent increase in the carbon content of the coal (Suárez-Ruiz and Ward, 2008). In addition, the other physico-chemical changes taking place with rank increase are porosity and calorific value. Many of the fundamental properties of coal which are crucial to the utilization of this solid fossil fuel are rank related. Experiments by King and Wilkins (1944) have shown that there is a reduction in porosity with increasing rank. According to their experiment, porosity falls to a minimum when carbon content ranges from about 87% to 90% (King and Wilkins, 1944; Berkowitz, 1994). With further increase in coal rank to the anthracitic stage, there is an apparent increase to porosity. The resulting coals

have useful properties, but may however require upgrading and technological matching. Whilst the origin and formation of coal as described above is generally similar the world over, specific differences exist in coal basins around the world. These arise from variations in basin structures, tectonic controls, vegetation, climate and subsequent factors, all of which impact on the coal forming processes in each region (Bauerman, 1911; Cao *et al*., 2000). These factors, in turn, result in different qualities and properties of the coals in each region. This is discussed further in Chapter 2.

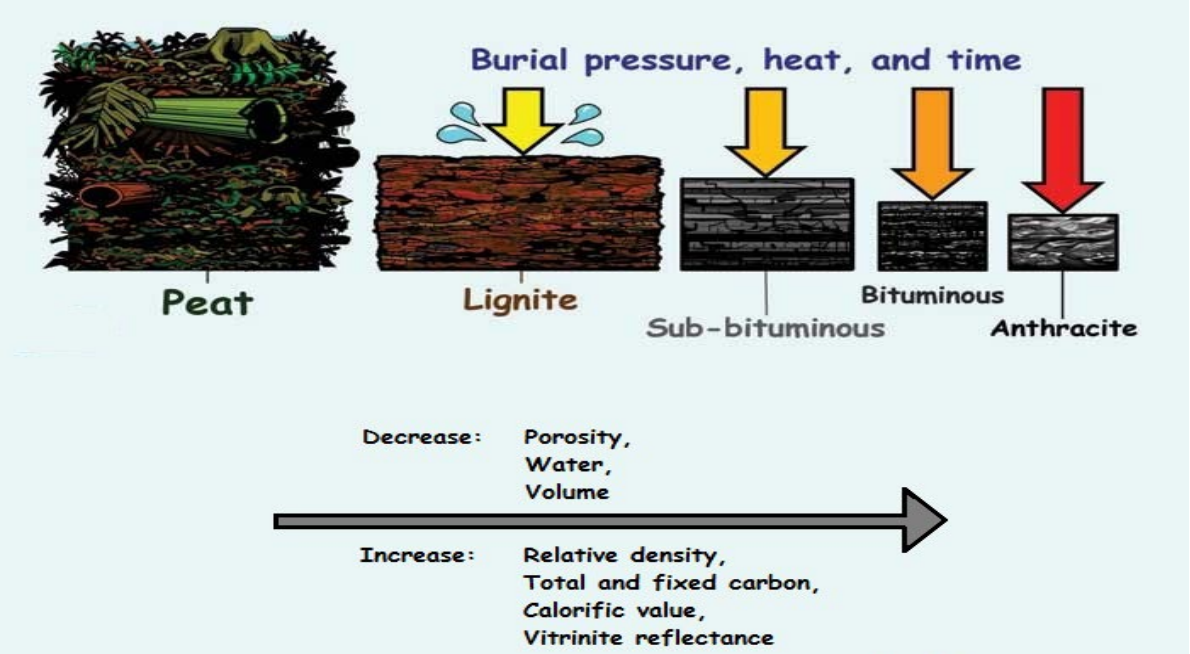


Figure 1.8: Coal rank and physico-chemical changes associated with the coalification process (By Steve Greb, © Kentucky Geological Survey, 2013).

1.4 Generalisation of the Zimbabwe Coal Deposits

Geological information generated from exploration programmes by various mining houses reveals that, to a greater or lesser extent, Zimbabwe's coal seams exhibit the following characteristics:

I. Lithostratigraphically the economic seams occur in the Ecca Group of the Karoo Supergroup.
II. The economic seams are correlateable, particularly across the Mid-Zambezi Basin (Figure 1.9).
III. The seams range in depth from outcrop to as deep as 1 000 m, with the deepest seams occurring in the Lupane area of Zimbabwe.
IV. They are generally horizontal and moderately deformed, and therefore relatively easy to extract.

V. In many cases only one seam (the bottom oldest seam) is economically viable (with low ash and usually high volatiles). There is usually a vertical variation in quality parameters. Ash and phosphorus contents increase, while volatile and sulphur contents decrease with distance above seam base. However, these attributes are particularly marked with respect to the Hwange Main Seam (Figure 1.10) which has a horizon ranging from 1 to 6 m of good quality coal at the base which usually has coking properties. This is overlain by a relatively high ash, non-coking coal which is fed to the Hwange Thermal Plant located on the Hwange Coalfield near the mine mouth. This is, in turn, overlain by a high ash carbonaceous mudstone which currently is discarded as part of the overburden. Some low-sulphur coking coal has been identified in the Tuli Coalfield (Thomas, 2013).

VI. The coals generally range in rank from low to medium-rank bituminous with minor anthracitic bodies in the vicinity of dolerite dykes and sills, a phenomenon that is prevalent in the Save-Limpopo coals.

VII. The deeper seams, (those more than 200 m from surface) are hosts to substantial, but not necessarily economic, quantities of coal-bed methane; and

VIII. The coal deposits in the Save-Limpopo Basin are, in the main, multi-seam types as typified by Tuli coal which has six thin high ash seams which are extensively disrupted by east-northeast trending faulting and dolerite intrusions. The Mid-Zambezi Basin coals, on the other hand, are generally single thick coals with no major partings, save thin discontinuous intercalations of carbonaceous material and siltstone.

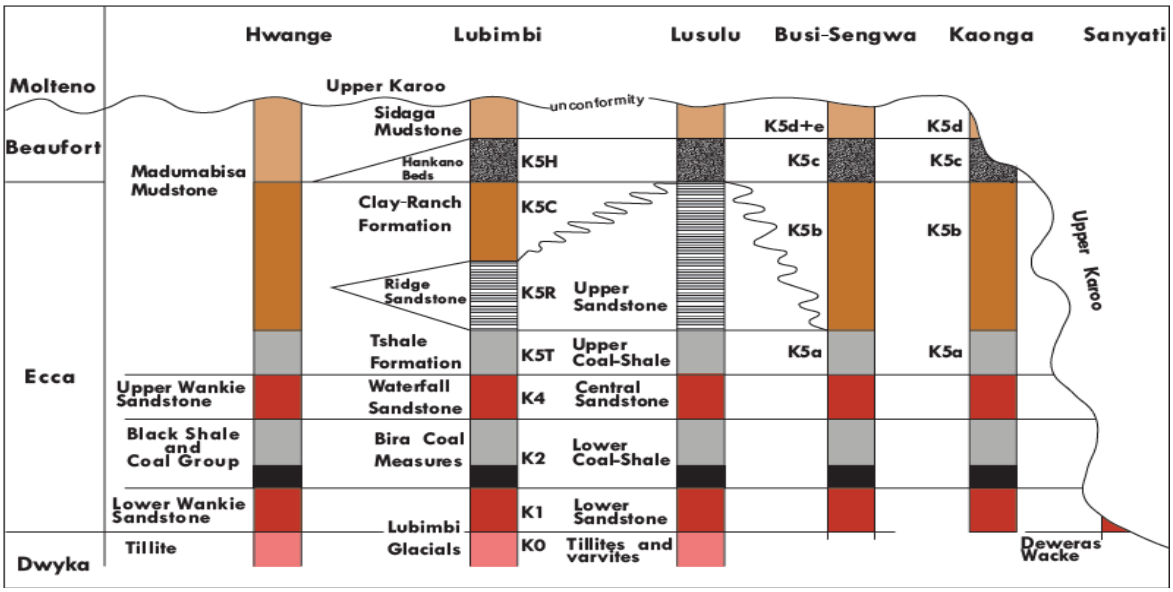


Figure 1.9: Lithostratigraphic correlation of the Lower Karoo in the Mid-Zambezi Basin (Adapted from Lepper, 1992). Not to scale.

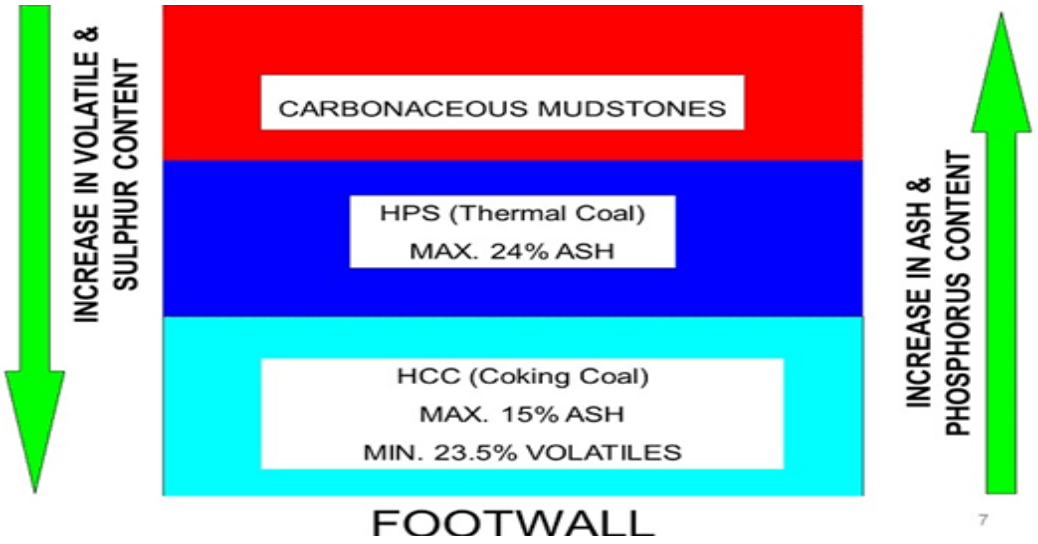


Figure 1.10: Economic Aspects of Hwange Main Seam (Source: Maponga 2014).

1.5 Aim and objectives of the study

The aim of the research is to establish the link between the geological environment of the deposition of the Hwange coals and their selected characteristics. Towards this end, the study aims to achieve the following objectives:

I. To carry out an in-depth study of the geology, composition, and characteristics of the Hwange coal deposit with specific reference to coal quality; and

II. To establish and understand those factors that controlled the distribution of the coal quality, the coking properties, as well as those factors that will affect the exploitation of the Hwange coal deposit and its techno-economic value.

1.6 Research Questions

The study seeks to provide answers to, and explanations for, the following questions:

I. What controlled the deposition of such a unique thick main coal seam characterized by a systematic vertical variation in chemical and physical composition in Hwange?

II. What is the maceral composition, how are the constituent macerals distributed, and what controlled their distribution within the seam (maceral profile)?

III. What are the main microlithotypes and how do these affect the combustion and coking behaviour of the Hwange coal?

IV. What is the quantified coal rank of the Hwange coal, and does it change vertically or laterally over the Hwange coal deposit?

V. What is the relationship between the petrographic constituents, chemical analyses, rank, and the mechanical and coking properties of the Hwange coal?

VI. Hwange “coking coal” has been described as “mind boggling” in that, although the swelling index of the coal in some sections of the mine is as low as 1.5, this coal still has good coking properties in practice. What is the reason for this?

VII. What model of geological deposition is indicated by the above attributes?

1.7 Hypothesis

The structural and sedimentary settings within which coal was deposited and the subsequent geological processes that the coal was subjected to had a major influence on the ultimate coal characteristics which, in turn, now have implications for the amenability to beneficiation and utilization of that coal.

1.8 Intended Outcomes

The intended outcome of this research is to develop a full understanding of the origin, formation, and nature of the Hwange coals in order to enhance the value and use of the coals produced from that major geological deposit.

1.9 Structure of the thesis

The thesis commences in Chapter One with an introduction outlining the significance of the study area, the purpose of the study, and the research objectives. Chapter Two covers the review of the available literature relevant to the study objectives. This focuses on: i) factors influencing coalfield development, ii) micro-factors controlling attributes of seams within a locality; iii) characterisation and analysis of coal with impacts on beneficiation and utilisation.

The methods used to achieve the objectives of the study are provided in Chapter Three, while the results obtained, and discussion thereof are presented in Chapter Four. The remaining coal resources and techno-economic assessment of that part of the Hwange Coalfield held by the Hwange Colliery is the subject of Chapter Five.

The thesis ends with Chapter Six in which the conclusions are presented based upon the research undertaken with recommendations for further work.

CHAPTER TWO: LITERATURE REVIEW

2.1. Introduction

New discoveries and understandings build upon the findings of previous experiences and investigations. This chapter is an analysis of similar works carried out on Gondwana coals in general, and in south-central Africa in particular, with the latter focussing on Zimbabwe coals as represented by the type deposit at Hwange. The goal of the chapter is to identify the knowledge that exists to date, to build on theories developed so far and to establish the gaps that still exist.

The review is structured into specific topic areas, as shown below, with summaries of existing literature undertaken with a view to linking past information to the topics of the current thesis.

2.2 General background knowledge to the Zimbabwe coal industry.
2.3 Macro factors in coalfield development (with specific reference to the Mid-Zambezi tectonic model and stratigraphy).
2.4 Coal characterisation and analysis of coal.
2.5 Coal beneficiation.
2.6 Coal utilisation; and
2.7 Conclusion.

2.2. The Zimbabwe Coal Industry

Coal has been known to mankind for thousands of years. It has been used for over 3 000 years in China, in Bronze Age Europe and by Plains Indians in America (Cassidy, 1973). Coal's application as an energy source has not only been varied, but has also been on the increase over the years. During the Middle Ages, coal was commonly used for heat and power in forges, kilns and breweries as well as for domestic heating (EIA, 2002). The role of coal for electricity production began circa 19th century, and countries such as South Africa, USA, Poland and indeed Zimbabwe, are amongst the most heavily dependent on this commodity as a feedstock for thermal power generation. (IEA, 2017).

While coal may have been known by the inhabitants of north-western Zimbabwe before the 20th century, outside interest in the country's coal only started around 1893, when Albert Geise, a German Geologist, came into the country after hearing of the "black stones that burned" described by a delegation from the Amananzva of the Hwange District, Zimbabwe (Bwerinofa and Brennen, 1989). Geise's geological work culminated in the commissioning of the No.1

Shaft at Hwange in 1902, an event which marked the beginning of the Coal Mining Industry in Zimbabwe (Bwerinofa and Brennen, 1989). Since then, several geological campaigns have been mounted and these have culminated in the discovery of at least 26 coal-bearing areas in the country's two major sedimentary depressions: the Mid-Zambezi Basin to the north and north-west, and the Save-Limpopo Basin to the south and south-east of the country's geographic watershed as shown on Figure 1.1 in Chapter 1. More coal bearing areas may lie in the ground yet to be discovered.

The coal deposits occurring in the Mid-Zambezi and Save-Limpopo Basins have been documented to varying degrees by several individuals and organisations in research studies and as part of their coal exploration programmes. These include Watson, (1960), Duguid, (1986a); Palloks, (1984) and Lepper, (1992). The Hwange coal deposit has been the most exploited coal deposit in Zimbabwe. In fact, from 1902, when the first tonne was extracted out of the No.1 Shaft at Hwange, until National Independence in 1980, the story of coal mining in Zimbabwe was synonymous with Hwange Colliery Company mining operations at Hwange. The company met the country's solid fossil fuel demands and produced various products which included thermal coal for power generation, general industrial coal for food and beverage manufacture and tobacco curing, and the more specialised coking coal for the metallurgical industry. Hwange Colliery Company continues to produce these products up to this day.

Hwange Colliery Company's operations are located within a 22 100-ha piece of ground called the Reduced Hwange Concession and Option Area (Figure 2.1). Mining operations commenced at No 1 Colliery in 1902 using the manual method referred to as the hand-got system. The increase in coal demand, particularly from the Copperbelt in Zambia, led to the commissioning of another shaft at No.2 Colliery in 1927. A third shaft was subsequently commissioned at No.3 Colliery as part of a major expansion programme which started in 1949. The three shafts were successively decommissioned for different reasons. No.1 Colliery was decommissioned in 1961 due to decreased coal demand following the commissioning of the Kariba Hydro-electric power generation. Unfortunately, a major mine disaster struck at No.2 Colliery on 6 June 1972 in which 427 men perished underground forcing it to close completely. To gain tonnage lost due to this unfortunate event, No.4 Colliery was hastily established in 1976 and was closed in 1981 for economic reasons. To increase power generation internally, the National Government decided to establish a major thermal power generation plant at Hwange. This led to Hwange Colliery embarking on a major opencast operation which came on stream in 1983. This introduced the Dragline with supplementary stripping operation

method of coal mining in Zimbabwe. With increased national coal demand and the need to mine the coal more efficiently, Hwange Colliery adopted the fully mechanised mode of coal mining at the M-Block underground mine in September 1998. The block ceased operations in 2004 following exhaustion of its coal reserves. Meanwhile, mining operations at the No.3 Colliery battled with bad ground conditions and other viability issues leading to its closure in 1999.

To replace the closed No.3 and M-Block underground mines, new mining blocks were commissioned at Chaba Opencast Mine and 3 Main Underground Mine, respectively. The two mines and J-K-L Opencast Block are currently operating.

Following the de-regulation of the coal industry in the late 1980s, more coal mines were commissioned by other players. Exploitation of the Sengwa coal deposit which was discovered in 1973 by what was then Rio Tinto (Rhodesia) following exploration work in the Gokwe District, commenced in the late 1980s to supply the ferrochrome industry. However, operations were suspended following the fall in the National ferrochrome industry in the early 1990s. Production resumed in 2005 when Rio Tinto (Zimbabwe) permitted a contractor, Coalzim, to commence operations. For a period of several years, the contractor produced coal at the rate of 200 000 tons per month, producing various coal types and grades. The operation stopped in 2008 due to viability issues.

In 2007, Steelmakers Zimbabwe commenced a small opencast operation in the Chiredzi area to exploit the Mkwasine coal deposit which the company blended with the superior Hwange coal for a direct reduction operation to produce sponge iron. In 2010, Makomo Resources commissioned a relatively large operation over part of the Entuba Coalfield, Hwange. The other part of the coalfield was reserved for Zambezi Gas which planned to exploit coal-bed methane. In 2014, Makomo resources reached production levels of 300 000 tons per month and the mines is still in operation, but production has been on a downward trend, like the rest of the currently coal producing mines. Zambezi Gas Coal Mine was subsequently awarded a mining licence for coal instead and commissioned coal mining operations in June 2016. Since 2012, the Government of Zimbabwe has awarded no less than twenty new coal concessions, and these are at various levels of development as shown on Figure 1.3 in Chapter 1.

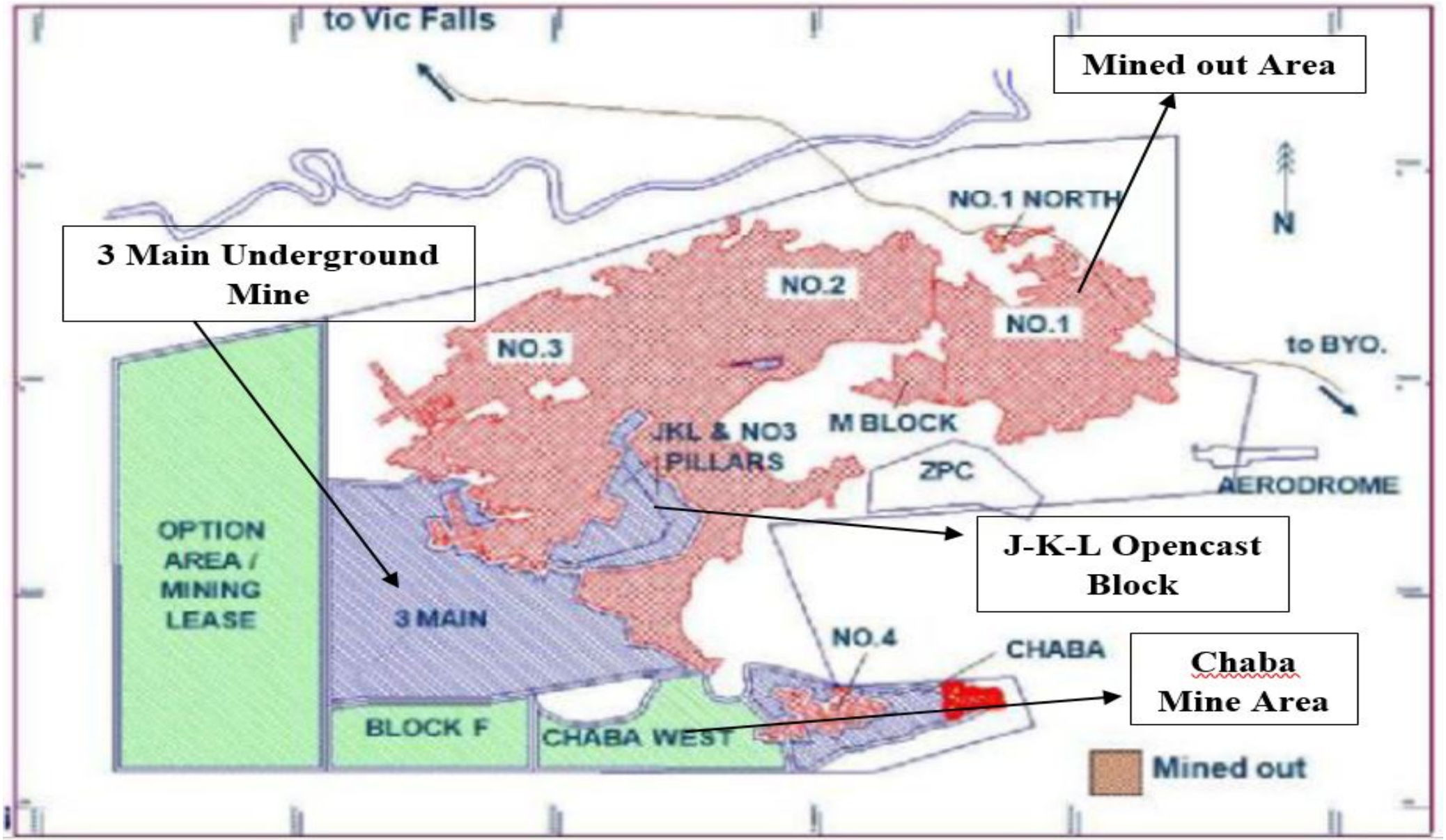


Figure 2.1: Hwange Colliery Company Concession mining blocks.

The country's coal reserves are reported to be at least 26.5 billion tonnes (Clutten, 1982). However, Clutten's report is fraught with technical deficiencies. A considerable amount of what is classified as the coal reserve is the coal resource. In addition, the report does not give any details on the quality of the "reserve". Results of the hive of coal exploration activities that commenced following the issuing of new exploration licences by the Governement of Zimbabwe in 2012 are yet to be reported; hence the effect of these activities on the coal resource base as reported by Clutten in 1980 is yet to be known.

2.3. Factors controlling or influencing coalfield development and coal seam attributes in southern Africa

Global coal deposits were laid down in specific but varied structural and sedimentary settings globally and under unique climatic conditions prevailing at the time of peat formation. The peat deposits were subsequently subjected to varying geological processes which had major influences on the ultimate qualities of the coal in each coalfield. The deposits, particularly those in Southern Africa, are highly variable in terms of their quality as well as their distribution. This section looks at the reasons for and nature of these variations.

Falcon, (1989) groups the factors that can be used to identify the differences in coal deposits at two levels: i) the macro-level, incorporating factors that influence the broad-scale nature and distribution of coal-bearing strata throughout the region; and ii) the micro-level, which refers to those factors that control or influence, within a particular locality, coal seam attributes such as geometric extent, the in-seam stratigraphy, and the detailed distribution of various coal-quality parameters such as ash content, volatile matters, total sulphur, phosphorus, etc. These factors are discussed in the following subsections.

2.3.1. Macro-level Factors Affecting Coalfield Development

Catuneau *et al*., (2005) state that the Gondwana sedimentary fill accumulated under the influence of two main *allogenic controls*: tectonism and climate, and these are discussed in the following sections.

2.3.1.1. Tectonic Framework

The importance of the tectonic control on sedimentation in the Karoo Basins of Southern Africa was first proposed by Rust, (1975). Subsequent research work refined this thinking (Tankard *et al*.,1982; Turner, 1986; Veevers *et al*., 1994a, b, c; Johnson *et al*., 1996; Visser and Praekelt, 1996; Selley, 1997; Catuneanu *et al*., 1998; Pysklywec and Mitrovica, 1999). The following

paragraphs discuss the role of tectonics in the creation of depositories for Karoo time sediments in southern-central Africa.

The development of a basin is an essential component in creating a depositional setting for peat accumulation and the subsequent coalification process. Tectonism that took place during the first-order cycle of supercontinent assembly and break-up of Pangea culminated in the development of Karoo basins over south-central Africa (Catuneanu *et al.,* 2005). Two distinct tectonic regimes are recognised. On the one hand, there is the one sourced from the southern margin, which was related to processes of subduction and orogenesis along the Panthalassan (palaeo-Pacific) margin. This was responsible for the formation of a retroarc system now known as the main Karoo Basin (Visser, 1992; Catuneanu, *et al.,* 2005) as well as other smaller Karoo basins as far as to the north as the Tuli Basin (Johnson *et al*., 1996; Catuneanu *et al*., 1999; Bordy and Catuneanu, 2001, Catuneanu, 2004a and b). In this geological system, the flexural and dynamic loading represents the primary subsidence mechanism. Shallow-angle subduction of the palaeo Pacific plate below the supercontinent characterises the southern convergent margin of Gondwana (Lock, 1980). The compressional region which is associated with a combination of collision and accretion resulted in the formation of some 6 000 km long Gondwanian Cape Fold Belt (Visser, 1992; Catuneanu *et al*., 2002).

The sedimentary fill that accumulated in the main Karoo Basin and the other smaller basins to the north of it (Figure 2.2) between the Palaeozoic and early Mesozoic has a lithostratigraphic rank of Supergroup (Catuneanu *et al*. 2005). Bound to the north by the Cargonian Highlands and to the south of the Cape Fold Belt (Isbell *et al*., 2008), the main Karoo Basin is regarded as a type-locality for the southern African coals (Cadle *et al*., 1993); while Haughton, (1970) describes it as a type region for the Karoo system. This opinion is based on the fact that this basin is preserved and noted as the most complete succession of the Karoo sedimentary strata and the largest coal resources (Cairncross, 1987). The Karoo Supergroup has been subdivided into five Groups which from below upwards are: Dwyka, Ecca, Beaufort, Stormberg and Drakensberg (Figure 2.3) which were deposited during a period of 120 million years spanning from the Late Carboniferous to the middle Jurassic, and terminated by the outpouring of the Drakensberg basalts. The other basins outside South Africa include the Limpopo Trough and the Mid Zambezi Valley in present day Zimbabwe, as well as other such depressions in other African territories. The positions of a number of these basins coincide with areas which later became part of the present-day Rift Valley system and their formation may have represented

early phases of earth movements which subsequently took the form of extensive rift faulting (Bond and Stocklmayer, 1966; Ghosh and Mitra, 1967).

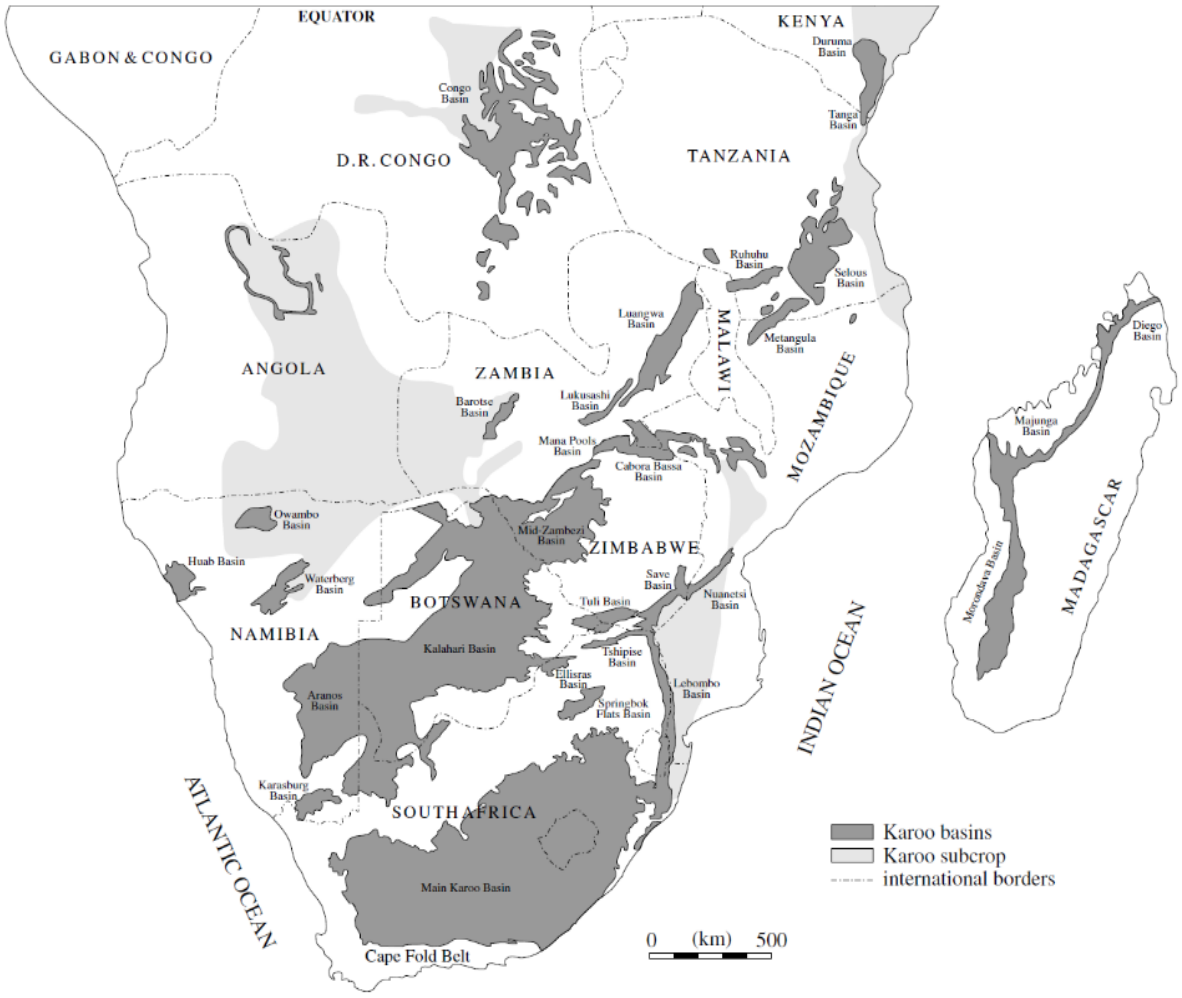


Figure 2.2: Distribution of Karoo basins in south-central Africa (source: Catuneau *et al*. 2005; modified from Johnston *et al.*, 1996; Wescott and Diggens, 1998; Nyambe, 1999; Wopfner, 2002).

The stratigraphic sequences within the main Karoo Basin have been extrapolated and correlated from this basin to sediments in other basins of the same age across southern African and the greater supercontinent of Gondwana (Cairncross, 1987, 2001; Falcon, 1989; Catuneau *et al.*, 2005;). In terms of sedimentary strata and facies, some of the basins north of the main Karoo basin consist of facies that are different from that of the major type basin.

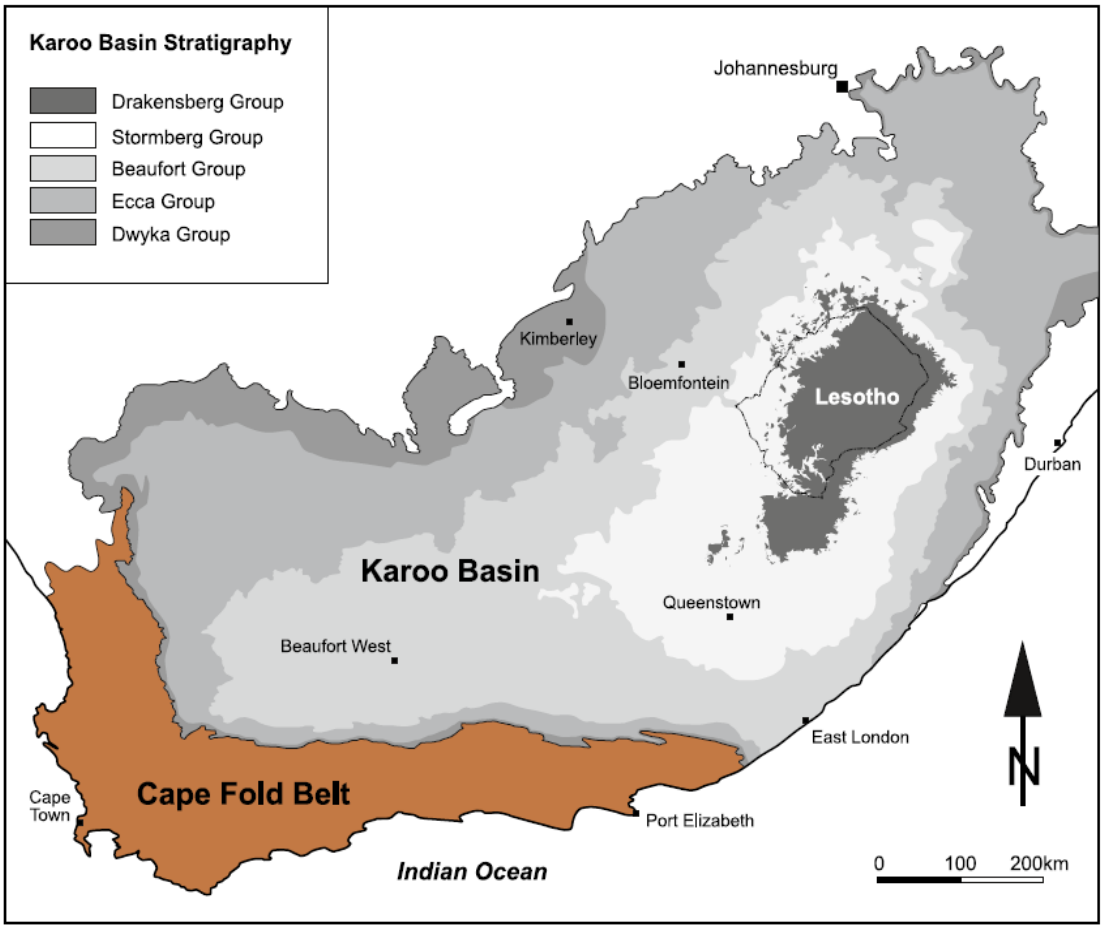


Figure 2.3: Distribution of the main stratigraphic groups of the main Karoo Basin (source: Wheeler and Götz, 2016; modified after Catuneau, *et al.* 1998)

North of the main Karoo Basin the tectonic regimes were dominated by extensional or transtensional stresses that spread southwards into the supercontinent from the divergent Tethyan margin of Gondwana (Wopfner, 1994, 2002; Cairncross, 2001, Catuneau *et al.*, 2005). The structural control gave way to extensional regimes along the eastern part of the African Gondwana and syneclistic type regime on the western portion (Catuneau *et al.*, 2005). The present watershed of the Congo River is considered as the dividing line of the two geological terranes and the demarcation is linked to the north-northeast trending ridge created by the initial thermal upwarp in the Late Carboniferous (Catuneau *et al*., 2005). This elevated area is the origin of glaciers issuing into west-central and eastern Africa (Rust, 1975; Wopfner, 1991).

To the east of the dividing line developed a complex rift system that extends from the Zambezi in the south to the Ogaden and up to the southern rim of Arabian Peninsula. Wopfner, (1993, 1994) described this extensional zone the “Malagasy Trough” and considered it as the initial fractures coming from the Tethyan margin of Gondwana. The zone coincides with the northern part of “Falkland-East African-Tethys shear system suggested by Visser and Praekelt (1996)

and the rift structure between Africa/Arabia and Madagascar/India identified by Reeves *et al*, (2002). The rift system runs from the Zambezi River (Cabora Bassa Basin) to the Horn of Africa and the southern margin of the Arabian Peninsula. The extensional feature comprises from south to north the Lukasachi and Luangwa basins of Zambia, some minor remnant basins in the northern part of Malawi, the Metangula Basin straddling Mozambique and Tanzania, the Ruhuhu, Ilima, Galula, Selous basins in Tanzania and the Tanga/Duruma Basin which straddles the Tanzania-Kenya border (Wopfner, 2002). All those are considered typical intracratonic rifts, although some, like the Tanga-Duruma, evolved into pericratonic basins during the opening of the Indian Ocean.

Elsewhere, investigations present arguments to the fact that the eastern margin of southern Africa broke away from Antarctica during early to mid-Jurassic (Cannon *et al*., 1981; Martin and Hartnady, 1986). After the late Carboniferous/Permian period leading up to the onset of the sea-floor spreading, major developments relating to the opening up of the proto-Indian Ocean took place largely as a result of tensional stress in the southern African region of Gondwana (Orpen *et al*., 1989). The resulting extensional fracturing of the supercontinent was largely accommodated along pre-existing mobile belts (Kroner, 1977) which were recognised to lie between ancient cratonic masses (Bryan, 1986). Several such mobile belts occur in south-central Africa, including Zimbabwe.

The tectonic history of the above rifts is strongly reflected in the lithofacies succession; while the similarity of the latter across the rifts indicates that the development of these extensional features was controlled by similar processes (Catuneau *et al.* 2005). Owing to the specific structural history of these basins, the oldest Karoo deposits were laid and preserved in the deepest parts of the Graben structures. With the increasing expansion of the rift, younger sedimentary sequences progressively overstepped onto the tilted horsts and young grabens. Turning to the Karoo basins west of the dividing highland, the basins in this part of the continent are less well known than their counterparts in the east. They appear to be sag basins that developed in depressions between the demarcation and a hypothetical rift shoulder or thermal swell related to the opening history of the Atlantic Ocean (and most of the Karoo deposits in this region are concealed below younger sediment cover. Thus, the information on the deepest parts of the basin can only be obtained from the few bore-holes sunk in the area and published by Hübner, (1965). Thus, the unique combination of tectonic stresses derived from the convergent and divergent margins of the Gondwana accounts for the variations in

basin attributes across Africa, primarily tectonic and dynamic loads in the south and rifting to the north (Catuneanu *et al*., 2005).

2.3.1.2. Climate and Flora

Climate, through its main elements, i.e., temperature, precipitation and to a lesser extent wind, is a significant parameter influencing the formation and accumulation of peat, the precursor of coal. You end up

The Karoo succession is a sedimentary archive of climate change from the late Palaeozoic to the Cenozoic (Götz and Ruckwied, 2014). Superimposed on the tectonic control on basin development, climatic fluctuations left their mark in the stratigraphic record. First inferred from palynological data by Falcon *et al*, (1984a), and Falcon (1986a), the Permo-Carboniferous glaciation was succeeded by a continuous climatic amelioration (Götz and Ruckwied, 2014). The data showed that, after the melting of the Dwyka ice, cold to cool temperate climatic conditions prevailed during the Early Permian and that there was a continuous change to hot and dry climate during the Late Permian and Triassic. More evidence in the literature suggests a general shift from cold, semi-arid conditions during the Late Carboniferous-earliest Permian interval to warmer and eventually hot climates with fluctuating precipitation during the rest of the Karoo period (Keyser, 1966; Johnston, 1976; Frakes, 1979; Visser and Dukas, 1979; Stavrakis, 1980; Tankard *et al*., 1982; Visser, 1991a, b). Such major trends are believed to have been mediated by a combination of continental drift, atmospheric composition, solar radiation and attitude of the Earth's axis of rotation (Condie, 1982).

A review of information available in the literature indicates that the Gondwana continents drifted relative to the South Pole into progressively lower latitudes (Visser, 1986). The Karoo Basin margin is considered to have migrated from 80^0 S during the Late Carboniferous to 40^0 S during the Early Jurassic (Visser, 1986). It is suggested that during the Carboniferous the South Pole was located approximately in the Transvaal and migrated to the Antarctica by the Triassic (Anderson and Anderson, 1985; Falcon, 1986b; Visser, 1986). During this 120 Ma period, Gondwana is considered to have drifted through several distinct *vegetational phases* as represented by macro-factors and palaeo-botanical evidence (Falcon, 1975b; 1978b; Falcon *et al*., 1984b; Visser, 1986). Further work has been carried out by other researchers (Falcon, 1986b; Hancox and Götz, 2014; Wheeler and Götz, 2016) and the results are summarized in Figure 2.4. The changes in vegetation were attributed to a combination of plant evolution and palaeo-climatic changes that were considered to have taken place over this time span (Falcon,

1989). Some researchers have attributed the floral changes to macroclimatic or migrating vegetation belts that may have existed around the polar region during the Permian and Triassic Periods (Plumstead, 1957, 1966; Falcon, 1978b, 1980, 1986b; McRae, 1984). From their works, it is envisaged that, as continental glaciation rapidly declined and Africa drifted away from the South Pole, the climatic belts would have passed over southern Africa in rapid succession, followed by increasingly slow paces, until stable positions of the continents had been reached.

It was under this setting and influence of tectonism and climate that the Gondwana sedimentary infill accumulated. The infill or sequence has earned the stratigraphic rank of Supergroup (Catuneau *et al.* 2005) and, as established in the main Karoo Basin, comprises several groups defined according to the overall sedimentological attributes. The shift in tectonic and climatic conditions from the southern to the northern margins of Africa during the Karoo time resulted in significant changes in the lithostratigraphic character of the "Karoo sequence" (Catuneau *et al.* 2005). For this reason, the Karoo basins *sensu stricto* which show clear similarity to the main Karoo Basin of South Africa are restricted to south-central Africa (Catuneanu *et al*. 2005).

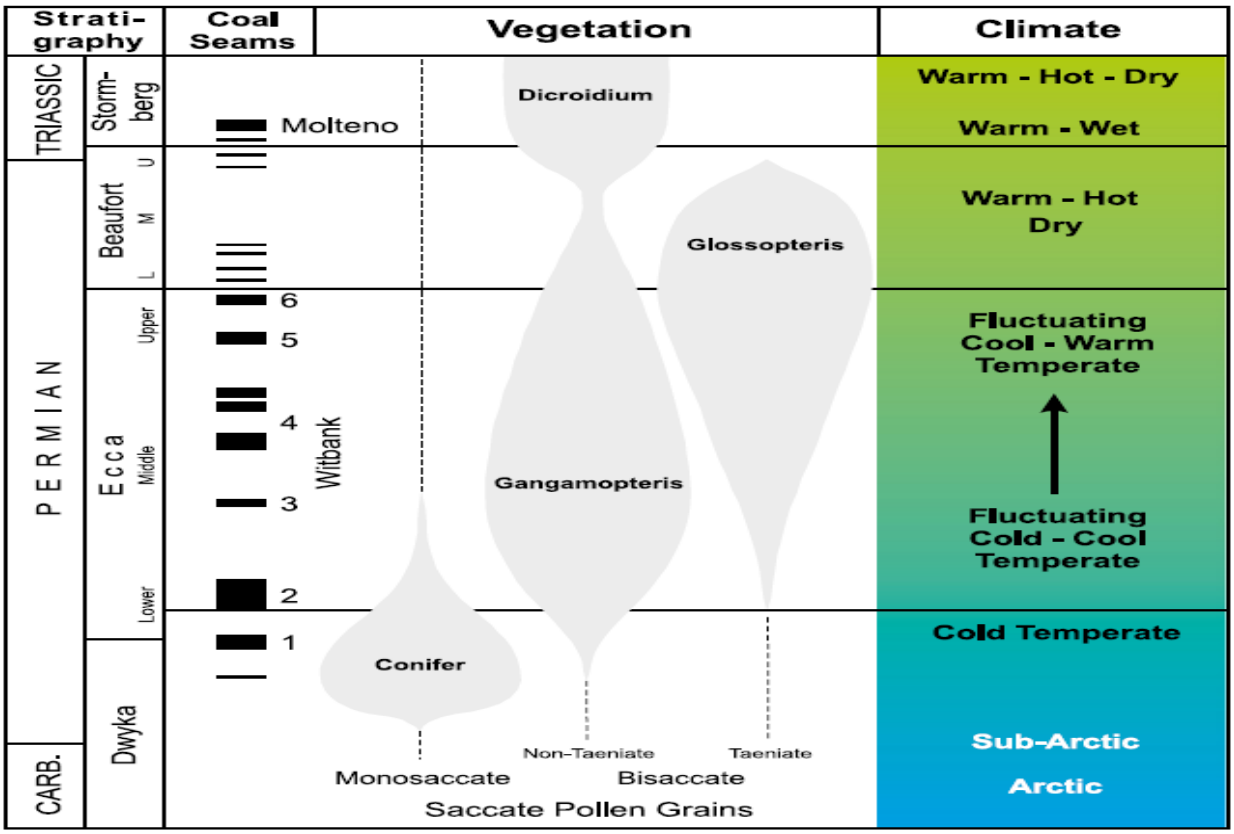


Figure 2.4: Climate reconstruction of the main Karoo Basin based on pollen-producing flora (from Hancox and Götz, 2014; modified after Falcon 1986).

On a global scale, there are marked differences between the types of vegetation that grew in the Northern Hemisphere (Laurasian) and those found in the Southern Hemisphere (Gondwanaland). These differences, and the climatic and sedimentary conditions in which they grew, imposed significant differences in coal properties in the two continental areas (Falcon, 1989). Laurasian coals were formed in vast, relatively undisturbed, hot and humid shallow swamps where specific equatorial-type vegetation accumulated. Such conditions led to rapid growth in similar environments over wide areas during the accumulation of the peats. Slow sinking of the terrain occurred at the same rate as vegetation deposition, which resulted in the accumulation of almost pure organic material with little or no river-born fine mineral matter (ash forming minerals) such as was characteristic of most Gondwana coal swamps (Horsfall, 1993). In contrast, Gondwana coal swamps vegetation grew in varied wet and dry conditions and were characterised by cold to cool temperate plant species growing in annual climatic cycles with spring floods populated by snow melts (and other cyclic inundations) bringing high mineral and sediment-bearing materials into the swamps (Falcon, 1989).

Focussing on the macro-factors influencing coalfield development Falcon, (1989) presents the following account. As the major part of the African continent remained stable, large deposits of coal-bearing and associated clastic sediments accumulated in then topographically low-lying areas between the cratons and, in some cases, in downfaulted areas within the cratons during pre-Gondwana split-up in Permian, Triassic and Jurassic periods. It was during the early to mid-Karoo times (Permian and early Triassic) that the major coal-bearing strata in the Karoo sequence was deposited (Falcon, 1989). Within this structural framework, some specific features appear to have exerted a major influence on the nature and form of Karoo sedimentation (Whateley and Turner, 1983; Whateley and Hopkins, 1985). The features include the following:

I. According to Falcon (1989), the ancient continental nuclei (cratons) seem to have represented major areas of positive relief, or mountainous regions, with each providing a specific source for Karoo sedimentation;
II. The intervening areas between the ancient cratons became sinks for specific Karoo deposition and sediment and coal seams accumulation (Figures 2.5 and 2.6). In this way, different types of basins developed. Whateley and Hopkins (1985) divided the basins in the region into four main types,

i) ***Large paralic basins*** ("inland seas") between cratons usually with stable cratonic shelves, i.e., Angola, Botswana, and Karoo basins 1, 2, and 3 in Figure 2.5;

ii) ***Intracratonic lineament zones or mobile belts*** along with the Karoo strata occur in narrow, elongated fault-bounded grabens or valleys, e.g., the Zambezi and Limpopo belts (4, 5, 6, and 7, in Fig. 2.5);

iii) ***Localised cratonic grabens or fault blocks*** such as Springbok Flats and Waterberg basins (Figures 2.5 and 2.6) and rifted and downwarped continental margins**,** e.g., along at least part of the Mozambique Belt (9, in Fig 2.5); and

iv) ***Major and minor crustal fractures*** which subdivided the region into several composite segments, as illustrated in Figure 2.6. The fractures represented major source areas for palaeo-geothermal gradients and conduits for igneous intrusion during late the Karoo period (Falcon, 1989).

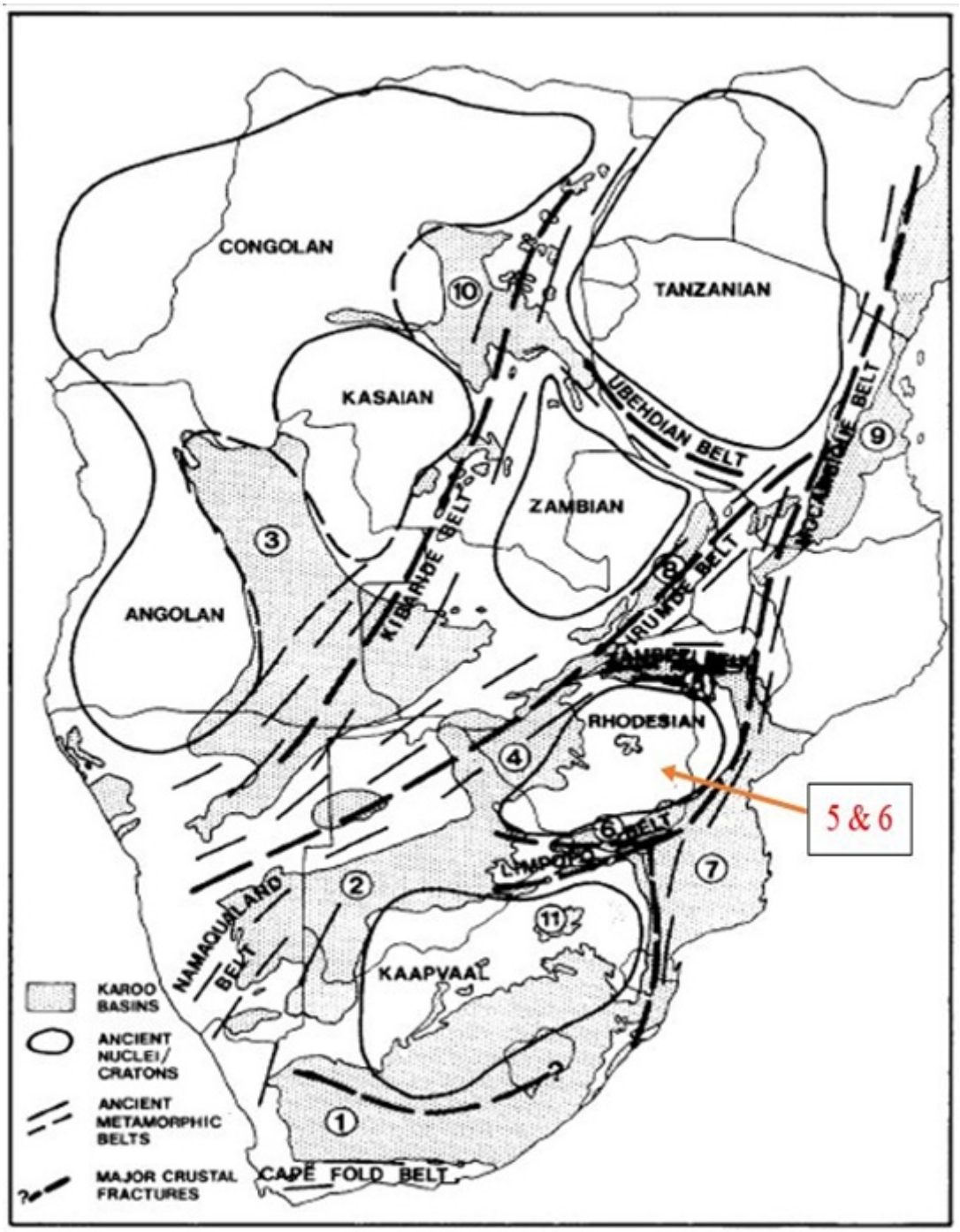


Figure 2.5: Major structural features affecting Karoo deposition in Southern Africa during Late Palaeozoic and Early Mesozoic Times (Falcon, 1986). Basins 1: Main Karoo Basin; 2: Botswana Basin; 3: Angolan Basin; 4: Mid Zambezi; 5: Lower Zambezi Basin; 6: Limpopo Basin; 7: Mozambique Basin; 8: Luangwa Basin; 9: Tanzanian Basin; 10: Zaire Basin.

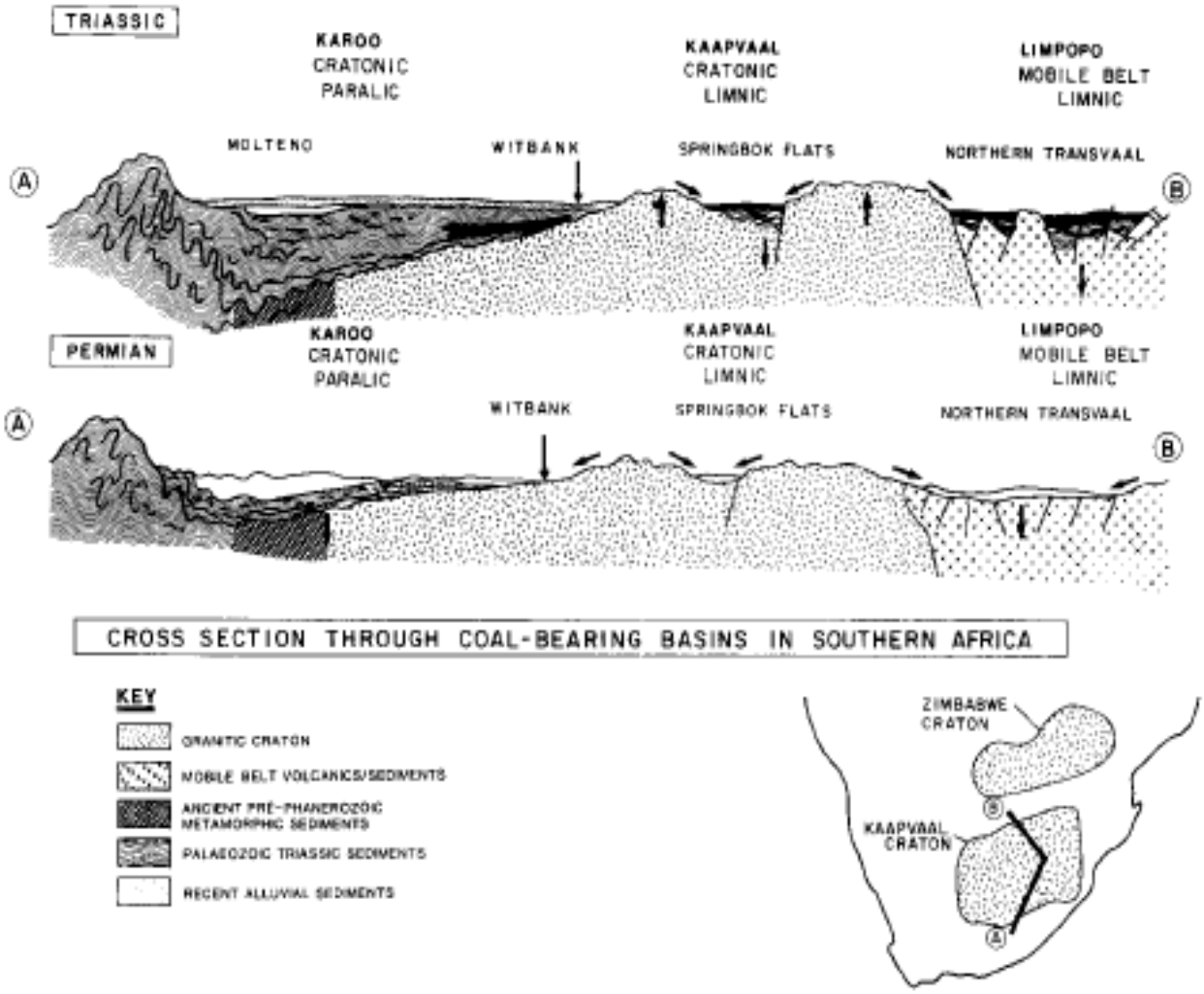


Figure 2.6: A cross section through different types of coal-bearing basins associated with the Kaapvaal Craton, South Africa, during the Permian and Triassic Times (after Falcon, 1978c, 1986b; Whateley and Hopkins, 1985).

Each of the factors described above produced specific outcomes in terms of the development of each coalfield as described below.

First, in basins such as the Great Karoo Basin of South Africa, the Botswana Basin and the Angola Basin in the north-western section of the region, sedimentation occurred partly on shallow cratonic shelf regions and partly over deep-crustal fracture zones. This resulted in laterally extensive stratigraphic sequences with relatively consistent patterns of sedimentation and well defined, distinct, and limited numbers of seams within the coal-bearing strata (Falcon, 1989). Generally, coalfields have only been in certain areas along the margins or shelves of these basins (Falcon, 1989).

Second, in the coal-bearing areas confined to elongated limnic basins along the metamorphic belts and crustal lineament zones, as well as those along the rifted and down-warped continental

margins along the Mozambique Belt, extensive warping occurred. This tectonic movement culminated in the accumulation of thicker sequences and greater numbers of coal seams during Karoo sedimentation, much of which exhibits extensive cyclic deposition (Falcon, 1980; Whateley and Turner, 1983). The seams in these areas may be more numerous, thin and usually discontinuous. In addition, the coal-bearing strata in these geographic areas characteristically extend into younger stratigraphic sequences (i.e., younger than the Lower Karoo). This contrasts with the central regions of the subcontinent where sedimentation stopped earlier (Falcon, 1978a, b, c, 1980; and Falcon *et al*., 1984b). In areas of localised cratonic grabens or fault blocks such as the Springbok Flats and Waterberg Basin, as depicted in Figures 2.5 and 2.6 above, thick extensive coal seams were formed as a result of slow and uninterrupted but progressive subsidence in these areas at a time when peat accumulation had ceased on the major cratonic shelves (Falcon, 1989). Peat forming activities temporarily halted in Permian-Triassic times in response to tectono-sedimentary and climatic conditions before resuming, albeit briefly, and in localised areas, in the early Triassic.

Third, the seam ***geometry and the rank*** of the coals appear to have been significantly influenced by the structural framework of the region. To cite examples, the Free State and eastern Botswana Coalfields which are situated on the stable cratonic shelves and far removed from sources of major palaeogeothermal heat are relatively uncompressed and shallow or through lack of burial, and the coals are generally of low rank due to low palaeogeothermal gradients in these regions (Falcon, 1986a, b). In some instances, the seams in such locations are of the ancient “lignitic” or sub-bituminous rank (Falcon, 1986a, b). Furthermore, the coal seams appear to be few, are thick, and tend to extend over relatively wide areas as defined by the topography of the region. In contrast, areas that straddle geological features, such as the major intercratonic crustal fractures, metamorphic belts, or lineament zones show wide variations in seam thickness, extent, and coal rank. Coal ranks in these regions characteristically range from low-rank bituminous coal on the margins, to extremely high-rank bituminous coal, leading to anthracitic and even graphitic types towards the source of higher palaeogeothermal heat and greater depth of burial. Save-Limpopo Basin in southern Zimbabwe and the Mucamba Vuzi region of Mozambique are typical examples of such coalfields (Falcon, 1977, 1978a; Falcon *et al*., 1984a, b).

In the Great Karoo Basin, a progressive increase in coal rank occurs eastwards, from the sub-bituminous coal ranks in the Free State, to anthracitic and meso-anthracitic coals in eastern KwaZulu-Natal. This is attributed to a regional increase in palaeogeothermal gradient related

to melting of the asthenosphere and the resulting large-scale magmatic activity which culminated in widespread outpouring of lavas arising from a crustal fracture in the depths of the Great Karoo Basin located closer to the KwaZulu Natal (KZN) coalfields. This occurred during the late Triassic and early Jurassic and coincides with the break-up of Gondwanaland (Snyman and Barclay, 1989). Triassic-Jurassic age igneous intrusions comprising dolerite dykes and sills which are seen passing through coal-bearing sediments in all Karoo basins have resulted in abrupt changes or variations in coal rank wherever they occur. Such local variations in rank can exhibit major quality variations from location to location, not only between coal basins and coalfield, but also from location to location within a mine.

2.3.1.3. Local Depositional Environments and Sedimentary Controls

The influence of local **topographic, palaeo-environmental, and sedimentological conditions** on the distribution and quality of coal has been documented by several investigators. These include Cadle (1982a, b); Cairncross, 1979, 1980, 1982, 1986, 1987); Cairncross and Cadle (1988); De Jager (1976); Duguid (1986); and Van Vuuren (1981). Topographically speaking, the pre-Karoo floor in southern African basins takes a variety of forms varying from deep glacially-incised valleys and highlands (e.g., the Kaapvaal and the Zimbabwean cratons arising from the more resistant Archaean and Proterozoic rocks) to back-swamp coastal swamps associated with deltaic environments. Besides providing different source areas for clastic sedimentation, the topographic features in the geographic areas are therefore different from area to area, and, as such, they would have exerted significant influence on the nature and form of peat accumulation (Falcon, 1989). In addition, the elevated areas of the coal-bearing basins are readily drained away thereby creating oxidizing environments. In these areas the organic maceral, inertinite, is likely to have developed from the woody plant accumulations as the dominant maceral. Such material is believed to lead to the development of a non-coking coal (Cadle *et al.* 1982).

Differential compaction has been cited as one of the phenomena resulting in subtle variations in seam thickness (Cadle *et al*., 1982). The authors state that in those areas where the coal seams closely overlie non-compactable pre-Karoo basement highs which are usually crystalline in nature, as often observed in Zimbabwe, loading and compaction effects caused thinning and even total pinching out of the coal seams. Elsewhere, seams occurring above channel sandstones have been reported to thin out for similar reasons (Winter, 1985). In contrast, in areas where significant thicknesses of such sediments as mud and silt have accumulated, e.g.,

palaeo-lows, differential compaction of the underlying clays provided depressed zones which promoted peat accumulation and hence thicker coal seams (Cadle *et a*l., 1982).

The rate of deposition and tectono-sedimentary history has influenced the thickness of sediments. For example, the relatively thicker sediment accumulation in the southern part of the Great Karoo Basin is attributable to rapid subsidence related to flexing of the continental crust in this area. Rates of accumulation of peats and sediments were relatively fast in the Natal coalfields, lying as they do have some distance away from the stable Kaapvaal craton. This resulted in increased cycles of sedimentation and the production of numerous laterally discontinuous coal seams in KwaZulu Natal (Falcon, 1989). In contrast, the Witbank and Free State coalfields which lie on the stable flanks of the Kaapvaal Craton, sedimentation was slower, and, following the initial topographic infilling of glaciated surfaces, coal seams and associated sediments were thicker and laterally persistent. Coals in this area are consequently more extensive and fewer in number than those in KwaZulu Natal.

Thus, pre-Karoo topography, rate of deposition and tectono-sedimentary history have, to a large extent, been shown to control coal depositional environments. These varied significantly from area to area, culminating in the development of unique and discrete coalfields with each coalfield exhibiting its own attributes as regards to coal seam development, geometry, and quality characteristics. Because of these features, and for the purpose of background information in this thesis, the coalfields of Zimbabwe have been divided into separate entities, such as those that occurred in the mid-Zambezi (Hwange, Lubu, Sengwa, Lubimbi, etc) and those formed in the Save-Limpopo basins (e.g., Bubi, Bendezi, and Mukwasine).

2.3.2. Micro-factors Affecting Coal Seams

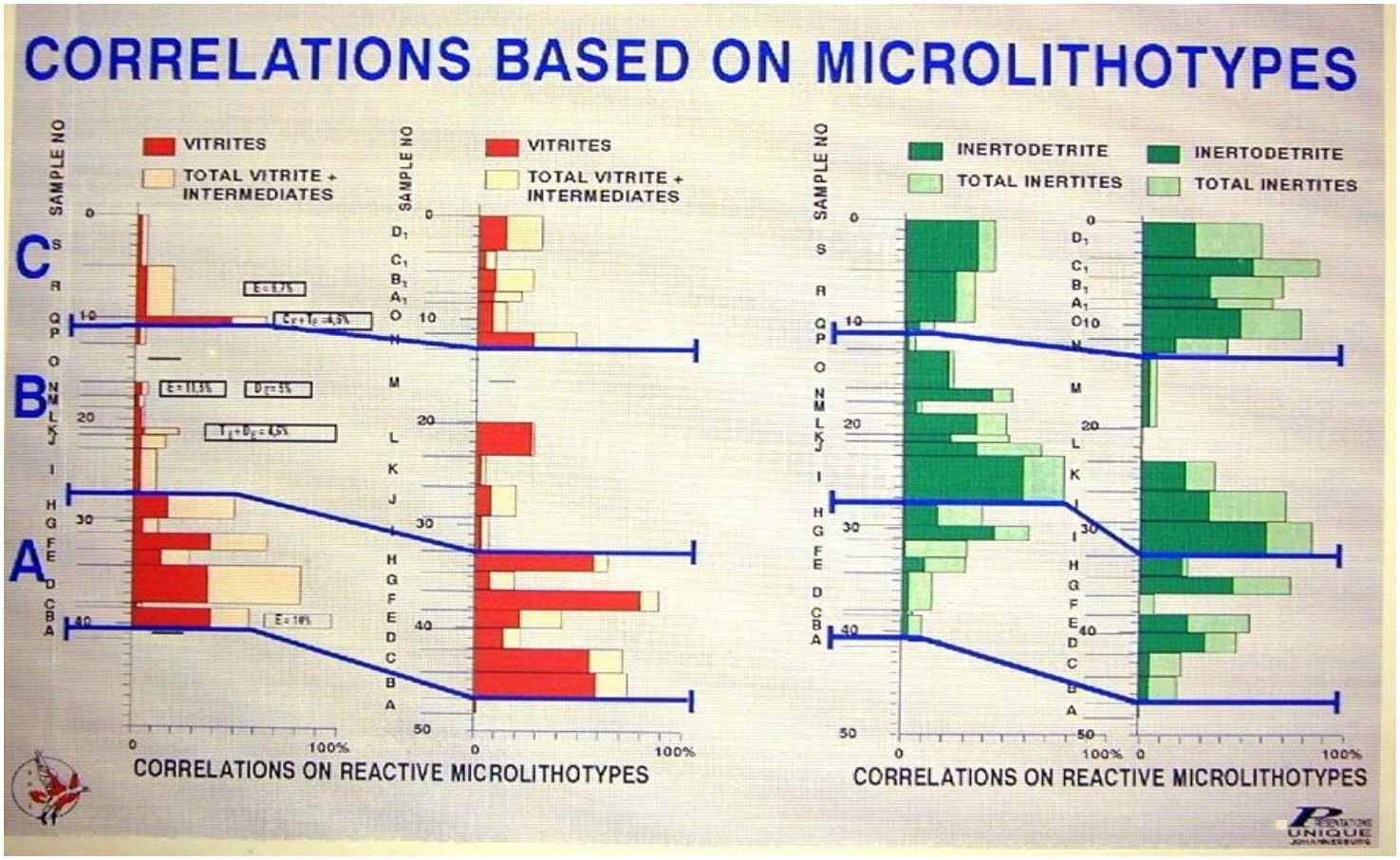
Several investigations relating to detailed in-seam development, stratigraphy and distribution in quality parameters have been carried out on various coalfields in southern Africa (Falcon, 1981, 1985a; Hagelskamp *et al.,* 1988; Hagelskamp and Snyman, 1988 among others). The following sub-sections provide an insight into the influence of these factors on; i) characterisation of the in-seam strata; and ii) in-seam biostratigraphic subdivision and correlation.

2.3.2.1 Characterisation of In-seam Strata

The No.2 seam, which is one of the main commercial seams in the Witbank Coalfield, has been one of the most investigated seams in southern Africa and is hereby used to demonstrate some

of the micro-factors affecting seams as reported by a few cited researchers. It is viewed as the correlative of most of the major commercially important seams in southern Africa. Snyman (1961, 1976); and Falcon (1981) investigated the vertical and lateral distributions of the coal quality regarding its petrography (Figure 2.7). The results from this analysis highlighted the different petrographic (maceral) components in this coal seam and revealed important variations in the in-seam development, quality distribution, as well as the vitrinite content between areas in this coalfield. Another investigation conducted on the channel samples from the No. 2 Seam coals, indicate that the coals fall within the low-rank Bituminous range (0.6 – 0.8 % mean random vitrinite reflectance). Maceral, microlithotypes and mineral-group analyses indicate wide variations in distribution and composition, both vertically in each channel profile and laterally between profiles. The widely varying ranges in the microlithotypes is attributed to coals having formed under strongly cyclic or fluctuating conditions, with minor fluctuations occurring within the broad trends (Falcon, 1981, 1989).

Falcon (1981), working in conjunction with a multidisciplinary team, which included sedimentologists, geochemists and chemists, studied the No.2 Seam in the Witbank Basin, considering four channels located in two separate locations. This work established a systematic vertical petrographic, chemical, and physical parameters and trace elements profile. Two main good-quality bands comprising low ash and high vitrinite material separated by monomineralic and inertodetrinite-rich bands of coal were recognised. In addition, the investigation indicated a close association between trace elements and shale partings within the seam and strong support for marine influence in the upper parts of the seam. From this, a marine transgression immediately above the No.2 seam is envisaged to have occurred (Hart and Leahy, 1983; Cairncross and Hart, 1988).



(a) Vitrites and Intermediates (b) Inertodetrite and Total Inertites

Figure 2.7 a and b: Summary of the No.2 seam stratigraphy using microlithotype petrographic profiles and illustrating vertical zones, subzones, and clastic partings. The sum of vitrite (and clarite) and intermediate categories (vitrinertite and trimacerite) and Inertite forms were used to draw the lithotype profiles. (Source: Falcon, 1989).

Correlations of the plies or zones identified in these profiles over distances more than 100 m revealed differences in thickness and lateral extent of the plies in which some eventually pinched out completely. These were considered to have been due to a variety of factors including: i) uneven basement topography; ii) the history and nature of sedimentation including water-table fluctuations and basin stability; iii) the nature and environment of peat accumulation, including fluctuating pH and Eh; and iv) proximity to major geographic features such as contemporaneous river channels, deltas and shorelines (Falcon, 1981; LeBlanc Smith and Falcon, 1982). These factors have been shown to influence the quality and yield of mineable seams. The palynological investigations conducted on several channel samples of the No.2 Seam indicate that the parent-plant communities varied in two ways: fluctuation on a cyclic basis; while others were observed to increase and develop progressively and irreversibly with time (Falcon, 1975a, b, 1978c, 1989). The wide variation in plant communities and palaeo-ecological environments are considered to have occurred at repetitive intervals during the peat accumulation. Fluctuating conditions are most likely to have been brought about by changes in water level, and, by inference, Eh and pH (Falcon, 1989).

The Triassic/Jurassic igneous intrusions (sills and dykes) have been demonstrated to have either "consumed" or thermally upgraded coal seams in the vicinity of these intrusive bodies in the Witbank area of South Africa and in the Save-Limpopo areas of Zimbabwe. Contact metamorphism of the coals within distances of approximately 0.6 to twice the thickness of the intrusive bodies has been recorded in these coal bearing areas, with Mkwasine Coal Mine in the Chiredzi areas in Zimbabwe being a typical example. This was observed during a site visit by the author, courtesy of Verify Engineering. In some parts of Zimbabwe, mudstone "dykes" have joined the contemporaneous river channels in playing havoc with coal seam continuity and quality (Swift et al., 1953; Duguid, 1978; Barber, 1987). The occurrence of these geological discordant structures has been interpreted as arising from the squeezing down of overlying sediments into the pre-existing faults or joints. Mudstone channels have also been encountered by geological mapping campaigns in both open pit and underground mining areas at Hwange Colliery.

2.3.2.2 In-seam Biostratigraphic Subdivisions and Correlations

Using data from petrological, palynological, chemical, and geochemical analyses detailed stratigraphic subdivisions of channel was achieved (Falcon, 1989), zones and subzones were formulated, followed by correlations of these units. At the end, an attempt was made to establish the sequence of historical developments during the process of peat accumulation in

the No.2 seam. From the petrographic profiles in selected adjacent channels, minor events of a localised nature were initially recognised from which broad-scale major events were subsequently identified. With diligent investigation, the latter were found to be recognisable in varying degrees in all the channel samples. The study established three major zones: Zone A, B and C, as seen in (Figure 2.7a and b) above and each zone appears to be representative of a specific sequence of events. Zone A is interpreted to have undergone two periods (possibly three) of relatively quiet, waterlogged reducing swamp conditions, interspersed with periods of organic detritus influx, but not accompanied by mineral-derived material. The end of this zone is marked by the first major carbominerite event as represented by lenses of high quartz and high clay content detected (Falcon, 1989).

In zone B, which occurs in the middle of the seam, conditions for stable quiet and waterlogged swamps resumed. The period is characterised by deposition of only minor granular, detrital organic matter with no significant detrital mineral matter. This is interpreted to present the period during which the best quality coal, i.e., low ash, high reactive macerals, was formed (Cairncross and Cadle, 1988; Falcon, 1989). A minor and brief return to quiet water-logged conditions (as evidenced by more extensive vitrinite appearance) followed a second major carbominerite event (represented by a significant carbonate lense). This constituted Zone C, the upper zone. All the three zones may be observed in all areas that were investigated, although their thicknesses vary. Investigations into the variations in thickness, both whole seams and of zones within them, indicate that these fluctuations may be linked to the topographic contours of the region and to differential compaction of the sediments underlying the seam (Falcon, 1989).

Available information on the Hwange Basin indicates that the No.2 Seam in the Witbank shares common attributes with the Hwange Main Seam. These common factors include:

i. The vertical variation in major quality parameters such as ash, volatile matter, and sulphur and coal type (bands of low ash, bright coal linked to vitrinitic macerals occur typically at the base of the seam giving rise to good quality coal which, usually, has coking properties);
ii. Using data from proximate analysis of Drill-hole 1067 (Table 2.1) Pallocks (1987) found that the Main Seam in the Hwange Concession consists of three sub-seams: the basal No.1 sub-seam with a cumulative ash content of 15%; overlain by sub-seam 2 with a cumulative ash content of 20%; which, in turn, is overlain by a horizon where

there is sudden increase in the ash content, yielding ash values in excess of 30%. Figure 2.8 is a graphic presentation of the data in Table 2.1.

iii. The upper part of both seams consist of bands of dull higher ash coal with grey mudstone inter spaced with small bands of shiny, presumably vitrinite-rich, material; and, both seams (No. 2 Seam at Witbank and Hwange Main Seam) are the most important seams in South Africa and Zimbabwe, respectively, from an economic perspective.

However, the two seams (No.2 Seam at Witbank and the main seam in the Hwange Concession) differ in two areas:

i. Vertical variation in the Main Seam at Hwange is apparently gradation and there are no visible physical indicators such as clastic partings (Table 2.1 and Figure 2:8) as observed in the No.2 Seam in the Witbank Coalfield;
ii. The Hwange Main Seam apparently is devoid of the igneous intrusions (which are localised features) that affected the No.2 Seam in the Witbank Coalfield. In addition, unlike the No.2 Seam in South Africa, which occurs above No.1 seam, the Hwange Main Seam does not have an underlying seam.

Table 2.1: Proximate analysis (ash and volatile matter contents) of drill-hole 1067 (after Pallocks, 1987).

Depth (m)		Ash (%)	Volatile matter (%)	Subseam	Definition of Subseam
From	To				
3.96	4.19	58.2	13.4	Roof	
4.19	4.42	35.5	16.9	3	Cumulative
4.42	5.03	30.9	16.9		Ash>25%
5.03	5.64	22.8	18.3		
5.64	6.25	25.1	18.7		
6.25	6.86	23.3	18.4		
6.86	7.47	16.9	20.3	2	Cumulative
7.47	8.08	12.9	20.9		Ash<20%
8.08	8.69	13.9	21.7		
8.69	9.30	13.3	22.0		
9.30	9.91	13.6	21.4		
9.91	10.52	13.3	21.1		
10.52	11.13	11.7	21.0		
11.13	11.74	12.9	22.1		
11.74	12.32	10.0	24.3		
12.32	12.93	7.4	26.5	1	Cumulative
12.93	13.24	8.6	26.3		Ash up to 15%
13.24	13.85	6.2	30.3		
13.85	14.46	7.0	29.2		
14.46	15.07	8.5	28.4		
15.07	15.68	5.4	32.3		
15.58	15.98	8.9	32.5		
				Floor	

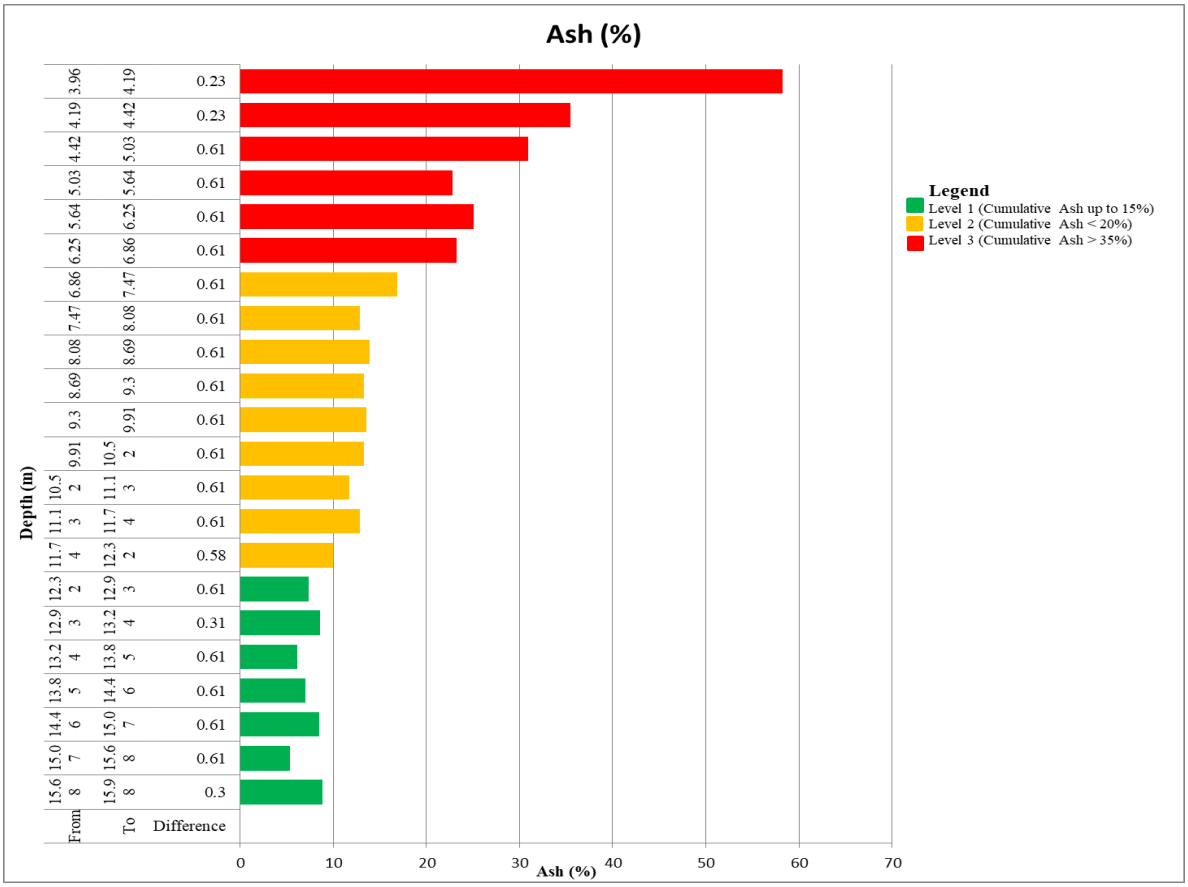


Figure 2.8: Graphic presentation of the Hwange Concession subseam development based on Drill-hole 1067 proximate analysis (after Pallocks, 1987).

2.3.3 Mid-Zambezi Basin Models

2.3.3.1. The Tectonic Model for the Mid-Zambezi Basin

The Mid-Zambezi Basin has attracted considerable attention mainly in view of its coal deposits, particularly the Hwange coal deposit, and a few models have been postulated by different researchers. To guide coal exploration programmes in Zimbabwe, Duguid (1980) looked at the geological and geomorphological settings of each of Zimbabwe's coal basins and developed depositional models for the coalfields. Duguid's models and their palaeogeomorphologic setting are summarised as follows:

I. **Basin-end Shoreline Plain**

Duguid (1980) cited the Hwange coal measures as the best example of the model. He describes the area of coal measures as a southern part of a very large palaeoshoreline plain, the northern part of which had been down faulted to a great depth by the Deka Fault. Duguid further notes that facies changes and strike directions within the Black Shale and Coal Measures exist at the south-east end of the north-east-trending, early Lower Permian, Mid-Zambezi Karoo intrabasin.

II. **Basin-side Shoreline Plain or Strip**

Duguid describes this as a coalification area trending parallel, and in close juxtaposition, with the palaeoshoreline along the side of one of the Lower Permian Karoo basins. He cited the Lubimbi-Hankano Coalfield as a good example of this model.

III. **Basin-confluence Inner-side Shoreline Plain**

This coal-bearing area was developed on a stable plain situated at the confluence of the north-trending Save-Lundi Basin and the west-south-west-trending Save-Lundi Basin, the Mkwasine Coal Measures are cited as the best example of this model. He describes the two basins as with the marginal shoreline facies indicating that they were individual interconnected basins during the Lower Karoo times.

IV. **Basin –embayment Shoreline Plain**

The Sessami Kaonga Coal Measures, which occur as an embayment that occupies a position along the main south-eastern shoreline oblique to the axis of the Zambezi-Karoo geosyncline, is a typical example of this model (Bohmnke and Duncan, 1974).

V. **Palaeoisland-side Shoreline Plain or Strip**

The Lusulu Coalfield (Duguid, 1980) is described as a good example of this model. With the main coal seam which occurs over a belt of 7 km wide and 28km long, the area occurs along the early Lower Permian palaeoshoreline on the southern side of the of the Sijarira palaeoisland.

VI. **Palaeoisland-protrusion Shoreline Plain or Strip**

A good example of this model is the Sengwe Coalfield which lies around the tip or protrusion of the Sijarira palaeoisland (Duguid, 1980). The Sebungu Coal Measures in this model occur at the south-western end, or protrusion, of the northern arm of the herringbone-shaped palaeoisland.

VII. **Palaeoisland-embayment Shoreline Plain**

Though little work has been carried out in the area, an embayment has been identified between the arms of the herringbone-shaped palaeoisland around Lubu, in Kariyangwe District" (Duguid, 1980). The area had suffered a great deal of faulting, and it was argued that this embayment was a wedge of the down-faulted Karoo sediments.

The Duguid's palaeo-shoreline model has been challenged by a new model, developed by Oesterlen, (1999); and Oesterlen and Lepper, (2005) as described below:

i) **Intrabasin model**, this was a model developed by Lepper (1987), which described the northeast – southwest trending Mid-Zambezi Basin as a depression made up of four intra-basins which are: the Upper and Lower Sengwa intrabasins; the Gwayi intrabasin and the Mlibizi intrabasin. Lepper, (1987) based this subdivision of the Mid-Zambezi Basin on the existence of inliers of either sedimentary rocks older than the Karoo, or Archaean basement rocks which essentially are of granitic composition. The Chizarira horst (essentially sedimentary) separates the Upper Sengwa intrabasin from the Lower Sengwa intrabasin. The same sedimentary horst is the main feature separating the Lower Sengwa intrabasin from the Mlibizi intrabasin. The Kamativi inlier of basement rocks, which are essentially granitic in composition, separates the Gwayi intrabasin from the Mlibizi intrabasin.

Within these intrabasins occur localised coal bearing areas which are separated from each other by topographically high areas. These coal bearing areas are shown in Figure 2.9 and their respective hosting intrabasins shown in Table 2.2.

Table 2.2: Mid-Zambezi coalfields and hosting intrabasins.

Intrabasin	Coalfield and coal occurrence
Upper Sengwa	Sengwa North, Busi, Kaonga, Sessam.
Lower Sengwa	Sengwa South,
Gwayi	Lusulu and Lubimbi
Mlibizi	Hwange, Lubu and Sebungwe

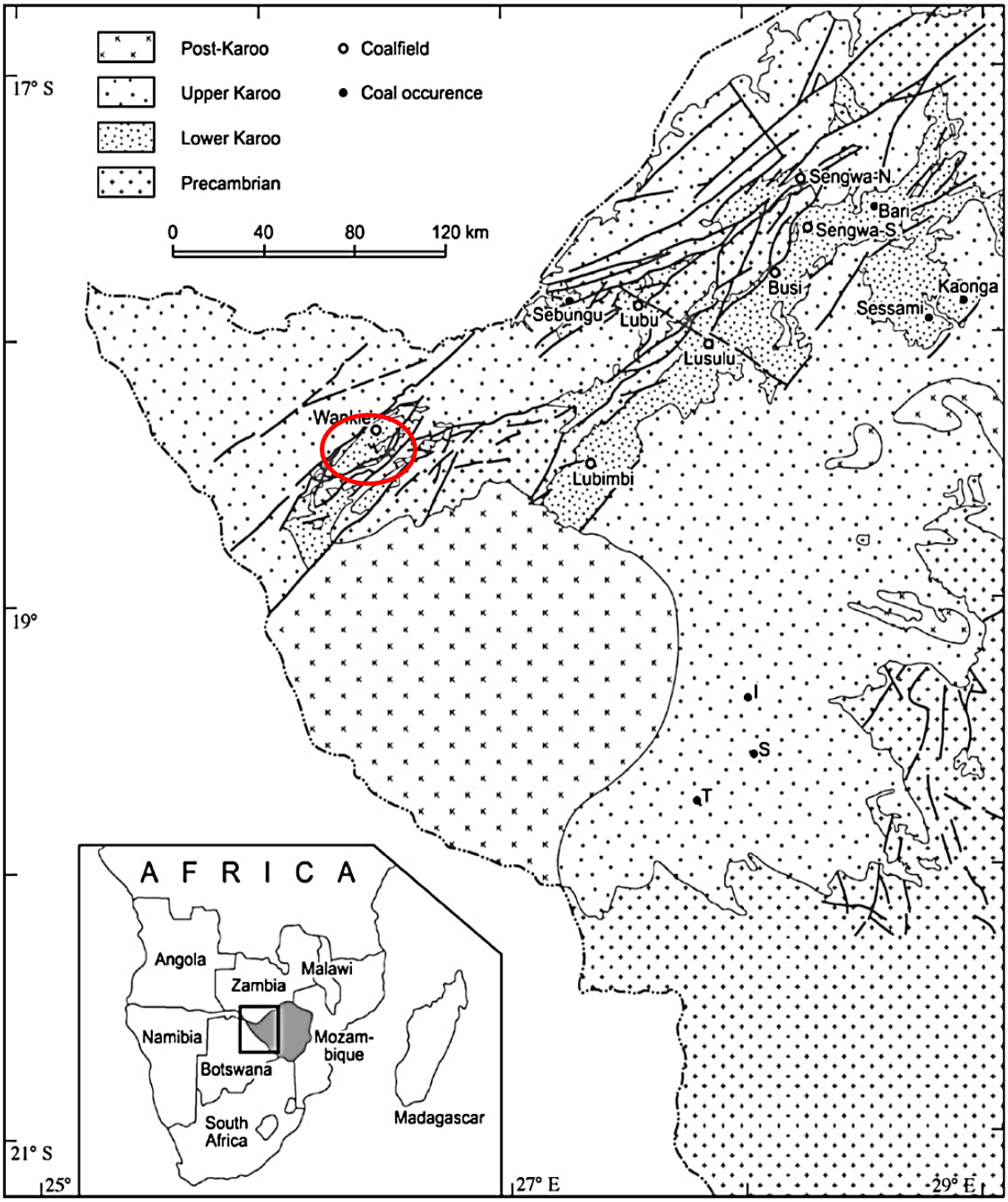


Figure 2.9: Location of the Hwange Coalfield in relation to other coalfields and coal-occurrences in the Mid-Zambezi basin, Zimbabwe (I=Insuza, S=Sawmills, T=Tsholotsho) (source: Oesterlen and Lepper, 2005).

Both the Lower Sengwa and the Mlibizi intrabasins are truncated on their northwestern boundary by the northeast-southwest trending "Boundary Fault" described by Orpen *et al.* (1989) and referred to earlier in this Chapter. This is traceable southwestwards as far as the Zimbabwe-Botswana border. The red circle (Figure 2.9) shows location of Hwange Colliery operations in the map.

ii) The Half Graben Model (Orpen, *et al*. 1989), focussed on the Karoo basins of Central Africa, particularly those formed along the northwestern and northern margins of the Zimbabwean Craton. Orpen *et al.* (1989) provide a corroborative interpretation of the Zambezi Karoo basin as having been developed because of wrench-faulting and half-graben tectonics during the Palaeozoic. The interpretation is derived from a review of geological and geophysical (aeromagnetic and gravity) data for the Central African basins (Taverner Smith, 1958; Tankard, *et al*., 1982; Daly, 1986) and specifically those areas formed along the north-western and northern margins of Zimbabwe Archaean Craton, i.e., the Mid-Zambezi and Lower Zambezi, respectively. These data have enabled the broad interpretation of the geometry of the basins, as depicted in Figure 2.10.

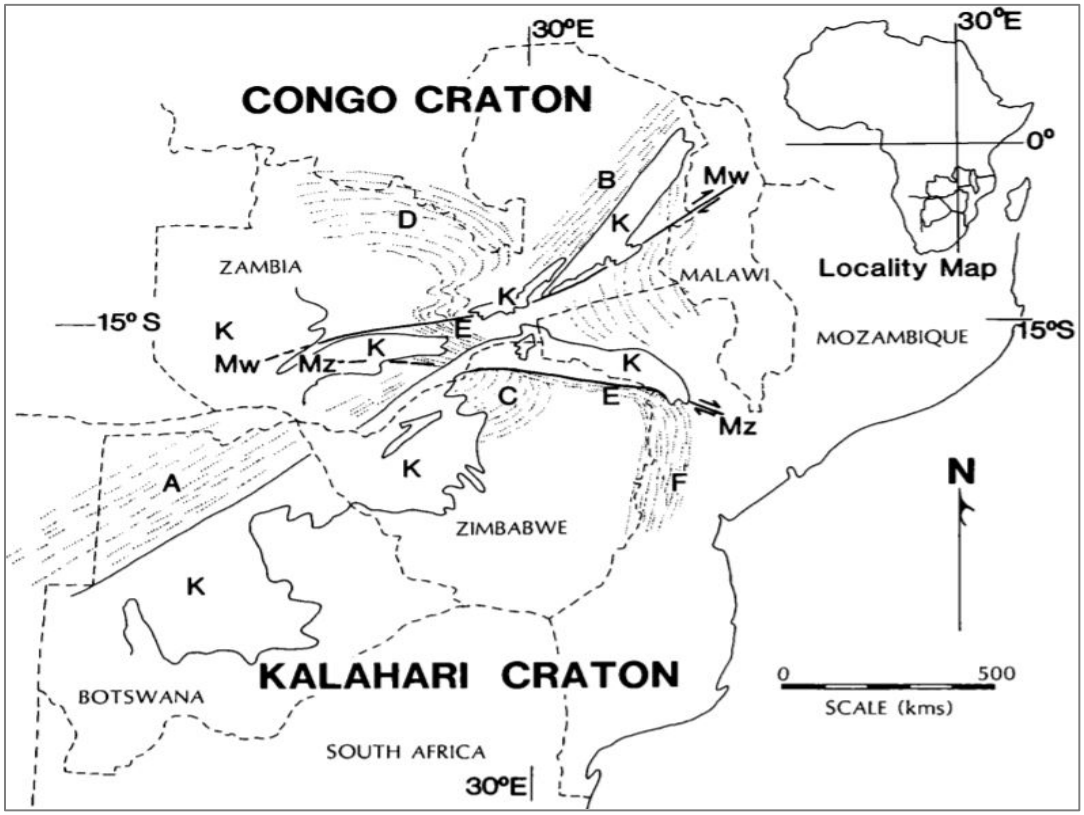


Figure 2.10: The mobile belts of Central Africa and the distribution of the Karoo Basins (after Orpen *et al*., 1989). Mw = Mwembesi Shear Zone; Mz = Mzarabani Shear Zone; K = Karoo. Mobile belts are identified as follows: A = Damaran; B = Irumide; C = Magondi; D = Lufilian Arc; E = Zambezi; and F = Mozambique Mobile Belt.

A horst of basement gneisses, known as the "Chiwore Inliers", trends southwards from Zambia into the Karoo sediments of northern Zimbabwe and forms the western margin of the Lower Zambezi Basin. To the west of the horst lies a small but prominent basin recently defined geophysically and is referred to as the "Mana Pools Basin" (Orpen, *et al*., 1989) and is

separated from the Mid-Zambezi Basin to the south. Towards the end of the Karoo period, the sedimentary fill of these three basins (i.e., Mid-Zambezi, Mana Pools and Lower Zambezi) coalesced (Orpen *et al*., 1989).

Referring to Figure 2.11, which is a sketch map of the Karoo basins and their broad-scale geometry, the author draws attention to the linear alignment of the faulted NW margins of the Luangwa, Mid-Zambezi and Passarge basins, with the last two having lobate south east margins that exhibit "a largely passive unconformable relationship between the sediments and the basement" while the Luangwa trough is fault-bound on both margins. A further feature of the Mid-Zambezi and the Passarge basin noted by Orpen *et al*. (1989) is that the depocentres of the two lie close to their faulted northwest margins resulting in both basins exhibiting "an asymmetric profile, perpendicular to the depositional axis". This was also previously noted by Watson, (1960) and, subsequently, described by Swardt, *et al*., (1965).

Major intrabasin normal faults with strike sub-parallel to the NW marginal fault have culminated in the development of isolated basement horsts such as the "Sijarira" horst within the basin in their conclusion (Figure 2.11). Orpen *et al.* (1989) state that the features of the Mid-Zambezi Basin which include major rift escarpment faults occurring on the NW margins of both this basin and that of Passarge, which they consider to be aligned along a plane of weakness in the earth's crust indicate a half-graben. They suggest this tectonic setting as the most plausible tectonic model of the basin's development. They further suggest that the well-developed NW marginal fault as presumably listric in profile.

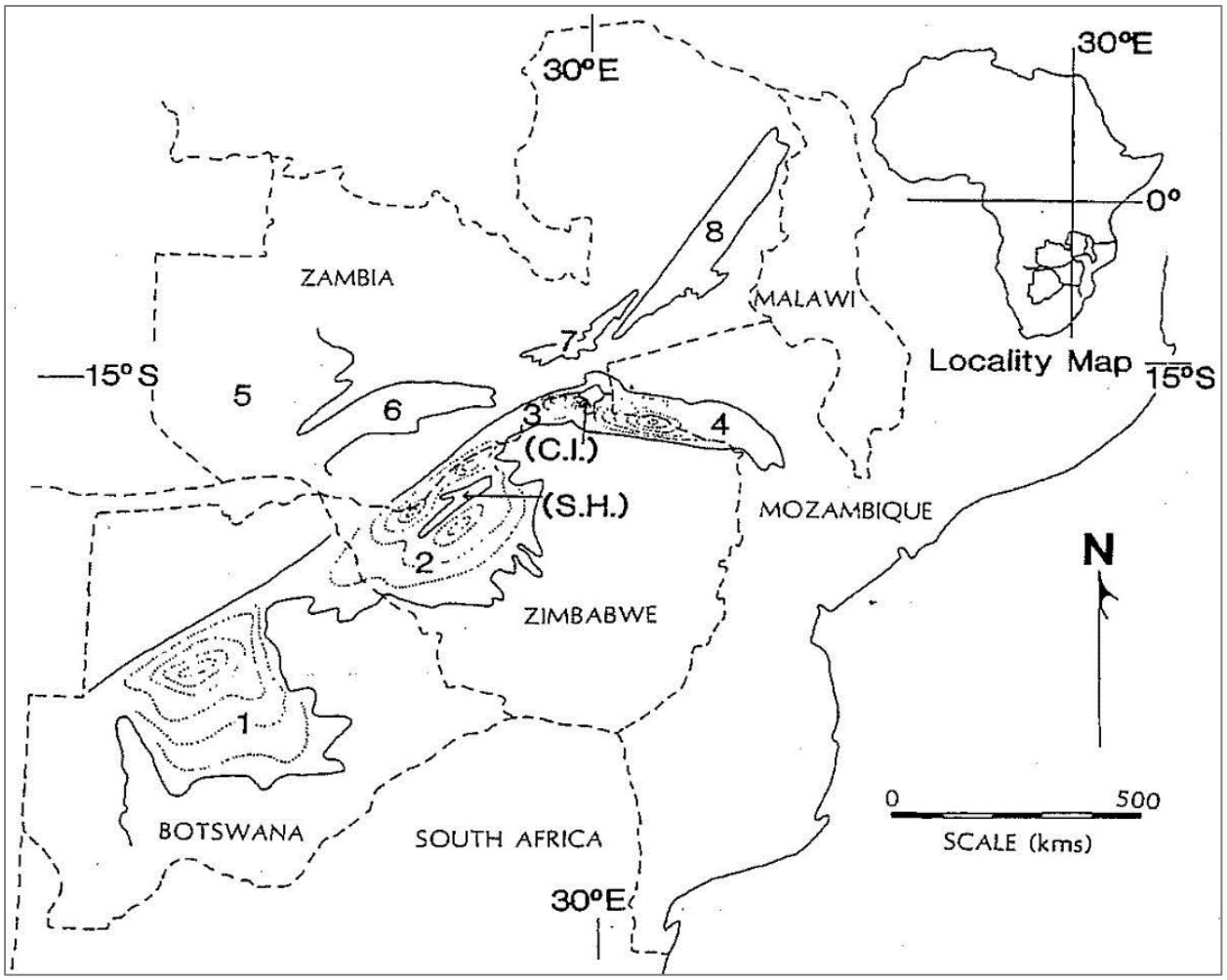


Figure 2.11: Sketch map of Central African Karoo basins showing their broad-scale geometry (Orpen *et al*., 1989).

As indicated on the map, 1 denote the - Passarge; 2 – Mid-Zambezi; 3 – Mana Pools; 4 – Lower Zambezi; 5 – Western Zambia; 6 – Kafue; 7 –Luano: 8 – Luangwa Basin. The Mid-Zambezi Basin consists of at least three sub-basins separated by the "Sijarira" Horst (S.H.). The Chiwore Inliers (C.I.) separate the Mana Pools and Lower Zambezi basins (adopted from Orpen et al., 1989). N.B. The corrupted name "Sijarira" has since been changed to "Chizarira.".

iii) The Kinematic-thermal model was postulated in a study carried out on the development of the Mid-Zambezi Basin and coal seams therein by Oesterlen and Lepper, (2005). Three main lines of evidence: the new rift concept, information from lithology and coal quality related to the depositional environment, and maceral distribution were investigated by the author.

2.3.3.2. The new rift concept of the Mid-Zambezi Basin

Oesterlen, (1999) applied the kinematic-thermal models of Mckenzie (1978) and other researchers for the rift basin to the Mid-Zambezi Basin. Oesterlen identifies three phases of

development of the present day Mid-Zambezi Basin and these are: i) the non- deformational phase of a sag basin brought about by the kinematic stretching of the crust and lithosphere during the Lower Karoo (Permian pre-rift phase); ii) the phase of formation of a subsiding central rift along boundary faults, due to crustal breakdown accompanied by rising rift shoulders during the Upper Karoo (syn-rift phase during the Triassic time); and iii) the phase of widening of the Mid-Zambezi Basin in Jurassic time due to thermal subsidence on the margins of the basin (post-rift phase). Figure 2.12 shows the suggested stages in the development of the Mid-Zambezi Basin by the Oesterlen (1999). This new model significantly contradicts the palaeogeographic settings previously described by Duguid (1977, 86) and Hosking (1981) in that it describes a large shallow basin which was not subdivided by an intrabasin high (Oesterlen and Lepper, 2005). Oesterlen and Lepper, (2005) argue that the Kamativi-Sijarira inliers were uplifted at the same time with the rifting and subsidence of the graben which only occurred in the Upper Karoo time from the Lower Triassic onwards. According to Oesterlen and Lepper (2005), this model is supported by several arguments among which are:

i. The inliers consisting of Precambrian rocks of various ages still possess a few Lower Karoo erosional remnants, which attest to the Lower Karoo roof sediments that overlie the Precambrian base (Chappell, 1969; Humphreys, 1969).
ii. Isopach trends for the Hwange Main Seam (K^2) Main Seam from Hwange and Sengwa coalfields and the ash contours calculated by Palloks (1984) do not reflect the boundary faults of the inliers.
iii. The coal seams at Hwange Concession, Lusulu and Sengwa, show a clear increase in thickness towards the uplifted blocks (Lepper, 1992).

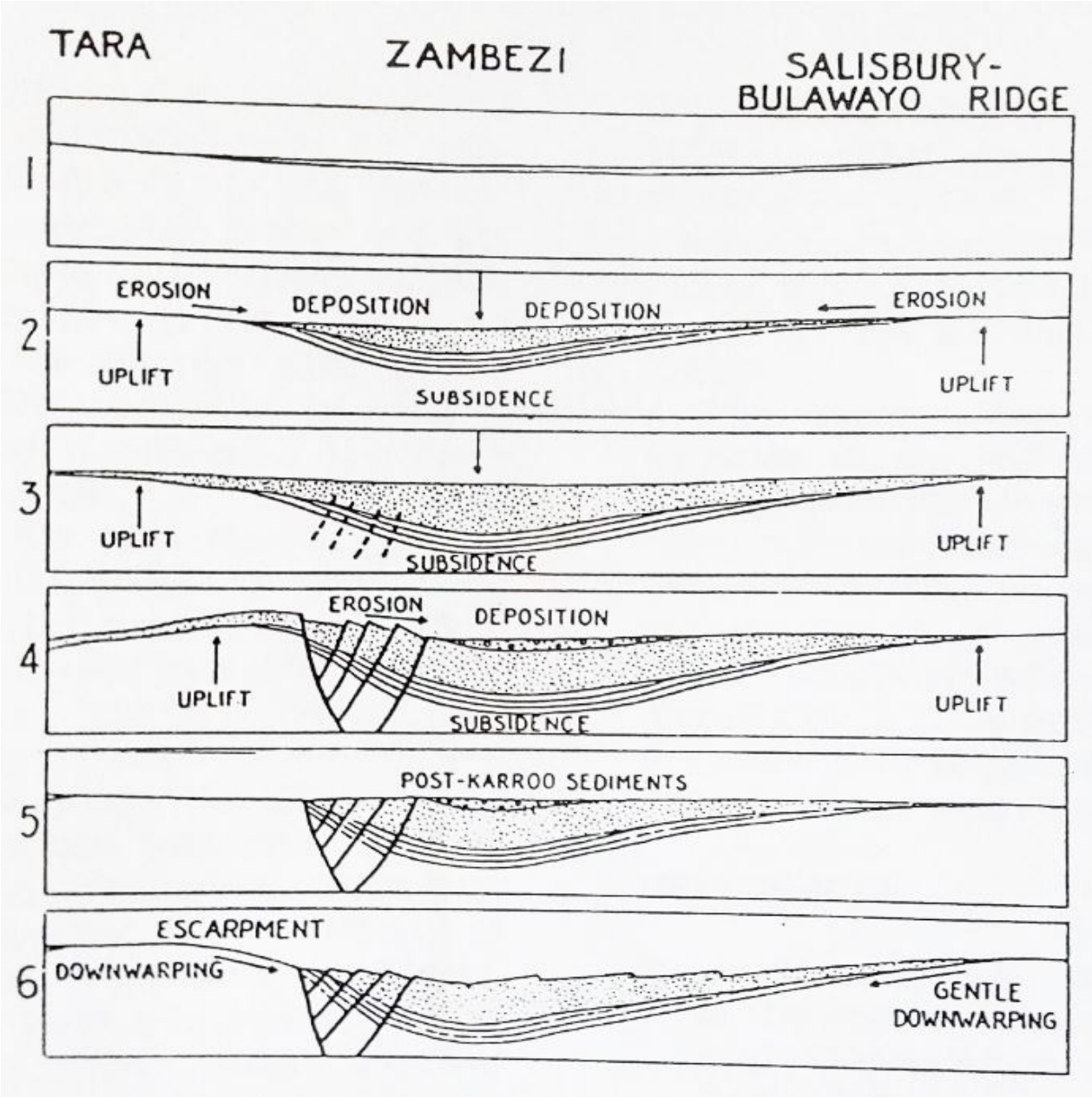


Figure 2.12: Suggested stages in the development of the Mid-Zambezi Basin (Diagrammatic and not to scale. Source: Oesterlen, 1999).

To buttress their argument in support of the new model of a large shallow Lower Karoo basin, Oesterlen and Lepper, (2005) turned to K^{2-3} coal-mudstone group of the Hwange Karoo sequence to generate a new palaeogeographic and depositional setting in view of the fact that the earlier model of a palaeoshoreline of Duguid (1986) was no longer appealing (Oesterlen and Lepper, 2005). The focus on K^2 was spurred by the fact that coals are good indicators for certain environments of sedimentation and regional tectonics on the one hand, and because of its importance as a source of energy in Zimbabwe, yet the knowledge of this fossil fuel in the country was rather limited (Oesterlen and Lepper, 2005)

The available literature then included publications by Duguid (1986); while the general Lower Karoo lithostratigraphy of this major basin was covered by Lepper (1992). New ideas have since been put forward mainly on the formation and evolution the Zambezi Basin and rift in general, and the Mid-Zambezi basin, which shed some new light on K^2 coal of Zimbabwe (Oesterlen and Blenkinsop, 1994; Oesterlen, 1998, 1999). Spurred by the need for an increase in knowledge on the depositional environment and palaeogeographic setting of this sedimentary deposit, Oesterlen and Lepper (2005) carried out a comprehensive lithological study and correlation of borehole data from the Coal-Back Shale Group (K^{2-3}) coalfields or known coal occurrences in the Mid-Zambezi Basin (Figure 2.9).

The study identified two types of coal: the alluvial plain coal and the freshwater lake coal. The former was only found in Gokwe and Nyamandlovu areas. The depth of the coal was more than 200 m below surface, its thinness, and the discontinuous nature of the seams, as well as its high ash content render the economic significance very small (Oesterlen and Lepper, 2005). In sharp contrast, lithologically and economically, is the freshwater lake type, which is found in the Hwange, Lubimbi, Lusulu, Busi and Sengwa coalfields, as seen in Figure 2.13. The coal is characteristically more or less massive (Hwange, Lusulu and Lubu) or thin coal bands alternating with carbonaceous mudstones (Lubimbi and Sengwa). The lateral lithofacies of the coal where it turns down-dip into sapropelic (massive and granular) mudstone of the lake, and up-dip into terrestrial sediments of the coastal plain are strong evidence for a shoreline environment (Oesterlen and Lepper, 2005). According to Oesterlen and Lepper (2005) the lake shoreline interpretation culminates in the delineation of a 20 to 40 km wide coal belt stretching from the Hwange Coalfield in the west to Sengwa in the east.

2.3.4 Lithology and coal-quality related to environment of deposition of the K^{2-3} Group

Oesterlen and Lepper (2005) went on to review the available literature on lithology and coal quality which might be related to the environment of deposition of the K^{2-3} group of the Mid-Zambezi Karoo sequence. Their study included a review of records of selected drill holes drilled over the known coal occurrences in the Mid-Zambezi Basin to identify the lithology and coal quality attributes that could shed light on the depositional environment of the K^{2-3} in this basin. With more than 3 000 drill holes sunk by the study period, Hwange Concession provided an excellent database for sedimentological interpretation. As had been pointed out earlier by Duguid, (1986 & 1993), the Hwange Concession K^{2-3} consists of the Main Seam of up to 14 m thick at the base. This seam is overlain by approximately 20 m of carbonaceous mudstone and in places replaced in the upper part by a thin coal seam (Seam 1), and Fireclay

of 6 m thick (Drill-hole W 1539, Figure 2.13). Towards the western areas this pelite-coal lithology changes gradually with the coal being replaced with clastic intercalation in the main seam as well as in the hanging wall mudstones and Fireclay. This occurred until eventually the main seam thins out, leaving only siltstone and Fireclay resting directly on the K^1 sandstone (Drill-hole 92, Figure 2.13). Going eastwards, the black shale and coal lithology becomes increasingly replaced by carbonaceous mudstone (Drill-hole 33, Figure 2.13).

This trend from sand-silt facies in the far WSW- part via a peat swamp-mud facies in the centre towards a pure mud facies in the far ENE was noted by Duguid (1986). Oesterlen and Lepper, (2005) interpreted this as a lake shoreline peat swamp environment, with its up-dip margin on one side representing the shore of the Mid-Zambezi lake and its down-dip lacustrine facies in the other direction.

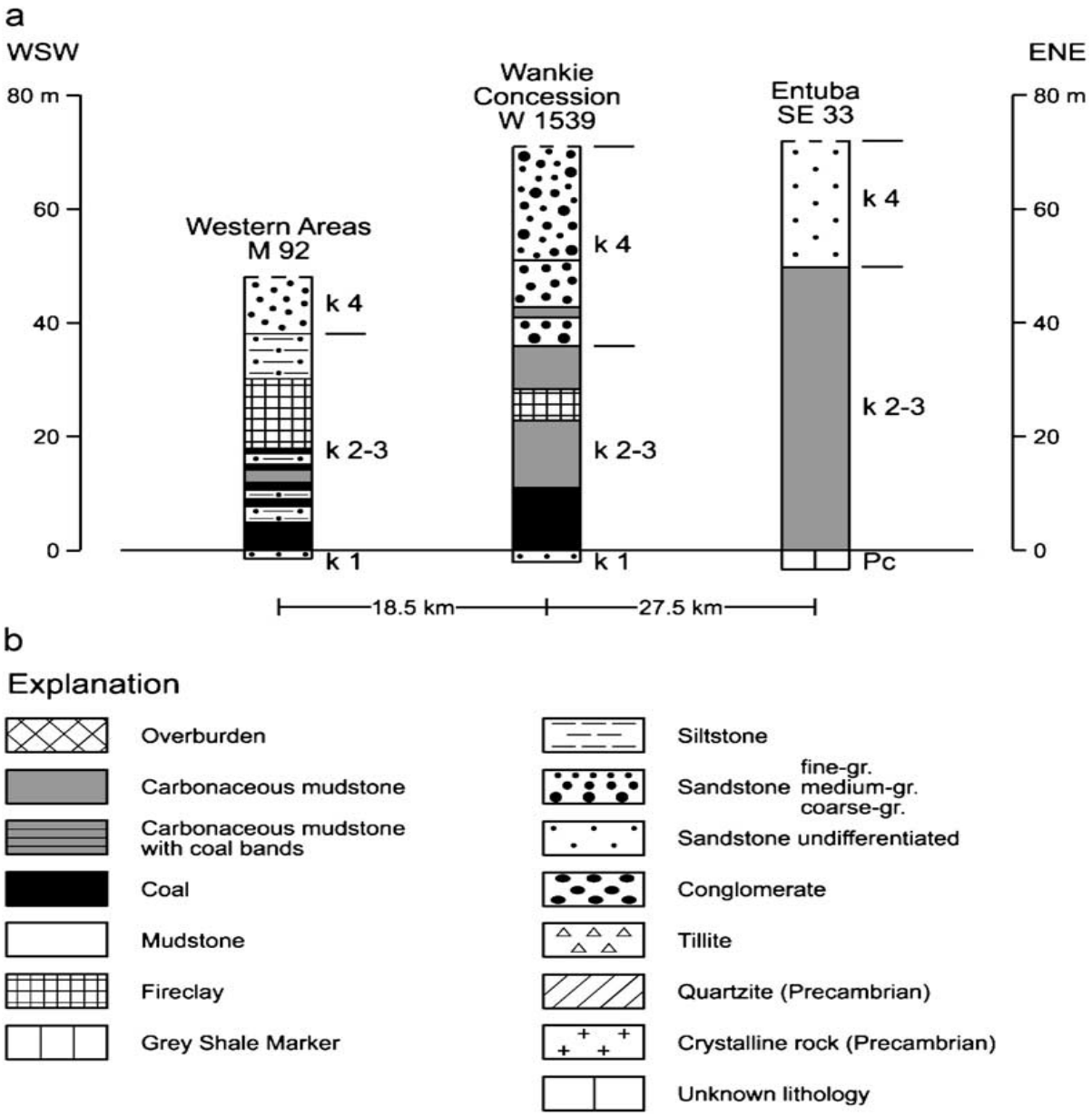


Figure 2.13: The K^{2-3} lithofacies changes at the Hwange coalfields including lithological legend (Source: Oesterlen and Lepper, 2005).

Watson, (1960) found that the coal quality of the Main Seam within the Hwange Concession has a low ash content between (5-7 %) at the base and increases to 30 % at the top. The same trend was report for the Entuba and the Western Areas by Thompson *et al*., (1982) and Pallocks (1987) respectively. The coal quality trend whereby the ash levels become progressively higher and lower in basal coking coal (Duguid, 1993) towards the edges of distribution, i.e., the up-dip margin at the Western Areas, and the down-dip edge at Entuba is consistent with lithofacies trend of the K^{2-3} sequence described above where the coal was replaced by clastic sediments. Oesterlen and Lepper, (2005) stated that the environment was composed of a large amount of inorganic material deposited in the peat swamp, forming mudstone partings, and resulting in higher ash content for the raw coal.

At Lubimbi the scenario is rather different from that of Hwange area coalfields. Typical features of the Lubimbi coal are the alternation of bright coal with dull coal horizons (Oesterlen and Lepper, 2005). This alternation of coal with bituminous mudstone layers, the common stratification of the coal i.e., banded coal with bands exhibiting a lenticular shape on a larger scale and the relatively high amount of silty mineral matter, led to the marked increase in the thickness of the K^{2-3} member from 32 m at Dhalia to 53.5 m at Lubimbi East (Thompson, 1981).

Looking at Lusulu, Oesterlen and Lepper (2005) suggest a shoreline swamp coal depositional environment, which grades rapidly into a carbonaceous flood plain towards the south. The two authors further argue that the very thick sapropelic mudstones, with a few sandstone tongues in the upper portion, which were reported in most drill-holes also point to a lacustrine origin resulting from a transgression of the lake.

2.3.4.1. Information from maceral analysis of coal.

Oesterlen and Lepper (2005) noted during their investigation that the petrography of the K^{2-3} coal was not well studied, and that the data obtained were incomplete with no information at all from Busi and Lubu coalfields, Gokwe coal occurrence, and the deep drill-holes at Nyamandlovu. However, they note that some data appears to exist at Hwange, Lusulu and Sengwa where one dominant maceral model for the coalfields is reported, while Lubimbi coalfields present a different scenario.

Watson, (1960) reported on two maceral analyses from the Main Seam in Hwange Concession at No.2 Colliery, although the author did not give any details of the sampling procedure utilized (Oesterlen and Lepper, 2005). One sample was reported to be bi-maceral coal comprising 54.35% vitrinite, 44.3% inertinite, 0.2% liptinite and 1.2% other components. This, presumably, was taken from the basal portion of the Main Seam, judging from the relative proportions of the macerals, high vitrinite and relatively low inertinite in the sample. The other sample reported 61.7% inertinite, 34.6% vitrinite, 0.5 liptinite and 3.2% other components, which Oesterlen and Lepper, (2005) concluded was most certainly from the upper portion of the Main Seam. Thompson, *et al.,* (1982) presented some data from the Entuba Coalfield from coal washed at specific gravity of 1.4. The basal 1.3 m of the Main Seam, which is classified as coking coal, is composed of 47.3% vitrinite, 27.0% inertinite, and 2.3% liptinite (and 23.4% minerals as suggested by Oesterlen and Lepper (2005). The overlying 1.4 m of coal classified as blend coking coal revealed only 29.7% volatile matter, 18.0% inertinite and 1.3% liptinite,

while the remaining 51.0% was not reported. Maceral values at the Western Areas Coalfield for the basal 2.3 m (coking coal) of the Main Seam were reported comprising 40.6% vitrinite, 20.2% inertinite, 2.7% liptinite, with the remaining 36.5% not reported (Thompson, *et al*., 1982).

Similar results are reported for Lusulu Coalfield (Shell Developments Zimbabwe (Pvt) Ltd., 1983), as reported by Osterlen and Lepper 2005), which indicates a vitrinite-rich coal comprising 64.0% vitrinite, 28% inertinite, 6% liptinite and 2% minerals). Oesterlen and Lepper (2005) revealed that Falcon Research Laboratory (Pvt.) Ltd. (1995) reported results for the Main Seam at Sengwa based on three drill-holes as a dominantly inertinite rich coal comprising 51-96% inertinite, 1.5-12% vitrinite, and 3-13% liptinite. These results represent a typical Gondwana coal (Oesterlen and Lepper, 2005).

The maceral analyses for Lubimbi as reported by Thompson, (1981) are presented in Table 2.3. These analyses are based on seven drill-holes. As revealed by the analyses, the two lithologies within the K^{2-3} sequence (the bright banded coal and the dull coal) differ in the maceral composition. The bright banded coal is in the main a vitrinite-rich; while the dull coal and carbonaceous coal are dominantly inertinite-rich and contain a higher mineral value than the vitrinite-rich coal (Table 2.3).

Table 2.3: Maceral analyses from drill-holes Nos. 101 and 107, Lubimbi coalfields (from Thompson, 1981).

	Bright banded coal (vol%)	Dull coal and carbonaceous mudstone (vol%)
Vitrinite	45-59	13-23
Liptinite	8-11	5-7
Inertinite	23-31	41-61
Minerals	10-13	19-31

The maceral profile for the whole K^{2-3}succession at Lubimbi does not correlate with the standard maceral model for other coal bearing areas reported above. The samples from B-horizon (Table 2.4) indicate inertinite rich coal with the nonreactive maceral constituting over 70% of the maceral constitution. These are overlain by a vitrinite rich coal of the C-horizon in the south, with values of 51% vitrinite, 33% inertinite, 11.1% liptinite and 5% minerals. Banded coal of the D-horizon shows similar results; while its carbonaceous mudstone coals are inertinite rich coal; which is typical of Gondwana coal. The banded coals of the E/F-horizons are vitrinite rich and consist of 64% vitrinite, 16% inertinite, 7% liptinite, and 13% minerals.

Table 2.4: Maceral analysis of the coal horizons from Lubimbi coalfields (source; Thompson, (1981).

Banded coals					Dull coals		Carbonaceous mudstones
Horizon	E/F	D	C		B	E/F	D
			South	North			
Vitrinite (vol.%)	64	51	51	37	6	35	14
Liptinite (vol.%)	7	10	11	9	10	6	7
Inertinite (vol.%)	16	27	33	44	71(?)	33(?)	53(?)
Minerals (vol.%)	13	12	5	10	13	26	26
Ash (wt.%)	23.7	25.8	14.9	22.4	28.7	42.6	41.5

Oesterlen and Lepper, (2005) conclude that the maceral data of the individual coalfields of the Mid-Zambezi are a result of deposition processes. They envisage a swamp formation which started as a paludification process, with the fluviodeltaic sandstones of K^1 sequence replaced by a swamp due to rising groundwater-table. The standard maceral profiles for the basal 2 m of the Main Seam at Hwange, Lusulu, and Sengwa coal were characterised by a wet forest swamp with *Glossopteris-Gangamopteris* flora, and high water-table (vitrinite –dominated coal). The two authors postulated that the first stage of coal formation changed gradationally by the fall of the water level, leading to oxidation and decomposition of the plants in the swamp (i.e., dry forest swamp). The second stage is described by Oesterlen and Lepper, (2005) as having been more stable than the first and produced the inertinite-dominated coal of the major part of the Main Seam. According to Oesterlen and Lepper, the second stage was succeeded by the deposition of carbonaceous mudstone (at Hwange) when the shoreline swamp was drowned either by higher subsidence of the ground or a rise of the lake water level due to the transgression of the shoreline towards the south.

2.4 Coal Characterisation

2.4.1. Introduction

Coal, “the black stone that burns” (Bwerinofa and Brennen, 1989) is probably one of the most complex materials that ever exist naturally on earth. The value of a coal deposit is measured not only by the quantity of the deposit, but more importantly by its quality, i.e., its specific properties (Miller, 2013). It is mainly if not entirely the quality of coal, which determines its usage.

Coals occur globally and they vary significantly in their physical and chemical attributes for a number of reasons, both with respect to their organic components, rank and to associated mineral matter that is always present in varying amounts (Chen, 1998). The vast number of coal types and the myriad of possible coal end-uses render it imperative to carry out detailed characterisation, classification, and evaluation of this heterogeneous commodity. Besides, thorough characterisation of the coal and associated waste materials is essential for the determination of the subsequent beneficiation process. In order to understand the behaviour of different coals, it is necessary to characterise the coals by involving additional analyses to determine the physical and chemical properties of coal prior to its exploitation (Xie, 2015). Section 2.4.2 describes the essential coal properties that must be determined.

2.4.2. Coal Characterisation

The potential use of coal depends on its physical and chemical properties, which, in turn, depend upon its composition (maceral and mineralogical components) rank, grade, and the condition of the coal (Falcon, 1978a). Thus, these must be determined prior to the exploitation of the coal deposit. These properties are described in brief below, starting with coal composition, followed by the natural inherent aspects of coal, i.e., coal condition (weathered or burnt), coal rank, coal type and coal grade.

Coal is made up of two main components. Firstly, there are organic components derived from original plant matter, i.e., macerals which are microscopic organic constituents. Then, there are the inorganic constituents or minerals in coal. The two components occur together in varying ratios forming microscopic bands of 50 microns or more termed microlithotypes. These may, in turn, form a succession of macroscopic bands known as lithotypes (Van Krevelen, 1981; Snyman *et al*., 1983; Falcon and Snyman, 1988).

2.4.3. Organic Constituent

The organic constituents, or ***macerals***, are the building blocks of a coal. These organic entities evolved from different tissues and organs of the original plant material during the primary vegetative accumulation and the early stages of the coalification process (Falcon and Snyman, 1988; Wagner, *et al*., 2018). They are classified into three groups based on major attributes pertaining to each group, namely, the vitrinite group, liptinite group and inertinite group. Each group consists of a series of macerals (Stach, *et al*. 1982; Wagner *et al.,* 2018) which can be considered as belonging together either because of similar origin (such as liptnite) or because of the mode of degradation and preservation (vitrinite and inertinite). The maceral groups have

been conventionally separated into “reactive and “unreactive” categories based on their change in form and structure, relative to one another when subjected to heat (Wagner *et al*., 2018).

The relative proportions of these groups of macerals and minerals determine the type and nature of coal (Taylor *et al*., 1998; O’Keefe *et al*., 2013). In addition, the nature of the macerals in the coal determines its value for its application either as an energy source (Suarez-Ruiz and Crelling, 2008a; Ward, 1984, 2013) or as a coal that can form a hard, porous, and devolatilised carbon-rich product i.e., coke, when heated. In fact, almost all the economic benefits accruing from coal such as its energy input in combustion, its role in metallurgical processes, its capacity for *in situ* methane adsorption, and its methane’s potential as an alternative hydrocarbon source is determined by the organic components (Ward, 2016). In terms of carbon content, inertinite has the highest carbon content, followed by vitrinite which, in turn, is followed by liptinite.

Another feature that distinguishes macerals from one another is density. Broadly speaking the organic components have low densities (e.g., pure vitrain has a density of 1.24gm/cc) as compared to inorganic components (minerals) which is significantly denser with density ranges of 2.6 to 5.0 gm/cc (O’Brien *et al*., 2011). The maceral groups among themselves have different densities, with densities changing with coal rank. In the bituminous rank, liptinite has the lowest density range of approximately 1.15 to 1.20gm/cc, with vitrinite in second position with a density averaging 1.24gm/cc. Inertinite is the densest with a density range of 1.45 to 1.60gm/cc (O’Brien *et al.*, 2011). The implication of this revelation is that the association of mineral and maceral components in individual particles gives a coal its relative density which, in turn, affects the washability of such coal (O’Brien *et al*., 2011). The maceral groups are discussed briefly in the following section;

2.4.3.1. Vitrinite Group

The vitrinite group is divided into three subgroups (telovitrinite, dentrovitrinite, and gelovitrinite) based on: i) relatively pure layers or lenses; ii) continuous phase of groundmass binding other coal components; and iii) amorphous filling of cells, pores, and fissures (ICCP, 1998). Macerals comprising of vitrinite group and their respective forms are listed in Table 2.5. Telinite and collotelinite constitute the telovitrinite subgroup; vitrodentrinite the detrovitrinite subgroup, while gelinite and corpogelinite constitute the gelovitrinite subgroup.

Table 2.5: Vitrinite maceral and their respective forms (source: Wagner, *et al*. 2018, adapted from ICCP System 1994).

MACERAL	FORM
Telinite	Coalified cell walls of recognisable plant tissues, more or less intact
Collotelinite	More or less homogeneous structureless layers; may show mottling in low-rank coals; widely used as rank indicator
Vitrodentrinite	Discrete, small vitrinitic fragments of varying shape; a secondary maceral
Collodetrinite	Mottled, compact vitrinitic groundmass binding other coal components
Gelinite	Pure colloidal gel, homogeneous infilling of cracks and other voids; secondary maceral
Corpogelinite	Structureless homogeneous and discrete bodies of humic cell infilling.

This group of macerals presented in Table 2.5 is formed from woody tissue such as bark, cortex and xylem. It is formed under water-logged anaerobic conditions (Figure 2.14). These macerals have an aromatic nucleus surrounded by aliphatic groups (i.e., -OH, -COOH, $-CH_3$); and the main properties of this group are as follows;

i. Compared to the other two groups, the chemical structure of vitrinite is characterised by relatively high oxygen levels (Wagner *et al*., 2018) which, like the liptnite and inertinite groups, decrease with increasing rank.
ii. The vitrinite group is defined by the level of reflectance.
iii. The entity is readily oxidized, and as such renders the maceral prone to spontaneous combustion.
iv. The density of vitrinite ranges from 1.27 to 1.8 g/cm^3, subject to rank (O'Brien *et al.*, 2011); and
v. Vitrinite's properties and its reactivity in various utilisation processes varies linearly with rank, hence the use of vitrinite reflectance is paramount to the determination of coal rank.

The vitrinite macerals are moderately aromatic and are reactive in that when heated they release volatiles (derived from the breakdown of aliphatic chains) relatively easily and the remaining carbon-rich molecular structure softens and swells before becoming porous in the bituminous range of rank (Falcon, 2013). Thus, they are essential macerals in coking coals and for rapid combustion. Vitrinite has a higher reflectance than liptinite, but a lower reflectance than inertinite in coals in the bituminous range of rank.

2.4.3.2. Inertinite Group

The inertinite maceral group is comprised of a wide range of plant materials including woody fibrous constituents, similar to vitrinite but in this case the plant material would have accumulated in drier environments characterised by exposure to varying levels of oxidation as seen in Figure 2.14 (ICCP System, 1994; Falcon, 2013). Where plant material was attacked by microbial fungi and bacteria such conditions lead to desiccation and decomposition of the botanical structures. Scott and Glasspool (2006) believe that most, if not all, inertinite macerals are formed through exposure to elevated temperatures. According to O'Keefe *et al*. (2013), some inertinite macerals were formed almost certainly from peat fires, aerobic or sub-aerobic decomposition during the process of oxidation and ultimate carbon-enrichment. As a result, some inertinite maceral formed have reflectance values that are higher than those of the vitrinite and liptinite groups (Wagner *et al*., 2018). Fire may also have been responsible for some highly reflecting carbon-rich fragments. Gondwana coals are typically characterised by very high percentages of inertinite, a fact that is consistent with a low water table. The inertinite maceral group is divided into three subgroups namely: i) those with plant cell structures; ii) those lacking plant cell structures; and iii) those which are fragmented.

The subgroup with the cell structures are classified into fusinite, semifusinite – inert (ISF) and semifusinite – reactive (RSF); while funginite, secretinite, micrinite and macrinite comprise the subgroup lacking plant cell structures. The fragmented which is the third subgroup, is composed of inertodetrinite (ICCP System 1994 and ICCP, 2001). Owing to the dominance of inertinite in South African coals (Wagner *et al*. 2018) the semifusinite is subdivided into reactive and inert semifusinite (Falcon, 1981; Meyers, 1982; Smith, 1984; Van Krevelen, 1981). The inertinite releases little or no volatile matter and is relatively difficult to ignite. The macerals are generally non-reactive or, in some cases, semi-reactive in combustion and coke-making (Falcon, 1978; Stach *et al*., 1982). Table 2.6 presents the macerals that constitute the inertinite group as well as their respective forms.

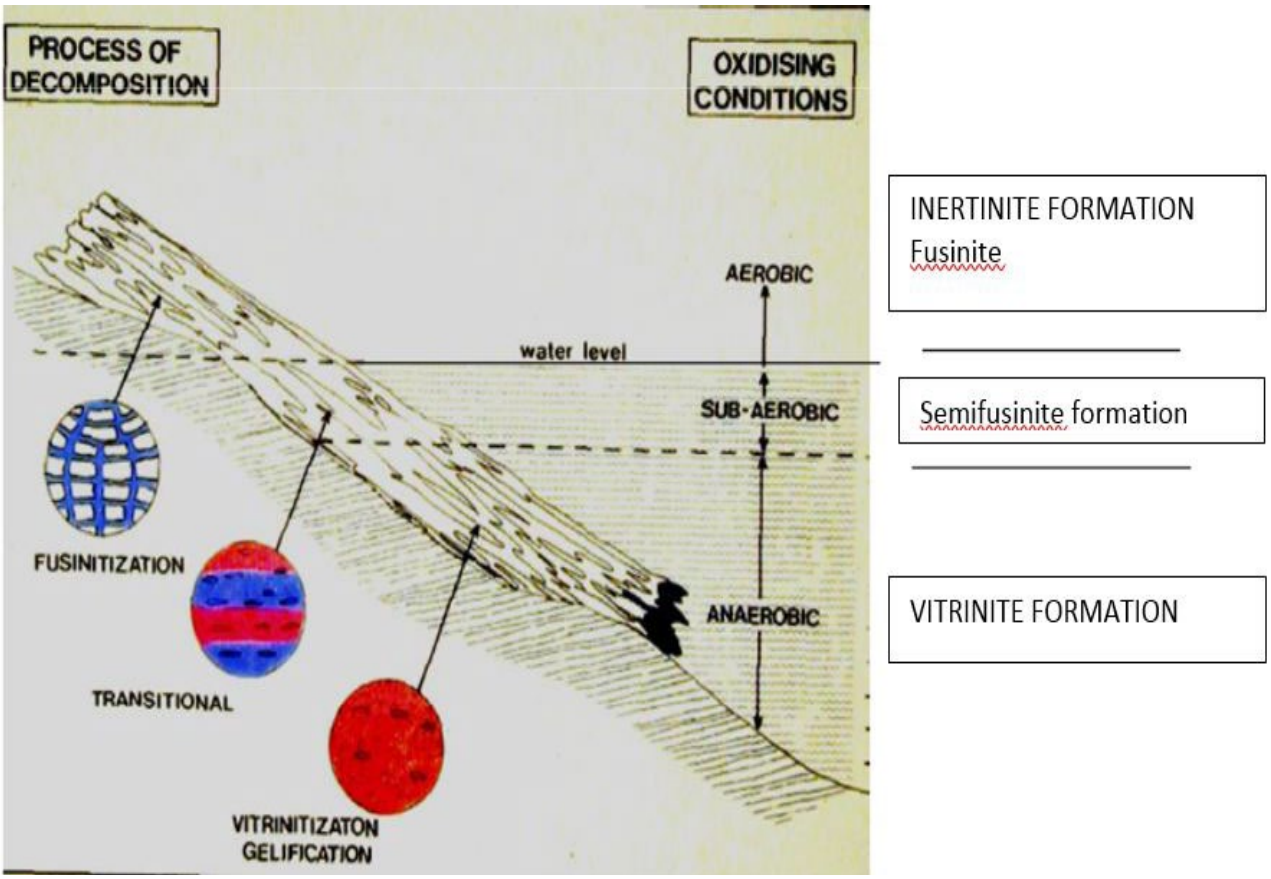


Figure 2.14: The formation of vitrinite and inertinite (from Falcon, 2013).

Table 2.6: Macerals in the inertinite maceral group (source: Wagner *et al.* 2018; adapted from ICCP System 1994 (ICCP, 2001), with some modification)

MACERAL	FORM
Fusinite	Highly reflecting, well-preserved cellular structure often intact or fragmented; no fluorescence; hard; exact origin debated between incomplete combustion in peat fires, and/or advanced oxidation.
Semifusinite – inert (ISF)	Intermediate structure and reflectance between vitrinite and fusinite in the same coal; derived from wood (Northern Hemisphere coals) or leaves (especially Gondwana coals); shows irregular anisotropy; common component of southern African coals.
Semifusinite – reactive (RSF)	Reflectance values close to vitrinite at the same rank, but the maceral exhibits structure and possibly partial anisotropy.
Funginite	Fungal remains; highly reflecting single or multi-cell fungal spores, almost completely absent in southern African coals, more common in Northern Hemisphere coals and low-rank coals of Asia and Nigeria.
Secretinite	Round to oblong, non-cellular, vesicled to non-vesicled forms, typically with high reflectance; may exhibit range of reflectances; previously referred to as sclerotinite; origin uncertain – may be oxidized resins; relatively common globally.
Micrinite	Very small, rounded organic grains occurring as aggregates, of inertinitic reflectance, generally considered as a secondary maceral; occurs in most coals globally, but not common; origin uncertain, possibly derived from liptinite, or inertinitic fragments.

Macrinite	Large, compact, amorphous, structureless inertinite of variable shape; variable origin, including metabolic products of fungi/bacteria, invertebrate excrement, or flocculated humic matrix substances partially oxidized, occurs globally, but generally rare.
Inertodentrinite	Discrete inertinitic fragments 2-10 microns of varying shape without microscopically recognizable structure; excludes fusinite fragments. Secondary maceral derived from oxidized/fusinized organic precursors that have undergone desiccation, mechanical crushing, attrition before/during decomposition and compaction; very common in Gondwana coals.

The inertinite macerals have the following properties listed below (Falcon, 1978; Stach *et al*., 1982; Falcon and Snyman, 1986).

I. They are the highest reflecting group in the bituminous coals.
II. They have low volatile matter content.
III. They are not readily oxidized/ignited.
IV. They are more aromatic and have a higher density than the vitrinite and liptinite groups in low and medium rank coals.
V. Their low hydrogen content renders hydrogenation impossible; and
VI. Save fusinite, which is relatively friable, the inertinite group macerals strengthen the coal bands in which they occur (incurring more resistant to compression and breakage).

2.4.3.3. Liptinite Group (Previously known as Exinite group)

This group of macerals was derived from hydrogen, waxy and oil-rich plant material, i.e., those parts of the plant that are generally chemically resistant and protective of the plant whilst growing. Taylor *et al*., 1998 and Pickel *et al*., 2017 describe the plant matter from which the group is derived as non-humifiable. This group includes spores, cuticles, suberine cells, resins, algae, and polymerized waxes, fats and oils of vegetable origin (Wagner *et al*., 2018). The liptinite maceral group exhibits the following properties (Falcon, 1978; Stach *et al*., 1982; Falcon and Synman, 1986; Pickel *et al*., 2017):

I. In low rank coals liptinite possesses a higher hydrogen content than vitrinite.
II. The maceral group has a high volatile matter content down to the rank of mid bituminous coal.
III. The density of liptinite varies between 1.18 to 1.25 g/cm^3.
IV. The maceral is less aromatic than vitrinite, with an aliphatic-aromatic skeleton and aliphatic side chains.

V. Liptinite gives high yields of tar and gas during pyrolysis and carbonisation in the low bituminous range of rank.
VI. It oxidizes more rapidly than both inertinite and vitrinite.
VII. Owing to its high hydrogen content, liptinite is highly suitable material for hydrogenation and liquefaction.

The liptinite group is sub-divided according to specific plants (algae), parts of plants (spores and cuticles), or products of plants (waxes and resins). Table 2.7 presents the list of liptinite maceral group and their respective forms.

Table 2.7: Macerals in the liptinite maceral group (after Wagner *et al*. 2018).

MACERAL SUBGROUP	FORM
Sporinite	Outer membranes (exines) of macro- and megaspores; usually compressed at higher rank and aligned with sediments, well-preserved, variable shape and wall thickness, distinct botanical forms. Most common form of liptinite
Cutinite	From leaf and stem cuticles. Elongated, usually serrated, well-preserved, distinct botanical forms, parallel to stratification. May show serrations on one edge.
Exudatinite	A secondary maceral, infilling voids, cavities, empty cells; strong fluorescence. Derived from hydrogen rich sources (e.g. liptinite).
Resinite	Pod-shaped, globular or irregular bodies occurring as discrete forms; may fill cellular cavities or amorphous shapes in vitrinitic lenses; origin is cell excretions; can show red internal reflections. Where the reflectance is comparable to vitrinite, is referred to as corpogelinite, or secretinite where the reflectance is higher.
Alginite	Algal colonies, or solitary, of planktonic and benthic origin; rounded, elongated, semi-compressed, distinct, and well-preserved in botanical form. Rare in humic coals; sub-categories: telalginite being larger, more structurally distinct than lamalginite.
Suberinite	A rare form in lignites, from suberous tissues; well –defined cell structure; intense fluorescence. Not encountered in southern Africa due to rank.
Bituminite	An amorphous degradation product distinguished from vitrinite by lower reflectance and higher fluorescent intensity. Occurs as fine-granular groundmass, or laminae, streaks, wisps, bands, threads. Extremely rare.

The organic composition of coal defines the *coal type*. There are three major descriptive types of coal, defined by the preponderance of one of the maceral groups over the other two; thus, we have: fusic, vitric, and liptic. Fusic is associated with aerobic decomposition; vitric with anaerobic decomposition (because of rising water level); and liptic with deeper or open water accumulation of detrital material forming sapropelic coals. Falcon (1986) states that there are two major groups defined by their locality of formation: *humic* (land or very shallow water-based) and *sapropelic* coal (deeper water based). Falcon (1986) puts the division between sapropelic coal and carbonaceous or oil shale at 50% mineral matter. There has been a move towards internationalising the classification of in-seam hard coals as summarised in Figure 2.15 (Falcon, 2013).

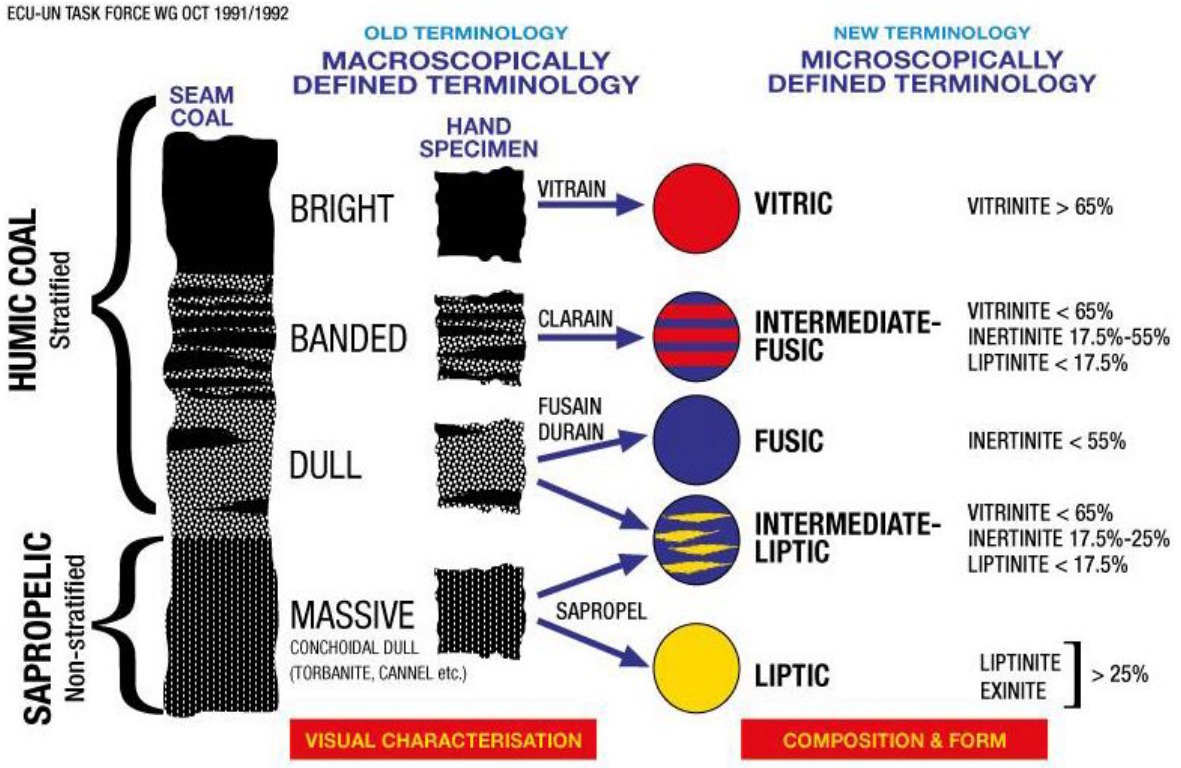


Figure 2.15: International classification of coal seam by type – hard coal (after Falcon, 2013).

2.4.4. Mineral Matter

Mineral matter in coal includes the total inorganic constituents, regardless of how it occurs or its origin (Gary *et al*., 1972; Given and Spackman, 1978). Standards Australia (1995, 2000) defines the mineral matter as representing the "sum of the minerals and inorganic matter in and associated with coal". Harvey and Ruch, (1986) and Finkelman (1994) provide similar

definitions. From these definitions one recognises that there are three fundamentally different types of inorganic coal constituents, which Ward (2002) categorises into the following:

I. Dissolved salts and other inorganic substances in the coal's pore water.
II. Inorganic elements incorporated within the organic compounds of the coal macerals; and
III. Discrete inorganic particles (crystalline or non-crystalline) which represent true mineral components.

According to Ward, (2002) the first two forms of mineral matter are perhaps best described as non-mineral inorganics. These constituents are usually prominent in the mineral matter of the lower rank coals (brown lignite and sub-bituminous materials (Kiss and King, 1977, 1979; Given and Spackman, 1978. These non-crystalline inorganic elements may be precipitated in the coal's pores from saturated groundwater or chemically bound in the organic matrix (Given and Spackman, 1978; Miller and Given, 1986; Matsuoka *et al*., 2002; Ward, 2002; Li *et al*., 2010). It is estimated that up to 50% of the ash-forming constituents in lower-rank coal could be represented by the non-mineral inorganic material. Expulsion of moisture, and any associated mineral in solution, and changes in the chemical structure of the organic matter usually combine to remove the non-mineral inorganics from the coal with increasing coal rank (Ward, 2002). Therefore, non-mineral inorganics are present in very small amounts, if at all, in the higher rank coals (bituminous and anthracites). On the other hand, discrete inorganic particles, or minerals, may be present in both lower- rank and higher- rank coals. In the absence of non-mineral organics, the group listed below constitutes the dominant, if not the sole component of the mineral matter in the higher-rank coal deposits (Ward, 2002).

2.4.4.1. Syngenetic minerals (primary mineral matter)

This constitutes primary mineral matter formed during crystallisation i.e., authigenic minerals, either within the peat deposits or shortly after its formation (primary or syngenetic precipitates), or in the cleats and fractures of the coal after its compaction and probably rank advance (secondary or epigenetic precipitates). These mineral forms are a very common component of coal seams (Ward, 2002). Minerals in the primary precipitates group include siderite nodules, feldspar, pyrite framboids and a range of cell and pore infillings (kaolinite, quartz, phosphate minerals and pyrite). Cleat infillings may include calcite, dolomite, ankerite and pyrite, marcasite, apatite, illite and chlorite (Raymond and Andrejeko, 1983; Ward, 2002).

2.4.4.2. Epigenetic minerals (secondary mineral matter)

These minerals were formed during rank advance (after peat formation). These minerals were precipitated from groundwater percolating through cracks and fissures and cleats in the coal seams after the coal had been almost compacted (Cobb, 1985). Another category of epigenetic minerals is the detrital group. This class of mineral matter in coal represents material washed or blown as detrital fragments into the accumulating peat deposit (Davis *et al*., 1984). This includes material from river water and flood loads, airborne dust etc., brought in by epiclastic processes, and volcanic debris deposited into the peat from pyroclastic activity (Ward, 2002). The epigenetic minerals are relatively easier to liberate by comminution than the syngenetic fraction (Bunt, 2006). However, epigenetic minerals can also fill cell lumens of the inertinite maceral, and these minerals are hard to liberate during coal beneficiation. Figure 2.16 is a summary of the sources and mode of introduction of mineral matter into the accumulating peat deposit.

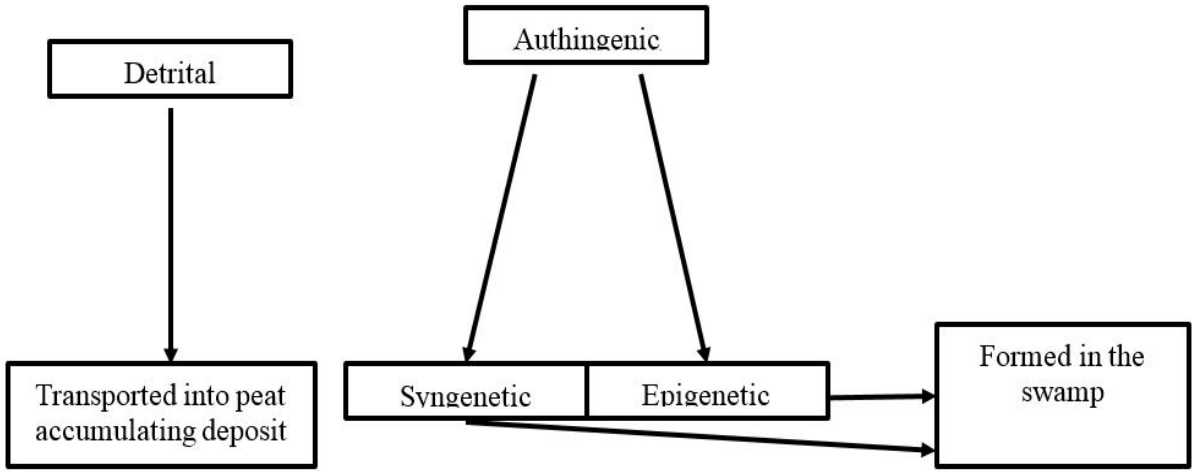


Figure 2.16: Mineral matter introduction into the peat swamp.

Among the minerals commonly found in coal are quartz, clays, carbonates, sulphides and apatite. Clay is the most abundant and widespread mineral in most coals and in Gondwana coals this often constitutes 80% or more of the minerals present (Falcon, 2013). Unlike the organic component, the inorganic fraction in coal characteristically contributes little to the value of the coal. At best it is a diluent, i.e., it displaces the otherwise more valuable organic matter with a non-combustible component which formed an ash after the coal has been combusted (Ward, 2002). Ash also absorbs heat, i.e., it is endothermic. In addition, mineral matter may be a source of unwanted abrasion, stickiness, corrosion or pollution associated with coal handling and use. Most of the problems associated with coal utilisation arise in some way from the incorporated mineral matter (Gupta *et al*., 1999b). Besides replacing the combustible

organic component of coal with non-combustible fraction, mineral matter has a host of other negative impacts among which are the following:

I. Quartz in coal increases the negative impact of dust in mining operations, particularly in underground mining environments (Schatzel, 2009; Erol *et al*., 2013; Schatzel and Stewart, 2012), and contributes to the generation of lung cancer via indoor combustion (Tian *et al*., 2008).
II. Mineral occurrence in coal is also associated with decreases in the coal's capacity for methane gas adsorption or with coal permeability (Gurba *et al*., 2003), thus potentially having a negative impact on the gas recovery of the coal seam methane resources (Pitman *et al*., 2003; Moore, 2012).
III. Arguably several trace elements may be intimately associated with the organic component (Finkelman *et al.*, 2002), but most of the trace elements in coal are associated with the mineral component (Gluskoter *et al.*, 1977; Kolker, 2012); and
IV. Oxidation of coal pyrite both in stockpiled as well as in mined areas, particularly shallow areas i.e., open pits, generates acid mine drainage (AMD) which has a number of negative implications on the environment such as pollution of streams whose waters affect aquatic life as well as humans and land animals that may depend on the streams for their water requirements. Oxidation of pyrite is an exothermic reaction has often led to spontaneous combustion in coal seams and on coal stockpiles as well as in coal product in transit to distant markets.

However, mineral matter can be credited for its action as a catalyst which influences the decomposition of a coal during various heating processes (Zhao, *et al*., 2003). It also influences the reactivity of the resulting coke or char. Furthermore, the resulting ash material from thermal power stations has now found use in brick and tile manufacturing industries (Zhao, *et al*., 2003). The amount of impurities or the composition of mineral matter in the coal defines the grade of the coal under consideration and the beneficiation potential of the coal. The latter is normally predicted by washability tests resulting in curves which are drawn from either drill-hole data or beneficiation plant results. Three washability products or divisions based on ash levels may be used to describe coal *in situ*, and these are (after Falcon, 1986):

I. Prime commercial washed products and Eskom coal - 0 – 30% ash.
II. Middlings with 30 - 80% ash; and
III. Discarded products including shale and sandstone with >80 % ash.

2.4.5 Microlithotypes

Organic and inorganic constituents often occur in various associations to form microscopic layers or bands which, when greater than 50 micrometres, are termed ***microlithotypes***. Microlithotypes are named according to the macerals contained in them (Falcon, 1978a; Stach, *et al* 1982; Falcon and Snyman, 1986; ISO, 1994; Taylor *et al* 1998; Falcon, 2013).

Table 2.8 presents the types of microlithotypes found in coal, and where a microlithotype is enriched, i.e., over 95% in a single maceral group, it is referred to as a monomaceral microlithotype; and where there is a mixed association of macerals with greater than 5% of two maceral groups, the microlithotypes is termed bimaceral. Where all three maceral groups occur, the association is termed a trimaceral microlithotype.

Properties of microlithotypes may be summarised as follows:

I. Their chemical properties are very similar to the maceral of which it dominantly consists; and
II. The attendant physical properties are a function of / or are linked to the macerals that constitute them as well as their combined effect.

Table 2.8: Microlithotypes in coal (Taylor, et al., 1998)

Microlithotype	Name	Maceral Association
Monomaceral	• Vitrite • Liptite • Inertite	Vitrinite greater than 95% Liptinite greater than 95% Inertite greater than 95%
Bimaceral	• Vitrinertite • Clarite • Durite	Greater than 95% Vitrinite + inertinite Greater than 95% Vitrinite + liptinite Greater than 95% Liptinite + inertinite
Trimaceral	• Duroclarite • Clarodurite • Vitrinertoliptite	Vitrinite greater than inertinite and liptinite All groups over 5%. Inertinite dominant All groups over 5%, liptinite dominant
Mineral-rich	• Carbominerite • Minerite	20 – 60% (vol) silicates and carbonates Or 5 – 20% (vol) sulphides Over 60% (vol) silicates and carbonates Or over 20% (vol) sulphides.

2.4.6 Coal Condition

Another attribute of coal that should be considered when determining its value and expected technological performance is the condition of that coal, i.e., its current state well after deposition. The conditions vary from macro-scale (discernible by naked eye) to micro-scale;

i.e. identifiable under a coal petrographic microscope (Falcon, 2013). A variety of such conditions are found arising from situations such as those described below:

I. **Surface Mining:** This often results in oxidation and weathering of shallow seams particularly by the open pit mining techniques where water and air easily ingress.
II. **Igneous Intrusions**: In these cases, hot magmatic materials are intruded into pre-existing coal seams as either sills or dykes heating up and even burning the coal *in situ***.**
III. **Groundwater Stored within the Seam:** This could be due to the presence of an aquifer or subterranean water bodies. This could result in pressure cracking and brittleness of the coal on handling, as well as excessive "apparent bed moisture" which is often difficult during the evaluation of the coal for market purposes (Falcon, 2013).
IV. **Earth Movement (folding and faulting):** The fracturing and bulking of strata may lead to abnormally brittle condition and excessive friability on handling a coal that has been subjected to these tectonic movements.
V. **Untended and Unprotected Stockpiled Coal:** A coal that has been stockpiled for a long time, particularly when untended and unprotected, is prone to self-heating, spontaneous combustion and possible burn-out of parts of that stockpile. This affects the quality of the stockpiled coal, which, in turn, would affect the performance of the coal during utilisation. Oxidation, particularly of vitrinite bands in a stockpiled coal, will also rapidly reduce its coking properties.

2.4.7 Coal Rank

Coal rank refers to the degree of maturation or metamorphism of coal as peat, the precursor of coal, and then subsequently transformed into a solid fossil fuel under the influence of temperature and pressure over time as described in Chapter One. The process of coalification commences with peatification which culminates in the breakdown of plant material into organic fragments within the original swamp. This process is *sensu stricto* not part of the maturing process or increase in rank (Stach, *et al*., 1982; Taylor *et al*., 1998; Falcon, 2013). The actual coalification process starts with the transformation of peat into brown coals i.e., lignite, sub-bituminous and bituminous coals and finally to anthracites and meta-anthracite.

With increasing temperature and pressure, the original organic matter loses water, volume and volatile matter, while increasing in carbon content, density and heat value. The American and European Carboniferous coals, which differ from the Gondwana coals, are rich in volatile matter and carbon, these two being the defining parameters for rank in those regions. On the

other hand, the mineral-rich and highly variable Gondwana coals require more parameters to determine its rank. This is because volatile matter varies with maceral composition in the same rank of coal. With the expansion of the international coal trading the need to come up with an internationally based method of identifying coal rank became inevitable. The idea was eventually initiated by the Coal Working Party of the United Nations Economic Commission for Europe (UNECE) during the 1970s. Results of subsequent investigations proved that increasing rank changed linearly in parallel with the proportion of light emanating from the surface of vitrinite particles (Falcon, 2013).

Petrographic studies reveal that in the lignitic and sub-bituminous levels of rank, vitrinite reflects medium to dark grey in relation to normal white light. As rank increases, vitrinite passes through various levels of grey, increasingly turning lighter and whiter as coalification proceeds, until meta-anthracite and graphite become bright white. These phenomena have been described by several researchers including (Snyman *et al*., 1983; Stach *et al*., 1982). It was upon this systematic regular change that drawing up of vitrinite reflectance values (as defined by ISO 11760, 2005) was based and vitrinite reflectance was adopted as the official international method for determining the rank of coal in the bituminous and anthracite range (Falcon, 2013).

2.4.8. Analytical Techniques

Coal analytical techniques may be classified into two categories: those that determine the empirical properties of coal and those that focus on the fundamental composition of coal. The techniques vary in the degree of sophistication. While some of the tests which are carried out are simple, others require manipulation, a high degree of sophisticated equipment and involve complex interpretations (Karr, 1978; Falcon and Ham, 1988; Johns and Harris, 2009) Empirical properties are determined using chemical and physical analytical methods, and the most common conventional methods are summarised in Table 2.9. These analytical methods are discussed in more detail in Chapter 3, while the determination of fundamental composition of coal is carried out using a coal petrological microscope.

For reliable results, it is imperative that both sampling and analytical techniques are performed as adequately and precisely as possible and in accordance with international standards. Proximate and ultimate analyses as well as those falling under calorific value and swelling index (Table 2.9) are crucial in characterising coal prior to its utilisation. These analyses involve the use of common and more sophisticated laboratory methods such as X-Ray,

Spectroscopy and Atomic Absorption. Ash composition analysis gives the chemical composition of (elements or oxides); while XRD give the proportion of mineral phases such as pyrite, quartz, carbonates, and clays and this gives the end-user some idea on the coal's propensity to form clinkers when combusted. In addition, the type, form and distribution of minerals in coal are critical: they may be trapped in the organic matter and could serve as contaminants, or inhibitors, in the devolatilisation and swelling processes.

Table 2.9: Most common conventional analyses (Falcon and Ham, 1988; Johns and Harris, 2009).

Proximate (%)	**Ultimate (%)**	**Ash Composition (%) major minerals**	**Others**
Moisture	Total Carbon (C)	Quartz (SiO_2)	Calorific Value (MJ/kg)
Ash Content	Hydrogen (H)	Pyrite (FeS_2)	Swelling Index (SI)
Volatile Matter	Oxygen (O)	Calcite ($CaCO_3$)	Hard Grove Index (HI)
Fixed Carbon	Nitrogen (N)	Dolomite CaMg $(CO_3)_2$	Ash Fusion Temp. (AFT,^{0}C)
	Total Sulphur (S)	Kaolinite $Al_2(S1_2O5)(OH)_4$ etc	Roga Index,
	Phosphorus (P)	Apatite	Dilatation

While empirical methods allow one to have a quick assessment of qualities of coal at hand, the information they offer on the actual performance of coal in some areas is limited. In other words, the conventional methods often need to be complemented by other analyses to accurately predict critical aspects of combustion such as flame stability, combustion rate, temperature distribution in the furnace, burn-out attributes, blending compatibility, and condition of coal (Van der Riet *et al*., 2010).

Among some of the economically important properties of coal are the coking attributes which are unique to bituminous ranked coals. Coking coals are coals which, when heated to sufficiently high temperatures soften, swell, and solidify into a grey, spongy solid mass called coke (Zimmerman, 1979). The caking power of a given coal is defined by the mechanical strength of the crucible coke obtained by carbonation under standard conditions of a mixture of 1 g of a sample of the coal and 5 g of standard anthracite. Special tests have been designed to carry out an evaluation and testing of the coking attributes of coals. These include plasticity tests (free swelling index, Gieseler fluidity and Audibert-Arnu dilatometer), Gray King coking index and Roga index (Zimmerman, 1979).

Additional analyses that involve the more fundamental constitution of coals are required to provide a full understanding of the behaviour of different coals (Falcon, 1989). Among such

analyses is coal petrography, which provides information on the type, grade and rank of the coal. Regrettably, coal petrography, maceral composition and vitrinite reflectance are not carried out as routine analyses mostly due to the costs involved and the coal producing mines do not always have the requisite equipment on site.

Another advanced analytical technique is thermogravimetric analysis (TGA) which is used to characterise materials in controlled environments (Brown, 2004; Soni, 2017). In the technique, the mass of a substance is monitored with respect to temperature or time as the sample is subjected to controlled temperature in a controlled atmosphere. Le Manquais *et al*., 2009, describe thermogravimetric analyses (TGA) and the drop tube furnace (DTF) as techniques for further laboratory scale testing of combustion performance to establish the rate of devolatilisation and reactivity of coal. The use of TGA, whereby a sample of coal is heated at a constant rate to 700 – 900^0C in a thermogravimetric analyzer to produce TGA and DTG curves for characterising coals, is increasing in prominence for use as a technique to provide information on the reactivity of individual coal samples and their blends under controlled conditions (Norton, 1993).

The curves so produced provide detailed information about a fuel from the onset of oxidation to complete burnout (Rostam-Abadi, *et al*., 1990). The technique has been described as particularly useful for evaluating unusual fuels in which the sample quantities are insufficient for full-scale burning tests (Waggoner and Winegartner, 1973). As coals with similar burning profiles are expected to behave similarly during full scale plant combustion, burning profiles can be used to predict combustion behaviour of coal in large boilers (Norton, 1993). Figure 2.17 represents typical examples of TGA and DTG curves obtained for Illinois No.6 coal (Norton, 1993), while Figure 2.18 shows the features of the burning profiles from the time a coal sample is ignited till it burns out completely. Investigations into the thermogravimetric analysis of different coal ranks, types, degree of oxidation and particle size contribute significantly to the activation energies needed to give rise to combustion.

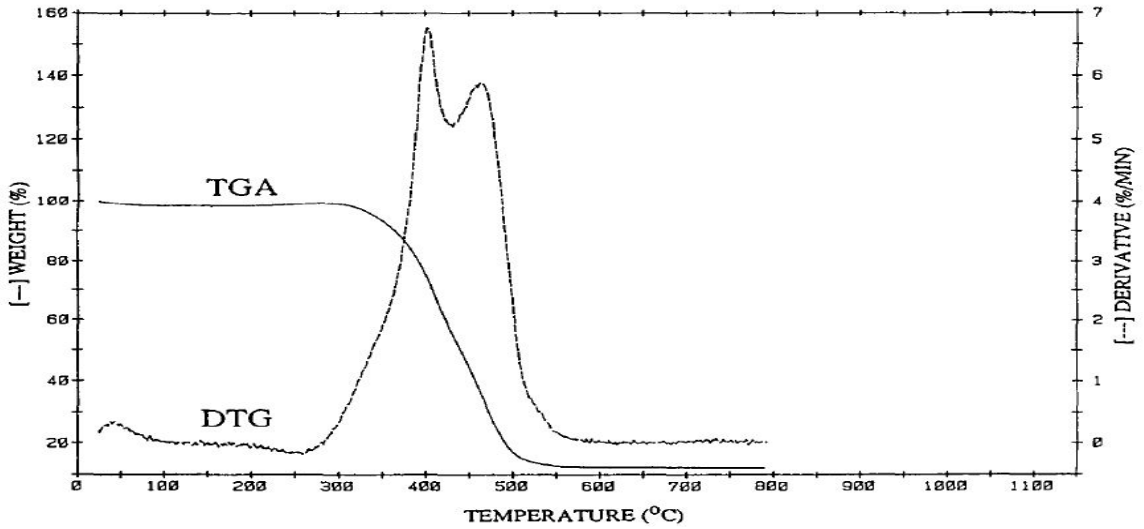


Figure 2.17: A Typical TGA and DTG (burning profile) curves (from Norton, 1993).

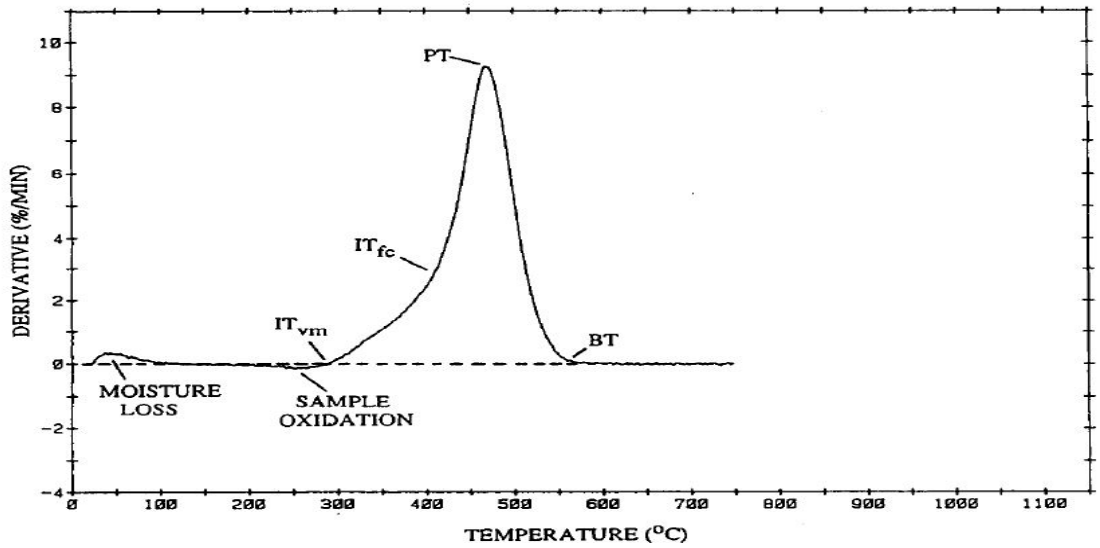


Figure 2.18: Simple burning profile (DTG) showing moisture loss, initiation temperature for volatile matter (IT_{vm}) and fixed carbon (IT_{fc}), peak temperature (PT) and burnout temperature (BT) (from Norton, 1993).

According to Norton, (1993) the results obtained from the thermogravimetric analysis of coal reveal that the following factors/material properties influence the temperature at which ignition, devolatilisation peak and burnout of samples take place:

i. Coal rank
ii. Increase in inertinite content.
iii. Particle size distribution and
iv. Presence of oxidised particles (including oxidised vitrinite).

2.5. Coal Beneficiation

2.5.1. Reasons for Coal Beneficiation

Coal as mined from the working face of the coal seam is a heterogeneous mixture of numerous types of altered plant materials originally laid in swamplands several hundred million years ago. Frequently, in its pristine state, coal as a commodity, has low value and is relatively less energy efficient during utilisation due mainly to: i) impurities or contaminants (i.e., inorganic material, and rock); and ii) the surface area/volume ratio effect (for example, the removal of volatile matter from the coal mass in the absence of oxygen produces coke, which is a higher value product (Horsfall, 1978). The process, or combination of processes, applied to remove the contaminants from the lower grade coal in order to achieve a product quality which meets the requirements of the end user, either as an energy source or as a chemical agent or feedstock, is called beneficiation. It is a compromise between the requirements, on the one hand, of the end user who requires a premium quality product and, on the other hand, a producer who makes much effort to ensure he sells as much of the mined product as possible (Horsfall, 1978).

In today's business environment, operational systems and user plant equipment are required to operate at maximum standards and efficiencies. In the coal value chain, there is an increase in the demand for consistent qualities of coal, for example, to provide high energy in terms of heat content, appropriate sulphur content and ash fusion temperatures is required for such end application. To this end, coal processing plants must rely on beneficiation to provide power utilities consistent coal quality. While initially it would appear that coal beneficiation increases the cost of the coal, depending on the geological and mining conditions among other factors, coal preparation provides the appropriate coal quality on a constant basis, which dramatically increases the efficiency of boilers (Beafore, 1983).

2.5.2 Broad Steps in Coal Beneficiation

While the term coal beneficiation is often restricted to the crushing, sizing, handling and washing of the run-of-mine coal, this thesis takes the views of several researchers and resource persons' presentations. Gauthier and Pelletier, (2015) argue coal beneficiation starts earlier in the whole coal exploitation process. They view it to start from exploration, through mining to thermal upgrade of the coal and in some cases to coke, i.e., carbonisation. The rationale is that the mineral value chain represents the stages and processes that a mineral project goes through to produce a mineral product, i.e. a build up to cash. Each stage represents a value-add on the previous one reducing uncertainties. This, therefore, provides opportunities for investor(s) to

make an informed decision to invest at any of the major stages. Figure 2.19 illustrates the broad steps in the beneficiation of coal and the subsequent paragraphs describe these stages.

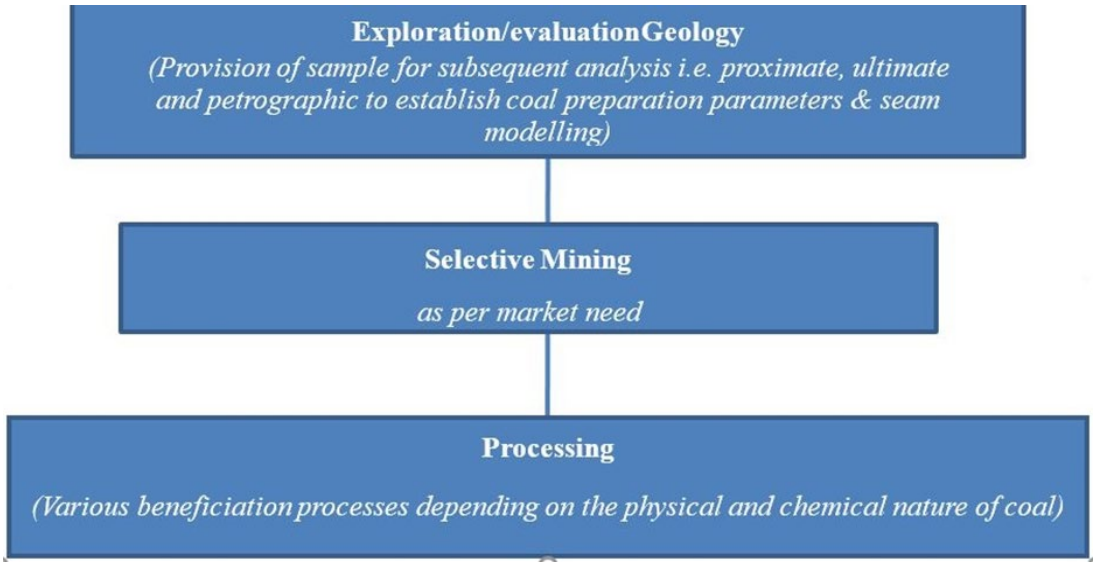


Figure 2.19: Broad steps in the beneficiation of coal.

The goal of coal exploration is two-pronged: i) to model the seam according to quality parameters as per market demands; and ii) to compute a coal resource/reserve. A typical example of this operation is given in Figure 2.20 where, on the basis of ash and volatile matter contents, the 30 m thick geological seam at Hwange Coal Basin is modelled into a basal good quality coking coal, an overlying thermal coal, and a supernatant high ash material or carbonaceous mudstone which is currently discarded as part of the overburden material. At the open cast mine, two qualities of commercial types of coals are mined separately (selective mining) and handled separately (Figure 2.19), with the underground mine having the coal with the good coking quality only. The thermal coal is fed to the Hwange thermal Power Plant for electricity generation, while the good quality coal is fed to the coke making batteries situated on the coalfield for carbonisation.

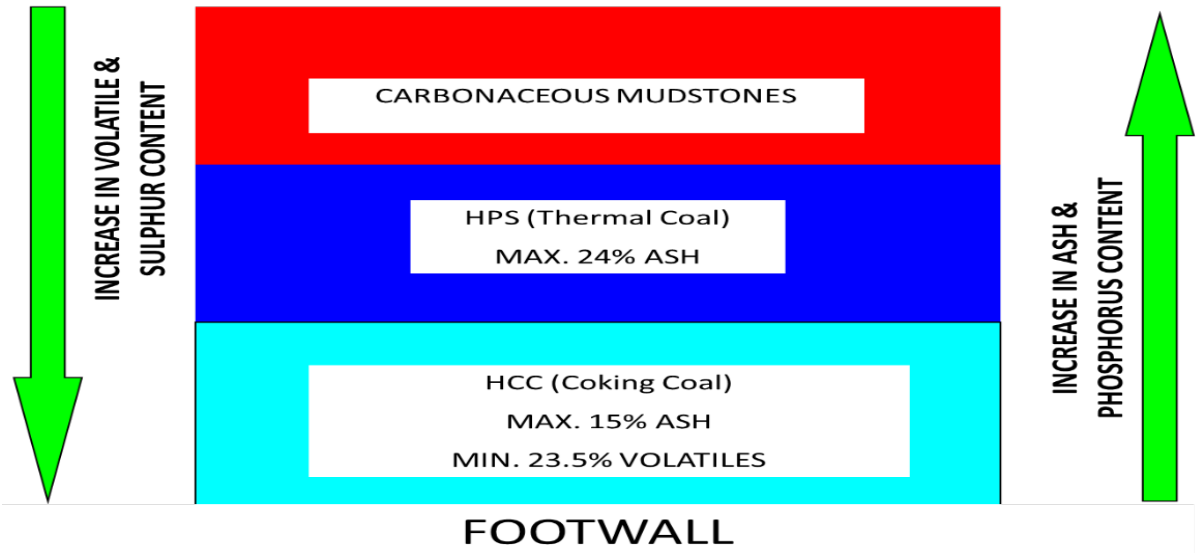


Figure 2.20: Geological modelling (as per major customers) of a seam during coal exploration.

2.5.3. Coal Beneficiation Methods (past and present)

A review of the available literature, and site visits to view industry best practice, reveals that a variety of techniques (ranging from simple and manual to the sophisticated chemical and mechanical utilities) are in use in coal beneficiation. These may be grouped into those techniques involving gravity separation of particles by physical means (gravity concentration), i.e. heavy medium separation (HMS), float and sink (density fractionation), and jigging, and those that separate particles of different attributes by chemical means (flotation).

2.5.3.1. Heavy Medium Separation and Float and Sink (Washability)

In coal beneficiation, the heavy medium separation, also known as dense medium separation (HMS) is employed as a coal beneficiation technique to produce a graded coal product which is separated from high carbonaceous materials such as shales and other in-organic components associated with the coal. It is probably the simplest of all gravity processes and has a long history of application in the separation of minerals of different specific densities (Amini, 2014). A typical heavy medium separation technique comprises the following:

i. The Norwalt bath vessel which uses gravity in a vessel containing a large enough volume of medium (usually water and magnetite); and
ii. A Hydrocyclone unit which uses the centrifugal force to separate particles of different densities from each other. Material lighter than the medium migrates to the inner spiral towards the vortex and leaves the cyclone at the overflow (i.e., negative driving force), while the heavier material moves to the wall and is entrained in the medium to the outlet.

Figure 2.21 illustrates a typical heavy media separation unit. The separator uses a mixture of fine magnetite and water as the require media for coal separation. This will allow density material to rise to the top and float, while the high-density material sinks (Kuback, 2012). The specific gravity of separation in the medium slurry, in the case of coal, can range from specific gravity of 1.35 to 2.00. The different coal components (organic and inorganic) have different densities, with vitrinitic and liptinitic material reporting to densities lower than 1.4 and inertinite greater than 1.4.

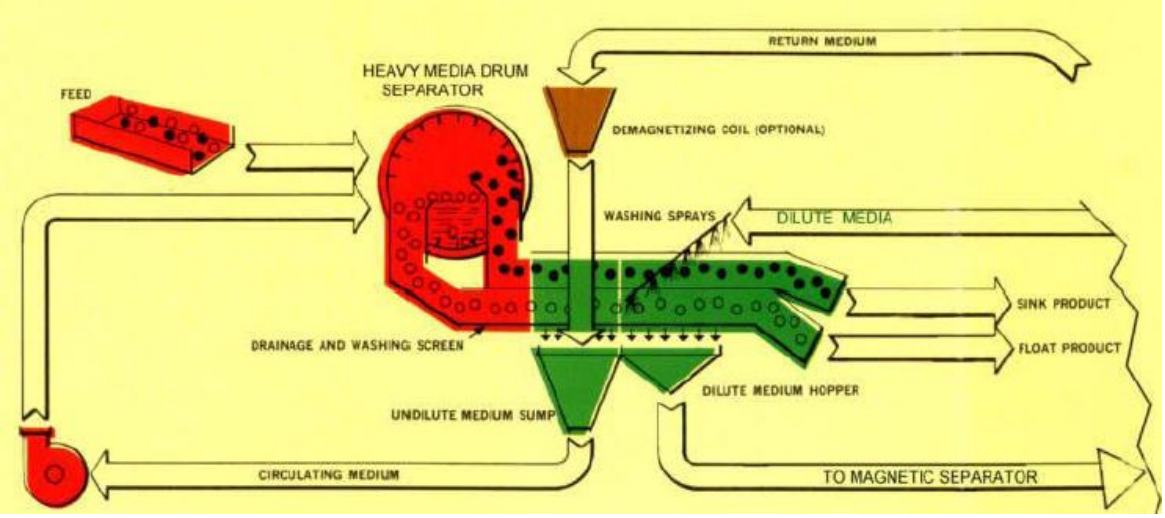


Figure 2.21: Heavy medium separation plant configuration (from Kubach, 2012).

Alternative to heavy medium separation is the heavy liquid separation (HLS) process. In HLS, particles of different specific gravities are separated into several relative density fractions using suitable heavy liquids such as solutions of inorganic salts like calcium chloride and zinc chloride. The steps involved in the float and sink process is depicted in Figure 2.22. Some explanatory notes are included to assist in the understanding of the product and waste output derivation.

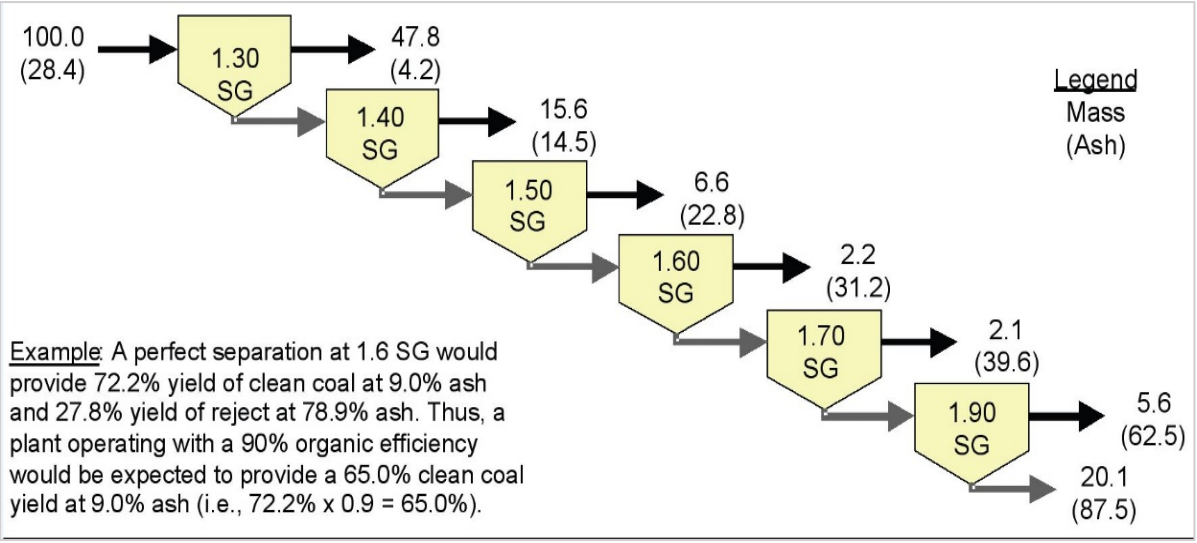


Figure 2.22: Diagram to illustrate the Float and Sink Process (from the US National Commission on Energy Policy, 2008).

The float and sink process can be described as a trade-off between coal recovery and quality. It involves placing flasks containing liquids (usually organic) of increasingly higher densities (ASTM, 1994) in a sequential arrangement. In the figure above, pure coal with density up to, but less than 1.30, is collected as the float product from the first flask; while pure rock with a high-density report as the sink product in the flask with density 1.9. According to Figure 2.22, ash value of 9.0 % at 1.60 SG is calculated by adding weighted averages proportionately from 1.30 SG.

The outcome of the exercise above is to determine the washability attributes of a coal sample and to determine the efficiency with which the coal could be washed. With the data obtained from the float and sink testing and associated ash determinations, a wash curve is generated. The curve so generated can be used to predict the yield of coal achieved at a given separation density (Stach *et al*., 1982; Osborne, 1988; Horsfall, 1993). However, application of this technique is fraught with a few challenges that include the following:

I. Some liquids are deemed toxic.
II. Organic liquids are expensive.
III. The liquids are often absorbed by particle surfaces and may contaminate the mineral particles.
IV. Loss of liquids is high due to volatility.
V. The liquids may not be recovered economically; and
VI. It is not always possible to get hold of the required heavy liquids.

2.5.3.2. Jigging

This process involves the separation of particles of different specific gravities, size and shape by introducing them on a perforated surface (or screen) through which water is made to flow by pulsion and suction strokes alternatively. The resulting oscillating motion separates the bed into layers of different densities: the heaviest concentrate forms the lowermost layer; while lightest product forms the highest layer (de Korte, 2010; 2015). However, this jigging process does not produce a thorough classification of the feed as the process cannot separate particles that are less than 1 mm.

2.5.3.3. Froth Flotation

The technique is applied when the intended mineral is water repellent, i.e., hydrophobic. To achieve favourable conditions for froth floatation, the pulp is treated with various chemical reagents known as flotation reagents, which are grouped into:

I. Collectors – which can either be an acid, base or salt and hetero-polar in nature.
II. Frothers – which are chemical reagents that are hetero-polar in nature.
III. Frother-collectors – which possess both frothing and collecting properties, i.e., fatty acids, sulphates and amines; and
IV. Depressants – inorganic chemicals that react chemically with the mineral particle surfaces to produce insoluble protective coatings of a wettable nature thereby making them non-floatable even in the presence of a proper collector.

On a world-wide basis, much success in using run of mine high ash coals has been attributed to these technologies of coal beneficiation (de Korte, 2010; 2015). Furthermore, the technologies are contributing immensely to the substantial reduction in sulphur, thus aiding in sulphur dioxide emission reduction from coal- burning thermal power stations. Froth floation has been found to be very effective for coal cleaning as coal is naturally hydrophobic. The collector disperses into droplets in the pulp and these droplets collide with and adhere to, and coat the coal particles, thus increasing their hydrophobicity (Polat *et al*., 2003). Because of the coal's hydrophobicity, froth flotation has employed mostly non-polar oil collectors such as kerosene, crude petroleum, fuel oil and certain coal-tar distillates (Wójcik *et al*., 1990; Solov'eva and Muklakova, 1995; Petukhov, 1995).

2.5.4 Beneficiation of Coal for Making Coke

2.5.4.1. Coal Beneficiation in Zimbabwe

In Zimbabwe, a country that depends heavily on coal for its energy needs, Hwange Colliery Company has mined the Hwange Main Seam for *circa* 113 years and over most of this period has supplied and met the nation's requirements for power generation. The company has managed to also meet the demands of a variety of markets each requiring different physical or chemical characteristics in their products. The technology employed by the Hwange Colliery Company for coking making generally follows worldwide trends. It commenced with the establishment of the first coal washing in 1928, introducing the Jig plant. Subsequently the company introduced a heavy medium separation plant in 1948 to produce clean coal with ash values of less than 10% (from a run-of-mine feedstock of 15% ash) for the beehive coke ovens which had been constructed in 1926 at the then-known No.1 Colliery. Then the sole coal and coke producer in the country, Hwange Colliery took another technological advancement step and introduced the Copper recuperative ovens in 1930 (Maponga, 2019). This was followed by the introduction of the more modern Otto Simon Curve, twin-flue, underjet-type ovens in 1971, which has subsequently been rebuilt and extended. For Zimbabwe, this probably marked the earliest definitive advance which had a profound effect on the country's economy. The beneficiation plants have since undergone subsequent improvements and now produce a variety of products, from upgraded steam coal to coking coal. Coke is made for the foundry and metallurgical industries both within Zimbabwe and the sub-region.

Technological developments in coal beneficiation have made a major positive impact on Zimbabwe's economy. The coke making process also produces valuable by-products such as tar, ammonia, benzol and spirits. Figure 2.23 is a simplified coke making flow chart from Hwange Colliery.

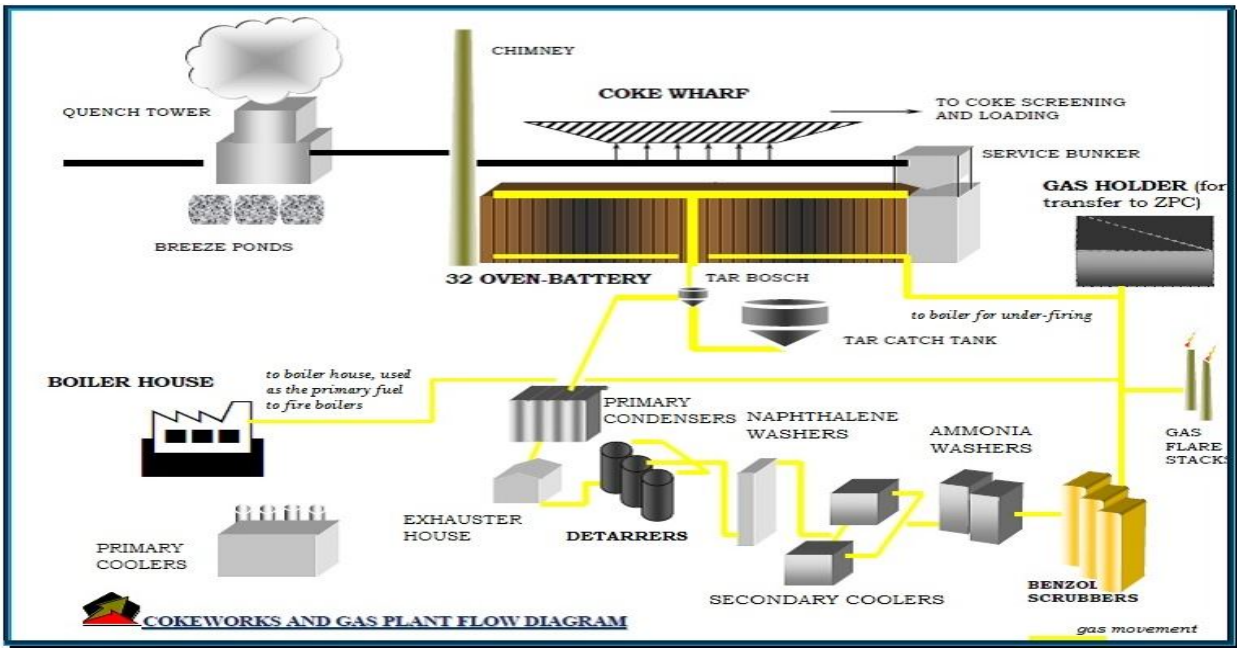


Figure 2.23: Diagrammatic presentation of the Hwange Colliery Coke works and gas plant operation. (Hwange Colliery Centenary Brochure, 1995).

2.6. Coal Utilisation

As indicated in Section 2.2, coal has been known for thousands of years, with China reported to have used this solid fossil fuel for over 3 000 years (Miller, 2011). Coal's use began with simple and basic applications in areas such as domestic heating and subsequently for transport, i.e. to fuel steam engines. Today the combustion of coal or its conversion into solid, liquid and gaseous products has advanced tremendously as new technologies have been developed. This section looks at the properties and factors that influence the utilisation of this fossil fuel before discussing the current uses of this heterogeneous commodity focussing on the two major uses which are power generation and carbonisation.

2.6.1. Properties/Factors affecting Coal Utilisation

The nature or type of utilisation of coal is influenced by several factors which can conveniently be categorised into intrinsic and external properties. It is essential that both categories are adequately analysed, understood, and appropriately adjusted before and during any field of use (Kural, 1994).

2.6.1.1. Intrinsic factors

Intrinsic factors are basically the inherent aspects of coal, its characteristics and nature (Falcon and Ham, 1988). The intrinsic factors or properties of coal that influence its combustion are further categorised below, with the summary of the properties of coal that is responsible for its metallurgical application presented in Table 2.10.

Table 2.10: Effects of selected coal properties on combustion (Falcon and Ham, 1988).

Property/Parameter	Effect
Moisture Content	Reduces calorific value and poses handling challenges.
Volatile Matter	High volatile matter coals ignite easily and are highly reactive.
Ash Content	Reduces heat value; mineral matter consumes heat; and minerals clinker at high temperatures.
Fixed Carbon	Higher values call for longer combustion times
Ultimate Analysis	Oxygen consumes; while nitrogen, sulphur, hydrogen and carbon release heat.
Macerals	Vitrinite and liptinite (rich in volatiles) are very reactive (cake); while inertinite is non-reactive (poor ignition, non-swelling, slow rate of degasification and restrictive combustion). Liptinite oxidizes more rapidly than inertinite.
Coal Rank	Temperature at which coal ignites increases with rank of coal.
Grindability (HGI)	Is a measure of resistance to crushing, affects crushing ability of the mills.
Porosity	Affects rate of reaction in a conversion process as internal surface area outstrips external surface area of coal particle.
Density	Bulk density depends on the particle size distribution of a coal and is critical to design of storage bins and silos.

i) Coal rank, i.e., its degree of maturity,
ii) Its composition (nature and relative proportions of organic and inorganic constituents).
iii) Proximate analysis (moisture, ash, volatile matter, and fixed carbon contents).
iv) Ultimate analysis (carbon, hydrogen, nitrogen, oxygen, total sulphur and phosphorus)
v) Calorific value; and
vi) Physical properties (particle size, Hardgrove index, Abrasive index, ash fusion temperatures, degree of weathering and state of oxidation, among others).

Several investigations have been carried out on the effects or influences of the above factors or properties on coal combustion in the boiler. These include Lee *et al*. (2009); Wang *et al*. (2011) among others.

Table 2.11: Effects of some coal properties on metallurgical processes (Zimmerman, 1979)

Property/Elements	Effect on Coal utilisation
Proximate Analysis	
• Moisture	Since it is inert, it requires heat to evaporate and lowers bulk density of coke oven charge; the lower the moisture the better. On the other hand, dry coal presents dust challenges in handling. The maximum range of 6-8% surface moisture is preferred.

• Ash	Ash levels determine effective carbon available. An increase in ash increases the coke rate and lag volume in blast furnace. A 1% increase in coke ash reduces blast furnace productivity from 2 to 3 %
• Volatile matter	Volatile matter contents affect effective carbon available, hence in the blast furnace volatile matter removed; a low volatile coal will yield a higher percentage of coke and more carbon per tonne of coal. Coals with volatile matter content of less than 14% (dry-ash will not coke; and coals with extremely high volatile matter will either make poor quality coke and will be low in fixed carbon content. 38% volatile matter may be considered the upper limit.
Ultimate Analysis	
• Sulphur	Sulphur will enter the steel crystal lattice and weaken the steel.
• Carbon	Carbon is what the coke game is about. It does the work of reducing iron ore to metal.
• Phosphorus	Has a deleterious effect in iron. The phosphorus in the blast furnace burden is reduced and enters the hot metal product. The lower the phosphorus value in coal (0.015%) the better.
Ash Fusion Analysis	It determines the melting points of coke ash in the blast furnace as it can slow down or enhance the slag formation.
Mineral Analysis	
• Determined in form of oxides	Some oxides are deleterious while others may assist in fluxing of the ore. Alkalis decrease burden permeability, lower productivity and cause high coke rates.

In summary, with proper beneficiation technique, the intrinsic properties of coal can be controlled, with the inherent mineral contaminants which contains the alkalis be reduced before being used for coke making.

2.6.1.2 External factors

External factors refer to those conditions that influence combustion. These include particle size distribution, loading levels, temperature and velocity of the combustion air, ratio of mixing fuel and air, and the design and spacing of burners (Van der Riet *et al*., 2010). Kitto and Stultz (2005) state that these factors are especially critical in the utilisation of some high ash fuel. Coal as ordered usually leaves the mine with particle top size of 5 cm or larger (against a lower top size required for an energy-related application (e.g., fuel slurry and power generation) who may require smaller top size than that leaving the mine. To comply with the customer feed coal specification, in terms of feed coal particle size, the coal top size might need to be reduced. Particle size does influence the residence time require for the coal to burn out completely in the boiler.

In terms of the fuel ratio require for combustion, a proper fuel mix, is necessary to generate combustion air, which is normally forced into the furnace. Generally, the combustion efficiency decreases with any increase in air velocity. Secondly, in order to ensure complete combustion, combustion chambers are fired with excess air, which leads to increased probability of oxygen

getting into contact with which it reacts. Addition of excess air also increases turbulence which in turn increases mixing of air and fuel in the chamber. This will also improve combustion efficiency by giving these components a better chance to react.

2.6.2 Coal use for Power Generation

The solid fossil fuel plays a vital role in the economic development of countries of southern Africa, particularly South Africa and Zimbabwe. Its use by far is to produce electricity, where it provides heat in the boilers for steam generation in the production of power. The standard cut-off values for critical quality parameters, e.g., ash content, volatile matter and sulphur, for coal feedstock to these thermal plants vary from country to country and for different boiler designs. Table 2.12 shows the typical characteristics of the coal feedstock to the power plants in South Africa and Zimbabwe.

Table 2.12: Comparative Thermal Coal Characteristics in South Africa and Zimbabwe. (Hwange Colliery Marketing Department, 2015).

Parameter	South Africa	Zimbabwe
Ash content	35-45%	26% maximum
Calorific Value	20 – 24 MJ/kg	25MJ/kg

From the current literature survey, several combustion systems were found to be currently in use, while new and more advanced systems have been introduced recently in selected power generation utilities. The most common coal-fired systems in use in the world are fixed bed combustion, circulating fluidized bed combustion, pulverised fuel and chain grate stoker boilers. These technologies are not discussed in detail since the focus of this study is to establish a correlation between the geological environment of the deposition of the Hwange coals and their selected characteristics/ coking coal quality.

2.6.3 Coal Carbonisation

Carbonisation is the thermal upgrading of coal into a high carbon material called coke using metallurgical grade coal. The process involves heating of coal in the absence of oxygen, i.e., out of contact with air (Stach *et al*., 1982). In the carbonisation process, all the volatile products are practically driven off as gases or liquids, leaving behind a solid residue consisting principally of carbon with minor amounts of hydrogen, nitrogen, and oxygen (which together constitute the fixed-carbon content of the coal (Miller, 2011). Carbonisation can be carried out at varying temperatures (low, medium, and high), and products vary accordingly, for example:

i. Low temperature carbonisation (i.e., 450 – 750^{o}C) produces lower quantities of gaseous material, while the liquid products are high. It is used to produce liquid fuels.
ii. In high temperature carbonisation (from 900^{o}C upwards), the yield of gaseous products is higher than liquid products, with low production of tar.

The carbonisation of coal involved the heating up of the coal, which then softens, becomes plastic, and swells before it solidifies into a porous grey mass, i.e., coke (Stach *et al.,* 1982; Zimmerman, 1979). Coals that exhibit such behaviour are referred to as caking coals. Strongly caking coals that produce a hard-porous mass (i.e., coke) are called coking coals and are derived from the mid bituminous range of rank provide this range. The softening, attainment of plasticity and swelling is a measure of reactivity of the constituents of the coking coal and this is a property of group of organic components of coal referred to as the reactive macerals, namely, vitrinite and liptinite and to some extent certain semi-reactive semi-fusinites (Stach *et al*., 1982; Zimmerman, 1979). Impurities such as mineral matter not only negatively affect the reactivity of the organic matter, but also reduce the carbon levels in the resultant coke. Therefore, coal destined for carbonisation must be low in inorganic mineral content and high in reactive macerals.

The normal prime coking coals generally have the following attributes:

i) Volatile matter of 20 – 32 % (low- to medium-volatiles, bituminous in rank);
ii) Ash content of less than 10%.
iii) Reactive macerals (vitrinite, liptinite) greater than 45%; and
iv) Swelling Index of at least 3, although some countries such as India prefer Swelling Indices of a minimum of 5 (author's personal communication with ESSAR of India, 2013). ESSAR is an acronym of an Indian company formed by Sashi and Ravi Rui, brothers from India. At the other end, coals with high swelling capacities of greater than 8 cannot be used to produce coke as the resultant coke is usually too weak to support the loads imposed on them within the furnace. They, however, are blended to produce the desired coke (Sahoo *et al.*, 2018).

N.B. Chemical composition alone cannot be used to predict whether a coal is suitable for coking but must be accompanied by petrographic as well as plasticity tests.

As mentioned above several crucial tests have been designed to determine whether a coal will yield coke or not. A selected number of these have been carried out during this study and are described below.

The first of these is free-swelling index (FSI), also known as crucible swelling index (CSI). The plant produces a coal with ash values of less than 10% from a run-of-mine feedstock of 15% free swelling index. It is a measure of increase in volume of a coal sample when the sample is heated with the exclusion of air. It is a qualitative test to evaluate the caking capacity of a coal. The analysis involves heating a small sample of coal in a standardised crucible to approximately 800^0C for a specified period until all the volatiles are liberated from the sample (ASTM D720-2010). At this stage, a small coke button remains in the crucible. The free swelling index is determined by comparing the cross-sectional profile of the remaining coke button to a series of standardised profiles. Swelling index ranges in value from 0 to 9 (Falcon, 1986; Sahoo *et al*., 2018). Figure 2.31 represents the standard profiles of buttons and the corresponding free swelling numbers (from ASTM D-720-2010).

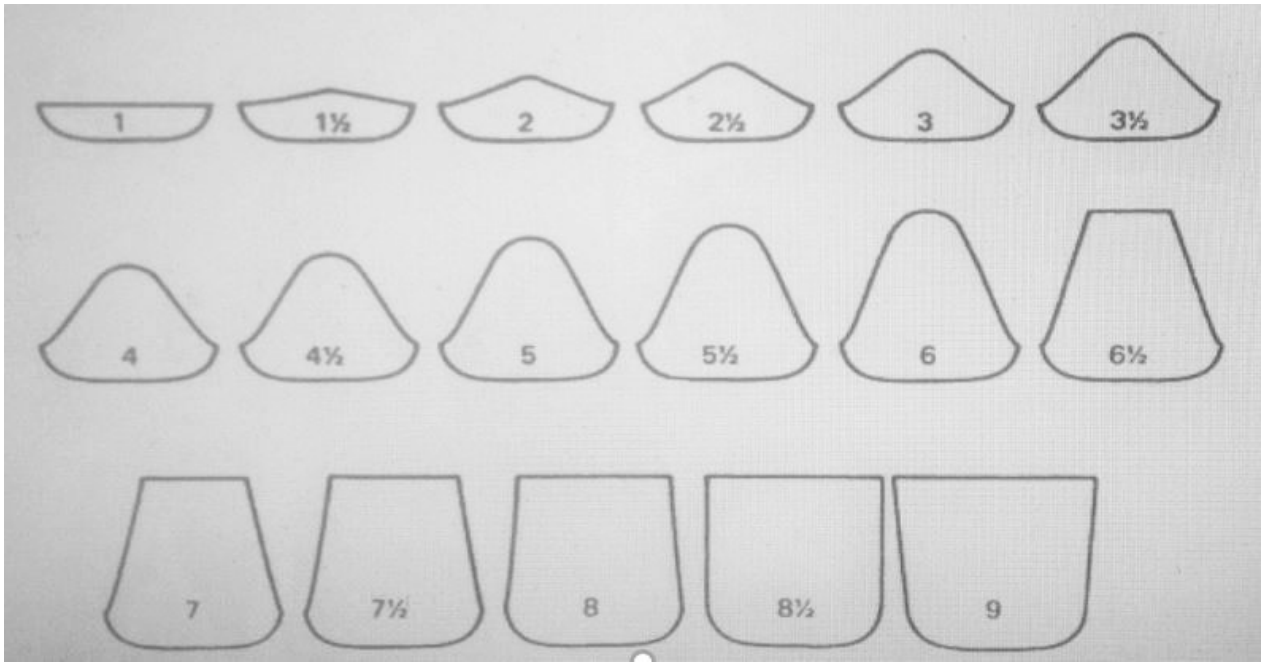


Figure 2.24: Standard profiles of coke buttons and the corresponding Free Swelling Index Number (from ASTM D-720-2010).

The caking behaviour of a coal is critical to the manufacture of coke, a key ingredient for the steel making process. Normally, coals with a low free swelling index of 0-2 are not suitable for coke manufacture and an FSI of 3.5 is considered as the lower limit for coking coal potential (Zimmerman, 1979). At the other extreme coals with high swelling of greater than 8 cannot be used by themselves to produce coke as their resultant coke is usually too weak to support the loads imposed on them within the furnace. These, however, are blended to produce the desired coke (Sahoo*, et al.,* 2018).

The second test carried out to determine cokeability of coal is dilatation. The test is carried out to determine the swelling of a coal when heated under standard conditions. There are several methods used to determine the dilatation of coals, but the principles are the same, there are, however, some variations in equipment and procedures. These include the Audibet-Arnu test which is the standard ISO test and is commonly used; the Ruhr dilatometer test, which is German Standard DIN-51-739; and the British Standards Institution.

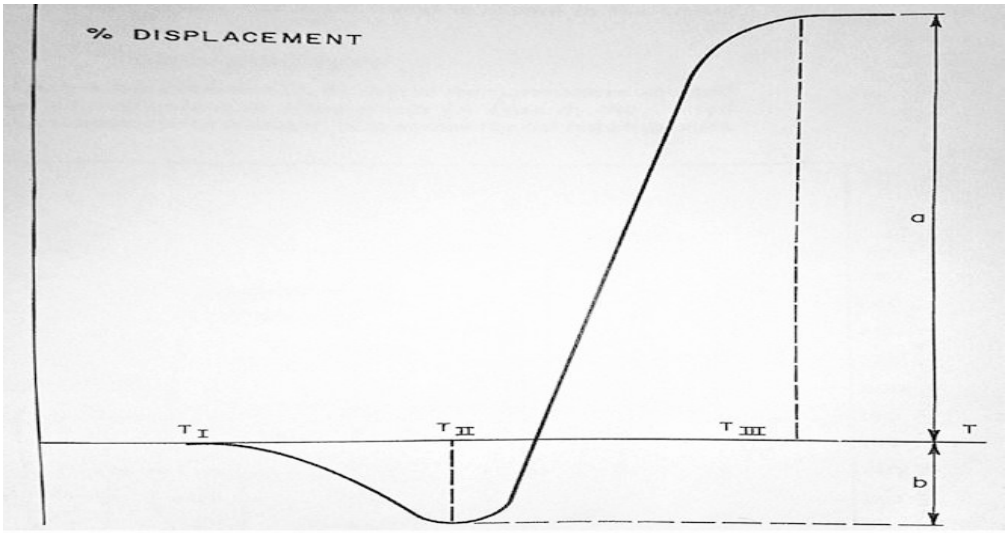


Figure 2.25: Audibert-Arnu dilatometer curve [ISO Standard 349-1975(E)].

The tests involve forming a 600 mm coal pencil from a 600 mm mesh coal and inserting the pencil into an accurately calibrated retort tube with a graduated piston on top. The sample is then placed in a furnace. The apparatus is heated at 3°C/minute and movement of the piston as it shrinks or expands is recorded. The data generated from the movement of the piston is used to generate curve seen in Figure 2.25. This is known as the Audibert Arnu dilatation method, in which the percentage of the original cylinder length is plotted against the corresponding temperature (SGS Minerals Services, 2013). The curves so produced provide valuable information regarding the suitability of the representative coal samples for use as coking coals, as the record produced is a characteristic of the swelling properties of the coal.

The important data on the curve are as follows [ISO Standard 349-1975(E)]:

i) Ti: Temperature at which the piston has moved down 0.5 mm (i.e., softening temperature)
ii) Tii: Temperature at which the piston reaches its lowest point (i.e., temperature of maximum dilatation.

iii) Tiii: Temperature at which the piston reaches its highest point (i.e., temperature of maximum dilatation).
iv) a: maximum contraction of length of pencil expressed as a percentage; and
v) b: maximum dilatation of length of pencil, per cent.

The maximum dilatation value is the critical parameter and the highest value possible is considered optimal. Typical ranges are as follows (SGS Group Management, 2013): i) high volatile matter coals = + 50 to 300 %; ii) medium volatile coals = + 100 to 250 %; and low volatile coals = <0 to 200 %.

A third test carried out to determine whether a given coal cokes or not is the Roga Index. In English, the Roga Index is abbreviated as R.I. In Poland the abbreviation is LR. It was developed by a Polish coal Chemist, B. Roca, a professor who in 1949 proposed a method for estimating the capacity of caking coal.

The bigger the LR, the stronger the caking capacity of a coal. In general, LR.5 coal has no adhesive force; LR between 5 and 20 indicates that the caking property of coal is poor or not having adhesion; LR between 20 and 45, the caking property of coal is partial or weak; LR between 45 and 80 indicates good caking coal and LR between 80 and 90 indicates the caking property of coal is strong.

A fourth test carried out to determine the caking properties of a coal is the Grey King test. Like the Roga test, the Gray King test was adopted to determine the coking properties of hard coals, although the two do not measure precisely the same parameters. The Grey-King test is a laboratory assay method which involves carbonising a small quantity of finely ground coal sample (ground to – 212mm under standard conditions. The test procedure involves heating a 20 g coal sample in a silica tube to 600ºC. The residual product is then compared with a standard series ranging from A to G with A representing non-coking; while G represents coking coal. The coals falling in the G grade are given a subscript (i.e., G-1 to G-8) that indicate the degree of swelling (ISO 502:2015 – Coal). G-8 represents the most strongly coking coal (Zimmerman, 1979).

Table 2.13 presents a comparison between the plastic properties of coal, while a rough comparison between FSI and Gray-King tests is given in Table 2.14. It is a rough comparison between FSI, and Gray-King test presented by Zimmerman (1979) as shown in Table 2.13.

Table 2.13: Representative data for the plastic properties of coals (Speight, 2013).

Coal Type	Swelling Index	Dilatation	Roga Index	Gray-King Test *
Non-coking	0	0	0 – 5	A to D
Weakly coking	1 – 2	0	5 – 20	D to E
Medium coking	2 – 4	0 – 40	20 – 50	E to G
Strongly coking	>4	>50	>50	G-2 to G-8

Table 2.14: Rough Comparison between FSI and Gray-King Test (after Zimmerman, 1979).

Crucible-Swelling Index	Gray-King Test
1	A to B
1.5	C to D
2 to 2.5	D to E
3	E to G
4 to 4.5	G-2
5 to 5.5	G-3
6.5 to 7	G-5 or higher
9	G-8

The carbonization of coal in producing a metallurgical coke is carried out in a high temperature coke oven. Historically, the oven was developed from just simple bee-hive type to modern large plants. Modern coke ovens are typically 6 m high, 15 m deep and 0.5 m wide, with each oven holding up to 36 tonnes of coal (Figure 2.26). The ovens are arranged in batteries (hence the term coke batteries), and each battery could contain up to 100 ovens (Crelling, 2008).

Modern coke batteries are highly mechanised, thus minimising atmospheric pollution and reducing labour requirements. Massive machines (Charge Cars) are utilised to load coal into each oven; a Ramp then pushes the coke sideways out of the oven, i.e., away from the oven into a Quench car; and the latter transfers the red hot coke to a quench station where it is cooled with water (wet quenching). Dry quenching is practised in some operations whereby the red-hot coke is cooled by circulating inert gases.



Figure 2.26: Coke Oven Operation: An oven has just been pushed and a quench car, full of incandescent coke, is *en route* to the Quench Station. (Photograph by Morrise, 2005).

During the last hours in the oven, coke shrinks and creates fissures. Upon discharge, the particles of coke may be discrete pieces of up to 200 mm long or more. After leaving the quencher, the coke is screened into various sizes as per market requirements which normally are as follows:

i. The 40 – 100 mm size (which forms the bulk of the product) is used in blast furnaces as a reductant (reducing the iron ore into iron).
ii. The exceptionally large and strong coke (i.e., foundry coke) is utilised in foundry cupolas to melt iron.
iii. The 10 – 25 mm size range is used in the manufacture of phosphorus and calcium carbide from which acetylene is made.
iv. Large quantities of the less than 12 mm size is termed coke breeze and is used in operations such as sintering of small iron ore prior to use in the blast furnace. Coke breeze can also be used as an industrial boiler fuel; and
v. A by-product plant within the coke plant complex captures by-products of the coke manufacturing process from which crude tar, ammonia, benzol, naphthalene and coke oven gas are produced. The by-products are utilised as feedstock for various industrial processes.

2.7 Chapter Summary

From the current literature review it is evident that much work has been carried out on the geology and formation of the coalfields in southern-central Africa. The coal measures and associated sediments are part of the Karoo Supergroup which was deposited in sedimentary

basins during a 100-million-year period commencing from the Upper Carboniferous to the early Jurassic. This major sedimentation covered the whole of the southern end of the continent, roughly the area south of latitude 25^0S. To the north of this are found other but relatively smaller basins which include the Limpopo trough and the Mid-Zambezi valley in Zimbabwe, with yet other basins occurring in other African countries. The area of the current study (the Hwange Basin) is part of the Mid-Zambezi Basin which has been described in the literature as having developed because of wrench-faulting and half-graben tectonics.

The coals in southern and central Africa show high variability in quality and occurrence. The quality attributes of the coals are a function of the original environment of deposition and the subsequent conditions that were imposed on the coal seams. These conditions have been described in the literature based on studies on specific coal deposits, with most studies centred on the South African coal deposits. There is a lack of information pertaining to the coals from the Hwange Basin.

The level of assessment and understanding of Zimbabwe coals in terms their composition (i.e., macerals, microlithotypes and inorganic constituents), all of which have a strong bearing on the exploitation of these coals, has remained practically low. This, regrettably, is against the background of the coal industry in Zimbabwe rapidly facing challenges which include increasing competition against a stagnant, if not shrinking home market. There is, therefore, a need to close the gap in the systematic knowledge of the country's coals, particularly the Hwange coals where the larger mines are in order for the Hwange coals to compete on the regional and international market as South African coal has done. More specifically, there is need to establish an understanding of the geology and formation of Hwange coals, and how such information will affect the exploitation and utilisation of this deposit. One of the most pressing matters is the consideration of the anomalous behaviour of the low swelling index of Hwange's coking coal. This needs to be investigated in depth in order to give assurance to the international coking coal market that Hwange coking coal does indeed provide strong coke despite the unusually low swelling index. Investigation of this anomaly is part of the objectives of this study.

The current research aims to fill the gaps in knowledge as outlined. No systematic full seam petrographic analysis and TGA/DTG analyses have been conducted on the Hwange coals. Available literature on petrographic analysis is only that reported by Watson (1960) where only two samples, all from one locality (No. 2 Colliery) were analysed for their macerals. A full

seam systematic sampling followed by the required petrographic analysis will facilitate delineation of coals into premium coking coal, blend coal, thermal coal as well as general industry coal. Mine plans could then be prepared, and production schedules made to ensure the right coal product is mined and delivered to the appropriate customer(s) timeously. In addition, the Hwange coal resource would realize its full potential.

CHAPTER THREE: METHODOLOGY

3.1 Introduction

As a commodity, coal is remarkable and indeed a rewarding material. It is a heterogeneous naturally occurring material with a myriad of uses in the energy-related applications. However, this heterogeneous naturally occurring material is often viewed as if it were a single and homogeneous substance (Schweinfurth, 2009). Whether this is intentional for convenience or not, the fact is that coal is a heterogeneous and complex substance. The relative proportions of coal type and rank determine the physical and chemical properties of the coal and the nature of its application as an energy source (Falcon and Ham, 1988). It is therefore imperative that the physical and chemical properties and proportion of organic and mineral components are established to determine its use, whether as single or as blended coals (Suarez-Ruiz and Ward, 2008). Furthermore, other factors such as the nature of dispersion of mineral matter within the coal have a bearing on the amenability of the coal to beneficiation prior to its utilisation. Thus, all such properties need to be understood prior to beneficiation and ultimate application.

The methods used for characterizing coal include specific standards, which have been established by consensus and approved and documented by recognised bodies (Ward, 1984; Falcon and Synman, 1986; Hessley *et al*., 1986; Smoog, 1992). These include British Standards (B.S), South African National Standards Association (SANS), American Standards for Testing Materials (ASTM), and the International Standards Organisation (ISO) and ICCP. The analytical work undertaken during this study occurred at various laboratories/institutions, namely: i) Hwange Colliery Company in Zimbabwe; ii) University of the Witwatersrand; iii) University of Johannesburg; and iv) commercial laboratories in South Africa (Mintek and Bureau Veritas). In addition, most of the analyses are conducted in Zimbabwe (Hwange Colliery Company Laboratory (certified to ISO 9001: 2008), and there was a good correlation in the results obtained from these laboratories.

These following procedures and analytical techniques applied during this research are as follow.

i. Geological mapping – surface and underground maps.
ii. Review and processing of historical data to complement the current study.
iii. Sampling and preparation of samples for various analyses
iv. Sample physicochemical analyses - proximate and ultimate analyses and calorific value.
v. X-ray fluorescence (XRF), and Ash Fusion Temperature analysis.

vi. Petrographic analyses – maceral and microlithotypes analyses, and rank by vitrinite reflectance
vii. Combustion prediction – Derivative thermo-gravimetric analysis (TGA & DTG)
viii. Basic coking tests using free swelling index, Roga Index, and dilatation; and
ix. Furnace Tests to determine which parts of the coal samples swell on heating.

3.2. Geological mapping

The geological mapping and drilling techniques used in this study to gather geological data complied with the established standards and codes such as South African Resource Committee Code (The SAMREC Code 2016 Ed) and the Joint Ore Reserve Code (The JORC Code, 2012 Ed.). The process involved surface mapping over the entire study area, as well as in the mine workings. Both surface maps and historical data from 6 000 drill cores were considered during this study.

3.2.1 Surface Geological Mapping

A surface geological map is analogous to a snapshot of the field distribution of rocks and geological structures such as faults and folds, and surface anomalies in each area. It may also be key to the unravelling of geologic history of an area, or a mineral deposit, being it fossil fuel such as coal, or a precious metal such as platinum. Geological mapping was incorporated as one of the techniques to achieve an objective of the current study for the following reasons

i. Mapping gives indications of depth of seam burial, i.e., if the stratigraphy of the area is known, the study of outcrop pattern will facilitate estimation of depth of overburden cover.
ii. It locates features such as faults and igneous intrusions which affect the seam and its quality; and
iii. It can be used to determine methods of exploitation, i.e., extraction by underground or opencast mining methods.

The current study utilised various techniques drawn from the literature (Allum, 1960; Compton, 1985). The field geological mapping involved ground traverses utilising marked collars of the over 6 000 drill holes sunk over the Hwange Concession, as well as bulldozer established tracks used as access to these drill holes. Aerial photography was also used, and this technique also benefitted from the aforementioned tracks, as the tracks were clearly visible on the aerial photographs. In the Western Areas part of the Hwange Coalfield where there are neither tracks nor marked collars of old drill holes, a hand-held global positioning system

(GPS) was used to locate and plot the positions of geological layers and their contacts as well as faults and other structural elements in. Surface mapping was carried out over the entire area covered by the Hwange Concession and the adjoining Western Area Coalfield, i.e., the area held by the Hwange Colliery Company (Figure 2.1), hence ease of access to the Hwange Colliery geologists.

3.2.2 Underground and Open Pit Geological Mapping

The geological mapping was carried out in accessible areas of active mine workings both in the opencast and underground sections of the mine. There are two basic methods of plotting geological features, and they may be combined or employed separately depending on the prevailing situation (Baron, 1985). The first is the off-set method, and the second is the compass clinometer method. The current study used the off-set method as it was the more appropriate for structural mapping. The procedures undertaken are as follows (refer to Figure 3.1)

I. A 50 m long tape was run between two survey pegs anchored in roof of drive/crosscut, and the tape was held vertically below each peg.
II. A traverse was made to identify the lithologies encountered, and then recorded in the field book with description/notes.
III. When a planar feature such as a joint, fault, mud-dyke, or geological contact was encountered, it was plotted as follows:
    i) Measured distance (a) – refer to Figure 3.2.
    ii) Measured distance (b) using a short (5 – 10 m) tape.
    iii) Plotted both distances on the underground mapping sheet as in Figure 3.2-point x;
    iv) Plotted the distance on the underground mapping sheet.
    v) Repeated with distances (c) and (d) –refer to Figure 3.1– point x.
    vi) Joined offset points x and y on the underground mapping sheet with a straight line.
    vii) Used a clinorule to measure dip of the planar feature (refer to Figure 3.1)
    viii) Recorded amount and direction of dip; and
    ix) If the feature was a fault, the dip and displacement magnitude (where possible) were similarly measured and recorded on the mapping sheet.

If the planar feature pinched out towards hanging wall or footwall, and therefore was not expressed on both sides of the drive/crosscut being mapped, then only one point was plotted. For an open pit mapping, a measuring tape was similarly laid down along the footwall rock

(sandstone) parallel to the pit face and 10 m away from it, for safety reasons. Geological features were projected to the tape and the actual positions were plotted using survey pegs positioned in a line running along the pit highwall. A clinorule was then used to measure the dip of the intersected planar feature and result entered on the opencast geological mapping sheet. In both cases, safety of personnel was paramount and communication with coal production personnel as well as adherence to mine procedures, were strictly adhered to.

Underground and opencast geological mapping were carried out only in accessible areas of the currently mined blocks. Some areas of the current blocks, as well as the entire now-decommissioned blocks, are closed to personnel for safety and statutory reasons. The results from the underground and opencast geological mapping are reported in Chapter 4 (Section 4.2.2.

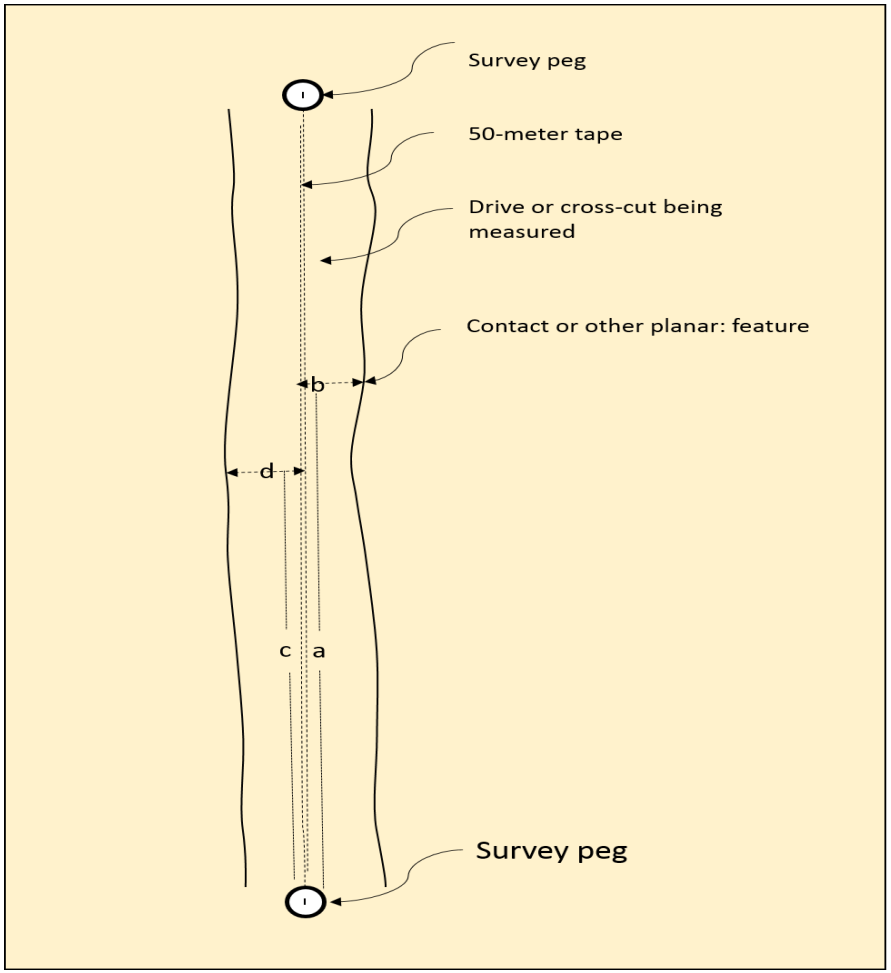


Figure 3.1: Diagram to illustrate the layout of the off-set mapping method.

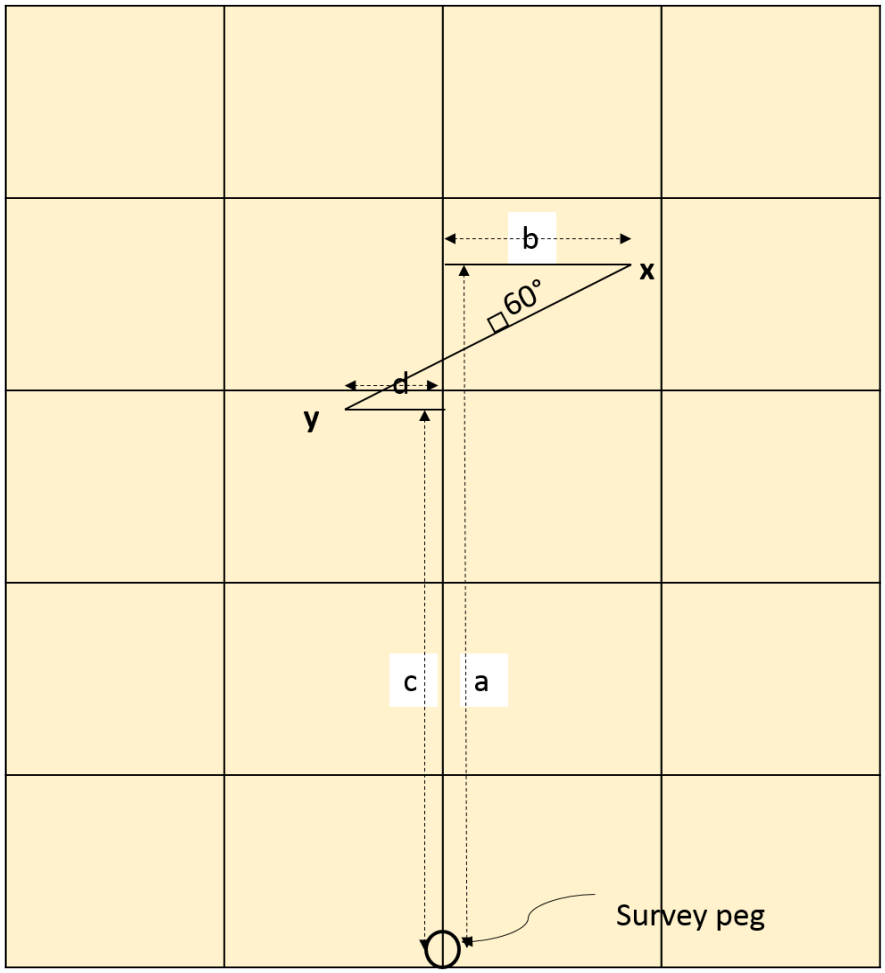


Figure 3.2: Diagram to illustrate the measurement and plotting of planar geological feature from the off-set Method.

3.3 Historical raw coal sample data review and processing

The current study incorporated raw data from core logs and linked coal analyses from coal exploration and evaluation drilling programmes conducted over the study area by the mine. Approximately 70% of this historical data was generated between 1996 and 2015 under the supervision of the author who was then Chief Geologist of the company. The drilling practice and the quality assurance and quality controls, the compositing procedure used to model the Hwange Main Seam into the two commercial coal horizons, i.e., coking coal and thermal coal, and the high ash carbonaceous material currently discarded as waste, are all described below.

3.3.1 Drilling practice

Diamond core drilling was carried out according to the requirements of the SAMREC Code of Practice for mineral resource evaluation and reporting, particularly with respect to core recoveries, core logging, coal sampling and handling (Refer to Assessment Criterion T3.2: sample method, collection, validation, capture and storage of the Code Version 2016). Procedurally, drill-hole spacing in deep underground coal areas commences with a 600 m grid, reducing to 300 m. In the shallow opencast areas, the coal exploration and evaluation drill-holes spacing is further reduced to a 100 m grid, closing in to 50 m in geologically complex areas. Drilling on a closer grid of 100 m in opencast areas facilitates a more accurate projection of the boundary between the thermal coal and the coking coal where the two coals are mined separately. Figure 3.3 is a drill-hole plan showing some of the 6 000 boreholes sunk over the study area during the period between 1983 and 2015.

All holes were drilled vertically from surface to at least 2 m below the Hwange Main Seam. Drilling runs were recorded accurately by trained and experienced drillers to ensure accuracy in terms of hole-depth. Coordinates of drill-hole collars were accurately surveyed in terms of UTM co-ordinates and Azimuth by trained and experienced surveyors to ensure accuracy of drill-hole location as well as elevation of both surface and footwall above sea level. The survey data was subsequently used to construct surfaces of geological layers of interest (e.g., footwall elevation contour plan). The exercise provided samples for coal assays, while logging of cores generated from the drilling programmes provided data such as depths, thickness of all geological layers intersected by each drill-hole as well as the attributes of the lithologies such as colour, degree of weathering as well as presence, frequency, and severity of structural elements. The generated data which included collar coordinates, collar elevation, depth to the coal/footwall sandstone boundary, geological logs, and coal analyses of at least 6 000 drilled

holes, was used to draw geological sections, footwall elevation profiles and coal type thickness contours following receipt of coal assay results. The results of these geological plans and sections are provided in Chapter 4 (Section 4.2.2.2).

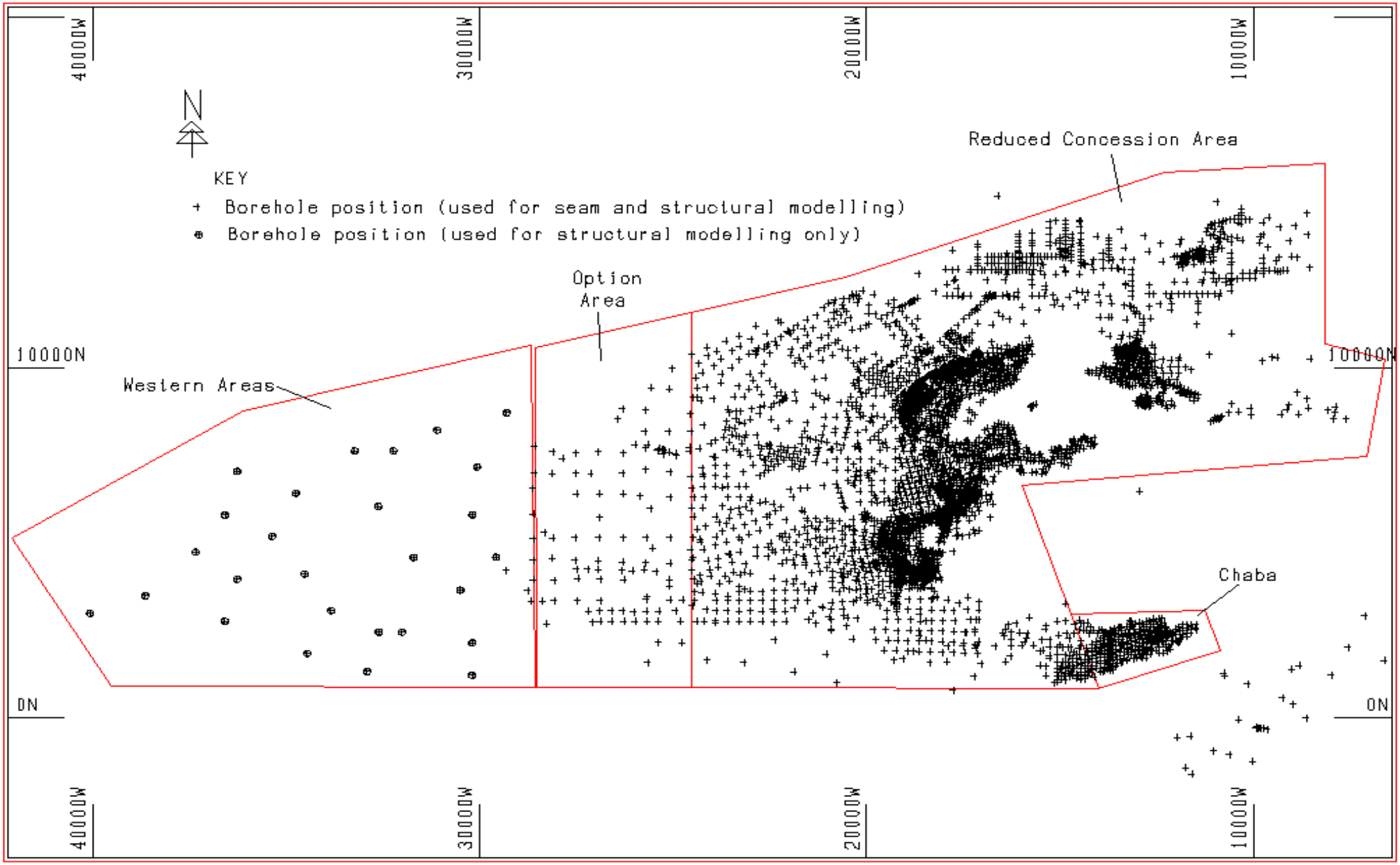


Figure 3.3: Location of diamond core drill holes sunk over the Hwange Concession between 1983 and 2015.

3.3.2 Drill core samples quality assurance and quality control

Coal horizon samples (placed in core boxes) were taken at 1 m intervals from the Fireclay–Main Seam boundary up to approximately 2 m above what the geologist perceived to be thermal coal (referred to as HPS). Here, the coal sampling interval was reduced to 0.5 m intervals, except where there were recognisable geological boundaries/inter-beds. However, 0.3 m was taken as the absolute minimum sample length to ensure enough material for laboratory testing. The samples were bagged and ticketed with each ticket showing drill-hole number, sample identification number (ID), "Depth From" and "Depth To". After labelling, the samples were taken to the laboratory for different analyses, with the procedures and data obtained subjected to several stringent checks to ensure it was error-free and meet the require coal quality assurance standards.

3.3.3 Hwange Main Seam Modelling

The Hwange Main Seam is a geological unit in which its main quality parameters, ash content, volatile matter, total sulphur and phosphorus, show characteristic and systematic vertical variations. The ash content and phosphorus content increase vertically, while volatile matter and sulphur content decrease with height above the seam base. On the basis of this variation, the coal seam was modelled into three benches: i) a basal high-quality coking coal horizon; ii) a relatively higher ash and low volatile matter thermal coal; and iii) a carbonaceous material which currently has no market due to its excessively high ash values.

Central to this modelling function is what is termed the "compositing procedure" designed for modelling coal seams such as that of Hwange Main Seam using Surpac, a computer software (Figure 3.4) designed by the South African vendor for Surpac Australia.

The coal quality parameters used during this exercise were:

I. Hwange Coking Coal (HCC): minimum of 23.5% volatile matter content; and maximum of 15% cumulative ash content. In the past, coal with this ash content and volatile matter content (cut-offs) did cake, but today this is not always the case, which is part of the motivation for this study.
II. Hwange Power Coal (HPS): maximum of 24% cumulative ash content

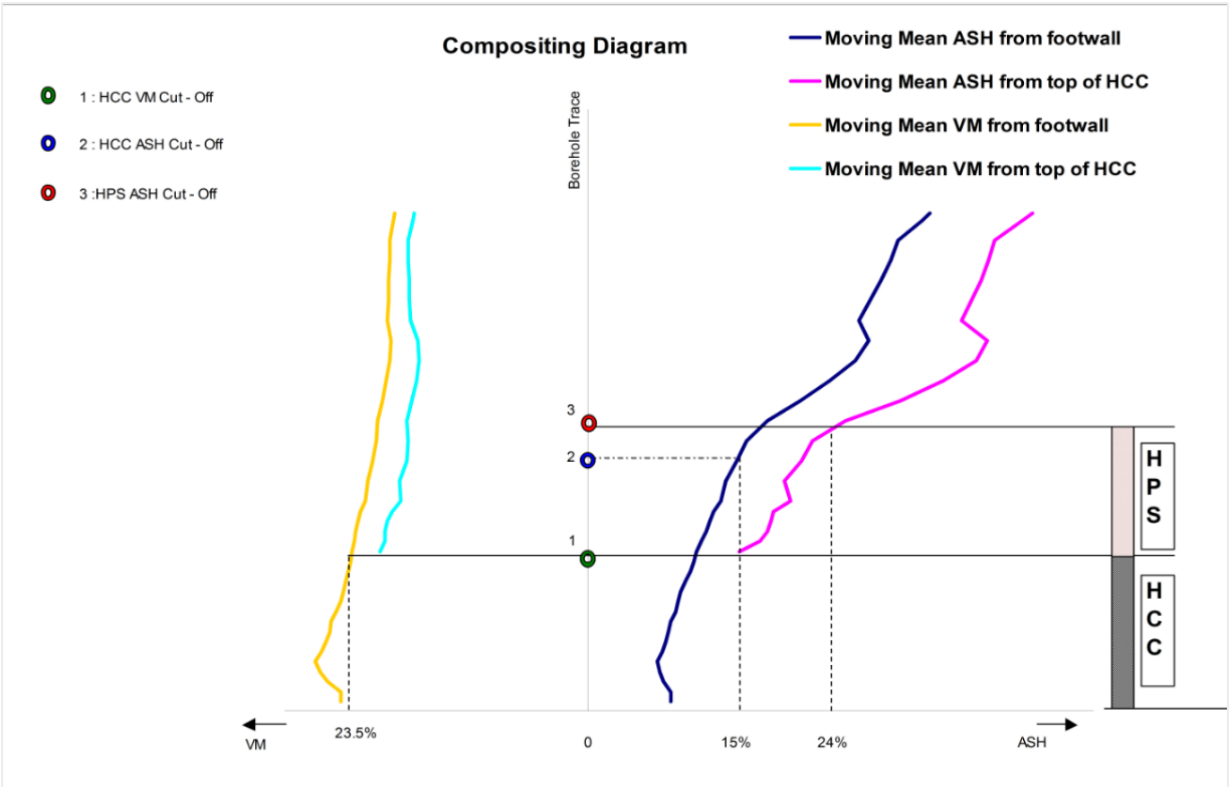


Figure 3.4: The coal quality compositing procedure

With reference to Figure 3.4, the proximate analysis values were cumulated upwards from the base of the coal, per borehole, until either the moving mean for volatile matter or ash content was reached (threshold value). At this point, the top of coking coal was defined. Accumulation then proceeded anew until the power coal (HPS) top was reached. This point defined the top of the power station coal horizon. The balance of the data into the high ash carbonaceous material was accumulated and recorded as well.

In this exercise, it is critical to note that in any of the above accumulating iterations, the moving mean could, and often it did, move beyond the coking coal cut-offs, only to drop back below these limits, to be followed by a subsequent rise above the limits. It was the final rise which was recorded and used to define the top of coal, hence the thickness. The exercise was repeated for samples from each of the over 6 000 boreholes. Using the digital terrain modelling (DTM) system inbuilt in the software, coal type thickness contours were drawn.

Approximately 150 000 coal horizon samples (an average of 25 samples per each of the 6 000 drill-holes, drilled from 1983 to 2015) were incorporated in this study to determine coal quality and seam thickness distribution of the Hwange Colliery Concession. All core samples generated before 1982 were routinely analysed for moisture, ash content and volatile matter

content, and as from 1986, total sulphur and phosphorus analyses became mandatory due to the market demands. The results are presented as thickness contours in Section 4.2.3 of Chapter 4.

3.4 Coal sampling and sample collection for the current study

To supplement the drill core data previously generated, and to address specific questions raised during this research, more samples were collected from 3 different localities, as indicated in Figure 3.5.

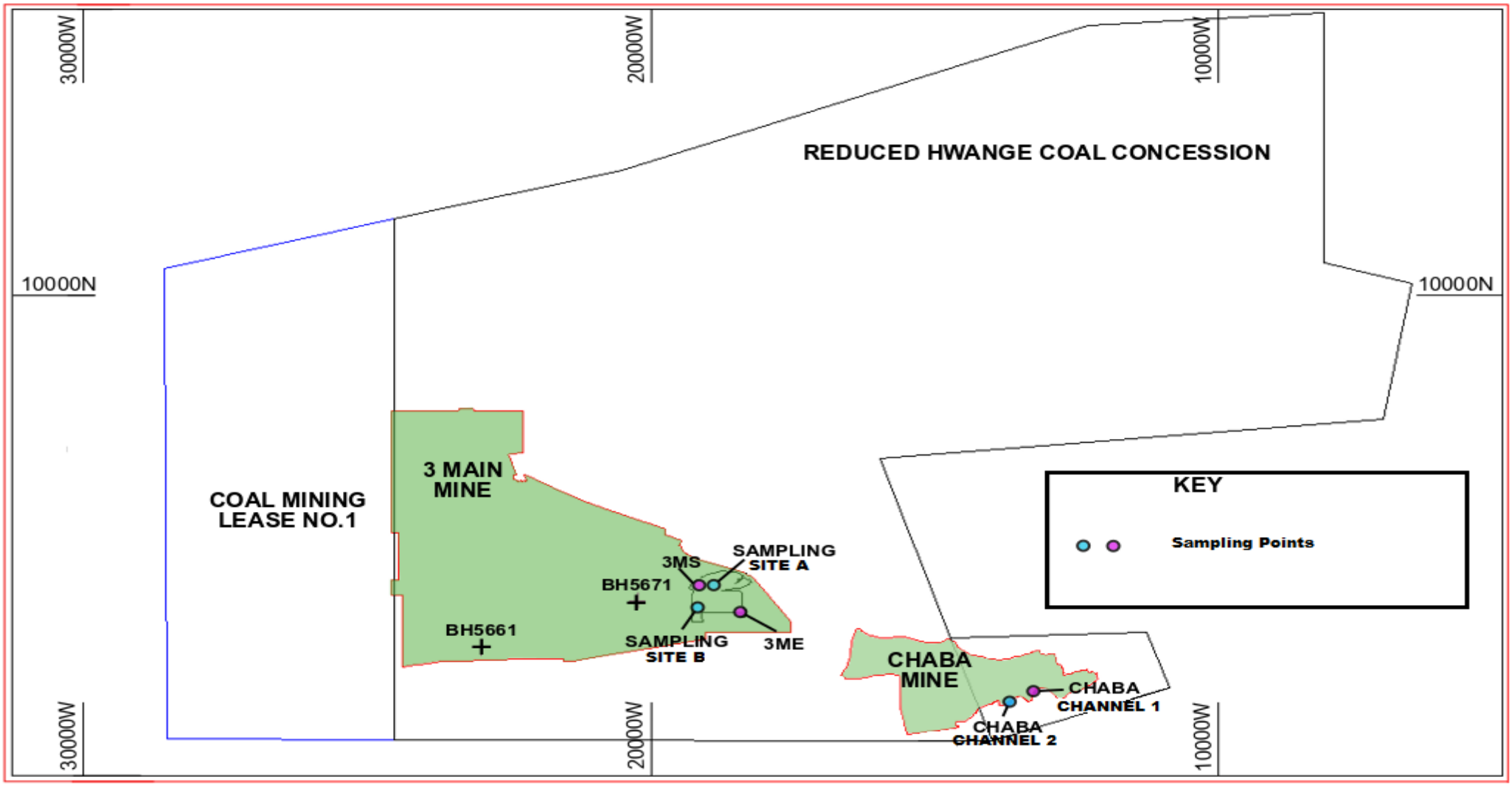


Figure 3.5: Localities for the channel samples at Chaba Opencast and 3 Main Underground Mine.

3.4.1 Description of sample localities

3.4.1.1 Chaba Opencast Mine:

Initial coal face sampling at Chaba was carried out at 3 m intervals along a vertical channel (Chaba Channel 1) running from top to bottom of the seam. This sampling campaign acquired three composite samples. Following the acquisition of appropriate and safe equipment, a further 8 samples were collected at 1 m intervals from bottom of the seam to the top (i.e., Chaba Channel 2). This included the thermal coal part of the Hwange Main Seam. The location of these samples in plan view is shown in Figure 3.5, while Figure 3.6 presents the coal face from Chaba with the locations (on the coal face) of the 8 samples. The coal face location of the initial 3 channel samples depicted in Figure 3.5 could not be shown as the face was blasted before the highwall was photographed.



Figure 3.6: Chaba Opencast highwall showing location of Channel 2 samples.

3.4.1.2 Main underground mine.

The 3 Main underground mine provided three sets of samples collected as follows: Channels 3MS and 3ME, as well as chip samples collected systematically along two vertically oriented lines at sites A and B (see Figure 3.5). The two vertical channels cut in the coal face from two different production areas are as follows:

i) 3 Main East (3ME) Channel comprised 12 samples collected at 30 cm intervals from seam base up to the roof of the underground tunnel for the sample site; and

ii) 3 Main South (MS) Channel contributed 11 samples also collected at 30 cm intervals also from bottom of the seam to the roof of the underground tunnel.

Note well, the underground mine workings only mine coal to predetermined mining heights to win the required coal quality. In addition, the mining height is constrained by the mining equipment in use or ground stability considerations. Consequently, the mining height ranges from 3 m to 5 m.

A further six samples were collected from selected positions along the vertical lines at two different sites in the underground mine coal face as follows:

i) Site A - 3 samples taken at intervals 0.25 - 0.75 m; 2.0 - 2.50 m; and 3.50 - 4.25 m, from above seam base; and
ii) Site B – 3 Samples taken at intervals 0.25 – 0.75 m; 2.50 – 2.75 m; and 4.0 – 4.25 m- also above seam base.

These six samples were collected primarily for furnace tests to observe physically which of the samples swell after heating under nitrogen in an airtight furnace. Hence, a total of 40 samples from these three locations were prepared and utilized in this study.

3.4.2 Sample preparation

The samples utilized in this study were collected from the working mining faces, free from oxidation or weathering. They were collected in a clean plastic sheet from each pre-marked interval, and along the vertical channels marked. Each sample was thoroughly mixed before it was quartered. The sub samples were collected and bagged in an airtight bad under nitrogen and clearly labelled (e.g., 3MS 1, 3MS 2, etc.) before being sent to the laboratory.

For the physicochemical and mineralogical analyses, the samples were further crushed and milled to different particle sizes in accordance with ISO 13909:2016.

3.5 Analytical techniques

As the samples were collected in phases, and due to logistical issues, which included budgetary constraints, accessibility of sampling points (particularly at 3 Main Underground Mine), delay in securing appropriate sampling equipment (i.e., mining excavator for highwall channel sampling at Chaba), three phases of analyses took place (as shown in Table 3.1). The samples were split (for the different techniques) before they were analysed following an array of procedures and analyses as indicated in Figure 3.7. Figure 3.8 shows the various analyses carried out on the Hwange coals during the current study.

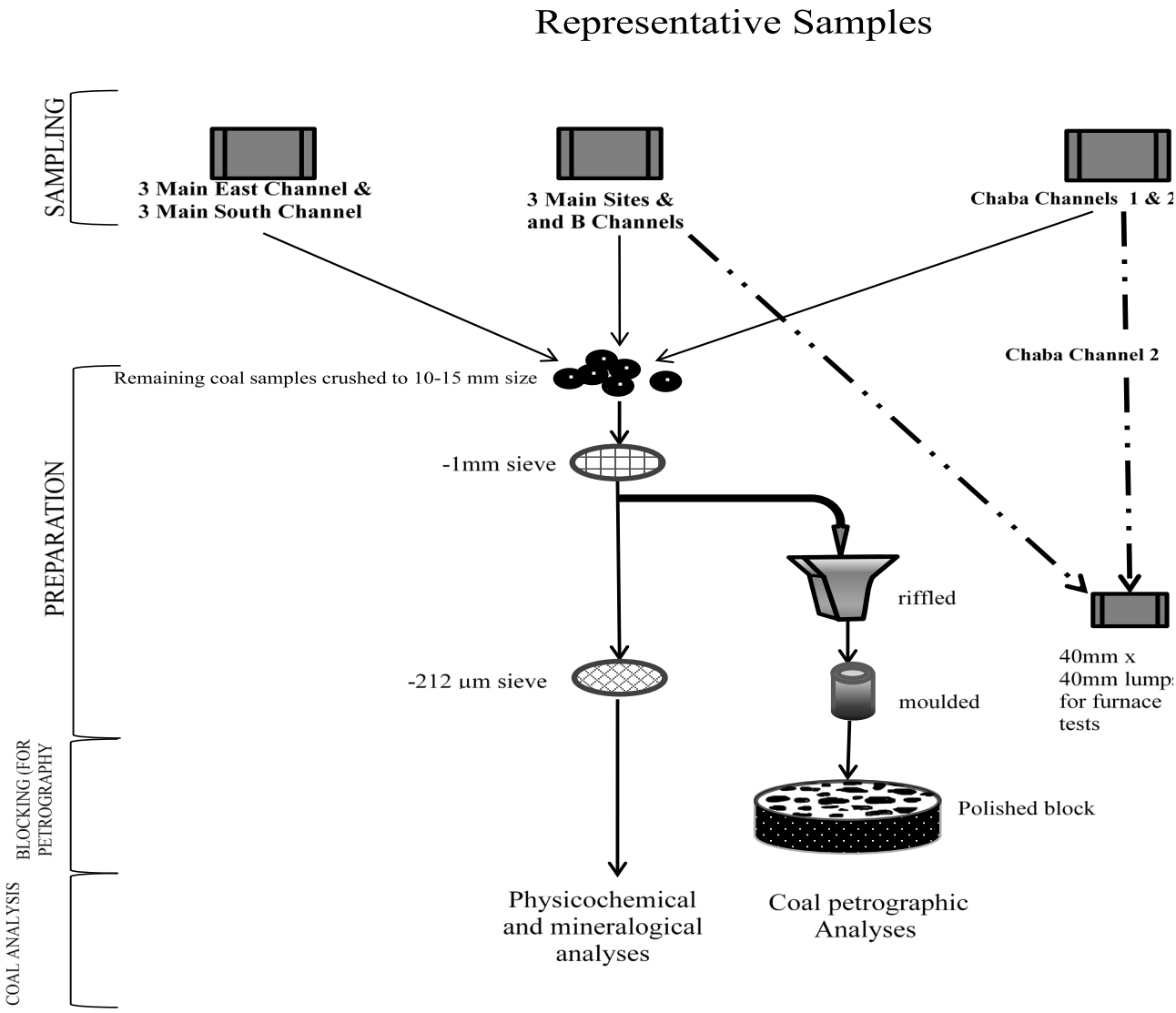


Figure 3.7: Summary of sampling and preparation steps taken Hwange coal analyses.

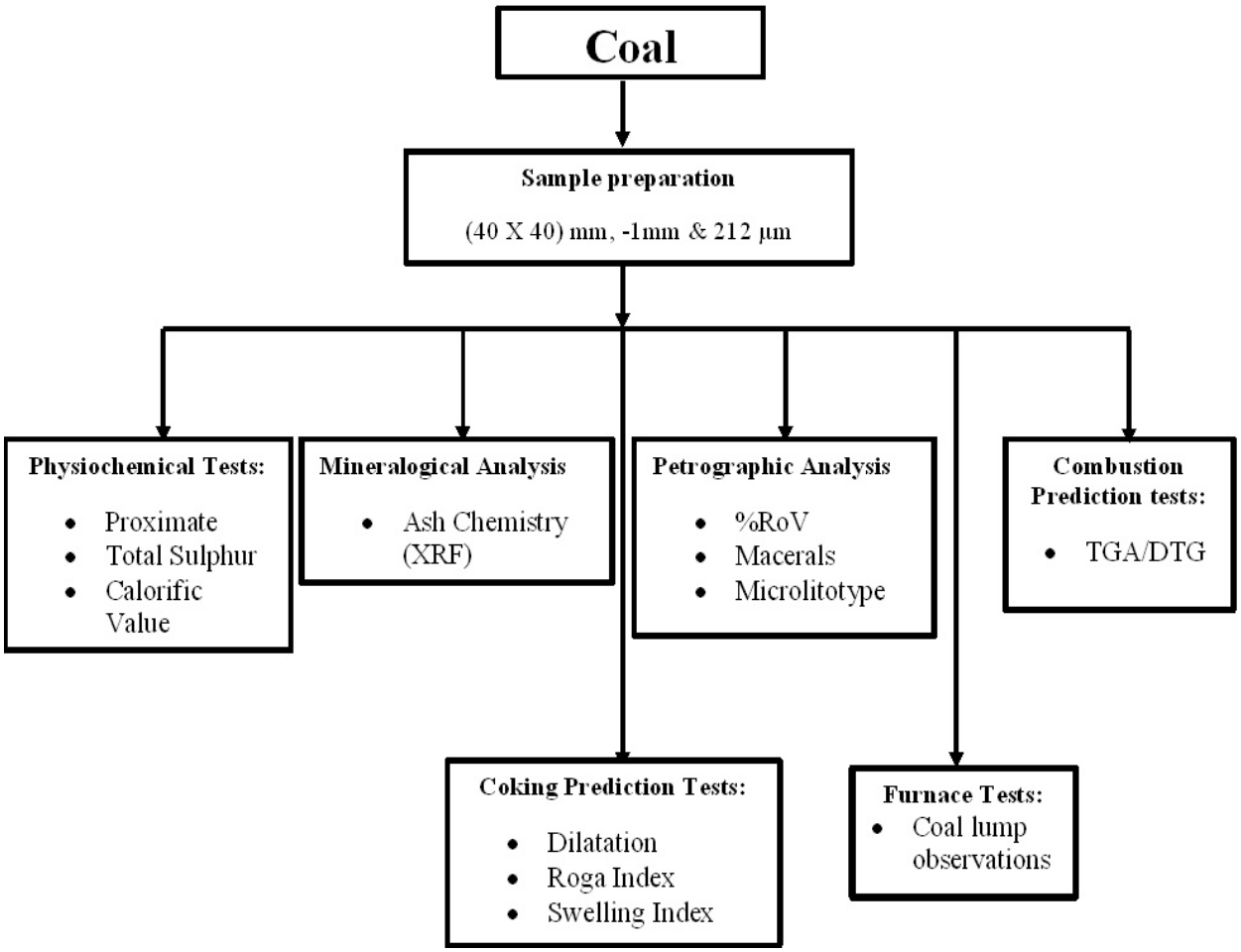


Figure 3.8: Flowsheet for Hwange coal samples

Table 3.1: Analyses and analytical phases (HCCL = Hwange Colliery Company Limited).

PHASE 1 Characterisation and combustion tests			
Sample Source	**Qty**	**Analysis Type**	**Standard Used**
3 Main (3ME & 3MS) & Chaba Channel 1	26	Proximate (air dried)	Hwange Quality Assurance Testing Method 3.03-3.05
		Total Sulphur (TS)	QATM 3.10 (In-house)
		Total Phosphorus	QATM 3.09 (In-house)
		Calorific value	ASTM D5865-04
		Coal petrography	ISO 7404: 1 – 5
		TGA combustion tests	in house procedure
		Swelling Index	British Standard
3 Main (3ME & 3MS)	23	XRF	ASTM D 4326
PHASE 2: Characterisation and coking tests			
3 Main Sites A & B	6	Proximate Analysis	ISO 11722:1999 (moisture); ISO 1171:2010 (Ash); ISO 562:2010 (Vol)
		Swelling Index	ISO 501:2003
		Total sulphur	ASTM D – 3177
		Roga Index	SANAS 881:2009
		Dilatation	ISO 23873
Chaba Channel 2	8	Proximate (air dried)	ASTM D5142
		Phosphorus	British Standard
		Petrography	ISO 7404: 1 -5
		Roga Index	SANA 881:2009
		Dilatation	ISO 23873
		Free Swelling Index	ISO 501:2003
PHASE 3 Furnace Tests			
Chaba Channel 2	8	Furnace Tests	Wits
3 Main Sites A & B	6		

3.5.1. Proximate Analysis

The proximate analysis was conducted in a Leco TGA 701 in accordance with ASTM D-5142. Approximately 1 g of -212 µm coal sample was used for the analyses in determining the inherent moisture, ash content and volatile matter present in the coal with fixed carbon

calculated by difference. The same samples were also subjected to the ISO 11722:1999 (moisture); ISO 1171:2010 (Ash content); ISO 562:2010 (Volatile matter), and similar results were obtained from both standard methods.

3.5.2 Total sulphur analysis

The sulphur analysis was carried out in two parts: total sulphur analysis, and determination of sulphate, pyritic and sulphur forms. The analyses were conducted at the Hwange Colliery Company using the Quality Assurance Test Method (QATM 3.10), an in-house procedure based on the British Standard 1016-106.4.2:1996 (Appendix 3.1).

3.5.3 Phosphorus

The phosphorus analysis was carried out at the Hwange Colliery Laboratory using an in-house procedure QATM 3.09 which is based on the British Standard BS 1016: Part 9:1077 (Appendix 3.2).

3.5.4 Heat Content Analysis

The calorific value which is known as the measure of the heat content of coal was determined in accordance with ASTM D5865-04, using a Leco AC500. The coal sample utilized was pulverized to -212 μm, and approximately 1 g was weighed into the crucible and then inserted into the combustion vessel. The system uses an electronic thermometer with an accuracy of 0.0001 ^{0}C to measure the temperature every six seconds, with the results obtained within 4.5 to 7.5 minutes.

3.5.5 Ash Chemistry (XRF)

The coal samples were ashed in an atmosphere of air according to the standard ISO 1171:2010 for 'Solid mineral fuels - Determination of ash'. The compositional analysis of the ash obtained from each coal was conducted in accordance with the ASTM D 4326 using XRF to determine the oxides of major elements for the coal ash (ashed to 815 °C), including SiO_2, Al_2O_3, CaO, K_2O, Na_2O, Fe_2O_3, MgO, TiO_2 and P_2O_5.

3.5.6 Petrographic Analyses

The petrographic analysis was carried out according to SANS 7404-3 (SABS ISO 7404-3) (2016) (2016-11-11), in which blocks of coal were prepared by mixing coal particles (-1000 μm) with resin and hardener. The mixture was allowed to solidify under ambient temperatures and atmospheric pressure. Prepared coal blocks were polished using a Struers TegraForce-1

polishing machine. The analysis of macerals, and microlithotypes composition as well as rank provide important information regarding the organic matter and its distribution/association with coal; while analyses of the inorganic matter give indications as to the broad type and dispersion of minerals matter in the coal sample. Besides allowing the investigator to detect the various components in the coal mass, petrographic analyses also allow for detection of coal conditions such as oxidation and weathering, micro-cracks, fissures (including their pattern) micropores, oxyrim formation and any other features within the coal specimen under examination. In this study, the polished blocks were analysed using a Leica DM 4500P reflected light microscope with a J and M spectrolytic system used for the vitrinite reflectance analysis.

3.6 Coking Tests

There are several appropriate methods applied to measure the plastic properties of coal, which have been described in detail in section 2.6.3. In the current study, the following methods were utilized.

3.6.1 Dilatation

The Ruhr dilatation tests were carried out by the Bureau Veritas according to SANAS 23873. In the test, a 60 mm coal pencil formed under pressure from minus 600 mm coal was inserted into an accurately calibrated retort tube with a graduated piston on top. The sample was then placed in a furnace. The apparatus was heated at 3 ^{0}C/minute and movement of the piston as it shrank or expanded was recorded.

3.6.2 Roga Index

The Roga Index was also conducted at the Bureau Veritas Laboratory; in accordance to ACT-TPM procedure based on SANAS 881:2009.

3.6.3 Free Swelling Index

The free swelling index measures the increase in the volume of coal when heated in the absence of air and reported in numbers from 0 to 9, with the higher value considered to be of higher quality for coking coal application. This caking characteristic of the coal samples were determined according to ISO 501:2012 (Hard coal Determination of the crucible swelling number).

3.7 Combustion tests using Thermogravimetric Analysis (TGA)

The thermogravimetry analysis (TGA) was carried out to predict the combustion performance of 26 coal samples under phase 1 (Table 3.1). The combustion tests were conducted in a thermogravimetric analyser, under an oxidising atmosphere using air. Approximately 100 mg of each sample (100% passing a 212 mm screen), was used for the experiment. The differential thermogravimetric (DTG) curves, i.e., combustion profiles were obtained at a constant heating rate of 6 ^{0}C/minute, from 25 ^{0}C to 850 ^{0}C and held until there was constancy in weight loss. The differential thermogravimetric curves (DTG) indicating the rate of weight loss (%/min) with increasing temperature were used to directly evaluate the combustion properties including initiation devolatilisation temperature (ITVM), peak temperature (PT) and burnout temperature (BT).

3.8 Furnace/Oven Tests

In order to determine the reasons for the anomalous behaviour of coals from some parts of the Hwange Seam during coking processes, lumps of coal (roughly 14 square blocks of approximately 4 cm x 4 cm), were subsequently split into two mirror images, making 28 samples. One block from each representative sample was heated in a furnace under a nitrogen atmosphere to 650 ^{0}C for an hour. After one hour in the furnace, the blocks were carefully removed and placed in a desiccator to preclude oxidation during the cooling period. The two mirror images comprising one fresh and the other heated in the oven (resultant char) were compared to see which areas of the samples had reacted and which ones had not. The mirror images were photographed for comparison and are presented in Chapter 4 Section 4.4.7. The samples utilized are, i) 6 samples from sites A and B at the 3 Main Underground Mine, and ii) 8 samples from Chaba Open-cast Mine Channel 2.

3.9 Challenges Faced.

A couple of challenges were encountered during the sampling and subsequent analytical phases. Among these challenges were:

i) Sporadic flooding of the mine which precluded reaching the intended sampling points, resulting in a decision to relocate to an alternative, but similar site.
ii) Power cuts which precluded underground sampling trips at appropriate times before the intended site was either sealed off or flooded.
iii) Financial and logistical constraints that hampered transportation of samples from Zimbabwe to Johannesburg as one batch.

iv) In addition, and due to complexity and requirements of specialised analytical equipment, analyses were not carried out under one roof, but at different, but recognised analytical centres in South Africa and in Zimbabwe, and
v) As a result, sampling and analyses were conducted in phases as indicated in Table 3.1.

3.10 SUMMARY OF THE COAL ANALYSES CONDUCTED DURING THE STUDY

Table 3.2 presents a summary of coal analyses conducted during this study.

Table 3.2: Summary of coal analyses conducted.

SOURCE		Coke Tests			Combustion Tests								
	No. of Samples	Proximate	Sulphur	Phosphorus	Mineralogy	Petrography	XRF	Roga	FSWI	Dilatation	Coal Lumps	CV	TGA
Chaba Channel 1	3	✓	✓	✓	✓	✓	X	X	X	X	X	✓	X
Chaba Channel 2	8	✓	✓	✓	✓	✓	✓	✓	✓	✓	✓	X	✓
3 Main East Channel	12	✓	✓	✓	✓	✓	X	X	X	X	X	✓	✓
3 Main South Channel	11	✓	✓	✓	✓	✓	X	X	X	X	X	✓	✓
3 Main Site A	3	✓	✓	✓	✓	X	✓	✓	✓	✓	✓	X	X
3 Main Site B	3	✓	✓	✓	✓	X	✓	✓	✓	✓	✓	X	X
Hwange Concession historical data	180,000	✓	X	X	X	X	X	X	X	X	X	X	X

CHAPTER THREE: RESULTS AND DISCUSSION

4.1 Introduction

This chapter presents the results and discussions of the practical geological work and the various coal tests carried out as discussed in Chapter 3. The chapter is structured into two major sections: Section 4.2 and Section 4.3.

In Section 4.2 the results of the practical geological investigations carried out over the study area are presented and discussed. These include regional and local geological studies, and the processing of data from previous coal exploration/evaluation programmes, i.e., historical data. More specifically, it looks at the structural set-up of the Hwange Coalfield, its stratigraphy and general seam attributes as revealed by recent geological mapping and the interpretation of core logs from previous core drilling campaigns by the Hwange Colliery Company. Thus, the geological environment during coal seam deposition is unraveled, and subsequent factors that may have affected the seam attributes are addressed.

Section 4.3 presents the analytical results of the samples collected and analysed using the analytical methods described in Chapter 3. These include proximate and ultimate analyses, mineralogical analyses, coal petrographic analyses, combustion prediction tests, coking tests, and furnace tests. The results are compared and discussed in Chapter 5.

4.2 Geology of the Hwange Basin

4.2.1 Background

As discussed in Chapter 2, Section 2.3.3, the Hwange coalfield is one of the coal bearing areas that lie in the Mlibizi intrabasin. In the Hwange area, the basin is dichotomous, with the dichotomy brought about by the occurrence of the northeast-southwest trending Entuba Inlier of crystalline basement rocks which divides the basin into two. That part of the Hwange Coalfield covered by the Hwange Reduced Concession and the adjoining Western Areas Coalfield constitute the northwestern branch, while the Entuba-Simatella Coalfield forms the southeastern branch (Figure 4.1).

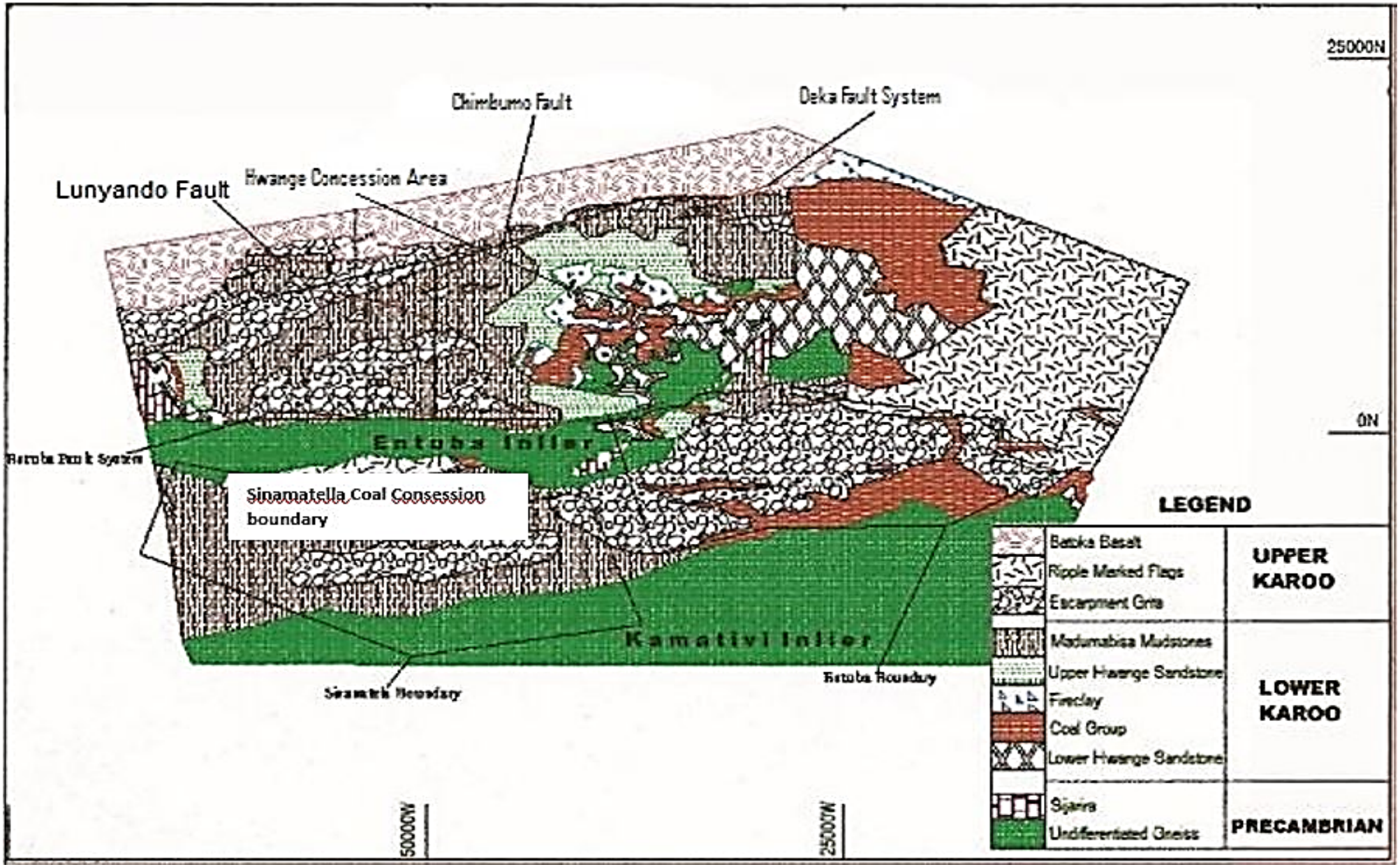


Figure 4.1: Geological map of the dichotomous Hwange Basin (modified from Watson, 1960)

The northwestern branch is bordered to the northwest by the Deka Fault, a regional geological feature that is traceable for several kilometres from the Zimbabwe-Botswana border in the southwest to Kariba in the northeast. The southeastern branch is bordered by the Kamativi Inlier which is made up of Archaean basement rocks, also essentially of igneous origin. The younger Karoo rocks successively overlap the older rocks until they rest directly on the Archaean basement rocks.

The Hwange Coal Basin has been drilled extensively; with no less than 6 000 diamond drill holes sunk vertically from the surface to intersect the Ecca-age Hwange Main Seam. From the drill cores, sufficient information is now known of the sedimentary basin to justify describing it a type area for the Karoo stratigraphy. Figure 4.2 presents the stratigraphy of the Hwange Basin drawn from the information generated by drill-holes sunk over the basin. The Karoo Supergroup is included for comparison. The stratigraphy of the Hwange Basin as noted in most, if not in all Karoo basins, reflects an amelioration of climatic conditions from the Later Palaeozoic to Cenozoic (Götz and Ruckwied, 2014). The succession records a change in climatic conditions leading to the melting of Dwyka ice to cold, cool temperate climate conditions during the Early Permian. The succession commences with glacial beds correlated with Dwyka and terminates in mafic lavas known locally as Batoka Basalts which are correlated with the Stormberg Group of South Africa. The intervening strata comprise normal sediments as shown in Figure 4.2.

The importance of this succession is the occurrence of the Coal Group (K^2), which is the focus of this paper. The K^2 formation is the main source of energy in Zimbabwe and has played and continues to play a critical role in the economic development of the country.

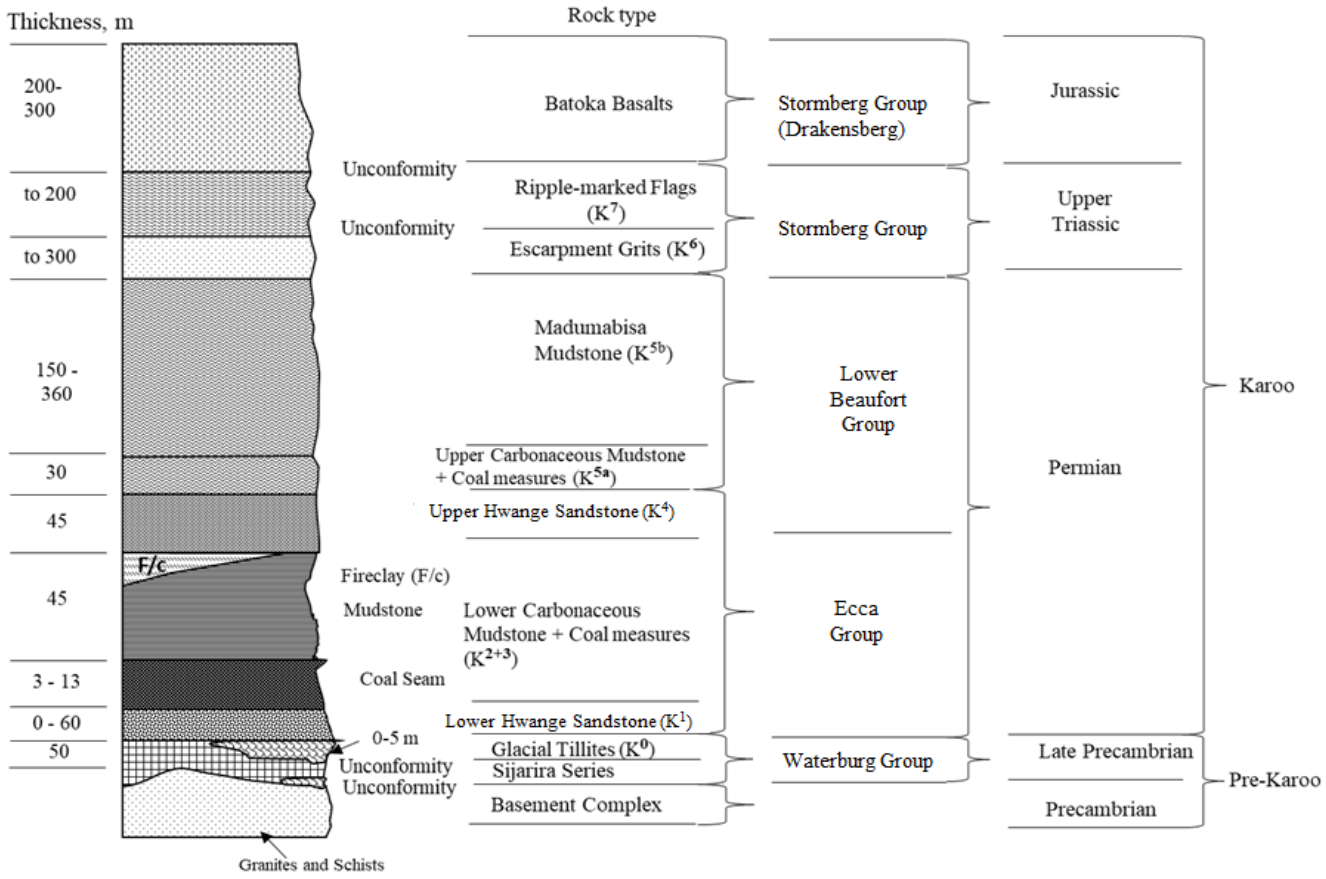


Figure 4.2: Hwange Karoo Basin stratigraphy.

The field geological mapping carried out during coal exploration over the Western areas' coalfield reveals the existence of glacial beds resting over the basement rocks. The sequence of the glacial beds is as follows:

I. Massive diamictites which are greyish, pebbly sandstone and are unsorted and massive.
II. Bedded diamictites which are greyish, pebbly sandstone, minor conglomerate with faint bedding and sorting.
III. Massive sandstone facies: grey, fine to medium grained, arkosic sandstone, laminated with x-bedding and ripple marks, pyritic, kaolinitic matrix; and
IV. Fine grained clastic facies: light-grey, very fine-grained sandstone, massive or cyclic in parts with rhythmites and lamination.

The glacial beds are overlain by sandstones at the base constituting what is known locally as the Lower Hwange Sandstone Formation. The formation generally ranges from a coarse to fine grained material with distance from base. The fine-grained material, which occurs at the top, is usually micaceous and laminated.

The limited drill-hole intersection of the Lower Hwange Sandstone Formation was a handicap to the ability to derive sufficient information from drill cores required to unravel tectonic activities related to the deposition of the Lower Hwange Sandstone. Elsewhere, Barber (2001), describing the formation in the Mlibizi Intrabasin, suggests that the Lower Hwange Formation was deposited in response to a tectonic activity that was probably associated with the isostatic rebound that followed the Dwyka ice-age. The rock represents a transition of the fluvial-glacial sediments of Dwyka into wholly fluvially deposited sediment (Barber, 2001). The Lower Hwange Sandstone Formation is designated K^1, with "K" standing for Karoo.

Overlying the Lower Hwange Sandstone is the Coal Group which comprises the Hwange Main Seam and the overlying Carbonaceous Mudstones. The change from the Hwange Main Seam to Carbonaceous Mudstones is, in the main, a gradational one, characterized mainly by the increase in the ash content generally from 10% at the coal seam base to approximately 70% at the top of the Coal Group. There are occasional intercalations of siltstone within the coal seam, particularly towards the top. Vertical to near vertical mud dykes have also been encountered within the seam during mining and geological mapping. However, dolerite dykes found in coal seams in the southern part of the country have not been found in the Hwange Coal Seam. The coal measures were derived from vegetation that thrived following warming of the region during the Carboniferous-Permian times and the remains of dead vegetative matter are envisaged to have subsequently been preserved in the low-lying and subdued topography that characterized the relief at that time. Leaves of giant flora such as *Glossopteris* have been observed within the coal measures in the underground mining workings.

Overlying the Coal Group, and in some cases replacing it, is a rock unit referred to as Hwange Fireclay. This is a light coloured khaki to creamy massive and often brecciated claystone. Where it outcrops and overlies burnt coal, it often also occurs as a burnt residue. The Hwange Fireclay ranges in thickness from zero to 15 m. It is designated K^3. Succeeding the Hwange Fireclay is a coarse to medium grained sandstone formation known locally as the Upper Hwange Sandstone Formation. The rock is essentially grey to white in colour and feldspathic. Lenses and specks of pyritic material occur here and there within the rock formation. Common sedimentary structures exhibited by the formation include both planar and trough-cross bedding, with the latter predominating. The formation also contains lenses of both argillaceous and rudaceous sediments. Occurring within this formation is a carbonaceous marker horizon known as Lightfoot Marker (named after Lightfoot, who was the investigator who first

recognized this persistent geological horizon). The deposits were overall derived from the surrounding provenance by the erosion process. The Upper Hwange Sandstone Formation, which has a thickness that ranges from a few centimeters to 30m, is designated K^4.

The Upper Hwange Sandstone Formation is, in turn, overlain by a thick layer of mainly fine grained mudrock which is comprehensively known as the Madumabisa Mudstone Formation. This formation represents the deposition of predominantly argillaceous material in a lacustrine environment as subsidence progressed. Attempts were made to follow the arduous work conducted elsewhere (e.g., in the Sengwa and Gwayi areas) by Bond (1955) where he differentiated the Madumabisa Formation into several horizons, namely $K^{5\ a\ to\ e}$.

However, differentiation of the Madumabisa Formation into the abovementiones horizons was not conducted during the current study. What could be achieved, and suffices for the current study, was the differentiation of the 280 m stratigraphic pile into two main horizons: the Lower Madumabisa Member and the Upper Madumabisa Member. The Lower Member is a carbonaceous coal-bearing mudrock consisting of thin vitrinite-rich bands of a few centimeters interspaced with dark grey mudrock. The presence of vitrinite in the Lower Member indicates that the horizon was deposited in an anaerobic environment around the basin margin.

The overlying Upper Member is frequently carbonate rich. The horizon is predominantly comprised of sequences of massive, homogeneous mostly green-grey mudstones and laminated silty mudstones and siltstone. Bone beds have also been observed in some drill cores. The horizon is interpreted as having accumulated in relatively shallow lacustrine environments. While logging one of the boreholes drilled in the same area, numerous coarsening upwards cycles as denoting a shoreline or delta progration into a relatively stable basin were observed. It is concluded from the occurrence of horizons of dark, bituminous-rich mudstone and limestone, which are often rich in plant fossils but in most cases devoid of sedimentary structures, that deposition proceeded in or adjacent to shallow aerated water where vegetation flourished. The Madumabisa Formation forms the top of the Lower Karoo, marking the end of the Lower Karoo Group. The formation's upper 10 m or so is characterized by greenish-brown mud rock that is weathered. The 10 m horizon has been particularly a challenge to diamond drilling operations, as it often results in the jamming of the down-the-hole drilling equipment. The surface represents a dominantly erosional period (an unconformity).

Deposited upon the above-mentioned unconformity and marking the beginning of the Upper Karoo Group were the Escarpment Grits. These rocks are coarse grained and pebbly. They weather a characteristic red-brown colour and therefore ieasy to distinguishin handspecimen from the Ecca Upper Hwange Sandstone Fromaton. The pebbles are rounded water-warn fragments and are predominantly of quartz. Trough cross-bedding is among the sedimentary structures identified in the formation. The Escarpment Grits are interpreted as having been deposited by a proximal system of alluvial fans and braided rivers (Barber, 2001) during the Triassic period. Geological logs of water exploration pilot holes, drilled ahead of large-diameter water abstraction holes, have recorded sediments that include Ripple Marked Flagstones intercalated with intercalated beds of red to white coloured fissile mudstone and siltstone. These rocks collectively form the Ripple-marked Flagstone Member which overlies the Escarpment Grits and underlie the Batoka Basalts on the downthrown side of the Deka Fault.

Succeeding the Ripple-marked Flagstone Member are the mafic volcanic rocks known locally as the Batoka Basalts. These are massive and pillowed, and contain amygdales, i.e., vesicles previously filled with gases, but now filled with calcite. The Batoka Basalts terminate the Karoo System in the area (Watson, 1960). Both the Ripple-marked Flagstone Member and the Batoka Basalts are absent from the coal-bearing study area, presumably having been eroded away. They were preserved in the core of a pilot diamond drill-holes sunk on the downthrown side of the Deka Fault.

4.2.2 Description of the area covered by the study.

The study focused on the northern branch of the Hwange Coalfield, the area covered by the Hwange Concession on the east, the Option Area in the middle, and the Western Areas on the west (Figure 4.3). The Hwange Colliery Company operations are spread over the “Concession Area” and the contiguous “Option Area”.

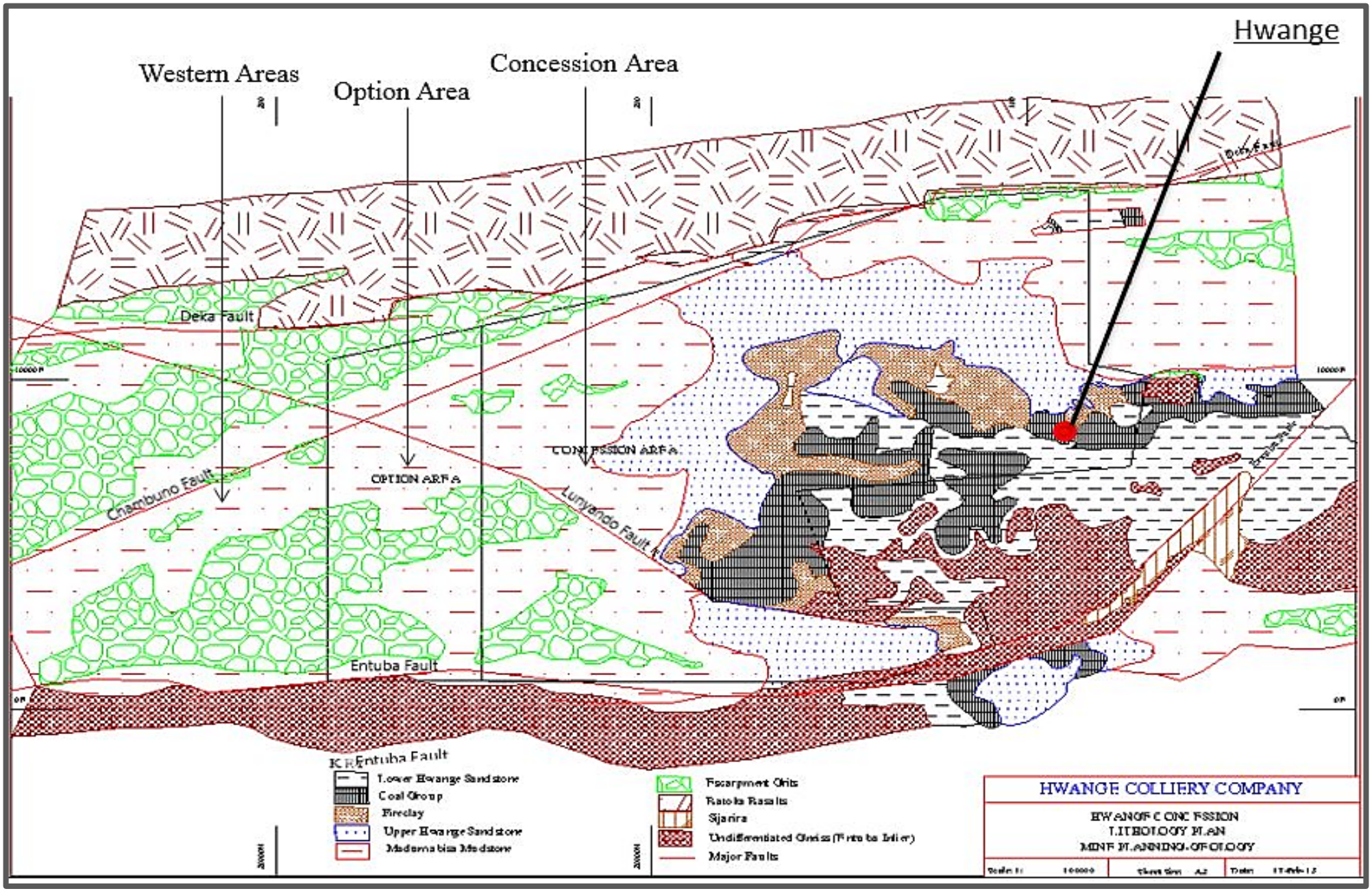


Figure 4.3: Geology of the area covered by the Hwange Colliery mining operations.

4.2.2.1 Stratigraphy of Hwange Colliery Operational Area

Figures 4.4 represents stratigraphic columns drawn from a geological log of a vertical drill-hole from surface, to intersect the coal seam, from the top of Matura Hill which sits above one of the Hwange Colliery Company underground mining blocks. The stratigraphic succession in this drill-hole is consistent with that presented in Figure 4.2 and this section focuses on the field relations of the main lithologies.

The stratigraphy of the northern branch (hereinafter referred to as the "Hwange Colliery operational area" commences with the basement rocks which are predominantly granitic in composition and their metamorphic derivative, the gneisses. These outcrop in the south as a linear inlier of old and hard rocks that stand above the generally subdued relief to form the Entuba Hills. The rocks extend eastwards as irregularly shaped out crops (Figure 4.3). Lying directly above the basement rocks is Late pre-Cambrian rocks referred to as the Sijarira Series. The members making up this formation include hard, flaggy, red brown quartzitic sandstones. In the area under study, the formation occurs as small outcrops in the south east (Figure 4.3). The glacial beds that were deposited on the Late pre-Cambrian basement rocks only outcrop in the extreme west of the Western Area part of the study area.

The Lower Hwange Sandstone Formation which succeeds the glacial beds outcrops on the extreme eastern portion of the Hwange Colliery operational area, where it occasionally occurs as block outcrops due to orthogonal jointing. This is observed immediately to the southeast of the Hwange town. In this locality the formation often contains scattered fragments of gneiss and quartz presumably derived from the pre-Karoo floor. Overlying the Lower Hwange Sandstone Formation, Coal Group also occurs as isolated irregularly shaped outcrops on the eastern portion of the Mine site (Figure. 4.3). Outcrop mapping and study of drill cores visibly show that the formation comprises a lower portion of black horizon which ranges from bright banded material and gradually becomes dull with height above base. The formation gradually becomes duller and grey coloured towards the top. Drill-hole data reveals that the formation becomes deeper westwards and its thickness ranges from zero to 30 m.

Overlying the Coal Group occasionally replacing the former is a white to creamy refractory material known as the Hwange Fireclay. This outcrops in the eastern part of the Hwange Concession (Figure 4.3) where it may be a variably burnt rock.

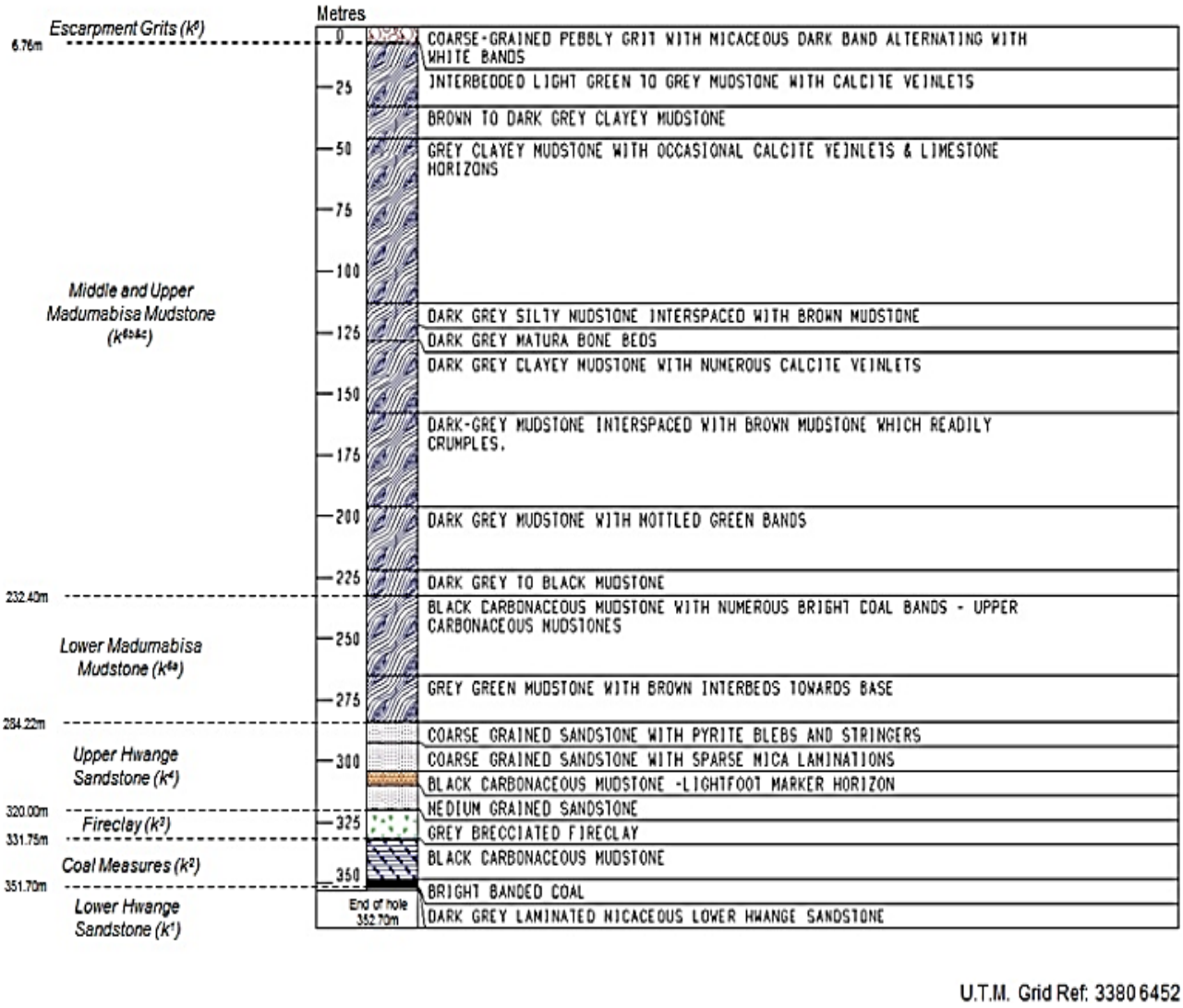


Figure 4.4: Log of BH 3901 (Matura Hills) showing the stratigraphy of Hwange Colliery Mining Area.

Also occupying the topographically low ground and overlying the Hwange Fireclay is the Upper Hwange Sandstone Formation. A persistent layer of black carbonaceous material known as the Lightfoot marker horizon, occurs within the Upper Hwange Sandstones Formation. This formation outcrops draping around the older Karoo members (Coal Group, Fireclay and Lower Hwange Sandstone Formation) in the Hwange Concession portion of the north branch, and, for coal mining purposes, currently marks the limit of the shallow opencastable coal. In the study area the formation has a maximum thickness of 30 m.

Overlying the Upper Hwange Sandstone is a thick pile of rock which in the mine site commences with grey green material containing brown intercalations at the base followed by black carbonaceous mudstone which contains several thin (5 to 10 cm) bands of bright banded coal (Figure 4.4). The remaining portion of the pile comprises rock material with various

attributes and colour as shown in Figure 4.4. Two important features of the supernatant horizon are the fish bones and dinosaur remain which were located on Matura Hill, some 200 m from the drill-hole BH 3901. Fish bone indicates a lacustrine environment. Diamond core drilling operations over the Matura Hills and other hills occurring to the west of the Hwange Concession, the adjoining Option Area and the Western Area have encountered a muddy horizon which has often led to the jamming down-the-whole drilling equipment. The muddy horizon is interpreted as representing an unconformity (Watson, 1960), a period of non-deposition. Immediately above this muddy horizon occur the Escarpment Grits which within the mine site is a plus or minus 10 m slab of rock which caps all the plateaux occurring on the Western part of the study area. Rocks younger than the Escarpment Grits (the Ripple marked flags, Forest Sandstones and the Batoka Basalts) are preserved on the downthrow side of the Deka Fault (Figure 4.3).

In summary, over the northern branch of the Hwange Coalfield, the Hwange Main Coal Seam outcrops on the eastern part and becomes buried under a progressively increasing overburden cover westwards with the deposition of younger rocks (Figure 4.3).

4.2.2.2 Structural Geology of Hwange Colliery Mining Area

The structural geology of the Hwange Hwange mining area is characterized by two major crustal features: the Deka Fault and Entuba Fault (Figure 4.5), which trend parallel to each other. The two faults impart a stepping down process, a feature that characterizes the sub-surface of the northwestern portion of the Hwange Basin as both faults are down thrown to the northwest. The intervening ground, i.e., the tract of ground geologically sandwiched between the Deka Fault and the Entuba Fault, is structurally characterized by a criss-cross of relatively smaller scale faults which have been encountered during mining operations.

The Deka Fault

The Deka Fault is a regional crustal geological feature which is traceable from the Zambian Border in the northeast, through Hwange District, to the Botswana border in the southwest. The “Boundary Fault” described by Orpen *et al.*, (1989) discussed in Chapter 2, Section 2.3.3 and shown on Figure 2.10 in Chapter 2 reveals that the “Boundary Fault” coincides with the

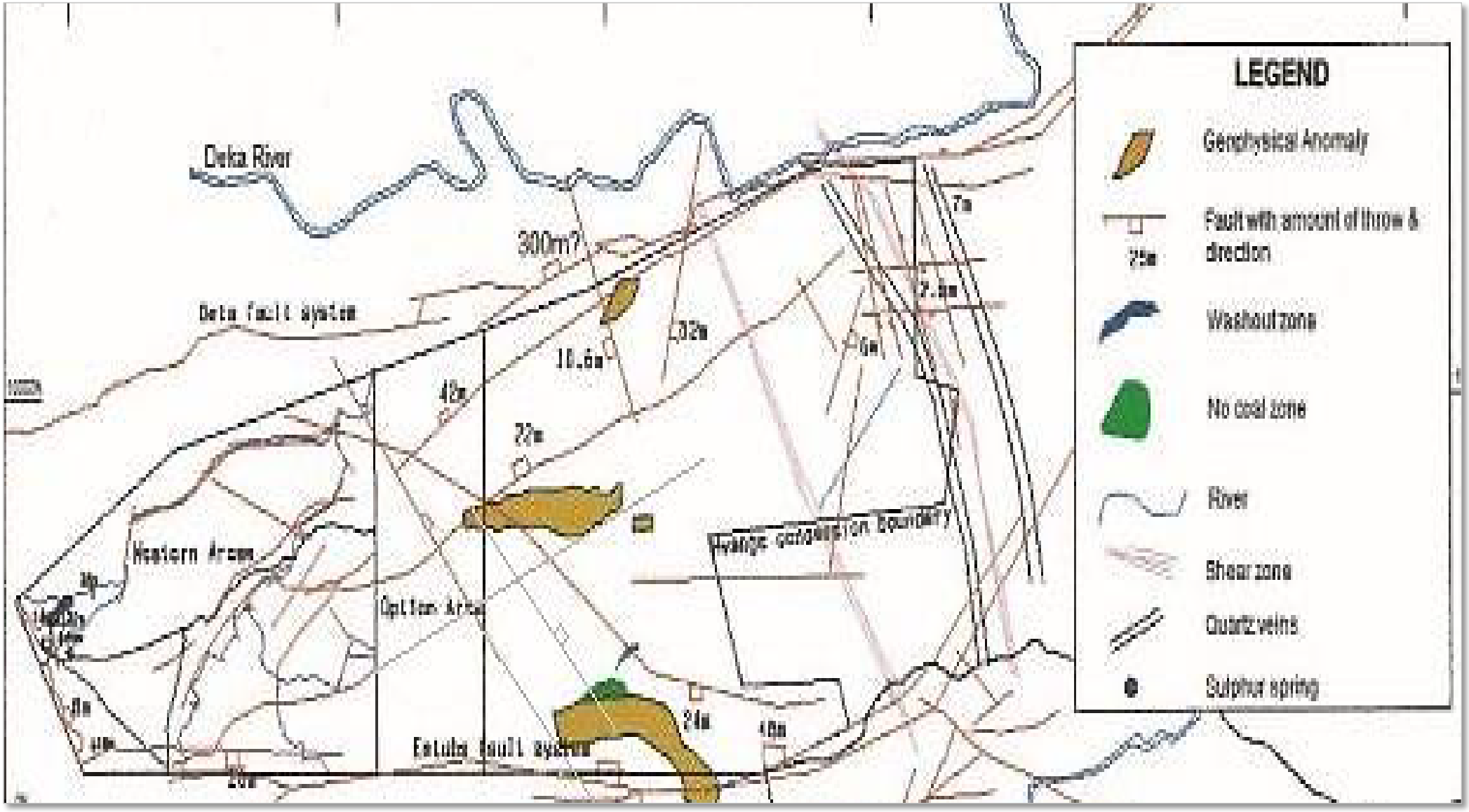


Figure 4.5: Structural plan of Hwange Concession and location of mined-out part of 3 Main showing mapped faults and joints. (Note some joints may well be listric faults).

position of the Deka Fault. It is a normal fault with a downthrow to the northwest. Based on the pilot water exploration drill-holes sunk on the downthrow side of the fault, displacement is estimated at approximately 300 m. The fault plane is observed at a road cutting across the Deka River, approximately 3 km north of Hwange Town. At this site, the Deka Fault justposes the pillowed Batoka Basalts against sediments of the Kondo Range (Figure 4.6).



Figure 4.6: Deka Fault juxtaposing pillow lavas of Batoka Basalts (on the left) against the Escapement Grits (on the right). Location: Deka Bridge to Angling Boating Club Camp at the Zambezi River. (blue pen is included for scale).

The Kondo Range, which stands high above the surrounding areas, is considered to be due to the heat from the Deka faulting event which led to the intense recrystallisation of the rocks close to the fault plane; thus, rendering them relatively more resistant to weathering than the rocks further away from the fault plane. A 75 m sheared zone defined by carbonate (mainly calcite) veinlets occurs on either side of the fault plane. Sympathetic faults occur over an 800 m wide zone occurring on either side of the fault plane. Coal mining within this zone is not only a challenge, but impossible due to severe ground conditions. One such fault, the Chambumo Fault which at the old and decommissioned No.3 Shaft occurs some 600 m south of the Deka Fault. All mining was halted as soon as the 200 m “cautional line” from the Chambumo Fault was crossed. Copious amounts of groundwater have been drawn from 250 m deep water abstraction boreholes sunk within the 75 m wide Deka Fault shear zone for domestic and industrial use by the Hwange Colliery Company. In fact, the Company draws

approximately 65% of water for its mining operations as well as for the 50 000 Hwange Town population from the boreholes drilled along the Deka Fault.

Entuba Fault

Trending NE-SW along the middle of the equally trending coal-bearing basin, the Entuba Fault is less well known than the Deka Fault. Indications from the meagre information available are that the fault is also downthrown to the northwest, as with the Deka Fault. However, while the amount of fault displacement is yet to be precisely established, it is less than that of the Deka Fault. This tentative conclusion is based on the differences between the heights above sea-level of the coal seam on either side of the fault.

The coal seam within 200 m of the fault, at both the Makomo Resources Colliery on the south east of the fault and Hwange Colliery's Chaba Opencast Mine, is highly cleaved and the area is difficult to mine due to severely fractured ground. Where it has been mined at the Chaba Opencast, the coal was out-of-specification for most end-user's requirements due to its high ash, low volatile matter or high sulphur content. Periodic earth tremors occur along both Deka and Entuba faults indicating the two are still active.

Other Faults

Surface and underground mapping in conjunction with interpretation of diamond drilling data reveals that away from the Deka and the Entuba faults, occur other relatively small-scale faults whose displacement magnitudes range from a few centimeters to as much as 20 m. Among these is the Lunyando Fault which runs through the Hwange Colliery's Chaba Opencast Mine in the northeast, to 3 Main Underground Mine in the southwest as shown on the geological and structural maps of Hwange Concession (Figure 4.3 and Figure 4.5, respectively). Displacement along this fault diminishes along strike to the southwest. Where it has been intersected by 3 Main underground mining to date, the fault has a displacement magnitude of 15 m in one mining section and the seam is almost entirely separated. In an adjacent mining section, the displacement magnitude diminishes to 4 m (Figure 4.7). From geological mapping, the shear zone along the fault is estimated to be 5 m on either side of the fault. The fault has also been associated with huge amount of water that has severely affected mining operations by flooding the coal mining faces. This has been exacerbated by the frequent power outage that has impacted the country since 2007; because with no power, water pumping is incapacitated.

Several faults have been mapped in the highwall at the Hwange Colliery's Chaba Opencast Mine and Hwange Colliery Dragline Pit and most of the faults mapped are listric faults. The displacements show a decline along strike. In addition, the faults are listric normal in profile, i.e., concave at the top and convex at the bottom. Another feature of the listric faults is that their displacement magnitudes diminish from top to bottom of the fault plane such that where the geological feature reaches the coal seam's contact with the footwall sandstones, no displacement is evident although there is shuttering of the rock/coal on either side of the fault plane. Figure 4.8 represents part of the Chaba Opencast Mine and the location of one of the listric faults mapped in the area (Figure 4.9); while Figure 4.10 is a photograph of the highwall JKL Opencast Mine (also known as the Dragline Pit), on the eastern side of the Entuba Inlier showing a listric fault. Regrettably, the upper part of overlying sandstone which showed displacement (from cleavage observation) had been mined out at the time of photographing the feature. Listric normal faults are associated with tensional tectonics. This is consistent with the half graben theory advanced by Orpen *et al*. (1989) and Oesterlen and Lepper (2005).

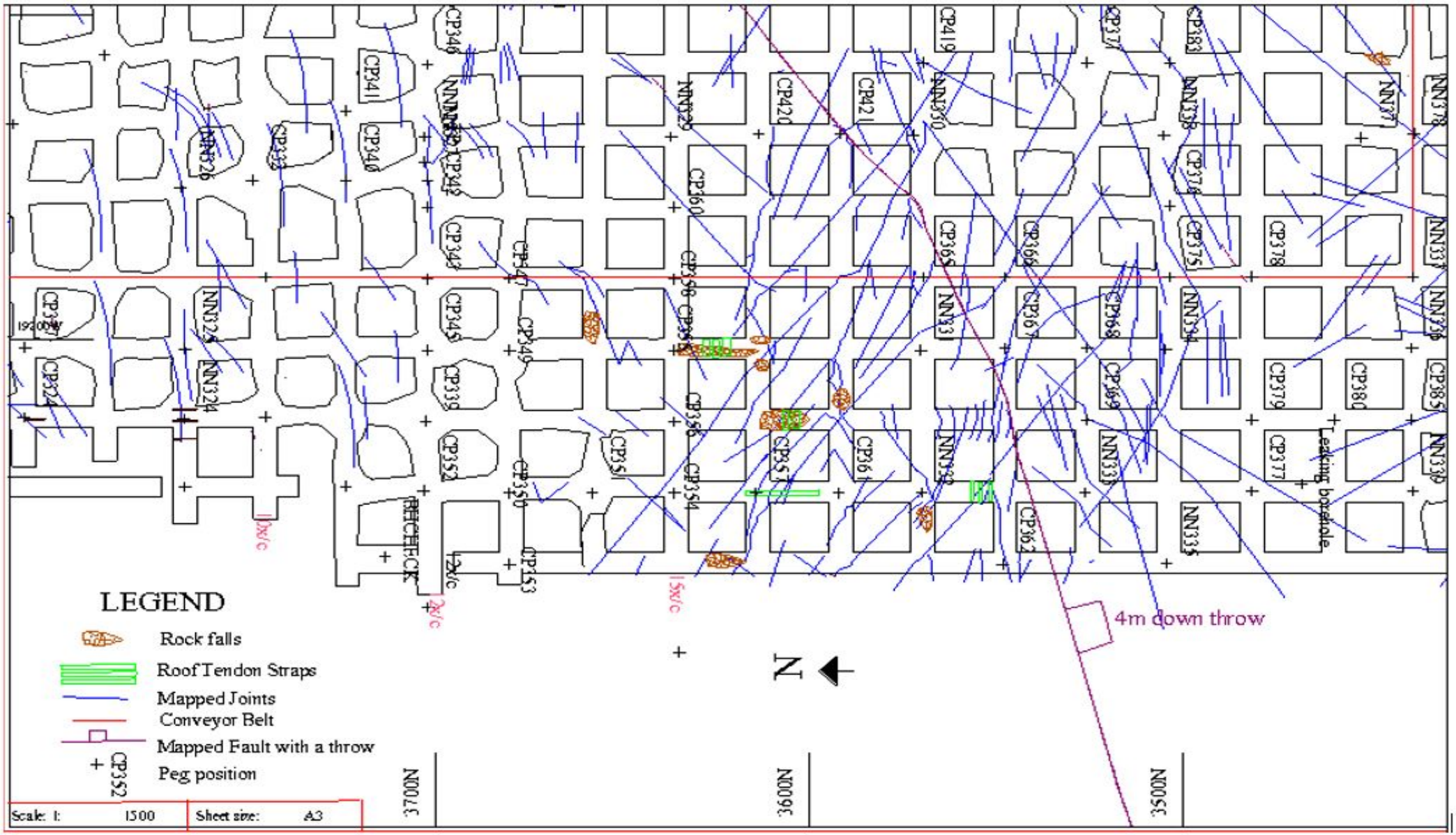


Figure 4.7: Structural map of part of 3 Main Underground Mine showing mapped joints and faults (current study).

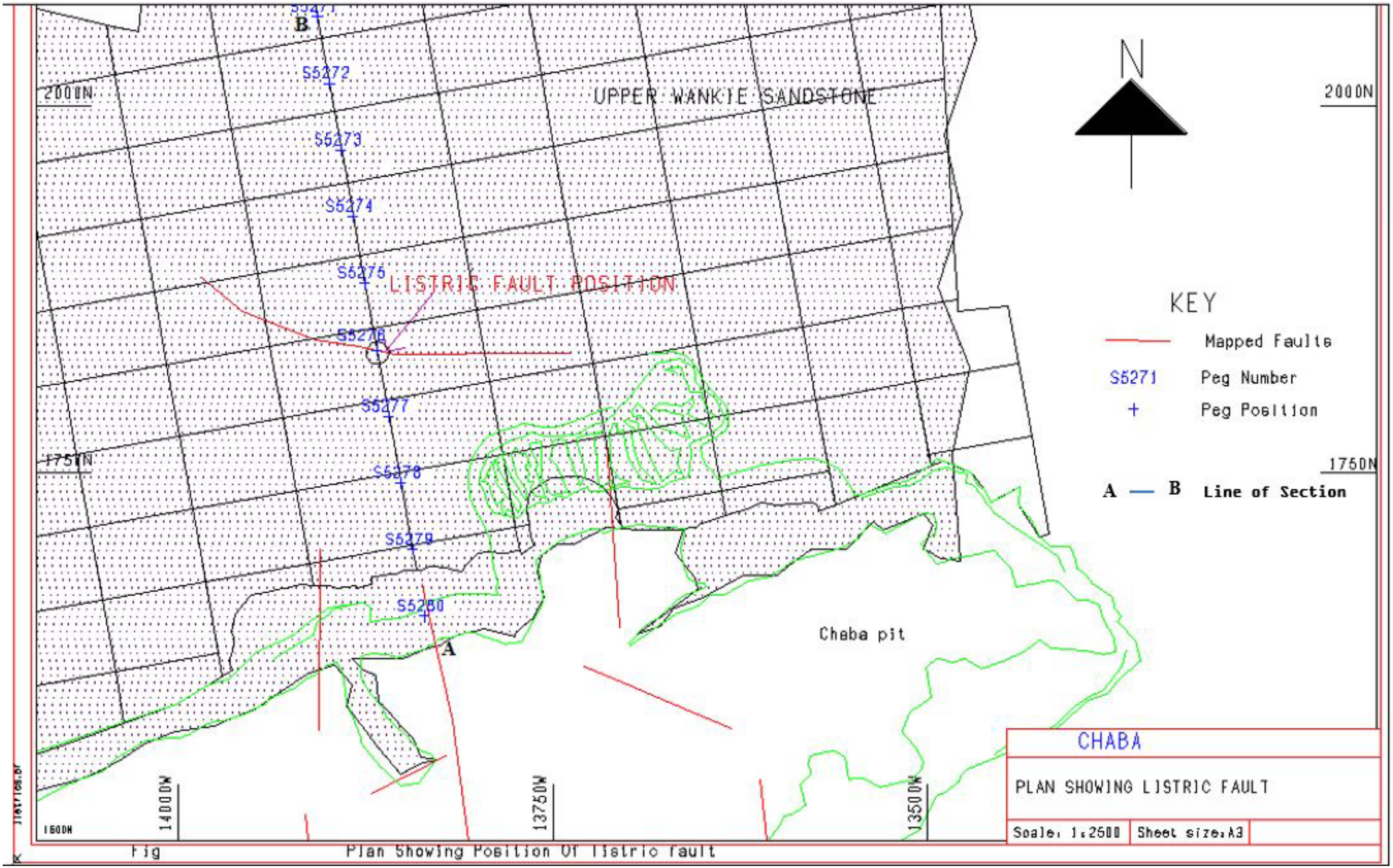


Figure 4.8: Geological plan of part of Chaba showing location of one of the listric normal faults encountered.

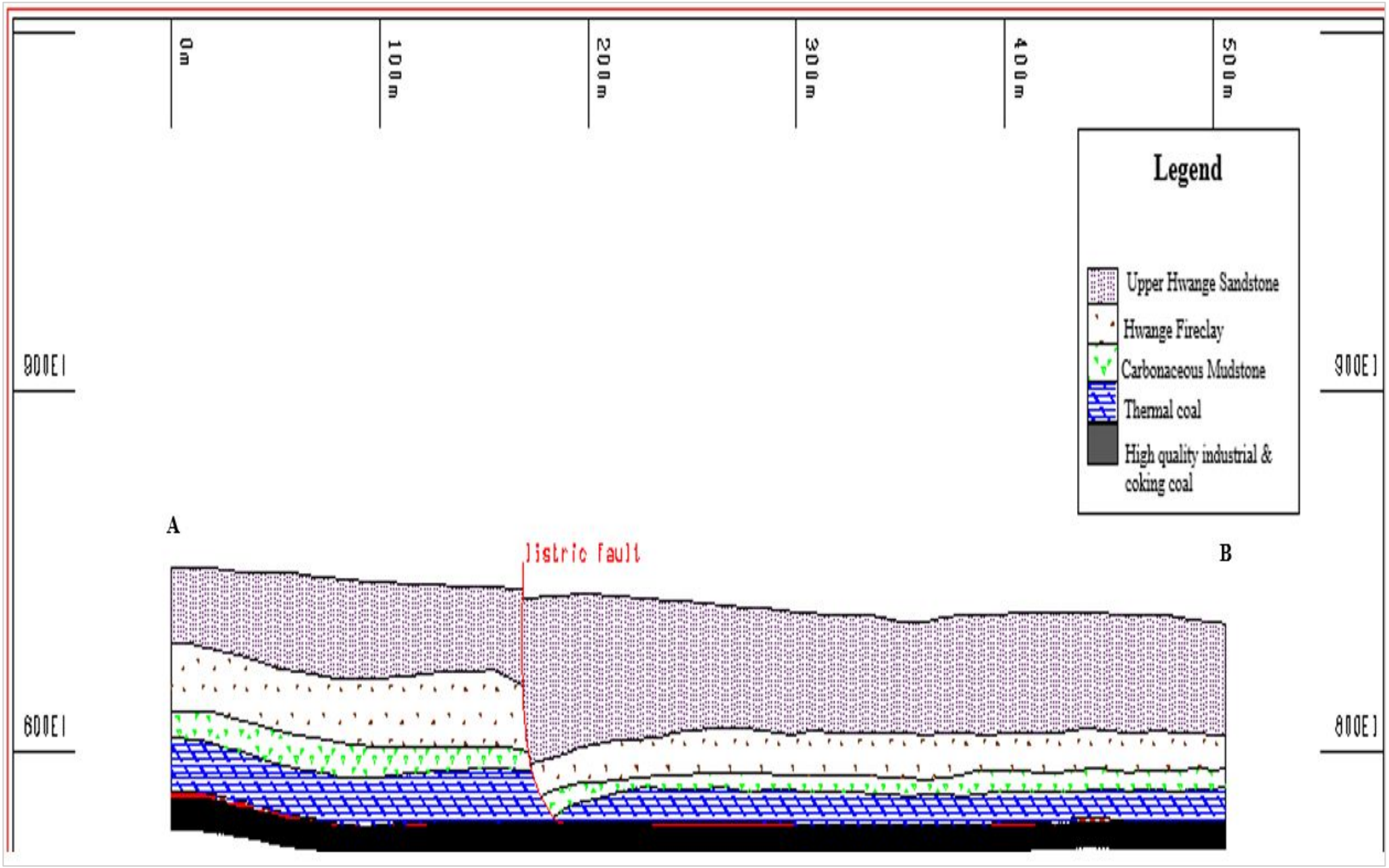


Figure 4.9 : Geological section along Chaba coal face to show a listric normal fault.

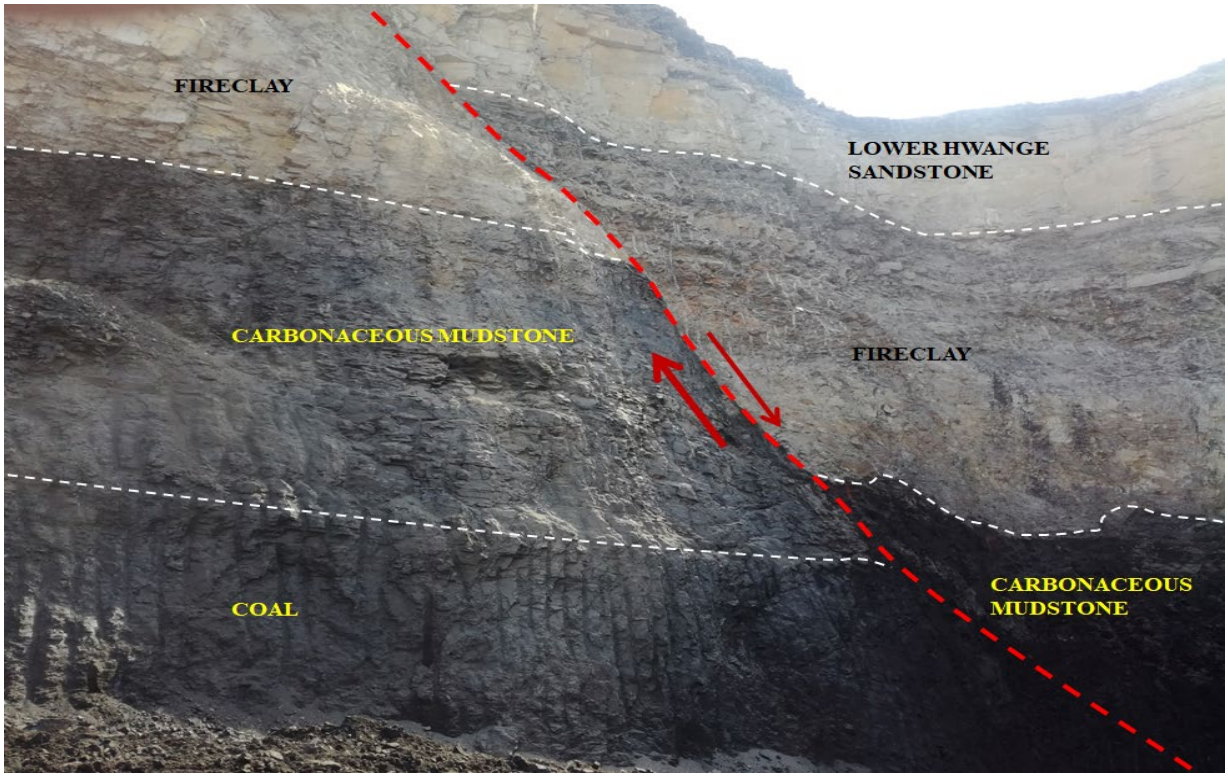


Figure 4.10: Photograph of a highwall at JKL Opencast Block (also known as the Dragline Pit) showing a listric normal fault.

4.2.2.3 Controls on the Hwange Main Seam Thickness

Coal Seam Base Profile

The current study interpreted the geological logs of holes drilled vertically from the surface during previous coal exploration programmes (part of historical data referred to in Chapter 3) conducted over the Hwange Concession and the Option area part of the northern branch of the Hwange Coalfield. The data were subsequently used to draw contours which represented footwall heights above sea-level which effectively generated a seam-base or footwall topography (referred to as footwall profile by Hwange Colliery personnel). Figure 4.11 presents the footfall topography constructed from this research.

The footwall over the Hwange Concession and the adjoining Option Area drops from approximately 720 m above sea level in the Chaba Opencast in the southeastern part of the mining area to below 520 m above sea level in the western boundary of the Option Area (Figure 4.11). Localised domes and depressions do occur here and there within the area.

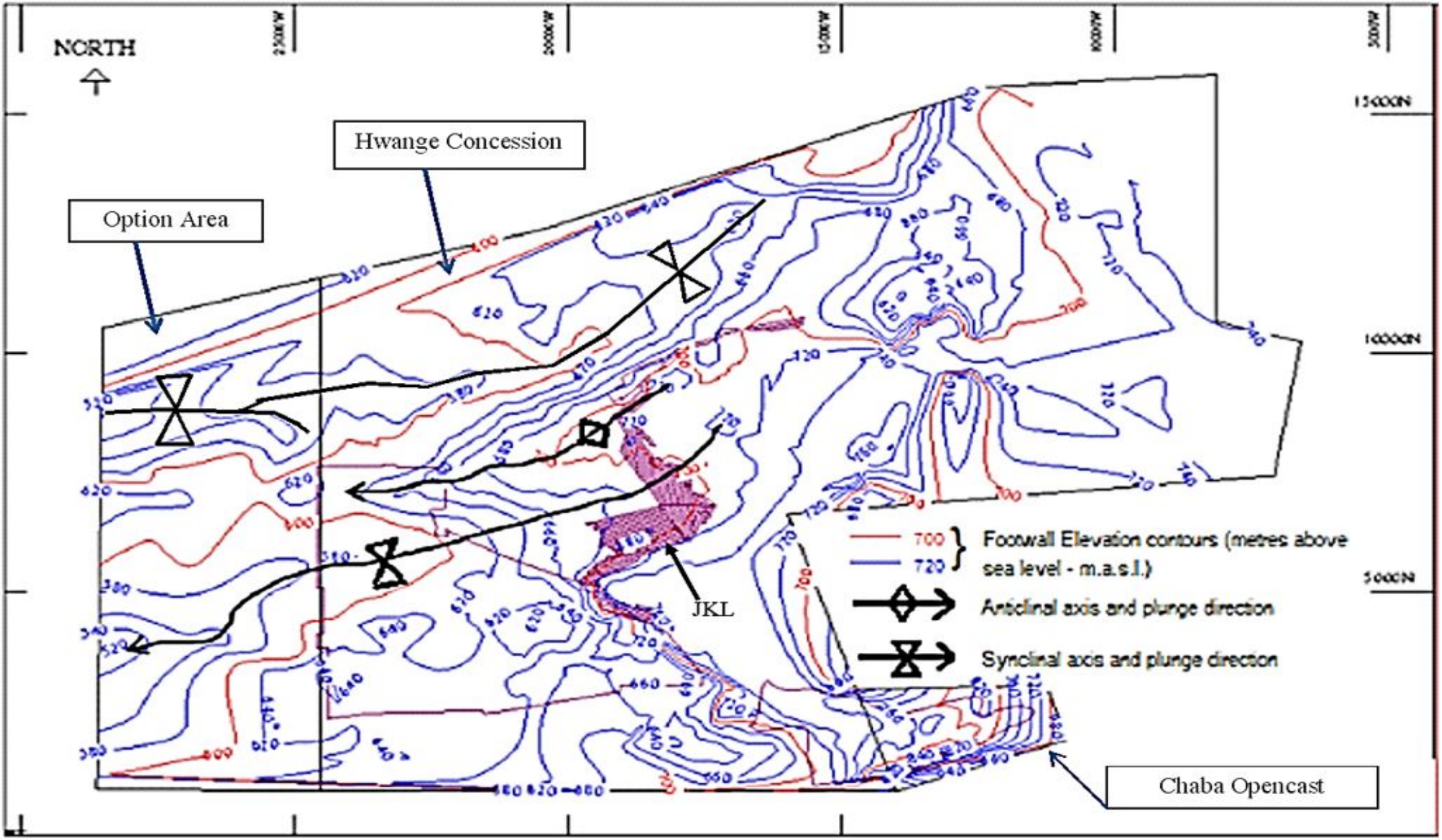


Figure 4.11: Hwange Main Coal Seam footwall profile over the Hwange Concession.

Geological Sections along Selected Lines

Geological logs of previously drilled exploration holes were further utilized in this research to draw geological sections along three selected lines as indicated in Figure 4.12. One section was drawn along the main axis of the northern section of the coal-bearing basin, and one at right angles to it. The third was drawn across a topographic high along the southern margin of the 3 Main Underground Mine. This was carried out to determine the factors that influenced the coal seam distribution and the subsequent exploitation of this fossil fuel deposit. The general drop in the footwall from the northeast to southwest, as well as its irregular profile, is evident along Section E - F. Section E –F (Figure 4.13) is a longitudinal section running parallel to the orientation of the concession.

The coal seam is thick in the topographically low areas (i.e., depressions), particularly from eastern border of the Option Area (future underground mining block) to the point in the Western Areas where the footwall commences to rise. This distribution pattern is particularly so for the good quality coking coal horizon which then thins out outside this zone. The overlying carbonaceous mudstones dominate in thickness in the topographical high ground in the northeast and southwest. In the extreme west and east, the coal seam also tends to split into multiple thin seams interspaced with grey to black mudstone layers. The short northeast-southwest trending Cross-section A – B (Figure 4.14) reveals a topographic high, against which the coal seam gradually thins before it eventually pinches out.

A NW-SE trending geological cross-section C-D drawn along the 3 Main Underground and Option Area blocks (Figure 4.15) reveals a prominent palaeotopographic depression. Within this depression the coal seam, particularly the bottom good quality coal, is significantly thicker than it is in palaeotopographic high ground. Interestingly, the deep-seated seam is devoid of any thermal coal, with the coking coal directly overlain by carbonaceous mudstones.

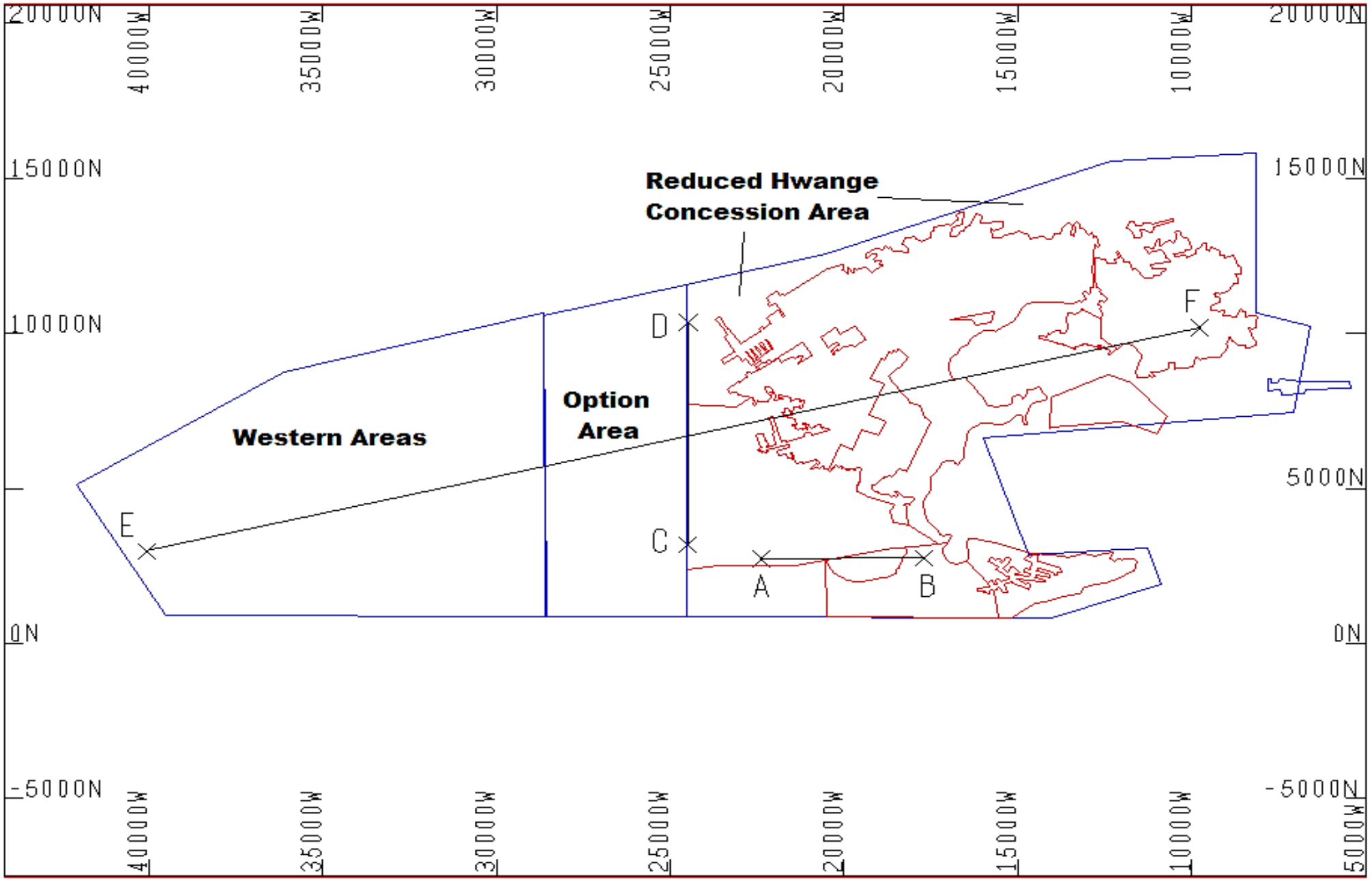


Figure 4.12: Hwange Concession and Western Areas Coalfield plan showing positions of selected section lines.

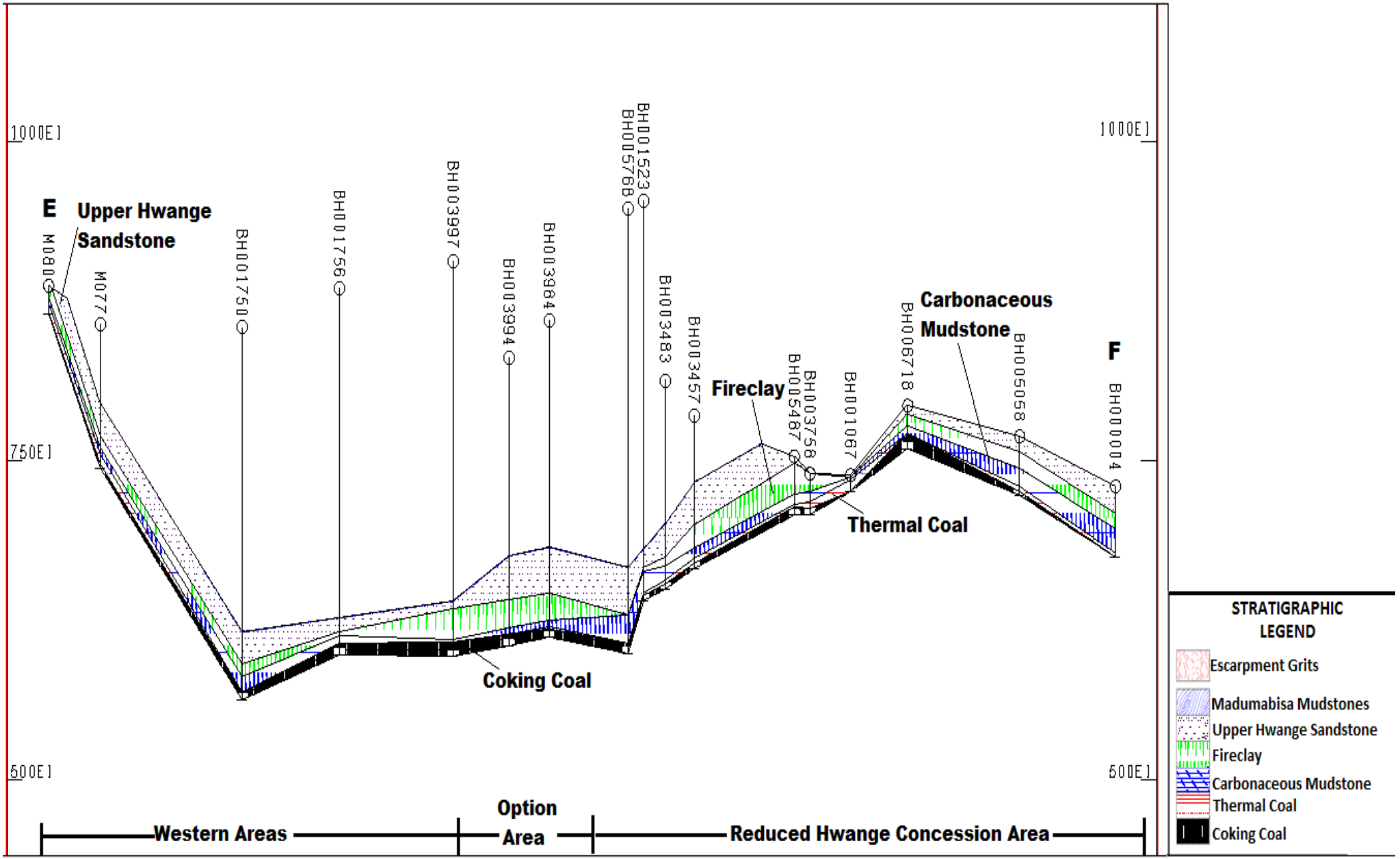


Figure 4.13: Geological section along section line E –F .

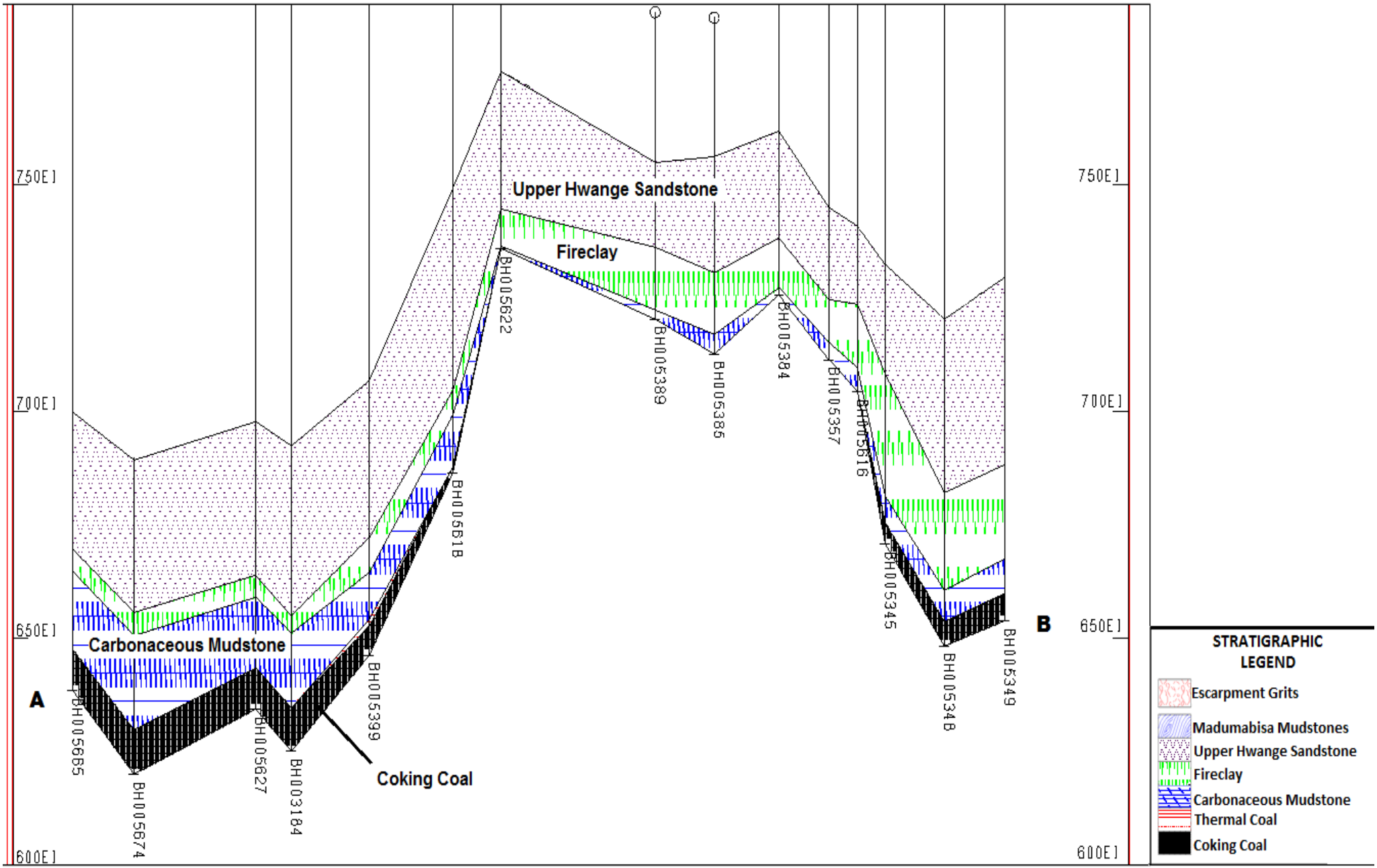


Figure 4.14: Geological section along section line A – B.

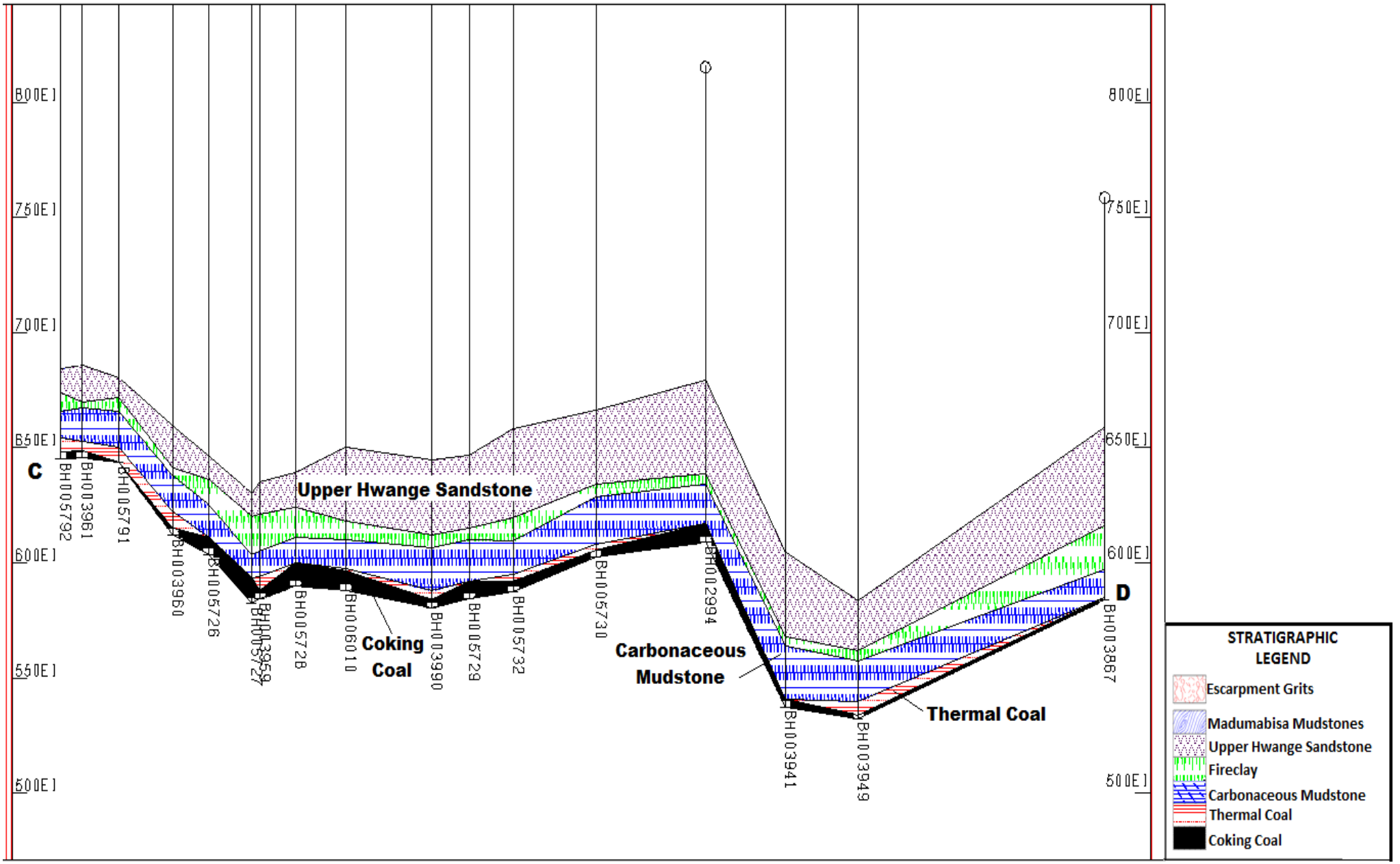


Figure 4.15: Geological section along section line C – D (drawn during this study).

4.2.3 Coal thickness Distribution over the Hwange Concession and Option Area

The analytical data from the 6 000 holes drilled over the Hwange Concession was processed and the coal seam was modeled into three horizons using the compositing procedure described in Chapter 3, Section 3.3.3 (Figure 3.4). These layers are: 1) a basal horizon of good quality coal (low ash and high volatile matter) generally with coking attributes; 2) a relatively higher ash and lower volatile matter horizon, suitable for power generation; and 3) an overlying high ash carbonaceous mudstone layer or black-shale horizon. The good quality basal portion and middle layer combined, make up what is referred to as the Commercial Seam. It averages 12 m in thickness, and relative partitioning at 12 m into thermal and coking coal, the pattern is not straight forward, but the general observation is that where one type increases in thickness, the other decreases, and vice versa. Unfortunately drill-holes sunk over the Western Areas were not systematically sampled and thus were not included in the contouring exercise. As a result, contours end against the Option Areas boundary with the Western Areas Coalfield.

Thickness contour plans for the two commercial coal horizons were drawn during this study using the cut-off grades of ash cumulative maximum of 15% and volatile matter cumulative minimum of 23.5% for high grade usually coking coal, and ash cumulative maximum of 24% for thermal coal to show the lateral distribution thickness of two coal grades. The results are shown in figures 4.16 and 4.17, respectively.

4.2.3.1 Coking Coal

A study of Figure 4.16, which is a high grade and usually coking thickness contour plan for the Hwange Colliery Concession, reveals the following:

I. A high-quality coal horizon (generally with coking attributes) ranges in thickness from 0 to 12 m.
II. A lateral zone of peak thickness values over the Hwange Concession is y-shaped.
III. When superimposed on Figure 4.11 (footwall contour plan), the main NW-SE trending axis of maximum coking coal thickness zone was found to coincide with a major southwest plunging trough or synclinal feature which evidently runs from the 3 Main Underground Block into the Option Area.

4.2.3.2 Thermal Coal

The thickness distribution pattern for the thermal coal, which is a coal with a cumulative maximum ash content of 25%, is interestingly similar to that of coking coal in that the "y" shape of the peak values of the coking coal thickness described above are also evident in thermal coal (Figure 4.17). The major differences between the thickness distribution contours for the two coal types are the three large patches devoid of thermal coal. These are:

i) The northeastern part of the Hwange Concession.
ii) The northwestern part of the Hwange Concession; and
iii) The near central part of the Option Area.

This pattern demonstrates the somewhat antipodal relationship between the two coal types: when one thickens, the other thins out.

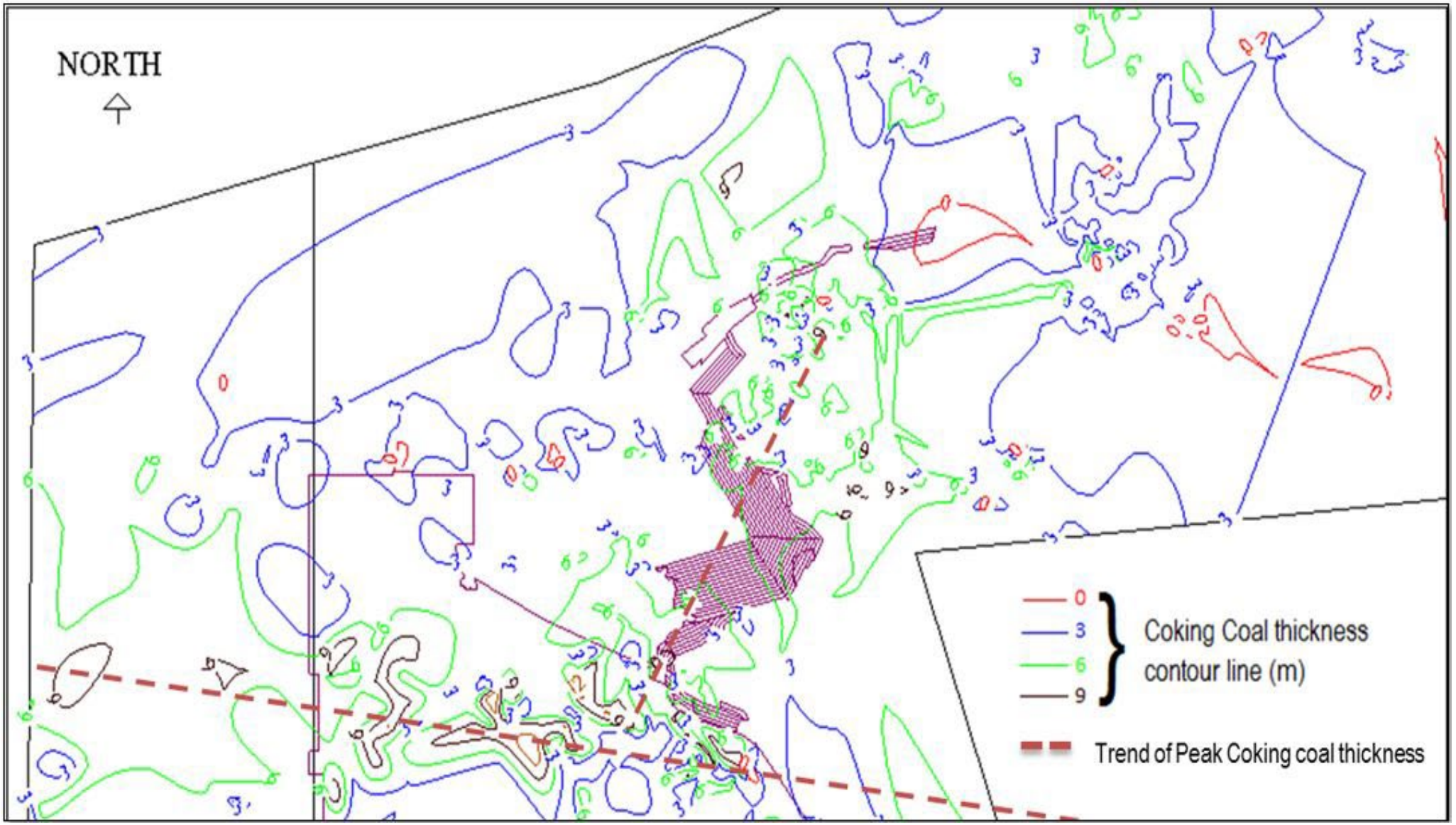


Figure 4.16: Hwange Concession thickness contour plan for the high grade coking coal.

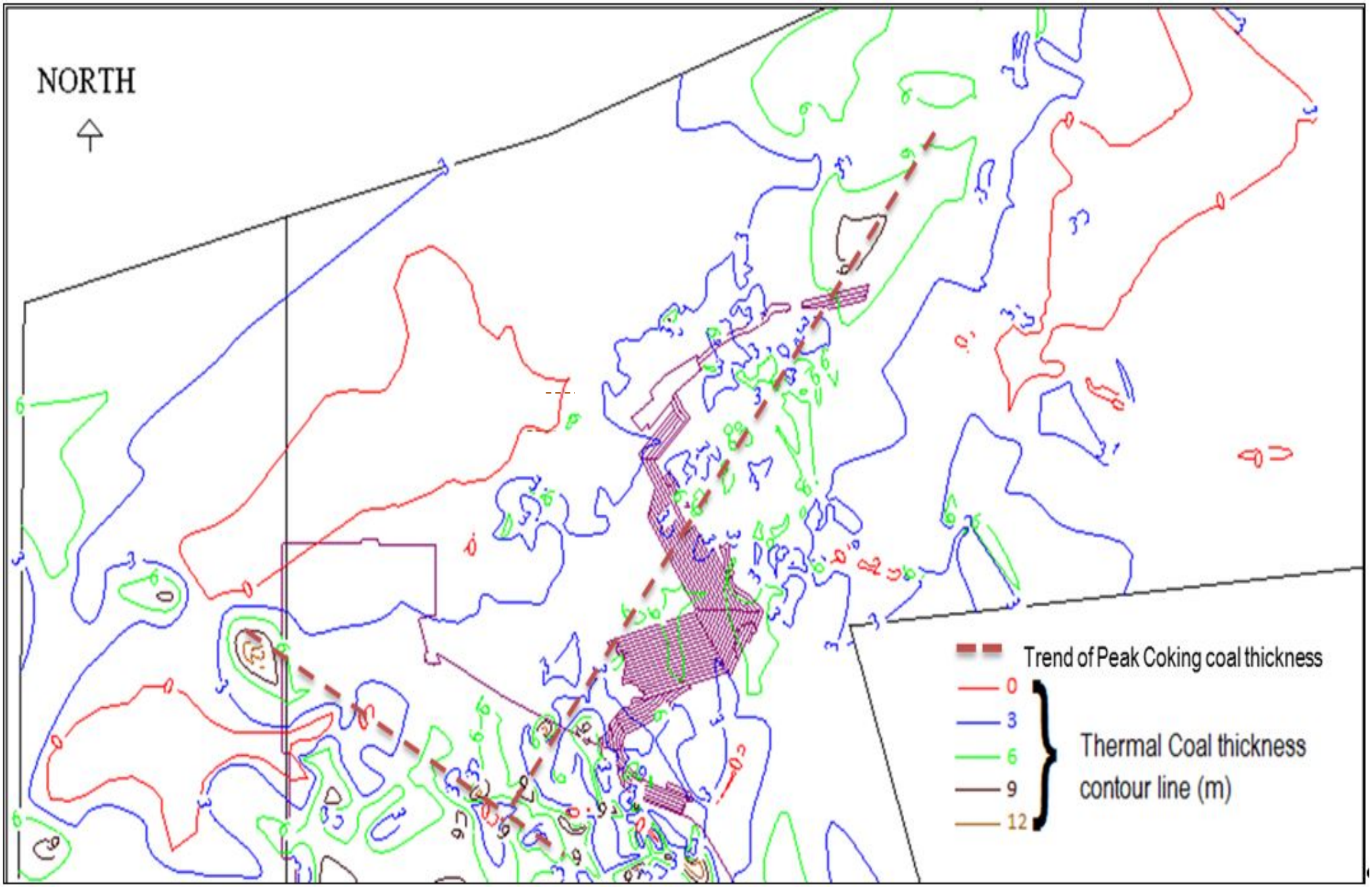


Figure 4.17: Hwange Concession thickness contour plan for the thermal coal.

4.2.3.3 Free Swelling Index Values of the Mine Site from Historical Drill-hole Data

Unlike proximate analyses which are mandatory and thus are carried out on a routine basis, the free swelling index (FSI), which is one of the key properties of coking coal, is not determined routinely on coal exploration and evaluation drilling at Hwange Colliery. As a result, FSI determinations were carried out on only a few drill-holes data available during this research. There is therefore a paucity of free swelling data to define the distribution of the value over the study area. As a result, the picture presented in figures 4.18 and 4.19, which are of swelling index value contour plans for the coking and coal horizon in 3 Main Underground and JKL Opencast mines, respectively, may not present the actual picture on the ground.

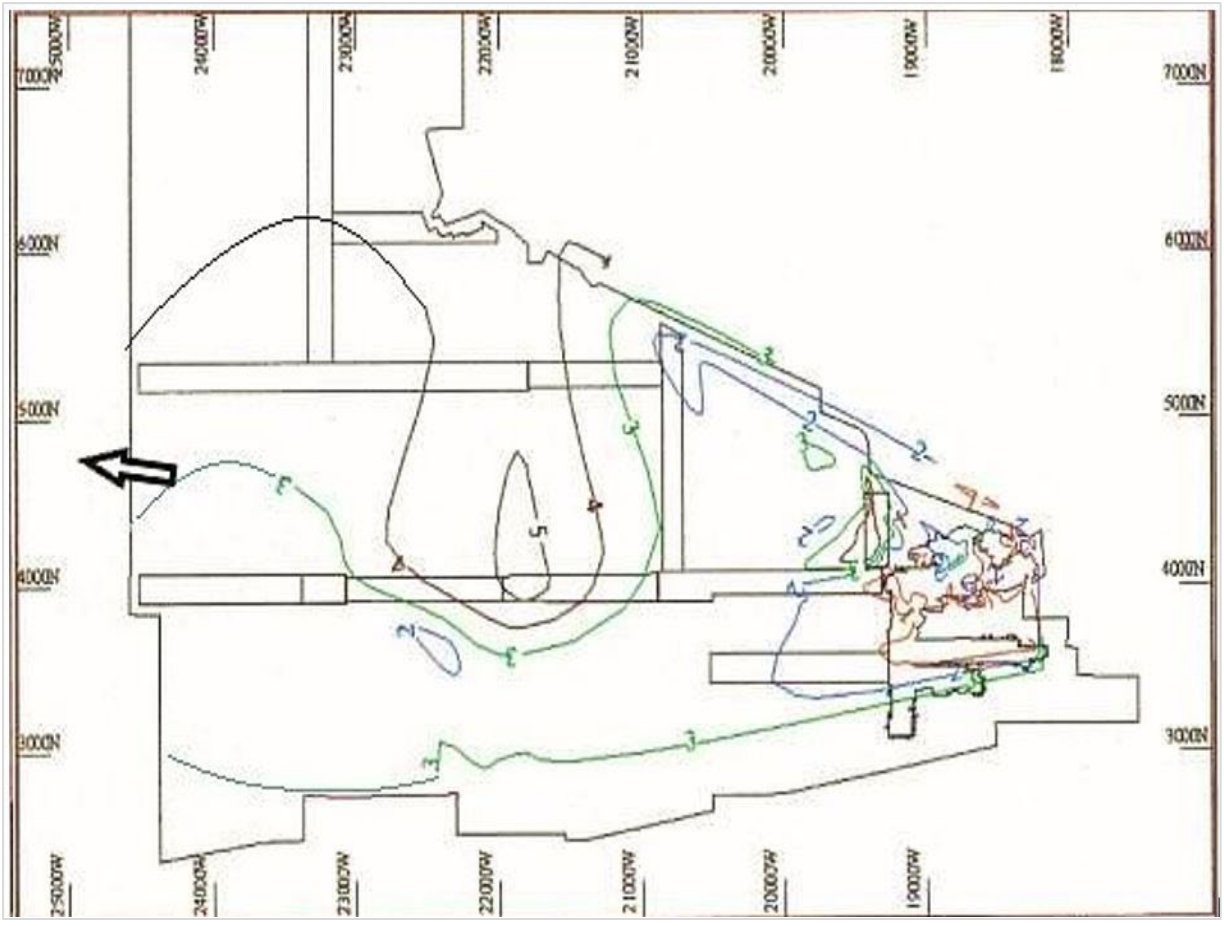


Figure 4.18: Free Swelling Index Value contour plan for 3 Main Underground Block based on borehole data available at time of study. The arrow points in the direction of overburden increase as well as direction of coal seam base plunge.

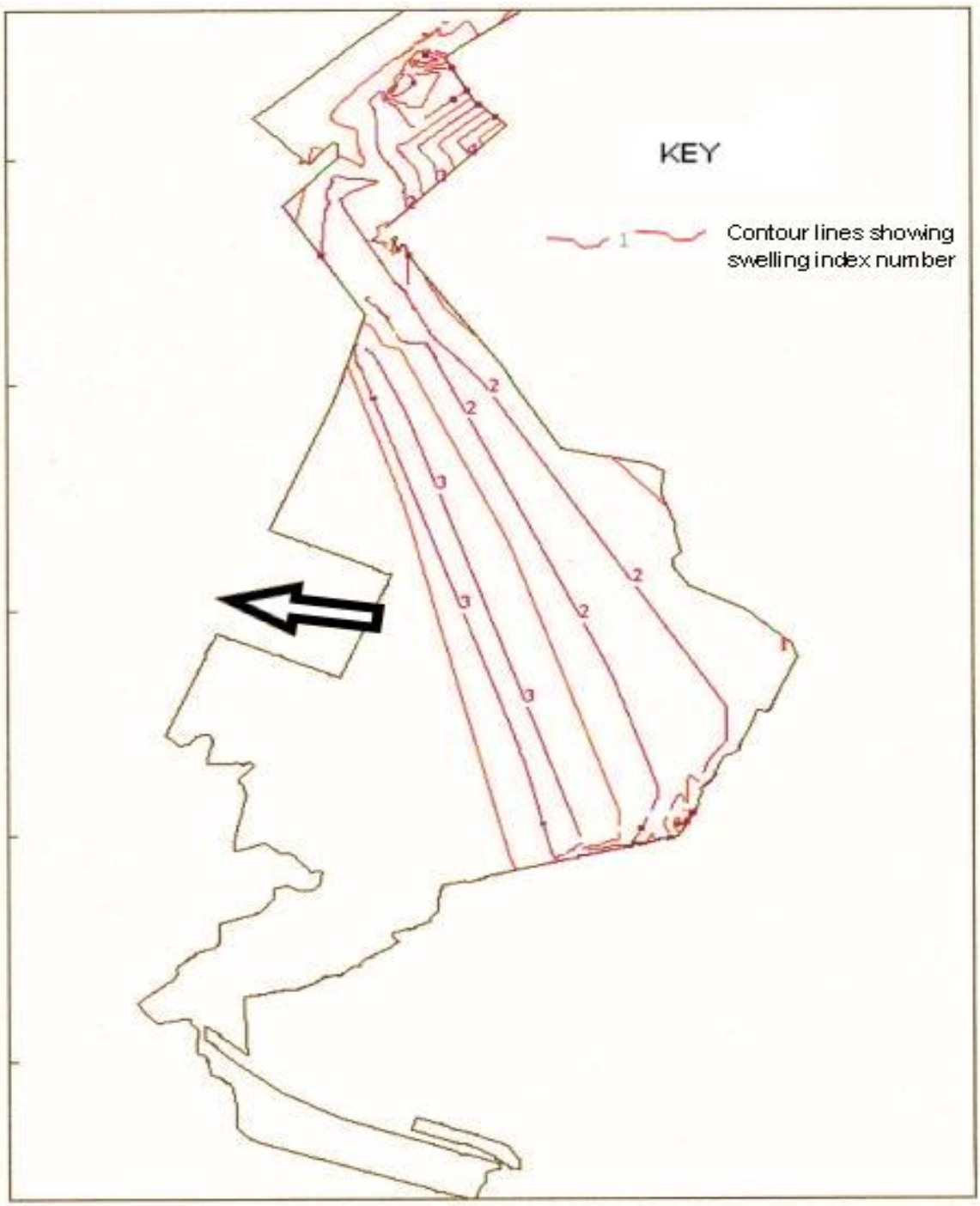


Figure 4.19: Free Swelling Index value contours for JKL Block based on data from historical drill-holes. The arrow points in the direction of overburden increase as well as direction of coal seam base plunge.

NB JKL is one of the Hwange Colliery operations' coal blocks, no samples were collected during the current study as operations over the block were on hold due to financial constraints.

Information generated from historical drill-holes drilled over the Hwange Concession is that over elevated areas, particularly in Chaba, the coal has a low swelling index. In the latter case, the Chaba coal was found with low ash. Where the coal occurs above the 620 m above-sea-level contour, and the overburden is relatively thin (less than 50 m), the swelling index number is less than one. On the other hand, where the footwall topography is depressed (i.e., below the 620 m above sea level), and the depth of overburden cover is significant, and the swelling number is found to be concomitantly higher. It is noted that the relationship between free swelling index is an antithetic one.

4.3. Implications of Geological Aspects of Hwange Coalfield on Coal Attributes

Geological work conducted over the Hwange Concession and the Western Areas coalfields has established that the site is a type-area for the Karoo Supergroup. The most economically important feature of the succession is the occurrence of the coal seam or K^2 towards the base of stratigraphic pile. Coal seams as sedimentary rocks were formed in a variety of geological environments. A study of the available literature reveals that tectonics, palaeotopography and depositional environments played a crucial role in determining coal type, rank, coal seam geometry and coal quality. The attributes of the coals of southern Africa were primarily controlled by their location relative to cratons and mobile belts, changes in groundwater regimes or gradual transgressions (Hobday, 1987). It is also observed that, while influencing the thickness and areal extent of the coal seams, these factors were even more important in determining microlithotypes, organic and inorganic composition of the coals.

4.3.1. Implications of Palaeotopography on Coal Formation

The footwall profile modelled from the historical drill-hole data indicates that the surface upon which the Hwange coal was deposited was irregular and consisted of localised depressions (presumably due to glacial erosion) and palaeo-topographic highs. Granitic and paragneissic rocks of the pre-Karoo floor outcrops, such as one which outcrops near the entry to the Hwange Colliery opencast mining operations and the Entuba crystalline inlier as described earlier in this chapter, are corroborative evidence for these topographic highs. The Hwange coal seam is observed to thin or pinch out over these topographic highs. On the other hand, thick layers of coaly material accumulated in the topographic lows, or depressions, forming relatively thick coal seams. Figure 4.14 (Section 4.2.2.3) presents these two scenarios with the west and east

parts of the section characterised by two depressions where the Hwange Main attains maximum thickness. A topographic high occurs in the middle of the section and the coal seam in this part thins out.

Topographically, swamp or lake waters would normally be expected to occur in the topographically depressed areas, covering or submerging the dead vegetative matter, subjecting the plant matter to reducing conditions such as those required for the formation of vitrinite. Slow subsidence in these depressed areas would have led to greater proportions (thickness wise) of plant matter accumulation and hence thicker peats and seams. With progression towards the topographically higher and more stable areas, such as the Chaba Opencast area, the accumulation of plant matter is envisaged to have slowed, while ground water regimes declined, with both aspects leading to thinner seams with vegetative matter becoming progressively more exposed to sub-aerial and oxidizing conditions. Such environments lead to the formation of the more inertinitic forms of organic matter which is consistent with Figure 2.15 (Chapter 2) which presents a model put forward by Falcon (2013).

The proposed scenarios outlined above are reflected in the Hwange Colliery. The 3 Main Underground and the adjoining Option Area coal mining blocks are occupied by a depression (lower than 620 m above sea level), and a significantly thicker coal seam, which also has a significantly thicker vitrinite-rich coal horizon at the base. The Chaba Opencast area exhibits three attributes: a) the coal was deposited 700m above sea level, unlike in 3 Main and Option Area mining blocks where the seam occurs at 620 m above sea level and below; b) the coal seam is significantly thinner than at the 3 Main Underground mine; and c) the seam is overlain by relatively thin overburden (approximately 30–60 m). This interpretation assumes that there has been no uplift in the coal base, neither has there been significant subsequent erosion of the rocks overlying the coal seam. The consequence of the latter scenario is that the remains of the vegetative matter at Chaba were, in the main, such that only the thin (1–2 m) basal portion of the Hwange Main Seam remained below the water table, (in reducing environment); while the rest of the supernatant part of the seam was above the water table, in an oxidising environment and also close to surface where sub-aerial oxygen occurring above the overburden rocks such as the Upper Hwange Sandstone Formation and the Hwange Fireclay had access to the peat. As a result, the Chaba coal is predominantly non-coking, as the environment is interpreted to

have been an oxidising one. At 3 Main, the two sites A and B are in topographically lower ground (approximately 620 m above sea level) than at Chaba (approximately 700m above sea level) as indicated on Figure 4.11. A relatively thicker (3.5 to 4 m) portion of the seam would have been under the water table, hence in a reducing environment. Under this environment vitrinite would be expected to be the dominant maceral.

Furthermore, rapid subsidence associated with graben tectonics would quickly bury the vegetative matter, shielding it from oxidation. This is particularly so where the remains of the vegetative matter are covered by a thick overburden in the depression areas. This would preclude access of oxygen to the dead vegetative matter.

4.3.2 Implications of Tectonics and Structural Geology on Coal Formation and Condition

As described earlier in Section 4.2.2, the Hwange Coalfield is traversed by several faults of varying displacement magnitude. The amount of displacement on the Deka Fault estimated at 300 m and the occurrence of subsidiary faults, among which is the Chambumo Fault, had a significant impact on the mineability of the coal seam on the northern part of Hwange Coalfield. The irregular northern boundary of the mined-out area of Hwange Colliery (Figure 2.1, Chapter 2) is due to abandoned mining headways towards the fault after operations encountered severe ground conditions coupled with a progressively thinning out coal seam as stated in the occasional reports by the company's technical staff (Maponga, 1989). Displacement magnitude on the northeast-southwest trending Entuba Fault which runs sub-parallel to the Deka Fault has severely affected mining operations in Chaba as mining advances towards the fault. The coal has been rendered out-of-specification for a number of user sectors, particularly agriculture where cobble-size coal is the preferred product as reported by the Hwange Marketing Department to the company's ISO 9001:2008 October 2009 Committee Meeting. The coal is heavily cleaved. The relatively smaller-scale faulting occurring in the intervening ground has also adversely affected mining operations. These become more numerous towards the southwest where the Deka and the Entuba faults draw nearer to each other as described earlier in this chapter. Faulting of such magnitude and frequency could have generated enough heat energy to alter some of the pre-existing coal attributes, although localised, such as the devolution of oil and methane base derivatives from the reactive macerals. Several coal

exploration drill-holes have intersected coal-bed methane in the Chambumo Fault area of the Hwange Concession (Maponga, 1989, 2014).

The presence of exudatinite, a solidified oil-based product, which has been observed in several of the Hwange coal samples during this study supports this concept. This has been proposed to be the case in methane and bitumen-rich coals such as those in the Lubimbi Basin to the east of Hwange (Falcon, personal communication, 2017). Geological mapping in the coal production areas has often encountered shear zones and sympathetic fractures mapped as joints (which could be listric faults), as well as hardened coal associated with the relatively larger-scale faults.

The Hwange Concession has been drilled and geologically mapped in detail, with the latter conducted as part of geological condition prediction ahead of mining, but no igneous intrusions have been encountered. However, an old geophysical survey plan (ground magnetics) drawn by the Anglo-American Corporation geological staff indicated that the survey had picked up three geophysical anomalies (Figure 4.20) which were interpreted as an igneous intrusive body below the coal seam, but there is no appreciable effect on the coal, if ever any. Regrettably, no follow up investigations were conducted on these anomalies.

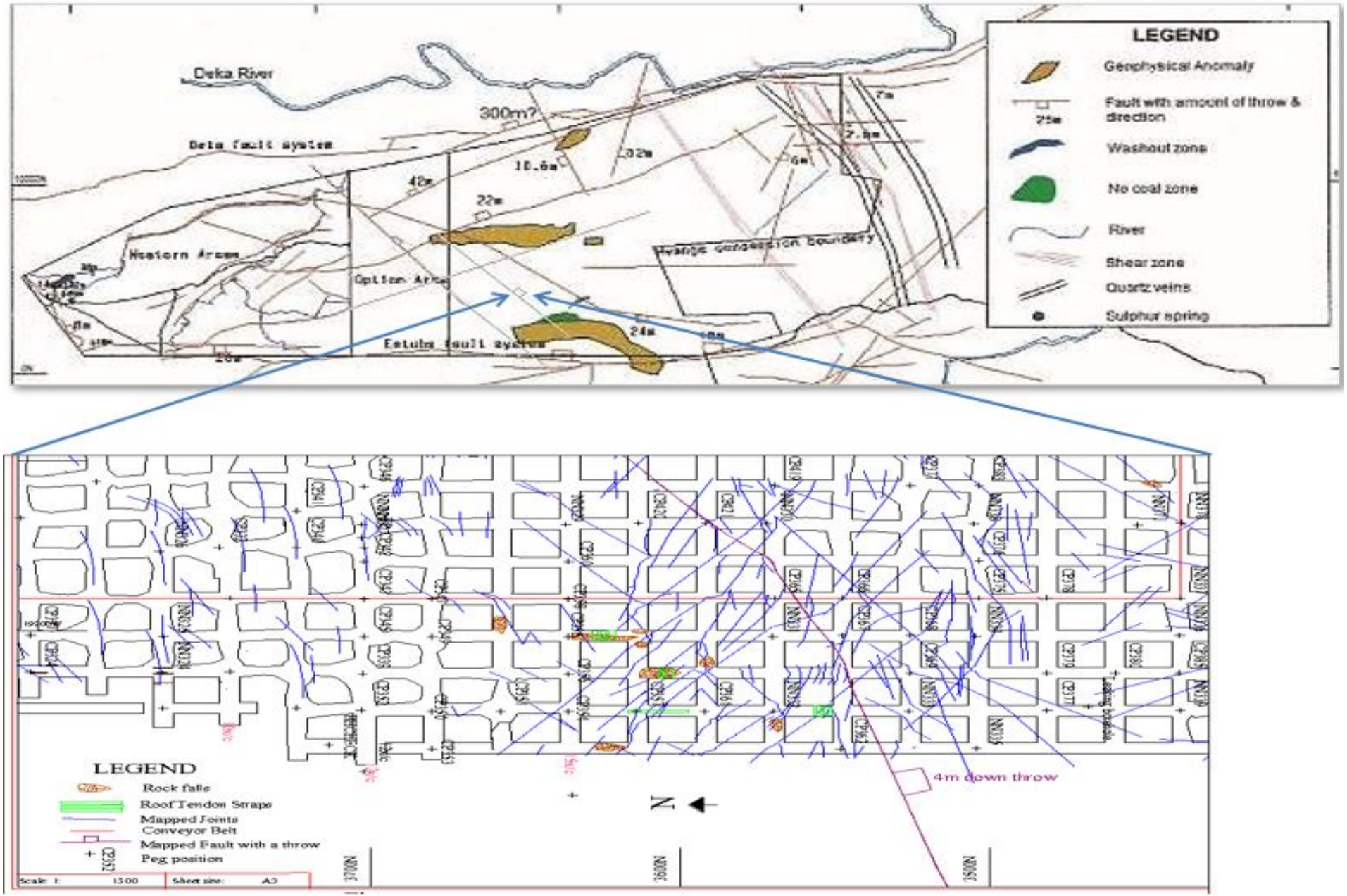


Figure 4.20: Structural plan of Hwange Concession and location of mined-out part of 3 Main showing mapped faults and joints. (Note some of joints may well be listric faults).

The results of the geological investigations may be summarised as follows:

I. The nature of faulting is essentially normal and listric normal.
II. Within the basin thick coals occur in topographically low areas, while coals thin out in topographically high areas.
III. Zones of thick coal seams occur, and these may represent areas where the palaeo-vegetation, which is the precursor to the coal seam, prolifically grew while that part of the basin subsided relatively fast and preserved the vegetal matter.
IV. The thicker coals in deeper areas exhibited good FSI whereas thinner coals in shallow areas (areas with thin overburden cover) and elevated heights (in terms of height above sea-level) are associated with dominantly non-coking coal properties.

4.4 Coal Characterisation

This section presents results of the various standard and specialised analyses carried out to provide data required to classify all the coal samples mentioned in Chapter 3 according to the end users' varied specifications. The reader is reminded to consult Table 3.1 and Table 3.2 to review the sample identification, locality, and different analyses conducted.

4.4.1. Proximate Analysis

Proximate analysis is the most applied analysis for the basic determination of any coal, including thermal and coking coals. It is the simplest and most commonly form of coal evaluation, and it forms the basis of many coals purchasing and performance prediction indices employed by utility operators (Zhu, 2014). As mentioned in Chapter 3 Section 3.5.1, the analysis is conducted to determine, by a prescribed method, the relative amounts of moisture, ash, volatile matter and, indirectly, by difference, fixed carbon (Zimmerman, 1979; Zhu, 2014). Proximate analyses for the coal samples collected from the two mines operated by the Hwange Colliery are reported below.

4.4.1.1. Proximate Analyses for Chaba Channel 1 and Channel 2 Samples

Table 4.1 presents analytical results of coal samples from Chaba Channel 1, while Table 4.2 presents results for Chaba Channel 2. As mentioned in Chapter 3 Section 3.4.1, Chaba Channel 1 was sampled at 3 m intervals, while Chaba Channel 2 was sampled at 1 m intervals. Appendix 4.1 presents the same data in Table 4.3 and 4.4 in graphical form.

In both sets of analytical results, there is a vertical variation in coal quality in terms of ash and volatile matter contents. In the Chaba Channel 1 samples which were sampled at 3 m intervals (Table 4.3), the basal sample 0-3 m comprises high-grade data and thereafter the quality progressively decreases towards the top of the seam.

In Chaba Channel 2 which was sampled at 1 m intervals, the basal 1 m (i.e., sample number 0-1 m) has very low ash and high volatile matter of 5.54% and 28.84%, respectively. In the overlying 1 m horizon, the figures are 8.64% for ash and 23.81% for volatile matter contents. In other words, the coal quality over the 2 m vertical interval deteriorates before improving in the third interval. Thence, and to the top of the seam, the coal quality variation shows a cyclic pattern. But, overall, and based on the ash content and volatile matter contents the coal quality is high in the 0-3 m samples at the base (ash content < 10% with volatile matter > 23%) and then deteriorates towards the top of the seam (i.e., ash content >10% and volatile matter < 20%).

Table 4.1: Proximate Analysis Results (air dry) for Chaba Channel 1.

Sample Code (m)	Moisture content (%)	Ash content (%) a.d	Volatile matter (%)	Fixed Carbon (%)
Chaba 6-9m	0.5	20.2	19.5	59.8
Chaba 3-6m	0.3	15.0	23.6	61.1
Chaba 0-3m	0.2	7.9	28.8	63.1

Air dry: a.d

Table 4.2**:** Results for proximate analyses of the Chaba Channel 2.

Sample Code (m)	Moisture (%)	Ash content (%) a.d	Volatile matter (%)	Fixed Carbon (%)
Chaba 7-8m	1.86	11.93	20.99	65.22
Chaba 6-7m	1.81	12.88	20.14	65.17
Chaba 5-6m	1.82	12.35	19.46	66.37
Chaba 4-5m	1.74	13.4	18.15	66.71
Chaba 3-4m	1.57	8.55	19.78	70.10
Chaba 2-4m	1.42	6.04	24.16	68.38
Chaba 1-2m	1.43	8.64	23.81	66.13
Chaba 0-1m	1.20	5.54	28.84	64.42

Sample Chaba 0-1 m: base of the seam; air dry: a.d

4.4.1.2. Proximate Analyses for 3 Main East Channel Samples

Table 4.3 presents proximate analyses for 3 Main East channel coal samples. The samples were taken at 30 cm intervals. The analyses reveal that the basal 210 cm (from 0-210 cm) of the coal seam along this channel is characterised by ash value of less than 10%. The exception is the sample with a sample code 1545 (representing sample range 90cm-120cm), which yielded an ash content of 12.1%. This, however, is within the limits of ash values (i.e., a maximum of 15%) for coking coal as defined at Hwange. The upper samples possess ash contents greater than 10% and volatiles matter less than 23%.

Table 4.3: Proximate analyses of 3 Main East Channel coal samples

Sample Code	Sample Interval (cm)	Moisture (%)	Ash content (%) a.d	Volatile matter (%)	Fixed Carbon (%)
1553	330 – 360	0.4	15	20.2	64.4
1552	300 – 330	1	11.1	20.7	67.2
1551	270 – 300	0.5	10.9	23	65.6
1550	240 -270	0.4	10.7	21.8	67.1
1549	210 – 240	0.5	12.2	27.3	60
1548	180 -210	0.8	8.7	25.5	65
1547	150 – 180	0.6	7.4	27.2	64.8
1546	120 – 150	1.1	7.9	23.5	67.5
1545	90 – 120	0.8	12.1	24.2	62.9
1544	60 – 90	0.6	9.3	27.4	62.7
1543	30 – 60	0.9	7.4	27.6	64.1
1542	0 -30	0.2	8.9	29.3	61.6

Dry basis: a.d

4.4.1.3. Proximate analyses for 3 Main South Channel coal samples

The proximate analysis results for the 3 Main South Channel samples are presented in Table 4.4 while the same data is presented in Appendix 4.1. In this suite of samples, better qualities in terms of ash content (< 10% ash) lie in the middle part of the seam; while lower grades are found at the base and in the uppermost samples. Volatile matter content is highly variable but generally higher than the other suites of samples so far presented. Volatile matter values range from an anomalously low 19.5% in one sample in the good quality low ash section, to unusually high values (over 30%) towards the base of the seam and up to 28% in the upper section. Samples tests were rerun to confirm the anomalies and the rerun confirmed the anomaly. In fact, the same sample interval (120-150cm) in Channel 3ME also records a moisture content

value which is above any other sample, although in this case it is 1.1.%, which is significantly less than the 3.9% recorded in 3ME Channel.

Table 4.4: Proximate analyses of 3 Main South Channel coal samples.

Sample Code	Sample Interval (cm)	Moisture (%)	Ash content (%) a.d	Volatile matter (%)	Fixed Carbon (%)
1564	300 – 330	0.6	7.9	25.6	65.9
1563	270 – 300	0.2	16.5	24	59.3
1562	240 – 270	0.2	11.8	26.8	61.2
1561	210 – 240	0.8	5.9	28.5	64.8
1560	180 – 210	0.9	7	26.6	65.5
1559	150 – 180	0.4	9	24.5	66.1
1558	120 – 150	3.9	9.6	19.5	67
1557	90 – 120	0.5	8.8	29.6	61.1
1556	60 – 90	0.5	7.8	30.1	61.6
1555	30 – 60	0.5	13.8	31.4	54.3
1554	0- 30	0.4	14	25.2	60.4

Dry basis: a.d

The parameters analysed in this study which were, moisture, ash, volatile matter, and fixed carbon (which was calculated), have important bearing on both a coal's cokability and combustion behaviour. Proximate and petrographic analysis determine the coal rank, and, in addition, determines coal type which, in turn, determines whether a coal falls into the coking coal category or not.

The ash content, which is essentially the mineral and related inorganic impurities in coal, is important regarding coal used in making coke. The usual practice is to acquire coals with lower ash contents, as an increase in ash increases the slag volume in a blast furnace and leads to reduced blast furnace productivity. Ideally for coke-making the feedstock to the coke ovens should be a coal with a maximum of 10% (Ekbote, 2020). Worldwide, for coke making, the feedstock is a coal of not more than 12% (Zimmerman, 1979). Coal with marginally higher (up to 15%) ash may be washed to yield a clean coal with 10% or less ash values, usually 8 to 9%. Ash values for samples analysed during the study range from 5.54% to 20.2% with the lowest ash content recorded in the lowest (basal) sample in Chaba Channel 2 and the highest ash value

recorded in topmost sample in Chaba Channel 1. The ash values in the lower portion of the Hwange coal seam therefore fall within the range of coking coal.

Volatile matter is an important parameter in the classification of coking coals and to a larger extent determines the fixed carbon limit. Carbon is essential for reduction in the blast furnace and removal of volatile matter which is largely removed in the coke ovens leaves a coal mass of higher carbon. Thus, low volatile matter coal will give more carbon per tonne of coal. The ideal range of volatile matter for coking coal is 28 to 30% for standard by-product slot-type ovens (Zimmerman, 1979). Proximate analysis carried out on the Hwange coals from 3 Main and Chaba shows that the basal 1 to 2.5 m of the seam at 3 Main yields volatile matter content which fall within the limits of straight coking coal; while at Chaba only the lowest sample (0-1 m) has volatile matter content that falls within the limits of coking coal. The higher samples (up to the mining roof in 3 Main with volatile matter contents falling within the 24 to 27% may be used as blending feedstock. Coal occurring higher up the seam (beyond 1 m) may not qualify as blend coking coal. Fixed carbon values range from 59.3% to 70.10%. Only two samples, one in Chaba Channel 1 (topmost sample) and the other in 3 Main South Channel (last but one sample from coal base), recorded fixed carbon values of below 60%. Thus, the ash and fixed carbon values of the Hwange coals at least for the lower half of 3 m of the seam meet the range for coking coal.

Volatile matter in coal also plays a critical role in electricity generation, with utilities preferring coals with narrow ranges of volatile matter of 25 – 35% for flame stabilisation (Thomas, 1992; Ekbote, 2020). Besides increasing flame length, volatile matter helps in easier ignition of coal and sets limits on furnace height and volume. In addition, it influences secondary air requirements as well as secondary oil support. Samples from the top part of the Hwange coal seam should be able to provide coal with a contractual volatile matter content of 19.3% (Schedule A2 of the 2003 agreement between Hwange Colliery and ZPC).

An important point to make here, which formed part of the motivation to conduct this research, lies in some changes in the performance of the Hwange coals after 2005. Prior to 2005, proximate analysis alone was used on a routine basis at Hwange Colliery to determine the cut-offs for two coal products: Zimbabwe Power Company's feedstock to their power generation (Agreement between Wankie Colliery Company Limited and Zimbabwe Power Company

(Private) Limited on the Supply and Purchase of Coal, 2003) whose cut-off is set at the cumulative ash maximum of 25%; and that for making coke for the metallurgical industry whose cut-off based on laboratory tests had been a cumulative ash maximum of 15% and a cumulative minimum volatile matter content of 23.5%. Until 2005 all other energy applications (other than electric power generation at Hwange) of coal had been using coking coal as their feedstock material. The commissioning of the Chaba Opencast Mine in 2005 brought in a technological challenge. Mining of the two products as defined above satisfied the thermal coal specification for the Zimbabwe Power Company, but the other product which, though it met the existing coking coal cut-off of cumulative ash content maximum of 15% and cumulative volatile matter content minimum of 23.5%, did not coke when fed into the coke battery on mine site. As a result, Hwange Colliery could not meet its coking coal agreement with its customers in metallurgical industries.

4.4.1.4 The Hwange Seam Ash Vertical Trend Current Samples and Drill Core Samples

While there is a general increase in the ash content with height above seam base, some" jumps" in the ash values are observable both in analyses carried out during this study, particularly in the 3 Main East Channel whose samples were analysed during the current and in both Tables 4.3 and Table 4.4 with the ash value showing a dramatic rise or fall. Working with quality data from elsewhere within the Hwange Coalfield, Pallocks (1987) considers this as due either to a sudden subsidence of the swamp floor or a rise in the water table.

Another feature of some significance in the interpretation of the palaeographic environment (during coal formation) is the significantly high ash content of 14 to 25% in the first 50 cm to 1 m above the coal footwall that has been recorded in analyses of core samples (Tables 4.5 and 4.6). Channel samples collected and analysed during this study also reveal this feature. In 3MS Channel the basal 30 cm shows an ash content of 14% followed by an ash content of 13% in the next 30 cm before the ash value significantly decrease to 7.8%.

Table 4.5: Hwange Main Seam proximate analysis, free swelling index (BH006750 core samples).

Borehole I.D	Sample I.D	Depth from (m)	Depth to (m)	Moisture (%)	Ash (%)	Volatile matter (%)	Sulphur (%)	Phosphorus %)	Swelling Index
BH00675	SM01	35.81	36.57	0.1	77.5	12.4	0.31	0.051	0.0
“	SM02	36.57	37.57	0.1	78.6	11.2	0.30	0.102	0.0
“	SM03	37.57	38.57	0.1	82.2	9.6	0.26	0.026	0.0
“	SM04	38.57	39.57	0.4	22.2	21.0	0.32	0.080	0.0
“	SM05	39.57	40.57	0.1	71.4	12.9	0.31	0.091	0.0
“	SM06	40.57	41.72	0.3	37.4	17.2	0.49	0.065	0.0
“	SM07	41.72	42.07	0.3	38.3	18.4	0.43	0.010	0.0
“	SM08	42.07	42.57	0.3	32.7	18.8	0.39	0.009	0.0
“	SM09	42.57	43.07	0.3	35.5	17.8	0.54	0.010	0.0
“	SM10	43.07	43.57	0.3	32.1	19.0	0.46	0.022	0.0
“	SM11	43.57	44.07	1.3	6.9	29.2	1.77	0.011	1.0
“	SM12	44.07	44.57	0.8	13.3	24.2	1.82	0.009	1.0
“	SM13	44.57	45.07	0.6	15.3	23.3	0.73	0.037	0.5
“	SM14	45.07	45.57	1.3	7.5	28.7	1.90	0.013	1.0
“	SM15	45.57	46.07	0.8	13.8	24.0	0.73	0.054	0.5
“	SM16	46.07	46.57	0.8	13.4	24.4	0.71	0.102	0.5
“	SM17	46.57	47.07	0.5	18.8	22.4	0.72	0.101	0.5
“	SM18	47.07	47.57	0.6	15.6	23.1	1.10	0.016	0.5
“	SM19	47.57	48.07	0.9	10.5	25.6	1.00	0.025	0.5
“	SM20	48.07	48.57	1.2	8.8	27.3	1.64	0.014	0.5
“	SM21	48.57	49.07	0.8	13.9	24.1	1.00	0.027	0.5
“	SM22	49.07	49.57	1.3	6.4	29.7	1.67	0.013	0.5
“	SM23	49.57	50.07	0.7	14.9	23.9	1.56	0.018	1.0
“	SM24	50.07	50.57	0.8	12.4	24.9	1.75	0.010	1.0
“	SM25	50.57	51.07	1.3	7.5	28.6	1.66	0.019	1.0
“	SM26	51.07	51.57	1.2	9.3	26.6	1.80	0.010	1.0
“	SM27	51.57	52.04	0.6	16.8	23.8	0.67	0.239	0.5

N.B. “Depth from” and “depth to” denotes depth of sample interval from the surface. Samples analysed were air dried.

Table 4.6: Hwange seam proximate analysis and Free Swelling Index Free for BH006404 core samples.

Borehole I.D	Sample I.D	Depth from (m)	Depth to (m)	Moisture (%)	Ash (%)	Volatile matter (%)	Sulphur (%)	Phosphorus (%)	Swelling Index
BH00640	SM01	76.52	77.02	0.4	49.3	15.4	1.06	0.017	0.0
“	SM02	77.02	77.52	0.4	32.0	15.0	0.75	0.018	0.5
“	SM03	77.52	78.02	0.5	35.3	16.7	0.75	0.018	0.0
“	SM04	78.02	78.52	0.5	36.8	17.5	1.58	0.076	0.0
“	SM05	78.52	79.02	0.5	26.6	19.6	1.63	0.079	0.0
“	SM06	79.02	79.52	0.6	16.6	22.4	0.79	0.043	0.5
“	SM07	79.52	80.02	0.7	13.7	23.7	0.77	0.042	0.5
“	SM08	80.02	80.52	0.7	20.0	20.0	0.77	0.043	0.5
“	SM09	80.52	81.02	0.7	13.4	23.6	1.20	0.043	1.5
“	SM10	81.02	81.52	0.6	15.3	23.0	1.19	0.041	1.0
“	SM11	81.52	82.02	0.8	12.1	24.1	1.19	0.042	1.5
“	SM12	82.02	82.52	0.9	7.7	26.6	1.00	0.012	1.5
“	SM13	82.52	83.02	0.8	10.9	25.2	1.03	0.012	1.5
“	SM14	83.02	83.52	0.9	8.3	26.2	1.33	0.005	2.0
“	SM15	83.52	84.02	0.9	8.0	26.3	1.57	0.006	2.5
“	SM16	84.02	84.52	1.0	7.1	26.8	1.58	0.009	3.0
“	SM17	84.52	85.02	0.8	9.6	25.7	1.76	0.009	2.5
“	SM18	85.02	85.52	1.0	8.9	26.0	1.79	0.008	3.0
“	SM19	85.52	86.02	0.6	14.0	23.0	1.79	0.008	2.5
“	SM20	86.02	86.52	0.6	15.6	22.6	1.76	0.008	3.0
“	SM21	86.52	87.12	0.5	25.9	19.5	1.79	0.005	2.0

The trend along 3ME Channel is similar, though the ash content 8.9% (of the basal 30 cm) is relatively lower compared to the basal 30 cm of the former. Pallocks (1987) considers this as evidence for a previous fluviodeltaic clastic depositional environment of the Lower Hwange Sandstone Formation (K^1) before this was replaced by a shoreline peat swamp-mud environment of the Hwange Main Seam (K^2).

4.4.2. Total Sulphur content in Chaba Coal Samples

In both Chaba Channel 1 and Chaba Channel 2, the total sulphur content was found to be high (3.0% and 3.06%, respectively) at or near the base of the coal seam (Table 4.7). This is followed by a decline (to 1.17% in sample interval 3-6 m in Chaba Channel 1 and 0.89% in sample interval 3-4 m in Chaba Channel 2). An increase in the total sulphur content was observed in coal samples higher up the coal seam as seen in Table 4.7 and Figure 4.21 for Chaba Channel 2.

Table 4.7: Total sulphur analyses for Chaba Channels 1 and 2 coal samples.

CHABA CHANNEL 1		CHABA CHANNEL 2	
Sample Identification (m)	Total sulphur (%)	Sample Identification (m)	Total sulphur (%)
6-9	1.55	7-8	1.77
		6-7	1.27
3-6	1.17	5-6	1.21
		4-5	1.23
		3-4	0.89
0-3	3.0	2-3	1.13
		1-2	2.13
		0-1	3.06

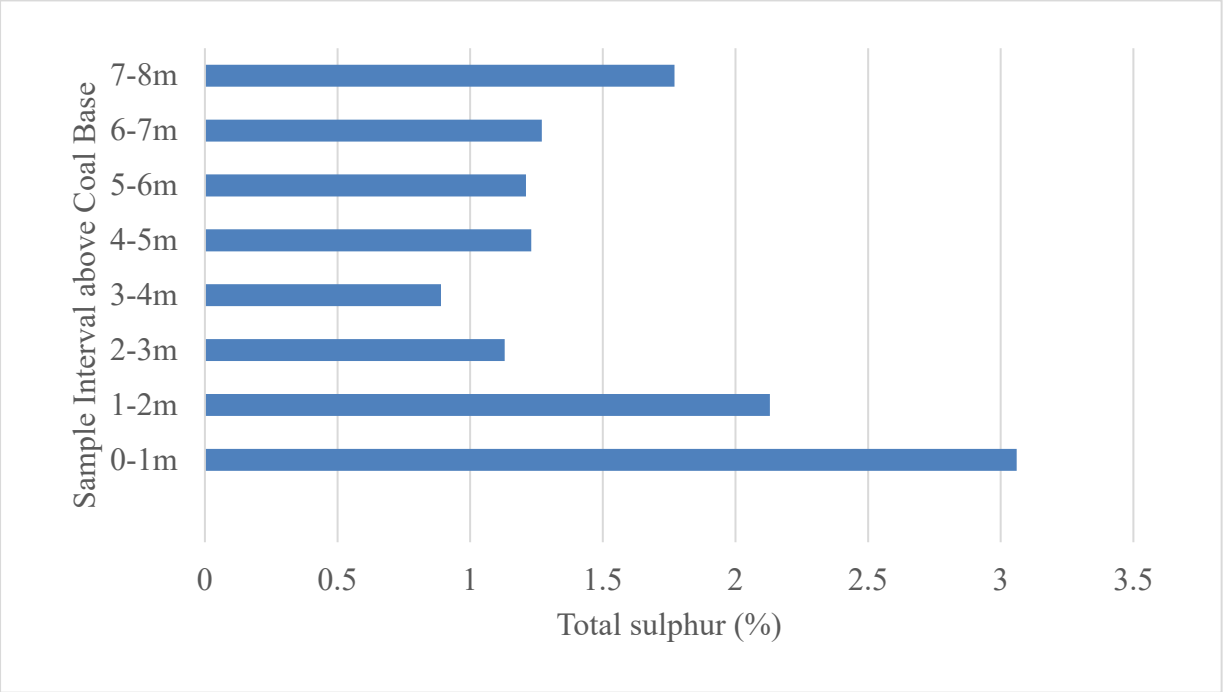


Figure 4.21: Variation of total sulphur along Chaba Channel 2.

4.4.2.1. Variation of total sulphur along 3 Main East and 3 Main South channels

The total sulphur content of the coal at the 3 Main Underground Mine is high near the coal seam base and declines towards the middle before it increases towards the top of the seam. Data presented in Table 4.8 shows a sulphur content of 2.08% in the basal 0-30 cm coal sample and the sulphur content declines steadily to 0.90% in sample 210-240 cm, before it starts to increase with height above coal seam base to 2.09 in sample interval 330-360 cm along Channel 3 Main East. A similar scenario is revealed along 3 Main South Channel. The total sulphur is shown to be 2.15% in the basal sample (0-30 cm) and declines steadily to 0.86% in sample 270-300 cm, after which the total sulphur content gradually increases to 0.95% in the last sample (sample 270-300 cm).

Table 4.8: Variation of sulphur content along 3 Main East and 3 Main South.

3MAIN EAST		3MAIN SOUTH	
Sample Identification (cm)	Total sulphur (%)	Sample Identification (cm)	Total sulphur (%)
330-360	2.09	300-330	0.95
300-330	2.01	270-300	0.86
270-300	1.87	240-270	0.87
240-270	1.75	210-240	1.88
210-240	0.90	180-210	1.08
180-210	1.10	150-180	1.18
150-180	1.60	120-150	1.18
120-150	1.75	90-120	1.19
90-120	1.77	60-90	2.01
60-90	1.82	30-60	2.00
30-60	1.85	0-30	2.15
0-30	2.08		

4.4.2.2. Variation of sulphur at 3 Main sites A and B

Two sites A and B from the 3 Main Underground Mine (see Figure 3.5 in Chapter 3 for location) contributed three samples each for total sulphur analysis. Their analytical results are shown in Table 4.9. The table reveals that from both sites, the total sulphur diminishes in content from the top of the coal seam to the bottom for both sites.

Table 4.9: Total sulphur content in coal samples from 3 Main sites A and B.

SITE	Sample Identification (m)	Total sulphur (%)
SITE A	3.50-4.25	2.08
	2.00-2.50	2.1
	0.25-0.75	1.58
SITE B	4.00-4.25	0.9
	2.50-2.75	1.0
	0.25-0.75	2.12

Sulphur plays a crucial role in both coking and thermal coal. Sulphur in coal increases the blast furnace fuel consumption and is a highly deleterious element in steel making where it adversely affects the mechanical properties of steel and is the cause of brittleness in steel (Lu, *et al*., 2013). Lattice defects in steel are typical adverse features in steel products. Low sulphur contents are therefore vital for the coal used in metallurgical applications. Ideally the coal for metallurgical applications should have less than 1% sulphur (Zimmerman, 1979; Stach, *et al.,* 1982; Lu, *et al*., 2013).

The total sulphur values in coal in the 3 Main coal range from 0.85 to 2.15% with most of the samples recording values marginally above 1%. In Chaba total sulphur values range from 0.80% to 3.06%. In both mining blocks the high sulphur values are recorded in the basal samples (50 cm in 3 Main and 1 m in Chaba). These values, apart from the fact that the sulphur could be washed significantly to low lower levels, renders Hwange coals suitable for metallurgical applications in terms of sulphur levels. Determination of sulphur levels in coal is also vital as the element has negative effects on the environment where it has been linked to the generation of acid mine generation as well as the emission of sulphur dioxide gases.

4.4.3. Phosphorus Analyses

This section presents results obtained from the phosphorus analysis carried out on the coal samples from different locations of the two mines which are in operation during the study period (Chaba Opencast Mine and 3 Main Underground Mine).

4.4.3.1. Phosphorus analysis for Chaba Channel 1 and Channel 2 Samples

Table 4.10 presents the results obtained from the phosphorus analyses of Chaba Channel 1 and Chaba Channel 2. The data for both channels reveals that the basal part of the coal seam has low phosphorus content. At an interval of 0-3 m horizon in Channel 1, phosphorus content of

0.021% was reported, while a comparable seam horizon (average of the first three samples) has an averaged value of 0.020%. In Channel 1, the phosphorus value decreases to 0.019%, after which it increases to 0.046% with distance from seam base. The vertical distribution of phosphorus content in Chanel 2 shows a decrease from 0.031% in the basal 1 m to 0.013% in the sample interval 2-3 m. Thereafter there is a steady and continuous increase in the phosphorus value to 0.058% at the top of the coal seam (Table 4.10).

Table 4.10: Vertical distribution of phosphorus values along Chaba channels 1 and 2.

CHABA CHANNEL 1		CHABA CHANNEL 2	
Sample Identification (m)	Phos. in Coal (calculated from P_2O_5) (%)	Sample Identification (m)	Phos. in Coal (calculated from P_2O_5) (%)
6-9	0.046	7-8	0.058
		6-7	0.051
3-6	0.019	5-6	0.027
		4-5	0.018
		3-4	0.014
0-3	0.021	2-3	0.013
		1-2	0.015
		0-1	0.031

Phos: Phosphorous

4.4.3.2. Phosphorus content in 3 Main East and 3 Main South channels

Table 4.11 presents the phosphorus analysis results for the coal samples collected at 30 cm intervals along 3 Main East and 3 Main South channels. There is a general increase in the phosphorus content with distance above the coal footwall for both channels.

Table 4.11: Phosphorus analysis for coal samples collected at 3 Main East and 3 Main South.

3MAIN EAST		3MAIN SOUTH	
Sample Identification (cm)	Phosphorus content (%)	Sample Identification (cm)	Phosphorus content (%)
330-360	0.012	300-330	0.011
300-330	0.011	270-300	0.010
270-300	0.006	240-270	0.009
240-270	0.005	210-240	0.008
210-240	0.005	180-210	0.006
180-210	0.004	150-180	0.005
150-180	0.005	120-150	0.004
120-150	0.003	90-120	0.005
90-120	0.002	60-90	0.004
60-90	0.003	30-60	0.003
30-60	0.003	0-30	0.003
0-30	0.005		

4.4.3.3. Phosphorus content in 3 Main sites A and B coal

Table 4.12 presents the phosphorus content for the six coal samples collected from 3 Main sites A and B. Both sites A and B are in what may be described as a low phosphorus coal area, with the elemental composition of the phosphorus found below 0.010%. At Site A, there is a steady and continued increase of the element from the bottom of the coal face to the top. Around Site B, however, the vertical variation is cyclic, commencing with phosphorus values of 0.0045%, and decreasing to 0.0023%, before increasing to 0.005%.

Table 4.12: Phosphorus analysis for 3 Main sites A and B coal samples.

SITE‘	Sample Identification (m)	Phosphorus content (%)
SITE A	3.50-4.25	0.006
	2.00-2.50	0.003
	0.25-0.75	0.003
SITE B	4.00-4.25	0.005
	2.50-2.75	0.002
	0.25-0.75	0.005

Like sulphur, phosphorus is a highly deleterious element in coal which is used as a fuel and reductant in the steel manufacturing blast furnace. In the steel making process, phosphorus increases the propensity of a metal to become brittle at low temperatures (Lu, *et al.*, 2013). Together with non-metallic inclusions and sulphur, level of phosphorus is used to draw distinctions between commercial quality, high quality and very high-quality steel (Lu, *et al.*,

2013). Phosphorus levels in coal used in the steel making processes as well as the ferrochrome industries in Zimbabwe and South Africa ideally need coal with a maximum of 0.010% (Hwange Marketing Department, 1995).

Hwange coals from the 3 Main Underground Mine therefore fall within the desirable limits of the phosphorus levels entering the blast furnace. The coals with marginally higher phosphorus contents of up to 0.015% could be blended with very low phosphorus levels of 0.003% to yield a coal product of 0.010% desired by most of the blast furnace plants in southern African.

4.4.4. Calorific Value analysis

This analysis was carried out to determine the heating value of the coals from different parts of the Hwange Colliery mines, and the correlation was drawn between the calorific values and the ash, volatile matter, and fixed carbon contents of the samples.

Table 4.13: Calorific values (MJ/kg) ash content (%) for Chaba and 3 Main Mines.

Sample I.D (cm)	3MS (MJ/kg)	3ME (MJ/kg)	3MS (Ash%)	3ME (Ash%)
0-30	30.40	32.49	14.0	8.9
30-60	32.55	33.14	13.8	7.4
60-90	32.16	32.29	7.8	9.3
90-120	31.95	30.47	8.8	12.1
120-150	33.35	32.83	9.6	7.9
150-180	33.06	33.07	9.0	7.4
180-210	33.31	34.72	7.0	8.7
210-240	30.93	31.17	5.9	12.2
240-270	28.93	Not determined	11.8	10.7
270-300	32.19	32.03	16.5	10.9
300-330	31.15	31.70	7.9	11.1
330-345	Not determined	29.84	Not determined	15.0
Chaba Channel 1				
Sample I.D (m)	(MJ/kg)		Ash %	
0-3	34.90		7.9	
3-6	31.07		15.0	
6-9	31.36		20.2	

The results of the Chaba 1, 3ME and 3MS calorific values (heat contents) are summarized as follows:

I. In Chaba Channel 1 the calorific value ranges from 31.07MJ/Kg to 34.90MJ/Kg. The basal sample (0-3m) exhibiting the lowest ash content reports the highest CV value of 34.90MJ/Kg; The CV value decreases in the samples higher in the coal seam as ash contents increase as shown in Table 4.12 and Figure 4.22.
II. At the 3 Main Underground Mine, samples with ash values of 10% and below show CV values greater than 32 MJ/Kg (Table 4.12).

Unfortunately, there was no calorific value determined on Chaba Channel 2. The samples were collected from Hwange in Zimbabwe during Phase 3 by which time the mine budget had been overrun.

Calorific value (CV) determines, in part, the value of a coal as a fuel for combustion application (Sun., *et al*., 2010). It is an important parameter for which coal is mined for combustion application and is the most used benchmark of coal quality (Zhu, 2014). It is the basis for the purchase of coal for all but metallurgical industries. For example, the coal supply purchase agreement between Zimbabwe Power Company (ZPC), which operates the 920MW thermal power plant at Hwange, and the various producers of coal feedstock to this coal-fired thermal utility, is based on 24.75MJ/Kg and a volatile matter content of between 18 and 22% averaging 19.3% (Schedule A2 of the agreement between Hwange Colliery and ZPC, 2003) In major coal utilizing and trading countries such as India, calorific value is used for the gradation of non-coking coal; for example Grade 1, Grade 2 and Grade 3 coals are coals with CV values of 29.28 MJ/kg; 28.03-29.28; and 26.78- 28.03MJ/kg, respectively (Ministry of Coal, Government of India, 2019).

The source of heat in a coal is ultimately the carbon in the coal. Hence the higher the carbon in the coal, the higher the CV value of the coal. Thus, coal rank affects calorific value (Taylor *et al*., 1998; Suárez-Ruiz and Ward, 2008b; Wagner *et al*., 2018), with the value increasing in correlation with the increasing rank. Another coal property that affects calorific value is coal type. Of the three maceral groups, liptinite reports the highest calorific value at lower ranks, with the value increasing with rank in vitrinite; and inertinite reports a high calorific value in all ranks (Wagner *et al*., 2013). The relationship of coal rank and coal type is discussed in

Section 4.4.6. Furthermore, the amount of inorganic impurities (i.e., the ash levels) in coals determines the ultimate calorific value of a coal. There is, therefore, an inverse relationship between the ash levels and the CV. In the Hwange coals, it has been established that a CV value of 24.25 MJ/kg translates to an ash value of the coal of 25%.

The calorific values of Hwange coals collected from Chaba and 3 Main mines range from 28.93 to 34.90 MJ/kg (Table 4.13). Thus, Hwange coals fall within the limits of grades 1 and 2 which makes India as a potential market for the Hwange non coking coal.

The relationships between ash yield, volatile matter and fixed carbon for the Hwange coals are shown in figures 4.22, 4.23 and 4.24, respectively. Correlation coefficient between ash yield and calorific value (R^2) is 0.211; while the R^2 of that between the heat value and the two parameters of volatile matter and fixed carbon is 0.0397 and 0.0612 respectively. Thus, the R^2 between the ash yield and calorific value is significantly higher than the R^2 between calorific value and any of the other proximate analysis elements. The negatively synchronous variation obtained between ash yield and calorific value may be attributed to the negative impact of mineral matter in the Hwange coal.

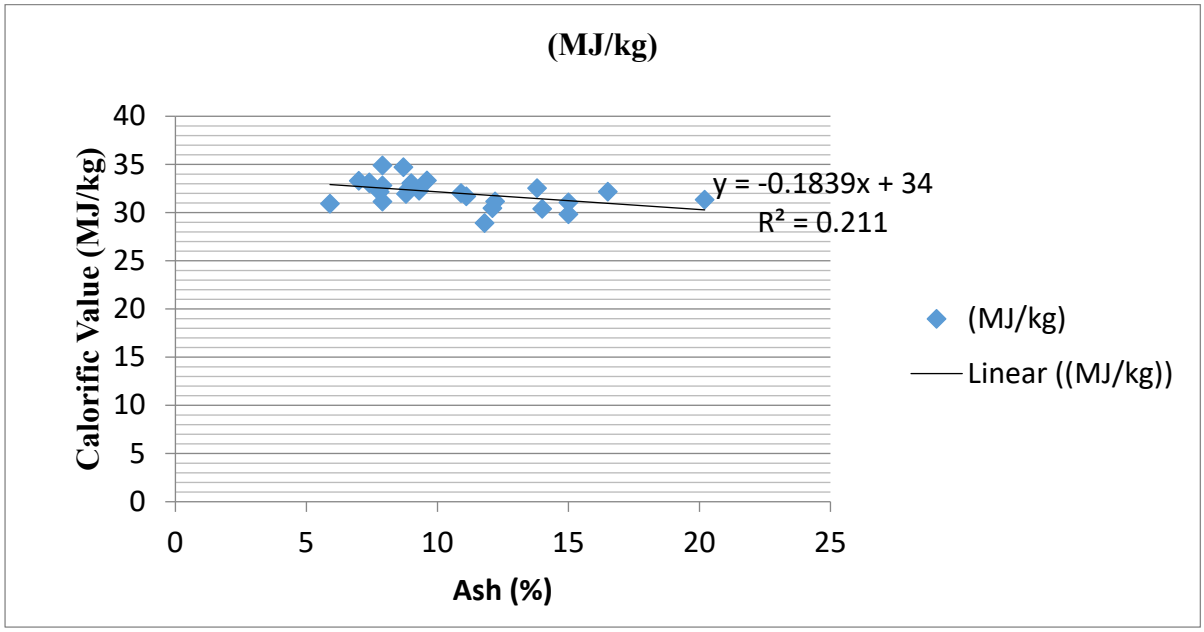


Figure 4.22: Cross-correlation plot of ash yield (%) and calorific value (MJ/kg).

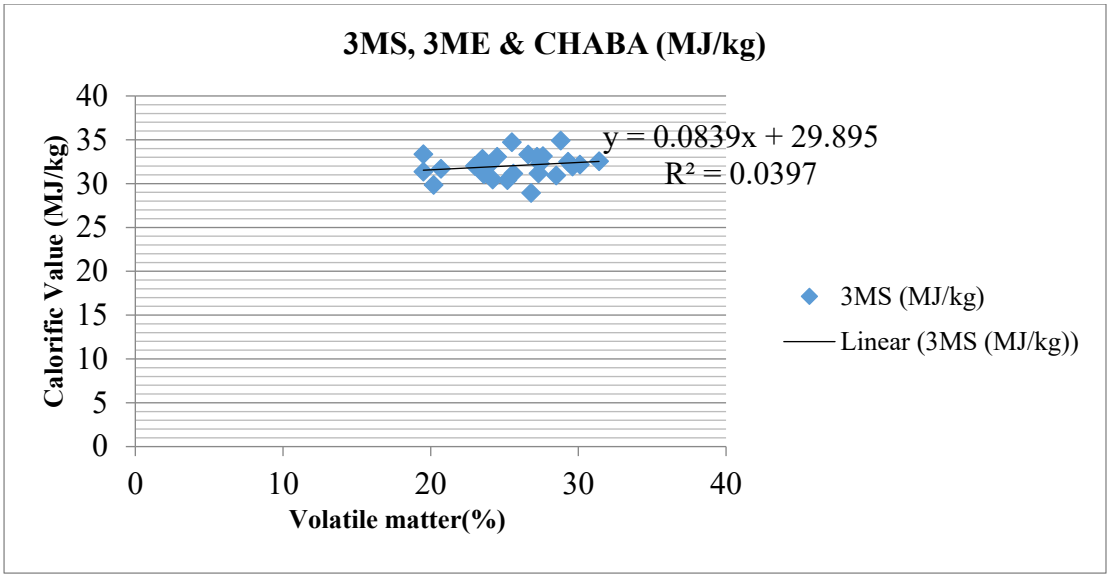


Figure 4.23: Cross-correlation plot of volatile matter (%) and calorific value (MJ/kg).

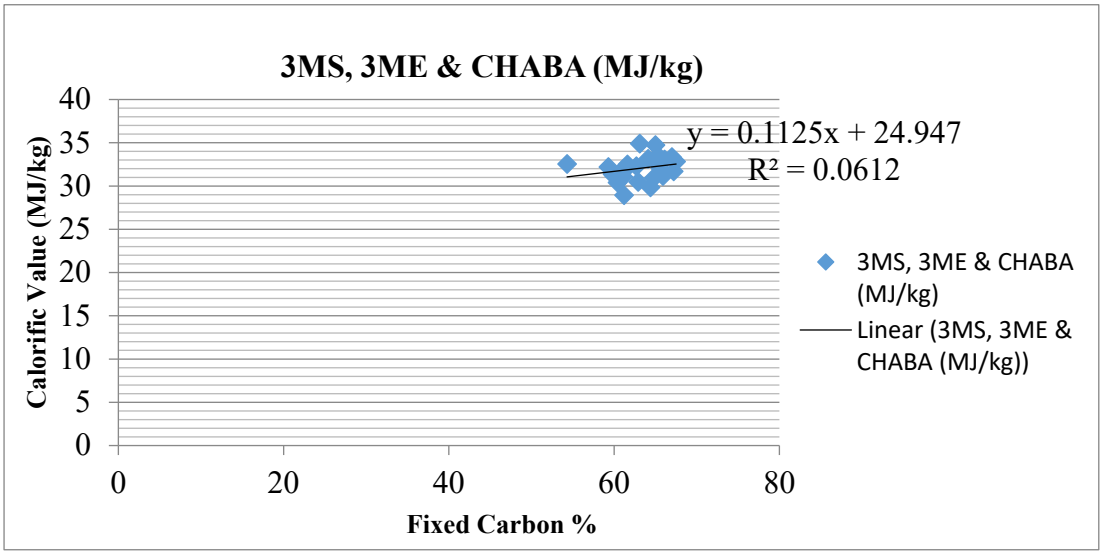


Figure 4.24: Cross-correlation plot of fixed carbon (%) and calorific value (MJ/kg).

4.4.5. XRF Analyses

XRF analyses are required to determine the mineralogical analysis of coal ash for both thermal and metallurgical coals. In this study, the analysis determined the form of oxides in the Hwange coal. The results are presented as Appendix 4.1 and are summarized in figures 4.25 to 4.29, which are graphic presentations of values for selected major oxides found in the coal ash samples which were analysed during the study. The results are described below according to the observation made from each graph.

The SiO_2 (quartz) is the most abundant of the oxides, attaining values more than 50% compared to other oxides analysed. From Figure 4.25, the 3ME sample has the highest composition of silicon dioxide, which does not conform to any trend with respect to the sample height or depth.

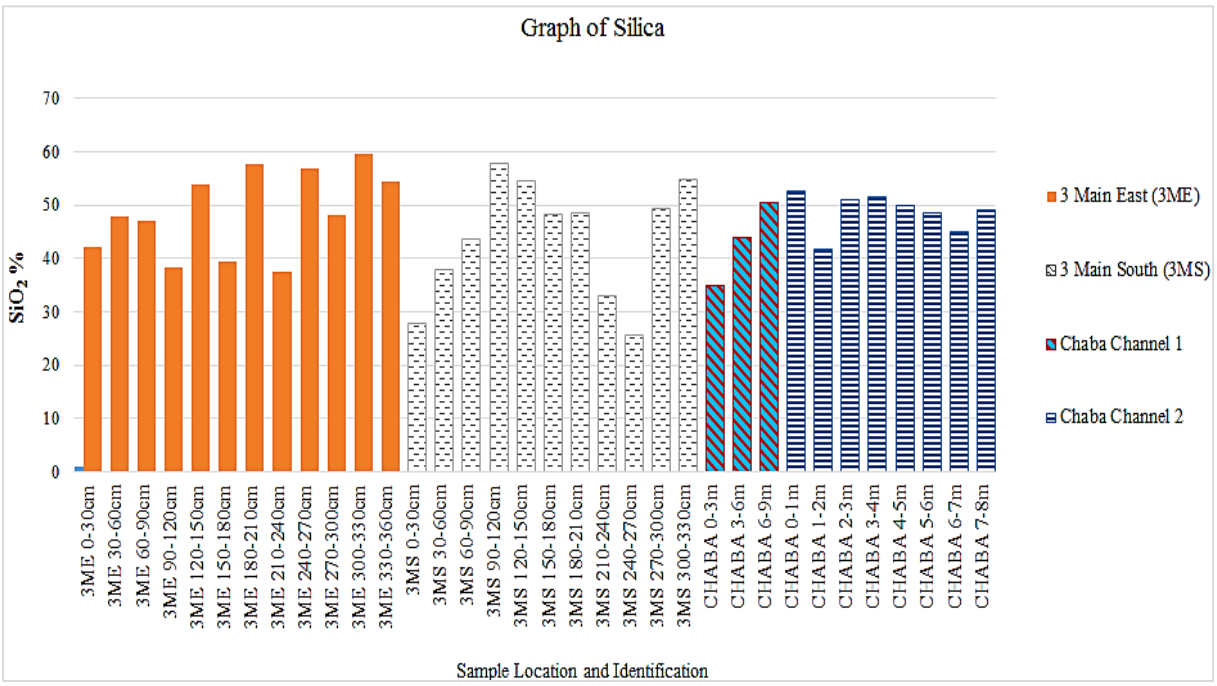


Figure 4.25: Graph for SiO_2 in coal samples from Chaba and 3 Main channels

The second most abundant oxide present in the coal ash analysed is Al_2O_3, and this was found in Chaba coal sample (Figure 4.26), an oxide that indicates the presence of clay. There is a noticeable build up in Al_2O_3 between 2 m and 6 m up the Chaba Channel 2 where values above 38% occur. In Chaba Channel 1, where samples were taken at 3 m intervals, there is a steady increase in alumina composition from bottom to top of the coal (i.e., from 28.31 at the base, followed by 36.36% before attaining a value of 39.97% at the top of the seam). But as with SiO_2, there is a general increase in Al_2O_3 towards the middle of the seam in all three sets of samples.

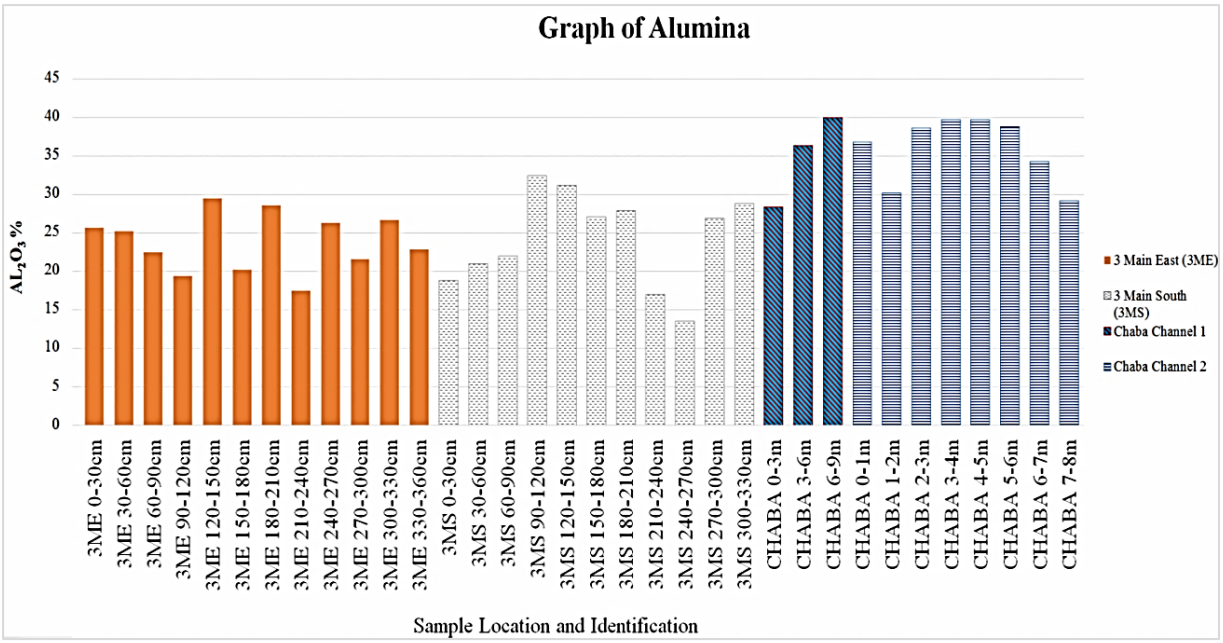


Figure 4.26: XRF analysis for Al_2O_3 in coal samples from Chaba and 3 Main channels.

The third most abundant oxide is CaO (Figure 4.27) which has a maximum value of 28%, as found in 3MS 0-30 cm sample. The presence of CaO indicates calcite. The vertical variation of oxide values is generally irregular. A notable feature is the spike in the oxide in the basal sample (3MS). This is consistent with observations of some coal analyses as well as examination of drill-cores of some holes sunk over the Hwange Concession where the ash content is high and calcite veneers are observed on the Hwange Main Coal Seam/ Lower Hwange Sandstone boundary. In another words, CaO values are synchronously high with the ash in some areas of the Hwange Concession. The mineral species detected under the petrological microscope are presented in Section 4.4.6.3.

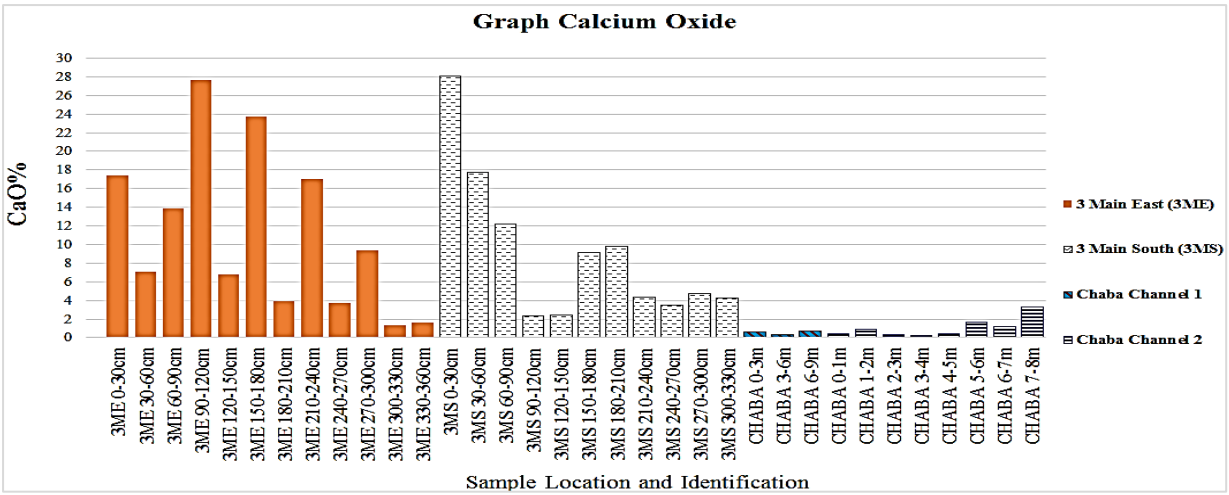


Figure 4.27: Graph for CaO in coal samples from Chaba and 3 Main channels.

According to Figure 4.28, the Fe_2O_3 composition ranges in value from less than 0.58% in Chaba Channel 2 (sample ID 3-4 m), to 51.91% in 3 Main South Channel (sample ID 240-270 cm).

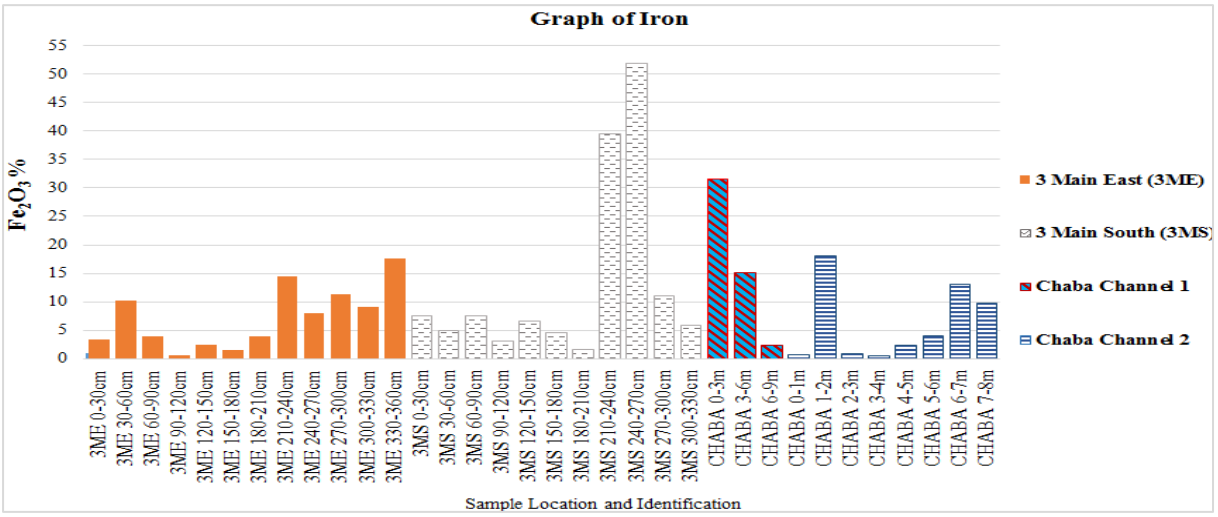


Figure 4.28: Graph for Fe_2O_3 (ferric oxide) in coal samples from Chaba and 3 Main channels.

The TiO_2 (Figure 4.29) was found as one of the major oxides analysed in the coal ash utilized, and its composition ranges from 0.7% in 3 Main South, sample ID 0-3cm, to a maximum of 2.84% in Chaba Channel 2, sample ID 2-3m. The average value is 1.41%. A closely similar trend is observed in the Chaba Channel 1 samples (Table 4.1), with the 0-3 m basal sample reflecting the same high-grade data as the 0-3 m samples in Chaba Channel 2 (Table 4.2) and progressively decreasing in grade to the top of the seam.

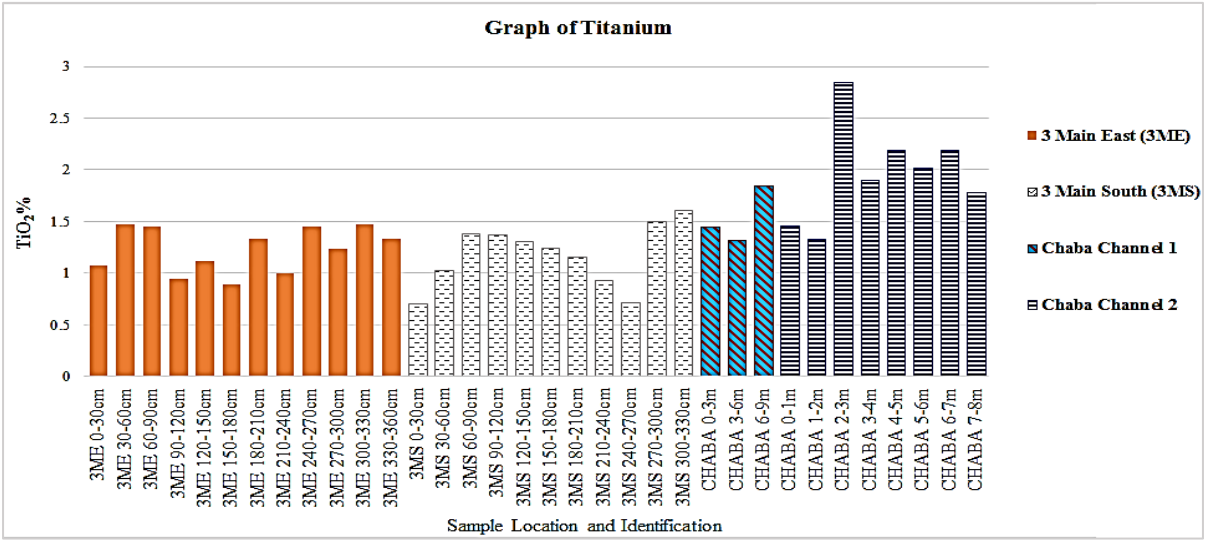


Figure 4.29: Graph for TiO_2 in coal samples from Chaba and 3 Main channels.

When coal is burnt, the mineral constituents form an ash residue composed mainly of the oxides of silicon, aluminium, iron, calcium, titanium, magnesium, sodium, potassium, partly combined as silicates, sulphates and phosphates (Zhu, 2014). These ten oxides are indicative of common minerals that occur in coals (Wagner, *et al*., 2018) As result, the mineral analysis of coal ash is usually determined in the form of oxides (Zimmerman, 1979; Zhu, 2014). Table 4.13 lists the ten major ash oxides typically reported in coal ash analyses (Wagner, *et al*., 2018; Zhu, 2014). The concentration and composition of the minerals occurring in coals may reflect the environment in which the coals were initially deposited and the subsequent tectonic and geological processes, as well as climatic factors.

There is an increasing requirement to determine major, minor and trace elements associated with minerals and organic matter in coal due to their effects in coal utilisation (Wagner, *et al*., 2018). SiO_2 in the ash has a strong impact on silicon content of hot metal in furnace while Al_2O_3 affects the slag fluidity. Alkalis sublime in high temperature areas of the furnace and re-condense in the low temperature zones of the furnace resulting in the reduction of the coke strength in the lower part of the furnace as well as creating formation of scaffolds on the furnace lining and attaching on the furnace refractory (Lu, et *al*., 2013). Coal ash constituents such as Na_2O and K_2O have been observed to have serious effects in the blast furnaces whereby they decrease burden permeability and cause high coke rates (Fisher, 1971) in addition to their negative impacts on coal combustion in boilers. The presence of trace elements in coal also has

a negative impact on health of humans as well as animals (Swaine, 1990, 2000). Therefore, the oxides, or the mineral matter in coal destined for both metallurgical and combustion, must be kept at low levels.

The current study focused on oxides derived from minerals in the Hwange coal ash (Appendix 4.1). The results are complemented by and reasonably agree with those reported by Mapani *et al.,* (2013) who conducted a study on the Hwange coals using analyses of core samples from three drill holes (BH6254A, BH6254B and BH 6254C). Table 4.14 presents averaged values for selected major oxides in Hwange coal obtained during this study and those recorded by Mapani, *et al*., (2013).

Table 4.14: Major oxides in Hwange coal ash (incorporating data from Mapani, *et al*., 2013).

Sample ID	Ash	SiO_2	Al_2O_3	Fe_2O_3	CaO	MgO	Na_2O	K_2O	SO_3	P_2O_5	TiO_2
E-202322	36	56.5	33.5	0.35	0.07	0.15	1.4	0.46	0.04	0.06	1.9
E-202323	27.6	55.3	30.8	3.2	0.54	0.24	1.4	0.29	0.34	0.06	2.6
E-202324	6.5	45.1	38.2	0.76	1.4	0.23	3.1	0.60	0.93	0.60	2.6
3ME	10.13	48.6	23.8	7.2	10.56	0.26	0.29	0.49	4.87	0.09	1.24
3MS	10.28	43.8	24.2	0.04	8.97	0.53	0.43	0.43	7.16	0.08	1.18
Chaba 1	14.37	43.1	34.9	16.33	0.54	0.29	0.33	2.52	0.38	0.18	1.53
Chaba 2	9.91	48.7	35.9	6.16	1.05	0.61	0.07	3.59	0.32	0.90	1.96

The results are also compared to the global analysis of the major inorganic constituents found in coal (Table 4.15)

Table 4.15: Global major inorganic constituents of coal ash (after Speight, 2013).

Inorganic Constituent	Representative %
SiO_2	40-90
Al_2O_3	20-60
Fe2O3	5-25
CaO	1-15
MgO	04-4
Na_2O	0.5-3
K_2O	0.5-3
SO_3	0.5-10
P_2O_5	0-1
TiO_2	0-2

In summary the values of the oxides as determined both in this study and that by Mapani *et al*., (2013) fall within the ranges reported by Speight (2013). Fe_2O_3, as well as CaO content, are strongly influenced by local geology, e.g. in Chaba (this study), pyrite has been observed petrographically to constitute a significant portion of the mineral matter.

4.4.6 Petrographic Analyses

4.4.6.1. Coal Rank determination by Vitrinite Reflectance Analysis (ISO 7404)

The ranks of the coal samples utilized were determined through the vitrinite reflectance analysis (using collotelinite maceral). This provides an insight into the difference between the coal horizons and the understanding of the variation observed in the coking behavior of the coal samples tested. The reflectance results for all samples are presented in Tables 4.16, 4.17 and 4.18, while the graphical representation of the results is presented in the Appendix 4.2.

Table 4.16 depicts the mean random vitrinite reflectance results for Chaba coal samples, i.e., sample 1 to 3 with the random vitrinite reflectance values obtained in the range of 0.94 to 0.95,

Table 4.16: Vitrinite reflectance results for Chaba Channel 1 Samples

	Sample Name		
	CHABA1 (Sample 0-3m)	CHABA2 (Sample 3-6m)	CHABA3 (Sample 6-9m)
RoV mean	0.94	0.95	0.95
St.Dev	0.065	0.067	0.07
Max	1.1	1.07	1.09
Min	0.81	0.81	0.81
Rank Category	MrC	MrC	MrC

Key: MrB = Medium rank B bituminous coal; MrC = Medium rank C bituminous coal

Table 4.17 shows the reflectance results for sample 3ME 1 to 12 (also from 3 Main). The Random reflectance of vitrinite displays a range of 0.94 to 1.05, which is slightly higher than that of Chaba coal samples.

Table 4.17: Vitrinite reflectance results for 3 Main East Channel.

Sample Name	RoV mean	St.Dev	Max	Min	Rank Category
3ME1 (0-30cm)	1.02	0.05	1.13	0.9	MrB
3ME2 (30-60cm)	0.99	0.056	1.14	0.88	MrC
3ME3 (60-90cm)	0.99	0.059	1.1	0.85	MrC
3ME4 (90-120cm)	0.94	0.073	1.07	0.81	MrC
3ME5 (120-150cm)	0.99	0.072	1.1	0.83	MrC
3ME6 (150-180cm)	0.99	0.071	1.16	0.85	MrC
3ME7 (180-210cm)	0.99	0.069	1.15	0.82	MrC
3ME8 (210-240cm)	0.98	0.061	1.09	0.85	MrC
3ME9 (240-270cm)	0.94	0.059	1.1	0.82	MrC
3ME10 (270-300cm)	0.99	0.069	1.19	0.85	MrC
3ME11 (300-330cm)	0.97	0.063	1.1	0.85	MrC
3ME12 (330-360cm)	1.05	0.071	1.17	0.9	MrB

Key: MrB = Medium rank B bituminous coal; MrC = Medium rank C bituminous coal

Values of mean random reflectance of vitrinite in 3MS Channel (Table 4.18) show a range from 0.90 to 0.98, which are generally slightly lower than those of 3ME Channel, but slightly higher than those of Chaba Channel 1.

Table 4.18: Vitrinite reflectance results for 3MS Channel samples.

Sample Name	RoV mean	St.Dev	Max	Min	Rank Category
3MS1 (0-30cm)	0.9	0.054	1.04	0.74	MrC
3MS2 (30-60cm)	0.93	0.055	1.08	0.82	MrC
3MS3 (60-90cm)	0.9	0.063	1.06	0.79	MrC
3MS4 (90-120cm)	0.97	0.054	1.09	0.85	MrC
3MS5 (120-150cm)	0.9	0.067	1.04	0.76	MrC
3MS6 (150-180cm)	0.93	0.066	1.05	0.75	MrC
3MS7 (180-210cm)	0.96	0.059	1.08	0.85	MrC
3MS8 (210-240cm)	0.96	0.077	1.13	0.82	MrC
3MS9 (240-270cm)	0.96	0.073	1.1	0.82	MrC
3MS10 (270-300cm)	0.98	0.074	1.11	0.82	MrC
3MS11 (300-330cm)	0.93	0.075	1.09	0.77	MrC

Key: MrB = Medium rank B bituminous coal; MrC = Medium rank C bituminous coal

Determination of coal rank is crucial, as the parameter relates both to the coalification history and the potential of a coal (Lu, *et al.*, 2013). Vitrinite reflectance remains the most definitive indicator of coal rank. This is because, unlike proximate analysis, it is not affected by changes

to coal type (variations in maceral content) or mineral content. As coal rank increases, so do the vitrinite reflectance values and the carbon content in vitrinite.

Isoreflectance maps drawn for selected stratigraphic horizons in the Bowen Basin reveal regular rank trends and a general parallelism between reflectance contours and structural contours. These features have been concluded (Beeston, 1986) to imply that coalification in the Bowen Basin is due to increasing depths of burial. Referring to the bituminous coals in the Appalachians, Arnold, (2013) concludes that with a geothermal gradient of 0.556^{0}C per 30.5 m, temperature must have added greatly to the coalification of these coals in the region. The role of temperature due burial over time (with effect pressure considered minimal) is consistent with other workers' (Hood *et al.*, 1975; Shibaoka and Bennet, 1976) arguments, with yet others, such as Strauss, *et al.*, (1976) adding tectonism and depth of basement and thermal conductivity to the list of factors influencing coal rank attainment.

Prime coking coals are considered to have narrow vitrinite reflectance range of 1.1 to 1.45% (Diesel and Pickel, 2012). However, the blending of high, medium, and low volatile matter coal types has yielded properties better than any of the cokes produced from individual coals (Mitchell, 1999a and b). Vitrinite reflectance determination puts the Hwange coals into a blend of Medium Rank C and B bituminous coal, with mean random vitrinite reflectance values ranging from 0.90 to 0.98% (Figure 4.15). From a sample population of 26, all from 3ME (which are 3ME1 and 3ME12) fall in the Medium Rank C, with two exceptions falling in the Medium Rank B category. The values fall just outside out of the narrow range of 1.1 to 1.45% considered to define the limits of prime coals (Diessel and Pickel, 2012) and could be considered as blend coking coals.

However, in terms of coal classification and utilisation, the results corroborate well with requirements of global and locally acceptable blend coking coal and are marginally acceptable for some prime coking coal ranges of rank. Blending of coals from different parts of the mine could produce good coke. Rank is not of major consequence to the thermal markets, other than to state that, swelling coals may not be acceptable to specific industrial boilers in cases where swelling and agglomeration could cause blockage to the flow of air through the combusting burden.

Regrettably, the random reflectance data, unlike the Bowen Basin data which was spread throughout the Basin, was limited to the two rather shallow areas of the Hwange Coalfield. The possibility of recording higher reflectance data with increasing depth of burial and faulting westwards (Option Area and the adjoining Western Areas), albeit not very significantly, is believed to be possible.

4.4.6.2. Maceral Analyses

Maceral analyses were carried out to determine the organic components in the Hwange coals. This analysis is crucial as the organic components determine coal type and performance in various sectors of utilisation; in other words, maceral components control devolatilisation, ignition, combustion, and burnout in steam coals, and cokability in metallurgical coals. The results are presented in Tables 4.19 to 4.24.

Maceral analysis of Chaba Channel 1 and Chaba Channel 2 coal samples

Table 4.19 presents detailed maceral analyses of Chaba Channel 1 and Chaba Channel 2 coal samples, respectively. Table 4.20 is a summary of the three maceral groups. The results are summarised as follows:

I. There is a vertical variation in the maceral constitution along both channels with the vitrinite group dominating at the base of the channels (i.e., vitrinite comprises 52% in Chaba 1 sample 0-3 m and 36.5% of the maceral constituent in sample 0-1 m in Chaba 2 channel). Chaba 1 is therefore the more reactive of the two channels.
II. The inertinite group progressively becomes the dominant maceral group with increasing distance from the seam base.
III. In both channels, collotelinite constitutes the main vitrinite maceral followed by collodetrinite.
IV. In both channels, inertinite group of macerals is dominated by inert semifusinite with fusinite coming second in the case of channel 1. In channel 2 inertinite is followed by inertodetrinite.
V. Liptinite is represented by three macerals: sporinite, resinite, and exudatinite. Sporinite dominates the liptinite group and occurs in all Chaba samples. The sporinite values show a cyclic variation with height above seam base. For example, along channel 1, it

commences with a high value of 2.1% in sample 0-3 m followed by a lower value of 0.2% in the middle sample (3-6 m) and increases to 2.1% in the top samples (6-9 m).

VI. The existence of exudatinite in a number of samples, albeit in small quantities, is unusual in southern African coals and is a point of interest. This secondary maceral is produced from vitrinite and liptinite macerals during coalification and also when exposed to some degree of heat. It has been suggested that the source of such heat in the Hwange Colliery could have emanated from geothermal heat generated from the multiple faults prominently evident in the western areas of the mine. The presence of such hydrogen-rich material has been reported to provide enhanced fluidity and swelling when heated, and, in this manner, aid in coking capacity.

VII. The sulphides dominate the mineral group in Channel 1, while in Channel 2 silicates (clay/quartz) dominate the mineral component. These results agree with the XRF results. In Chaba Channel 1 (Figure 4.28) the Fe_2O_3, presumably hematite ranges from 15% to a spike of 30 %; the later value occurring in the basal 0-3 m sample. The Fe_2O_3 values in Chaba Channel 2 fall below 20%, with only one sample yielding Fe_2O_3 value above 15%. On the other hand, Al_2O_3 and SiO_2 which represent clay and quartz, respectively, have SiO_2 values which are all above 40% with majority yielding 50% (Figure 4.25); while the majority of the samples have Al_2O_3 values falling between 20% and 40% (Figure 4.26).

Table 4.19: Detailed maceral analyses (% by volume) of Chaba channels 1 and 2.

		Chaba Channel 1						Chaba Channel 2															
Sample identification:		Chaba-1 0-3m (1565)		Chaba 1 3-6m (1566)		Chaba 1 6-9m (1567)		Chaba 2 0-1m		Chaba 2 1-2m		Chaba 2 2-3m		Chaba 2 3-4m		Chaba 2 4-5m		Chaba 2 5-6m		Chaba 2 6-7m		Chaba 2 7-8m	
MACERAL GROUP	MACERAL (vol%)	inc. mm vol%	Mmf vol %	inc. mm vol%	Mmf vol %	inc. mm vol%	mmf vol %	inc. mm vol%	mmf vol %	inc. mm vol%	mmf vol %	inc. mm vol%	Mmf vol %	inc. mm vol%	Mmf vol %	inc. mm vol%	mmf vol %	inc. mm vol%	mmf vol %	inc. mm vol%	mmf vol %	inc. mm vol%	mmf vol %
Vitrinite	Telinite	1.6	1.7	0.4	0.4	0.4	0.4	0.2	0.2	0.2	0.2	0.2	0.2	0	0	0.6	0.6	0	0	0	0	0.6	0.6
	Collotelinite	42.8	44.3	18.8	19.4	5.4	5.5	20.1	20.8	10	10.1	14.5	14.6	3.2	3.3	5.4	5.6	1.8	1.8	2.8	3	0.8	0.8
	Vitrodetrinite	1.2	1.2	0.4	0.4	0.4	0.4	0	0	0	0	0.2	0.2	0	0	0.4	0.4	0	0	0	0	0	0
	Collodetrinite	2.6	2.7	2.4	2.5	2	2.1	11.2	11.6	6.6	6.6	2.9	3	8.9	9.2	4.2	4.4	1.6	1.6	1	1.1	0	0
	Corpogelinite	2	2.1	2	2.1	0.2	0.2	2.5	2.6	1.2	1.2	0.4	0.4	0	0	0.2	0.2	0	0	0	0	0	0
	Gelinite	0	0	0.4	0.4	0.2	0.2	1.2	1.2	1.6	1.6	1.2	1.2	0.8	0.8	0.4	0.4	1.4	1.4	0.2	0.2	1.2	1.2
	Pseudovitrinite	0	0	0	0	0	0	0	0	0	0	0	0	0	0	0	0	0	0	0	0	0	0
Inertinite	Fusinite	6.2	6.4	6.2	6.4	4.8	4.9	18.2	18.8	15.3	15.5	10.4	10.4	8.7	9	6.4	6.6	8.2	8.5	1.8	1.9	0.4	0.4
	reactive semifusinite	4.8	5	9.8	10.1	7.6	7.8	5.6	5.8	6.6	6.6	5.3	5.3	3.8	3.9	8.6	8.9	3.9	4	6.6	7	3.6	3.7
	inert semifusinite	17	17.6	30.6	31.5	45	46.2	23.8	24.6	28.5	28.8	33	33.3	31.4	32.6	30.9	32	37.8	38.9	39	41.1	39.2	40.8
	Micrinite	4.4	4.6	1	1	0.6	0.6	0.2	0.2	1.6	1.6	0.2	0.2	1.2	1.2	2.2	2.3	0.2	0.2	1.8	1.9	0.8	0.8
	Macrinite	1.4	1.4	1.2	1.2	1.4	1.4	0.8	0.8	0	0	0	0	0	0	0	0	0.2	0.2	0.2	0.2	0	0
	Secretinite	5	5.2	10	10.3	8	8.2	5.2	5.4	9.4	9.5	6.8	6.9	7.1	7.4	3	3.1	6.3	6.5	4	4.2	7	7.2
	Funginite	0	0	0	0	0	0	0	0	0	0	0	0	0	0	0	0	0	0	0	0	0	0
	inertodetrinite R	1	1	3.6	3.7	4.8	4.9	0.6	0.6	2.8	2.8	2	2	3.6	3.7	8	8.3	5.1	5.2	1	1.1	5.8	6
	inertodetrinite I	3.2	3.3	8.2	8.5	13.8	14.2	4.3	4.4	12.7	12.9	20.5	20.7	26.3	27.3	24.6	25.5	29.7	30.6	34.2	36.1	36.3	37.7
Liptinite	Sporinite	2	2.1	0.2	0.2	2	2.1	0.4	0.4	0.8	0.8	1.2	1.2	1.4	1.4	1.4	1.5	0.8	0.8	1.8	1.9	0.4	0.4
	Cutinite	0.2	0.2	0	0	0	0	1.2	1.2	0.4	0.4	0	0	0	0	0.2	0.2	0.2	0.2	0.4	0.4	0.2	0.2
	Resinite	0	0	1.8	1.9	0	0	0	0	0	0	0	0	0	0	0	0	0	0	0	0	0	0
	Alginate	0	0	0	0	0	0	0	0	0	0	0	0	0	0	0	0	0	0	0	0	0	0
	Liptodetrinite	0	0	0	0	0	0	0	0	0	0	0	0	0	0	0	0	0	0	0	0	0	0
	Suberinite	0	0	0	0	0	0	0	0	0	0	0	0	0	0	0	0	0	0	0	0	0	0
	Exudatinite	1.2	1.2	0	0	0.8	0.8	1.2	1.2	1.4	1.4	0.6	0.6	0.2	0.2	0	0	0	0	0	0	0	0
Mineral matter	silicate (clay/qz)	0		0.2		0.8		0		0		0.2		1.8		3		2.2		3.4		3.6	
	Sulphide	3.4		2.8		1.2		3.5		0.4		0.2		1.4		0		0.2		1		0.2	
	Carbonate	0		0		0.6		0		0.6		0.2		0.4		0.4		0.4		0.8		0	
	Other	0		0		0		0		0		0.2		0		0		0.2		0		0	

Table 4.20: Summary of detailed maceral analyses of Chaba channels 1 and 2.

		Chaba Channel 1						Chaba Channel 2													
Sample identification:		Chaba-1 0-3m (1565)		Chaba 1 3-6m (1566)		Chaba 1 6-9m (1567)		Chaba 2 0-1m		Chaba 2 1-2m		Chaba 2 2-3m		Chaba 2 3-4m		Chaba 2 4-5m		Chaba 2 5-6m		Chaba 2 6-7m		Chaba 2 7-8m	
MACERAL GROUP	MACERAL (vol%)	inc. mm vol%	mmf vol%	inc. mm vol%	mmf vol%	inc. mm vol%	mmf vol%	inc. mm vol%	mmf vol %	inc. mm vol%	mmf vol%	inc. mm vol%	Mmf vol%	inc. mm vol%	mmf vol%	inc. mm vol%	mmf vol%	inc. mm vol%	mmf vol%	inc. mm vol%	mmf vol%	inc. mm vol%	mmf vol%
MACERAL GROUP	VITRINITE	50.2	52	24.4	25.2	8.6	8.8	35.2	36.5	19.5	19.7	19.3	19.5	12.8	13.3	11.2	11.6	4.7	4.8	4	4.2	2.6	2.6
TOTALS (vol%)	INERTINITE	43	44.5	70.6	72.8	86	88.3	58.6	60.7	76.9	77.7	78.1	78.7	82	85	83.8	86.7	91.4	94.2	88.6	93.5	93	96.7
	LIPTINITE	3.4	3.5	2	2.1	2.8	2.9	2.7	2.8	2.6	2.6	1.8	1.8	1.6	1.6	1.6	1.7	1	1	2.2	2.3	0.6	0.6
	MINERAL MATTER	3.4		3		2.6		3.5		1		0.8		3.6		3.4		2.9		5.2		3.8	
	TOTAL INERTINITE	43	44.5	70.6	72.8	86	88.3	58.6	60.7	76.9	77.7	78.1	78.7	82	85	83.8	86.7	91.4	94.2	88.6	93.5	93	96.7
	TOTAL REACTIVE MACERALS	59.4	61.5	39.8	41	23.8	24.4	44.1	45.7	31.5	31.8	28.3	28.5	21.7	22.5	29.5	30.5	14.7	15.1	13.8	14.6	12.6	13

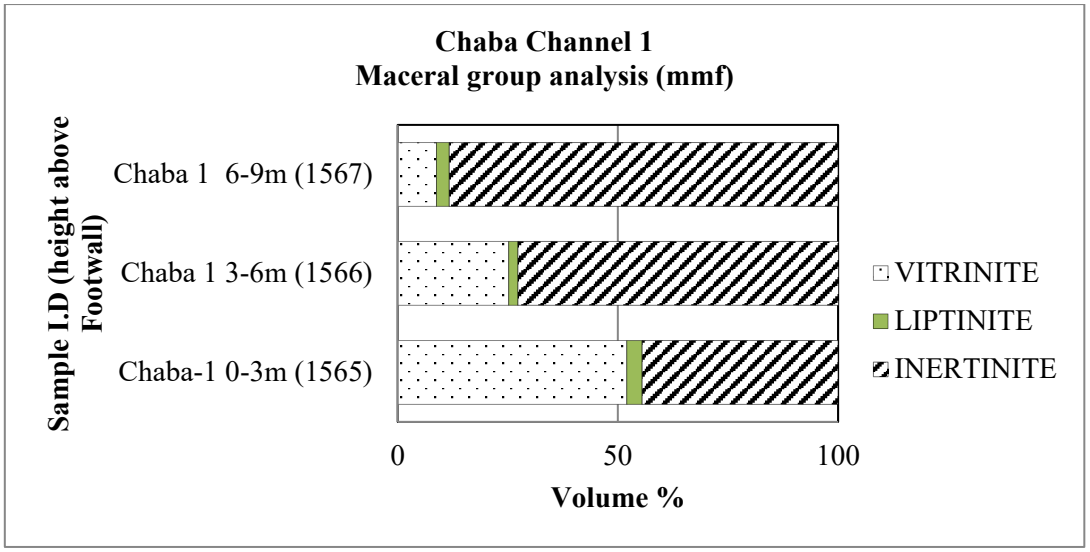


Figure 4.30: Maceral group analyses (m.m.f) for the three Chaba Channel 1.

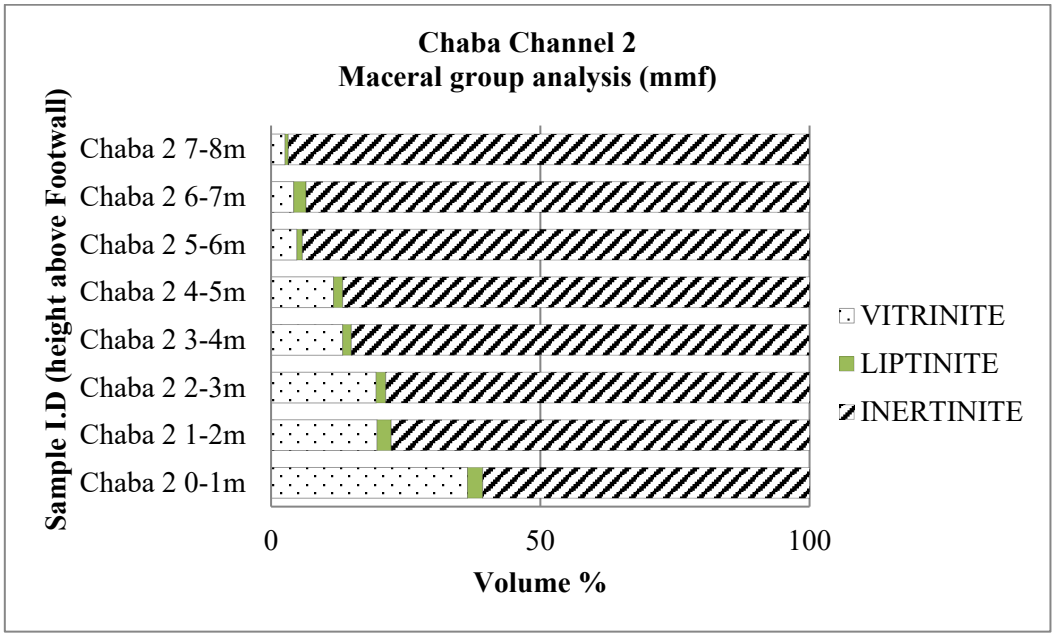


Figure 4.31: Maceral group analyses (m.m.f) for the three Chaba Channel 2.

3 Main Channel 3ME the summary on maceral analyses:

Table 4.21 presents detailed maceral analyses of 3 Main Channel 3ME coal samples; while Table 4.22 is a summary of the three maceral groups. The results are summarised as follows:

I. Vitrinite is dominant in the lower samples particularly the 0-30 cm from base of coal while inertinite becomes the dominant in the upper samples (commencing from the 30-60 cm samples.

II. Collotelinite is the main vitrinite maceral, with collodetrinite occupying the second position.
III. The inertinite group is dominated by inert semifusinite, followed by fusinite.
IV. Reactive semifusinite is significant in sample intervals 30-60 cm and 180-210 cm.
V. Exudatinite is the main liptinite maceral in sample 30-60 cm. It occurs in all samples in the channel except in sample 60-90 cm.
VI. The mineral group is dominated by carbonates which occur in fractures, followed by sulphides which occur as framboids.
VII. There are vertical and cyclic variations in the proportions of different macerals. Vitrinite shows a steady decrease from 55% in the basal 0-30 cm samples to 28.4% in sample 90-120 cm, followed by an upward trend to 49.4% in sample 180-210 cm before it starts to decrease towards the top. Inertinite, on the other hand, steadily increases from 41.4% in the basal 0-30 cm sample to 69.1 in the 90-120 cm samples followed by a downward trend before increasing steadily towards the top.

Maceral analysis results for 3 Main Channel 3MS

Table 4.23 presents detailed maceral analyses of 3 Main Channel 3MS coal samples; while Table 4.24 presents a summary of the three maceral groups. The results are summarised as follows:

i) Vitrinite is dominant at the base and fluctuates in content up the sequence.
ii) Collotelinite dominates the vitrinite maceral group, followed by collodetrinite.
iii) Inert semifusinite dominates the inertinite group beyond 30 cm above seam base, followed by the inertodetrinite beyond 90 cm.
iv) Sporinite is generally the dominant liptinite maceral. Exceptions are with the 30-60 cm and 120-150 cm above seam base where exsudatinite is in second position.
v) Carbonates dominate the mineral group, followed by sulphides within the first 60 cm above seam base. Thereafter sulphides are the most abundant of the mineral group.

Table 4.21: Maceral group analysis (% by Volume) of 3ME Channel samples.

Sample identification:		3ME1 0-30cm (1542)		3ME2 30-60cm (1543)		3ME3 60-90cm (1544)		3ME4 90-120cm (1545)		3ME5 120-1150cm (1546)		3ME6 150-180cm (1547)		3ME7 180-210cm (1548)		3ME8 210-240cm (1549)		3ME9 240-270cm (1550)		3ME10 270-300cm (1551)		3ME11 300-330cm (1552)		3ME12 330-345cm (1553)	
MACERAL GROUP	MACERAL (vol%)	inc. mm vol%	Mmf vol %	inc. mm vol %	Mmf vol %	inc. mm vol %	mmf vol %	inc. mm vol %	mmf vol %	inc. mm vol %	mmf vol %	inc. mm vol%	mmf vol %	inc. mm vol %	mmf vol%	inc. mm vol%	mmf vol %	inc. mm vol%	mmf vol%	inc. mm vol%	mmf vol%	inc. mm vol%	mmf vol %	inc. mm vol%	mmf vol%
Vitrinite	Telinite	0.0	0.0	0.0	0.0	0.0	0.0	0.0	0.0	0.2	0.2	0.0	0.0	0.2	0.2	0.0	0.0	0.2	0.2	0.2	0.2	0.0	0.0	0.0	0.0
	Collotelinite	43.8	45.1	35.2	36.3	35.4	36.4	17.4	18.5	26.1	26.4	23.4	24.1	39.8	40.8	25.5	25.9	30.6	32.9	12.5	13.1	7.2	7.5	5.0	5.4
	Vitrodetrinite	0.0	0.0	0.0	0.0	0.0	0.0	0.0	0.0	0.0	0.0	0.0	0.0	0.0	0.0	0.6	0.6	0.4	0.4	0.2	0.2	0.0	0.0	0.4	0.4
	Collodetrinite	11.6	11.9	3.6	3.7	10.7	11.0	10.6	11.3	3.6	3.7	4.0	4.1	7.0	7.2	6.8	6.9	9.4	10.1	6.2	6.5	9.3	9.8	4.9	5.2
	Corpogelinite	0.0	0.0	1.8	1.8	0.4	0.4	0.0	0.0	0.0	0.0	0.2	0.2	0.6	0.6	0.6	0.6	0.2	0.2	0.6	0.6	0.2	0.2	0.6	0.6
	Gelinite	0.0	0.0	0.6	0.6	0.4	0.4	0.4	0.4	0.4	0.4	0.8	0.8	0.6	0.6	0.6	0.6	0.6	0.6	0.0	0.0	0.6	0.6	0.6	0.6
	Pseudovitrinite	0.0	0.0	0.0	0.0	0.0	0.0	0.0	0.0	0.0	0.0	0.0	0.0	0.0	0.0	0.0	0.0	0.0	0.0	0.0	0.0	0.0	0.0	0.0	0.0
Inertinite	Fusinite	8.8	9.1	14.8	15.3	11.0	11.3	10.8	11.5	6.6	6.7	7.2	7.4	16.8	17.2	12.2	12.4	11.4	12.3	7.0	7.4	7.6	7.9	6.4	6.8
	Reactive Semifusinite	1.6	1.6	8.3	8.6	4.2	4.3	3.8	4.0	5.2	5.3	3.0	3.1	6.8	7.0	4.8	4.9	4.6	4.9	5.8	6.1	5.6	5.8	5.0	5.4
	Inert Semifusinite	14.8	15.2	17.8	18.3	18.0	18.6	32.2	34.3	33.9	34.3	36.9	37.9	13.6	13.9	24.0	24.5	21.6	23.2	34.4	36.0	37.4	39.1	42.0	44.5
	Micrinite	2.8	2.9	1.2	1.2	1.8	1.8	0.6	0.6	0.8	0.8	1.4	1.4	0.8	0.8	0.8	0.8	2.8	3.0	0.2	0.2	1.2	1.2	0.2	0.2
	Macrinite	0.0	0.0	1.2	1.2	0.2	0.2	0.4	0.4	0.0	0.0	0.2	0.2	0.0	0.0	1.2	1.2	0.6	0.6	0.4	0.4	0.6	0.6	0.4	0.4
	Secretinite	7.0	7.2	5.2	5.3	7.0	7.2	4.4	4.7	7.8	7.9	3.4	3.5	6.8	7.0	7.4	7.6	3.0	3.2	7.6	8.0	7.0	7.3	4.5	4.7
	Funginite	0.2	0.2	0.0	0.0	0.0	0.0	0.0	0.0	0.2	0.2	0.0	0.0	0.0	0.0	0.0	0.0	0.0	0.0	0.0	0.0	0.0	0.0	0.0	0.0
	Inertodetrinite	1.6	1.6	1.4	1.4	1.8	1.8	5.0	5.3	1.2	1.2	3.2	3.3	1.0	1.0	3.2	3.3	1.4	1.5	4.8	5.1	7.6	7.9	3.7	3.9
	Inertodetrinite	4.6	4.7	4.4	4.5	5.8	5.9	7.8	8.3	11.4	11.6	11.8	12.2	2.6	2.7	8.6	8.8	4.0	4.3	13.7	14.3	9.7	10.2	19.2	20.4
Liptinite	Sporinite	0.2	0.2	0.4	0.4	0.4	0.4	0.0	0.0	0.4	0.4	0.4	0.4	0.4	0.4	0.4	0.4	1.2	1.3	1.4	1.5	0.8	0.8	0.8	0.8
	Cutinite	0.0	0.0	0.0	0.0	0.2	0.2	0.2	0.2	0.0	0.0	0.4	0.4	0.2	0.2	0.2	0.2	0.6	0.6	0.0	0.0	0.2	0.2	0.0	0.0
	Resinite	0.0	0.0	0.0	0.0	0.0	0.0	0.0	0.0	0.4	0.4	0.2	0.2	0.2	0.2	0.4	0.4	0.0	0.0	0.0	0.0	0.2	0.2	0.0	0.0
	Alginate	0.0	0.0	0.0	0.0	0.0	0.0	0.0	0.0	0.0	0.0	0.0	0.0	0.0	0.0	0.0	0.0	0.0	0.0	0.0	0.0	0.0	0.0	0.0	0.0
	Liptodetrinite	0.0	0.0	0.0	0.0	0.0	0.0	0.0	0.0	0.0	0.0	0.0	0.0	0.0	0.0	0.0	0.0	0.0	0.0	0.0	0.0	0.0	0.0	0.0	0.0
	Suberinite	0.0	0.0	0.0	0.0	0.0	0.0	0.0	0.0	0.0	0.0	0.0	0.0	0.0	0.0	0.0	0.0	0.0	0.0	0.0	0.0	0.0	0.0	0.0	0.0
	Exudatinite	0.2	0.2	1.2	1.2	0.0	0.0	0.4	0.4	0.4	0.4	0.6	0.6	0.2	0.2	0.8	0.8	0.4	0.4	0.4	0.4	0.6	0.6	0.6	0.6
Mineral matter	Silicate (clay/qz)	0.0		0.0		0.4		1.0		0.4		0.8		0.8		0.6		0.8		0.8		1.2		1.7	
	Sulphide	1.0		0.4		1.0		0.0		0.6		1.0		0.8		1.2		2.6		2.6		2.0		3.3	
	Carbonate	1.8		2.6		1.4		5.0		0.4		1.0		0.8		0.0		3.6		1.0		1.2		0.8	
	Other	0.0		0.0		0.0		0.0		0.0		0.0		0.0		0.0		0.0		0.0		0.0		0.0	

Table 4.22: Summary of detailed maceral analyses of 3ME Channel samples.

Sample identification:		3ME1 0-30cm (1542)		3ME2 30-60cm (1543)		3ME3 60-90cm (1544)		3ME4 90-120cm (1545)		3ME5 120-1150cm (1546)		3ME6 150-180cm (1547)		3ME7 180-210cm (1548)		3ME8 210-240cm (1549)		3ME9 240-270cm (1550)		3ME10 270-300cm (1551)		3ME11 300-330cm (1552)		3ME12 330-345cm (1553)	
MACERAL GROUP	MACERAL (vol%)	inc. mm vol%	Mmf vol%	inc. mm vol %	Mmf vol %	inc. mm vol %	mmf vol %	inc. mm vol%	mmf vol %	inc. mm vol%	mmf vol %	inc. mm vol %	Mmf vol %	inc. mm vol %	mmf vol %	inc. mm vol%	Mmf vol %	inc. mm vol %	mmf vol %	inc. mm vol %	mmf vol %	inc. mm vol %	mmf vol %	inc. mm vol %	mmf vol %
TOTALS (vol%)	VITRINITE	55.4	57	41.2	42.4	46.9	48.3	28.4	30.2	30.3	30.7	28.5	29.3	48.2	49.4	34.1	34.7	41.4	44.5	19.7	20.6	17.3	18.1	11.5	12.2
	INERTINITE	41.4	42.6	54.3	55.9	49.7	51.2	65	69.1	67.1	68.1	67.1	69.1	48.4	49.6	62.3	63.5	49.4	53.1	74	77.5	76.6	80.1	81.4	86.4
	LIPTINITE	0.4	0.4	1.6	1.6	0.6	0.6	0.6	0.6	1.2	1.2	1.6	1.6	1	1	1.8	1.8	2.2	2.4	1.8	1.9	1.8	1.9	1.4	1.4
	MINERAL MATTER	2.8		3		2.8		6		1.4		2.8		2.4		1.8		7		4.4		4.4		5.8	
	TOTAL INERTINITE	41.4	42.6	54.3	55.9	49.7	51.2	65	69.1	67.1	68.1	67.1	69.1	48.4	49.6	62.3	63.5	49.4	53.1	74	77.5	76.6	80.1	81.4	86.4
	TOTAL REACTIVE MACERALS	59	60.7	52.5	54.1	53.5	55	37.8	40.2	37.9	38.4	36.3	37.3	57	58.4	43.9	44.7	49.6	53.3	32.2	33.7	32.2	33.7	21.6	22.9

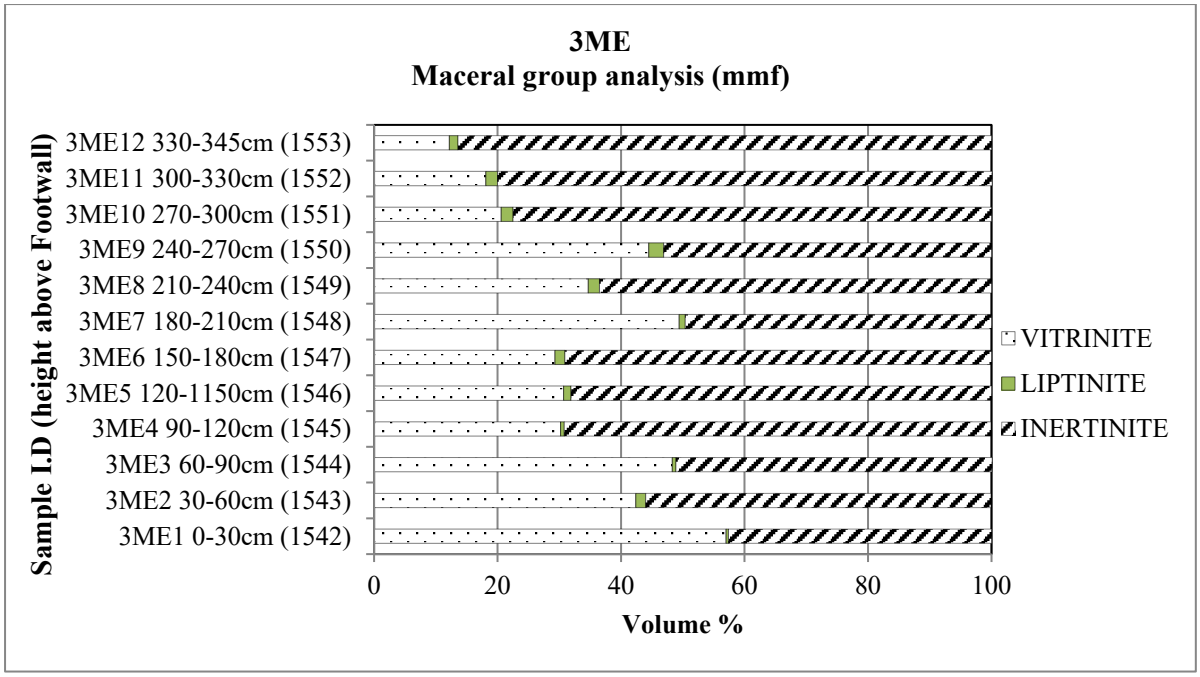


Figure 4.32: Graph to show analyses (m.m.f) for the three maceral groups along 3ME Channel samples.

Table 4.23: Maceral group analysis (% by volume) for 3MS Channel samples.

Sample identification:		3MS1 0-30cm (1554)		3MS2 30-60cm (1555)		3MS3 60-90cm (1556)		3MS4 90-120cm (1557)		3MS5 120-150cm (1558)		3MS6 150-180cm (1559)		3MS7 180-210cm (1560)		3MS8 210-240cm (1561)		3MS9 240-270cm (1562)		3MS10 270-300cm (1563)		3MS11 300-330cm (1564)	
MACERAL GROUP	MACERAL (vol%)	inc. mm vol%	mmf vol%	inc. mm vol%	mmf vol%	inc. mm vol%	mmf vol%	inc. mm vol%	mmf vol%	inc. mm vol%	Mmf vol%	inc. mm vol%	mmf vol%	inc. mm vol%	mmf vol%	inc. mm vol%	mmf vol%	inc. mm vol%	mmf vol%	inc. mm vol%	mmf vol%	inc. mm vol%	Mmf vol%
Vitrinite	Telinite	0.6	0.7	0.0	0.0	0.2	0.2	0.0	0.0	0.0	0.0	0.2	0.2	0.2	0.2	0.0	0.0	0.2	0.2	0.2	0.2	0.0	0.0
	Collotelinite	46.8	52.1	35.4	36.5	40.2	41.6	10.4	10.4	16.0	16.1	24.6	24.8	49.0	49.3	29.6	34.5	14.4	16.9	23.6	23.9	8.2	8.6
	Vitrodetrinite	1.0	1.1	0.0	0.0	0.6	0.6	0.7	0.7	0.0	0.0	0.0	0.0	0.2	0.2	0.0	0.0	0.0	0.0	0.0	0.0	0.2	0.2
	Collodetrinite	4.6	5.1	3.6	3.7	4.4	4.6	0.5	0.5	3.4	3.4	7.6	7.7	3.4	3.4	5.0	5.8	4.8	5.6	8.2	8.3	4.0	4.2
	Corpogelinite	0.2	0.2	1.8	1.9	1.0	1.0	0.0	0.0	0.0	0.0	0.6	0.6	0.6	0.6	0.0	0.0	0.6	0.7	1.0	1.0	0.4	0.4
	Gelinite	0.0	0.0	0.6	0.6	0.4	0.4	0.2	0.2	0.0	0.0	0.4	0.4	0.0	0.0	0.2	0.2	0.4	0.5	0.2	0.2	1.6	1.7
	Pseudovitrinite	0.0	0.0	0.0	0.0	0.0	0.0	0.0	0.0	0.0	0.0	0.0	0.0	0.2	0.2	0.0	0.0	0.0	0.0	0.0	0.0	0.2	0.2
Inertinite	Fusinite	12.4	13.8	14.6	15.1	12.4	12.8	3.7	3.7	7.0	7.1	11.0	11.1	9.4	9.5	6.6	7.7	5.4	6.3	10.0	10.1	8.4	8.8
	Reactive Semifusinite	2.8	3.1	8.4	8.7	3.2	3.3	3.0	3.0	5.4	5.4	5.8	5.9	7.2	7.2	4.6	5.4	2.8	3.3	29.4	29.8	4.4	4.6
	Inert semifusinite	7.6	8.5	17.6	18.1	19.0	19.7	47.4	47.6	41.6	41.9	30.4	30.7	17.8	17.9	19.8	23.1	33.2	38.9	5.2	5.3	37.4	39.3
	Micrinite	2.4	2.7	1.2	1.2	1.0	1.0	0.7	0.7	1.2	1.2	3.2	3.2	3.8	3.8	2.0	2.3	1.0	1.2	2.8	2.8	0.8	0.8
	Macrinite	0.8	0.9	1.2	1.2	0.8	0.8	0.7	0.7	1.0	1.0	0.8	0.8	0.0	0.0	1.2	1.4	0.2	0.2	0.6	0.6	1.8	1.9
	Secretinite	3.4	3.8	5.2	5.4	4.8	5.0	11.9	11.9	4.6	4.6	5.2	5.3	3.4	3.4	5.6	6.5	7.2	8.4	2.2	2.2	6.0	6.3
	Funginite	0.0	0.0	0.0	0.0	0.0	0.0	0.0	0.0	0.0	0.0	0.0	0.0	0.0	0.0	0.0	0.0	0.0	0.0	0.0	0.0	0.0	0.0
	Inertodetrinite R	1.2	1.3	1.4	1.4	0.8	0.8	4.0	4.0	4.2	4.2	1.8	1.8	0.2	0.2	2.6	3.0	2.8	3.3	2.4	2.4	4.0	4.2
	Inertodetrinite I	3.0	3.3	4.4	4.5	6.0	6.2	15.1	15.1	12.0	12.1	6.8	6.9	3.4	3.4	6.4	7.5	10.0	11.7	10.6	10.8	14.4	15.1
Liptinite	Sporinite	1.0	1.1	0.4	0.4	0.6	0.6	0.2	0.2	1.6	1.6	0.4	0.4	0.4	0.4	0.2	0.2	1.0	1.2	1.0	1.0	1.8	1.9
	Cutinite	0.0	0.0	0.0	0.0	0.2	0.2	0.5	0.5	0.0	0.0	0.0	0.0	0.0	0.0	0.2	0.2	0.0	0.0	0.0	0.0	1.0	1.1
	Resinite	1.2	1.3	0.0	0.0	0.2	0.2	0.0	0.0	0.2	0.2	0.0	0.0	0.2	0.2	0.8	0.9	0.0	0.0	0.4	0.4	0.6	0.6
	Alginite	0.0	0.0	0.0	0.0	0.0	0.0	0.0	0.0	0.0	0.0	0.0	0.0	0.0	0.0	0.8	0.9	1.0	1.2	0.2	0.2	0.0	0.0
	Liptodetrinite	0.0	0.0	0.0	0.0	0.0	0.0	0.0	0.0	0.0	0.0	0.0	0.0	0.0	0.0	0.0	0.0	0.0	0.0	0.0	0.0	0.0	0.0
	Suberinite	0.0	0.0	0.0	0.0	0.0	0.0	0.0	0.0	0.0	0.0	0.0	0.0	0.0	0.0	0.0	0.0	0.0	0.0	0.0	0.0	0.0	0.0
	Exudatinite	0.8	0.9	1.2	1.2	0.8	0.8	0.5	0.5	1.0	1.0	0.2	0.2	0.0	0.0	0.2	0.2	0.4	0.5	0.6	0.6	0.0	0.0
Mineral matter	Silicate (clay/qz)	1.2		0.0		0.2		0.0		0.0		0.2		0.2		0.0		0.2		0.2		0.8	
	Sulphide	2.2		0.4		2.6		0.5		0.6		0.4		0.0		14.0		14.0		0.6		3.6	
	Carbonate	6.8		2.6		0.6		0.0		0.0		0.4		0.4		0.2		0.4		0.6		0.4	
	Other	0.0		0.0		0.0		0.0		0.2		0.0		0.0		0.0		0.0		0.0		0.0	

Table 4.24: Summary of detailed maceral analyses for 3MS Channel.

SUMMARY TABLE																							
Sample identification:		3MS1 0-30cm (1554)		3MS2 30-60cm (1555)		3MS3 60-90cm (1556)		3MS4 90-120cm (1557)		3MS5 120-150cm (1558)		3MS6 150-180cm (1559)		3MS7 180-210cm (1560)		3MS8 210-240cm (1561)		3MS9 240-270cm (1562)		3MS10 270-300cm (1563)		3MS11 300-330cm (1564	
		inc. mm vol %	mmf vol %	inc. mm vol %	mmf vol%	inc. mm vol %	mmf vol%	inc. mm vol %	mmf vol%	inc. mm vol %	Mmf vol%	inc. mm vol %	mmf vol%	inc. mm vol %	mmf vol%	inc. mm vol %	mmf vol%	inc. mm vol %	mmf vol%	inc. mm vol %	mmf vol%	inc. mm vol %	Mmf vol%
MACERAL GROUP	VITRINITE	53.2	59.2	41.4	42.7	46.8	48.4	11.9	11.9	19.4	19.6	33.4	33.7	53.6	53.9	34.8	40.6	20.4	23.9	33.2	33.7	14.6	15.3
TOTALS (vol%)	INERTINITE	33.6	37.4	54	55.7	48	49.7	86.4	86.8	77	77.6	65	65.7	45.2	45.5	48.8	56.9	62.6	73.3	63.2	64.1	77.2	81.1
	LIPTINITE	3	3.3	1.6	1.6	1.8	1.9	1.2	1.2	2.8	2.8	0.6	0.6	0.6	0.6	2.2	2.6	2.4	2.8	2.2	2.2	3.4	3.6
	MINERAL MATTER	10.2		3		3.4		0.5		0.8		1		0.6		14.2		14.6		1.4		4.8	
	TOTAL INERTINITE	33.6	37.4	54	55.7	48	49.7	86.4	86.8	77	77.6	65	65.7	45.2	45.5	48.8	56.9	62.6	73.3	63.2	64.1	77.2	81.1
	TOTAL REACTIVE MACERALS	60.2	67	52.8	54.4	52.6	54.5	20	20.1	31.8	32.1	41.6	42	61.6	62	44.2	51.5	28.4	33.3	67.2	68.2	26.4	27.7

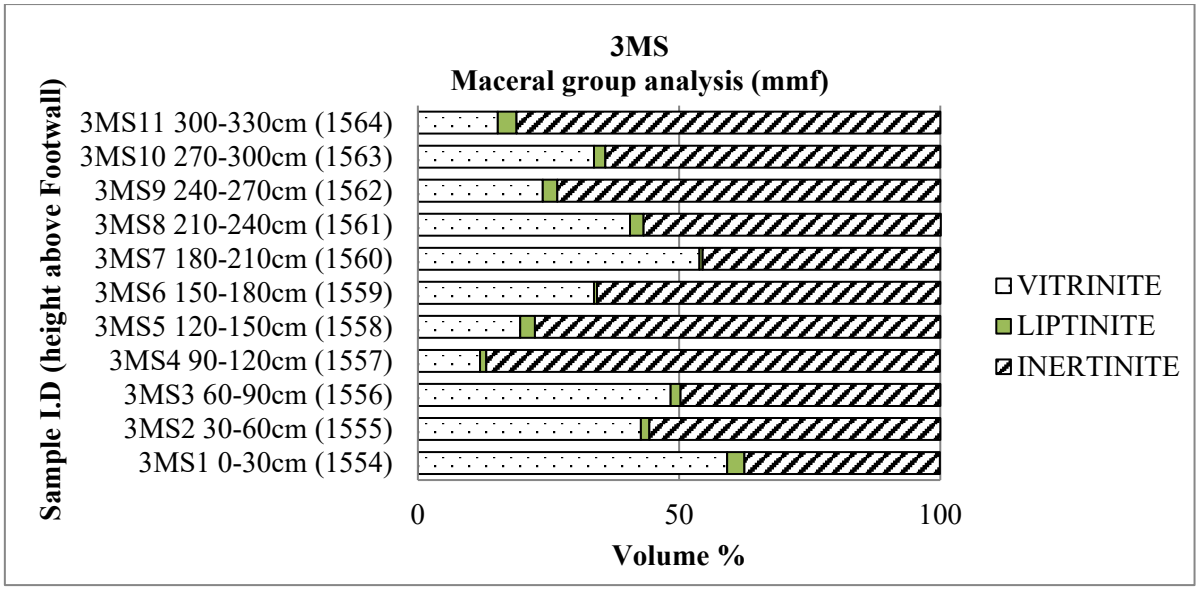


Figure 4.33: Graph to show analyses (m.m.f) for the three maceral groups along 3MS Channel samples.

4.4.6.3 Mineral Species in Hwange Coal

A petrographic examination of the mineral species distribution reveals an interesting picture which is as follows.

I. The sulphide component is the only mineral component detected in the bottom sample (0-3 m) and it subsequently dominates in all three higher samples up Chaba Channel 1 (Figure 4.34), with steady decrease towards the top of the seam. The silicate species (clay and quartz) appear from second samples (3-6 m) and show an increase upwards the seam. The carbonate species only appears in the topmost sample (6-9 m).

II. In Chaba Channel 2 (Figure 4.35), the sulphide component is, once again, the only mineral species detected in the basal sample (0-1 m) and is detected in all samples up the channel. The silicate component appears from the middle of the seam and shows a steady increase towards the top of seam. The carbonate species has the least abundance and occurs from sample 1-2 m to sample 6-7 above coal base.

III. Along 3ME Channel (Figure 4.36), both the sulphide and carbonate components occur in the basal 0-30 cm (with the carbonate being the more dominant) with the sulphide showing a steady increase towards the roof of the coal face. Silicates start appearing in the third (6-9 cm) sample showing a steady increase towards the mining roof.

IV. All the three mineral species appear in the basal (0-30 cm) samples in 3MS Channel (Figure 4.37) with the carbonate being the most dominant, followed by sulphides. The mineral component decreases in the middle of the channel before a spike dominantly of sulphide and a very small amount of carbonate appears between 210 and 270 cm above coal base.

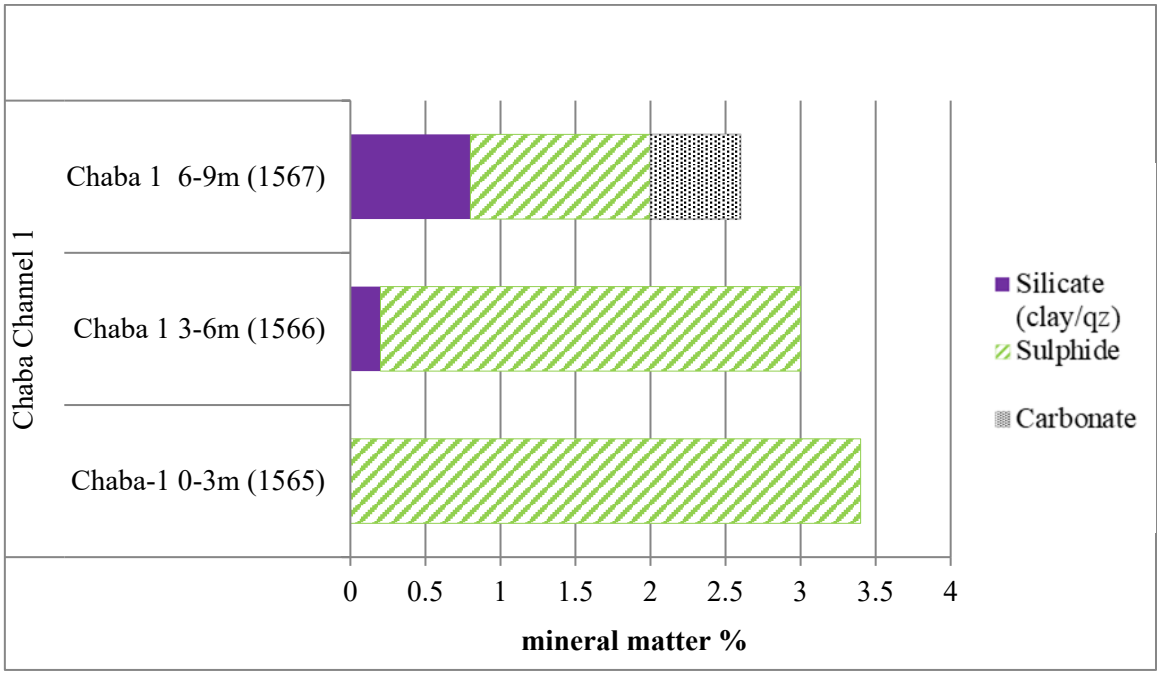


Figure 4.34: Mineral species petrographically observed in Chaba Channel 1 samples.

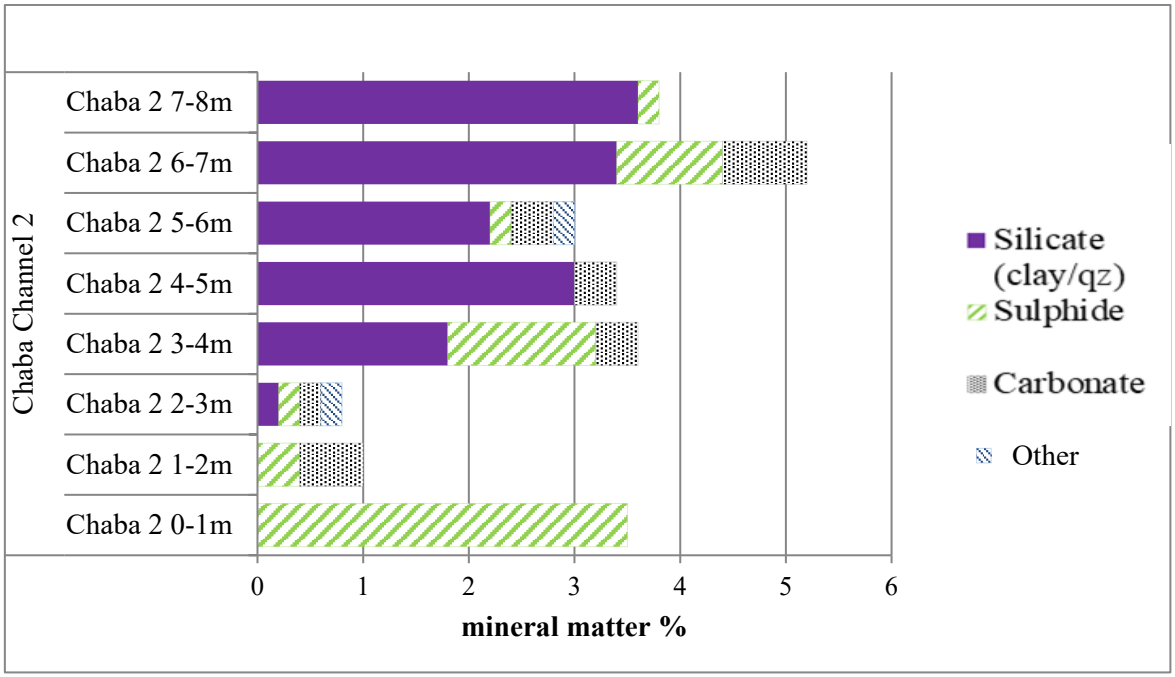


Figure 4.35: Mineral species petrographically observed in Chaba Channel 2 samples.

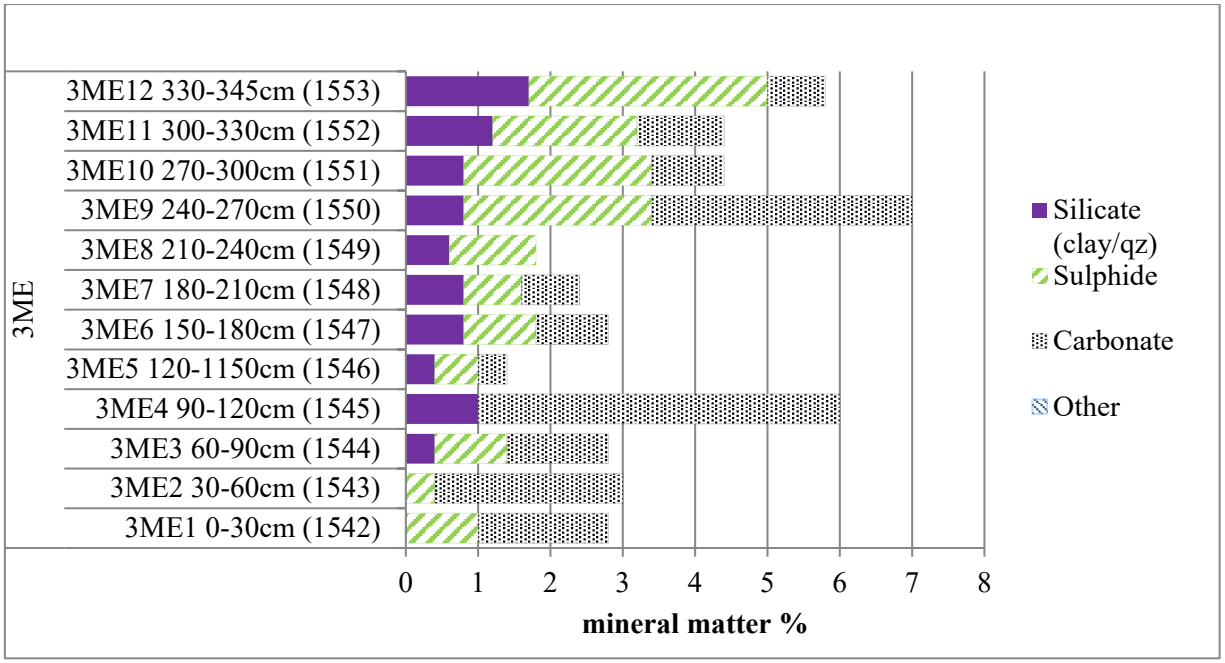


Figure 4.36: Mineral species observed in 3 Main East samples.

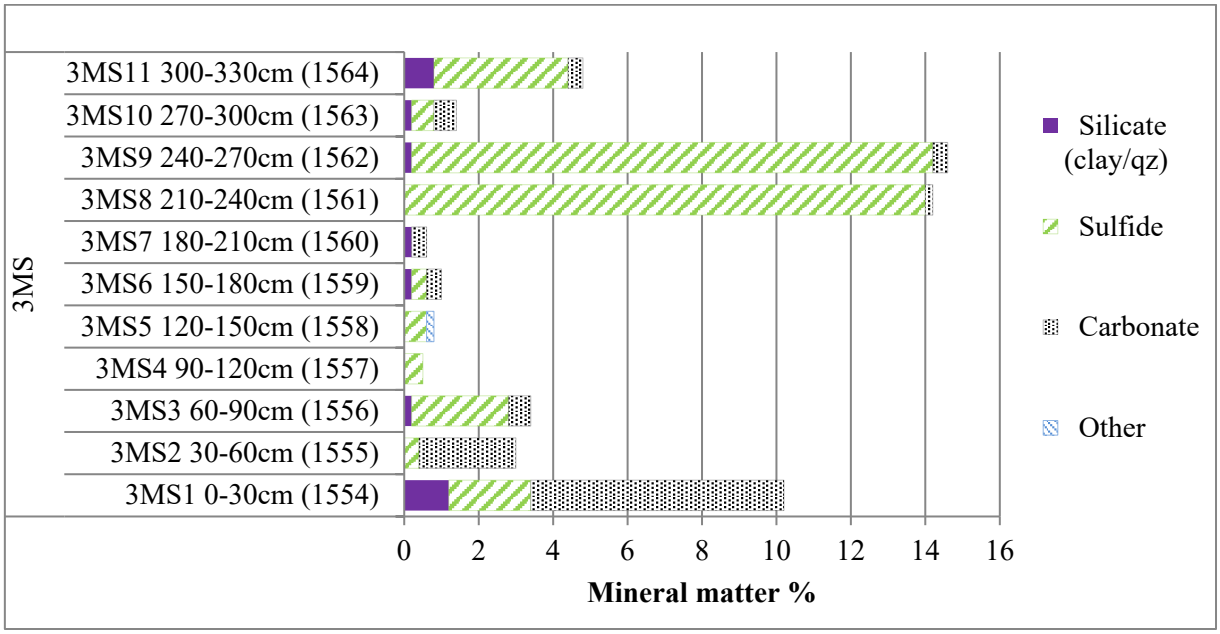


Figure 4.37: Mineral species in 3 Main South samples.

Data from coal petrography, which provides details on the observable mineral and basic mineral composition, and the ash value from the proximate analysis of the coal was used to draw a graph for each sampling channel to establish whether there is an agreement between the mineral matter content and ash value vertical trend (figures 4.38 to 4.41). The graphs also provide details on species that constitute the mineral matter. There is a somewhat crude agreement between the ash and mineral matter vertical variation trends. This is more evident in the 3ME and 3MS channels. However, not all mineral matter can be determined petrographically mainly due to the unavoidable inaccuracy

resulting from the fineness of some minerals, particularly clay. Hence the ash value is considered a better indicator of total mineral matter although XRD (a technique not used in this study) is a better indicator of mineral composition. However, all three complement each other (usually all three analyses are conducted). The mineral matter as conducted petrographically shows a trend that agrees with the trend of the ash value as determined by proximate analysis. The silicates, namely clay and quartz, generally show an increase towards the top (figures 4.38 to 4.41). However, the study did not establish whether the mineral towards the top of the seam included detrital material. The presence of clays and quartz in southern African coals, however, generally assumes their detrital provenance.

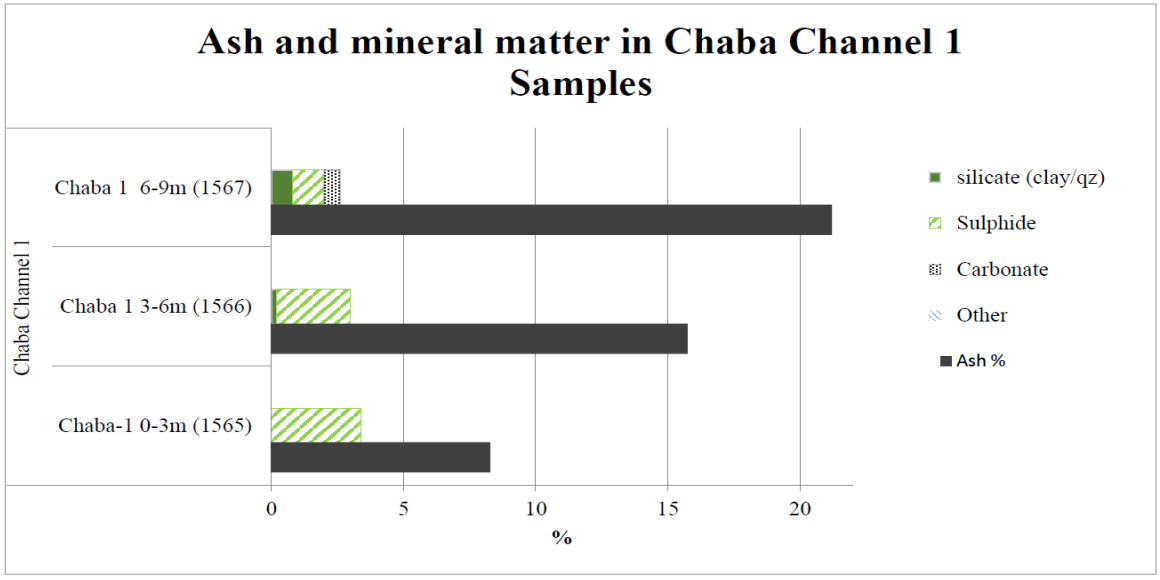


Figure 4.38: Ash and observed mineral species in Chaba Channel 1 samples.

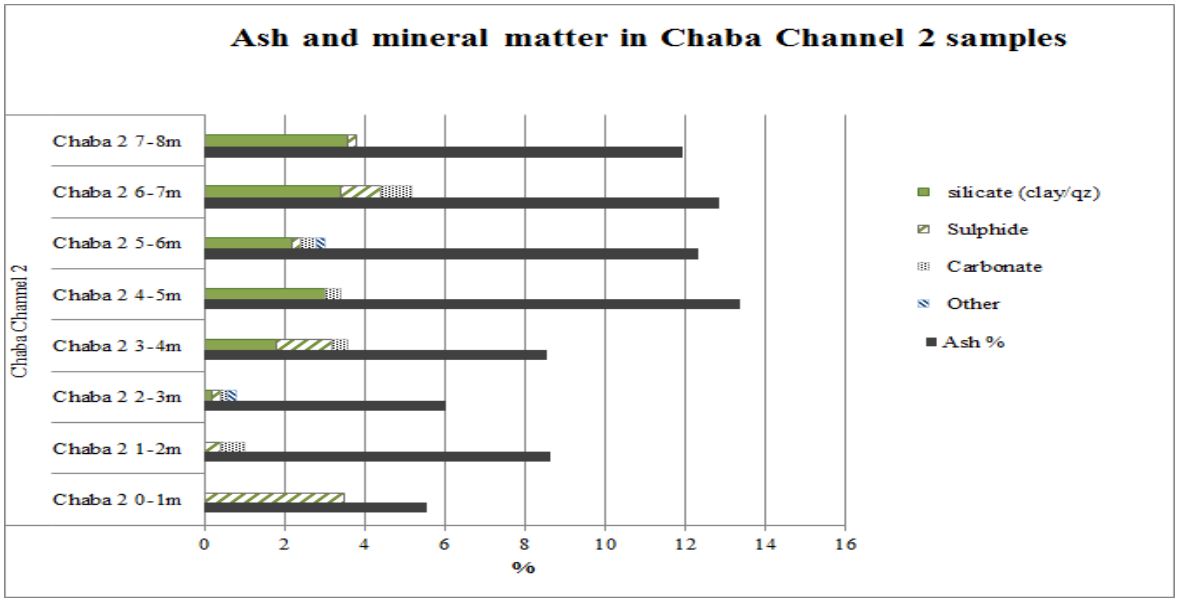


Figure 4.39: Ash and observed mineral species in Chaba Channel 2 samples.

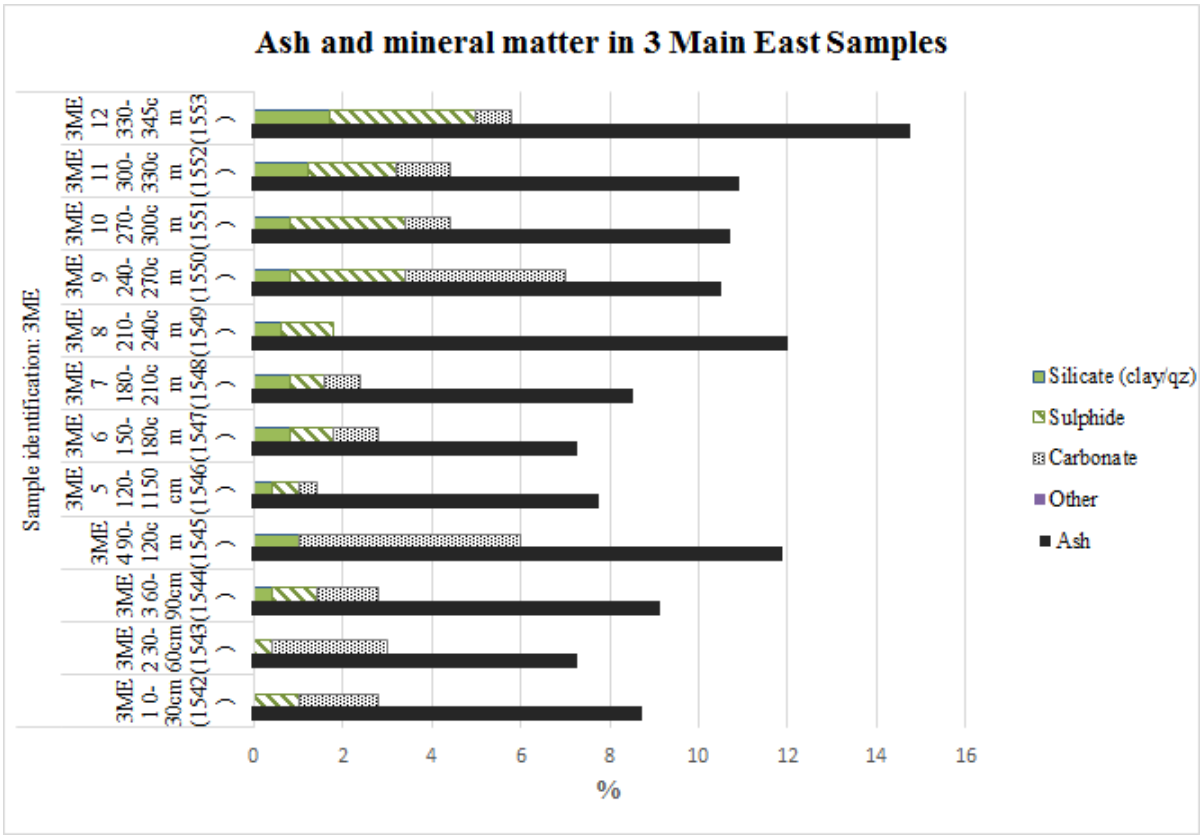


Figure 4.40: Ash and observed mineral species in 3 Main East samples.

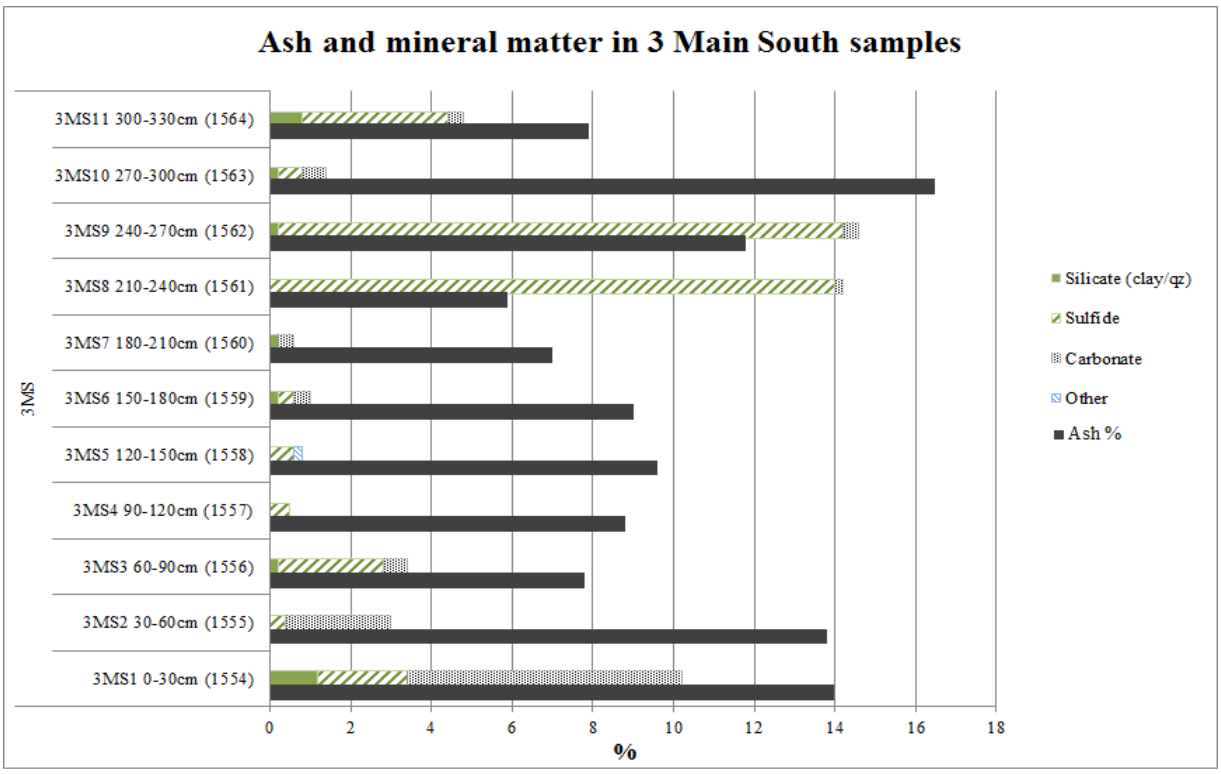


Figure 4.41: Ash and observed mineral species in 3 Main South samples.

4.4.6.4 Macerals Microscopy

Polished blocks of samples from Chaba channels 1 and 2, as well as samples from 3 Main South and 3 Main East samples were viewed under the coal petrographic microscope. This section presents a total of 16 photomicrographs (made up of six from the 3 Main East Channel, six from 3 Main South Channel, and four from Chaba Channel 1) of some of the macerals as well as mineral matter observed under the coal petrographic microscope. The rest of the photomicrographs are presented under Appendix 4.5.

Plate 1: Six photomicrographs of 3ME Channel samples.
Scale bar = 50 microns

A. Plate 1A: Part of SME 1545 showing collotelinite (co) and cutinite (c) (fusinite, semifusinite and liptinite macerals)
B. Plate 1B: Fluorescent image showing infilling of exudatinite (the yellow pieces) in fusinite.

C. Plate 1C: Photomicrograph of 3ME sample code 1549 containing exudatinite (E) held in secretinite (Secr) vesicles. The exudatinite is assumed to have migrated through the coal mass after coalification.

D. Plate 1D: A large carbonate mineral in 3ME sample code 1550.

E. Plate 1E: Pyrite in fusinite honeycomb structure in 3ME sample code1550. Pyrite is inflling cell lumens with some lumens appearing empty. There are two possibilities: either the pyrite did not accumulate in all cavities, or that some of the pyrite has subsequently been leached out.

F. Plate 15B: A photomicrograph of 3ME sample 1553 showing quartz, and semifusinite and inertodetrinite (silicates within inertinite).

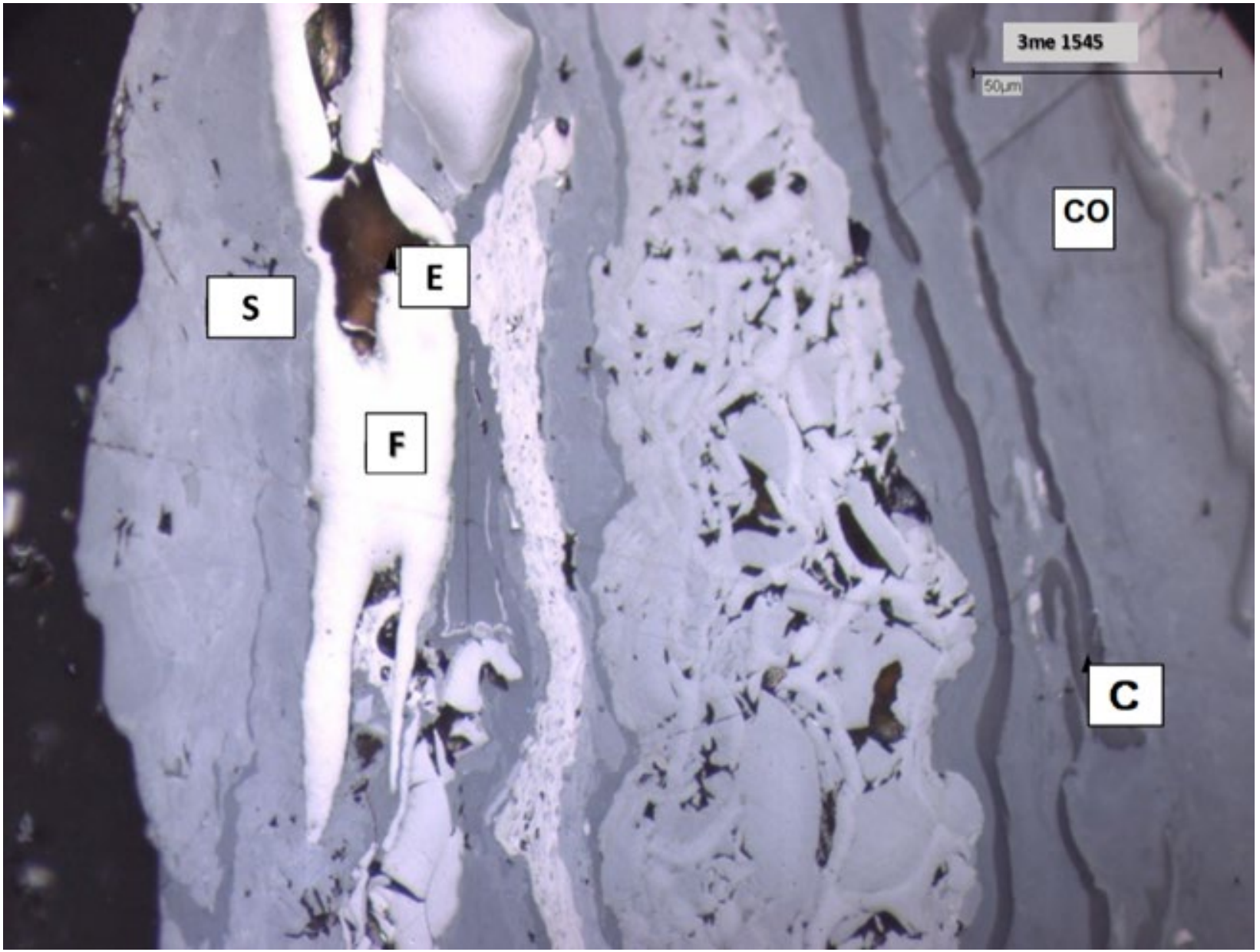


Plate 1A

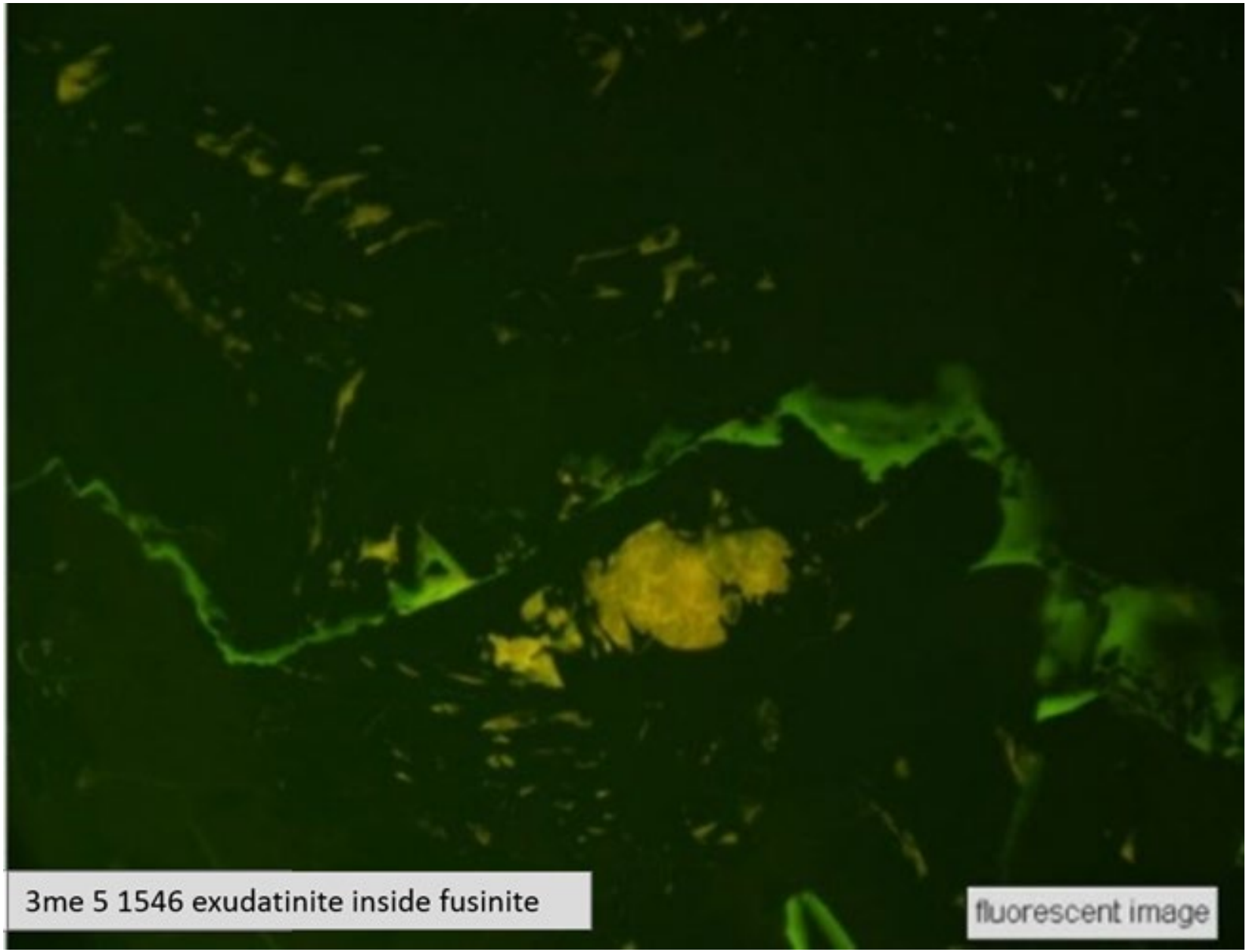


Plate 1B

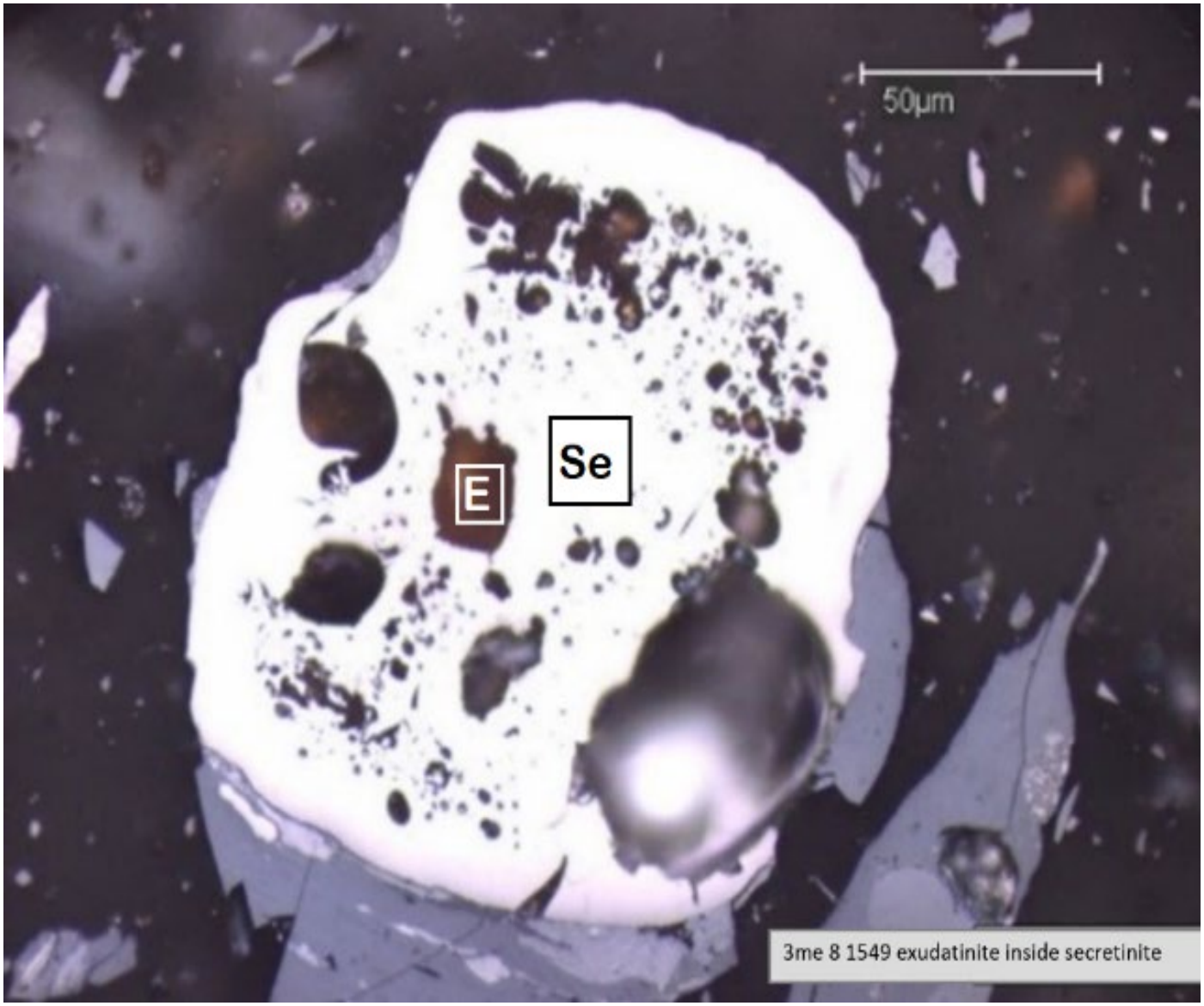


Plate 1C

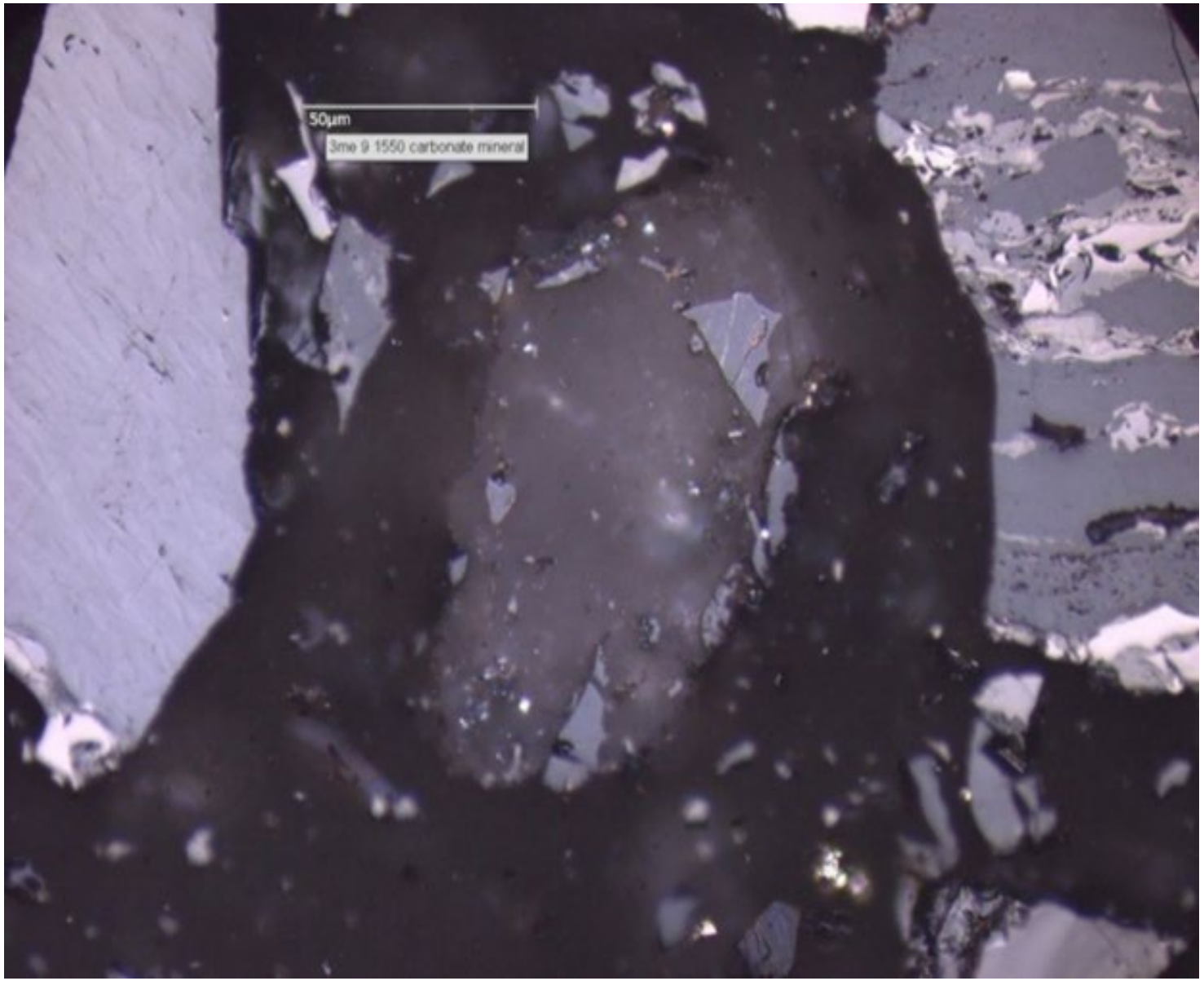


Plate1D

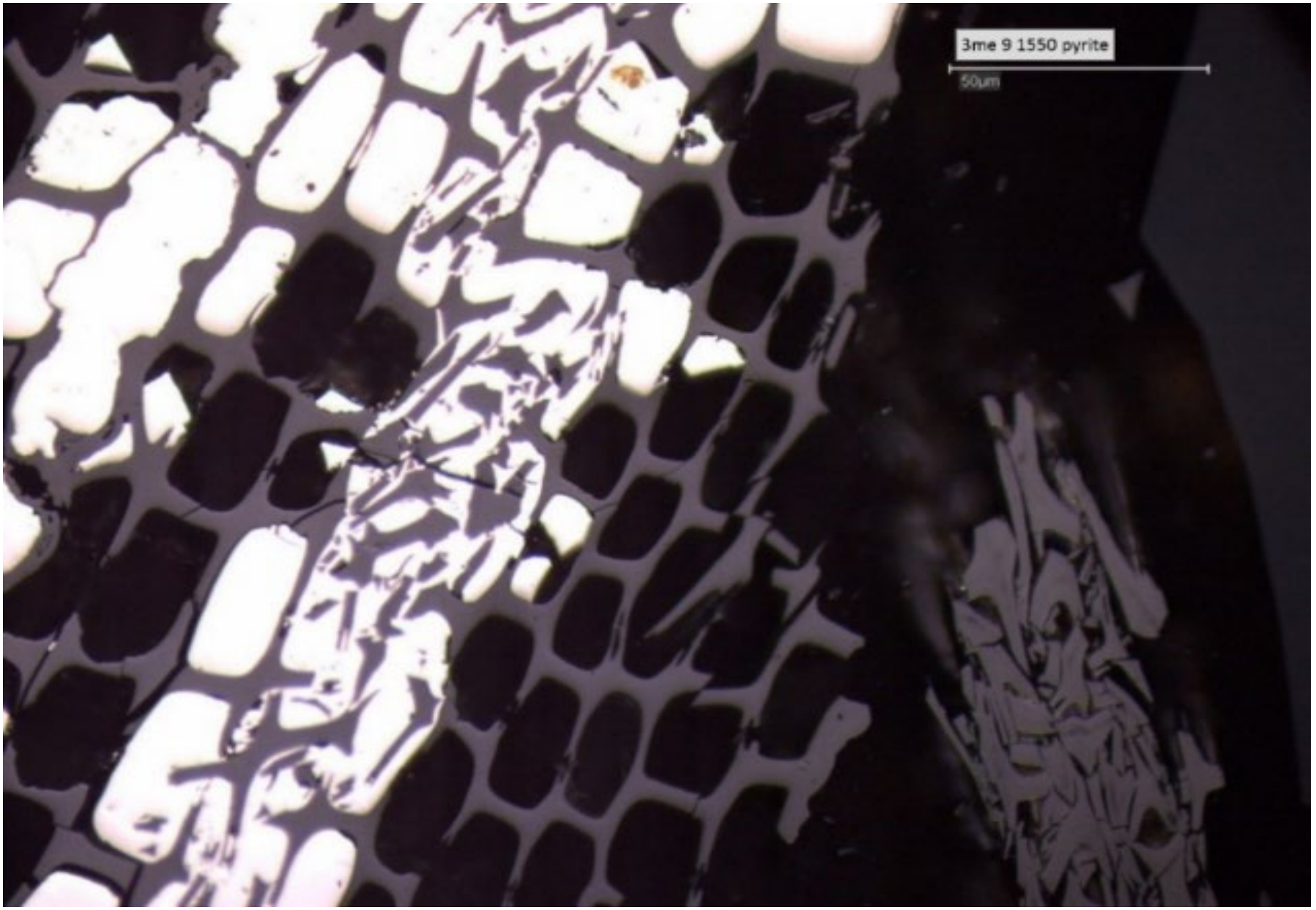


Plate1E

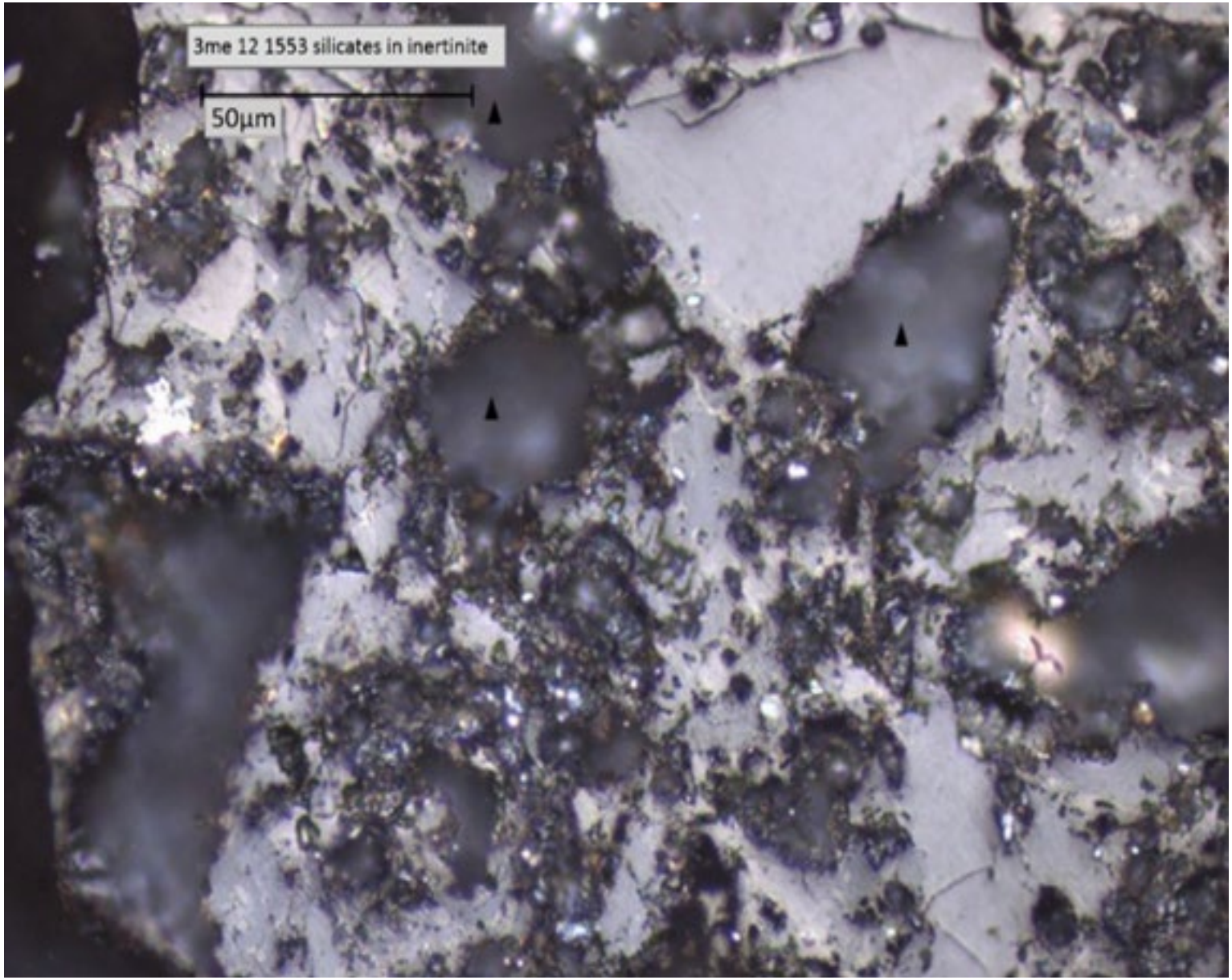


Plate1F

Plate 2: 3MS

A. Plate 2A: A large carbonate particle in 3MS sample code 1554.

B. Plate 2B: A photomicrograph of 3MS sample code 1556 showing typical particle of collotelinite, secretinite and inertinite (secretinite, vitrinite and inertinite).

C. Plate 2C: An association of vitrinite and inertodetrinite and micrinite in 3MS

D. Plate 2D: Cuticle and reactive semi fusinite particles in 3MS sample code 1559.

E. Plate 2E: Extensive pyrite infilling of cell lumen 3MS sample code 1561. The infilling could be syngenetic, or epigenetic; in the latter case pyrite may have replaced clay minerals.

F. Plate 2F: A photomicrograph showing infilling of organic matter by pyrite in 3MS sample code 1561.

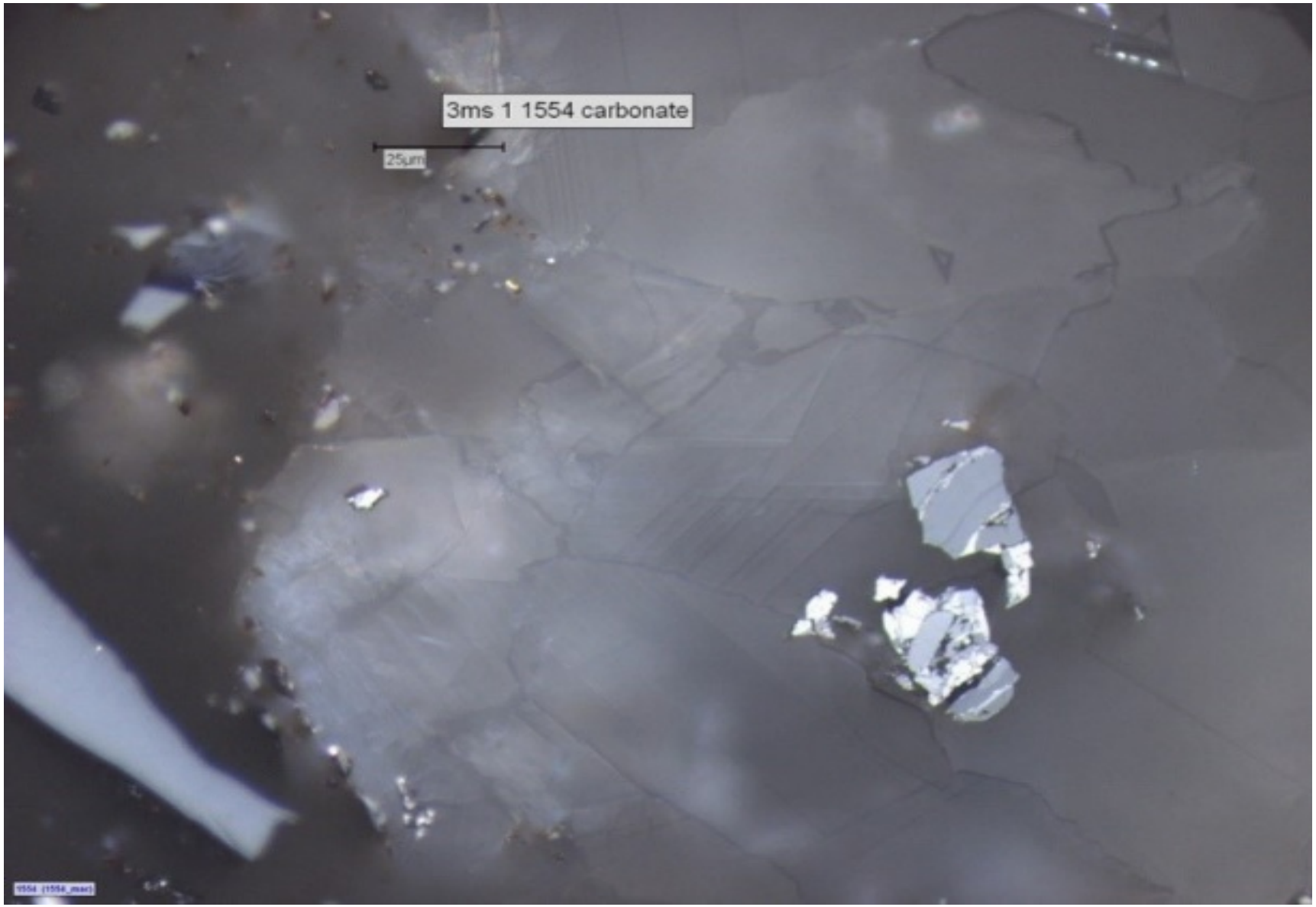


Plate 2 A

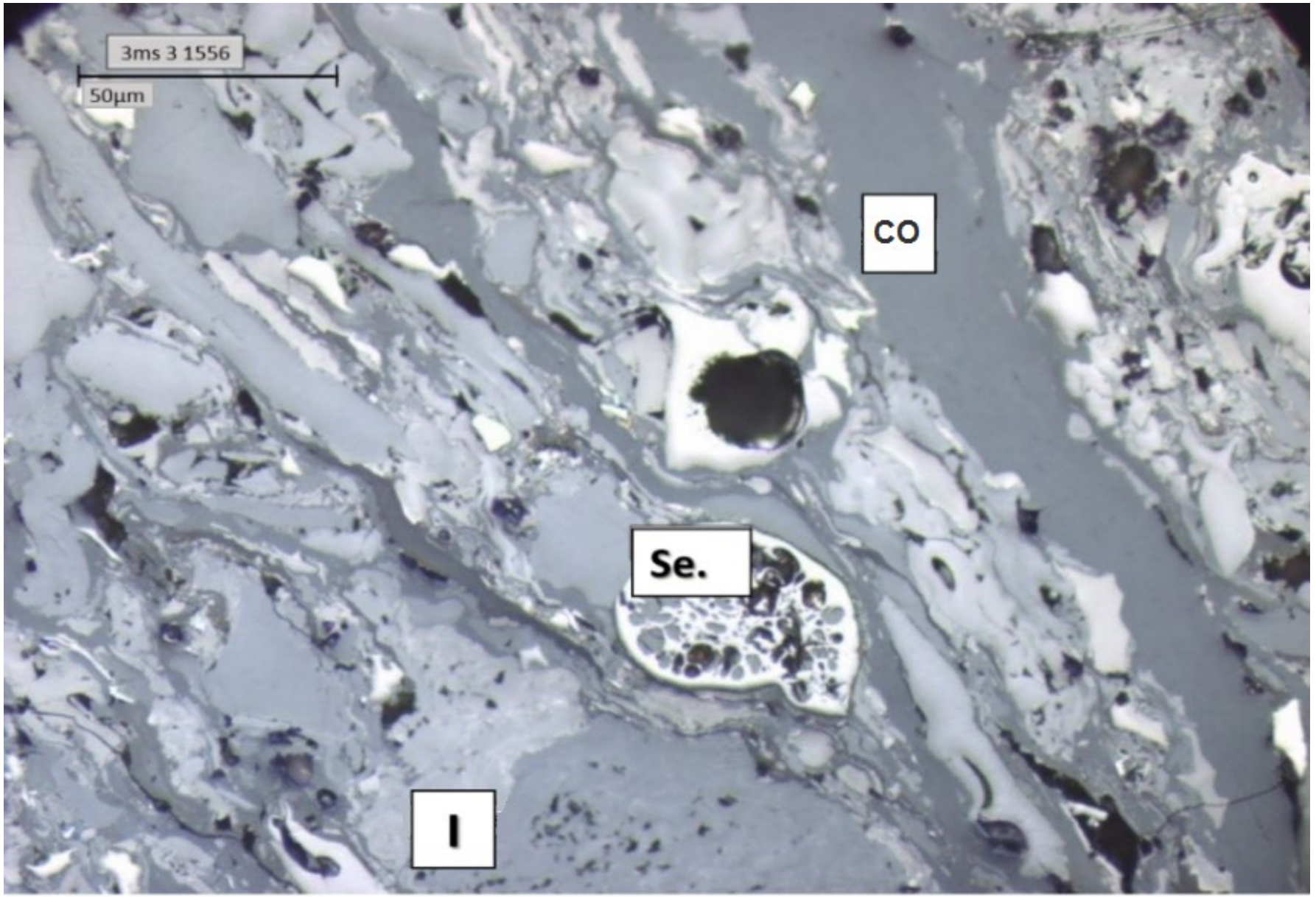


Plate 2B

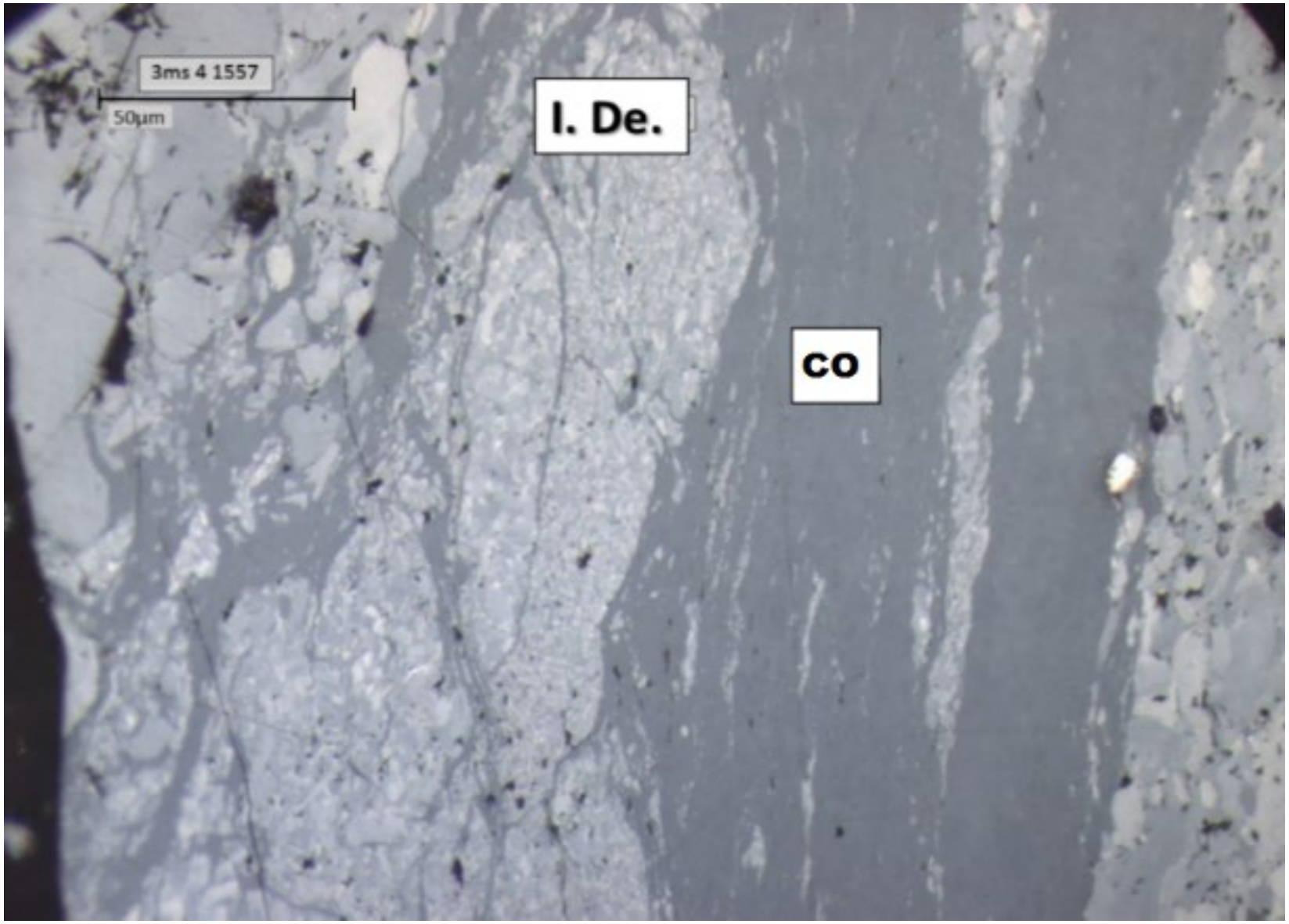


Plate 2C

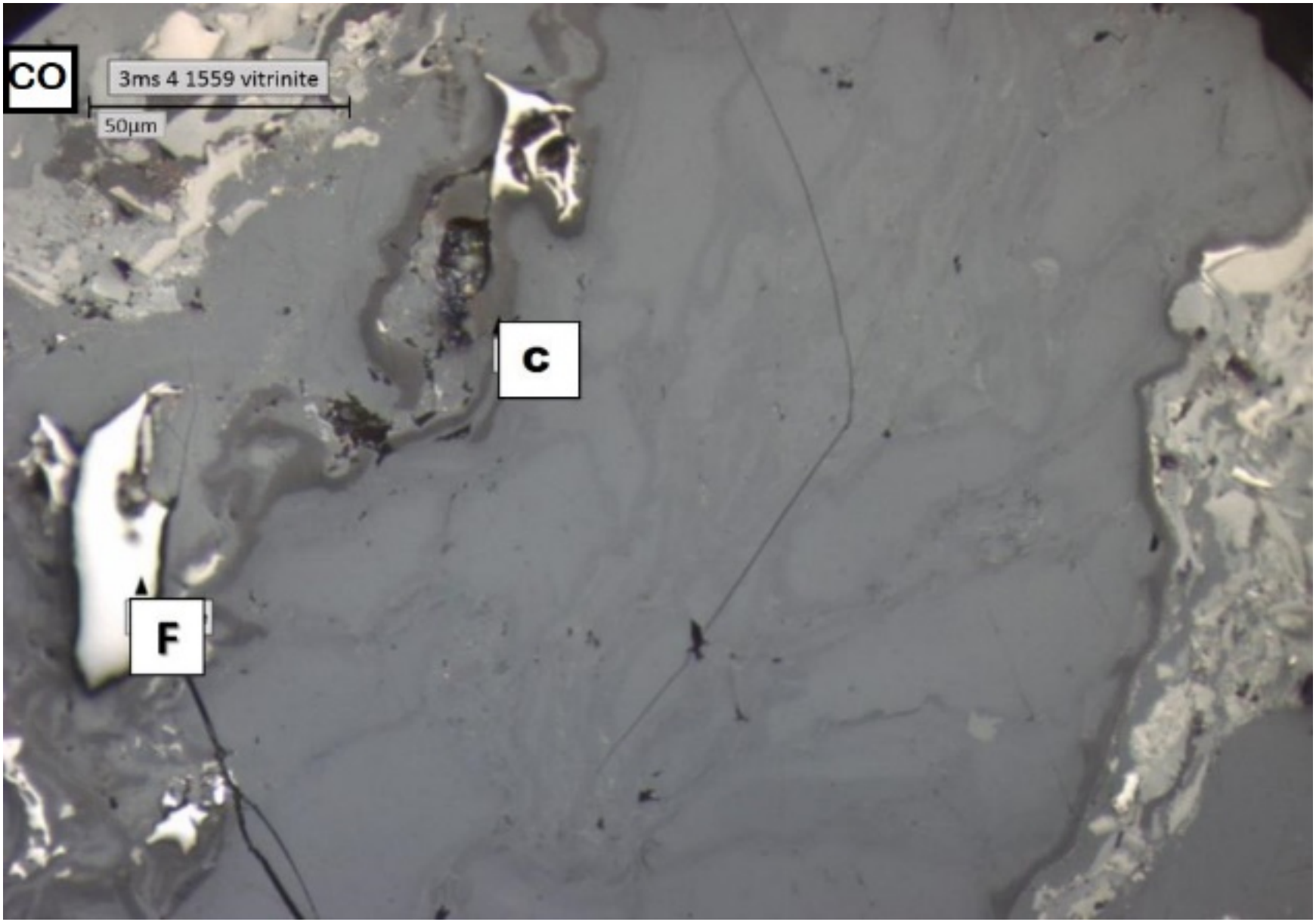


Plate 2D

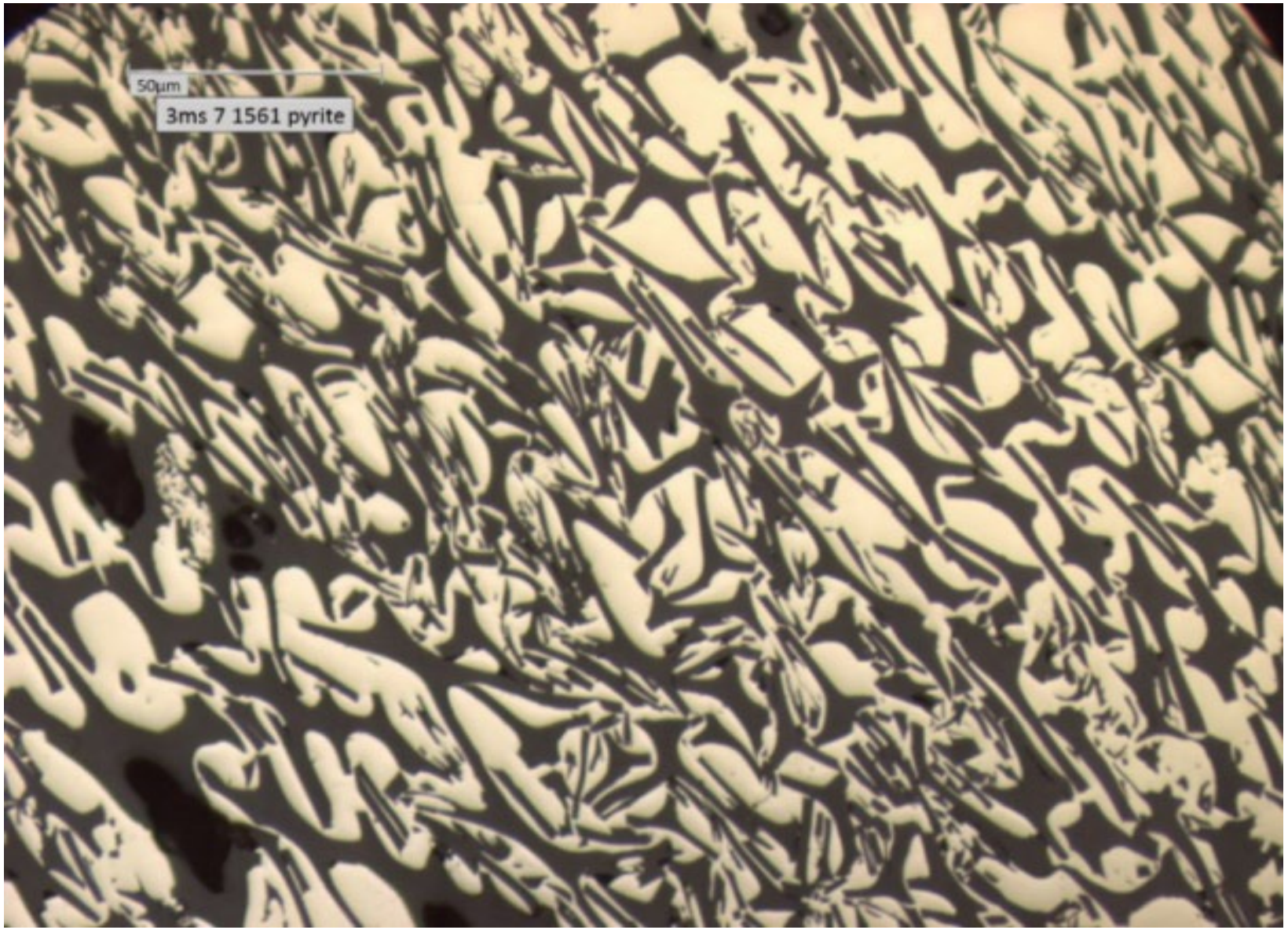


Plate 2E

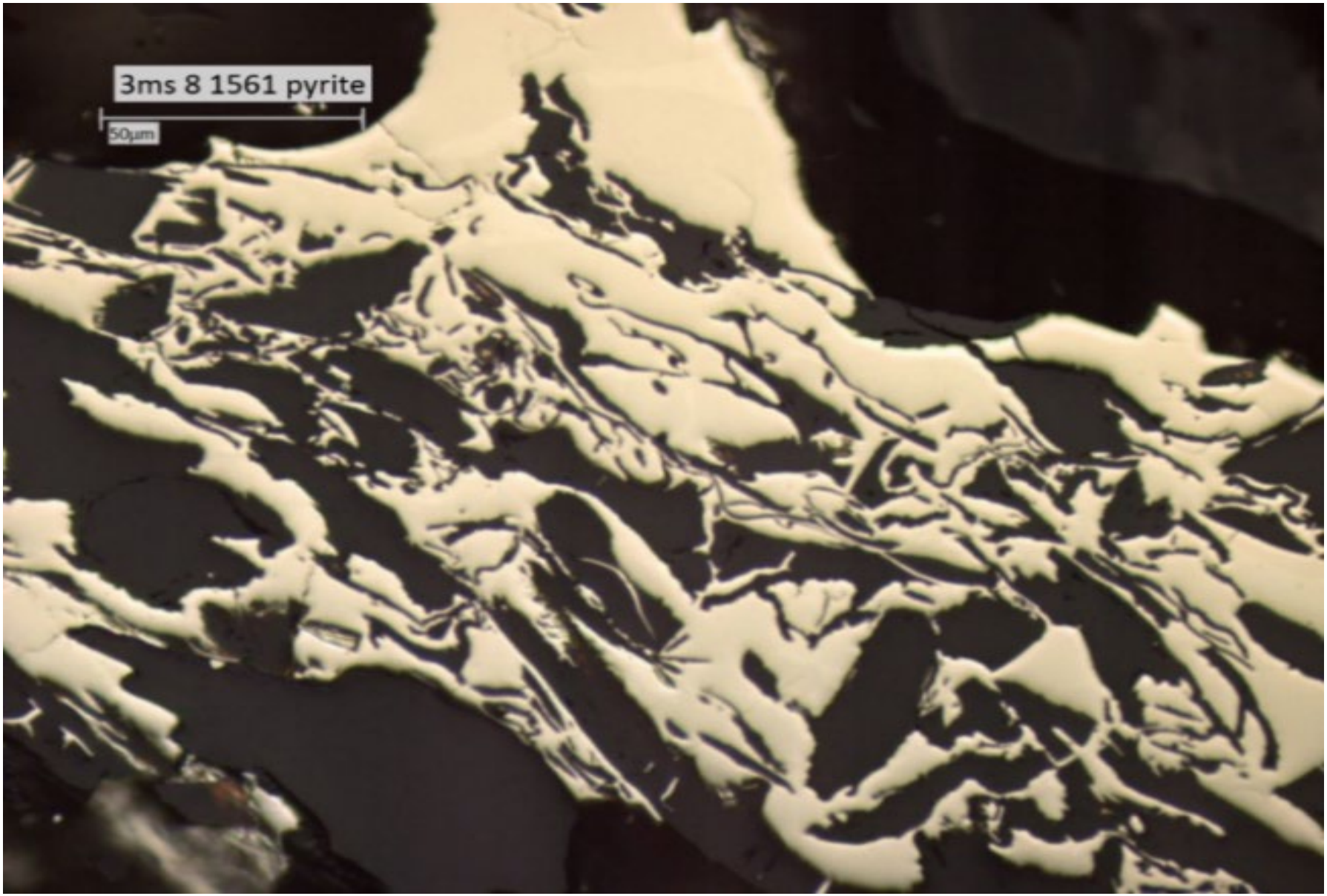


Plate 2F

Plate 3 Chaba

A. Plate 3A: Pyrite in Chaba sample code 1565.

B. Plate 3B: A photographmicrograph of Chaba sample code 1566 showing fusinite and collotelinite.

C. Plate 3C: Reactive semifusinite and inert semifusinite.

D. Plate 3D: Inertodetrinite particles in Chaba sample 1567 showing dominance of inert macerals in higher samples at Chaba.

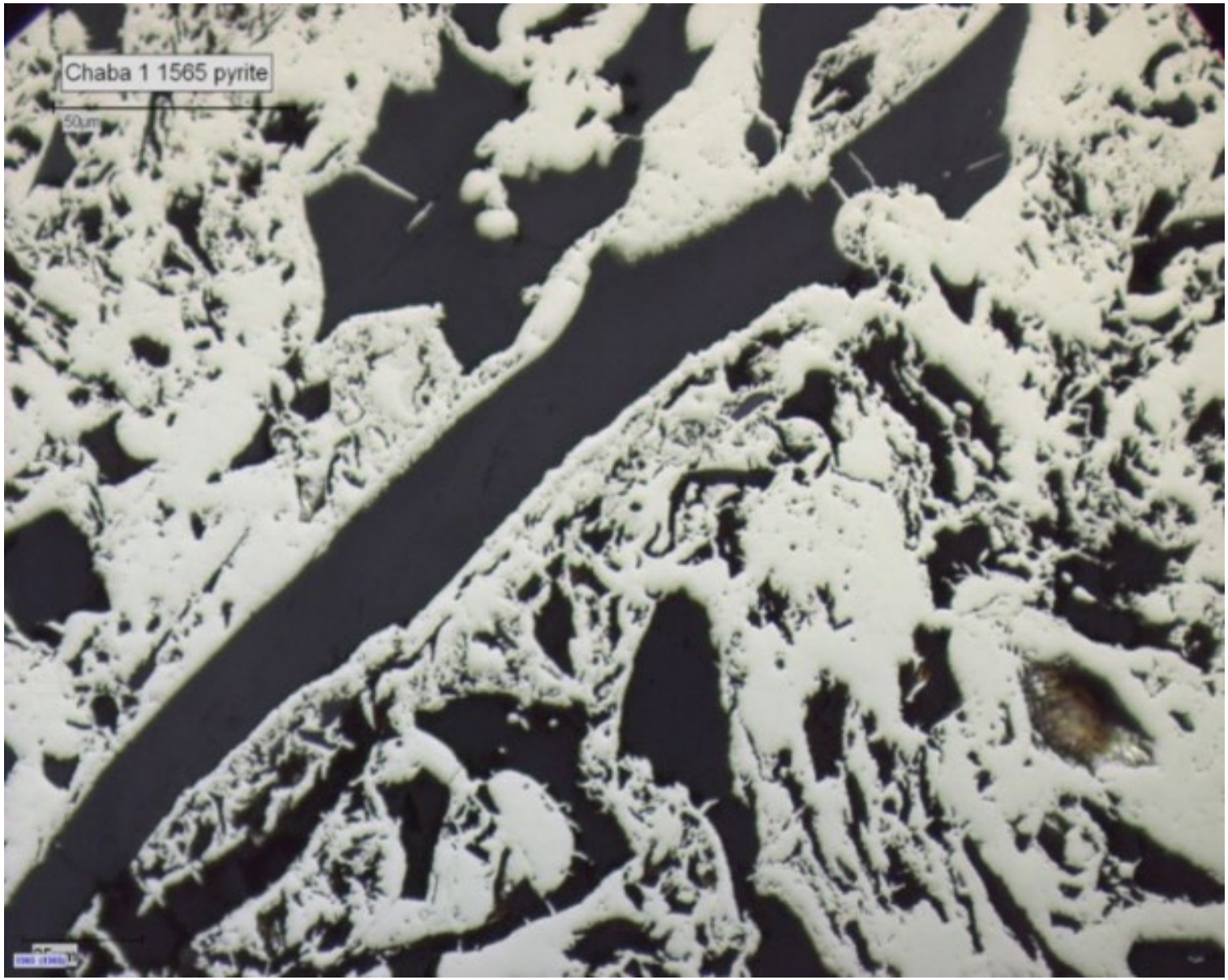


Plate 3A

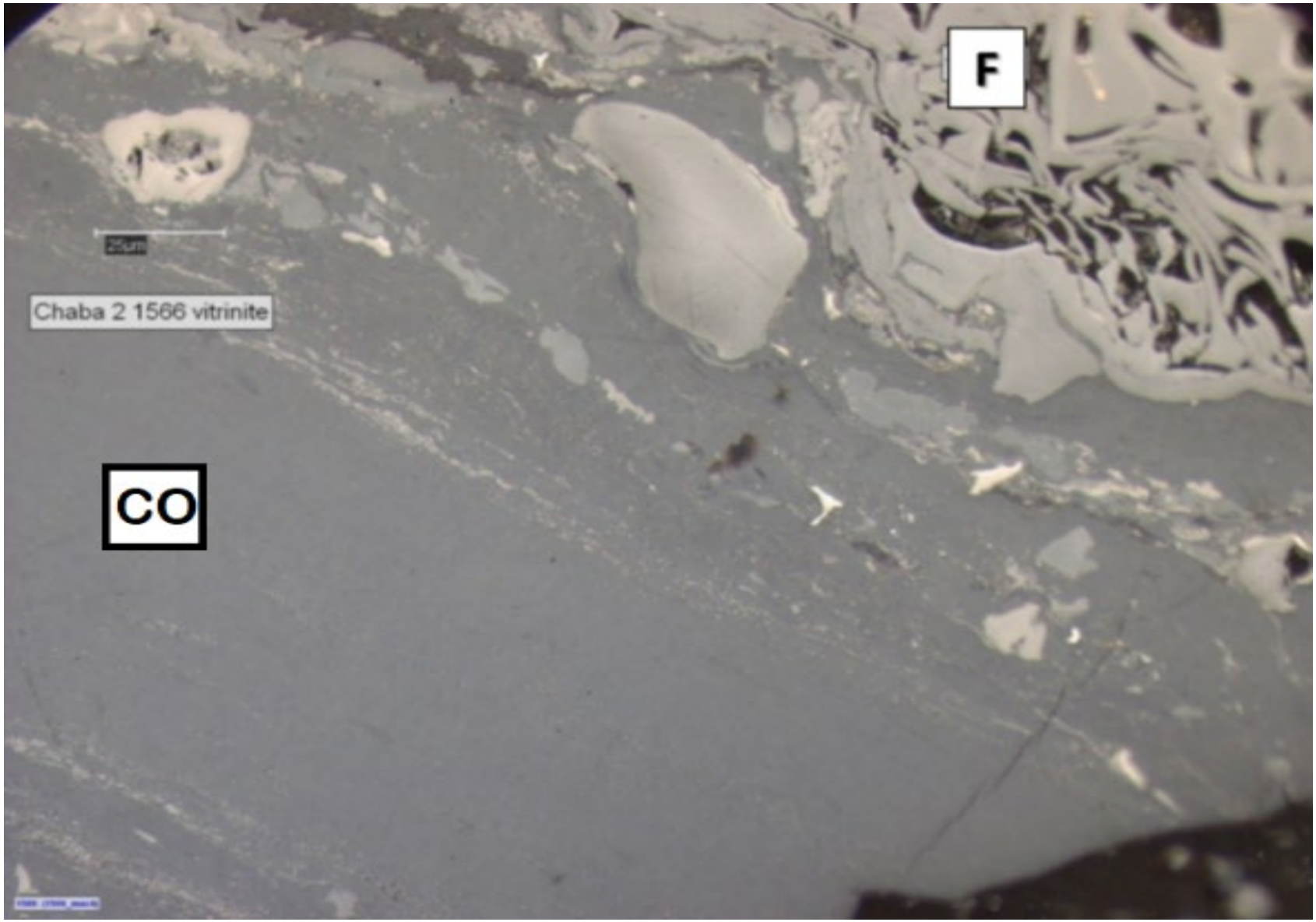


Plate 3B

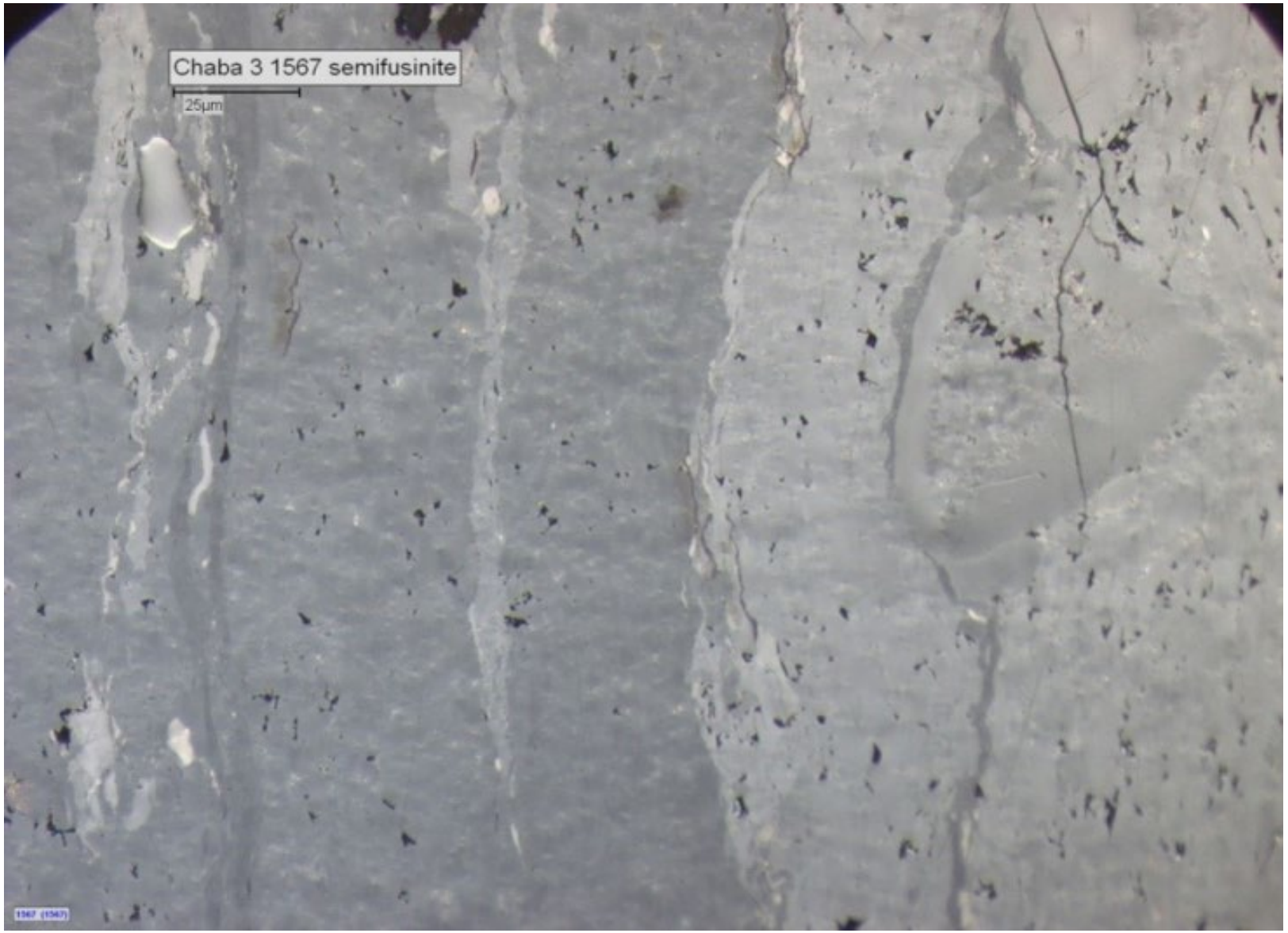


Plate 3C

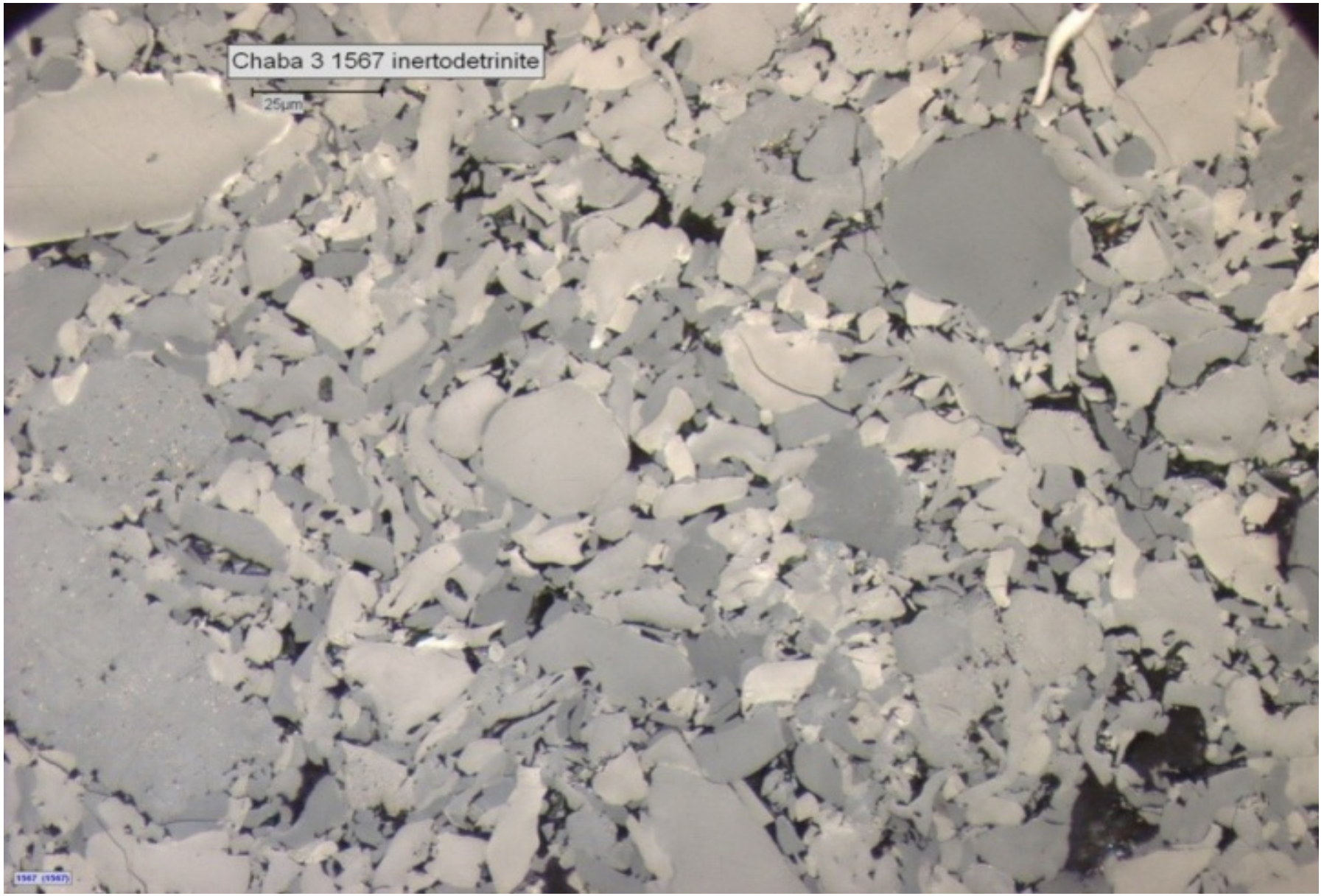


Plate 3D

4.4.6.5 Microlithotype Analysis

Tables 4.25 to 4.28 present the results of the microlithotype analysis of coal samples collected from the four channels, i.e., Chaba Channels 1 and 2, and 3 Main Underground Mine channels 3ME and 3MS. The data are also presented graphically in Figures 4.42 to 4.45, and the observation made from the microlithotype analysis of the samples summarized as follows:

I. A steady decrease was observed in the vitrite content with the distance above coal foot wall along both channels 1 and 2 at Chaba. The basal sample (0-3 m) shows a vitrite content of 38.3% which decreasess to 3.2% in sample taken at 6-9 m from the top of the seam (Table 4.25 and Figure 4.42). Along Chaba Channel 2, the basal sample (0-1 m) yielded a vitrite value of 17.4%, while the microlithotype is recorded as 0% in the top most sample (i.e., 7-8 m) as seen in Table 4.26 and Figure 4.43.

II. In the two underground mine channels (3ME and 3MS), vitrite (composed predominantly of vitrinite) predominates at the base, with inertodetrite becoming more signficant towards the top of the seam. However, a cyclic pattern giving rise to vertical variation is also evident. Along both channels, there is a significant spike in the vitrinite content in samples 1548 (3ME) and 1560 (3MS) both of which represent the 180-210 cm height interval (tables 4.27 and 4.28 respectively). This is more pronounced in Figure 4.44 and Figure 4.45, respectively.

Table 4.25: Microlithotype analysis for Chaba Channel 1 samples.

Sample no: Sample identification:		**1565 0-3 m**	**1566 3-6 m**	**1567 6-9 m**
Microlithotype group	Microlithotype (vol%)	vol%	vol%	vol%
Monomaceral	vitrite	38.3	10.6	3.2
	semifusite	14.8	38.3	47.0
	fusite / secretinite	4.8	7.9	12.0
	inertodetrite	0.7	3.7	10.5
	liptite	0.0	0.2	0.5
Bimaceral	vit+sf/f	11.6	18.7	7.0
	vit+int	16.2	3.4	6.3
	sf+int	1.5	7.4	6.0
	vit+lipt	0.0	0.0	0.0
	int+lipt	0.0	2.0	2.5
Trimceral	trimaceral	6.8	3.9	3.0
Carbominerite	cbm arg/clay	0.0	0.2	0.2
	cbm pyrite	2.2	1.7	0.5
	cbm ank/carb	0.0	0.0	0.8
	cbm sil/qz	0.0	0.0	0.0
	cbm poly	0	0.0	0.0
Rock (minerite)	rock	3.1	2.0	0.5

vit = vitrite; sf =:semifusinite; int = inertodetrite; lipt = liptite; sil = silicate; qz = quartz; ank = ankerite; carb = carbonate; cbm = carbominerite; arg = aragonite; poly = polydymite.'

Table 4.26: Microlithotype analyses for Chaba Channel 2 samples.

Sample identification:		**0-1 m**	**1-2 m**	**2-3 m**	**3-4 m**	**4-5 m**	**5-6 m**	**6-7 m**	**7-8 m**
Group	Microlithotype (vol%)								
Monomaceral	Vitrite	17.4	11.0	9.0	7.3	6.8	1.0	0.6	0.0
	Semifusite	26.2	25.5	22.0	28.3	25.8	26.1	26.0	25.1
	fusite /secretinite	10.5	10.2	16.6	4.7	5.0	9.1	4.8	1.6
	Inertodetrite	1.2	9.0	21.2	39.6	25.8	24.7	40.3	36.8
	Liptite	0.0	0.0	0.0	0.0	0.0	0.4	0.2	0.0
Bimaceral	vit+sf/f	11.6	6.1	7.0	2.6	2.2	1.4	1.1	0.8
	vit+int	12.8	9.6	9.2	3.5	7.1	6.0	4.8	4.0
	sf+int	3.8	17.2	10.3	5.3	15.7	17.9	16.2	20.1
	vit+lipt	1.6	0.2	0.0	0.4	0.0	0.2	0.0	0.0
	int+lipt	1.8	7.3	2.9	1.6	1.8	2.3	2.9	1.6
Trimceral	Duroclarite	7.7	2.5	0.8	1.8	0.0	0.8	0.2	0.2
	Clarodurite	0.8	0.4	0.4	0.0	0.2	0.2	0.2	0.2
	Vitrinertoliptite	0.0	0.0	0.0	0.0	0.0	0.0	0.0	0.2
Carbominerite	cbm arg/clay	0.0	0.0	0.0	0.2	0.0	0.6	0.0	0.0
	cbm sil/qz	0.0	0.0	0.0	3.1	5.6	6.6	1.7	8.6
	cbm pyrite	1.6	0.6	0.0	0.6	2.2	1.7	0.4	0.6
	cbm ank/carb	0.0	0.0	0.6	0.0	1.0	0.2	0.2	0.0
	cbm poly	0.0	0.0	0.0	0.0	0.0	0.0	0.0	0.0
Rock (minerite)	rock 60%	3.0	0.0	0.0	1.0	0.8	0.8	0.4	0.2

vit = vitrite; sf =:semifusinite; int = inertodetrite; lipt = liptite; sil = silicate; qz = quartz; ank = ankerite; carb = carbonate; cbm = carbominerite; arg = aragonite ; poly = polydymite.'

Table 4.27: Microlithotype analyses for 3 Main East Channel samples.

Sample No:		**1542**	**1543**	**1544**	**1545**	**1546**	**1547**	**1548**	**1549**	**1550**	**1551**	**1552**	**1553**
Sample Identification:		**3ME1 0-30m**	**3ME2 30-60cm**	**3ME3 60-90cm**	**3ME4 90-120cm**	**3ME5 120-150cm**	**3ME 6 150-180cm**	**3ME 7 180-210cm**	**3ME 8 210-240cm**	**3ME 9 240-270cm**	**3ME 10 270-300cm**	**3ME 11 300-330cm**	**3M E12 330-360cm**
Microlithotype group	**Microlithotype (vol%)**	**inc. mm**	**inc. mm**	**inc. mm**	**inc. mm**	**inc. mm**	**inc. mm**	**inc. mm**	**inc. mm**	**inc. Mm**	**inc. mm**	**inc. mm**	**inc. mm**
		vol%	**vol%**	**vol%**	**vol%**	**vol%**	**vol %**	**vol %**	**vol %**	**vol%**	**vol %**	**vol %**	**vol %**
Monomaceral	**Vitrite**	**32.1**	**31.7**	**30.5**	**14.5**	**22.7**	**20.8**	**37**	**25**	**28.6**	**13.9**	**7.7**	**2.7**
	semifusite	**10.2**	**13.2**	**13.3**	**29.2**	**36.6**	**30.1**	**12**	**19**	**9.3**	**26.4**	**36.3**	**37.3**
	fusite / secretinite	**11**	**7.4**	**4.4**	**4.1**	**4.9**	**5.1**	**13**	**14**	**9.3**	**13.9**	**9.5**	**7.5**
	inertodetrite	**0.2**	**0.2**	**4.1**	**7.7**	**5.4**	**15.4**	**1**	**4**	**3.2**	**12.5**	**10.4**	**22.4**
	Liptite	**0**	**0.0**	**0**	**0**	**0**	**0.5**	**0**	**0**	**0**	**0**	**0**	**0.2**
Bimaceral	**vit+sf/f**	**13.9**	**17.8**	**15.5**	**13.5**	**11.2**	**8.1**	**14**	**9**	**10.2**	**9.1**	**10.2**	**5.8**
	vit+int	**22.4**	**21.1**	**22**	**12.9**	**10.7**	**7.6**	**9**	**14**	**13.7**	**10.3**	**8.5**	**4.6**
	sf+int	**1**	**0.7**	**2.2**	**3.7**	**4.9**	**5.6**	**2**	**3**	**5.6**	**3.1**	**3.9**	**1.4**
	vit+lipt	**0.2**	**0.5**	**0**	**0**	**0**	**0.5**	**0**	**0**	**0.2**	**0**	**0.2**	**0**
	int+lipt	**1.5**	**1.0**	**0.7**	**2.6**	**0**	**0.5**	**5**	**5**	**3.4**	**5**	**4.6**	**5.1**
Trimceral	**trimaceral**	**3.9**	**5.0**	**4.1**	**4.5**	**1**	**3.2**	**4**	**4**	**6.3**	**2.2**	**4.4**	**1.4**
Carbominerite	**cbm arg/clay**	**0**	**0.0**	**0**	**0.8**	**0.5**	**0.7**	**0**	**0**	**0.2**	**0**	**0.7**	**3.4**
	cbm pyrite	**0.7**	**1.0**	**0.5**	**0.2**	**0.7**	**0.7**	**1**	**1**	**2.2**	**2.4**	**3.2**	**4.1**
	cbm ank/carb	**1.5**	**0.2**	**1.5**	**2**	**0.7**	**0.2**	**1**	**0**	**2.7**	**0.5**	**0.2**	**0.5**
	cbm sil/qz	**0.2**	**0.0**	**0.5**	**0**	**0.5**	**0**	**0**	**1**	**0.2**	**0**	**0**	**0**
	cbm poly	**0**	**0.0**	**0**	**0.2**	**0**	**0**	**0**	**0**	**1**	**0**	**0**	**0**
Rock (minerite)	**rock 60%**	**1.2**	**0.2**	**0.7**	**4.1**	**0.2**	**1**	**1**	**1**	**3.9**	**0.7**	**0.2**	**3.6**

Table 4.28: Microlithotype analyses for 3 Main South Channel samples.

Sample No:		1554	1555	1556	1557	1558	1559	1560	1561	1562	1563	1564
Sample Identification:		3MS 1 0-30cm	3MS 2 30-60cm	3MS 3 60-90cm	3MS 4 90-120cm	3MS 5 120-150cm	3MS 6 150-180cm	3MS 7 180-210cm	3MS 8 210-240cm	3MS 9 240-270cm	3MS 10 270-300cm	3MS 11 300-330cm
		inc. mm	inc. mm	inc. mm	inc. mm	inc. mm	inc. mm	inc. mm	inc. Mm	inc. mm	inc. mm	inc. mm
Microlithotype group	Microlithotype (vol%)	vol %	vol %	vol %	vol %	vol %	vol %	vol %	vol%	vol %	vol %	vol %
Monomaceral	Vitrite	41.2	26	30.7	7.0	9.0	18.5	53.0	19.5	12.2	22.5	4
	Semifusite	4.7	22.7	15.5	38.8	35.7	29.5	14.2	14.2	29.7	28.5	37
	Fusite / secretinite	9.3	7.8	7.5	5.3	7.0	8.5	2.3	5.0	4.5	6.3	6
	Inertodetrite	0.3	1.8	1.3	17.2	9.0	4.8	0.5	1.0	5.3	5.3	12
	Liptite	1.8	0.3	0.0	0.3	0.3	0.0	0.0	0.2	0.0	0.0	0
Bimaceral	vit+sf/f	12.3	17.5	14.5	6.3	11.8	17.0	12.8	16.0	9.0	13.5	9
	vit+int	11.7	16.7	14.0	8.5	10.2	12.7	13.5	13.2	9.5	10.5	8
	sf+int	0.8	0.5	3.5	10.0	8.2	2.0	1.0	3.5	4.3	6.0	6
	vit+lipt	0.5	0.5	0.3	0.0	0.0	0.8	0.0	0.0	0.3	0.2	0
	int+lipt	0.5	1.3	2.0	2.7	2.8	1.3	0.3	0.5	2.0	1.3	5
Trimaceral	Trimaceral	5.7	2.2	5.5	3.0	4.0	3.7	1.2	2.5	1.7	2.5	7
Carbominerite	cbm arg/clay	0	0	1.2	0.0	0.0	0.5	0.0	0.0	0.0	0.2	1
	cbm pyrite	1	0	1.5	0.2	1.0	0.0	0.0	7.0	9.5	2.0	3
	cbm ank/carb	1.5	1	0.8	0.0	0.0	0.2	1.0	0.0	1.3	0.7	0
	cbm sil/qz	0	0	0.0	0.2	0.0	0.0	0.0	0.2	0.0	0.0	1
	cbm poly	0	0	0.0	0.0	0.0	0.0	0.0	0.0	0.0	0.0	0
Rock	rock 60%	8.7	1.7	1.7	0.5	1.0	0.5	0.2	17.2	10.7	0.5	1

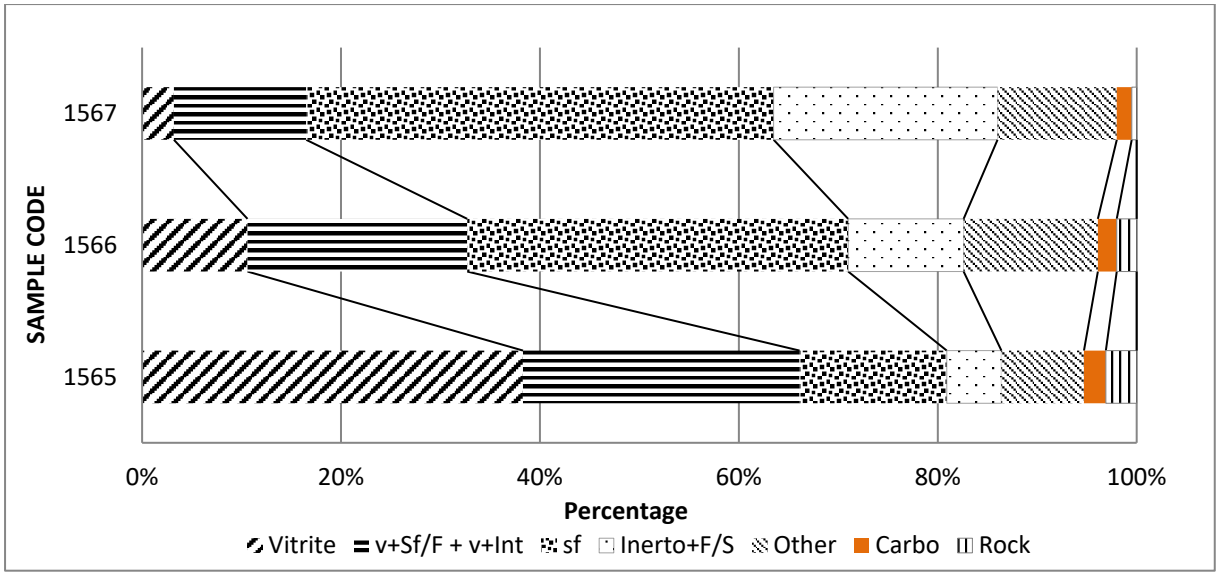


Figure 4.42: Microlithotype vertical variation along Chaba Channel 1 (%vol). NB, samples were taken at 3 m intervals vertically up the seam with 1565 representing the lowest sample (0-3 m), and the 1567 representing the top three metres of the seam.

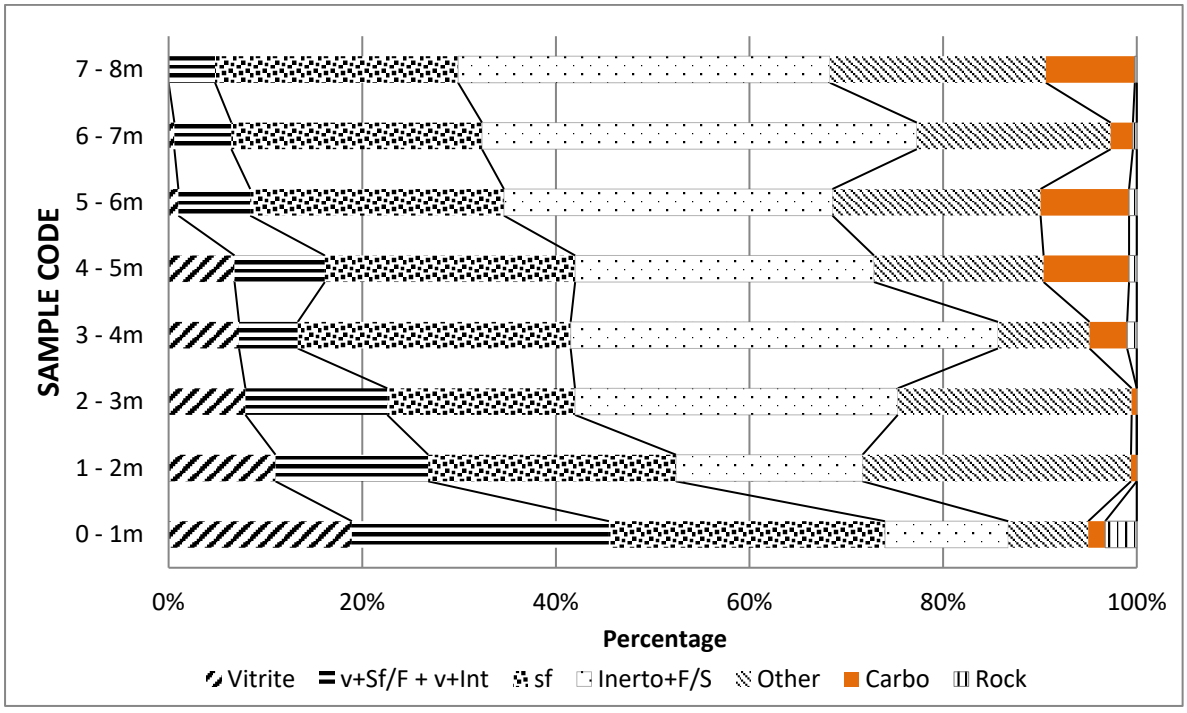


Figure 4.43: Microlithotype vertical variation along Chaba Channel 2 (%vol). NB., samples were collected at 1 m intervals from base to top with 0-1 m representing the basal sample and 7-8 m representing the top of coal sample.

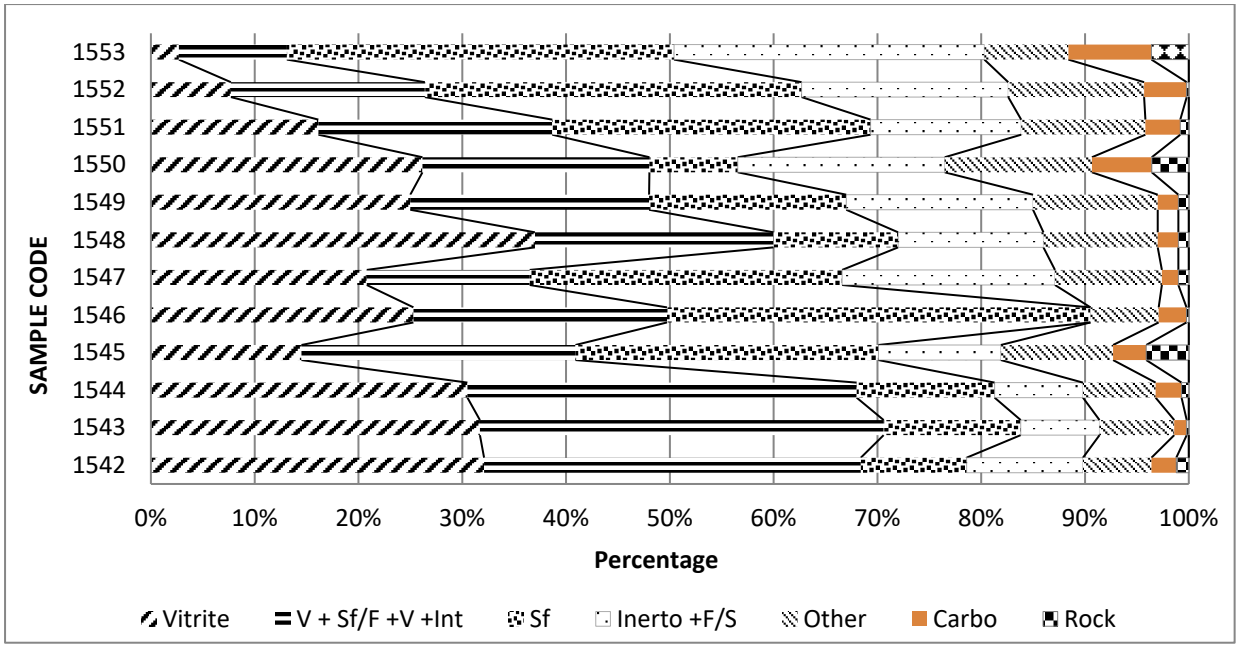


Figure 4.44: Microlithotype vertical variation along 3 Main East Channel. NB, samples was taken at 30 cm intervals vertically up the seam with 1542 being representing the basal sample (0-30 cm), and the 1553 representing top 30 cm of the channel.

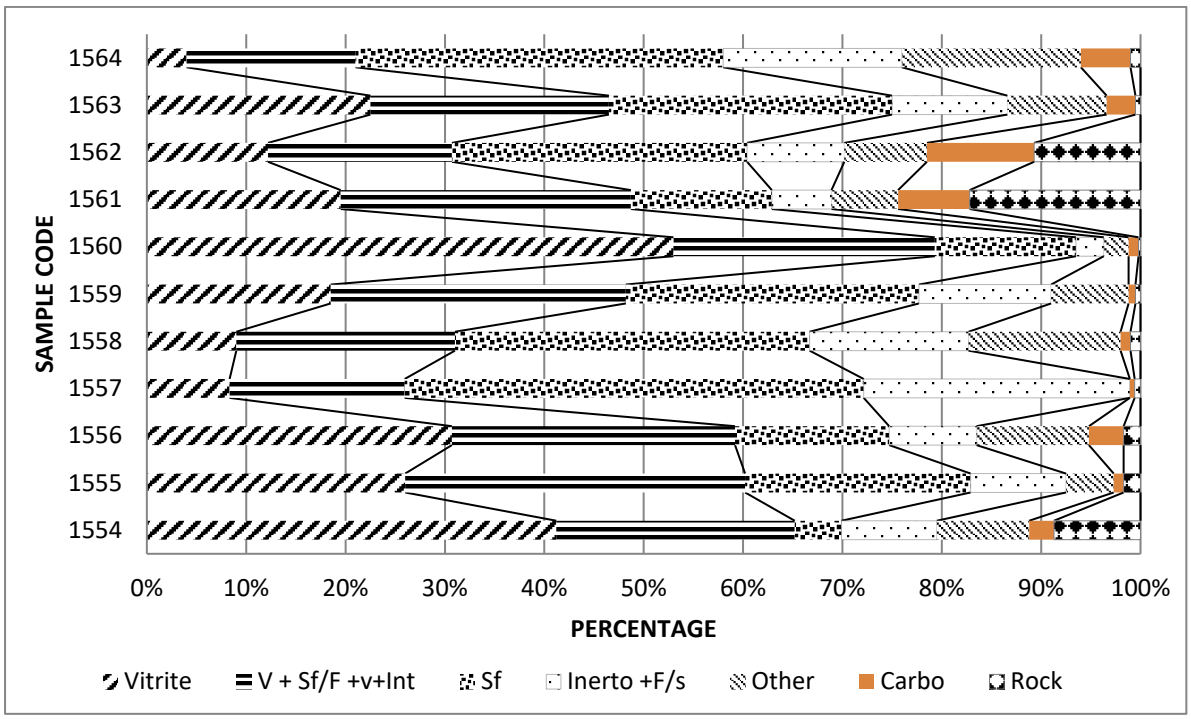


Figure 4.45: Microlithotype vertical variation along 3 Main South Channel.

4.4.7 Thermogravimetric Analyses: (TGA & DTG)

In this study, the thermogravimetric analyses were conducted on selected samples from 3ME, 3 Main South and Chaba Channel 2. The combustion profiles of the samples were presented in Figure 4.46 to 4.51, and this test was conducted using a thermogravimetric analyser (TGA), at 6 ^{0}C/min under (air) atmosphere. The results of the thermogravimetric analyses are summarized as follows:

i) The mass loss curves for the initial peak moisture loss lie between 25 and 100 ^{0}C. This is followed by a slight gain in mass in all samples with the adsorption of oxygen as the burning profiles dipped below the zero on the DTG X- axis. The initiation of volatile for the samples in Figure 4.46 occurs between the range of 240 - 270 ^{0}C as the samples crosses the X axis, with the loss of the masses. Thereafter, the lower samples in each channel show slight differences in their mass loss combustion curves relative to the remaining samples. 3MS sample (Figure 4.51) at 0-30 cm was observed as the most reactive and the temperatures at which the initiation of volatiles and fixed carbon occurred was 246^{0}C and 349.55^{0}C, respectively; while peak and burn out temperatures were 468^{0}C and 600^{0}C, respectively.

ii) In all cases, the DTG profile of all the samples presented a single peak and similar shaped burning profiles.

iii) The lower samples in each channel devolatilise more rapidly and reach their peak temperatures sooner than the higher-level samples. This pattern of combustion also reflects the higher volatile and vitrinite contents, and lower ash content of the lower samples.

iv) In general, the upper channel samples (in particular beyond 4m in Chaba 2) with higher ash content and inertinite contents, have similar combustion curves showing a slower and lower rate of devolatilisation and higher peak burning temperatures.

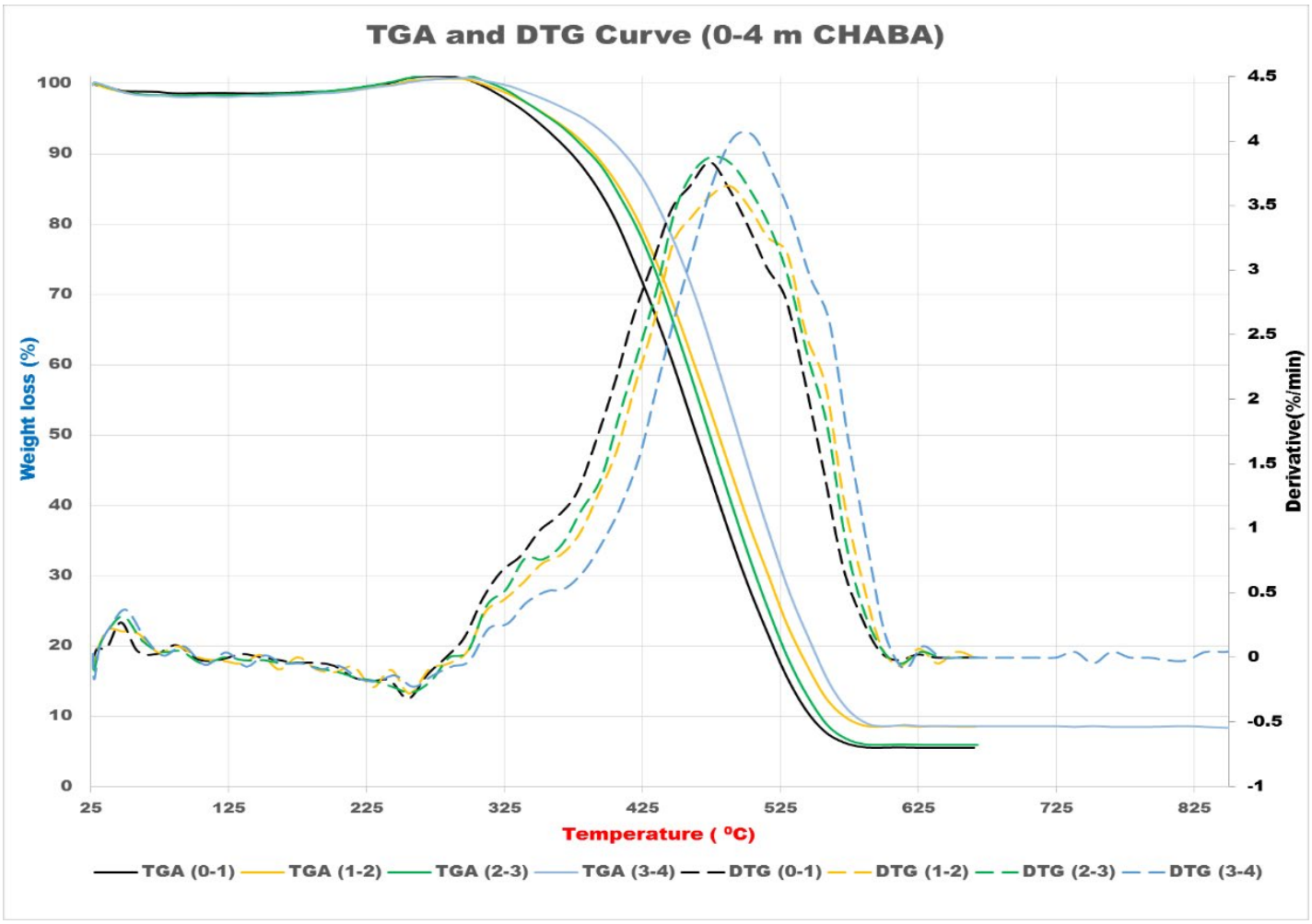


Figure 4.46: TGA and DTG for Chaba Channel 2 samples from 0-1 to 3-4 m.

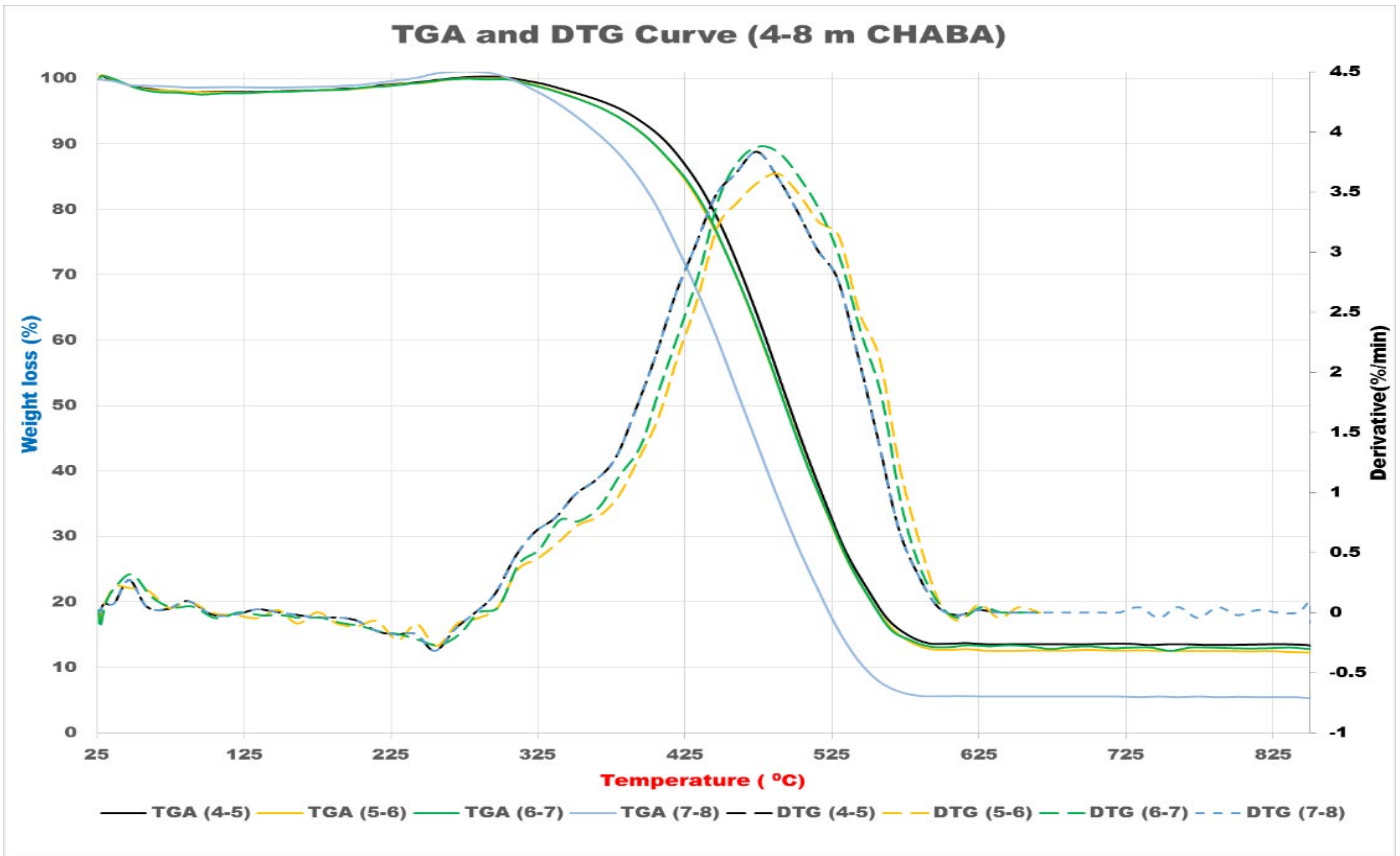


Figure 4.47: TGA and DTG for Chaba Channel 2 samples from 4-5 to 7-8 m.

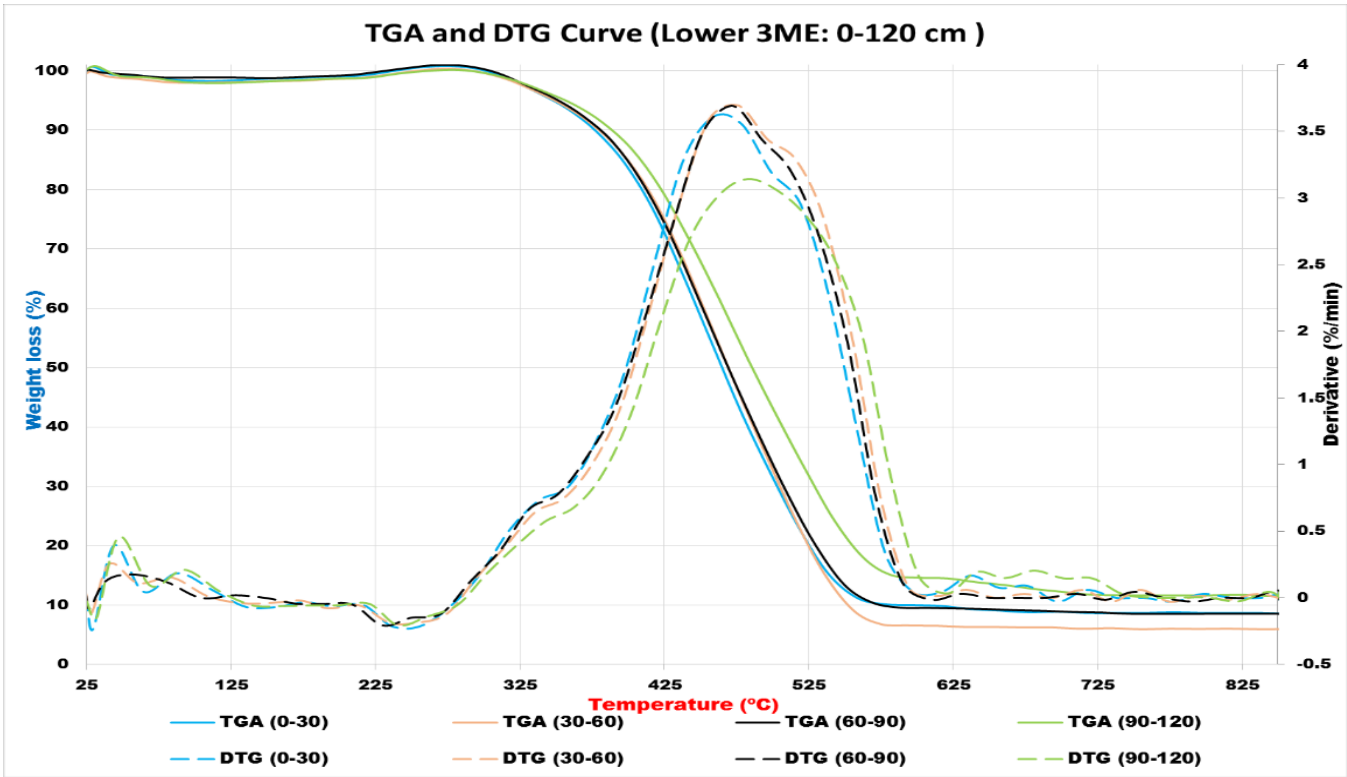


Figure 4.48: TGA and DTG for 3ME samples from 0-30cm to 90 -120 cm.

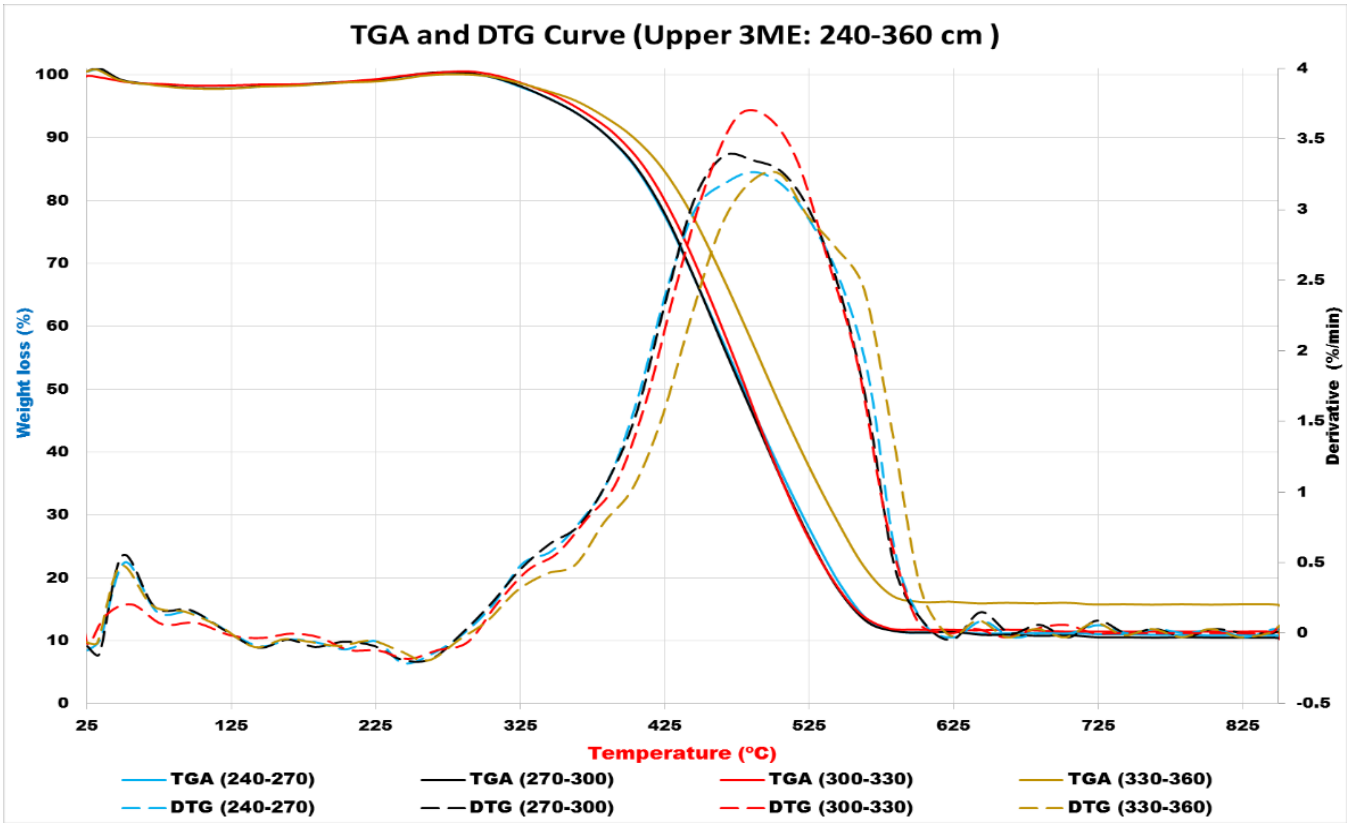


Figure 4.49: TGA and DTG for 3ME samples from 240 -270 to 3.30-360 cm.

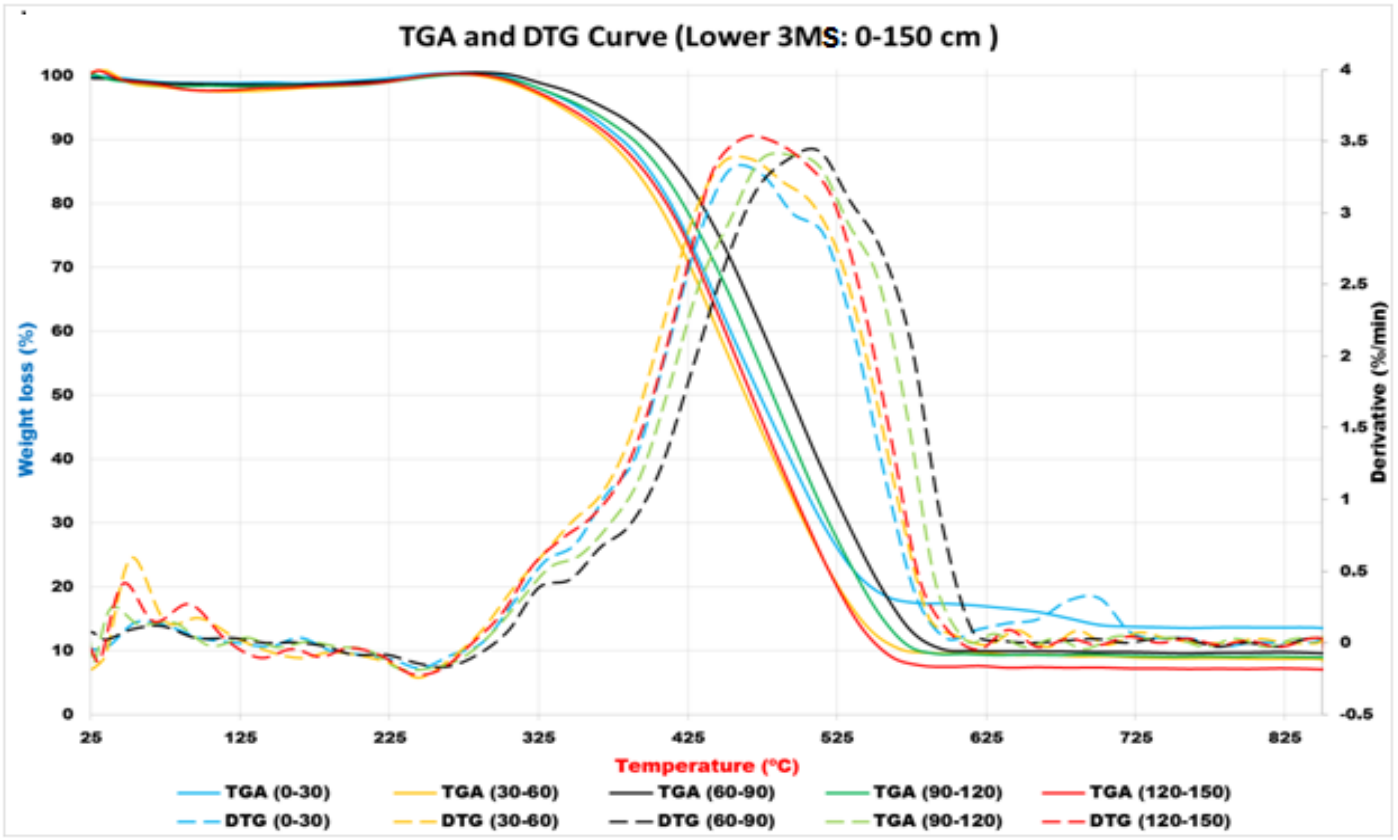


Figure 4.50: TGA and DTG for 3MS samples from 0 -30 to 120-150cm.

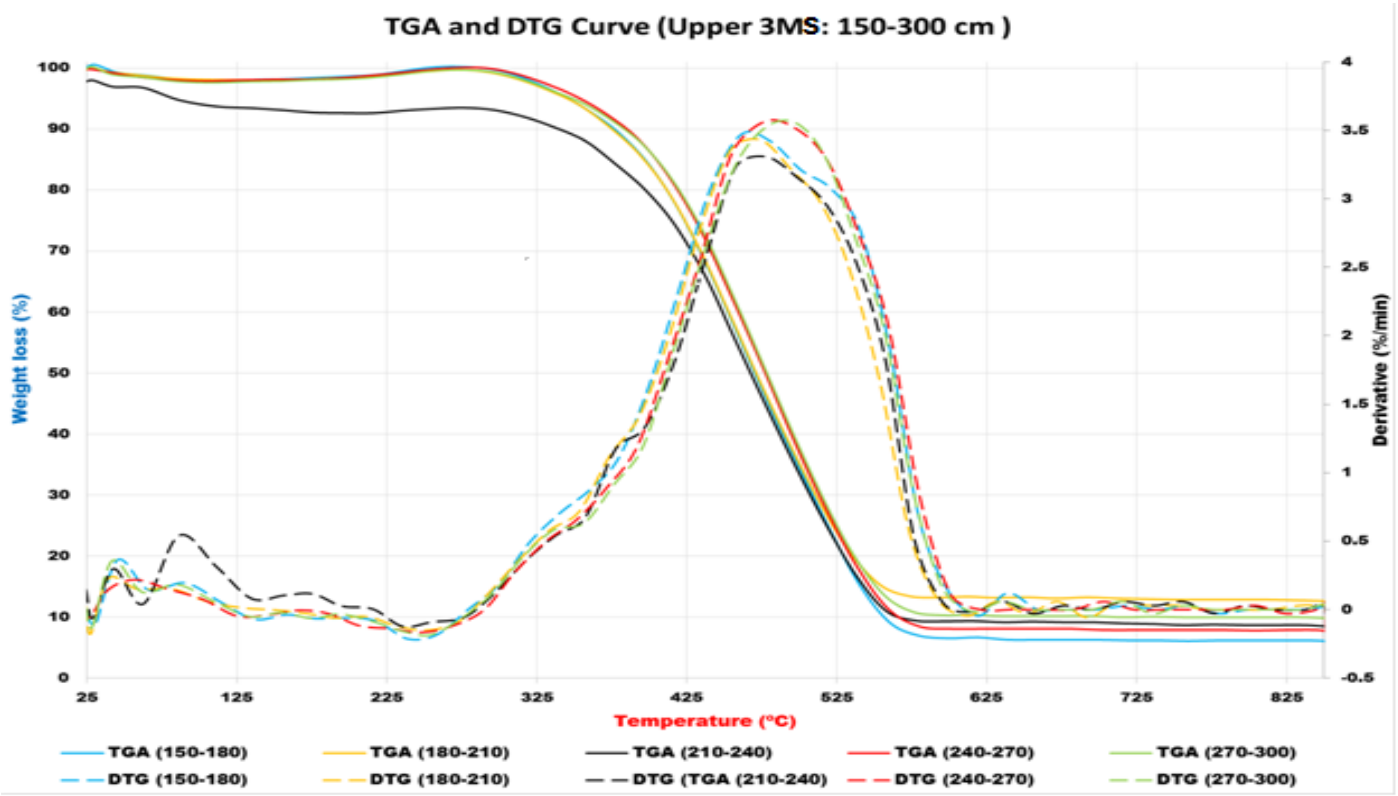


Figure 4.51: TGA and DTG for 3MS samples from 150 -180 cm to 270-300 cm.

4.4.8 Coking Coal Analysis Tests

As stated in Chapter 3, three methods were employed to determine the coking properties of the Hwange coals. These are i) dilatation, ii) the Roga Index, and iii) the Crucible Swelling Index. The coking tests involved the 8 samples from Chaba Channel 2 and 6 samples from sites A and B at the 3 Main Underground Mine. These samples were selected based on the accessibility to the coal during the study period. The coking results for these coal samples are shown in Table 4.29 and Table 4.30.

4.4.8.1 Dilatation

As indicated in Table 4.29, the first sample in Chaba Channel 2 (0-1 m) has the lowest softening temperature of 334^{0}C, indicating an earlier reaction than any of the overlying samples. Thereafter, the softening temperatures steadily increased with height above the seam, up to sample at 6-7 m. Sample taken at the depths of 5-6 and 7-8 m broke the trend and softened at 436^{0}C and 432^{0}C, respectively. The basal sample also shows a positive maximum contraction percentage of 21%, which is significantly higher than any other samples. This indicates that coal in the basal 0-1 m of Chaba channel 2 would provide a significant source of highly plastic coking material with a moderate contraction after reaction, making it a good coking coal.

Table 4.29: Coking tests for Chaba Channel 2.

Sample ID (m)		DILATATION					RI	SW
		ST (°C)	Temperature of maximum contraction °C	Temperature of maximum dilatation °C	Maximum contraction %	Maximum dilatation %		
CHABA	7-8	432	501	501	3	-3	11	1
	6-7	464	501	501	3	-3	13	1
	5-6	436	501	501	5	-5	11	1
	4-5	453	500	500	4	-4	11	1
	3-4	437	500	500	7	-7	16	1
	2-3	425	500	500	11	-11	18	1.5
	1-2	402	452	458	16	-15	21	2.5
	0-1	334	403	465	21	119	79	7

ST: Softening temperature; SW: Swelling Index; RI: Roga Index

Dilatation tests for samples at both sites A and B at 3 Main (Table 4.30) show a cyclic scenario about softening temperatures. The basal sample at Site A (0.25-0.75 m) reports a softening temperature of 394 ^{0}C, increasing to 444 ^{0}C before decreasing to 370 ^{0}C near the roof (sample 3.50-4.25 m). At Site B the basal sample (0.25-0.75 m) records a softening temperature of 386 ^{0}C, rising to 417 ^{0}C before decreasing to 387 ^{0}C in the topmost sample (4.00-4.25 m). The maximum contraction percentages at

both sites show cyclicity as well. Thus, in short, for both 3 Main sites A and B, the lowermost samples (i.e., samples close to the base of seam) and the uppermost samples (i.e., near the roof) softened at lower temperatures than samples in the middle of the coal face.

The maximum contraction for samples at Site A is initially 18%, declining to 8% in the middle sample before rising to 20% in the samples occurring at the top of coal mining face. As for the samples at Site B, there is steady increase in the maximum contraction from 12%, through 16% to 18% near the roof. The coal samples which softened at lower temperatures (i.e., 0.25 - 0.75 m and 3.5 - 4.25 m at Site A; and 0.25 – 0.75 m and 04.0 – 4.25 m at Site B) are good for coking.

Table 4.30: Coking tests for 3 Main sites A and B Samples.

Sample ID (m)		DILATATION					RI	FSW
		ST (°C)	Temperature of maximum contraction °C	Temperature of maximum dilatation °C	Maximum contraction %	Maximum dilatation %		
SITE A	3.50-4.25	370	433	462	20	35	76	7.5
	2.00-2.50	444	499	499	8	-8	20	1.5
	0.25-0.75	394	443	485	18	33	72	6.5
SITE B	4.00-4.25	387	500	500	18	-18	30	2
	2.50-2.75	417	462	485	16	-14	37	4
	0.25-0.75	386	439	458	12	-4	37	4.5

ST: Softening temperature; FSW: Swelling Index; RI: Roga Index

In the case of Chaba Channel 2, the basal sample (0-1 m) has by far the highest RI of 79 (Table 4.29) compared to the RI for the rest of the samples which recorded RI of 21 and below. For the 3 Main channel samples, the RI values are cyclic at Site A, commencing with RI of 72 for the lowest, most samples, declining to RI of 20, before increasing to RI of 76. At site B the Roga Index values for the first two samples are the same with both at RI of 37, but the last sample (sample towards the roof) has a low value at 30. The coal samples 0-1 m along Chaba Channel 2; and samples 0.25-0.75 m and 3.5-4.25 m are likely to be good coking coals.

Dilatation, which determines the coal's expansion and contraction capacity, is considered as a crucial property of this fossil coal when it is considered as a feedstock to the coke making process. Based on the dilatometer results, the following characteristics are derived:

I. Softening temperature.
II. Maximum contraction
III. Maximum dilatation temperature; and
IV. Degree of contraction and dilatation based on the initial length of sample.

Mitchell (1999a) considers that coal with 50-140% dilatation has a good coking power. In China the equivalent is referred to as 'b' value and a coal with a'b' value of more than 20% is considered to possess a good coking capacity (Jia, *et al*., 2011). Reporting on the Shankodi-Jangwa coals of Nigeria, Ryemshak and Jauro (2013) report that the coal had a softening temperature of 380^0C attained a maximum of contraction of 19.9% at 420^0C and then dilated maximally at a temperature of 475^0C. The free swelling index of the coal is reported at 3. This coal is placed in the medium coking class. Zimmerman (1979) quoting the US Bureau of Mines (Information Circular 8010) gives the following as the limits of Eastern coking coal blend:

I. Contraction at 30%
II. Dilatation at 210 %
III. Softening Temperature at 356 ^{0}C
IV. Temperature of maximum contractions at 400 ^{0}C
V. Temperature of maximum dilatation at 467 ^{0}C

The dilatometric data for Hwange coal, samples from 3 Main which are 0.25 - 0.75 m and 3.5 - 4.25 m at Site A; and 0.25 – 0.75 m and 04.0 – 4.25 m at Site B as well as the basal sample (0-1 m) in Chaba fall in ranges of coal classified as medium-coking coals in Shankodi-Jangwa as well as in the Eastern coal blend as reported by Zimmerman, (1979). The Hwange coals are also compared based on its dilatation data from selected coking coal areas of South Africa and Mozambique compiled by Kruger (2013). Data from three of the coking coal producing areas is presented in Table 4.31. The Hwange coal samples from 3 Main 0.25 - 0.75 m and 3.5 - 4.25 m at Site A; and 0.25 – 0.75 m and 04.0 – 4.25 m at Site B as well as the basal sample (0-1 m) in Chaba are in agreement with those reported for coking coals from the three selected areas of South Africa and Mozambique.

Table 4.31: Dilatation data for coking coals from areas in the sub-region (Kruger, 2013).

Parameter	Benga - Mozambique	Grootegeluk South Africa	Tshikondeni- South Africa
Softening Temperature ^{0}C	383	373	376
Maximum Contraction Temp. ^{0}C	421	417	413
Maximum Dilatation Temp. ^{0}C	501	439	439
Maximum Contraction %	27	30	-25
Maximum Dilatation %	208	11	198

4.4.8.2 Free Swelling Index

The results obtained from the Free Swelling Index are summarised as follows:

I. The basal sample (0-1 m) in Chaba Channel 2 has a high free swelling index of 7, as seen in Table 4.29 followed by a swelling index of 2.5 in the overlying sample. The rest of the samples have free swelling indices below 2. Thus, the free swelling index and the potential to provide a coking capacity declines with distance above seam base.
II. Similar to the data from the Roga test, the pattern of free-swelling index varies at the 3 Main Channel Site A: namely, 3 Main is cyclic; commencing with a swelling number of 6.5 in the first sample from base of coal, declining to free swelling number of 1.5 followed by a high swell number of 7.5. At Site B there is a steady decline from 4.5 to 2 towards the roof. Thus, as at the Chaba channel 2 site, free swelling tests at 3 Main indicate an upward decline of the free-swelling capacity of the Hwange coals.

As one of the tests conducted to determine the suitability of a coal for use as coking coal, the free swelling index is useful in determining the plastic properties of the solid fossil fuel. The industry standard for free swelling index ranges from zero indicating no increase in size, to 9 which indicates the greatest increase in size. A free swelling index of 3 is considered as the minimum for coking coal. Kruger, 2013 puts the free swelling index for coal used by Arcelor Mittal as coking coal at a minimum of 4, with a coal with a free swelling index of 7 indicating a high-quality coal.

The basal sample (0-1m) of Chaba Channel 2, with a free swelling index of 7.5, is categories the basal 1 to 2 m of Chaba as a good high-quality coking coal. Similarly, all samples at 3 Main Underground Mine, save two: 2.0- 2.50 m at 3 Main Site A and 4.0-4.25 m at Site B, meet the minimum free swelling index value and are therefore, potentially coking coal horizons.

4.4.8.3. Roga Index

Roga Index is considered as the ability of coal to agglutinate. The RI of coals ranges from zero, to well over 45 with higher values giving the coal higher potential as coking coal. Reporting on coals used as coking coal by ArcelorMittal in South Africa, Kruger (2013) puts the RI of at least 45 as equivalent to a coal with a free swelling index of 4, which is the lower limit for a coking coal.

The basal sample (0-1 m) from Chaba Channel 2 and the two 3 Main Site A samples (0.25-0.75 m and 2.50-2.75 m) with RI values of 72 and 76, respectively meet the RI limits of coking. The two lower samples (0.25-0.75 m, and 2.50-2.75 m) at 3 Main Site B with RI values marginally lower that the minimum of 45 may be sources of blend coking coal, especially that the two samples have free swelling index values of 4 and 4.5, respectively.

4.4.9 Furnace tests/Observations

Before both Chaba Opencast and the 3 Main Underground Mine were commissioned in 2005, Hwange coals with a cumulative ash maximum of 15% and a cumulative volatile matter content minimum of 23.5% was defined as coking, and indeed had coking properties. When the 3 Main Underground Mine was commissioned in 2005, it was found out that the coal from this part of the Hwange Coalfield with a cumulative volatile matter minimum of less than 23.5% and a free swelling index of 2 when delivered to the coke making batteries did provide softening, swelling and binding advantages. At that same time, coal modeled as coking coal based on the ash and volatile matter cut-offs as stated earlier, was delivered to the Hwange Colliery coke making battery from the Chaba sites that was found to be non-coking. As an integral part of efforts to find answers to the question as to why some Hwange coals produce such good coke capacity and therefore are an acceptable blend coking coals, yet do not respond well in conventional coking tests, a unique experiment was devised. Selected coal lumps from Chaba Channel 2 and the sites A and B at 3 Main were cut into cubes each of which was subsequently split into two mirror halves. As described in Chapter 3, one half was placed in a furnace and heated at 650 ^{0}C in the absence of oxygen for one hour.

The results from these tests are presented in Figure 4.52 and Figure 4.53. To view the complementary sets of information, certain proximate and coking test results are presented with photographs of the relevant non-heated and heated coal lumps. In addition, indications are given of the horizon from which the samples were taken. Observations show that the bright vitrinite-rich bands in the non-heated samples correspond to the bubbly bands showing swollen characteristic in the heated counterpart samples (see Chaba 0-1 m, 1-2 m and 2-3 m) (Figure 4.52). The dull coal, which is

essentially inertinite-rich, appears not to have reacted at all (samples 3-4 m, 5-6 m, 6-7 m, and 7-8 m) although sample 4-5 m did show incipient reaction. Some swollen bands are more dramatic in appearance than others. For example, in Chaba samples 0-1 m and 2-3 m, the swelling or "bubbles" appear as large ball-like structures, whereas other such swellings as in samples (5-6 m) and (6-7 m) indicate limited swelling, but to a much lower degree.

These tests prove that the samples in the lower sections of the seam swell considerably (i.e., they exhibit greater reaction) but, more significantly, they also indicate that some samples in the higher levels do undergo some degree of swelling which has not been indicated in earlier coking tests. The key observations made from the test are as follows.

I. In Chaba sample 0-1 (basal metre) and 2-3m, the heated coals have strongly reacted and bubbled; the bubble formation has altered the shape of the coal lump so that it appears completely different from the unheated lump.
II. The Chaba sample 1-2 m has also reacted, but less pronounce than 0-1 m and 2-3 m.
III. Bubbles occur in lump 3-4 m showing slight swelling. The shiny vitrain in sample 3-4 occurs as thin bands, as shown by the thin lines of bubbles on the surface of the heated lump.

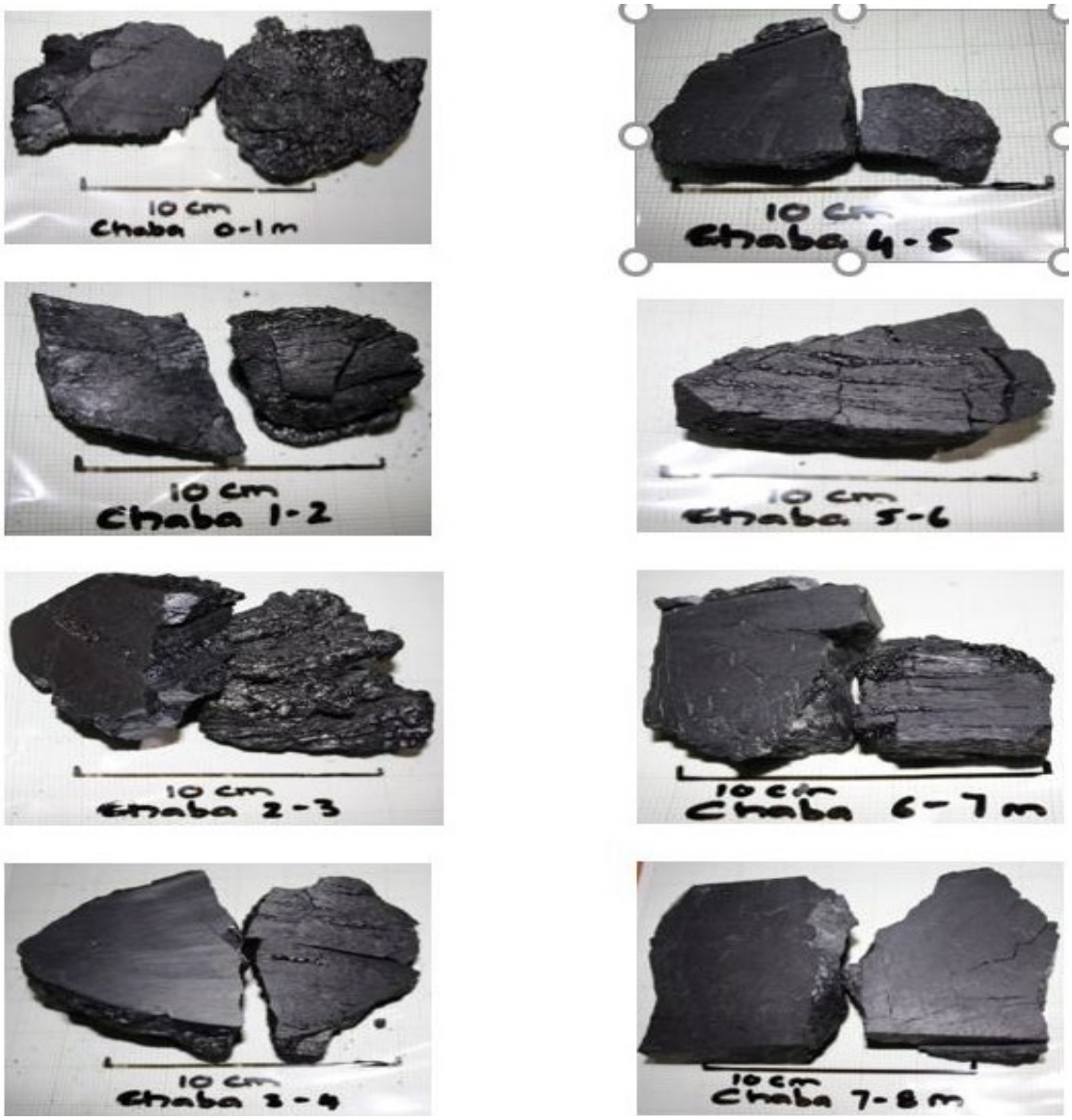


Figure 4.52: Coal lumps from lower half (i.e., from base to 4m above seam base) of Chaba Channel 2 showing varying levels of bubble (swellings) development. The lumps on the right in each pair were heated in the furnace, while the ones on the left were unheated original samples.

The Chaba Channel 2 samples, photographs (Figure 4.52) are linked to the results from their respective proximate analyses (figures 4.53 - 4.56).

In summary, free welling index, Roga Index and volatile matter are correlateable for key coking samples but swelling (bubbling) to various levels occurs in samples that do not possess significant volatile matter contents, free welling indices and Roga indices, for example, Chaba samples 0-1m and 2-3m.

Name/sample code	Initial Mass	Moisture	Volatile	Ash	Fixed Carbon	Swelling Index	Roga Index
CHABA 7-8M	1.0037	1.86	20.99	11.93	65.22	1.0	11
CHABA 6-7M	1.0105	1.81	20.14	12.88	65.17	1.0	13
CHABA 5-6M	1.0026	1.82	19.46	12.35	66.37	1.0	11
CHABA 4-5M	1.0052	1.74	18.15	13.4	66.71	1.0	11
CHABA 3-4M	1.006	1.57	19.78	8.55	70.1	1.0	16
CHABA 2-3M	1.0031	1.42	24.16	6.04	68.38	1.5	18
CHABA 1-2M	1.0054	1.43	23.81	8.64	66.13	2.5	21
CHABA 0-1M	1.0048	1.2	28.84	5.54	64.42	7.0	79

Elements	Average	Std. Deviation	RSD	Count
Initial Mass	1.0052	0.002	0.245	8
Moisture	1.6047	0.23915	14.9	8
Volatile	21.9161	3.49046	15.93	8
Ash	9.9174	3.13034	31.56	8





Figure 4.53: Coal lumps 0-1m and 1-2m and their respective proximate analyses and coking tests results. Arrows point to the sample interval.

Name/sample code	Initial Mass	Moisture	Volatile	Ash	Fixed Carbon	Swelling Index	Roga Index
CHABA 7-8M	1.0037	1.86	20.99	11.93	65.22	1.0	11
CHABA 6-7M	1.0105	1.81	20.14	12.88	65.17	1.0	13
CHABA 5-6M	1.0026	1.82	19.46	12.35	66.37	1.0	11
CHABA 4-5M	1.0052	1.74	18.15	13.4	66.71	1.0	11
CHABA 3-4M	1.006	1.57	19.78	8.55	70.1	1.0	16
CHABA 2-3M	1.0031	1.42	24.16	6.04	68.38	1.5	18
CHABA 1-2M	1.0054	1.43	23.81	8.64	66.13	2.5	21
CHABA 0-1M	1.0048	1.2	28.84	5.54	64.42	7.0	79

Elements	Average	Std. Deviation	RSD	Count
Initial Mass	1.0052	0.002	0.245	8
Moisture	1.6047	0.23915	14.9	8
Volatile	21.9161	3.49046	15.93	8
Ash	9.9174	3.13034	31.56	8





Figure 4.54: Coal lumps 2-3m and 3-4m and their respective proximate analyse and coking tests resultst Arrows point to the sample interval.

Name/sample code	Initial Mass	Moisture	Volatile	Ash	Fixed Carbon	Swelling Index	Roga Index
CHABA 7-8M	1.0037	1.86	20.99	11.93	65.22	1.0	11
CHABA 6-7M	1.0105	1.81	20.14	12.88	65.17	1.0	13
CHABA 5-6M	1.0026	1.82	19.46	12.35	66.37	1.0	11
CHABA 4-5M	1.0052	1.74	18.15	13.4	66.71	1.0	11
CHABA 3-4M	1.006	1.57	19.78	8.55	70.1	1.0	16
CHABA 2-3M	1.0031	1.42	24.16	6.04	68.38	1.5	18
CHABA 1-2M	1.0054	1.43	23.81	8.64	66.13	2.5	21
CHABA 0-1M	1.0048	1.2	28.84	5.54	64.42	7.0	79

Elements	Average	Std. Deviation	RSD	Count
Initial Mass	1.0052	0.002	0.245	8
Moisture	1.6047	0.23915	14.9	8
Volatile	21.9161	3.49046	15.93	8
Ash	9.9174	3.13034	31.56	8



Figure 4.55: Coal lumps 4-5 and 5-6 and their respective proximate analyses coking tests results. Arrows point to the sample interval.

Name/sample code	Initial Mass	Moisture	Volatile	Ash	Fixed Carbon	Swelling Index	Roga Index
CHABA 7-8M	1.0037	1.86	20.99	11.93	65.22	1.0	11
CHABA 6-7M	1.0105	1.81	20.14	12.88	65.17	1.0	13
CHABA 5-6M	1.0026	1.82	19.46	12.35	66.37	1.0	11
CHABA 4-5M	1.0052	1.74	18.15	13.4	66.71	1.0	11
CHABA 3-4M	1.006	1.57	19.78	8.55	70.1	1.0	16
CHABA 2-3M	1.0031	1.42	24.16	6.04	68.38	1.5	18
CHABA 1-2M	1.0054	1.43	23.81	8.64	66.13	2.5	21
CHABA 0-1M	1.0048	1.2	28.84	5.54	64.42	7.0	79

Elements	Average	Std. Deviation	RSD	Count
Initial Mass	1.0052	0.002	0.245	8
Moisture	1.6047	0.23915	14.9	8
Volatile	21.9161	3.49046	15.93	8
Ash	9.9174	3.13034	31.56	8



Figure 4.56: Coal lumps 6-7m and 7-8m and their respective proximate analyses and coking test results. Arrows point to the sample interval.

The coal lumps from Site A, 3 Main Underground (Figure 4.54) show diminishing bubbling with height above coal seam:

i) Lumps from 0.25-0.75 m have strongly reacted, and bubbling was dramatic and distorted the shape of the heated lump.

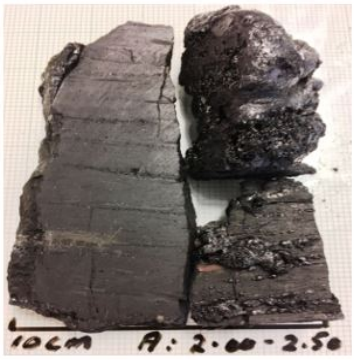
ii) Lumps from 2-2.5m and 3.5-4.25 show progressively reduced bubbling.



Figure 4.57: Coal lumps from 3 Main sites A and B.

For 3 Main Site A, the results obtained show diminishing bubbling with height above coal seam base (left side). Coal lumps from Site B, 3 Main Underground (right), show samples which all reacted, with the most reaction observed in the lower most sample (i.e., 0.25-0.75 m). As with the Chaba Channel 2 furnace test, the photographs for Site A and Site B are married with their respective coking test results as shown in Figures 4.58 and Figure 4.59, respectively.







Site A		Height Interval (m)	Roga	Swelling Index	Softening Temps (°C)
Sample	A-1	0.25-0.75	76	7.5	394
	A-2	2.00-2.50	20	1.5	444
	A-3	3.5-4.25	72	6.5	370

Figure 4.58: Furnace and coking tests for 3 Main Site A







Site B		Height	Roga	Swelling Index	Softening Temps (°C)
Sample	B-1	0.25-0.75	30	2.0	386
	B-2	2.50-2.75	37	4.9	417
	B-3	4.00-4.25	37	4.5	387

Figure 4.59: Furnace and coking tests for 3 Main Site B.

The lowest sample (0.25-0.75m) at Site A bubbled the most to the extent of distorting the shape of the original coal lump. Bubbling evidently becomes progressively less with height of sample above coal base. However, the three coking tests show that the middle sample (2.00-2.5 m) has the lowest free swelling and Roga indices, and the highest softening temperature of 444^0C. The softening temperature breaks the trend.

At Site B, again a diminishing amount of swelling (bubbling) is evident with distance from coal base. Both RI and FSI show sympatheic trends, decreasing with distance above the coal base. However, the middle sample (2.50-2.75 m) records the highest softening temperature of 417^0C compared to 387^0C and 386^0C for the basal lowest and the highest samples, respectively.

4.4.10 Selected Quality Parameters and Coal Classification

A series of scatter diagrams have been drawn to illustrate the relationship between selected pairs of quality parameters and one is shown below, with the rest shown in Appendix 4.4.

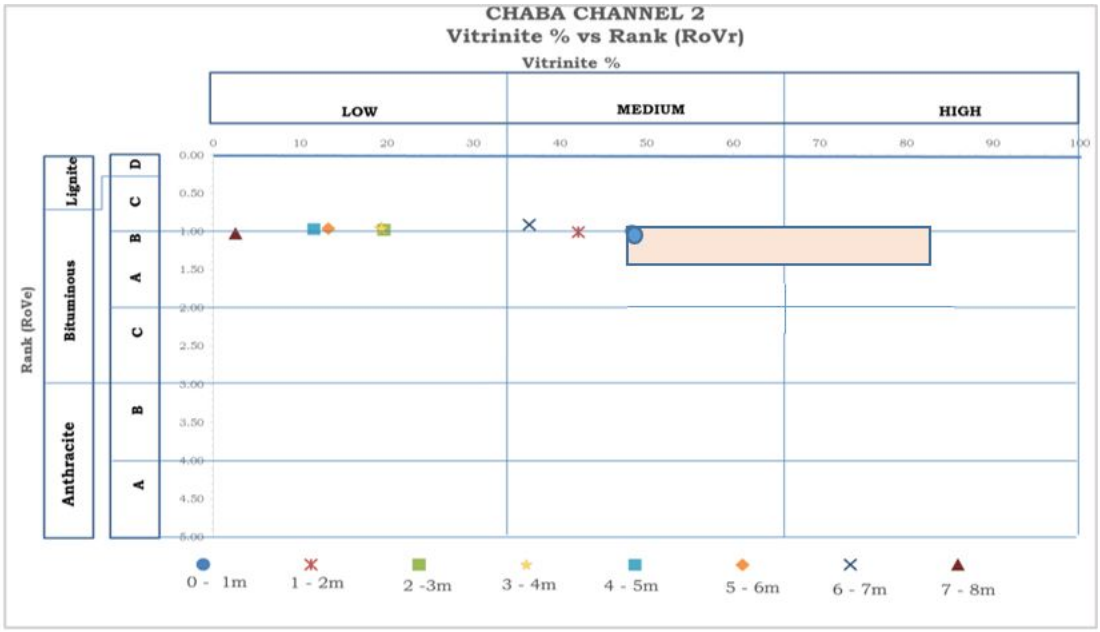


Figure 4.60: Vitrinite % vs Rank (RoVr) for Chaba Channel 2 samples.

This scatter diagram illustrates the fact that the Chaba Channel 2 samples are predominantly low in vitrinite content (low %) with one exception, the lowest sample in the seam profile, which

appears in the Medium vitrinite content (bottom sample at a depth of 0-1 m), while the rank values of the coals are all borderline Bituminous B and Bituminous C. The shaded area indicates the location where the best swelling and coking capacities are found. i.e., high swelling coking capacity coals lie in the higher vitrinite content levels and fall within the Bituminous B level of rank. The result above infers that only the lowest sample in this seam sequence with sufficiently high vitrinite content approaches the area in which relatively good swelling indices are found. It lies borderline on the correct level of rank. None of the remaining samples possess enough vitrinite content (despite being borderline and in the correct rank level (Bituminous B) to generate high swelling coking coals.

Of the proximate parameters, volatile matter content is shown to be the most closely related to swelling index. Volatile matter content also shows a negative relationship which, in turn, affects swelling number. Fixed carbon and ash contents show little or no relationship to swelling index.

4.5 Depositional Environment of the Hwange Coal

The environments of coal deposition range from upper and lower delta plains on the shorelines of marine seas or inland freshwater basins, in wide low and coastal swamps, in lakes and valleys, in mountainous regions, as well as river-cut mature plains (Falcon, 2013). The nature of the sedimentary environment and the related topography under which the peat swamp originated controlled the lateral and vertical coal quality distribution within the swamp. Some areas may have been wet, some dry while others were in areas subjected to transitional geochemical conditions. Oestern and Lepper (2005) note that swamps are known to form under certain conditions which are: a) a subsiding floor, b) a stable water level, and c) lack of of peat contamination due to clastic influx (Oesterlen and Lepper, 2005). In a maceral development model by Falcon (2013) described earlier in Chapter 2 of this thesis, vitrinite forms under reducing conditions while inertinite forms under oxidizing environment.

From the proximate and coal petrographic analyses conducted during this study, there is a general trend of ash values and maceral development which shows a low-ash vitrinite rich coal in the lower portion of the seam giving way to a high-ash inertinite-rich coal in the upper portion of the seam (typical Gondwana high ash inertinite-rich coals). This vertical profile, particularly in terms of maceral constitution, indicates that the low-ash vitrinite rich lower part of the seam represents a

wet forest swamp (of mainly *Glossopteris* as described by Watson, 1960) characterized by a high water table. This was subsequently followed by a gradual drop in the water table resulting in the wet forest changing to dry forest where the swamp vegetation was subjected to oxidation and decomposition (Oesterlen and Lepper, 2005).

CHAPTER FIVE: ECONOMIC POTENTIAL OF THE HWANGE COAL CONCESSION

5.1 Introduction

Coal mining technique, processing and utilisation can be forecasted knowing the geological condition of the deposit, the physicochemical properties of the coal in-situ and what is responsible for the various attributes observed during exploration. The geometallurgical assessment of the Hwange coal has been conducted as a multidisciplinary approach with the aim of integrating geological and coal properties (physicochemical, petrological, and coking) of this solid fossil fuel to yield a predictive model for the exploitation of the coal resource. This is consistent with the belief that in commercial operations, the price of coal not only reflects the quantity, but also the relationship of a desirable property or a combination of properties to performance of the coal under service conditions (Zhu, 2014). To this end, it was considered appropriate to include in this research a quantification of the resource whose properties have been determined, its possible life span as a mine and its monetary value.

Conventionally, coal in the southern African sub-region is used in combustion processes by various industries, such as paper, cement and lime, brick making industries, agriculture, in schools, hospitals, laundries to generate heat, power and for general domestic heating. Alternatively, the coal is carbonised for the manufacture of metallurgical coke for the steel manufacturing industry. In technologically developed and developing countries, coal is also used for gasification, producing precursors for other materials (tar, waxes, oils), in the production of chemicals, solid carbons, petrol, diesel and/or energy. In all sectors of use, coal must be characterised and must match the process it is to be used in, irrespective of the conversion process.

In Chapter 3 of the current study, the methods and techniques employed to characterise the Hwange Coalfield coals were described. The results of the coal characterisation, the distribution of the coals with specific properties over the Hwange Coalfield, and discussion of these results were presented in Chapters 4 and discussed in Chapter 6. Using the information generated, an evaluation of the techno-economic aspects of the coalfield is provided in this chapter by assessing the current expected value(s) of the coals yet to be mined in terms of:

I. Tonnages of coals that meet various current and future/ potential markets (Table 5.1):
II. The prices the various coal products will be marketed at, based on the production costs and current marketable values (Table 5.7); and
III. The remaining life of mine over the Hwange Coal Concession, assuming sustained production rates to meet the targeted markets (Table 5.3).

5.2 Estimated in Situ Coal Resource of the Hwange Coal Concession

Hwange Colliery coal resource/reserves are generally categorised according to the current market specifications. Coal reserve estimation procedure and reserve categorisation used in this study was consistent with this market-based practice. Table 5.1 presents the coal reserves categorised according to the coal type and height above current sea-level for the Hwange coal concession. The coal reserves have been categorised as follows:

5.2.1 Straight Hwange coking coal (HCC)

High quality coal used in metallurgical industries requires the following properties:

I. Free Swelling Indices and Roga Indices with a lower limit of 4 and 29, respectively.
II. Ash content of a cumulative maximum of 15%; and
III. Volatile matter content of a cumulative minimum of 23.5%.

The current study has revealed that, in Hwange, straight coking coal generally occurs in areas that are topographically below the current 600 m above-sea-level contour. Virtually all the straight coking coal reserve occurs in areas where the Hwange Main Seam is at depths of more than 70 m from surface (i.e., underground mining areas). Refer to Table 5.1.

5.2.2 Blend coal

Blend coking coal is a coal with swelling index of less than 4 which must be blended with coals of higher swelling index in order to be used in a blend with true coking coal sourced from other parts of the Hwange Concession. The proximate analysis values are like those of straight coking coal. Within the Hwange Concession, the blend coking coal occurs in areas that are topographically between 600 and 840 m above-sea-level contours. This category of coal occurs

both in shallow opencast and underground coal mining areas with the coal seam at depths from surface of up to 70 m and at depths from surface more than 70 m, respectively.

5.2.3 Hwange industrial coal (HIC)

Hwange Industrial Coal is generally a non-coking thermal coal which is used in industries other than metallurgical industry such as manufacturing, agriculture, hospitals, mines, schools, and laundries. Zimbabwe's small thermal plants in Bulawayo, Munyati and Harare are designed to combust this type of coal. Most of this coal occurs in the Chaba Opencast coal areas of Hwange Concession and has the following attributes:

I. Ash content cumulative maximum of 15%.
II. Volatile matter content with a cumulative minimum of 23.5%
III. Free Swelling of less than 1; and
IV. Calorific value averaging 26 MJ/kg.

5.2.4 Thermal coal (Hwange 920 MW coal-fired electricity generation plant - HPS):

The Hwange thermal coal, also known as the Hwange Power Station coal (HPS coal) is the type of coal defined by the design of the main coal-fired 920 MW power plant at the Zimbabwe Electricity Supply Authority (ZESA) located on the Hwange Concession. The coal has the following attributes:

I. Ash content cumulative maximum of 24% as per current Hwange Thermal plant design.
II. Volatile matter content is normally between 19% and 22% by mass; and
III. Calorific value ranges between 23 and 26 MJ/kg.

Table 5.1: summarises the in-situ resource in categories, by type and height above sea level as calculated from the borehole data used in this thesis.

	HCC		HIC		HPS	
	BELOW 600 m	ABOVE 600 m	BELOW 600 m	ABOVE 600 m	BELOW 600 m	ABOVE 600 m
BLOCK	TONNAGE	TONNAGE	TONNAGE	TONNAGE	TONNAGE	TONNAGE
CHABA EAST	0	3,455,582	0	14,298,226	0	17,101,284
CHABA WEST	0	1,733,963	0	7,174,653	0	8,581,189
JKL	0	8,282,237	0	0	0	8,903,903
3 MAIN	29,448,623	144,873,007	0	0	20,543,480	101,063,999
OPTION AREA	152,088,931	74,643,979	0	0	89,483,628	43,917,818
3 NORTH	25,263,262	6,321,511	0	0	17,025,287	4,260,160
TOTAL	**206,800,816**	**169 310 179**	**0**	**21,472,879**	**127.052,395**	**183,828,353**

HCC: Hwange coking coal; HIC: Hwange Industrial coal and HPS: Hwange Power Station coal

5.3 Resource Conversion to Mineable Reserve

Certain modifying factors are applied to the estimated coal resource at Hwange Colliery to convert the resource to mineable coal reserve tonnage. These factors are outlined as follows;

5.3.1. Strip Mining:

I. Geological factor of 0.95
II. Mining factor of 0.95

5.3.2. Underground Bord and Pillar Mining:

I. Geological factor varies according to geological complexity, but averages 0.20
II. Extraction factor varies according to depth of coal from surface with critical inputs being coal mine design table known as Salamon's Table.
III. Assumed coal strength of 7.2 Mpa
IV. Safety factor of 1.6.

The factors listed above, particularly in the underground section, are fed into a model, the Surpac Software. The final factors have been applied to compute the mineable figures in Table 5.2.

Table 5.2: Mineable coal reserves categorisation by source, type & extraction technology.

COAL SOURCE	COAL TYPE	TECHNOLOGY	IN SITU TONS	FACTOR	MINEABLE TONS
3 Main	Straight Coking	Bord and Pillar Mining	**29 449 000**	**0.20**	**5 890 000**
3 Main	Blend Coking	Bord and Pillar Mining	**144 873 000**	**0.20**	**28 975 000**
3 Main	Thermal Coal	Bord and Pillar Mining	**121 608 000**	**0.25**	**24 322 000**
3 North	Straight Coking	Bord and Pillar Mining	**25 264 000**	**0.25**	**6 316 000**
3 North	Blend Coal	Bord and Pillar Mining	**6 322 000**	**0.25**	**1 581 000**
3 North	Thermal Coal	Bord and Pillar Mining	**21 585 000**	**0.25**	**5 396 000**
Option Area	Straight Coking	Bord and Pillar Mining	**152 089 000**	**0.20**	**30 418 000**
Option Area	Blend Coking	Bord and Pillar Mining	**74 644 000**	**0.20**	**37 322 000**
Option Area	Thermal Coal	Bord and Pillar Mining	**133 402 000**	**0.20**	**26 680 000**
JKL Block	Blend Coal	Strip Mining	**8 282 000**	**0.9025**	**7 475 000**
JKL Block	Thermal Coal	Strip Mining	**8 904 000**	**0.9025**	**8 236 000**
Chaba East	Straight coking	Strip Mining	**3 456 000**	**0.9025**	**3 119 000**
Chaba East	Industrial Coal	Strip Mining	**14 298 000**	**0.9025**	**11 474 000**
Chaba East	Thermal Coal	Strip Mining	**17 101 000**	**0.9025**	**15 434 000**
Chaba West	Blend Coal	Strip Mining	**1 734 000**	**0.9025**	**1 565 000**
Chaba West	Industrial Coal	Strip Mining	**7 175 000**	**0.9025**	**6 637 000**
Chaba West	Thermal Coal	Strip Mining	**8 581 000**	**0.9025**	**7 744 000**

NB The factor of 0.9025 for opencast /strip mining areas is the product of 0.95 x 0.95.

Table 5.3 is a summary of the mineable reserves according to coal type. It will be noted that the highest quantities of marketable coal available in the Hwange are the Blend Coking and Thermal coals. The lowest are the Industrial coal followed by Straight Coking coal.

Table 5.3: Hwange Colliery summary of mineable coal reserves in metric tonnes.

COAL CATEGORY	ESTIMATED TONNAGE
Straight Coking	45 743 000
Blend Coking Coal	76 918 000
Industrial Coal	18 111 000
Thermal Coal	87 812 000
GRAND TOTAL	**228 584 000**

5.4. Anticipated Coal Product Demand and Raw Coal Supply

Zimbabwe's relationship with the international community is improving following the advent of the new dispensation in the country. As a result of this development, foreign direct investment (FDI) is poised for dramatic increase, therefore, primary, secondary, and tertiary industries are expected to grow. The growth will require a concomitant increase in energy requirements. In addition, organisations should be able to retool with equipment/technology which is appropriate for each respective industry. The Hwange Colliery Company will be able to purchase replacement

spares for the refurbishment of the giant Dragline, Rope Shovels and support equipment all of which are sourced from the United States. This technology will be the most ideal for the strip-mining method for the open-cast extraction of the Hwange coal deposit, i.e., the equipment most suitable for the geology of the coal seam as it will permit mining an overburden bench of up to 30 m and has a large bucket of 57 m^3 compared to the currently used excavators whose buckets are 4.5 m^3 in size. Furthermore, this type of equipment will enable Hwange Colliery's production capacity to match the anticipated coal demands as indicated below. Similarly, the company will be able to purchase the required units of mining equipment for the mechanised bord and pillar mining technique. Ideal for optimum production rates, an underground bord and pillar section requires a mining equipment suite comprising one Continuous Miner, three Shuttle Cars, one Roof Bolter and a high capacity Feeder Breaker. The company has battled to maintain its equipment during the previous regime's (Mugabe's) dispensation.

5.5 Projected Coal Product Sourcing Requirements

The make-up of the various products determines the required sources of the raw coal. Table 5.4 presents the various product requirements for coking coal and blend coal while Figure 5.1 is the associated coal process flow to satisfy the product demand. Table 5.5 presents the anticipated requirement for the thermal coal product.

Table 5.4: Anticipated coking coal and blend coal products and extraction sourcing requirements

	TONNAGE	**DESCRIPTION**
HCC & Blend Raw Coal mined	3.62 Mt	Direct from Underground and Opencast mines
Less – 6 mm Duff	0.24 Mt	From Opencast HCC Screening plant to HPS
Total HCC & Blend Coal Processed	3.38 Mt	Processed at the No. 2 Processing Plant
HCC & Blend Sized Coal Grades	1.985 Mt	Product of the Screening Plants
Coking Coal	1.059 Mt	Product of the Coal Washing Plants
Process Rejects	0.336 Mt	Fines, Shale, and Washing Plant Rejects

Hwange coking coal: HCC

Rejects: carbonaceous material with ash contents more than 30% plus siltstone.

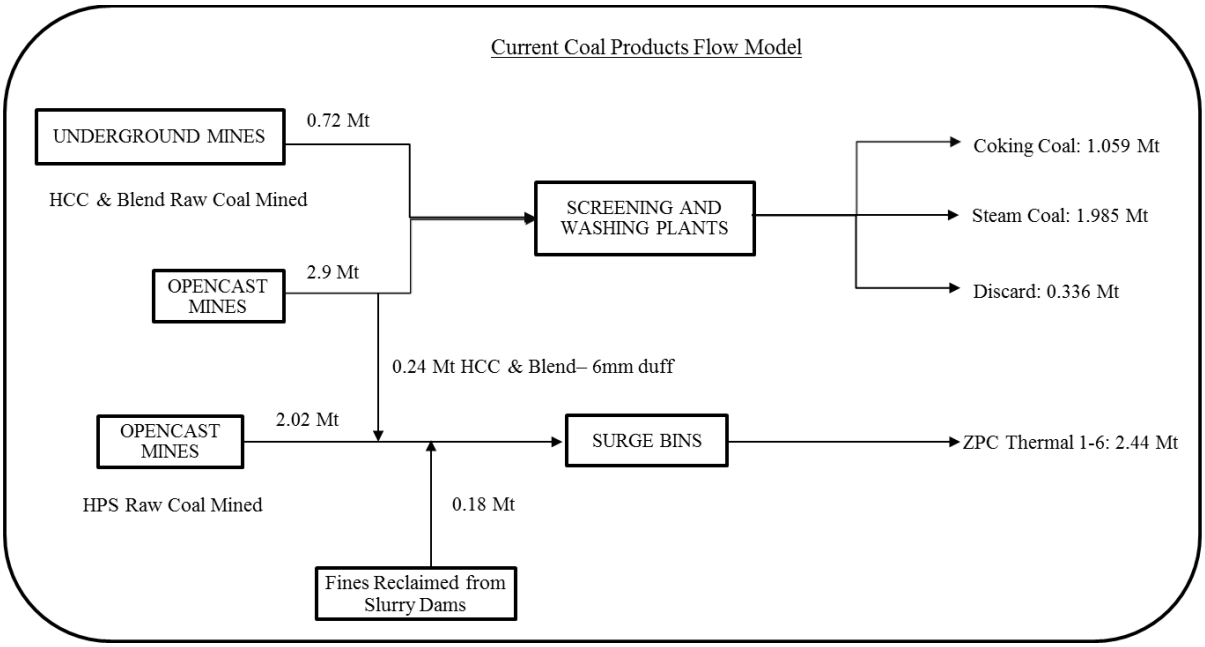


Figure 5.1: Anticipated coal products flow model.

5.6 Hwange Colliery Market Structure for coking, blend coal and industrial coal

Figures from the market indicate that Hwange's coal markets could absorb as much as 3 380 000 tonnes per year. The market comprises the government controlled Kwe Kwe metallurgical plant (formerly ZISCO), small thermal plants (Bulawayo, Munyati and Harare), industry, cement, agriculture, brickmaking, Chinese run coke batteries, and export markets to South Africa.

Table 5.5 and Figure 5.2 presents the distribution of the 3.38 million tonnes between the mentioned markets.

Table 5.5: Potential market requirement for Hwange coking coal, blend coal, and industrial coal.

Market	Tonnage/ Year
Zimbabwe Industry	693,000
Small Thermal Plants	420,000
Kwe Kwe Met. Coal	360,000
Local Asian Coke Batteries	180,000
Agriculture	180,000
Brick Making	60,000
Premium Coking coal (SA)	1,487,000
Total	3,380,000

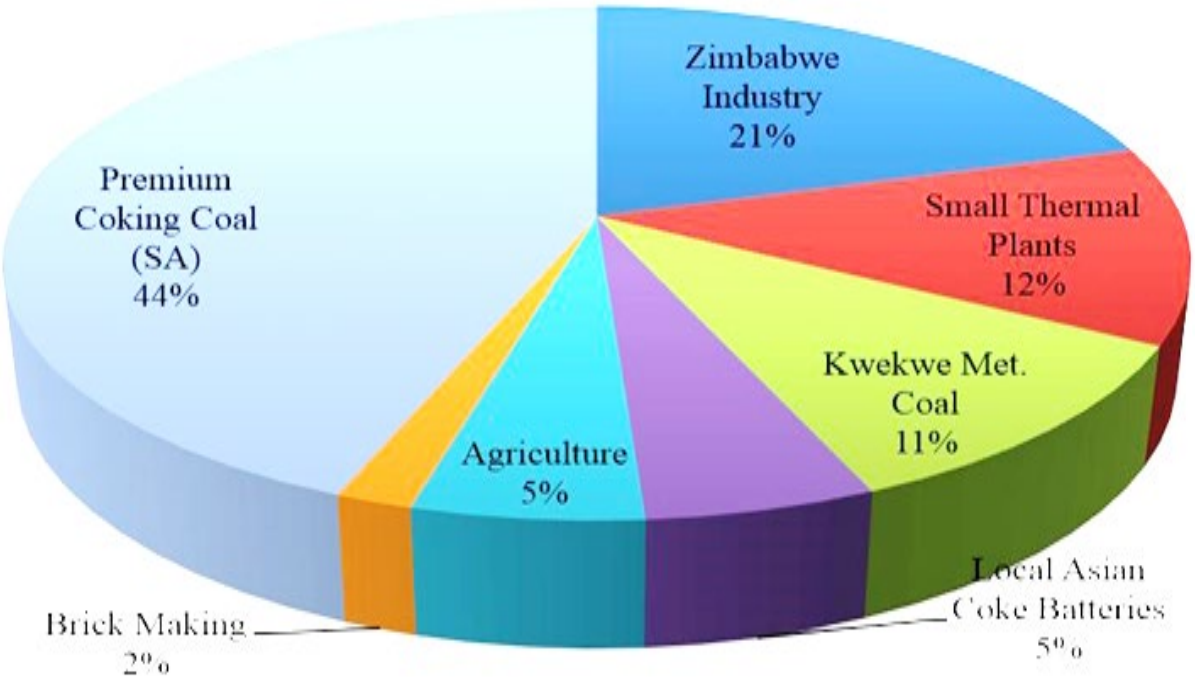


Figure 5.2: Hwange coking coal, blend coal, and industrial coal distribution by market.

5.7 Hwange Thermal Coal Market

Virtually all the thermal coal as defined earlier, is absorbed by the 920 MW coal fired plant at Hwange. This plant, which is the largest of the four-coal fired thermal plants in Zimbabwe, is designed to burn this coal product. The other three burn the low ash industrial coal. Table 5.6 presents feedstock material to the Zimbabwe Power Company thermal power plant.

Table 5.6: Anticipated thermal coal (HPS) product and demand (in tonnes).

	TONNAGE	DESCRIPTION
HPS Raw Coal mined	**2.02 Mt**	Direct from Opencast mines
Add – 6mm Duff	0.24 Mt	From Opencast HCC Screening plant
Add Slurry	0.18 Mt	Fines reclaimed from Slurry Dams
Total HPS Product	2.44 Mt	Delivered to ZESA Hwange Power Station

5.8 Estimated Remaining Life of Mine

The Hwange Colliery's life of mine (LOM) is estimated herein based on three assumptions:

I. That the industry will perform as anticipated hence the local coal market will materialise and be profitable.
II. That Hwange Colliery Company's business performance will likewise perform as anticipated following the advent of the new dispensation and will be able to retool appropriately; and
III. That the anticipated demand and supply as summarised in Tables 5.5 and 5.6 above will be sustainable at production rates of:
    i) A total of 3.62 million tonnes of coking and blend coal per year; and
    ii) A total of 2.02 million tonnes of thermal coal per year.

Therefore, the estimated life of mine for that part of the Hwange Coalfield for which Hwange Colliery Company has mining rights is estimated as follows:

I. Coking coal, blend coal and Industrial Coal: 140 772 000 divided by 3 620 000 = 39 years
II. Thermal (Hwange Power Station) Coal: 87 812 000 divided by 2 020 000 = 43 years

NB. There is potential for increasing the LOM for thermal coal if the country's power supply authority (Zimbabwe Power Company) modifies its boiler design to burn coal of higher ash content. By only combusting coal with a maximum ash content of 25% when other countries (South Africa and India)) are burning coals with up to 45% ash, Zimbabwe is underutilising its coal resources. In addition, if the Company embraces the clean coal technologies such as circulating fluidised bed combustion, it will not only reduce environmental pollution during energy production but will dramatically increase the utilisation of the available resource, thereby increasing the life of the mine (particularly the high ash non-coking thermal coal) considerably.

5.9 Financial Appraisal

In terms of a summary of the long-term value of Hwange Colliery, Table 5.7 presents an estimate of the value of the remaining coal reserves held by the Hwange Colliery, based on current average marketing figures for year 2020 as shown in Table 5.7. Assuming all the coal reserves, as calculated in this thesis and summarised in the tables above, are mined and sold, the results indicate

that the Colliery could generate USD 1 277 254 300 over the next 43 years, and more if lower grade coal coals can be used in the future.

NB. The average selling price for the various coal products and the production costs (Table 5.7) was obtained from the company's marketing and operations departments, respectively.

Table 5.7: Estimated net value of Hwange Colliery's remaining coal reserve.

PRODUCT	TONNAGE	SELLING PRICE	PRODUCTION COST	RESERVE NET VALUE
Coking and Blend Coal	122 657 000	95USD/ton	26USD/ton	845 333 300
Industrial Coal	18 111 000	45USD/ton	26USD/ton	344 109 000
Thermal Coal	87 812 000	27USD/ton	26USD/ton	87 812 000
GRAND TOTAL				**1 277 254 300**

NB: Because of confidentiality/proprietary issues, calculation of the above figures did not entail the details of the mine financial accounting, but, instead, has used the production costs and market selling figures to estimate the value of the reserve.

CHAPTER SIX: CONCLUSIONS AND RECOMMENDATIONS

6.1. Overall summary of the Approach and Methodology to this Research

This study was motivated by the need to establish the reasons for certain anomalies that arose in the performance of the Hwange coals since the commissioning of two mines, the 3 Main Underground and the Chaba Opencast in 2005. These anomalies were particularly as regards to coking capacity. Questions posed included:

a) Why does the Chaba coal reserve previously classified as coking coal, based on cut-offs of a cumulative ash maximum of 15% and cumulative volatile matter minimum of 23.5%, fail to produce coke in the plant?

b) Why does good coking coal produced in some areas of Hwange Colliery not respond well to conventional coking tests?

A compelling need arose to characterise the Hwange coals as an integral effort to answer the above questions. In addition, there was a need to estimate the tonnages of the mineable reserves for each of the established three coal categories, to ascertain Hwange Colliery's preparedness to supply the coal as per current and future market demands both in terms of coal product quality and quantity.

In order to provide sufficient background information, an extensive **review** was conducted on a number of aspects relevant to this research. This included a review of the Zimbabwe coal industry in general, and the macro- and micro-factors controlling or influencing coalfield development and coal seam attributes in southern Africa. Mid-Zambezi basin models were described and compared to the Hwange colliery and coalfield. Coal characterisation and the different parameters used to understand the coals of southern Africa were reviewed with specific emphasis on the petrographic factors applicable to southern African coals. This was followed by a summary of coal beneficiation and its impact on coals destined for coke making and the products required for various users in the different fields of coal utilisation.

The thesis then outlined the **methodologies** used in assessing the geological background and the data acquisition for the coal seams, coal samples and coal products in Hwange Colliery. This was followed by description of the sampling methods and analytical procedures to be undertaken for the samples chosen for further test work. This included conventional physicochemical analyses and the more specialised petrographic, combustion and coking tests and an innovative furnace test

for the specifically chosen representative sections of Chaba and 3 Main Underground mines operated by the Hwange Colliery Company.

The **results of the geological research** revealed highly relevant geological features in the Hwange Coalfield. These included paleotopographical highs and lows within which, or against which, the original peat swamps would have formed, and a series of multiple faults occurring on the western sector of the Coalfield which were considered to be associated with the mobile belt between the Zimbabwean and Congolese granitic cratons. Some faults were considered to still be active and to possibly have given rise to the generation of heat in localised areas as well as to being the source of geothermal heat from depth in the crust. Three suspected igneous bodies below the Hwange Main Seam were also highlighted which may have been a further source of heat at some stage in the development of the Coalfield. Deeper and thicker seams with good coking coals bands were found to have formed in topographic low areas towards the western sector of the mining areas whereas thinner seams with non-coking coals were found on, or abutting against, the topographic highs in the Chaba sector.

The **results of all the analytical and test work** performed on the selected samples in the mining areas were presented in detail. Clear trends in coal qualities were shown to occur in all analyses and tests. In general terms, this included vertical changes from better quality coals at the base of the coal seams to decreasing qualities as samples progressed up the seam. The more detailed analyses established the reasons for the anomalies in coals expected to be good coking coals based upon conventional ash and volatile matter specifications, but which failed to provide coking capacity, relative to coals that were indeed good coking coals. These details will be expanded below.

The **economic potential of the Hwange Coal Concession** was evaluated based upon explained assumptions, an extensive review on previously drilled borehole data to establish by calculation the reserves of the various qualities and grades of coal suitable for the marketplace, and the potential costs involved their production. In this regard, the life of mine for two valuable products ranges from 39 to 45 years under given conditions.

The key findings of the major aspects to this research are as follows:

6.2. Controls on the deposition of Hwange Main Seam and its impact on coal quality

The development of a depression, or basin, is a pre-requisite for the accumulation and preservation of the plant remains. This condition was satisfied by development of the half graben structure, the Mid-Zambezi Basin. The area of study, which comprises the Hwange Concession, the Option Area, and the adjoining Western Areas Coalfield, is traversed by a network of faults which are dominantly listric normal in profile. Such structures are signatures of tensional forces and their presence in the area of study is consistent with the half graben model developed for the Mid-Zambezi Basin.

The basin was occupied by a giant freshwater lake and on the shoreline of this lake developed peat swamps. It was in one such swamp that the Hwange Main Coal Seam developed from luxurious vegetation which included the giant *Glossopteris* vegetation. Subsequent subsidence buried and preserved the thick pile of accumulating vegetable matter. The location was protected from the influx of impurities by either wind, mineral-laden swollen rivers or water currents.

The base on which the coal seam was deposited was irregular. It was characterised by a series of troughs (depressions) and crests. As a result, thick coal horizons occupy the depressions, while the topographically high areas are associated with thin coal layers as the latter either shelve over or thin out completely against these topographic highs. Results from proximate analyses which show thick, low ash and high volatile matter contents in the low-lying areas of 3 Main, Option areas and, to a lesser extent, in Chaba, agree with this model.

In addition, the coal footwall profile reveals a gentle plunge south-westward from approximately 840 m above sea-level in the eastern part of the area of study to below 600 m above sea level in the middle of the study area. Thus, coal at Chaba occurs on topographically high ground and under a thinner overburn (10 - 40 m thick) compared to the coal at 3 Main and the adjoining Option Area where the seam occurs at 600 m and under an overburden thickness of up to 360 m. As a result, more of the coal seam in the Chaba area (in terms of thickness) was above the water table than in the progressively deeper 3 Main and Option Area coals. Thus, the greater part of the Chaba coal was subjected to an oxidising environment and the coally material to decomposition leading to the development of dominantly inertinite group of macerals. The coals in the depressions would, on

the other hand, be mostly below the water table, in a reducing environment. Such an environment is conducive for the development of the vitrinite maceral group. Results of maceral analyses for 3 Main and Chaba are consistent with this model.

In summary, from the profiles obtained from maceral development and proximate analyses obtained from this study, it is concluded that the low ash, vitrinite-rich basal horizon of the Hwange Main Seam represents a wet, forest swamp characterised by a high-water table. A gradual fall in water table exposed the later accumulating vegetative matter to increasing levels of oxidation indicating an increasingly dry forest environment with a greater influx of mineral matter, possibly by water or wind.

The thicknesses of the vitrinite-rich layers have therefore been shown to vary according to topographic location, namely, degrees of accumulation are controlled by location in a depression or against highland topography, with thicker accumulation in depressions and thinner in highland topography. A strong link has therefore been established between the attributes of the Hwange coals and the original environments of deposition.

Furthermore, as vitrinite is the prerequisite maceral for coking capacity (within specific ranges of rank), where such vitrinite is present, coking capacity is likely. This fact links coking capacity with the Hwange environments of deposition.

Furthermore, the petrographic study has established that the Hwange coals fall borderline between the Medium B to Medium C Bituminous range of rank, with Bituminous B rank being the prime coking and liquid-product-emitting range in vitrinite-bearing coals. In this borderline range of rank, vitrinite-rich bands of coal may well be expected to provide swelling properties and other coking capacity to a certain degree and indeed this is the case in the vitrinite-rich bands in 3 Main and Option Area coals. This establishes the link between coking capacity, deeper and thicker bands of vitrinite in the 3 Main and Option Area coals and the Hwange environments of deposition.

6.3. Conclusions regarding the Coking Anomalies

More specifically, this study sought to provide explanations for the anomalies with regard to why the Chaba coal reserve, previously classified as coking coal based on cut-offs of a cumulative ash

maximum of 15% and cumulative volatile matter minimum of 23.5%, fail to produce coke in the plant? And furthermore, why does good coking coal produced in some areas of Hwange Colliery not respond well to conventional coking tests? Answers to the following questions were sought:

6.3.1 Chaba coal anomaly

The question here was "Why does the Chaba coal reserve, previously classified as coking coal based on cut-offs of a cumulative ash maximum of 15% and cumulative volatile matter minimum of 23.5%, fail to produce swelling indices and coke in the plant?"

The study of the scatter diagrams generated show that volatile matter content is closely related to free swelling index. However, in some samples this shows a negative relationship resulting in an anomalous low swelling index. The lowest sample in the seam (Chaba Channel 2) with sufficiently high vitrinite content of 36% (mmf) and volatile matter content of 28.84% appears to possess a good free swelling index of 7. However, samples higher up the seam, despite being acceptably high in volatile matter (=/>23,5%), have **low vitrinite contents** and low swelling indices. Such samples *lack the maceral which would give rise to swelling capacity*. This explains why some Hwange coals swell to some extent while others do not despite possessing the acceptable volatile matter contents.

6.3.2 Why do some Hwange Low Volatile Coals produce Swelling indices and Coke.

While this has not been demonstrated conclusively in the study, it is tentatively considered that enough geothermal energy emanating from the deeper parts of the earth has found its way via faults into the Hwange Main Coal Seam effecting changes mainly to the organic component of the Hwange coals. This is particularly true for the western part of the Hwange Concession, where there is an apparent increase in faulting intensity.

The presence of **exudatinite**, originally a liquified hydrocarbon product emanating from reactive organic components in the coal seam, in the 3 Main and Chaba coal samples lends support to this suggestion. Exudatinite is a secondary maceral generated during coalification and usually found occupying empty spaces such as fissures, cracks and other cavities where it intruded (Taylor, *et al*., 1998; Teichmüller, 1974). The possibility is that geothermal heat emanating via faults and cracks (with increased frequency of faulting westward) may have enhanced the generation of exudatinite which intruded into the cracks and other porous structures in the Hwange coals. Under

such conditions, liquid hydrocarbons (oils) as well as methane (gas) would certainly have been produced from coals exposed to long-term raised temperatures. Both methane and exudatinite have been reported in various sectors of the Hwange Coalfield and in other coalfields in areas in close proximity to Hwange Colliery. The presence of such hydrogen-rich material is expected to provide enhanced fluidity and swelling capacity when heated, and, in this manner, aid in coking capacity.

6.4. Economic Value of Hwange Coal Resource and Life of Mine

The study established that the remaining life of mine (i.e., the area for which Hwange has rights) is 43 years for coking coal (straight coking and blend coking coals combined) and for 39 years thermal coal. This assumes that the production rates will be sustainable at 3.62 metric and 2.02 metric tonnes per year for coking and thermal coal, respectively. Based on the characteristics of the Hwange coals established during the current study, and assuming the production rates will be sustained, and that exploitation will continue to utilise the current financial model and the preferred mining technologies, Hwange will be generating in excess of USD 1 277 000 000 per year over the next 43 years.

6.5. Recommendations

Based upon the results of this study, several recommendations may now be drawn, namely:

I. The presence of exudatinite observed in several samples, particularly in 3 Main Underground mine samples, needs investigation as there may be a link to the high volatile matter content. There is a strong case for investigating the occurrence of exudatinite in more detail. A drill core sampling programme in the virgin areas of both 3 Main Underground mine and the future Option Area mining block should be planned and implemented.

II. A geophysical survey programme is also suggested to precisely locate faults and to take core samples of the coal falling within the fault zones. This will give an added advantage of determining the effects of faulting on coal properties such as the coal rank, maceral composition and mineral matter, in addition to exudatinite prevalence and form of occurrence.

III. Hwange should consider drilling test holes on a systematic grid ahead of mining to model the seam according to its quality. The model will culminate with the coal seam horizon of up to 7 m indicated to be of low ash and high volatile matter contents split into two benches which are: a) a lower bench of coking coal; and b) an upper bench comprising low ash and high volatile matter content, but non-coking coal. This will be in contrast to the current practice at Hwange of mining the entire lower seam bench of up to 7 m as non-coking, which the organisation sends to the general industry at a price lower than that of the coking coal.

IV. Hwange Colliery should consider carrying out petrographic tests, in addition to the current practice of the routine proximate analysis, to characterise the Hwange coal into coking and thermal coal, as proximate analyses alone are not sufficient to indicate that a coal will coke or not.

V. In addition to the above which are directly linked to the aim and objectives of this thesis, for Hwange Colliery financial benefits it is recommended that: Hwange carries out a systematic core drilling exercise to delineate more precisely the areas of its property that lie at various heights above sea-level, namely: a) up to 600m, b) 600 to 720m; and those above 720m which this study has established are intervals where straight coking coals, blend coking coals and general purpose non-coking industrial coals occur, respectively.

VI. Hwange should make a conscious effort to design their mining plans such that the coal categories as listed above are readily and timeously available for exploitation when the market requires respective products.

VII. Hwange Colliery Company should seriously consider employing the Longwall mining method which can achieve coal extraction rates close to 100%. This would increase recovery of the resource at Hwange, whose coking attributes and quantity are paralleled with none in Zimbabwe.

VIII. Hwange should reconsider its financial model (e.g., to highly mechanise and downsize the labour force) to increase mining efficiency and/or reducing costs so that the established economic value of the coal reserve is enhanced for the benefit its stakeholders.

IX. Hwange should consider washing the upper part of the Hwange Main Seam which is currently being discarded as waste due to its ash levels being more than the current boiler

design specifications for the thermal power plant at Hwange. Or, alternatively, that the power utility considers designing new boilers to burn the higher ash material; and

X. The Hwange power utility should consider embracing clean coal technologies such as Circulating Fluidised Bed Combustion in order to (i) combust the high ash coals at Hwange Colliery and (ii) reduce environmentally unfriendly CO_2 and Greenhouse Gas emissions such as SOx and NOx. This will permit the extension of reserves through the utilisation of the high ash products from Hwange colliery which are currently discarded as waste. Research in progress indicates the technique could utilise coals with ash levels as high as 65%. This could lead to exploitation of the entire geological seam. In this way, Hwange Colliery could supply clean coal-based energy to Zimbabwe and the region for many decades to come. This could also reverse the notion that "once a super fuel coal is now a super polluter".

CHAPTER SEVEN: REFERENCE LIST

Agreement between Wankie Colliery Company Limited and Zimbabwe Power Company (Private) Limited on the Supply and Purchase of Coal, 2003.

Allum, J.A.E. (1960). Photogeology and Regional Mapping. Pergamon Press, Great Britain, pp. 62

Amini, S. H. (2014). Ultra-clean coal production using dense medium separation for the silicon market, Lexington, Kentucky: University of Kentucky.

American Society for Testing Materials (ASTM). (1972). Standard Methods of Laboratory Sampling and Analysis of Coal and Coke. D271-70 in 1972 Annual Book of ASTM Standards: Part 19, Gaseous Fuels; Coal and Coke. Philadelphia, Pa., pp. 10-31

ASTM (1994). Standard Test Method for Microscopical Determination of the Reflectance of Vitrinite in a Polished Specimen of Coal. D2798-91 in Annual Book of ASTM Standards: Gaseous Fuels; Coal and Coke, sec. 5, v. 5.05. ASTM International, pp. 280–283.

Anderson, J.M. and Anderson, H.M. (1985). Paleao flora of Southern Africa – Prodomus of South African megafloras, Devonian to Lower Cretaceous. A.A. Balkema, Rotterdam, pp. 52 – 55.

Arnold, B. J. (2013). Coal Formation. In: D. Osborne, ed. The Coal Handbook: Towards Cleaner Production. Burlington. VT: Elsevier Science, pp. 31-52.

ASTM D720-91, (2010). Standard Test Method for Free-Swelling Index of Coal, ASTM International, West Conshohocken, PA, 2010, www.astm.org

Barber, B. (1987). The Save-Runde coal area, Save-Limpopo basin. Records of Zimbabwe Coalfields, vol. XV1. Zimbabwe Geological Survey, Harare.

Barber, B., (2001). The geology and coal potential of the Karoo Supergroup and younger rocks in Zimbabwe. (MSc Thesis). University of Zimbabwe.

Baron, L. (1985). The Transition from contractor to in-house evaluation diamond drilling in Shangani Mine. Association of mine managers of Zimbabwe. Presentation. 1985

Bartholomew, D.S. (1992). Base metal and industrial mineral deposits of Zimbabwe. Mineral Resources Series, 22. Zimbabwe Geological Survey (A government publication).

Bauerman, H. (1911). Anthracite. In: H. Chisholm, ed., Encyclopaedia Britannica, 11th ed. Cambridge University Press, pp.105–106.

Beafore, F.J., (1983). Coal Preparation Can be Cost Effective, CQ Spring 1983.

Beeston, J.W. (1986). Coal rank variation in the Bowen basin, Queensland. International journal of coal geology, 6: 163 - 179.

Berkowitz, N. (1994). An introduction to coal technology. San Diego: Academic Press, p.345.

Bohmke, F.C., and Duncan, R.G., (1974). Final report on EPO No. 378, Exploration for Coal and Natural Gas, Rio Tinto (Rhodesia) Ltd, Mining Division, Eiffel Flats, Zimbabwe.

Bond, G., (1955). The Madumabisa (Karoo) Shales in the Middle Zambezi Region, Trans. Geological Society of South Africa 58, pp.71 – 99.

Bond, G., and Stocklmayer, V. (1966). Possible Ice-Margin Fluctuations in the Dwyka Series in Rhodesia. Palaeogeography, Palaeoclimatology and Palaeoecology. Volume 3 (1967), pp.433 – 446.

Bordy, E.M. and Catuneau, O. (2001). Sedimentology of the Upper Karoo Fluvial Strata in the Tuli Basin, South Africa. J. African Earth Science, 33, pp.605–629.

Brown, M. E., (2004). Introduction to thermal analysis. New York: Kluwer Academic Publishers.

Bryan, W.B., (1986). Tectonic controls on initial continental rifting and evolution of young ocean basins – a planetary perspective. Tectonophysics 24, pp. 1 - 4.

Bunt, J. R., (2006). A New Dissection Methodology And Investigation Into Coal Property Transformational Behaviour Impacting On A Commercial-Scale Sasol-Lurgi Mk. Potchefstroom: North-West University.

Bwerinofa, O.K. and Brennen, R.G. (1989). Wankie - the Zimbabwe Coalmine. In: Annual Joint Meeting of the Institution of Mining Engineers and the Institution of Mining and Metallurgy. Annual joint meeting of the Institution of Mining Engineers and the Institution of Mining and Metallurgy. The Mining Engineer, pp.558–567.

Cadle, A.B. (1982a). Sedimentary control on coal distribution in the north-western Highveld Coalfield. Sedimentology ’82, Abstr., 3rd Symp. Sedimentological Div., Geol. Soc. S. Afr., Johannesburg, pp. 13 -14.

Cadle, A.B. (1982b). Sedimentary control on coal distribution in the north-western Highveld Coalfield. Sedimentology ’82, Abstracts, 3rd Symp. Sedimentological Division, Geol. Soc. S. Afr., pp. 667 – 670.

Cadle, A.B., Hobday, D.K., Smyth, M. and Van Rensburg, W.C.T. eds., (1982). Coal Exploration, Economics and Assessment- Short course. University of Witwatersrand, p.30.

Cadle, A.B., Cairncross, B., Christie, A.D.M. and Roberts, D.L. (1993). The Karoo Basin of South Africa: type basin for the coal-bearing deposits of southern Africa. International Journal of Coal Geology, 23(1–4), pp.117–157.

Cairncross, B. (1979). Depositional Framework and Control of Coal Distribution and Quality. Van Dyks Drift area, northern Karoo basin. MSc Thesis. p.83.

Cairncross, B. (1980). Anastomosing river deposits: palaeo environmental control in coal quality and distribution, northern Karoo basin. Trans. Geol. Soc. S. Afr., 83, pp.327–332.

Cairncross, B. (1982). Coarse-grained anastomosed river deposits from the Witbank Coalfield,

South Africa. In: Sedimentology ’82 Abstr.,. 3rd Symp. Sedimentology Div. Johannesburg: Geol. Soc. S. Afr., pp.8–10.

Cairncross, B. (1986). Depositional Environments of the Permian Vryheid Formation in the east Witbank Coalfield; a Framework for Coal Seam stratigraphy, Occurrence and Distribution. PhD Thesis, University of Witwatersrand. p.232.

Cairncross, B. (1987). Permian coal deposits of Southern Africa (Incorporating Botswana, Malawi, Mozambique, Namibia, Republic of South Africa, Swaziland, Tanzania, Zambia, and Zimbabwe). BHP-Utah International Co. Report, Herndon, VA, USA, p. 187.

Cairncross, B. (2001). An Overview of the Permian (Karoo) coal deposits of southern Africa. Journal of African Earth Sciences 33 (2001) pp. 529 – 562.

Cairncross, B. and Cadle, A.B. (1988). Palaeoenvironmental control on coal formation, distribution and quality in the Permian Vryheid Formation, East Witbank Coalfield, South Africa. Int. J. Coal Geol., 9: pp. 343 – 370.

Cairncross, B. and Hart, R.J. (1988). Coal black but neutron clear. Nuclear Active, No. 39, July, pp. 8 – 12.

Cannon, R.T., Siminyu Siambi, W.M.N., and Karanjani, F.M. (1981). The Proto-Indian Ocean and a probable Palaeozoic/Mesozoic triradial rift system in Africa. Earth planet. Sci. Lett, 52, pp. 419 – 426.

Cao, Y., Mitchell, G.D., Davis, A. and Wang, D. (2000). Deformation metamorphism of bituminous and anthracite coals from China. International Journal of Coal Geology, 43(1–4), pp.227–242.

Cassidy, S.M., 1973. History of coal mining. In: Cassidy, S.M., (Ed.), Elements of Practical Coal Mining. Coal Division, SME-AIME, New York, pp. 1–10.

Catuneanu, O. (2004a). Basement control on flexural profiles and the distribution of foreland facies: The Dwyka Group of the Karoo Basin, South Africa. Geology, 32(6), p.517.

Catuneanu, O. (2004b). Retroarc foreland system - evolution through time. J. African Earth Sciences, 38, pp.225–242.

Catuneanu, O., Hancox, P.J., Rubidge, B.S. (1998). Reciprocal flexural behaviour and contrasting stratigraphies: a new basin development model for the Karoo retroarc foreland system, South Africa. Basin Res. Volume 10, pp. 417 – 439.

Catuneanu, O., Kun-Jager, E.M., Rubidge, B.S., Hancox, P.J. (1999). Lateral changes of the Dwyka facies: implications for the initiation of the Cape Orogeny and the associated Karoo foreland system. In: Abstracts of proceedings, American Association of Petroleum Geologists Annual Meeting, 11–14 April, San Antonio, TX, p. A22.

Catuneanu, O., Hancox, P.J., Cairncross, B. and Rubidge, B.S. (2002). Foredeep submarine fans and forebulge deltas: orogenic off-loading in the underfilled Karoo Basin. Journal of African

Earth Sciences, 35, pp.489–502.

Catuneanu, O., Wopfner, H., Eriksson, P.G., Cairncross, B., B., Rubidge, B. S., Smith, R. M. H. , Hancox, P. J. (2005). The Karoo basins of south-central Africa. Journal of African Earth Sciences, Volume 43, pp. 211 – 253.

Chappell, J. (1969). The Geology of the Eastern Portion of the Chizarira Game Reserve and Adjacent Country, Rhodesia. Unpublished report, PhD-thesis Univ. Zimbabwe, pp. 216.

Chen, P. (1998). Classification of Coal. Coal, Oil Shale, Natural Bitumen, Heavy Oil and Pea – Vol. 1.

Clutten, J.M. (1980). Coal in Zimbabwe. Zimbabwe: Anglo American Corporation.

Cobb, J. C. (1985). Timing and development of mineralized veins during diagenesis in coal beds. In: Cross, A. T. (Ed), Compte Rundu of 9th International Conference on Carboniferous Stratigraphy and Coal Geology, Washington, D. C. and Champaign-Urbana, May 1979. Economic Geology-Coal, Oil and Gas, vol. 4 Southern Illinois Univ. Press, Carbondale, pp 371-376.

Committee for Coal and Organic Petrology (ICCP, International. (1998). The new vitrinite classification (ICCP System 1994). Fuel. 77. 10.1016/s0016-2361(98)80024-0.

Compton, R.R. (1985). Geology in the Field. Cape Town, South Africa: John Wily & Sons.

Condie, K., 1982, Plate Tectonics and Crustal Evolution. Pergamon Press, London, p. 288.

Crelling, J. C. (2008). Coal Carbonization. In: Applied Coal Petrology: The Role of Petrology in Coal Utilization. Burlington(Massachusetts): Academic Press, pp. 173-192.

Daly, M. (1986). Crustal shear zones and thrust belts: Their geometry and continuity in Central Africa. Royal Society of London Philosophical Transactions Series A, 317, 111- 127.

Damberger, H.H., Harvey, W.A., Ruch, R.R. and Thomas Jr, J. (1984). Coal characterization. In: B.R. Cooper and W.A. Ellingson, eds., The Science and Technology of Coal and Coal Utilization. Plenum Press, pp.7–45.

Davis, A., Russell, S.J., Rimmer, S.M. and Yeakel, J.D. (1984). Some genetic implications of silica and aluminosilicates in peat and coal. International Journal of Coal Geology, 3(4), pp.293–314.

De Jager, F.S.J. (1976). Coal. In: C.B. Coetzee (Editor), Mineral Resources of the Republic of South Africa. Handbook., Geol. Surv. S. Afr., 7: pp. 289 – 330.

de Kort, G. J. (2010). Coal preparation research in South Africa. The Journal of the Southern African Institute of Mining and Metallurgy, Volume 110, pp. 361-364.

de Korte, G. (2015). Processing low-grade coal to produce high-grade products. The Journal of the Southern African Institute of Mining and Metallurgy, July, Volume 115, pp. 569-572.

Diessel, C. and Pickel, W. (2012). Carbonisation and coke petrology. In: 5th International

Committee for Coal and Organic Petrology Course in Organic Petrology. International Committee for Coal and Organic Petrology (ICCP), pp.53–129. Course Notes, Volume 2.

Duguid, K.B. (1977). A cross-section through the Lusulu coalfield. In: Thompson, A.C. (Ed.), The Lusulu (and Sengwe) Coalfields. Zimbabwe Geological Survey, Records of Rhodesian Coalfields.

Duguid, K.B. (1978). The Geology of the Karoo System the Sabi and Lundi-Sabi basins. (Unpublished D.Phil. thesis). University of Rhodesia (University of Zimbabwe), Salisbury (Harare). 356 p.

Duguid, K.B. (1980). Coal and coal exploration. Chamber of Mines J., 26 (8).

Duguid, K.B. (1986a). The coal resources of Zimbabwe. In: Annhauessar and Maske, S (Eds). Mineral Deposits of Southern Africa. Vol. 11. Geol. Soc. S. Afr., Kelvin House, Johannesburg, pp. 2091 – 2098.

Duguid, K.B. (1986b). Wankie district coal measures. In: C.R. Anhaeusser and S. Maske, eds., Mineral Deposits of Southern Africa. Johannesburg: Geological Society South Africa, pp.2099 – 2104.

Duguid, K. B. (1993). The potential for coalbed methane gasfields in Zimbabwe. Proceed. 1993 Coalbed Methane Symposium, pp. 37-55.

EIA (2002). Energy in the United States: 1653-2000. Energy Information Administration. [online] Available at: http://www.eia.doe.gov/emeu/aer/eh.

Ekbote, P. (2020). Session 2 Module 2 Coal Properties and Effect on Cobustion. [Online] Available at: https://www.eecpowerindia.com/codelibrary/ckeditor/ckfinder/userfiles/files/Session%202%20Module%202%20Coal%20Properties%20and%20Effect%20on%20Cobustion.pdf [Accessed 13 June 2020].

Erol, I., Aydin, H., Didari, V., Ural, S. (2013). Pneumoconiosis and quartz content of respirable dusts in the coal mines in Turkey. Inst. J. Coal Geol. 116 – 117, pp. 26 – 35.

ExxonMobil Corporation (2008). 2008 Financial and Operating Review. Exonnmobil Corporation 2008 Financial and Operating Review. [online] Available at: https://www.sec.gov/Archives/edgar/data/34088/000095013409006406/d66829exv99.htm#tocpage [Accessed 21 Mar. 2019]. Archives.

Falcon, R.M.S. (1975a). Palyno-stratigraphy of the Lower Karoo sequence in the Central Sebungwe District, Mid-Zambezi Basin, Rhodesia. Palaeontologica Africana, 18, 1-29.

Falcon, R.M.S. (1975b). Application of palynology in subdividing the coal-bearing formations of the Karoo sequence in southern Africa. South African Journal Science, 71, 336-344.

Falcon, R.M.S. (1977). Coal in South Africa – Part 1: The Quality of South African Coal In Relation to its Uses and World Energy Resources. Minerals Sci. Engng, Vol.9, No. 4, Oct., 1977.

Falcon, R.M.S. (1978a). Coal in South Africa, Part 2 – The application of petrography to the characterisation of coal. Miner. Sci. Eng., 10 (1), pp. 28 – 52.

Falcon, R.M. S. (1978b). Part 3 – Summary proposals – the fundamental approach to the characterization and rationalization of South Africa's coal. Miner. Sci. Eng., 10 (2), pp. 130 – 153.

Falcon, R.M.S. (1978c.) A palynological comparison of Karoo sediments on opposite sides of the Rhodesian Watershed with stratigraphic application. (PhD Thesis) University of. Witwatersrand, Johannesburg, pp. 480.

Falcon, R.M.S. (1980), Palynofloristic trends in the Permo-Triassic of Southern Africa. In: International Palynofloristics Symposium (Lucknow, 1976, 1977 (2). Proc., 1V, pp. 208 -218.

Falcon, R.M.S. (1981). The petrographic characterization of coals from the No.2 seam, Witbank Coalfield: In: Bureau for Mineral Studies: Characterisation of South African coals. Rep. 6, pp. 193.

Falcon, R.M.S. (1985). Report of the Petrographic and Palynological Analyses Conducted on one borehole from the Waterberg Coalfield of South Africa. Gold Fields of South Africa. Int. Rep. Falcon Research Lab., p.33.

Falcon, R.M.S. (1986a). A brief review of the origin, formation and distribution of coal in Southern Africa. In: Anhaeusser, C.R., Maske, S. (Eds), Mineral Deposits of Southern Africa, vols. 1 and 11. Geological Society of South Africa, Johannesburg, pp. 1879 – 1898.

Falcon, R.M.S. (1986b). Classification of coals in Southern Africa. In: Anhaeusser, C.R., Maske, S. (Eds.), Mineral Deposits of Southern Africa, vols. 1 and 2. Geological Society of South Africa, Johannesburg, pp. 1899 – 1921.

Falcon, R.M.S. (1989). 'Marco- and micro-factors affecting coal-seam quality and distribution in southern Africa with particular reference to the No.2 seam, Witbank coalfield, South Africa'. International Journal of Coal Geology, 12 (1989), pp. 681 – 731.

Falcon, R. (2013). Coal petrography. In: D. Osborne, ed. The Coal Handbook: Towards Cleaner Production. Cambridge: Woodhead Publishing Limited, pp. 53-79. Falcon, R.M.S. and Snyman, C.P. (1986). An Introduction to coal petrography: Atlas of petrographic constituents in the bituminous coals of Southern Africa. 1st ed. Johannesburg: Geological Society of South Africa.

Falcon, L. M., and R. M. S. Falcon. 1987. The petrographic composition of Southern African coals in relation to friability, hardness, and abrasive indices. Journal of South African Institution of Mineral and Metallurgy 87 (10): pp. 323–36.

Falcon, R.M.S. and Ham, A.J. (1988). The Characteristics of South African Coals. Journal of the South African Institute of Mining and Metallurgy, 88(5), pp.145 – 161.

Falcon, R. M.S., Pinheiro, H. J., Shepherd, P. (1984a). Palynobiostratigraphy of the major coal seams in the Witbank Basin with lithostratigraphic, chronostratigraphic and palaeoclimatic

implications. Comun. Serv. Geol. Port.; (Portugal); Journal Volume: 70:2; Conference: Symposium on Gondwana coals, Lisbon, Portugal, pp 215-243.

Falcon, R.M.S., Lemos de Sousa, M.J., Pinhero, H.J. and Marques, M.M. (1984b). Petrology and palynology of Moçambique coals, Mucanha Vuzi Region. In: M.J. Lemos de Sousa, ed., Symposium on Gondwana Coals. Lisbon Proc. and Papers, pp.321–338.

Falcon, R.M.S. and Snyman, C.P. (1986). *An Introduction to coal petrography: Atlas of petrographic constituents in the bituminous coals of Southern Africa*. 1st ed. Johannesburg: Geological Society of South Africa.

Falcon Research Laboratory (Pty.) Ltd., 1995. Petrographic analyses and report on three borehole cores M 94 G, M 129 G, and M 178, Sengwa Coalfield Exploration Project, for Rio Tinto Zimbabwe. Unpublished report.

Finkelman, R. B. (1994). Abundance, source and mode of occurrence of the inorganic constituents in coal. In Kural, O. (Ed), Coal. Istanbul Technical University, Istanbul, pp. 115-125.

Finkelman, R.B., Orem, W., Castranova, V., Tatu, C.A., Belkin, H.E., Zheng, B., Lerch, H.B., Maharaj, S.V., Bates,A.L. (2002). 'Health impacts of coal and coal use: possible solutions'' International Journal of Coal Geology. 50, pp. 425 – 443.

Fisher, A.D. (1971). Metallurgical Coals for the Future. In: Twenty-Third Canadian Conference on Coal. Twenty-Third Canadian Conference on Coal. Ottawa, Ontario, Canada: The Steel Company of Canada, Ltd.

Frakes, L.A. (1979). Climates throughout Geological Time. Elsevier, Amsterdam, p.310.

Gary, M., McAfee, R. and Wolf, C.L. eds., (1972). Glossary of Geology. Washington, DC.: American Geological Institute, p.805.

Gauthier, F. and Pelletier, P. (2015). The mining industry value chain: Characterization and mapping of the Northwest Territories mining sector's value chain. Publications. [Online] CDÉTNO - Conseil de development économique des Territoires du Nord-Ouest. Available at: http://cdetno.com/wp-content/uploads/2016/11/enCVSM.pdf [Accessed 18 Nov. 2018]

Ghosh, P. K. and Mitra, N. D. (1967), Talchir sedimentation in West Bokaro Basin, Ind. Minerals 21 1–9.

Given, P.H., Spackman, W. (1978). Reporting of Analyses of Low-rank Coals on the Dry, mineral-matter-free basis. Fuel 57, pp. 319 – 320.

Gluskoter, H.J., Ruch, R.R., Miller, W.G., Cahill, R.A., Dreher, G.B.Kuhn, J. K.. (1977). Trace Elements in Coal: Occurrence and Distribution, Illinois State Geological Survey Circular 499, p. 154.

Götz, A. E., & Ruckwied, K. (2014). Palynological records of the Early Permian postglacial climate amelioration (Karoo Basin, South Africa). Palaeobiodiversity and Palaeoenvironments, 94(2), 229–235.

Greb, S. (2013). How Coal Forms and Coal Rank Diagrams by Stephen Greb, © Kentucky Geological Survey. Kentucky Geological Survey. Available at: http://www.uky.edu/KGS/coal/ [Accessed 23 Jan. 2020].

Gurba, A. J., Gurba, L. W., Ward, C. R., Wood, J. (2003). Gas drainability and outburst risk assessment based on the distribution of micro-makers in coal seams. Australian Coal Association Research Programme (ACARP), End of Grant Report, Project C11057. ACARP, Brisbane, p. 84.

Gupta, R., Wall, T. F., Baxter, L. A. (Eds.). (1999b). The Impact of Mineral Impurities in Solid Fuel Combustion. Plenum, New York, p 768.

Hagelskamp, H.H.B., Eriksson, P.G. and Snyman, C.P. (1988). The Effect of Depositional Environment on Coal Distribution and Quality Parameters in a Portion of the Highveld Coalfield, South Africa. Int. J. coal Geol., 10, pp. 51 – 78.

Hagelskamp, H.H.B. and Snyman, C.P., 1988, On the origin of low reflecting inertinites in Coals from the Highveld Coalfield, South Africa. Fuel, 67, pp. 307 – 314.

Hancox, J. P., & Götz, A. E. (2014). South Africa's coalfields – a 2014 perspective. International Journal of Coal Geology, 132, pp 170–254.

Hart, R.J. and Leahy, R. (1983). The geochemical characterization of coal seams from the Witbank Basin. Geolog. Soc. Doc. S. Afr., Spec. Publ., 7, p. 169.

Harvey, R. D., Ruch, R. R. (1986). Mineral matter in Illinois and other US coals. In Vorres, K. S. (Ed.), Mineral matter in coal Ash and Geochemistry 3, pp 343-349.

Hatcher, P.G. and Clifford, D.J. (1997). The organic geochemistry of coal: from plant materials to coal. Organic Geochemistry, 27(5–6), pp.251–257, 259–274.

Haughton, S.H. (1970). The Gondwana (Karoo) System In Southern Africa. Second Gondwana Symposium: Proceedings and Paper.

Hessley, R. K., Reasoner, J. W., and Riley, J. T. (1986). Coal Science, Wiley, New York.

Hobday, D. K., (1987). Gondwana coal basins of Australia and South Africa: Tectonic setting, depositional systems and resources. Geological Society London Special Publications, 32(1), pp. 219-233.

Hood, A., Gutjahr, C.C.M. and Heacock, R.L. (1975). Organic Metamorphism and the Generation of Petroleum. AAPG Bulletin, 59(6), pp.986–996.

Horsfall, D.W., (1978). Coal preparation in South Africa: present position and future prospects. S.A. Mining & Engineering Journ. November 1978.

Horsfall, D.W., (1993). "Ed Coal Preparation and Usage – Coal Processing for Management," 3 Volumes, Coal Publications (Pty) Ltd.

Hosking, B.C., (1981). The stratigraphy and sedimentation of the Karoo Supergroup in the Mid-Zambezi Valley, Zimbabwe. Unpublished M.Sc thesis Univ. Zimbabwe, 194 pp.

Hübner, H. (1965). Permo-Carboniferous glacial and periglacial deposits from the central part of the Congo basin. Stockholm Contributions in Geology. Stockholm Contributions in Geology, 13, pp.41–61. 14 plates.

Humphreys, M. (1969). The geology of the western portion of the Chizarira Game Reserve and adjacent country, Rhodesia. Unpublished report PhD thesis Univ. Rhodesia, 297 pp.

Hwange Colliery Company Hundred Years Anniversary. Company centenary proncure, 1995.

Hwange Colliery Company Strategic Plan. (2014). Hwange Colliery Company, Zimbabwe. A report.

ICCP (International Committee for Coal and Organic Petrology). (1994). The new vitrinite classification (ICCP System 1994). Fuel, 77(5), pp.349–358.

ICCP, (1998). The new vitrinite classification (ICCP System 1994). Fuel 77, pp 349–358.

ICCP, (2001). The new inertinite classification (ICCP System 1994). Fuel 80, pp 459–471.

International Energy Agency (IEA). (2004). World Energy Outlook. France: OECD/IEA.

IEA Statistics. (2016). www.iea.org

IEA. (2017). Percentage coal dependency in electricity mix. www.iea.org

IEA. (2020). World Energy Balances: Data and statistics - Coal final consumption by sector, Zimbabwe 1990-2017. [online] International Energy Agency. Available at:https://www.iea.org/statistics/?country=ZIMBABWE&year=2016&category=Electricity&indicator=ElecGenByFuel&mode=chart&dataTable=ELECTRICITYANDHEAT [Accessed 23 Jan. 2020].

ISO 9001:2008 Quality Management System;.https//www researchgate.

ISO 502:2015 (2015). Coal Determination of caking power - Gray-King coke test. International Organization of Standardization- ISO.

ISO 11760:2005 (2005). Classification of coals. Available
at:https://www.iso.org/obp/ui/#iso:std:iso:11760:ed-1:v1:en.

ISO Standard 349-1975 (E) (1975). Hard coal - Audibert-Arnu dilatometer test. International Organization of Standards - ISO.

Isbell, J. L., Cole, D. I., & Catuneau, O. (2008). Carboniferous-Permian glaciation in the main Karoo Basin, South Africa: stratigraphy, depositional controls, and glacial dynamics. GSA Special Paper, 441, 71–82.

Jia, J., Xie, C. and Wang, Y. (2011). Factor analysis and raising measures about the coke quality.

In: 8th CSM annual meeting. Beijing: Chinese Society for Metals.

Johns, A.R. and Harris, M. (2009). Boiler Efficiency Calculations. Lecture notes: Coal Combustion and Power Generation course, University of Witwatersrand, Johannesburg, 31 August 2009.

Johnston, M.R.(1976). Stratigraphy and sedimentology of the Cape and Karoo sequences in the Eastern Cape Province. (PhD thesis), Rhodes University, Grahamstown, pp. 336.

Johnson, M.R., van Vuuren, C.J., Herzenberger, W.F., Key, R., Shoko, U. (1996). Stratigraphy of the Karoo Supergroup in southern Africa: an overview. Journal of African Earth Sciences, 23, pp 3-15.

JORC. (2012). Australasian Code for Reporting of Exploration Results, Mineral Resources and Ore Reserves (The JORC Code) [online]. Available from: <http://www.jorc.org> (The Joint Ore Reserves Committee of The Australasian Institute of Mining and Metallurgy, Australian Institute of Geoscientists and Minerals Council of Australia).

Karr, C. (1978). Analytical Methods for Coal and Coal Products. New York: Academic Press.

Keyser, A.W. (1966). Some indications of an arid climate during deposition of the Beaufort Series. Ann. Geol. Survey S. Africa 5, pp. 77 – 80.

Kiss, L. T., King, T. N. (1977). The expression of results of coal analysis: the case for brown coals. Fuel, 56, pp 340-341.

Kiss, L. T., King, T. N. (1979). Reporting of low-rank coal analysis- the distinction between minerals and inorganics. Fuel, 58, pp 547-549.

King, J. G., Wilkins, E. T. (1944). The internal structure of coal. Proc, Conf. Ultrafine. Structure of Coals and Cokes. Brit Coal Utilization Research Assoc. 46-56

Kögel-Knabner, I. (1993). Biodegradation and humification processes in forest soils. In: Soil Biochemistry. New York: M. Dekker, pp.101–135.

Kitto, J.B. and Stultz, S.C. (2005). Burners and combustion systems for pulverised coal. In: J.B. Kitto and S.C. Stults, eds., Steam/its generation and use. Barberton, Oh: Babcock & Wilcox Company, pp.14-1-14–21.

Kolker, A., (2012). Minor element distribution in iron di-sulphides in coal: a geochemical review. Int. J. Coal Geol. 94, 32 – 43.

Kroner, A. (1977). Precambrian mobile belts of southern and eastern Africa - ancient belts of southern and eastern Africa – ancient sutures or sites of ensialic mobility? A case for crustal evolution towards plate tectonics. Tectonophysics 40, pp. 101 -136.

Kruger, H. (2013). Coking Coal. [online] ArcelorMittal South Africa. Available at: http://www.fossilfuel.co.za/conferences/2013/CoalCokeCarbon/Day-One/02-Hannes-Kruger_Coking-Coal.pdf [Accessed 28 Nov. 2020].

Kubach, C. (2012) Heavy Medium Gravity Separation. Mining Engi. Communication 2012 L

Kural, O.C. (1994). Coal : resources, properties, utilization, pollution. Istanbul, Turkey: Istanbul Technical University.

Lee, B. H., Song, J.-H., Lee, C.-S., Chang, Y.-J., & Jeon, C. H. (2009). Effect of Coal Properties on Combustion Characteristics in a Pulverized Coal Fired Furnace. Transactions of the Korean Society of Mechanical Engineers B, 33(10), pp. 737-747.

Le Blanc Smith, G. and Falcon, R.M.S. (1982). Aspects of relationships in Gonwanan coal quality, distribution and palaeoenvironment. In: Witbank Coalfield, South Africa. Sedimentology '82. Abstr. 3rd Symp. Sedimentological Div. Johannesburg: Geol. Soc. S. Afr., pp.5–7.

Le Manquais, K., Snape, C., McRobbie, I., Barker, J. and Pellegrini, V. (2009). Comparison of the Combustion Reactivity of TGA and Drop Tube Furnace Chars from a Bituminous Coal. Energy & Fuels, 23(9), pp.4269–4277.

Lepper, J. (1987). Study on the Lower Karoo in the Mid-Zambezi Basin. Hannover: Bundesantalt fur Geowissenschaften und Rohstoffe.

Lepper, J. (1992). The Lower Karoo in the Mid-Zambezi basin (Zimbabwe). Geologisches Jahrbuch, Series B, Issue 82, p.38

Li, Z., Ward, .R., Gurba, L.W.(2010). Occurrence of non-mineral inorganic elements in low-rank coals. Int. J. Coal Geol. 81, pp. 242 – 250.

Lock, B.E. (1980). Flat-plate subduction and the Cape Fold Belt of South Africa. Geology 8, 35–39.

Lu, L., Devasahayam, S. and Sahajwalla, V. (2013). Evaluation of coal for metallurgical applications. In: D. Osborne, ed., The Coal Handbook: Towards Cleaner Production. Sawston, Cambridge, UK: Woodhead Publishing, pp.352–386.

Mapani, B., Finkelman, R. and Ravengai, S. (2013). Trace and heavy element distribution of the Hwange Coals in Zimbabwe: indicators of source rock chemistry, climatic conditions and deposition mechanisms during their formation in Southern Africa. Int. Sci. Technol. J. Namibia, 1(1).

Maponga, O.J. (1989). The Geology and Coal Reserves of the No.3 North Reserve Block, Hwange Colliery. Hwange: Hwange Colliery Company. Hwange Colliery internal company report.

Maponga, O. J. (2014). Zimbabwe's Coal-Bed Methane Potential, Johannesburg: Fossil Fuel Foundation.

Maponga, O.J. (2019). Coal. In: Mining in Zimbabwe. Harare: Chamber of Mines of Zimbabwe, pp.207–234.

Martin, A.K. and Hartnady, C.J.H. (1986). Plate tectonic development of South West Indian Ocean: a revised reconstruction of East Antarctica and Africa. J. Geo-phys. Volume 91, pp 4767 – 4786.

Matsuoka, K., Rosyadi, E., Tomita, A. (2002). Mode of occurrence of calcium in various coals. Fuel 81, pp. 1433 – 1438.

Mckenzie, D. (1978). Some remarks on the development of sedimentary basins. Earth Planet. Sci. Lett, 40, pp. 25 - 32.

McRae, C.S. (1984). Age relationships in the Gondwana glacial and fluvioglacial deposits. Abstract. Newslett. Palaeontol. Soc. S. Afri., 4 (1), pp. 6 – 7.

Meyers, R. A. (1982). "Coal Structure," Academic Press, New York.

Miller, B.G. (2011). Clean coal Engineering Technology. Elsevier. Pp 251 -296.

Miller, K. (2013). Coal analysis. In: Osborne, D., (Ed), The Coal Handbook: Towards Cleaner Production. Woodhead Publishing Company, pp 151–189

Miller, R.N., Given, P.H. (1986). The association of major, minor and trace elements with lignite: 1 – experimental approach and study of North Dakot lignite. Geochim. Cosmochim. Acta 51, pp. 2033 – 2043.

Miller, R.N., Given, P.H. (1987). A geochemical study of the inorganic constituents of some low-rank coals. Report, Contract E-76-C-01-2494, U.S. Department of Energy, Coal Research Section, Pennsylvania State University (unpublished), p 314.

Ministry of Coal (2019). Coal Grades | Ministry of Coal, Government of India. [online] Coal.nic.in. Available at: https://coal.nic.in/content/coal-grades [Accessed 10 Jul. 2020].

Mitchell, G. (1999a). Selecting coals for quality coke -" Part VIII: measurements of rheological/thermoplastic characteristics of coal. Iron and Steel Maker ,101-103.

Mitchell, G. (1999b). Selecting coals for quality coke -" Part X: coal selection strategies. Iron and Steel Maker, 67-69.

Moore, T. A. (2012). Coal-bed methane: a review. Int. J. Coal Geol. 101. Pp. 36 – 81.

Morrise, M., 2005. How is crude coal tar derived coopers creek chemical corporation, s.l.: Truthaboutcoaltar.com.

Moyo, F. (2012). The Hwange Coal Deposit, Johannesburg: Fossil Fuel Foundation.

Mukhopadhyay, P.K., and W.G. Dow, eds. (1994), Vitrinite reflectance as a maturity parameter: applications and limitations: Washington, D.C., American Chemical Society Symposium Series 570, 294 p.

National Commission on Energy Policy (2008). Meeting Projected Coal Production Demands in the U.S.A – Upstream Issues, Challenges, and Strategies. December 2008.

Norton, G.A. (1993). A review of the derivative thermogravimetric technique (burning profile) for fuel combustion studies. Thermochimica Acta, p. 214.

Nyambe, I.A. (1999). Tectonic and climatic controls on sedimentation during deposition of the Sinakumbe Group and Karoo Supergroup, in the mid-Zambezi Valley Basin, southern Zambia. J. Afr. Earth Sci. 28 (2), 443–463.

O'Brien, G., Firth, B. & Adair, B. (2011). The Application of the Coal Grain Analysis Method to Coal Liberation Studies. International Journal of Coal Preparation and Utilization, Volume 31, pp. 96-111.

O'Keefe, J. M. K., Betchel, A., Christanis, K., Dai, S., DiMichele, W. A., Eble, C. F., Esterle, J. S., Mastalerz, M., Raymond, A. L., Valentim, B. V., Wagner, N. J., Ward, C. R., Hower, C. J., (2013). On the fundamental difference between coal rank and coal type. International Journal of Coal Geology, 118, pp 58-87.

Oesterlen, P.M. (1998). The geology of the Dande-West area, Lower-Zambezi valley. Bulletin-Zimbabwe Geological Survey 98. 85 pp.

Oesterlen, P.M. (1999). Some new results from the Mid-Zambezi basin. Annals of the Zimbabwe Geological Survey XIX, 16– 20.

Oesterlen, P.M., Blenkinsop, T.G. (1994). Extension direction and strain near the failed triple junction of the Zambezi and Luangwa rift zones, Zimbabwe. Journal of African Earth Sciences 18, 175–180.

Oesterlen, P. M., and Lepper, J. (2005). The Lower Karoo coal (k2-3) of the Mid-Zambezi basin, Zimbabwe: depositional analysis, coal genesis and palaeogeographic implications.International Journal of Coal Geology, 61, pp 97-118.

Orpen J.L.,Swain, C.J., Nugent, C., Zhou, P.P. (1989). Wrench-fault and half-graben tectonics in the development of the Palaeozoic Zambezi Karoo Basins in Zimbabwe- the "Lower Zambezi" and "Mid-Zambezi" basins respectively – and regional implications. Journal of African Earth Sciences, Vol. 8. Nos. 2/3/4, pp. 215 -229.

Osborne, D. G. (1988), "Coal Preparation Technology – Volume One" Graham and Trotman, London.

Pallock, H-H. (1984). An assessment of some of the coal deposits in the north-west Zimbabwe Zimbabwe Geological Survey, Mineral Resources Series 19. 39 pp.

Palloks, H.-H. (1987). The Wankie Concession area. Zimbabwe Geol. Survey, Records of Zimbabwe Coalfields V. 14 pp.

Petukhov, V. (1995). Conditioning of coal for froth flotation with kerosine collector. Fuel and Energy Abstract, 36(4), 245–245.

Pickel, W., Kus, J., Flores, D., Kalaitzidis, S., Christanis, K., Cardott, B.J., Misz-Kennan, M., Rodrigues, S., Hentschel, A., Hamor-Vido, M., Crosdale, P. and Wagner, N. (2017).

Classification of liptinite – ICCP System 1994. International Journal of Coal Geology, Volume 169, pp. 40-61

Pitman, J.K., Pashin, J.C., Hatch, J.R., Goldhaber, M. B. (2003). Origin of minerals in joint and cleat systems of the Pottsville Formation, Black Warrior Basin, Alabama: implications for coal-bed methane generation and production. AAPG Bull. 87, pp. 713 -731.

Plumstead, E.P. (1957). Coal in Southern Africa. Witwatersrand University Press, Johannesburg, p. 24.

Plumstead, E.P. (1966). The story of South Africa's coal. Optima, 16 (12), pp. 387 – 402.

Pohl, W.L. (2011). Economic Geology: Principles and Practice. 1st ed. John Wiley & Sons, Inc.

Polat, M., Polat, H. & Chander, S. (2003). Physical and chemical interactions in coal flotation. International Journal of Mineral Processing, Volume 72, p. 199–213.

Pysklywec, R.N. and Mitrovica, J.X. (1999). The role of subduction-induced subsidence in the evolution of the Karoo Basin. J. Geol. 107, pp. 155 – 164.

Raymond, Jr., R., Andrejeko, M.J. (Eds) (1983). Proceedings of Workshop on Mineral Matter in Peat: Its Occurrence, Form and Distribution, Los Alamos National Laboratory, Los Alamos, New Mexico, September 26 – 30, Los Alamos National Laboratory Report LA9907 OBES, p. 242

Reeves, C.V., Sahu, B.K., de Wit, M. (2002). A re-examination of the paleo-position of Africas neighbours in Gondwana. J. Afr. Earth Sci.34, 101–108.

Rostam-Abadi, M., DeBarr, J.A., and Chen, W.T. (1990). Combustion studies of coal derived solid fuels by thermogravimetric analysis: III. Correlation between burnout temperature and carbon combustion efficiency. Thermochim. Acta, Volume 166, p. 351.

Rust, I.C. (1975). Tectonic and sedimentary framework of Gondwana basins in southern Africa. In: Campbell, K.S.W. (Ed.), Gondwana Geology (3rd Gondwana Symposium). Australian National University Press, Canberra, pp. 537 – 564.

Ryemshak, S.A. and Jauro, A. (2013). Proximate analysis, rheological properties and technological applications of some Nigerian coals. International Journal of Industrial Chemistry, 4(1), p.7.

Sahoo, B.K., Ghosh, B., Abhijnan, A., Kumar, A. and Kumar, A. (2018). Effect of different size fractions on Coal Quality. Asian Journal of Science and Technology, 9(4), pp.8032–8035.

SAMREC (2016). The South African Code for the Reporting of Exploration Results, Mineral Resources and Mineral Reserves (the SAMREC Code. [online] SAMCODE. SAMREC (South African Mineral Resource Committee). Available at: https://www.samcode.co.za/codes/category/8-reporting-codes?download=231:202001_SAMREC%20Code%20with%20Table%201 [Accessed 11 Jul. 2020].

Schatzel, S.J. (2009). Indentifying sources of respirable quartz and silica dust in underground coal mines in southern West Virginia, western Virginia, and eastern Kentucky. Int. J. Coal Geol. 78, pp. 110 – 118.

Schatzel, S.J., Stewart, B.W. (2012). A provenance study of mineral matter in coal from Appalachian Basin coal mining regions and implications regarding the respirable healthof underground coal workersa geochemical and Nd isotope investigation. Int. J. Coal Geol. 94, pp. 123 – 136.

Schweinfurth, S.P. (2009). An Introduction to Coal Quality, in Pierce, B.S., and Dennen, K. O., eds., The National Coal Resource Assessment Oveview: U.S. Geological Survey Professional Paper. 1625 – F Chapter C, p. 16.

Scott, A. C., and Glasspool, I. J. (2006). The diversification of Paleozoic fire systems and fluctuations in atmospheric oxygen concentration. Proceedings of the National Academy of Sciences of the United States of America, 103:29, pp 10861-10865.

Selley, R.C. (Ed.) (1997). Sedimentary Basins of the World. African Basins, vol.. 3. Elsevier, Amsterdam, p. 394.

Sengor, A.M.C. and Burke, K. (1978). Relative timing of rifting and volcanism on earth and its tectonic implications. Geophys. Res. Lett. 5, pp. 419 – 421.

SGS Group Management SA (2013). Metallurgical Coal and Coke Testing. [Online] Available at: https://www.sgs.com/-/media/global/documents/flyers-and-leaflets/sgs-min-wa058-lab-testing-metallurgical-coal-and-coke-en-11.pdf [Accessed 20 February 2019].

Shell Developments Zimbabwe (Pvt.) Ltd. (1983). Summary Geological Report Lusulu Project, E.P.Os No. 573, 606 and 607. Unpublished report, pp. 69.

Shibaoka, M. and Bennet, A.J.R. (1976). Effect of Depth of Burial and Tectonic Activity on Coalification. Nature, 259(5542), pp.385–386.

Smith, W. H. (1984). “The Constitution of Coal”, Lecture for the South African Coal Processing School, April 1984.

Smoog, M.D. (1992). Correlation of coal combustion in a drop tube furnace to a full size boiler. Eskom Report TRR/P92/027.

Snyman, C.P. (1961). A Comparison between the petrography of South African and some other Palaeozioc coals. Pretoria Univ. Pretoria, NuweReeks, p15.

Snyman, C.P. (1976). The Petrographic Composition and the Origin of Coal. *Trans. Geol. Soc. S. Afr.*, 79(2), pp.242–252.

Snyman, C.P. and Barclay, J. (1989). The coalification of South African coal. International Journal of Coal Geology, 13(1–4), pp.375–390.

Snyman, C.P., Vuuren, V. and Barnard, J.M. (1983). Chemical and physical characteristics of

South African coal and a suggested classification system. Pretoria: Council For Scientific And Industrial Research, National Institute For Coal Research.

Snyman, C.P., Barclay, J. (1989). The coalification of South African coal. Inst. J. Coal Geol. 13, 375 – 390, pp 89 – 102.

Snyman, C.P., Van Vuuren, M.C.J. and Barnard, J.M. (1983). Chemical and physical characteristics of South African coal and a suggested classification system. NICR Report. ISBN No. 0 7988 2799 8, 110p.

Soni, N. (2017). Thermal Methods of Analysis. Modern applications in Pharmacy & Pharmacology, 1(2), pp. 1-8.

Solov'eva, T., & Muklakova, A. (1995). Method for determination of flotation activity of apolar reagents during flotation of coals. Fuel and Energy Abstracts, 36(4), pp 246–246.

South African National Standards (SANS) 7404-3:2016 (ISO 7404-3:2009). Methods for the petrographic analysis of coals-Part 3: method of determining maceral group

Speight, J. G. (2013). The Chemistry and Technology of Coal (3rd ed.). Boca Raton, Florida, USA: CRC Press.

Stach, E., Mackowsky, M.Th., Teichmüller, M., Taylor, G.H., Chandra, D., Teichmüller, R., (1982). Stach's Textbook of Coal Petrology, 3rd ed. Gebrüder Borntraeger, Berlin.

Standards Australia (1995). Coal and coke-glossary of terms. Australia Standard 2418, p 180.

Standards Australia (2000). Higher rank coal-mineral matter and water constitution. Australia Standard 1083, Part 22, p 20.

Stavrakis, N. (1980). Sedimentation of the Katberg sandstone and adjacent formations in the south-eastern Karro Basin. Trans. Geol. Soc. S. Afr. 83, pp. 361 – 374.

Strauss, P. G., Russell, N. J., Bennett, A. J. R. & Atkinson, C. M. (1976). Coal petrography as an exploration aid in the West Circum-Pacific. In: W. Muir, ed. Coal Exploration. Proc. First International Symposium. London: First International Symposium, pp. 401-447.

Suárez-Ruiz, I., Crelling, J.C., (Eds.) (2008a). Applied Coal petrology. The role of petrology in coal utilization. Elsevier, Amsterdam, pp 398.

Suárez-Ruiz, I. and Ward, C.R. (2008b). Basic factors controlling coal quality and technological behavior of coal, In: Suárez-Ruiz, I., Crelling, J.C. (Eds.), Applied Coal Petrology: the role of petrology in coal utilization. Academic Press, New York, pp.19–59.

Sun, R., Liu, G., Zheng, L. and Chou, C.-L. (2010). Characteristics of coal quality and their relationship with coal-forming environment: A case study from the Zhuji exploration area, Huainan coalfield, Anhui, China. Energy, 35(1), pp.423–435.

Swaine, D.J. (1990). Trace elements in coal. London: Butterworths, p.278.

Swaine, D.J. (2000). Why trace elements are important. Fuel Processing Technology, 65–66, pp.21–33.

Swardt, A.M.J., Garrar, P. and Simpson, J.G. (1965). Major zones of transcurrent dislocation and superposition of orogenic belts in part of Central Africa. Geol. Soc. Am. Bull. Volume 76.

Swift, W. H., White, W. C, Wiles, J. W. and Worst, B. G., (1953). The geology of the Lower Sabi Coalfield. Sth. Rhod. geol. Surv., Bull. No. 40

Tankard, A.J., Jackson, M., Erikssen, K.A., Hobday, D.K., Hunter, D.R., Minter, W.E.L. (1982), Crustal Evolution of Southern Africa: 3.8 Billion Tears of Earth History. Springer-Verlag, Berlin, p 523.

Taverner-Smith, R. (1958). The development of the Mid-Zambezi Valley in Northern Rhodesia since early Karoo times. Geol Mag. Volume 45, 105-118.

Taylor, G.H. Teichmüller, M. Davis, A. Diessel, C.F.K. Littke, R. Robert, P. Organic Petrology, 1998. Gebrüder Borntraeger, Berlin-Stuttgart

Thomas, L. (1992). Handbook of practical geology. New York: Wiley.

Thomas, L. (2013). Age and Occurrence of Coal. In: Coal Geology. Chichester, West Sussex ; Hoboken, Nj: John Wiley & Sons.

Thompson, A.O. (1981). The geology of the Lubimbi, Dahlia and Hankano coalfields, Wankie and Lupane districts. Bulletin- Zimbabwe Geological Survey 88. 88 pp.

Thompson, A.O., Broderick, T.J., Palloks, H.-H. (1982). The Entuba coalfield. Zimbabwe Geological Survey, Records of Zimbabwe Coalfields VIII. 12 pp.

Tian,L., Dai, S Wang, J., Huang, Y., Ho, S.C., Zhou, Y., Lucas. D., Koshland, C.P. (2008). Nanoquartz in Late Permian C1 coal and high incidence of female lung cancer in the Pearl River Origin area: a retrospective cohort study. BMC Public Health 8, pp. 398.

Turner, B.R. (1986). Tectonic and climatic controls on continental depositional facies in the Karoo Basin of northern Natal, South Africa. Sediment. Geol. 46, pp.231 – 257.

Teichmüller, M. (1974). Generation of petroleum-like substances in coal seams as seen under the microscope. In: Tissot, B.; Beinner, F. ed. Advances in organic geochemistry 1973; Paris, Technip. Pp 321-343.

United Nations Development Programme (UNDP). 2004. World energy assessment: Overview 2004 update. New York, NY: UNDP, Bureau for Development Policy.

Van der Riet, M., Falcon, L and R.M.S. (2010). 'Coal qualities – from formation to consumption', Lecture notes distributed in the course, Coal Quality and Utilisation, University of Witwatersrand, Johannesburg on 15 February 2010.

Van Krevelen, D.W. (1981). "Coal Typology – Chemistry – Physics – Constitution"' Coal Science Technology 3, London, Elsevier p. 402.

Van Krevelen, D.W. (1981). Coal. New York: Elsevier.

Van Vuuren, C.J. (1981). Depositional models for the Vryheid Formation in the north-eastern part of the Karoo Basin - a Review. Ann. Geol. Surv. S. Afr., 15(1), pp.1–11.

Veevers, J.J., Cole, I.D., Cowan, E.J. (1994a). Karoo Basin and Cape Fold Belt. In: J.J. Veevers and C. McA. Powell (Eds.) Permian-Triassic Basins and Foldbelts along the Panthalassan Margin of Gondwanaland, Geological Society of America Memoir, 184, pp. 223–280.

Veevers, J.J., Conaghan, P.J., Powell, C. McA (1994b). Eastern Australia. In: Veevers, J.J., McA. Powell, C. (Eds.), Permian-Triassic Basins and Foldbelts along the Panthalassan Margin of Gondwanaland, Geological Society of America Memoir, 184, pp. 11–172.

Veevers, J.J., Powell, C. McA., Collinson, J.W., López-Gamundí, O.R. (1994c). Synthesis. In: Veevers, J.J., McA. Powell, C. (Eds.) Permian-Triassic Basins and Foldbelts Along the Panthalassan Margin of Gondwanaland, Geological Society of America Memoir, 184, pp. 331–354.

Visser, J.N. J., Dukas, B.A. (1979). Upward fining fluvial megacycles in the Beaufort Group north of Graaff Reinet, Cape Town Province. Trans. Geol. Soc. S. Afr. 82, pp. 149 – 154.

Visser, J.N.J. (1986). The palaeogeography and palaeoclimatology of the Karoo Basin in south-western Gondwana. Abstract of papers presented. 4th Biennial Conference held at the South African Museum, Cape Town (Sept. 2 – 25, 1986), p 11

Visser, J.N.J. (1991a). Geography and climatology of the late Carboniferous to Jurassic Karro Basin in south-west Gondwana. Anna. S. Afr. Museum, Volume 99, pp. 415 – 431.

Visser, J.N.J. (1991b). Geography and climatology of the Late Carboniferous to Jurassic Karoo Basin in south-western Gondwana: Annals of the South African Museum, 99, pp.415–431.

Visser, J.N.J. (1992). Basin tectonics in southwestern Gondwana during the Carboniferous and Permian. In: de Wit, M.J., Ransome, I.G.D. (Eds.), Inversion Tectonics of the Cape Fold Belt, Karoo and Cretaceous Basins of Southern Africa. Balkema, Rotterdam, pp. 109–115.

Visser, J.N.J., and Praekelt, H.E. (1996). Subduction, mega-shear systems and Late Paleozoic basin development of Gondwana. Geol. Rundsch. 85, 632–646.

Wagner, N. J., Malumbazo, N., & Falcon, R. M. (2018). Southern African Coals and Carbons: Definitions and Applications of Organic Petrology. Cape Town: Struik Nature.

Wagoner, C.L., and Winegartner, E.C. (1973). Further Development of the Burning Profile. Journ. Eng. Power, Volume 95 , pp. 119-123.

Wagner, N. J., Malumbazo, N. and Falcon, R. M. (2018). Southern African Coals and Carbons: Definitions and Applications of Organic Petrology. Cape Town: Struik Nature.

Wang, C., Liu, Y., Zhang, X. and Che, D. (2011). A Study on Coal Properties and Combustion Characteristics of Blended Coals in Northwestern China. Energy & Fuels, Volume 25, Issue 8, pp. 3634–3645.

Wankie Act (1950). Wankie Colliery Company, Hwange, Zimbabwe.

Ward, C.A. (2002). Analysis and Significance of Mineral Matter in Coal Seams. Int. J. Coal Geology, Volume 50, Issued 1- 4, May 2002, pp135-168.

Ward, C. R. (Ed.) (1984). Coal Geology and Coal Technology. Blackwell. Oxford, p 345.

Watson, R.L.A. (1960). The Geology and Coal Resources of the Country around Wankie, Southern Rhodesia. Southern Rhodesia Geological Survey Bulletin, Volume 48.

Ward, C.R. (2013). Coal Geology. In: S. Elias, ed., Reference Module in Earth Systems and Environmental Sciences. Encyclopedia of Physical Science and Technology, pp.45–77.

Ward, C.R. (2016). Analysis, origin and significance of mineral matter in coal: An updated review. International Journal of Coal Geology, 165, pp.1–27.

Wescott, W.A., Diggens, J.N. (1998). Depositional history and stratigraphic evolution of the Sakamena Group (Middle Karoo Supergroup) in the southern Morondava Basin, Madagascar. J. Afr. Earth Sci. 27 (3/4), 461–479.

Whateley, M.K.G. and Turner, B.R. (1983), Structural and sedimentological controls on coal deposition in the Nongoma graben, Northern Zululand, S.A. Int. Ass. Sedimentology. Spec. Pub., 6, pp. 457 -471.

Whateley, M.K.G. and Hopkins, D.A.S. (1985), A proposed classification of the Permo-Triassic coal basins of Southern Africa based upon tectonic setting and depositional environment. Johannesburg, p. 30.

Wheeler, A., & Götz, A. E. (2016). Palynofacies patterns of the Highveld coal deposits (Karoo Basin, South Africa): clues to reconstruction of palaeoenvironment and palaeoclimate. Acta Palaeobotanica, 56, 3–15.

Winter, M.F. (1985). Lower Permian palaeoenviroments of the northern Highveld Coalfield and their relationship to the characteristics of coal seams. (PhD thesis). University of the Witwatersrand, Johannesburg, p. 254.

Wójcik, W., Jan′czuk, B. & Bialopiotrowicz, T. (1990). The influence of an apolar collector on the contact angle, detachment force and work of adhesion to the coal surface in agglomeration flotation of a low rank coal. Fuel, Volume 69, p. 207–210.

Wopfner, H. (1991). Extent and timing of the late Palaeozoic glaciation in Africa. Geologisches Institut, Universität Köln, Sonderveröffentlichungen 82 (Brunnacker Festschrift), pp. 447–453.

Wopfner, H. (1993). Structural development of Tanzanian Karoo basins and the break-up of Gondwana. In: Findlay, A. et al. (Eds.), Gondwana Eight: Proceedings of the Eighth Gondwana Symposium Hobart. Balkema, pp. 531–539.

Wopfner, H. (1994). The Malagasy Rift, a chasm in the Tethyan margin of Gondwana. J. Southeast Asian Earth Sci. 9, pp. 451 – 461.

Wopfner, H. (2002). Tectonic and climatic events controlling deposition in Tanzanian Karoo basins. J. Afri. Earth Sci. 34, pp. 167 – 177

Xie, K.-C. (2015). Physical Characteristics of Coal. In K.-C. Xie, Structure and Reactivity of Coal Berlin: Springer, p. 29.

Zhao, Z., Qiu, J., Li, W., Chen, H. and Li, B. (2003). Influence of mineral matter in coal on decomposition of NO over coal chars and emission of NO during char combustion. Fuel, 82(8), pp. 949-957.

Zhu, Q., 2014. Coal sampling and analytical standards. IEA Clean Coal Centre, CCC/235 www.iea-coal.org (accessed 3 October 2016).

Zimmerman, R.E. (1979). Evaluating and testing the coking properties of coal. Miller Freeman Publications, Inc. San Francisco.

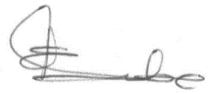
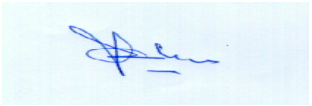
APPENDICES

Appendix 1.1 Sulphur Analysis by Wet Method

QUALITY ASSURANCE SERVICES

Title: SULPHUR ANALYSIS BY WET METHOD TEST METHOD N° : QATM 3.10	Page 1 of 4 Revision N°: 1 Issue Date: 15 June 2010

REVISION STATUS	
Revision No.: **Issue date:**	*1* 15 June 2010

PREPARATION & APPROVAL	
Reviewed by: **Name:** **Signature:** **Designation:**	*E. Dube*  **Quality Control Chemist**
Approved by: **Name:** **Signature:** **Designation**:	**C. Dube**  *Quality Assurance Superintendent*

Title: SULPHUR ANALYSIS BY WET METHOD TEST METHOD N° : QATM 3.10	Page 2 of 4 Revision N°: 1 Issue Date: 15 June 2010

1.0 SCOPE

This test method is for the determination of total sulphur in coal and coke samples.

2.0 PRINCIPLE

A known mass of sample is burnt in a stream of oxygen at a temperature of 1350 °C. The oxides of sulphur formed together with any chlorine present are absorbed in a neutral H_2O_2 solution and determined volumetrically. Aluminium Oxide is added to allow for a gradual oxidation of the sulphur as without the protective layer, the sample would immediately burn leading to retention of the sulphur in the ash.

Reaction is as follows:

$$SO_{2\,(g)} + H_2O_{2\,(aq)} \longrightarrow H_2SO_{4\,(aq)}$$

3.0 RESPONSIBILITY

The Quality Control Chemist is responsible for ensuring implementation and maintenance of this test method the Lab Tech for carrying out the analysis. Approved technical signatories are responsible for approval of records generated because of test method.

4.0 DESCRIPTION OF ITEMS

4.1 REAGENTS AND MATERIALS

a. 1 - 2% H_2O_2 AR grade
b. 0.05M H_2SO_4 AR grade
c. 0.05M Na_2CO_3 AR grade
d. 0.05M NaOH AR grade
e. Indicators - purple or methyl red, screened methyl orange and phenolphthalein.
f. Al_2O_3 (Aluminum Oxide AR grade with sulphate less than 0.0005%). Used Al_2O_3 can always be recycled by sieving through a 250 µm sieve and heating in a furnace at 815ºC for at least 4 hours)
g. 250 µm sieve
h. Coal standard(s)
i. Certified Reference Material

4.2 EQUIPMENT AND APPARATUS

a. Oxygen cylinder

b. Oxygen baffle

c. Carbolite Furnace

d. Combustion tube and boats.

e. Analytical balance

f. Boat puller

g. Purification train

h. Magnetic stirrer

i. Volumetric flasks (A grade)

j. Pipettes (A grade)

k. Burettes (A grade)

l. Dreschel bottles - absorption vessels (A grade)

m. 100ml Measuring cylinder (A grade)

4.3 SAMPLE(S)

Pulverized coal and coke samples passing through a sieve of 200 μm are used. Samples should be kept in airtight containers to prevent contamination.

5.0 DESCRIPTION OF THE PROCEDURE

a. Raise the temperature of the furnace to 1350°C and pass purified oxygen through combustion tube.
b. Perform a blank daily before analysing samples as a way of purging the system.
c. Accurately weigh a standard sample of coal and coke that is 0.5000 ± 0.0001g in a combustion boat.
d. Spread it evenly over the surface and cover with aluminium oxide.
e. Measure 100 ml of neutralised H_2O_2 into the absorption vessel and assemble the apparatus.
f. Insert the boat and place it just further the entrance then insert the oxygen baffle.
g. Push the sample boat further after one minute to a point where the outer end of the boat is just inside the outer furnace wall and then reinsert the oxygen baffle.
h. Allow the sample to burn for 3 minutes.
i. After this period push the sample boat into the central or hot zone with the end of the boat puller and leave it at this location for a further 3 minutes.
j. At the end of this time, all the sulphur in the coal or coke should have been oxidised to SO_2/SO_3. Both of these will dissolve in H_2O_2 forming H_2SO_4.
k. Wash down any oxides of sulphur that may have absorbed on the inner part of the absorption vessel into the titration flask.
l. Titrate the solution is then with standardized 0.05M NaOH.
m. Record the titres in the Calculations book.
n. Determine the percentage sulphur in the test sample.

6.0 QUALITY CONTROL AND ACCEPTANCE CRITERIA

Always standardize NaOH (0.05M) with 0.05M H_2SO_4 before analysis.

Wet sulphur analysis is done against recommended standard samples (certified reference materials and round robin samples). The results of the standard samples must be within ± 0.8% for every batch of 10 samples.

7.0 CALCULATIONS AND EXPRESSION OF RESULTS

% Sulphur = Sulphur factor × volume of NaOH.

Sulphur factor = 3.2066 x Molarity of NaOH obtained after standardization.

Uncertainty of measurement is ± 0.1%

8.0 SAFETY PRECAUTIONS

a. Sulphuric acid is corrosive.

b. Hydrogen peroxide

i. Causes burns and should be kept away from explosive material.

ii. Keep in a cool place at temperatures less than 20 ºC, if possible in a refrigerator

iii. After contact with skin wash immediately with plenty of water and seek medical help

c. Oxygen cylinders

i. They should be located outside the building and gas tapped from outside. In general a face shield should always be worn as the potential of explosion exists.

ii. Acid proof Laboratory coats, protective gloves and safety shoes should be worn at all times. For more information, refer to the MSDS file.

9 APPENDICES AND ATTACHMENTS

a Appendix 1: Calculation of Sulphur Factor

10. RECORDS

a. Wet Sulphur Analysis Logbook.

b. Reagents Logbook

11. REFERENCE

BS 1016-106.4.2:1996

CALCULATION OF SULPHUR FACTOR

Determination of No. of moles

Sulphur is oxidized to SO_2 which reacts with H_2O_2 to form H_2SO_4

$$SO_{2\,(g)} + H_2O_{2\,(aq)} \longrightarrow H_2SO_{4\,(aq)}$$

Reaction ratio is 1:1

Therefore, no. of moles of SO_2 = No. of moles of H_2SO_4 formed.

From standardization of NaOH with standardized H_2SO_4

$$H_2SO_{4\,(aq)} + 2NaOH_{\,(aq)} \longrightarrow Na_2SO_{4\,(aq)} + 2H_2O_{\,(l)}$$

Reaction Ratio is 1:2

No. of moles of H_2SO_4 = 2 x No. of moles of NaOH

No. of moles of H_2SO_4 after standardization with Na_2CO_3 = 0.00075mols

Therefore, number of moles of NaOH = Molarity of NaOH x $\frac{\text{Volume of NaOH}}{1000}$

Let number of moles be *y*

Number of moles of H_2SO_4 = 0.5 x No. of moles of NaOH

= 0.5 x *y*

No. of moles of Sulphur = No. of moles of H_2SO_4 = 0.5 x *y*

Mass of Sulphur = Atomic mass of Sulphur x Number of Moles

= 32.066 x 0.5 x *y*

= 16.033*y*

$$\% \text{ Sulphur} = \frac{\text{Amount of Sulphur in test sample}}{\text{Initial amount of test sample}}$$

$$\% \text{ Sulphur} = \frac{16.033y}{0.5} \times 100$$

= 32.066*y* x 100%

$$= 32.066 \times \text{Molarity of NaOH} \times \frac{\text{Volume of NaOH}}{1000} \times 100\%$$

% Sulphur = 3.2066 x Molarity of NaOH x Volume of NaOH

Sulphur factor = 3.2066 x Molarity of NaOH obtained after standardization.

Therefore, **%** Sulphur = Sulphur factor × Volume of NaOH.

APPENDIX 1.2: PHOSPHORUS ANALYSIS

QUALITY ASSURANCE SERVICES

Title: PHOSPHORUS ANALYSIS BY WET METHOD TEST METHOD N° : QATM 3.09	Page 1 of 5 Revision N°: 1 Issue Date: 15 June 2010

REVISION STATUS	
Revision No.: **Issue date:**	*1* 15 June 2010

PREPARATION & APPROVAL	
Reviewed by: **Name:** **Signature:** **Designation:**	E. Dube **Quality Control Chemist**
Approved by: **Name:** **Signature:** **Designation**:	C. Dube *Quality Assurance Superintendent*

Title: PHOSPHORUS ANALYSIS BY WET METHOD TEST METHOD N° : QATM 3.09	Page 2 of 5 Revision N°: 1 Issue Date: 15 June 2010

1.0 SCOPE

This test method is for the determination of phosphorus in coal and coke.

2.0 PRINCIPLE

The principle used in the determination of phosphorus in coal / coke involves the removal of carbonaceous matter by ashing in a furnace and then extraction of the phosphorus from the ash by using a mixture of Hydrofluoric acidand Sulphuric acid. Silica is eliminated as silicon tetrafluoride. The ammonium molybdate reagent is then added to complex the phosphorus producing the phosphomolybdic complex. The complex in solution is then selectively reduced with ascorbic acid to give molybdenum blue colouration.

The optical density of the blue solution is then measured by the absorptiometer and is proportional to the amount of the phosphorus present. The measured optical density is proportional to the amount of phosphorus present. The actual value of phosphorus present is obtained from a previously calibrated chart.

Detection limits for the method are 0.005%.

3.0 RESPONSIBILITY

The Quality Control Chemist is responsible for ensuring implementation and maintenance of this test method. The laboratory technician based at Central laboratory is responsible for carrying out this test method. Approved technical signatories are responsible for approval of records generated as a result of this test method.

4.0 DESCRIPTION OF ITEMS

4.1 REAGENTS AND MATERIALS

a. Reagent mixture (25ml of 6% Ammonium Molybdate solution, 10ml of 5% Ascorbic acid and 5ml of Antimony Potassium Tartrate, all AR grade)

b. 5M Sulphuric acid, 5M Hydrofluoric acid (HF), working phosphorus standard

c. Coal Standards

d. Certified Coal Reference Material

e. Potassium Dihydrogen Orthophosphate**,** KH_2PO_4, AR grade

4.2 EQUIPMENT AND APPARATUS

a. Hot plate

b. Fume Cupboard

c. Analytical balance 0.1mg accuracy.

d. Shimadzu – UV-Vis Spectrophotometer

e. 50ml Teflon beakers

f. 5ml and 10ml pipettes, 100ml and 50ml volumetric flasks (A grade glassware)

g. Agate mortar and pestle

h. Crucible Tongs

4.3 SAMPLE(S)

The samples used in this test method are obtained from ash determination method. A Certified Reference material, or any accepted standard should also be subjected to the same conditions as the samples to be used in this test.

5.0 DESCRIPTION OF THE PROCEDURE

5.1 Preparation of solution A

a. Grind the ash in an agate mortar with a pestleto pass 63 micron sieve.

b. Accurately weigh 0.0500 ± 0.001g of the ground ash as well as the standard ash, into separate 50ml Teflon beakers. Carry out a blank by omitting the sample.

c. Add 2ml of 5M sulphuric acid and 2ml of HF.

d. Digest the ash for thirty (30) Minutes on a hot plate at heater setting between 300 - 400^{o}C, in a fume cupboard, until all the HF has been removed and to white fumes of sulphuric acid.

e. Add 0.5ml of 5M sulphuric acid and evaporate to white fumes for 2 minutes and then remove and cool in the fume cupboard.

f. Add 20ml of distilled water and digest again for 30 minutes and then remove, cool and filter the contents of the Teflon beakersinto 100ml volumetric flasks.

g. Dilute to the mark with distilled water.

5.2 Preparation of colour solution B

a. Pipette out 10ml of each of the solution A`s so produced including the blank and the ash standard as well as the salt working phosphorus standard into separate 50ml volumetric flasks.

b. Add 5ml of the freshly prepared reagent mixture, swirling the contents during addition and then dilute to the mark with distilled water and stand for 20 minutes.

c. After the 20 minutes have elapsed, read the Absorbance (Abs) of the colour solution B against water using the UV-Vis Spectrophotometer set at calibration wavelength around 888nm. Use the 10mm cell for all readings.

5.3. Coal Calibration Standards

If using coal calibration standards, choose a suitable standard, the one with phosphorus content close to 0.100%. Prepare the sample as in 5.1 above. Proceed as in 5.2 above varying the standard concentrations by pipetting into 50ml volumetric flasks varying volumes of the solution e.g. 0, 1, 2, 3, 4, 5, 7, 8, 9 & 10ml to make 10 samples. Determine k from the calibration graph and use it to determine concentrations of the unknown.

5.4. Potassium Dihydrogen Orthophosphate, KH_2PO_4 Calibration Standards

If using Potassium Dihydrogen Orthophosphate calibration standards; in a molecular formula of the standard, for 1 mole of KH_2PO_4 there is also 1 mole of Phosphorus (P). In preparing the standard 0.1098g is weighed and so the number of moles (n) of P in 0.1098g is

$$n = m / Mr\ (KH_2PO_4)$$

$$= \frac{0.1098}{136.09} = 0.000806819 \text{ moles}$$

Therefore the mass of P in 0.1098g is

$$m = n * Mr\ (P)$$

$$= 0.000806819 * 30.974 = 0.02499g$$

Since 0.1098 is dissolved in 250ml of distilled water then the mass of phosphorus in mg per ml is

$$= \frac{0.02499}{250ml} * 1000$$

$$= 0.0999 = 0.1mg/ml$$

To get the standards concentrations e.g. we dilute 5ml of the above solution in 500ml and then the mass of P becomes:

$$m = \frac{0.1 * 5}{500} = 0.001mg / ml$$

Obtain the constant k from the calibration graph using the Abs and the corresponding concentration of P in % from equation y = mx + c where k = m.

Calculation %P = $\frac{Abs}{k}$

6.0 QUALITY CONTROL AND ACCEPTANCE CRITERIA

Standards or certified reference materials should be analysed together with the test samples, and these should give expected results within acceptable limits. If not, results should be discarded and the test re-done.

7.0 CALCULATION AND EXPRESSION OF RESULTS

$$\%Phosphorus = \frac{Abs \times Ash\ of\ sample}{K \times Ash\ of\ Standard}$$

Uncertainty of measurement is ± 0.026%.

8.0 SAFETY PRECAUTION

a. Hydrofluoric acid is toxic. Avoid inhalation or ingestion, it is readily absorbed through the skin and skin contact may be fatal. It also acts as a systemic poison, causes severe burns. Reaction may be delayed. Any contact with this material, even minor, requires immediate washing on running tap water.

b. A well-ventilated fume hood should be used at all times as well as respirators.

c. PVC chemical resistant gloves should be used, and **NEVER** pipette acid by mouth.

d. Water should never be added to acid but acid to water – **AAA (Always Add Acid).**

e. Sulphuric acid should be treated with the same respect and containers should be kept tightly closed.

f. Nylon or polyester clothing should be avoided all the time.

9.0 APPENDICES AND ATTACHMENTS

Nil

10.0 RECORDS

a. Reagents Preparation Book

b. Wet analysis Results Book

c. Calibration Curves

11.0 REFERENCE

BS 1016: Part 9:1977

Appendix 1.3: Leco Carbon and Sulphur Analyser Test

a) A crucible was thoroughly cleaned a placed into a weigher.

b) The weigher scale was zeroed.

c) A 0.250gm coal sample was placed into the crucible and the apparatus was subsequently taken to the Analyser.

d) The sampled was logged onto the PC (e.g. 3MS 0 -15cm);

e) The PC was instructed (by pressing F5 and "Enter") to analyse.

f) The sample was slid into the Analyser as far into the instrument as possible (until one could not push anymore), followed by the withdrawing of the pushing rod and closing of the chamber;

g) The sulphur and carbon values were displayed on and read from the PC screen; and

h) After every three analyses, the Analyser was checked against a "Standard" by going through the above process, after taking precaution that the standard was strictly 0.250gm and that the standard was logged as "Standard Test" instead of "Hwange coal".

On a couple of occasions, the Standard Test indicated "sulphur outside the limit" and this was rectified by going through the following steps:

- Clicking on the Sulphur and Carbon result;
- Followed by going to "configuration";
- Then to "drift"; and
- Clicking "ok".

NB. After each sample make sure you wash and dry bomb before the next sample.

Appendix 1.4: Calorific Value Determination by Bomb Calorimeter

Sample Specification: The test required a particle size of 250 micrometers.

Special Requirement: Calibration was required prior to instrument use to ensure integrity of instrumentation. A reference standard (Benzoic Acid) in the form of a tablet weighing +- 0.4g was used to calibrate the equipment.

Procedure:

a. One tablet was placed into a crucible and weighed.

b. The mass was immediately logged into the instrument and the sample name was logged as CAL.

c. An "O" ring was placed around the Bomp cap and thoroughly sealed with a DC4 electrical insulating compound to ensure no air entered in or out of the Bomb Calorimeter once closed.

d. A cotton string was hooked onto the ignition wire and subsequently placed into the sample.

N.B. It is critical for a connection to exist between the sample and the ignition wire; as the sample will not ignite if the connection is not achieved.

e. The bomb cap was then slowly and carefully placed inside the Bomb and locked in clockwise direction.

f. Oxygen was run up to 3.5 bars into the Bomb Calorimeter.

g. The latch (of the instrument) was pushed in to completely seal the Bomb Calorimeter.

h. The bomb was then slowly placed inside the calorimeter, and the experiment began immediately after the lid was closed.

The Calorific Value reading was displayed on and read from the screen once the run was completed and recorded as MJ/kg.

Appendix 1.5: Preparation of Polished Blocks for Petrographic Analyses





Sample Analysis Report

Prepared For: Mr. Oliver Maponga	**Date**: 23 March 2015
ojmaponga@hwangecolliery.co.zw	**Investigation**: Vitrinite Random Reflectance Analysis (RoV)
Petrographer: Patience Mavhengere	
patience.mavhengere@wits.ac.za	
ICCP ACCREDITATION: ICCP/SCAP-228/A (Exp 12/2016)	

1. Introduction

Twenty six coal samples from Zimbabwe were received for vitrinite random reflectance analysis. This analysis was carried order to determine the each coal's rank. This report outlines the methodology adopted in executing the analysis and the results obtained.

2. Methodology

The sample was prepared into petrographic blocks as follows.

- Petrography sample cups were cleaned and lined with lubricant.
- The samples were poured halfway into each sample cup.
- Epoxy resin and hardener were mixed uniformly in the ratio 7: 1 respectively and added to the coal to form a thick paste.
- The sample was labelled remaining resin mixture poured over the label.
- Twelve hours of drying was then allowed for the sample to harden into a petrography block. At this point the sample was then removed from the sample cups and polished using a Struers Tegraforce Polisher for the reflectance analyses.

A Leica DM 4500P reflected light microscope with J and M spectrolytic system was used for the analysis. The reflectance analysis was carried out according to the ISO 7404 standard part 3. 100 readings were taken on the collotelinite maceral for each sample. The same blocks will be used for maceral content analysis.

Clean Coal Technology Research
School of Chemical and Metallurgical Engineering · University of Witwatersrand · 1 Jan Smuts Ave Braamfontein 2000 Johannesburg · South Africa
Tel:0027117177540

Appendix 1.6 XRF Analysis of Hwange Coal Ash

Bureau Veritas Testing and Inspections South Africa
Sunderland Ridge
Reg N° 2002/003217/07

University of Witwatersrand.
For Attention: Zama Mthabela
Tel: (011) 717 7511
Cell: 071 609 0803
Email: zama.mthabela@wits.ac.za

Ref No:	**1718-283**
Date Received:	17/03/2017
Contact Person:	Willem Swanepc
Report Status:	Final
Report Date:	31/03/2017

308 Barolong Street
Icon Industrial Park
Sunderland Ridge X10
PO Box 11498
Wierda Park South 0057
Tel: +27(0)12 940 0911
Fax: +27(0)86 631 4743

TEST REPORT / CERTIFICATE OF ANALYSIS

Sample Identification	Al2O3 %	CaO %	Cr2O %	Fe2O %	K2O %	MgO %	MnO %	Na2O %	P2O %	SiO2 %	TiO2 %	V2O %	ZrO2 %	BaO %	SrO %	ZnO %	SO3 %
3ME 0-30cm	25.63	17.39	0.04	3.31	0.91	0.36	0.16	nd	0.07	42.15	1.07	0.03	0.04	0.01	0.03	0.02	8.11
3ME 30-60cm	25.23	7.10	0.04	10.15	1.17	0.37	0.09	0.11	0.09	47.96	1.47	0.02	0.07	0.02	0.03	nd	6.32
3ME 60-90cm	22.52	13.88	0.03	4.00	0.82	0.29	0.22	0.21	0.06	47.12	1.45	0.01	0.06	0.02	0.03	0.03	9.81
3ME 90-120cm	19.40	27.68	0.03	0.62	0.39	0.24	0.44	0.28	0.04	38.22	0.95	nd	0.04	0.01	0.03	0.01	12.20
3ME 120-150cm	29.46	6.79	0.03	2.51	0.52	0.25	0.11	0.59	0.07	53.81	1.12	0.02	0.06	0.02	0.03	0.02	4.45
3ME 150-180cm	20.24	23.73	0.02	1.59	0.28	0.27	0.38	0.39	0.09	39.43	0.89	0.02	0.05	0.02	0.03	nd	12.72
3ME 180-210cm	28.55	3.91	0.02	3.89	0.35	0.24	0.08	0.42	0.09	57.82	1.33	0.02	0.06	nd	0.02	0.01	3.51
3ME 210-240cm	17.45	17.03	0.02	14.39	0.25	0.24	0.24	0.15	0.06	37.37	1.00	nd	0.04	0.01	0.02	nd	12.67
3ME 240-270cm	26.30	3.76	0.03	7.96	0.30	0.22	0.09	0.33	0.06	56.87	1.45	0.02	0.06	0.02	0.02	0.04	3.12
3ME 270-300cm	21.56	9.34	0.03	11.28	0.26	0.25	0.24	0.35	0.07	48.17	1.24	0.01	0.05	0.02	0.03	0.01	7.63
3ME 300-330cm	26.70	1.34	0.03	9.04	0.32	0.21	0.03	0.41	0.14	59.63	1.47	0.02	0.07	0.03	0.04	0.01	0.75
3ME 330-360cm	22.83	1.59	0.03	17.58	0.29	0.18	0.02	0.30	0.25	54.52	1.33	0.01	0.07	0.02	0.03	0.01	1.07
3MS 0-30cm	18.80	28.04	0.06	7.50	0.52	0.36	0.28	nd	0.04	27.73	0.70	0.01	0.03	nd	0.03	0.03	16.67
3MS 30-60cm	20.96	17.75	0.03	4.84	0.83	1.37	0.22	0.59	0.10	37.78	1.03	0.02	0.05	0.01	0.03	0.03	14.89
3MS 60-90cm	22.00	12.21	0.02	7.61	1.12	0.79	0.19	0.60	0.07	43.74	1.38	0.02	0.06	0.02	0.03	0.04	11.03
3MS 90-120cm	32.40	2.34	0.03	3.09	0.59	0.36	0.03	0.40	0.05	57.74	1.37	0.02	0.06	0.03	0.03	0.06	2.02
3MS 120-150cm	31.17	2.45	0.03	6.56	0.50	0.35	0.04	0.40	0.06	54.62	1.30	0.02	0.06	0.01	0.03	0.03	1.99
3MS 150-180cm	27.03	9.14	0.04	4.56	0.53	0.79	0.13	0.58	0.08	48.31	1.24	0.01	0.07	0.03	0.03	0.01	7.68
3MS 180-210cm	27.88	9.84	0.06	1.61	0.42	0.59	0.14	0.50	0.10	48.48	1.16	0.03	0.06	0.01	0.04	0.01	9.11
3MS 210-240cm	16.96	4.39	0.05	39.56	0.25	0.25	0.05	0.26	0.04	32.97	0.93	nd	0.03	0.01	0.02	nd	4.38
3MS 240-270cm	13.54	3.49	0.03	51.91	0.23	0.25	0.08	0.24	0.04	25.76	0.71	nd	0.02	nd	0.02	nd	3.58
3MS 270-300cm	26.91	4.72	0.04	10.99	0.31	0.35	0.05	0.63	0.16	49.39	1.50	0.02	0.06	0.02	0.05	0.01	4.57
3MS 300-330cm	28.76	4.26	0.04	5.91	0.31	0.37	0.05	0.56	0.19	54.95	1.61	nd	0.07	0.02	0.04	0.01	3.24
CHABA 0-1m	36.74	0.42	0.01	0.75	5.29	1.08	0.03	nd	0.36	52.54	1.46	0.01	0.10	0.05	0.04	0.03	0.33
CHABA 1-2m	30.14	0.89	0.09	18.02	4.74	0.58	0.05	0.05	1.11	41.64	1.33	0.02	0.06	0.07	0.06	0.04	0.38
CHABA 2-3m	38.56	0.31	0.05	0.85	4.23	0.80	0.02	0.11	0.30	50.99	2.84	0.03	0.12	0.05	0.04	0.03	0.30
CHABA 3-4m	39.70	0.26	0.02	0.58	3.81	0.66	nd	0.08	0.30	51.51	1.90	0.02	0.09	0.04	0.05	0.02	0.21
CHABA 4-5m	39.72	0.39	0.03	2.42	3.26	0.40	nd	0.07	0.43	49.97	2.19	0.01	0.10	0.07	0.04	0.03	0.27
CHABA 5-6m	38.77	1.65	0.02	3.92	2.56	0.35	0.03	0.07	1.37	48.58	2.02	0.02	0.09	0.12	0.05	0.04	0.41
CHABA 6-7m	34.25	1.19	0.03	12.99	2.54	0.41	0.04	0.09	0.78	45.07	2.19	0.02	0.09	0.04	0.04	0.02	0.34
CHABA 7-8m	29.14	3.28	0.04	9.72	2.28	0.60	0.06	0.10	2.54	49.13	1.78	0.02	0.08	0.10	0.05	0.09	0.35
CHABA 0-3m	28.31	0.60	0.02	31.50	1.92	0.30	0.02	0.01	0.15	34.82	1.44	0.01	0.08	0.03	0.03	0.05	0.50
CHABA 3-6m	36.36	0.32	0.01	15.07	2.68	0.28	0.02	0.02	0.12	44.01	1.32	nd	0.06	0.04	0.03	0.05	0.25
CHABA 6-9m	39.97	0.69	0.03	2.42	2.97	0.30	nd	0.07	0.28	50.34	1.84	nd	0.09	0.04	0.05	0.03	0.38

Description	**Procedure / Test Method**
Sample preparation	ACT-TPM-001 based on ISO 13909-4: 2001
Ash composition	ASTM D4326 XRF – By fusion bead (Subcontracted Test)

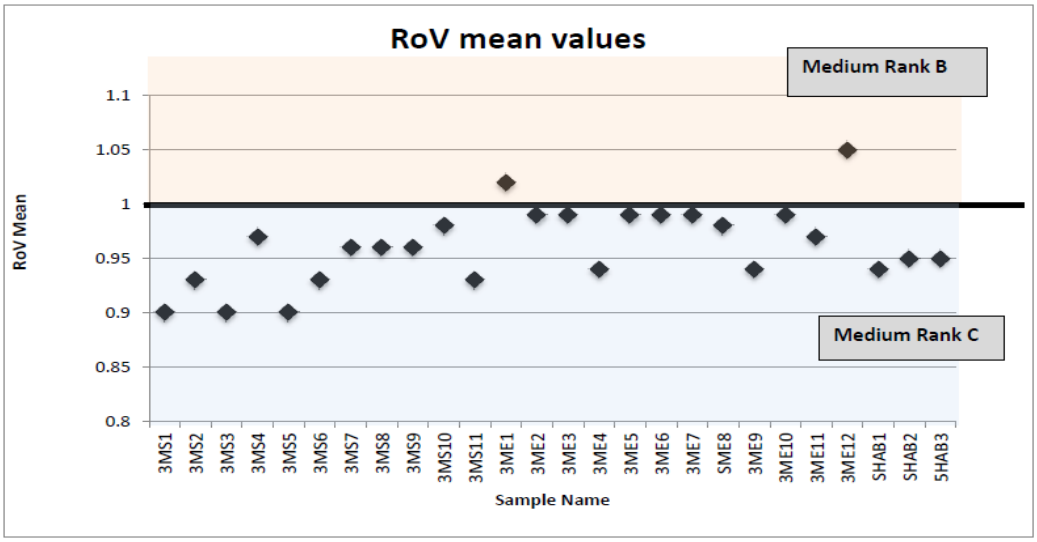
Results marked "Not SANAS Accredited" in this report are not included in the SANAS Schedule of Accreditation for this laboratory.
Results marked "Subcontracted Test" in this report are not included in the SANAS Schedule of Accreditation for this laboratory.

Results reported are only representative of the sample received for testing. Sample preparation will deviate from ISO13909-4: 2001(E) Table 1 (Minimum Mass of Samples After Division) where insufficient material was supplied or generated due to the nature of the requirements. While every endeavour has been made to ensure that the results reported are accurate, Bureau Veritas Testing and Inspections South Africa shall not be liable for any error nor for any damage or loss what so ever that may arise

sanas T0469

C.W. Swanepoel
Technical Signatory

Appendix 1.7: RoV Mean Values



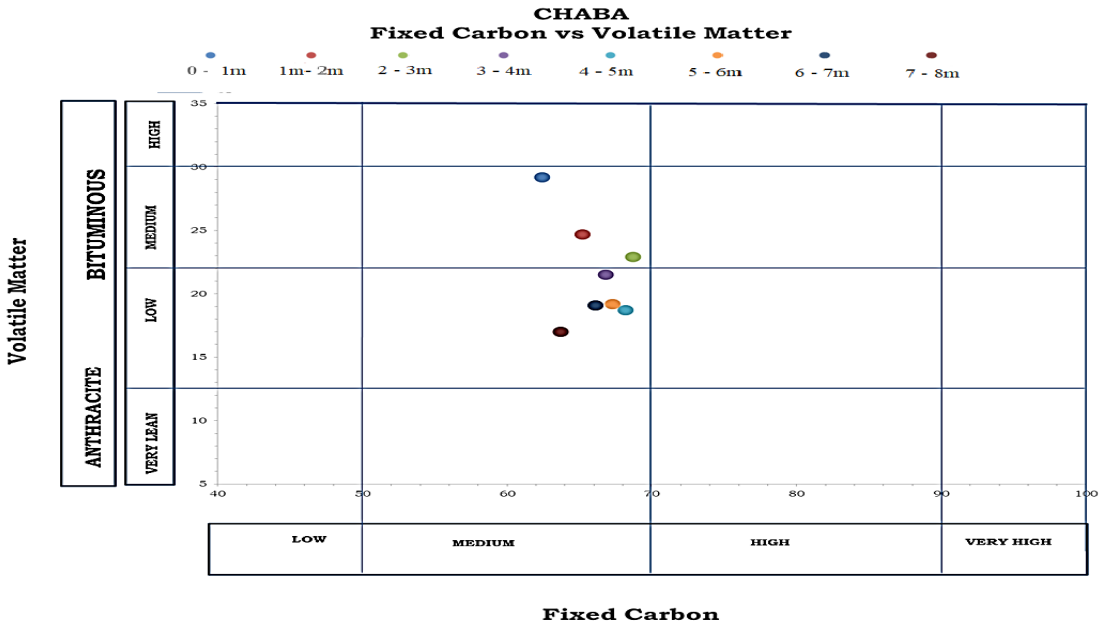
The standard deviation values for these samples range from 0.050-0.075. These charts present the count distribution of each of the samples. Majority of the samples present a fairly normal distribution whereas 6 of the samples (SMA10, SME4, SME5, SME11, and SME10 AND SHAB2) present a form of somewhat bimodal distribution.

Appendix 1.8: Microlithotype Analysis Hwange Coals

CLIENT:		OLIVER MAPONGA			
PROJECT:		PHD: ZIMBABWE WANKIE COALS - CHABA			
DATE:		9-Jun-15			
JOB / SAMPLE NUMBERS:					
ANALYST:		Prof NJ Wagner			
ICCP ACCREDITATION:		ICCP/SCAP-056/AB ; ICCP/CBAP/056			
Table 2: MICROLITHOTYPE ANALYSIS (% BY VOLUME)					
THESE RESULTS RELATE ONLY TO THE SAMPLES ANALYSED					
Sample no:		1565	1566	1567	
Sample identification:		**chaba 1 0-3m**	**chaba 2 3-6m**	**chaba 3 6-9m**	
MICROLITHOTYPE GROUP	MICROLITHOTYPE (vol%)	vol%	vol%	vol%	
MONOMACERAL	vitrite	38.3	10.6	3.2	
	semifusite	14.8	38.3	47.0	
	fusite / secretinite	4.8	7.9	12.0	
	inertodetrite	0.7	3.7	10.5	
	liptite	0.0	0.2	0.5	
BIMACERAL	vit+sf/f	11.6	18.7	7.0	
	vit+int	16.2	3.4	6.3	
	sf+int	1.5	7.4	6.0	
	vit+lipt	0.0	0.0	0.0	
	int+lipt	0.0	2.0	2.5	
TRIMCERAL	trimaceral	6.8	3.9	3.0	
CARBOMINERITE	cbm arg/clay	0.0	0.2	0.2	
	cbm pyrite	2.2	1.7	0.5	
	cbm ank/carb	0.0	0.0	0.8	
	cbm sil/qz	0.0	0.0	0.0	
	cbm poly	0	0.0	0.0	
ROCK	rock	3.1	2.0	0.5	

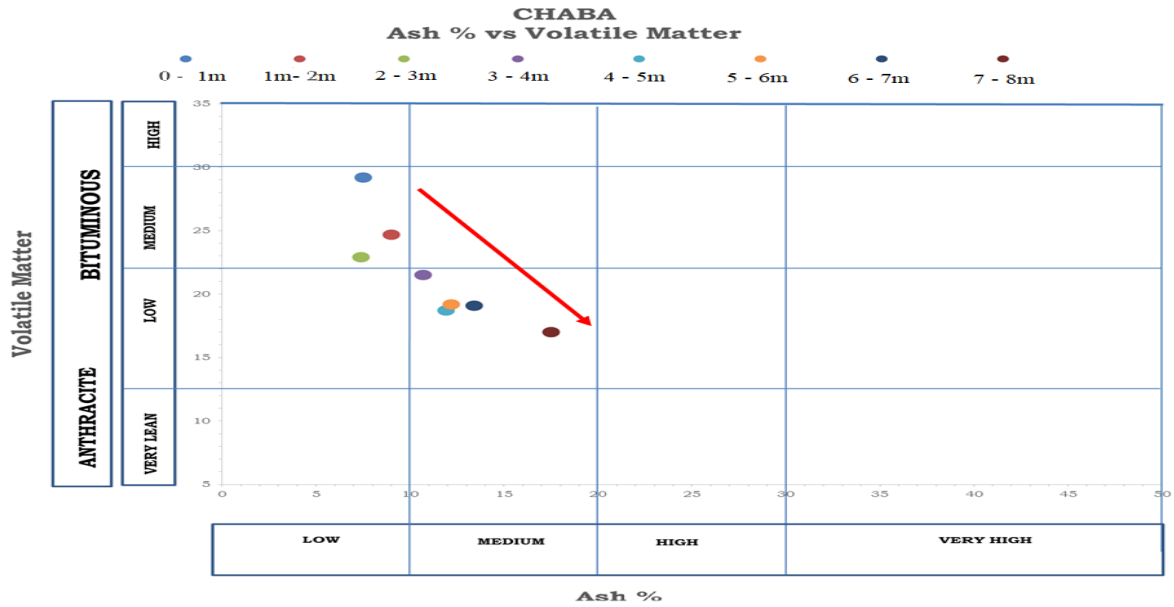
Table 2: MICROLITHOTYPE ANALYSIS (% BY VOLUME)									
THESE RESULTS RELATE ONLY TO THE SAMPLES ANALYSED									
Sample no:		**0-1**	**1-2**	**2-3**	**3-4**	**4-5**	**5-6**	**6-7**	**7-8**
Sample identification:									
GROUP	MICROLITHOTYPE (vol%)								
MONOMACERAL	vitrite	0.6	1.0	11.0	9.0	7.3	6.8	17.4	0.0
	semifusite	26.0	26.1	25.5	22.0	28.3	25.8	26.2	25.1
	fusite / secretinite	4.8	9.1	10.2	16.6	4.7	5.0	10.5	1.6
	inertodetrite	40.3	24.7	9.0	21.2	39.6	25.8	1.2	36.8
	liptite	0.2	0.4	0.4	0.0	0.0	0.0	0.0	0.0
BIMACERAL	vit+sf/f	1.1	1.4	6.1	7.0	2.6	2.2	11.6	0.8
	vit+int	4.8	6.0	9.6	9.2	3.5	7.1	12.8	4.0
	sf+int	16.2	17.9	17.2	10.3	5.3	15.7	3.8	20.1
	vit+lipt	0.0	0.2	0.2	0.0	0.4	0.0	1.6	0.0
	int+lipt	2.9	2.3	7.3	2.9	1.6	1.8	1.8	1.6
TRIMCERAL	duroclarite	0.2	0.8	2.5	0.8	1.8	0.0	7.7	0.2
	clarodurite	0.2	0.2	0.4	0.4	0.0	0.2	0.8	0.2
	vitrinertoliptite	0.0	0.0	0.0	0.0	0.0	0.0	0.0	0.2
CARBOMINERITE	cbm arg/clay	0.0	0.6	0.0	0.0	0.2	0.0	0.0	0.0
	cbm sil/qz	1.7	6.6	0.0	0.0	3.1	5.6	0.0	8.6
	cbm pyrite	0.4	1.7	0.6	0.0	0.6	2.2	1.6	0.6
	cbm ank/carb	0.2	0.2	0.0	0.6	0.0	1.0	0.0	0.0
	cbm poly	0.0	0.0	0.0	0.0	0.0	0.0	0.0	0.0
ROCK	rock 60%	0.4	0.8	0.0	0.0	1.0	0.8	3.0	0.2

Appendix 2.1 (A to I): Scatter Diagrams for Selected Coal Properties



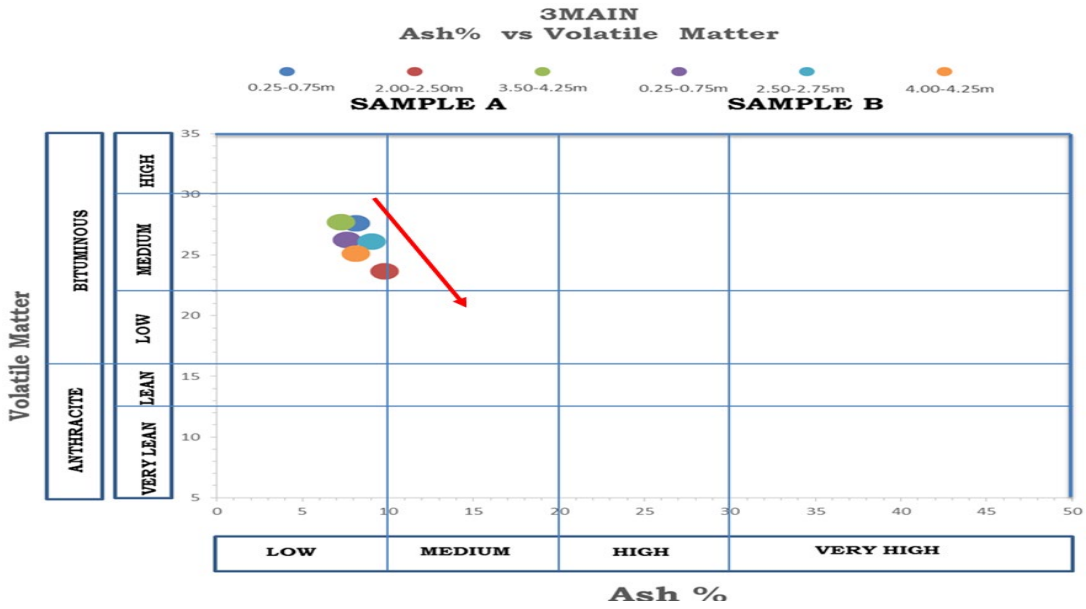
A: Fixed Carbon vs. Volatile Matter for Chaba Channel 2 samples

A illustrates that a relatively consistent fixed carbon content has little to do with varying volatile matter content. The change in volatile matter content will be associated more affectively by varying ash content (in B).



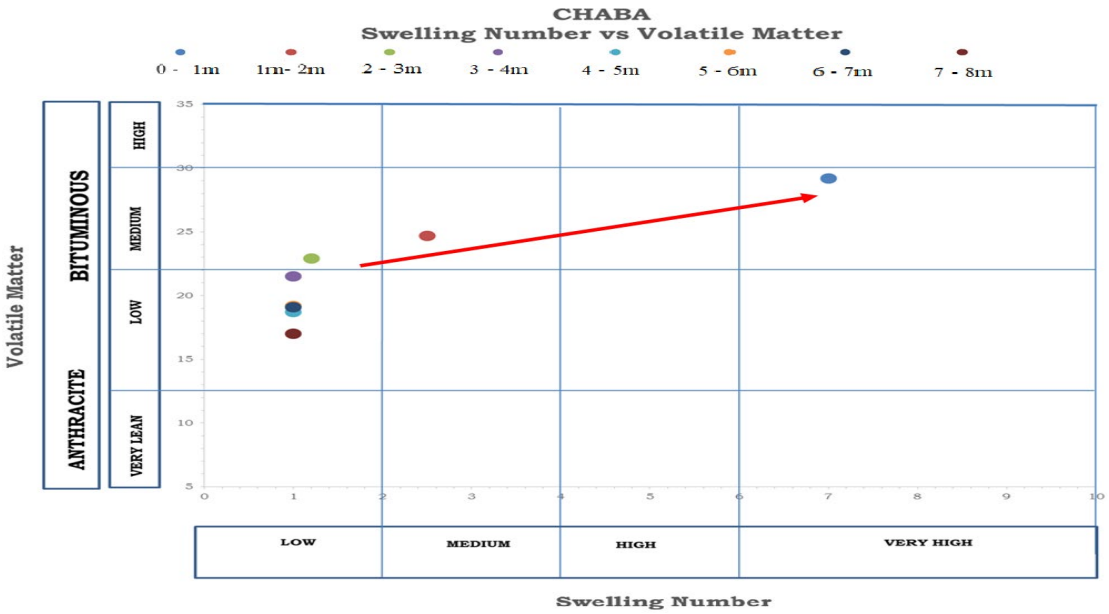
B: Ash % vs. Volatile Matter content for Chaba Channel 2 samples

B: shows a gradual increase in ash content with reducing volatile matter content.



C: Ash % vs. Volatile Matter for 3 Main sites A and B samples.

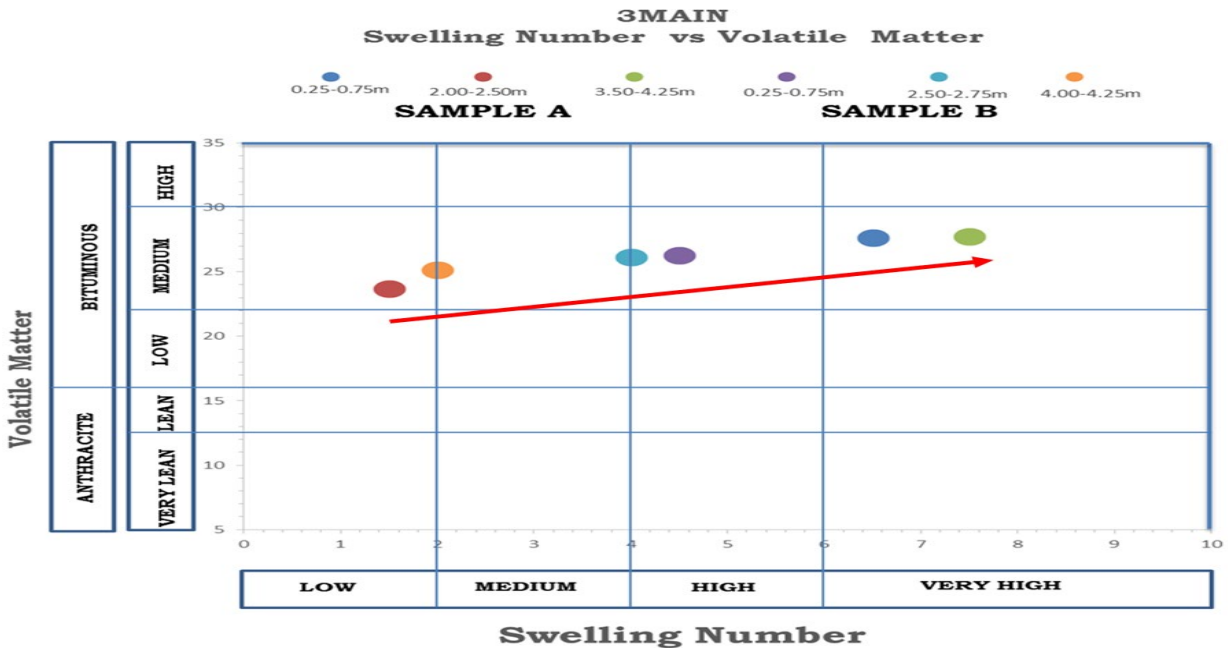
The trend in C is similar to that for Chaba Channel 2 samples shown in B.



D: Free swelling Number vs. Volatile Matter for Chaba Channel 2 Samples

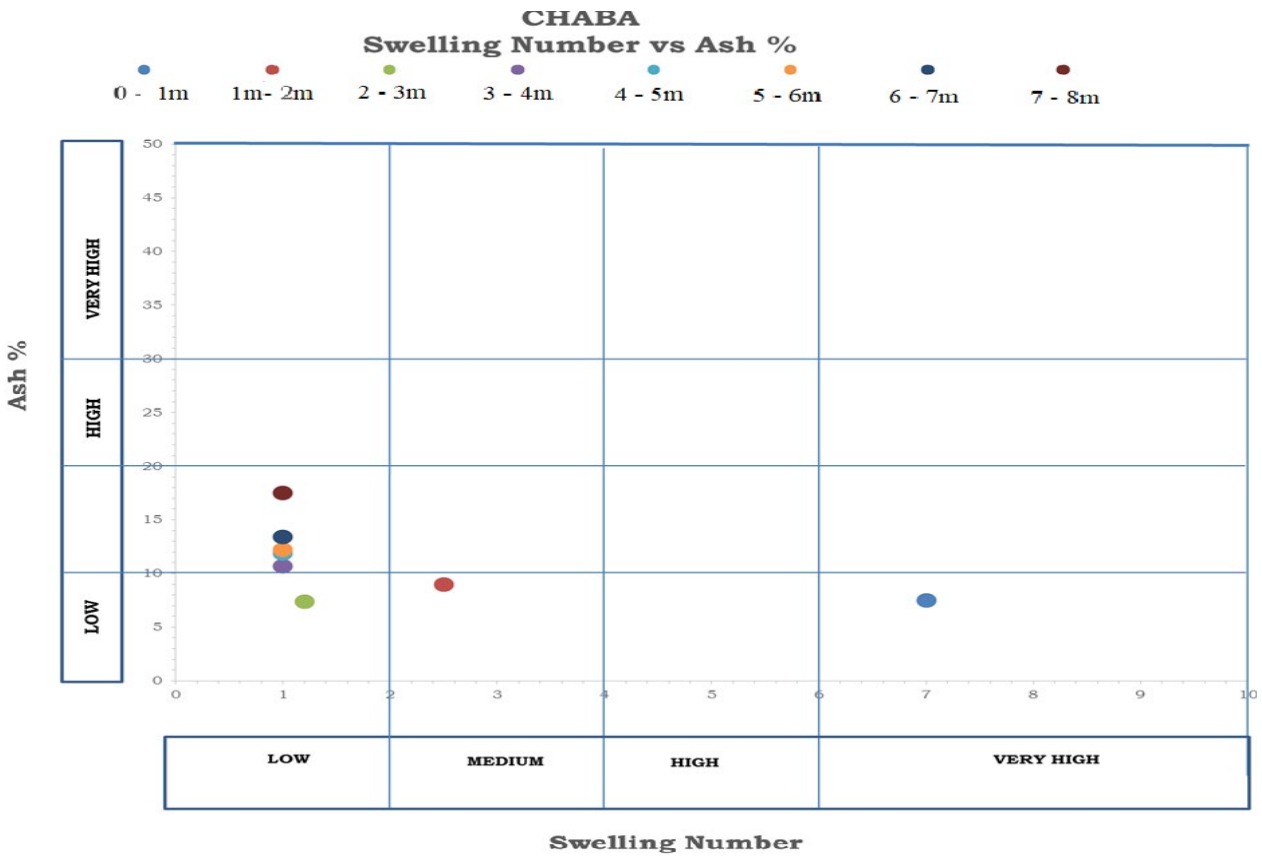
The results in D show that volatile matter content is moderately associated with swelling number in the first two samples from the bottom of the seam, with the highest volatile matter sample in the

lowest sample in the seam sequence. All remaining reducing volatile matter content samples show low swelling numbers.



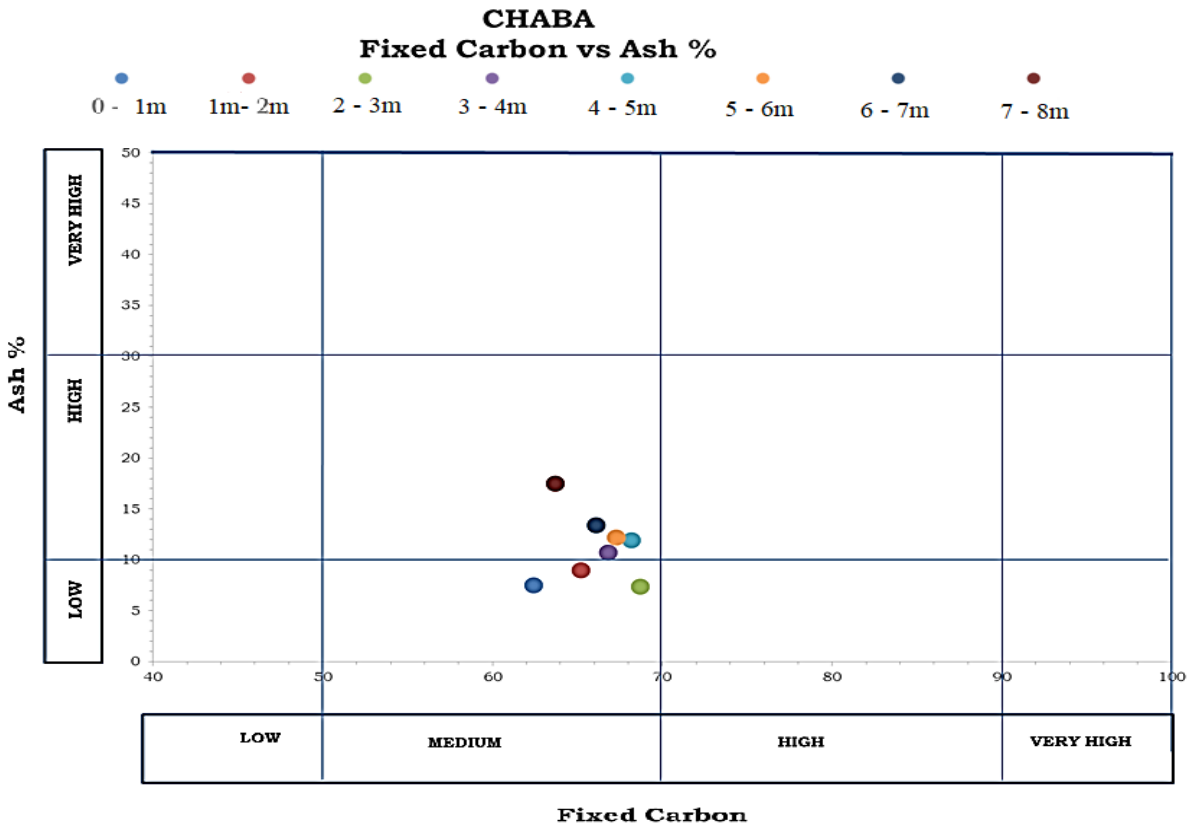
E. Free Swelling Index vs. Volatile Matter for 3 Main Sites A and B samples

Factors above to show that the relationship between free swelling index and volatile matter is similar with those in Chaba, particularly for the lower samples in both sample sites.



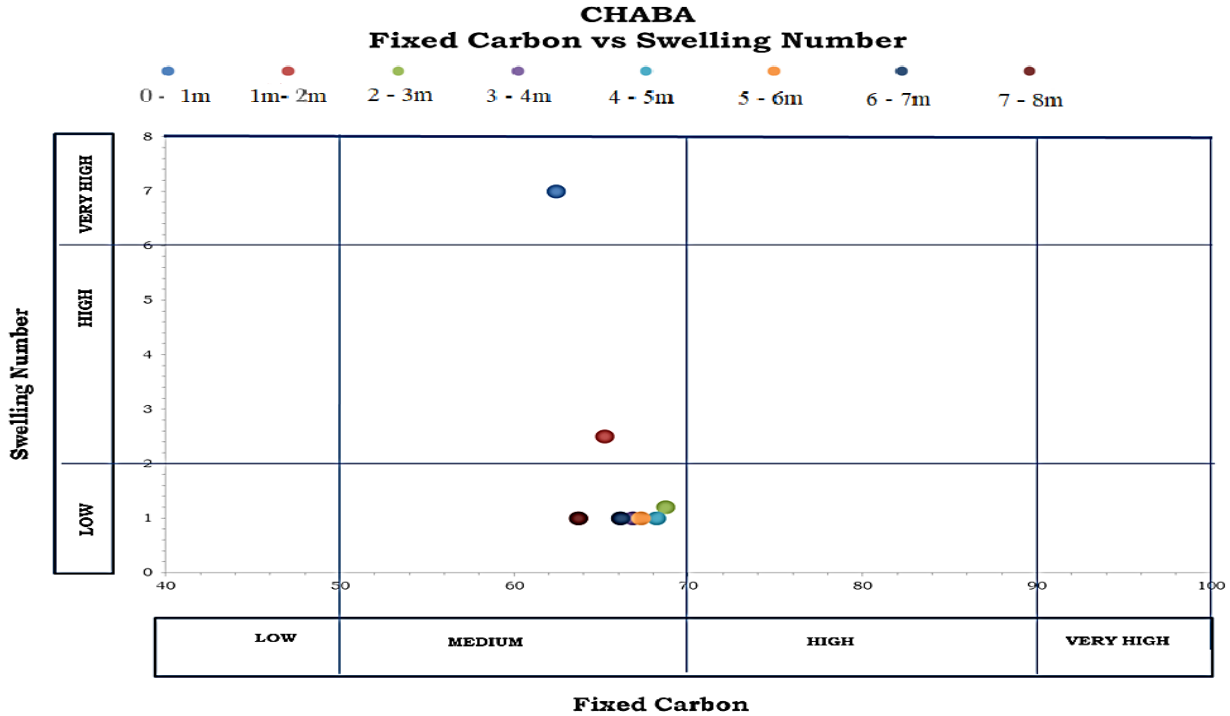
F: Free Swelling Number vs. Ash for Chaba Channel 2 samples.

The results in F show that ash content has little to do with swelling number, with the lowest three samples varying significantly in swelling content but all with similar low ash contents. The remainder of the samples higher up the seam sequence has increasingly higher ash contents and equally low swelling values.



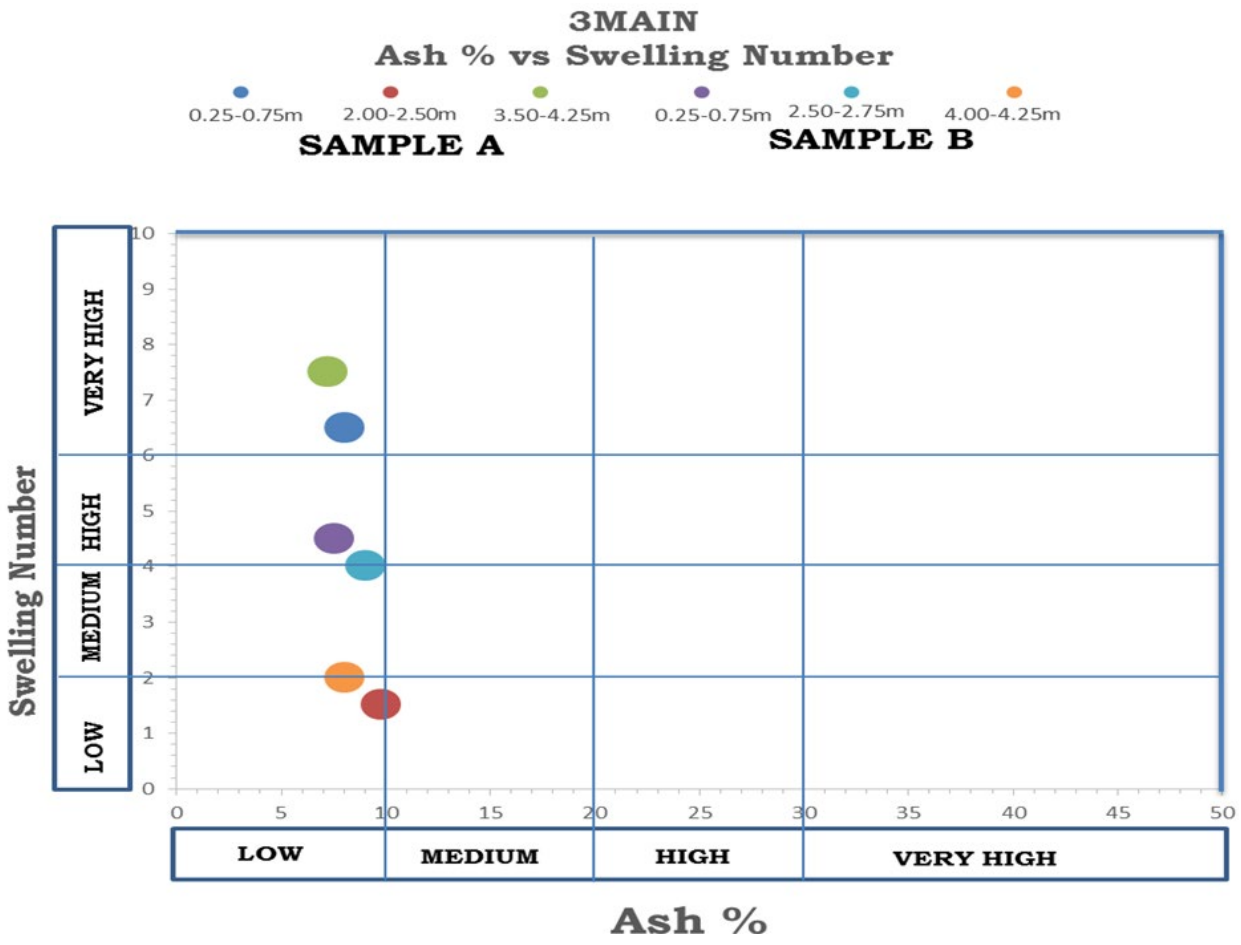
G: Fixed carbon vs. Ash for Chaba Channel 2 Samples

G illustrates that fixed carbon and ash content have little if any relationship.



H: Fixed Carbon vs. Free Swelling Number for Chaba Channel 2

Appendix 2.1H clearly illustrates that fixed carbon contents have no relationships to the highly variable free swelling number.



I: Ash% vs. Free Swelling Number for 3 Main sites A and B samples

In Appendix 2.1 I there is no apparent relationship between ash content and free swelling number.

Plate 1A: Photomicrograph of part of SME 1542 showing fusinite and collotelinite (vitrinite and fusinite)

Plate 2A: Photomicrograph of 3ME sample code 1546, which denotes an exudatinite (exudatinite infilling fusinite and secretinite (Fe). The image to the left is taken under fluorescent mode, image to the right under white light. (under oil emersion))

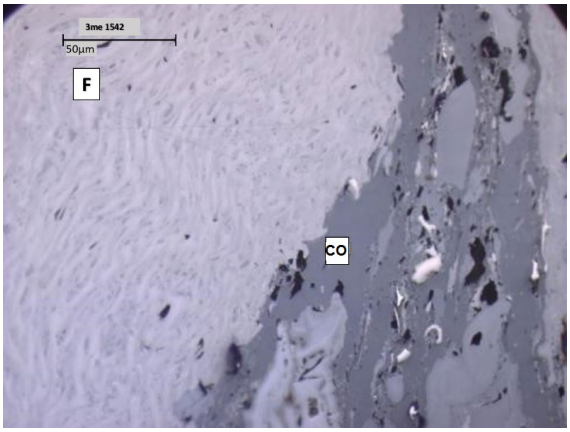


Plate 1



Plate 2 A

Plate 3A: Photomicrograph of 3ME sample code 1546 showing fusinite, collotelinite, semifusinite (exudatinite inside fusinite (normal light)).

Plate 4A: Photomicrograph of 3ME sample code 1547 showing typical macerals: vitrinite and inertinite.

Plate 4B: Photomicrograph of 3ME sample code 1546 showing collotelinite (a large (vitrinite particle)

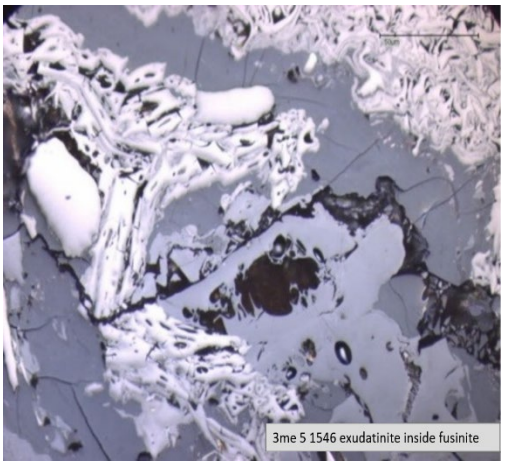


Plate 3 A

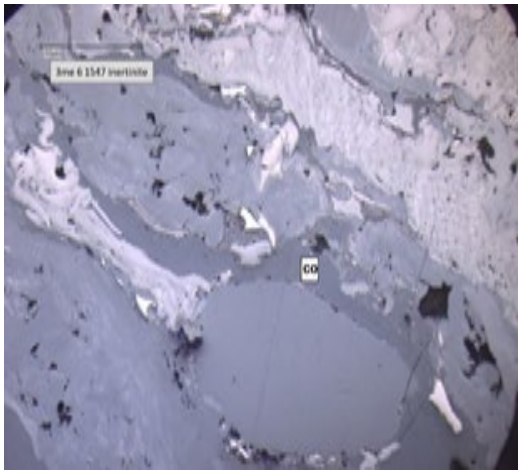


Plate 4 A

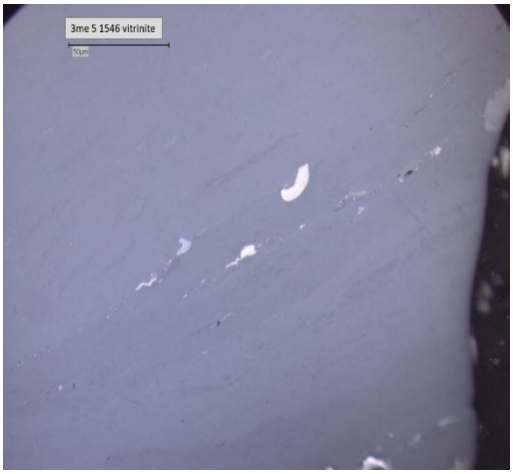


Plate 4 A

Plate 5A: Photomicrograph of 3ME sample code 1547 showing semifusinite (a large semifusinite particle)
Plate 5B. Photomicrograph of 3ME sample code 1547 showing secretinite, inertodetrinite, collotelinite, micrite (L-R) – (vitrinite and micrinite association)
Plate 6A: Photomicrograph of 3ME sample code 1547 showing secretinite exudatinite inside secretinite.
Plate 6B: Photomicrograph of same sample pores filled with exudatinite (the bright spot) and possibly a fluorescing mineral (in fluorescent light)



Plate 5 A

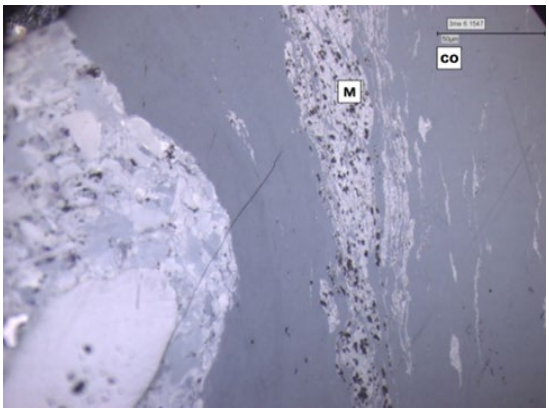


Plate 5 B

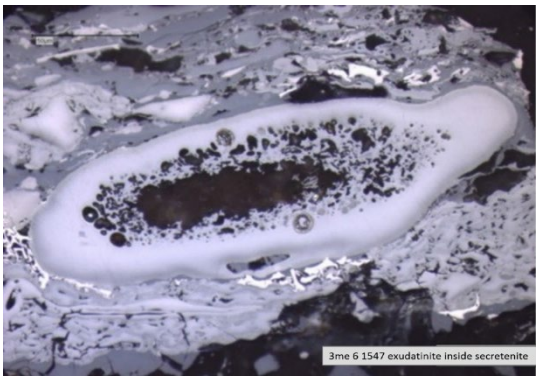


Plate 6 A

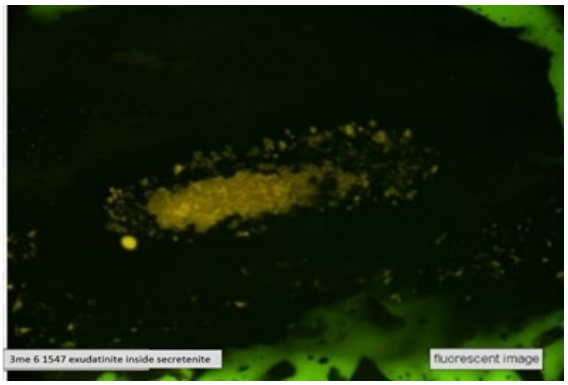


Plate 6 B

Plate 7A: A large particle of collotelinite with some pseudovitrinite (vitrinite with some parallel "cracks" and inclusions (3ME sample code 1548)

Plate 8A: Photomicrograph of 3ME sample code1548 showing a combination of fusinite, reactive semifusinite and inert fusinite

Plate 8B: Photomicrograph of 3ME sample code 1549 showing a large particle of semifusinite and inert fusinite

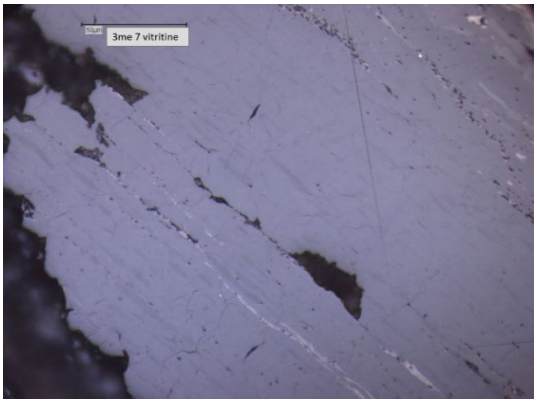


Plate 7 A

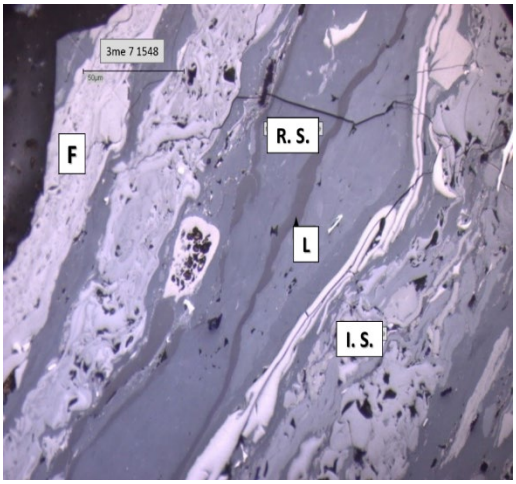


Plate 8 A

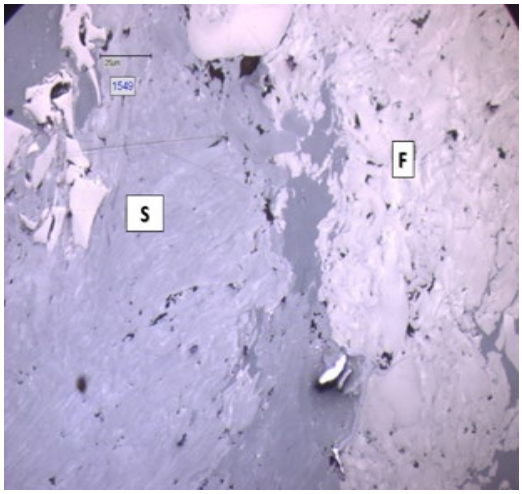


Plate 8 B

Plate 9B: Infilled with exudatinite (Fluorescent image of the same sample)

Plate 10A: 3ME sample code 1549 showing a fissure

Plate 10B: Inert semifusinite (A cracked semifusinite in 3ME sample code 1549)

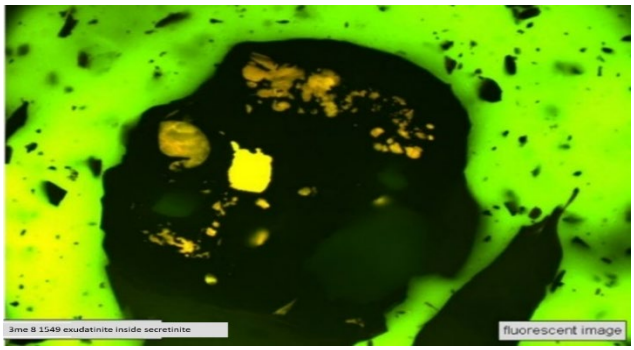


Plate 9 A

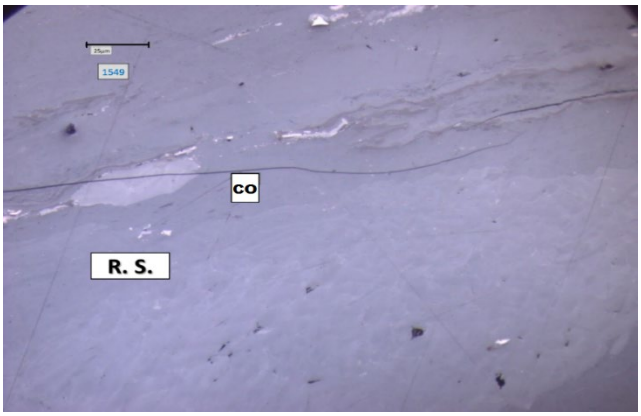


Plate 10 A

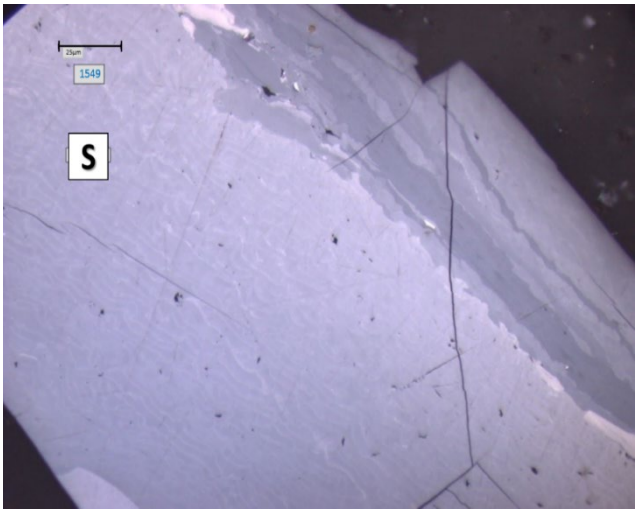


Plate 10 B

Plate 11B Reactive semifusinite, cutinite : (Field view of 1550 showing some liptinite.)

Plate 12A: Collotelinite, in between the fragments of collodetrinite (A large cracked vitrinite particle) in 3ME sample code 1550

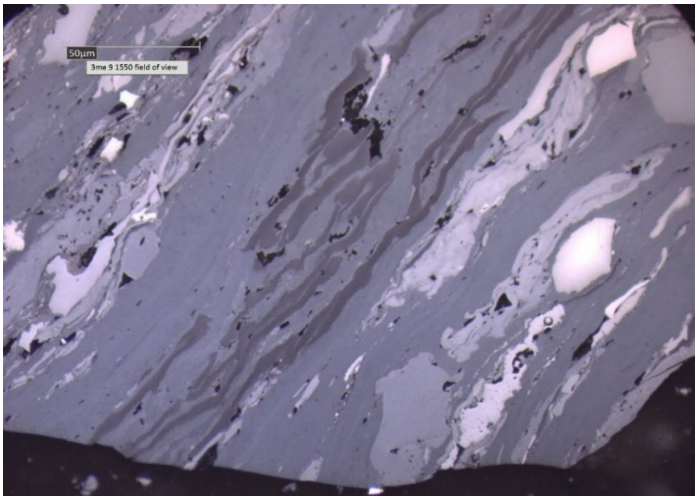


Plate 11 A

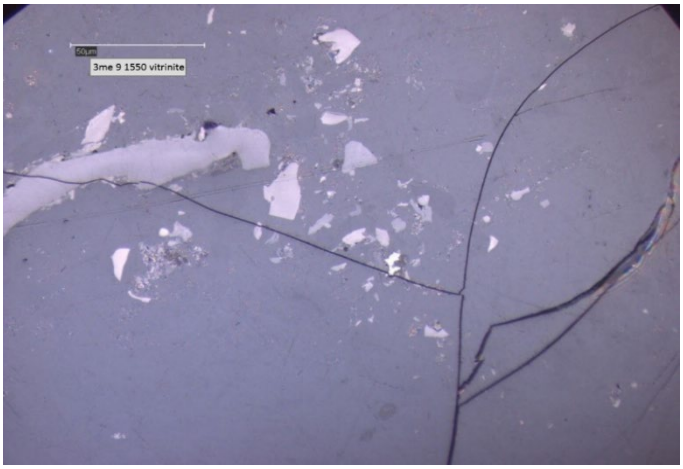


Plate 12 A

Plate 13A: A photomicrograph of 3ME sample code 1551 showing secretinite of various shades (different reflectance)

Plate 13B: Inert semifusinite (Semifusinite) particle in 3ME sample code 1551

Plate 14A: Collotelinite, fusinite, inertodetrinite Field of view of 3ME sample code 1552

Plate 14B: An association of Collotelinite band and micrinite (vitrinite and micrinite) in 3ME sample code 1552.

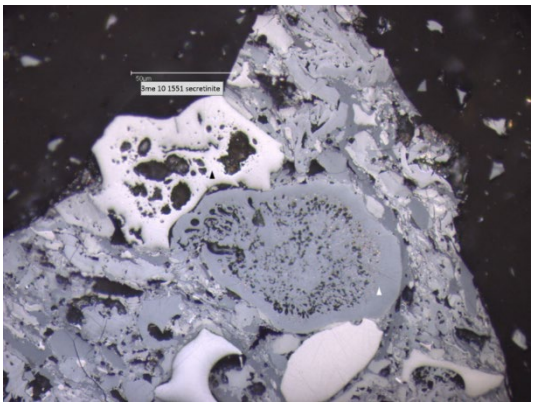


Plate 13 A

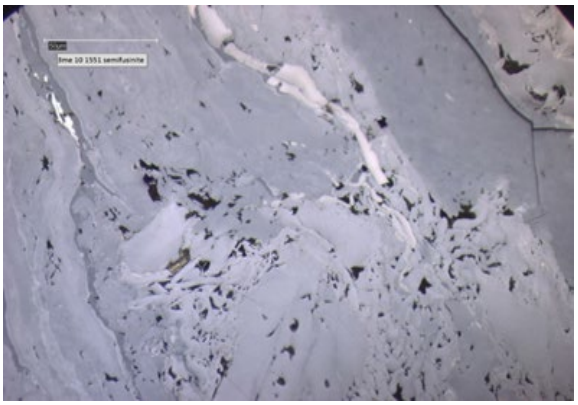


Plate 13 B

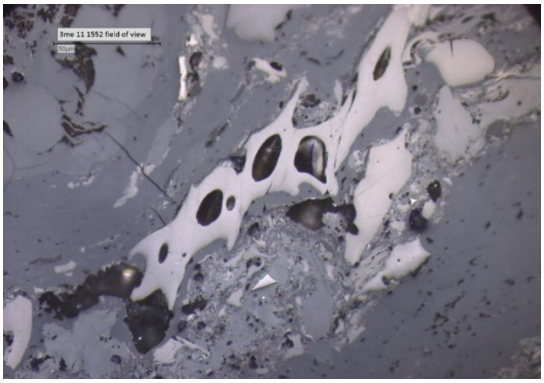


Plate 14 A

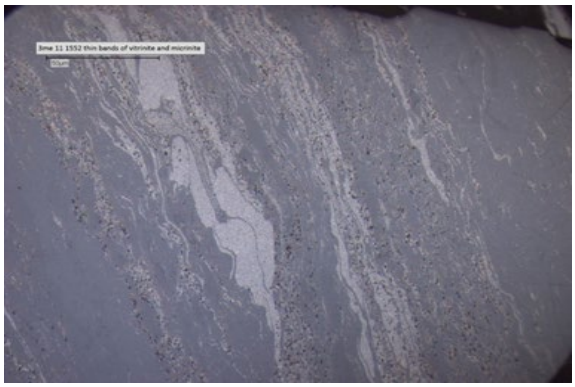


Plate 14 B

Plate 15A: A photomicrograph of 3ME sample code 1553 showing collotelinite, reactive semifusinite and inert semifusinite (vitrinite and both inert and reactive semifusinite)

Plate 16A: A photomicrograph of 3ME sample code 1553 showing large fusinite particle.

Plate 16B: A Photomicrograph of 3MS sample code 1554 showing collotelinite and fusinite (vitrinite and fusinite).

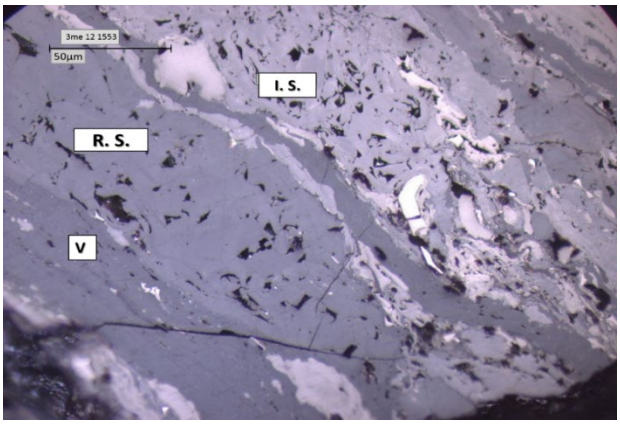


Plate 15 A

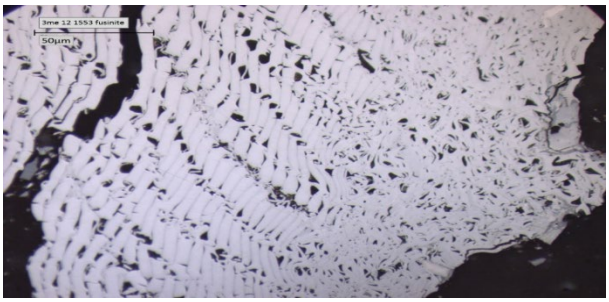


Plate 16 A

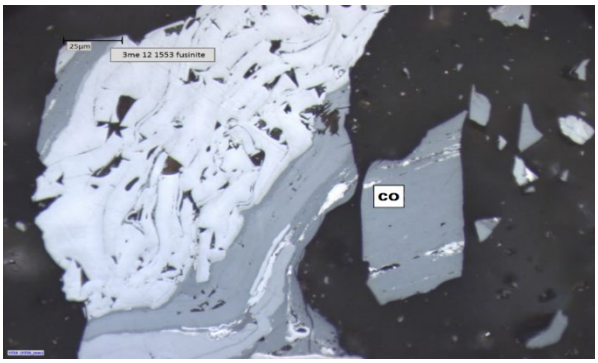


Plate 16 B

Plate 17A: A photomicrograph of 3MS sample code 1554 showing particle of collotelinite secretinite without resinite (vitrinite, secretinite and resinite).

Plate 18A: Some fusinite particles in 3MS sample code 1555

Plate 18B: A combination of Collotelinite and macrinite (vitrinite and fusinite particles) in 3MS sample code 1555

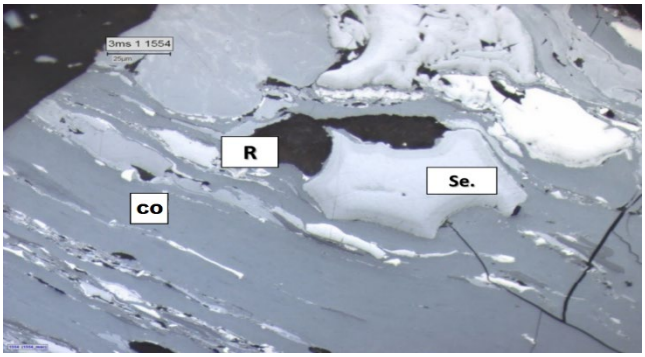


Plate 17 A

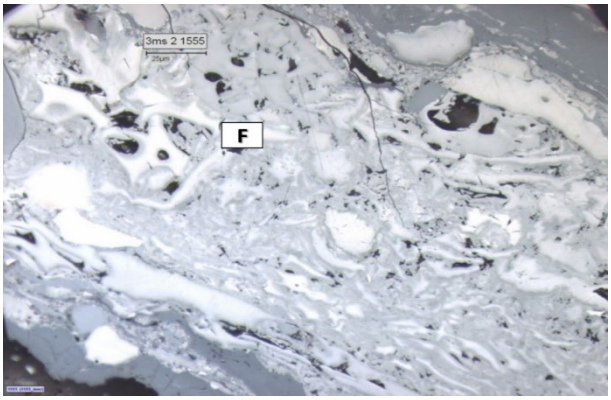


Plate 18 A

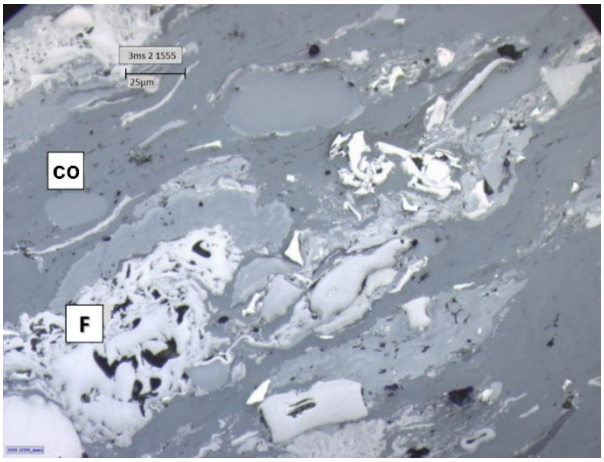


Plate 18 B

Plate 19A: Inert fusinite Semifusinite “interbedded” with vitrinite in 3MS sample code 1555.

Plate 19B: Carbonate in vitrinite

Plate 20B: A large Collotelinite (vitrinite) particle in 3MS sample code 1556

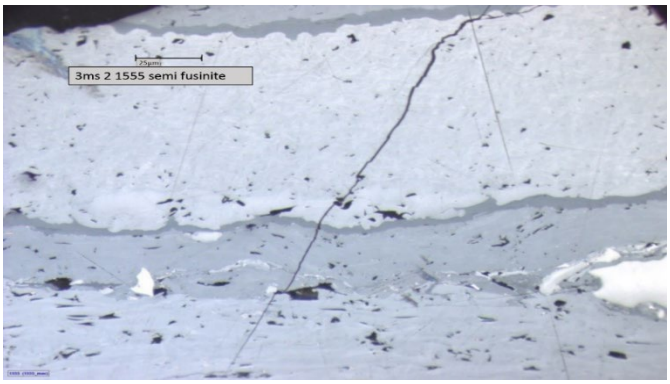


Plate 19 A

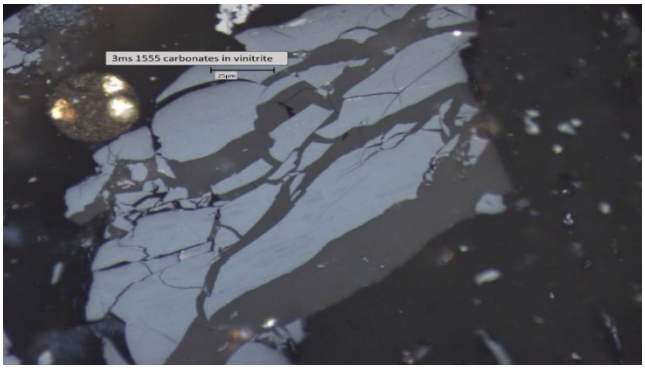


Plate 19 B

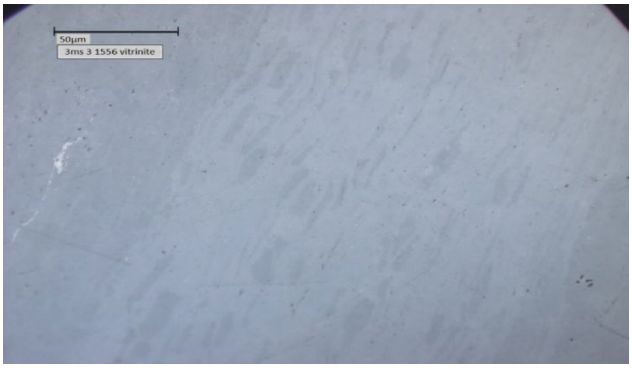


Plate 20 A

Plate 21A: Collotelinite and micrite band (A large vitrinite particle with some inertinite0

Plate 21B: A photomicrograph of 3MS sample code 1557 showing semifusinite and liptinite (L denote cutinite and with an inert semifusinite)

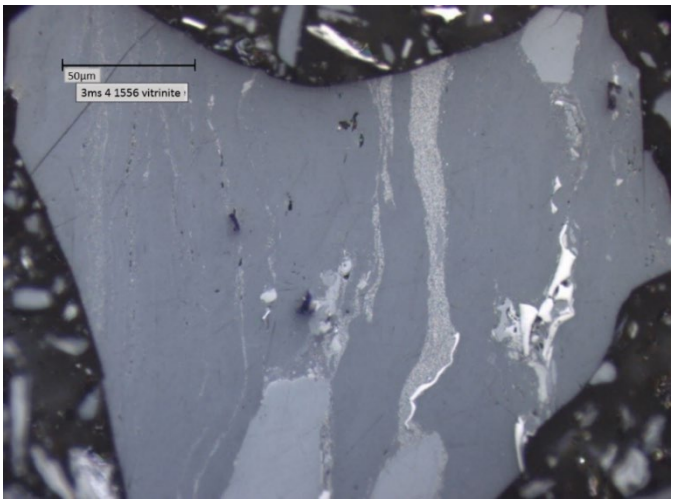


Plate 21 A

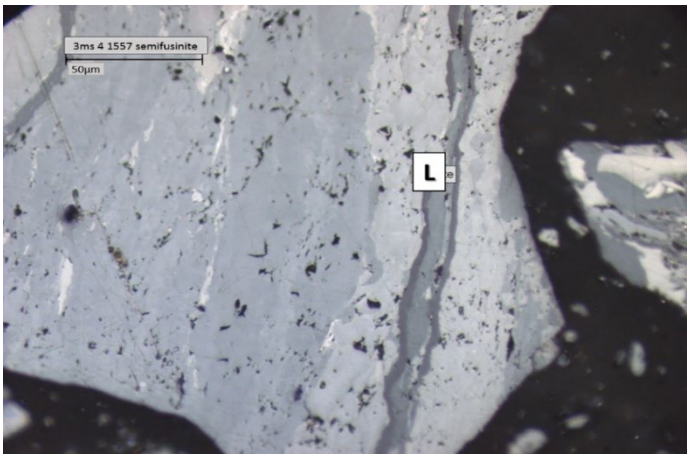


Plate 21 B

Plate 23A: various forms of inertinite (3MS sample code 1557)

Plate 23B: A large collotelinite and fusinite (vitrinite particle and fusinite) in 3MS sample code 1558

Plate 24A: Inert fusinite and fusinite (Semifusinite and fusinite) in 3MS sample code 1558

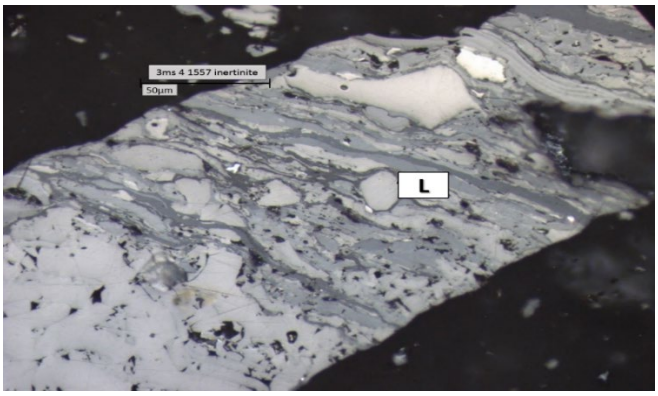


Plate 23 A

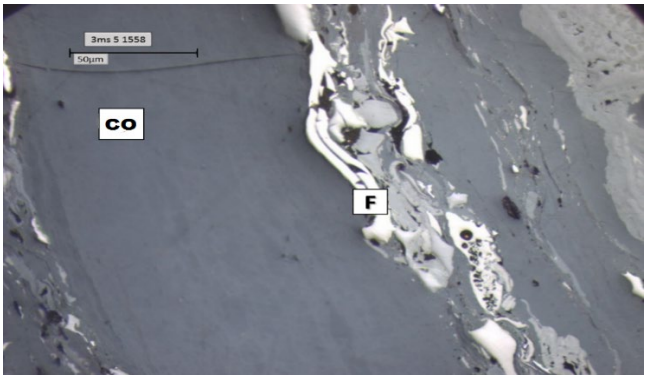


Plate 23 B

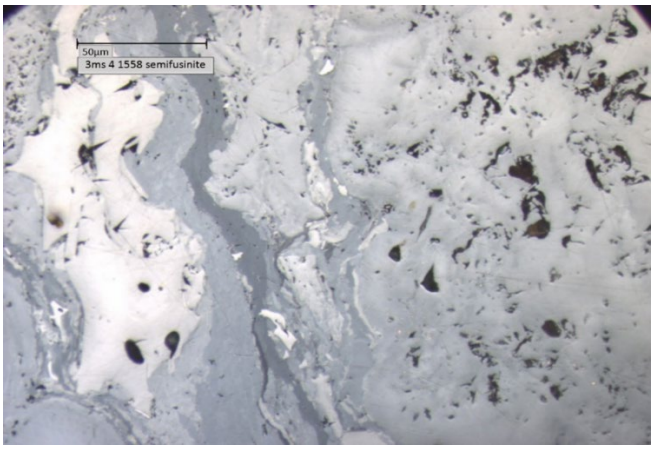


Plate 24 A

Plate 25A: Mixed maceral particle in 3MS sample code 1559; detrovitrinite and inertinite fragments
Plate 25B: Semifusinite and gelinite (Semifusinite and fusinite with gelinite) in 3MS sample code 1559
Plate 26A: Fusinite and secretinite in 3MS sample code 1559
Plate 26B: An association of vitrinite fusinite reactive fusinite (vitrinite, semifusinite and micrinite) in 3MS sample code 1560

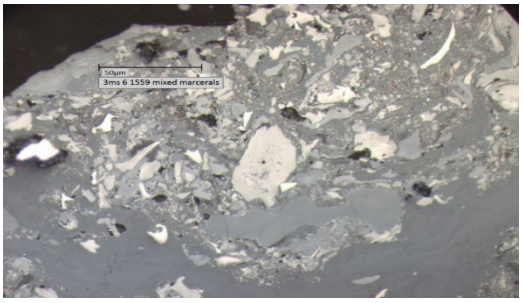


Plate 25 A

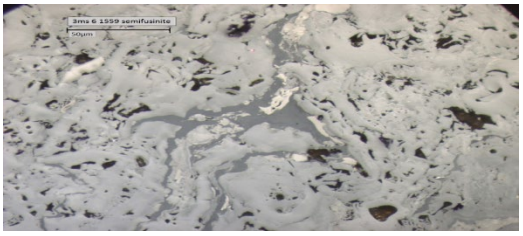


Plate 25 B

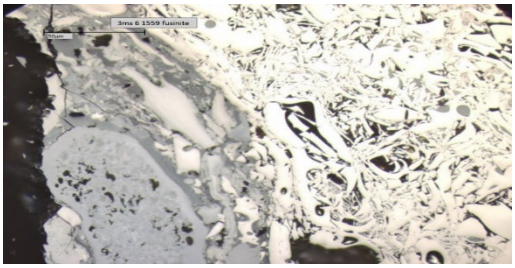


Plate 26 A

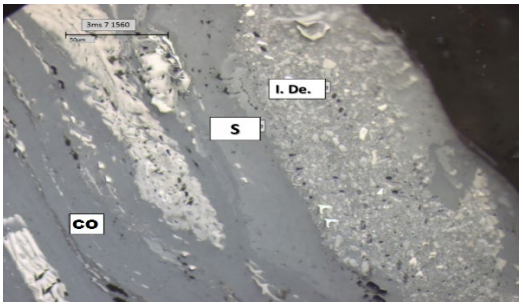


Plate 26 B

Plate 27A: A large collotelinite with gelinite filling (vitrinite particle) in 3MS sample code 1560

Plate 27B: Secretinite and mineral matter (Secretinite infilled with exudatinite)

Plate 28A: Field of view of 3MS sample code 1561 showing a combination of collotelinite, inert fusinite and secretinite (vitrinite (grey), inertinite (lighter grey) and fusinite.)

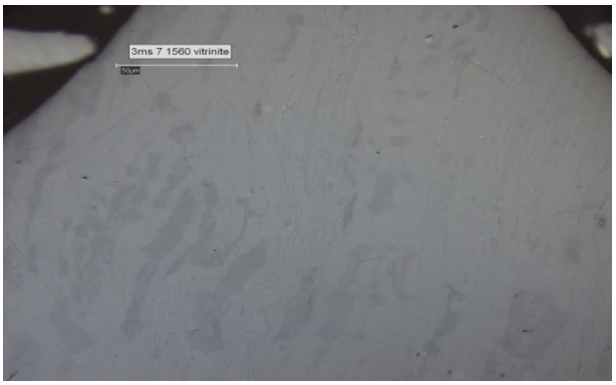


Plate 27 A

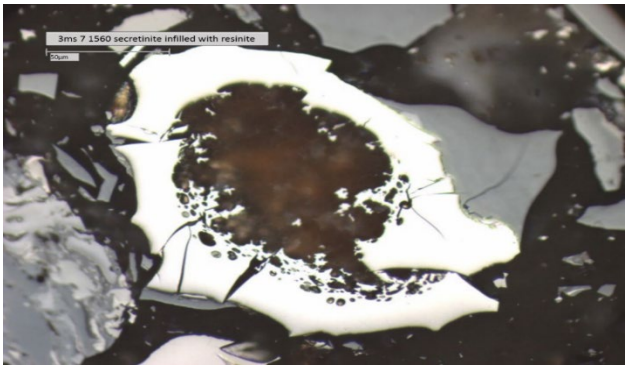


Plate 27 B

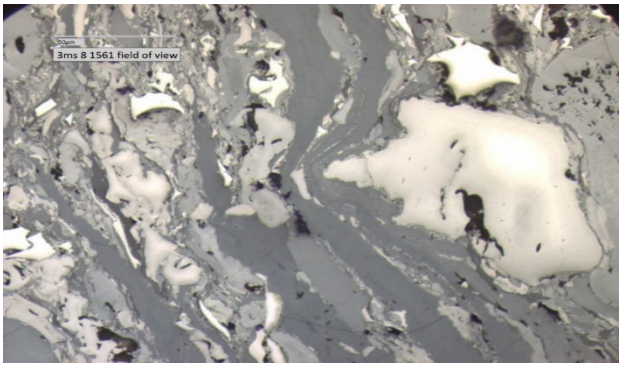


Plate 28 A

Plate 29B: Various secretinites (Inertinite) in 3MS sample code 1562

Plate 30A: A photomicrograph of 3MS sample code 1563 showing fusinite (exudatinite inside fusinite)

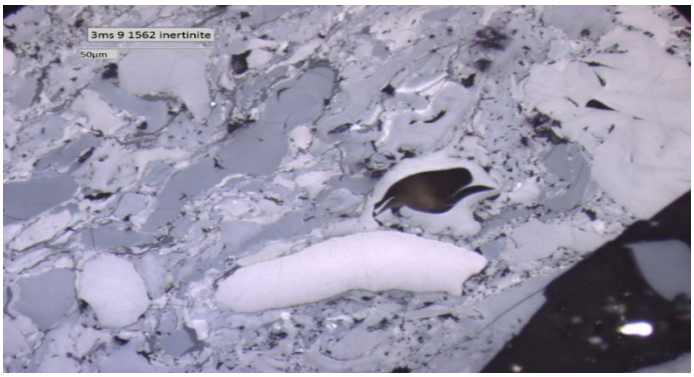


Plate 29 A

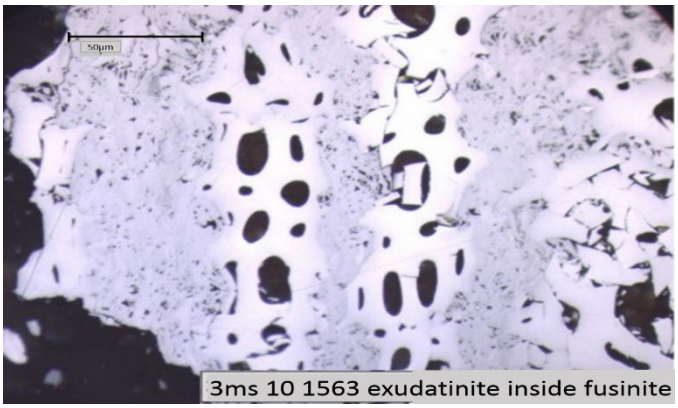


Plate 30 A

Plate 31A: Another fluorescent image of exudatinite in 3MS sample code 1564.

Plate 31B: Same field of view under normal light

Plate 32A: An association of (fusinite and inert fusinite (vitrinite and inertinite) in Chaba sample code 1565

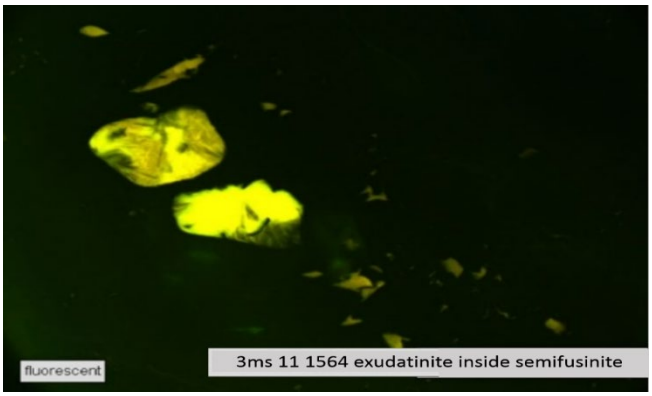


Plate 31 A

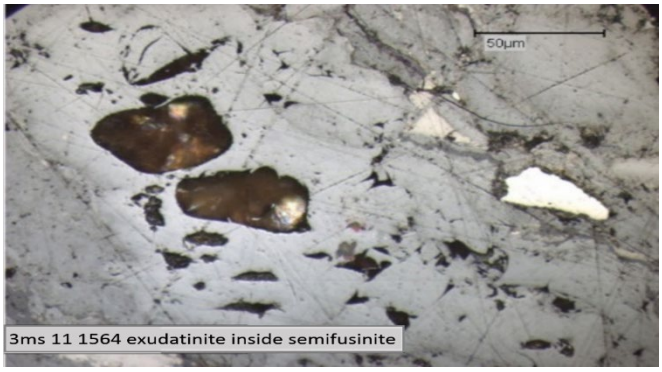


Plate 31 B

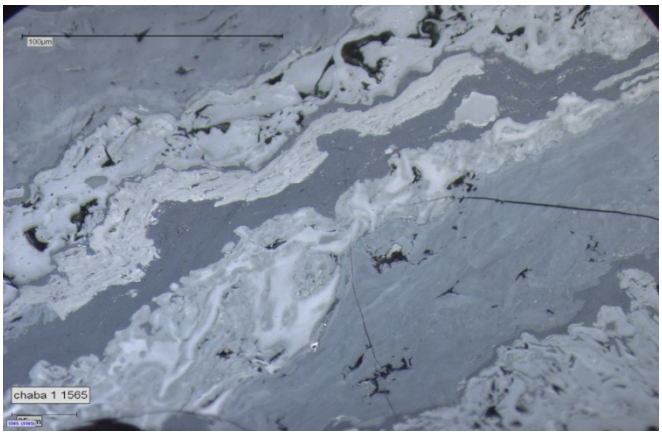


Plate 32 A

Plate 33A: Severely cracked particles (vitrinite) in Chaba sample code 1565

Plate 34A: A fluorescent image showing exudatinite Chaba sample code 1566

Plate 34B: Same field of view under normal light.

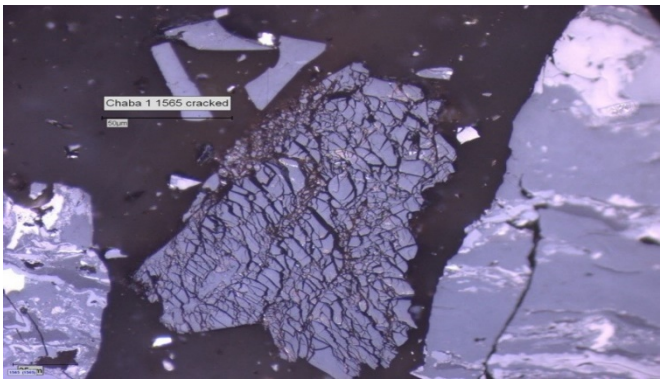


Plate 33 A

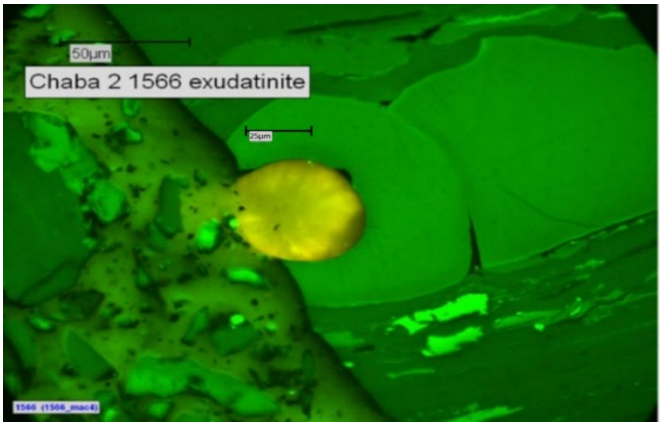


Plate 34 A

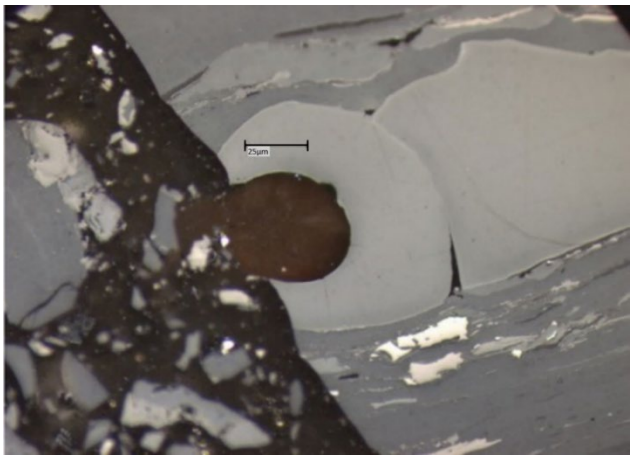


Plate 34 B

Plate 35B: Reactive semi fusinite and inert semi fusinite (Inertinite, with reactive semifusite) in Chaba sample code 1566.

Plate 36A: Inert semifusinite and fusinite in Chaba sample 1567

Plate 36B: Collotelinite, and inert semifusinite and reactive semifusinite in between (inertinite and vitrinite) in Chaba sample 1567

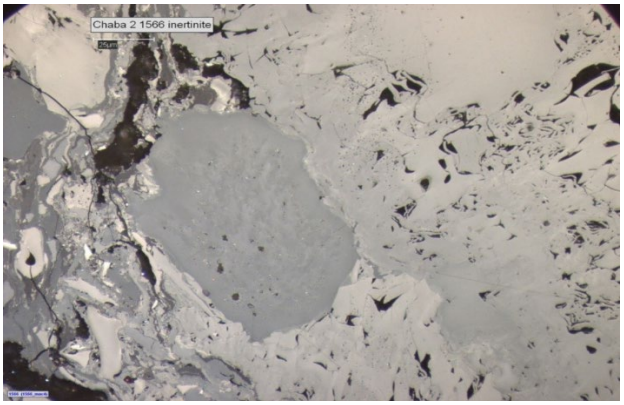


Plate 35 A

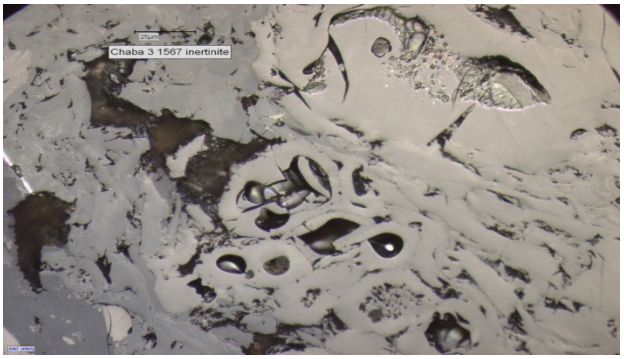


Plate 36 A

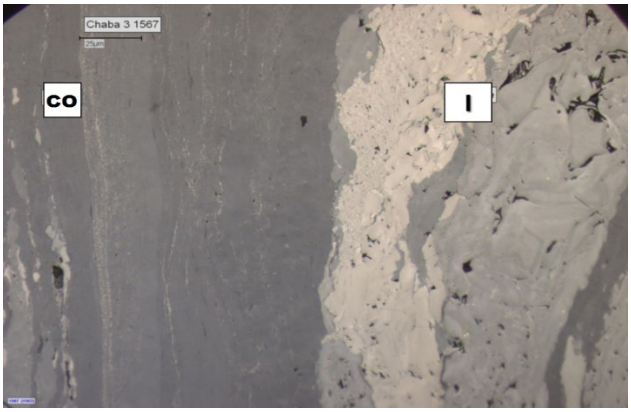


*Plate 36 B*Plate 37A:
A photomicrograph of Chaba sample code 1567 with reactive semifusinite and inert semifusinite (banded semifusinite)